



Alpizar Sosa, Edubiel Arturo (2020) *Polyomic characterisation of polyene drug resistance in Leishmania spp.* PhD thesis.

<https://theses.gla.ac.uk/79026/>

Copyright and moral rights for this work are retained by the author

A copy can be downloaded for personal non-commercial research or study, without prior permission or charge

This work cannot be reproduced or quoted extensively from without first obtaining permission in writing from the author

The content must not be changed in any way or sold commercially in any format or medium without the formal permission of the author

When referring to this work, full bibliographic details including the author, title, awarding institution and date of the thesis must be given

Enlighten: Theses

<https://theses.gla.ac.uk/>
research-enlighten@glasgow.ac.uk

**Polyomic Characterisation of Polyene Drug
Resistance in *Leishmania* spp.**

Edubiel Arturo Alpizar Sosa

**Doctor in Veterinary Medicine,
MRes. in Molecular Parasitology**

**Submitted in fulfilment of the requirements for the
degree of Doctor of Philosophy**

**Institute of Infection, Immunity and Inflammation
School of Life Sciences
College of Medical, Veterinary and Life Sciences**

University of Glasgow

October 2019

Abstract

Amphotericin B is the compound of choice for the treatment of leishmaniasis, however a definitive mode of action and full knowledge of causes of resistance to this polyene are still poor. The aim of this project is to use a polyomic approach to characterise laboratory generated mutant lines of *Leishmania* spp., selected for resistance against the polyene antifungals, amphotericin B and nystatin. While previous work has characterised multiple lines of *L. mexicana* resistant to amphotericin B, this is the first report of resistant lines selected against nystatin in *Leishmania* spp. Ergosta-7,22-dien-3-ol and cholesta-5,7,22-trienol, were the two main sterol intermediates replacing ergosterol in all eight polyene-resistant lines of *Leishmania* spp. The former sterol intermediate was associated with five novel mutations in sterol C5-desaturase, in two and six AmBR- and NysR-mutants and the latter resulted from changes in C24-sterol methyl transferase, along with deletion of the miltefosine transporter and its neighbouring gene downstream in two AmBR lines.

Interestingly, switching from ergosterol to these two sterol intermediates was associated with an increased and an attenuated inflammatory response *in vivo*, respectively. In all cases, viable parasites were recovered post-infection and the retention of resistance *in vivo* was confirmed. In addition, response to treatment with amphotericin B was observed only in wild type parasites. Untargeted metabolomics provided hints towards modes of action in addition to the binding to ergosterol. Upregulation of the pentose phosphate pathway plays a central role as a key provider of NADPH suggesting an immediate pulse of oxidative stress associated with addition of the drug. Amphotericin B treatment rapidly altered lipid metabolism, decreasing the abundance of Acetyl-CoA, NADPH, leucine and mevalonate.

In all mutants, the total or partial loss of the key membrane sterol ergosterol lead to amphotericin B resistance. All polyene resistant mutants were more susceptible to pentamidine and paromomycin. Conversely, miltefosine resistance was found in all mutants, with this increase being more pronounced in two lines showing a deletion of the miltefosine transporter. The grounds of cross-resistance to a new library of sterol inhibitors, 1,2,3-triazolylsterols, was also assessed. The most active hits showed a micromolar potency, albeit a mode of action independent of the inhibition of sterols is suggested. Considering the increase of resistance against the antileishmanials and the limited therapies available, this thesis provides valuable information on the MoA and resistance of polyenes in *Leishmania*, should the resistance against AmB, the drug of choice for leishmaniasis, increases in clinical settings, and to improve the discovery of potential new drug targets.

Table of Contents

ABSTRACT	2
LIST OF TABLES	5
LIST OF FIGURES	6
LIST OF ACCOMPANYING MATERIAL.....	8
ACKNOWLEDGEMENT	9
AUTHOR'S DECLARATION	10
DEFINITIONS/ABBREVIATIONS	11
1 INTRODUCTION	13
1.1 NEGLECTED TROPICAL DISEASES	13
1.2 <i>LEISHMANIA</i> PARASITES AND OTHER KINETOPLASTIDS.....	13
1.3 EPIDEMIOLOGY AND CLINICAL FORMS OF LEISHMANIASIS.....	14
1.4 BIOLOGY AND MOLECULAR BIOLOGY OF LEISHMANIA.....	18
1.5 LIFE CYCLE	19
1.5.1 <i>The sandfly vector</i>	21
1.6 USE, MODE OF ACTION AND RESISTANCE TO ANTILEISHMANIAL DRUGS	23
1.6.1 <i>Pentavalent antimonials</i>	25
1.6.2 <i>Pentamidine</i>	27
1.6.3 <i>Paromomycin</i>	28
1.6.4 <i>Miltefosine</i>	30
1.6.5 <i>Polyene antifungals</i>	32
1.6.6 <i>Amphotericin B</i>	35
1.7 <i>LEISHMANIA</i> METABOLISM	48
1.7.1 <i>The sterol biosynthetic pathway</i>	51
1.7.2 <i>The Pentose phosphate pathway</i>	59
1.7.3 <i>Polyamine-trypanothione pathway</i>	60
1.8 OMICS TECHNOLOGIES, GENE EDITING AND DRUG DISCOVERY.....	63
1.8.1 <i>Whole genome sequencing and transcriptomics in Leishmania</i>	63
1.8.2 <i>Gene editing of Leishmania spp. as a tool for drug discovery</i>	66
1.8.3 <i>Untargeted and targeted metabolomics</i>	67
1.9 AIMS OF THE STUDY.....	69
2 MATERIALS AND METHODS.....	71
2.1 CULTURE OF <i>LEISHMANIA</i> SPP. CELLS IN VITRO.....	71
2.2 SELECTION OF POLYENE RESISTANT <i>LEISHMANIA</i> SPP.....	72
2.3 CLONAL POPULATIONS BY LIMITING DILUTION CLONING.....	72
2.4 DRUG SCREENING ASSAYS	73
2.5 TIME-TO-KILL AND DOSE-TO-KILL IN WILD TYPE AND TWO RESISTANT CELL LINES.....	74
2.6 INFECTIVITY OF <i>LEISHMANIA MEXICANA</i> IN A MURINE MODEL	75
2.7 LIQUID CHROMATOGRAPHY/MASS SPECTROMETRY (LC/MS) BASED METABOLOMICS ANALYSIS	76
2.8 GAS CHROMATOGRAPHY/MASS SPECTROMETRY (GC/MS)	77
2.9 DNA AND RNA SAMPLE PREPARATION	79
2.10 GENERATION OF <i>LEISHMANIA</i> OVEREXPRESSION LINE OF C24SMT	79
2.11 QUANTITATIVE PCR	80
2.12 CRISPR CAS9 SYSTEM	82
2.13 DATA ANALYSIS OF GENOMICS AND TRANSCRIPTOMICS	88
2.13.1 <i>Next generation sequencing</i>	88
2.14 RNA-SEQ ANALYSIS	89
2.15 BIOINFORMATICS AND OTHER COMPUTATIONAL TOOLS.....	89
2.16 INFECTIVITY IN THE SANDFLY VECTOR.....	90
3 DRUGS SCREENING IN POLYENE RESISTANT LINES OF <i>L. MEXICANA</i>.....	91
3.1 INTRODUCTION.....	91
3.2 RESULTS.....	94
3.2.1 <i>Selection of polyene resistance in Leishmania spp.</i>	94

3.2.2	<i>Growth rate of polyene resistant promastigotes.</i>	100
3.2.3	<i>Drug screening of polyene-resistant lines</i>	102
3.3	DISCUSSION	112
4	CHARACTERIZATION OF POLYENE RESISTANT LINES OF <i>LEISHMANIA MEXICANA</i>: WHOLE GENOME SEQUENCING	113
4.1	RESULTS	113
4.1.1	<i>Chromosome changes</i>	114
4.1.2	<i>Gene copy number and changes in chromosome ploidy</i>	115
4.1.3	<i>Mutations triggering coding changes</i>	119
4.1.4	<i>Changes in the C-24 sterol methyltransferase gene</i>	120
4.1.5	<i>Changes in sterol C-5 desaturase</i>	124
4.1.6	<i>Predicted protein-protein interactions in the ergosterol biosynthetic pathway in Leishmania.</i>	130
4.2	DISCUSSION	138
5	STEROL PROFILING AND INFECTIVITY OF POLYENE RESISTANT LINES OF <i>LEISHMANIA MEXICANA</i>.	140
5.1	INTRODUCTION	140
5.2	RESULTS	142
5.2.1	<i>The sterol signature of AmB resistant lines</i>	147
5.2.2	<i>Sterol signatures of nystatin resistant lines</i>	153
5.2.3	<i>Infectivity of the AmBR lines in vivo</i>	158
5.2.4	<i>Response to treatment with AmB in vivo</i>	168
5.2.5	<i>Response to liposomal AmB (AmBisome®) in vivo</i>	169
5.2.6	<i>Retention of AmB resistance after infection in vivo</i>	172
5.2.7	<i>Histological analysis of mice infected with AmB resistant lines</i>	175
5.3	DISCUSSION	184
6	DRUG SCREENING OF A NEW CLASS OF STEROL INHIBITORS IN <i>LEISHMANIA</i> PROMASTIGOTES	186
6.1	INTRODUCTION	186
6.2	RESULTS	188
6.2.1	<i>Tricyclic antidepressants</i>	188
6.2.2	<i>Sterol inhibitors, 1,2,3-triazolylsterols</i>	191
6.2.3	<i>Effect of the 1,2,3-triazolylsterol inhibitors on the sterol profiling of Leishmania</i>	202
6.3	DISCUSSION	207
7	METABOLIC EFFECTS OF AMB IN THE <i>LEISHMANIA MEXICANA</i> PROMASTIGOTES.	210
7.1	INTRODUCTION	210
7.2	RESULTS	212
7.2.1	<i>Lipid metabolism</i>	217
7.2.2	<i>Carbohydrates and energy metabolism</i>	221
7.2.3	<i>Nucleotide metabolism</i>	228
7.2.4	<i>Amino acid and polyamine-trypanothione pathway</i>	230
7.3	DISCUSSION	234
8	GENERAL DISCUSSION	238
8.1	DRUG SUSCEPTIBILITY OF AMPHOTERICIN B RESISTANT LINES AGAINST DIFFERENT COMPOUNDS	239
8.2	UNTARGETED AND TARGETED METABOLOMICS IN AMBR LEISHMANIA	242
8.3	STEROL PROFILE AND VIRULENCE OF AMBR-RESISTANT LEISHMANIA IN VIVO	243
8.4	CONCLUSIONS AND FUTURE WORK	245
	LIST OF REFERENCES	247

List of Tables

Table 1-1. Number of cases of VL reported from 2013 to 2017 in regions with higher prevalence.	18
Table 1-2. Modes of action (MoA) of large and small polyenes.	34
Table 1-3. Sterol Biosynthetic Pathway (SBP) genes and enzymes in <i>Leishmania</i> spp. and orthologues in <i>Saccharomyces cerevisiae</i> .	55
Table 2-1. Primers sequences for PCR amplification of, sgRNA templates, and targeting fragments (plasmids with resistance cassettes) used to knockout <i>L. mexicana</i> C24SMT.	87
Table 3-1. Susceptibility to AmB and Nys of individual clones selected for resistance.	97
Table 3-2. Susceptibility of AmBR lines and clones (<i>L. mexicana</i>) to a series of compounds.	107
Table 3-3. Selectivity of NysR lines (<i>L. mexicana</i>) to antileishmanials, and other compounds.	110
Table 4-1. Samples for WGS of AmB resistant <i>Leishmania mexicana</i> promastigotes.	114
Table 4-2. Summary of genomic changes identified with WGS in AmBR lines of <i>L. mexicana</i> promastigotes.	122
Table 5-1. Metabolite profiling by GC-MS (derivatization with trimethylsilyl, TMS) in AmBR lines of <i>L. mexicana</i> promastigotes.	155
Table 5-2. Metabolite profiling by GC-MS (derivatization with trimethylsilyl, TMS) in AmBR lines of <i>L. mexicana</i> amastigotes.	156
Table 5-3. Metabolite profiling by GC-MS (derivatization with trimethylsilyl, TMS) in NysR lines of <i>L. mexicana</i> promastigotes.	157
Table 5-4. Susceptibility of AmBR lines of <i>L. mexicana</i> to AmB and AmBisome before and after infection in mice.	174
Table 5-5. Summary of the mutations identified in genes of the sterol pathway in AmB resistant promastigotes of <i>Leishmania</i> spp., coupled with their sterol profile (GC-MS) and their phenotype in a murine model.	182
Table 5-6. GC-MS profiling of <i>Leishmania</i> spp. amastigotes and promastigotes.	183
Table 6-1. Chemical structure of the library of heterocyclic steroids from pregnenolone.	195
Table 6-2. EC ₅₀ of the 1,2,3-triazolylsterol inhibitors (TAZ) in <i>L. mexicana</i> , and with the recombinant <i>L. mexicana</i> C24SMT-protein.	199
Table 6-3. Sterol profiling by GC-MS (derivatization with trimethylsilyl, TMS) in <i>L. mexicana</i> promastigotes treated with C24SMT inhibitors.	206
Table 7-1. Metabolites (identified / annotated) significantly (P<0.05) altered in wild type and AmBR lines treated with AmB.	216
Table 7-2. Effects of AmB on the Pentose Phosphate Pathway in a TKTKO of <i>L. mexicana</i> .	228

List of Figures

Figure 1-1. Global prevalence of cutaneous (CL) and visceral leishmaniasis (VL).....	15
Figure 1-2. The phylogenetic tree of the <i>Leishmania</i> species causing disease and other related Trypanosomatids.....	16
Figure 1-3. Life cycle of <i>Leishmania</i> spp.	20
Figure 1-4. Tropism of <i>Leishmania</i> species within the sandfly vector.....	21
Figure 1-5. The life cycle of <i>Leishmania</i> within the sandfly vector.....	22
Figure 1-6. Old and new life cycle of <i>Leishmania</i> within the insect vector.....	23
Figure 1-7. Compounds used for the therapy of leishmaniasis.....	24
Figure 1-8. Model of the MoA and MoR of antimonials in <i>Leishmania</i>	27
Figure 1-9. Chemical Structure and classification of polyenes and their target sterols.....	33
Figure 1-10. Model of the MoA of large and small polyenes in sterol-containing membranes.....	36
Figure 1-11. Model of structure and interaction of AmB and ergosterol-and phospholipid containing membranes.....	38
Figure 1-12. Molecular mechanisms of drug resistance in <i>Leishmania</i> spp.....	48
Figure 1-13. Enzymatic reactions of the Sterol biosynthetic pathway (SBP) in the budding yeast (<i>Saccharomyces cerevisiae</i>).....	52
Figure 1-14. Localisation of the SBP enzymes in the trypanosomatids.....	53
Figure 1-15. The Pentose Phosphate Pathway in <i>Leishmania</i>	60
Figure 1-16. The polyamine-trypanothione pathway in trypanosomatids.....	62
Figure 2-1. Detailed maps of pT plasmids of CRISPR-Cas9 used for generation of single and double knockouts of target genes in <i>Leishmania</i> spp.....	85
Figure 2-2. Workflow of the CRISPR-Cas9 toolbox in <i>Leishmania</i> spp.....	86
Figure 3-1. Selection of AmB resistance in <i>L. mexicana</i> promastigotes.....	95
Figure 3-2. Susceptibility of AmBR lines before the selection of individual clones.....	96
Figure 3-3 Selection of resistance to nystatin (NysR) in <i>L. mexicana</i> promastigotes and cross-resistance with AmB.....	99
Figure 3-4. Culture and growth rate and size of polyene resistant lines of <i>L. mexicana</i> promastigotes in HOMEM and Defined Medium (DM).....	101
Figure 3-5. Susceptibility of AmBR lines of <i>L. mexicana</i> against different inhibitors.....	106
Figure 3-6. Fold changes to a series of compounds of AmBR clones compared with the parental wild type.....	108
Figure 3-7. Susceptibility of NysR lines of <i>L. mexicana</i> to different inhibitors.....	109
Figure 3-8. Fold changes of NysR clones to a series of compounds.....	111
Figure 4-1. Ploidy changes derived from WGS data in AmBR lines and wild type <i>Leishmania mexicana</i>	117
Figure 4-2. Ploidy (absolute) changes of <i>Leishmania mexicana</i> derived from WGS data.....	118
Figure 4-3. WGS data showing coverage of the two copies of the C24SMT gene.....	119
Figure 4-4. Visualization of the genomic region of LmxM.13.1530 (miltefosine transporter) and LmxM.13.1540: (unknown function).....	120
Figure 4-5. Visualization of the genomic region of LmxM.36.2380 and LmxM.36.2390.....	123
Figure 4-6. Visualization of the genomic region of LmxM.23.1300 (LOX) (syn. of C5DS).....	125
Figure 4-7. Alignment of lathosterol oxidase LmxM.23.1300 (LOX) with orthologues (C5-desaturase) from kinetoplastids and other eukaryotes.....	127
Figure 4-8. Cladogram and synteny of <i>L. mexicana</i> C5DS and LOX genes.....	129
Figure 4-9. Structural 3D models of C14DM (ERG11 in yeast and fungi) in <i>Leishmania</i> spp.....	132
Figure 4-10. Docking of the predicted secondary structure of C24SMT LmxM.36.2380 (XP_003874589.1) of <i>L. mexicana</i>	135
Figure 4-11. Protein-protein interaction (PPI) network in yeast and trypanosomatids.....	137
Figure 5-1. Nomenclature of Sterols and the double bond system.....	144
Figure 5-2. Ion chromatogram for the mass of the fragment ion for the standard mix- and the <i>Leishmania</i> -sterol peaks.....	146
Figure 5-3. Metabolite profiling by GC-MS in AmBR lines of <i>L. mexicana</i> promastigotes.....	149
Figure 5-4. Metabolite profiling by GC-MS in AmBR lines of <i>L. mexicana</i> amastigotes.....	152
Figure 5-5. Metabolite profiling by GC-MS in NysR lines of <i>L. mexicana</i> promastigotes.....	154
Figure 5-6. BALB/c mice inoculated with <i>L. mexicana</i> metacyclic promastigotes and treated with AmB.....	161
Figure 5-7. Susceptibility to AmBisome of <i>L. mexicana</i> promastigotes in BALB/c mice.....	171

Figure 5-8. Susceptibility of AmBR lines of <i>L. mexicana</i> against AmB and AmBisome <i>in vitro</i> .	173
Figure 5-9. Histopathology of primary lesions (footpad) of BALB/c mice inoculated with AmBR lines of <i>L. mexicana</i> .	180
Figure 5-10. Histopathology of lymph nodes of BALB/c mice infected with AmBR lines of <i>L. mexicana</i> promastigotes.	181
Figure 6-1. Effect of ergosterol in wild type and AmBR lines of <i>L. mexicana</i> after the treatment with sterol inhibitors	191
Figure 6-2. Susceptibility of AmBR lines of <i>L. mexicana</i> to 1,2,3-triazolylsterol inhibitors.	193
Figure 6-3. Susceptibility of AmBR lines of <i>L. mexicana</i> to 1,2,3-triazolylsterol inhibitors.	194
Figure 6-4. Susceptibility of AmBR lines of <i>L. mexicana</i> to 1,2,3-triazolylsterol inhibitors.	196
Figure 6-5. Fold changes to 1,2,3-triazolylsterol inhibitors in different sterol resistant lines of <i>L. mexicana</i> promastigotes.	197
Figure 6-6. Activity of TAZ compounds with the recombinant C24SMT <i>L. mexicana</i> .	198
Figure 6-7. RNA-seq dataset of the C24SMT-overexpressor <i>L. mexicana</i> .	201
Figure 6-8. Growth curve of C24SMTKO of <i>L. mexicana</i> promastigotes in HOMEM and DM.	202
Figure 6-9. Treatment with TAZ inhibitors for 12 hours in wild type and two AmBR lines of <i>L. mexicana</i> promastigotes.	203
Figure 6-10. Characterisation of AmBR lines, and C24SMT and C24SMTKO mutants of <i>L. mexicana</i> , using GC-MS (sterols) and RNA-seq.	205
Figure 7-1. Principal component analysis (PCA) of two AmBR lines of <i>L. mexicana</i> promastigotes treated with AmB.	213
Figure 7-2. Volcano plots of metabolites with fold-change after the treatment with AmB in <i>L. mexicana</i> wild type and AmBR promastigotes.	215
Figure 7-3. Distribution of classes of metabolites in two resistant lines of <i>L. mexicana</i> promastigotes treated with AmB.	217
Figure 7-4. Lipid changes as detected by LC-MS.	220
Figure 7-5. Perturbation of metabolites related with the sterol biosynthesis.	222
Figure 7-6. Changes in carbohydrates metabolism.	224
Figure 7-7. Additional changes in the metabolism of carbohydrates in AmBRcl.14.	225
Figure 7-8. PCA and AmB EC ₅₀ of WT, ΔTKT and add-back-TKT <i>L. mexicana</i> promastigotes.	226
Figure 7-9. Metabolic changes in the PPP after the treatment with AmB in <i>L. mexicana</i> .	227
Figure 7-10. Changes in nucleotides (purines and pyrimidines) metabolism.	229
Figure 7-11. Metabolic changes in the PTP in <i>L. mexicana</i> after AmB-exposure.	231
Figure 7-12. Changes in amino acids and polyamines metabolism.	232
Figure 7-13. AmB abundance and susceptibility (EC ₅₀) in the experimental groups.	234
Figure 8-1. Graphical abstract of this Thesis.	238

List of Accompanying Material

Supplementary 1 Formulation of culture media. HOMEM and Defined Medium (DM).

Supplementary 2. Script workflow used for WGS in AmBR lines.

Supplementary 3. RNA-seq workflow). For visualization needs to be uploaded in the Galaxy server at (<http://heighliner.cvr.gla.ac.uk>). Galaxy file.

Supplementary 4. SNPs identified using WGS in *L. mexicana* and *L. infantum* (Text file).

Supplementary 5. Sterol profiling (GCMS) in AmBR *L. infantum*. (Word file).

Supplementary 6. EC₅₀ values (\pm SD) and statistics of Azasterols. (Word file).

Supplementary 7. qPCR analysis of C24SMT-overexpressor *L. mexicana* promastigotes.

Supplementary 8. RNA-seq analysis in C24SMT-overexpressor *L. mexicana* promastigotes. (Excel file).

Supplementary 9. LCMS data in WT and AmBR *L. mexicana*. (Word file).

Supplementary 10. IDEOM file AmBRcl.8. (Excel file).

Supplementary 11. IDEOM file TKTKO. (Excel file).

Acknowledgement

I hereby express my gratitude to Professor Michael Barrett for supervising this project. I do appreciate the freedom and full independence he granted me to perform my own ideas during this journey. His input has provided me with an essential critical thinking for understanding my research. Thanks to Dr Richard Burchmore for his input along our conversations. The invaluable intellectual and technical contributions provided by other colleagues and staff members are appropriately acknowledged throughout this Thesis. Equally thankful with everybody from the Barrett Lab, incomparable fellows.

I am so grateful with Dr Lisa Ranford-Cartwright, her human efforts were the beginning of my journey in Glasgow. Also, thanks to Dr Paul Denny for allowing me writing this work in parallel with other projects.

Special recognition to my mentors (and second parents) Prof. Alejandro Gonzalez Velez and Mtra. Marcia Elena Gutierrez Cardenas, both they forged the discipline and passion that I have for sports and science.

“Con amor para mi familia y amigos”

Project funded by the Brazilian government, Science without borders.

Author's Declaration

I declare that, unless otherwise stated, all results presented in this thesis are my own work.

Edubiel Arturo Alpizar Sosa

Definitions/Abbreviations

Abbreviation	Definition	Abbreviation	Definition
δ	delta or Difference between two values	mm	millimetres
γ GCS	γ -glutamyl cysteine synthetase	M	Molar (moles/litre)
$\Delta\Psi_m$	Mitochondrial membrane potential	m/z	Mass-to-charge ratio
$^{\circ}\text{C}$	Degrees Celsius	Mb	Megabase pairs
μ	Micro (10^{-6})	MDR	Multidrug resistance
μM	micromolar	MF	Miltefosine
μm	micrometer	min	Minutes
3'	3 prime end of DNA	mM	Milli-molar
5'	5 prime end of DNA	MMEJ	Microhomology-mediated end joining
Å	Ångström (10^{-10} m)	MoA	Modes of Action
A	Adenine	MoR	Modes of Resistance
AAT	African Animal Trypanosomiasis	mRNA	Messenger RNA
ABC	Adenosine triphosphate-binding cassette	mRNA	Messenger ribonucleic acid
ADP	Adenosine diphosphate	MRPA	Multidrug-resistant protein A
AmB	Amphotericin B	MS	Mass spectrometry
AmBR	Amphotericin B resistant	MSI	Metabolomics Standards Initiative
AmB-D	Amphotericin-Deoxycholate complex	MSL	Miltefosine Sensitivity Locus
ANOVA	Analysis of variance	MT	Miltefosine transporter
AOX	Alternative oxidase	n	Nano (10^{-9})
AQP1	Aquaglyceroporin 1	nM	Nano-molar (moles/litre 10^{-9})
ARG	arginase	NAC	N-Acetyl-L-cysteine
ATP	Adenosine triphosphate	NAD ⁺ or NAD ⁺	Oxidised nicotinamide adenine dinucleotide
BLAST	Basic local alignment search tool	NADH	Reduced nicotinamide adenine dinucleotide
BMDM	Bone marrow-derived macrophages	NADP ⁺	Nicotinamide adenine dinucleotide phosphate
BSF	Bloodstream form	NADPH	Reduced nicotinamide adenine dinucleotide phosphate
cm	Centi (10^{-2})	NGS	Next generation sequencing
C14DM	C14-Lanosterol demethylase	NIST	National institute of standards and technology
C24SMT	C-24 Sterol methyl-transferase	NO	nitric oxide
C5DS	C5-Sterol desaturase	Nys	Nystatin
C8SI	C-8 sterol isomerase	NysR	Nystatin resistant
cDNA	Complementary DNA	$^{\circ}\text{C}$	Degrees centigrade
CHX	Cycloheximide	Pa	Pascal (unit of pressure)
Ci	Curie	ODC	ornithine decarboxylase
CL	Cutaneous leishmaniasis	PAT	Potassium antimonyl tartrate
CMM	Creek's minimal medium	PAR	Paromomycin
CNV	Copy number variation	PBS	Phosphate-buffered saline
CoA	Coenzyme A	PCA	Principal Components Analysis
cRPMI	Complete RPMI	PCF	Procylic form
Ct	Cycle threshold	PCR	Polymerase chain reaction
Ct	Cycle threshold	PENT	Pentamidine
Cys	cysteine	PM	Peritrophic matrix
DA	Diminazene Aceturate	PPP	Pentose phosphate pathway
DAPI	4, 6-diamidino-2-phenylindole	PRP1	pentamidine resistance protein 1
dATP	Deoxyadenosine triphosphate	PSG	proteophosphoglycan
ddNTP	Dideoxynucleotide triphosphate	PPP	pentose phosphate pathway
DDT	Dichlorodiphenyltrichloroethane	PTP	polyamine-trypanothione pathway
DiCre	dimerizable Cre recombinase (DiCre)	QC	Quality control
DIGE	Difference gel electrophoresis	qPCR	Quantitative polymerase chain reaction
DMSO	Dimethylsulfoxide	qRT-PCR	Quantitative reverse transcription-polymerase chain reaction
DNA	Deoxyribonucleic acid	RNA	Ribonucleic acid
dTTP	Deoxythymine triphosphate	RNAi	RNA interference
dUTP	Deoxyuracil triphosphate	RNA-seq	RNA sequencing-based transcriptomics
EC ₅₀	Concentration at which 50% of inhibition is observed	ROS	Reactive oxygen species
ER	Endoplasmic reticulum	rpm	Rotations per minute
EtBr	Ethidium Bromide	RPMI	Roswell Park Memorial Institute (medium)
FACS	Fluorescence Activated Cell Sorting	rRNA	Ribosomal ribonucleic acid
FAD	Oxidised Flavin adenine dinucleotide	RT	Reverse transcriptase
FADH ₂	Reduced flavin adenine dinucleotide	s	Seconds
FBS	Fetal bovine serum	Sb ^{III}	Trivalent antimony
FC	Fold change	Sb ^V	Pentavalent antimony

FCS	Fetal calf serum	SBP	Sterols Biosynthetic Pathway
fg	Femtograms	SC5D	Sterol C5-desaturase
g	Gravitational force	SEM	Standard Error of the Mean
GAPDH	Glyceraldehyde 3-phosphate dehydrogenase	SHAM	Salicylhydroxamic acid
GC	Gas chromatography	SIDER	Small interspersed degenerate retrotransposon
GC-MS	Gas Chromatography/ Mass Spectrometry	SIT	Sterile insect technique
GFP	Green fluorescent protein	SL	Spliced leader
GO	Gene ontology	SMT	Sterol C24-methyltransferase
GOX	Glucose oxidase	SNP	Single nucleotide polymorphism
gRNA	guide Ribonucleic acid	SNPs	Single nucleotide polymorphisms
GSH	glutathione	SREBP	Sterol regulatory element binding protein
GWAS	genome-wide association study	TAO	Trypanosomal alternative oxidase
HAPT1	high-affinity pentamidine transporter	TCA	Tricarboxylic acid
HAT	Human African Trypanosomiasis	TDR1	thiol dependent reductase
HILIC	Hydrophilic interaction liquid chromatography	TRYP1	tryparedoxin peroxidase
HIV	Human immunodeficiency virus	TDPX	tryparedoxin dependant peroxidases
HMG-CoA reductase	3-Hydroxy-3-methylglutaryl-CoA reductase	TLR	Toll-like receptor
HR	Haploid Ratio	TORC1	Target of rapamycin complex 1
Hsp	Heat shock protein	tRNA	Transfer ribonucleic acid
IEF	Iso-electric focusing	TSH	trypanothione
Ig	Immunoglobulin	TRYR	Trypanothione reductase
InDel	Mutation involving a small insertion or deletion	TRYS	Trypanothione synthetase
k	Kilo (10 ³)	TRYX	Tryparedoxin
kDNA	kinetoplast Deoxyribonucleic acid	UTR	Untranslated region
KEGG	Kyoto encyclopaedia of genes and genomes	UV	Ultraviolet
l	Litres	V	Volts
LC	Liquid chromatography	VL	Visceral leishmaniasis
LC-MS	Liquid Chromatography/Mass Spectrometry	VSG	Variant surface glycoproteins
LB	Luria-Bertani	WGS	Whole genome sequencing
		WHO	World Health Organisation

1 Introduction

1.1 Neglected tropical diseases

Diseases that affect the poorest populations are mainly infectious diseases and to some extent, are preventable. Currently, there are twenty classified Neglected Tropical Diseases or NTDs and 70% of these are caused by parasites (Roger et al. 2017) (https://www.who.int/neglected_diseases/diseases/en/). Some parasitic NTDs are controllable by mass drug administration (MDA), but MDA has been restricted to NTDs caused by helminths given the safety of the antihelminthics (de Souza and C Dorlo 2018; Webster et al. 2018) (<https://www.cdc.gov/globalhealth/ntd/diseases/index.html>) and because for many years there were no oral compounds to treat leishmaniasis, Chagas Disease or African sleeping sickness, which are caused by trypanosomatid protozoans. Drug treatment remains a key step towards the control and elimination of leishmaniasis (Ponte-Sucre et al. 2017) and the advantages of oral treatments are key to achieve this goal. The first (and only) oral drug to treat leishmaniasis, miltefosine (Sunyoto, Potet, and Boelaert 2018), has provided some encouraging evidence regarding using oral formulations against these devastating diseases. More recently, fexinidazole, the first oral treatment for sleeping sickness (Torreele et al. 2010) was approved by the European Medicines Agency (EMA) (European Medicines Agency 2018) (<https://www.ema.europa.eu>) and is expected to improve the treatment management and the epidemiology of this disease.

1.2 *Leishmania* parasites and other kinetoplastids

In 1885, David Cunningham was the first to record *Leishmania* parasites but the first to recognise them as protozoa was Piotr Borovsky. In 1900, Sir William Boog Leishman and Charles Donovan identified the agent causing “Kala-azar”, which Ronald Ross named as “Leishman-Donovan bodies” and the disease leishmaniasis (Andrade-Narváez et al. 2001; Steverding 2017) (http://www.glaзgodiscoverycentre.co.uk/media/media_239689_en.pdf).

Leishmania species are intracellular parasites of the order Kinetoplastida and the family trypanosomatidae. These flagellated protozoan possess similar structural features including a single DNA-containing mitochondrion, the kinetoplast, specific organelles for glycolysis known as glycosomes and a microtubular corset. Other biochemical pathways such as the thiol metabolism and the synthesis of ergosterol are also unique of this grouping, which includes many species of *Leishmania* and *Trypanosoma* (Barrett and Croft 2012) and other

organisms such as *Crithidia* and *Leptomonas* (Chauhan et al. 2011). Among the Kinetoplastids are the causes of several key vector borne diseases in human and animals that are endemic in many tropical countries and represent a burden for the governments cause disease. The Leishmaniasis are a spectrum of diseases with various forms or clinical manifestations caused by infection with different species of *Leishmania*. Chagas Disease is caused by *Trypanosoma cruzi* and human African trypanosomiasis (HAT or African sleeping sickness) by subspecies of *Trypanosoma brucei*. In animals, infection by trypanosomes and leishmania is also complex (Dantas-Torres 2009; Otranto and Dantas-Torres 2013)(<http://www.leishvet.org/wp-content/uploads/2018/07/EN-Guidelines.pdf>). Understanding the biology of the Kinetoplastids is important in the quest for new treatments and other methods of control for these diseases (Daneshvar et al. 2003; Stuart et al. 2008).

1.3 Epidemiology and clinical forms of Leishmaniasis

Leishmaniasis is a vector-borne disease (VBD) and a major public and animal health issue that is related to poverty with over 1 billion people are at risk of infection in endemic areas. The World Health Organization (WHO) has estimated that between 600,000 to 1 million new cases of the cutaneous form, and 50,000 to 90,000 of Visceral leishmaniasis occur worldwide each year (Burza, Croft, and Boelaert 2018) (<https://www.who.int/news-room/fact-sheets/detail/leishmaniasis>). The epidemiology of leishmaniasis is complex and is determined by the interaction between the triad of “host-parasite-vector” with many factors including climate change, poverty, treatments available and the emergence of resistance, human and animal migrations, distribution of the vector, geography, season, etc. (Lewis 1971; Piscopo and C. 2006; Steverding 2017). Moreover, emerging genotypes (ISC1 of *L. donovani*) have been identified (Cuypers et al. 2018) and the prevalence of leishmaniasis is unknown in areas where sand flies are not the main vector (e.g. fomites, needles, blood transfusions), asymptomatic carriers or secondary modes of transmission (vertical) between hosts (Dantas-Torres, 2009; Michel, et al., 2011), and where routine diagnosis is not active, particularly risk areas like suburban settings where the prevalence has been reported to be increasing (Table 1-1 ; LSHTM, 2019, <https://www.futurelearn.com/courses/visceral-leishmaniasis/2/todo/39413>) (https://www.who.int/research-observatory/analyses/gohrd_analysis_leishmaniasis.pdf).

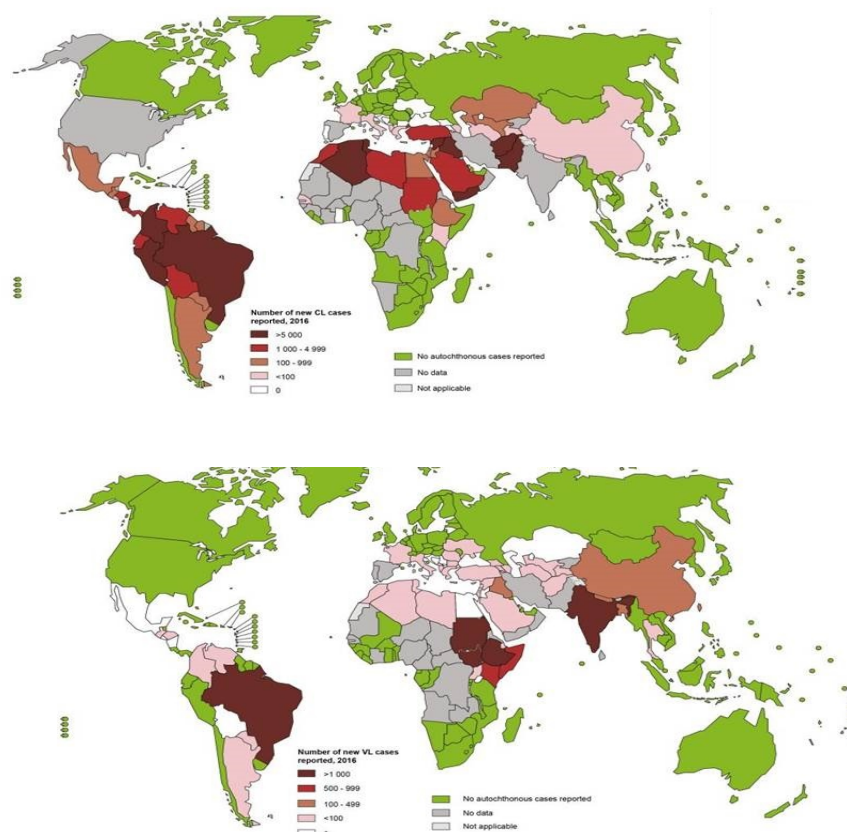


Figure 1-1. Global prevalence of cutaneous (CL) and visceral leishmaniasis (VL). CL (top) is present in the Mediterranean Basin, the Middle East, Africa and the Indian subcontinent (Old World species) and Central and South America (New World species). VL (bottom) exists in Asia and Africa (*L. donovani*) and in the Mediterranean Basin, Middle East, central Asia, South America and Central America (*L. infantum*) (Data source: WHO, 2016 <https://www.who.int/leishmaniasis/burden/en/>)

Leishmaniasis appears in different clinical forms that are caused by at least twenty species of the genus *Leishmania*, divided into Old World and New world varieties (Burza et al. 2018). Recently, *L. infantum* and some species of the newly added *L. enriettii* complex have been found to cause infections in both regions (Akhoundi et al. 2016).

Cutaneous leishmaniasis (CL) is the most common form of leishmaniasis with 90% of the cases occurring in nine countries (<https://www.who.int/news-room/fact-sheets/detail/leishmaniasis>) (Burza et al. 2018). CL is clinically polymorphic and is characterised by skin ulcers that are often misdiagnosed (Karimkhani, et al., 2017) or mistaken for fungal infections. The most frequent form of CL is a “localized” (LCL) form also known as American leishmaniasis (ACL) which represents between 50 and 75% of the new clinical cases globally. Lesions are often disfiguring and have an impact on the economy and quality of life of the patients. As it is often self-healing or can be

asymptomatic, CL has received less attention than other forms of leishmaniasis. CL also appears as other variants that are less frequent, including a “diffuse” form (DCL) characterised by non-ulcerative lesions, disseminated cutaneous leishmaniasis and *Leishmania recidivans* (Ghazanfar and Malik 2016).

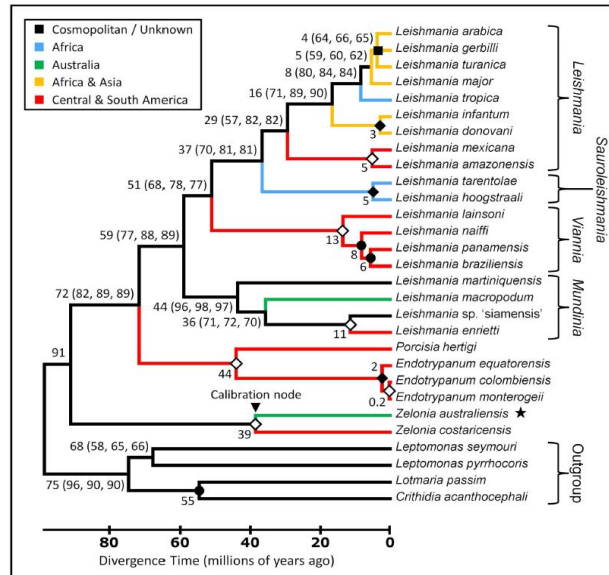


Figure 1-2. The phylogenetic tree of the *Leishmania* species causing disease and other related Trypanosomatids. The construction was made using 29 trypanosomatids and combining different methods. This tree includes species from the *L. enriettii* complex and a novel Australian trypanosomatid (*Zelonia australiensis*, 2017), a common ancestor of trypanosomatids, including the genus *Leishmania*. Text adapted from Barratt, et al. 2017 and Cotton, 2017. Source (Barratt et al. 2017).

In the Old-world CL is caused by species from the *L. major* complex (*L. aethiopica*, *L. major* and *L. tropica*) and in the New World by the *L. mexicana* complex (e.g. *L. mexicana*, *L. amazonensis*, *L. venezuelensis*), and members of the *Viannia* subgenus (e.g. *L. braziliensis*, *L. panamensis*, *L. peruviana*). Species causing CL are mainly restricted to the skin and are seldom described within lymphoid tissues (e.g. spleen, liver, lymph nodes, bone marrow) as is typical VL caused by *L. donovani* and *L. infantum*. However, viable amastigotes of cutaneous species (e.g. *L. mexicana*) have been observed and reisolated from lymph nodes in a murine experimental model, which may be due to inflammatory monocytes trafficking parasites via the draining lymph nodes (Kaye and Scott 2011) (see Chapter 5, section 5.2.7). It is also believed that patients with CL develop a curative immune response (Stuart et al. 2008) which leads to self-healing lesions. CL lesions can also be treated with locally with intralesional injections (antimonials), topical formulations (paromomycin)(Burza et al. 2018), and thermotherapy should also be considered (Cardona-Arias, Vélez, and López-Carvajal 2015; Gonçalves and Costa 2018).

Mucocutaneous leishmaniasis (MCL) is a potentially life-threatening condition caused by *L. braziliensis*. MCL is a highly disfiguring and disabling condition, also known as Espundia, characterized by the destruction of the oronasopharyngeal tissues. If untreated, this form of the disease can lead to secondary complications like pneumonia and can evolve or coexist with CL (Burza et al. 2018; Ghazanfar and Malik 2016).

Visceral leishmaniasis (VL) is the most severe form of the disease and is known as “kala-azar” (taken from the Hindi word meaning darkened skin, which is an occasional symptom of the disease). Humans are the main reservoir for infections caused by *L. donovani*. The course of the disease is often accompanied by hepato and splenomegaly, fever, lymphadenopathy, anaemia and severe weight loss and can also evolve and coexist with CL (Ghazanfar and Malik 2016). VL is caused by members of the *L. donovani* complex (*L. donovani* and *L. infantum*) in the Old world and *L. chagasi* (*L. chagasi* and *L. infantum* are synonymous) and *L. (Viannia) braziliensis* in the Americas (Dantas-Torres 2009; Michel et al. 2011). In the old world, VL species can also cause a condition known as post-kala-azar dermal leishmaniasis or PKDL which involves the skin, where plaques, nodules or papules are often seen months after a VL has apparently resolved clinically. PKDL results from the host immune response against residual parasites that are usually absent from lymphoid organs and which survived treatment and now manifest in the dermal lesions. For this reason, PKDL is considered a reservoir and important in the transmission of VL (Das et al. 2017). Other conditions as associated with *Leishmania* coinfection with helminths, HIV, tuberculosis or fungal diseases are also associated with PKDL (Martínez et al. 2018). Ninety per cent of the cases of VL exist in only six countries, Bangladesh, Brazil, Ethiopia, India, South Sudan and Sudan (Figure 1-1) (Burza et al. 2018).

Although the global prevalence of VL has been reduced significantly since 2005 when India, Nepal and Bangladesh, which used to have more than 50% of the global burden, committed to an elimination programme for leishmaniasis. However, in some countries the figures from the WHO showed an increase in prevalence between 2013 and 2017 (see Table 1-1). Additionally, countries where VL was non-endemic have reported human VL caused by *L. infantum*, in Uruguay the first autochthonous case occurred in a four-year-old girl in Uruguay ([Ministerio de Salud Publica Uruguay, 2018](#), consulted in December 2018). A month later, the second case of human VL was reported in the same region of Uruguay (Salto District), however, the Uruguayan Health Minister confirmed that transmission within this region is not active ([Ministerio de Salud Publica Uruguay, 2019](#), consulted in January 2019). The previous year an outbreak of autochthonous canine VL

was reported also in Uruguay, and *L. infantum* was isolated from sandflies in this region, revealing the presence of the complete life cycle (Satragno et al. 2017).

Table 1-1. Number of cases of VL reported from 2013 to 2017 in regions with higher prevalence.

Country	2013	2014	2015	2016	2017
Brazil	3,253	3,453	3,289	3,200	4,297
Sudan	2,389	3,415	2,829	3,810	3,894
South Sudan	2,364	7,472	2,840	4,285	3,541
Ethiopia	1,732	2,705	1,990	1,593	1,490
Kenya	181	880	894	692	954
Somalia	936	1,045	1,165	911	858
China	120	292	514	321	190

Numbers in bold and red reflect an increase in prevalence in relation with the previous year. ©WHO 2018. Consulted in January 28th, 2019, and WHO 2013 (map):

http://apps.who.int/neglected_diseases/ntddata/leishmaniasis/leishmaniasis.html,
http://gamapserver.who.int/mapLibrary/Files/Maps/Leishmaniasis_VL_2013.png?ua=1&ua=1

Although canine VL caused by *L. infantum* (*L. chagasi*) has been progressively diagnosed in this region of Uruguay since 2010, leishmaniasis needs to be reconsidered as a major health risk in Uruguay (Grill and Zurmendi 2017; Roger et al. 2017), particularly because dogs are the main reservoir of *L. infantum*, and the disease is also fatal. Interestingly, hunting Foxhounds (American) present higher prevalence in areas (United States) where outbreaks have occurred, possibly due to vertical (trans placental/trans-mammary) (Boggiatto et al. 2011; Petersen and Barr 2009). Other factors such as the genetics of the animal, are also related with the outcome of the disease (Ribeiro et al. 2018). More recently, a case report of a 3-year-old male Shih Tzu cross, possibly, the first reported case of Leishmaniosis (thus named by Veterinarians) in the United Kingdom, due to the presence of another dog that was euthanised due to severe Leishmaniosis, the authors raised the possibility of direct dog-to-dog transmission through bites or wounds (Mckenna et al. 2019).

1.4 Biology and molecular biology of *Leishmania*

Leishmania are heteroxenous (digenetic) parasites characterised by two main morphologically distinct stages of multiplication: the amastigote and the promastigote. The parasites are transmitted between several mammal hosts (animals and human) by the bite of female sand-flies. To complete their life cycle, parasites must adapt and survive across a wide range of environmental conditions, e.g. pH, temperature, etc. (Roque and Jansen 2014). The haploid genome of *Leishmania* spp. (~32 Mb) contains between 7,400 and 8,200 predicted genes (Kazemi 2011; Rogers et al. 2011), which are organised in 34, 35 or

36 chromosomes that varies between species. For instance, in *L. mexicana* two fusion events (linkage group) are known between Chr8 and Chr29, and between Chr20 and Chr36, which are merged into Chr8 and Chr30, respectively (Valdivia et al. 2017). In *L. mexicana* and in *L. (L.) amazonensis*, Chr30 (the homologue of Chr31 in the old world species *L. major*, *L. infantum* and *L. donovani*, and in the new world *Viannia* species (*L. braziliensis*), is frequently supernumerary (Rogers et al. 2011). The latter of these species also has a fusion between Chr20 and Chr34 (Kazemi 2011).

The protein-coding genes lack introns (most of them), transcription factors and promoters, instead, gene expression is controlled by means of polycistronic transcription and trans-splicing (Clayton and Shapira 2007; Ivens et al. 2005a). Different than in bacteria, transcripts in *Leishmania* are split into various mRNAs, followed by the attachment of a common leader sequence named spliced leader sequence (SL), and a poly-A tail, to the 5'- and the 3' ends, respectively (Lebowitz et al. 1993)(Ginger 2005). Some evidence suggests that the 3' untranslated region (UTR), is involved in post-transcriptional and post-translational gene regulation. Although the role of RNA polymerase II in regulation of protein coding genes is unclear (Ginger 2005), some sequences of subunits of RNA polymerases I, II and III, homologous to other eukaryotes has been described in trypanosomatids (Martínez-Calvillo et al. 2010).

Another unique feature of the genome in trypanosomatids is the plasticity. *Leishmania* spp. can adapt to different conditions (e.g. drug selection) through several genomic changes, such as gene dosage, up- and downregulation of mRNA transcripts (Ubeda et al. 2008), SNPs, gene amplification, gene duplication (Mukherjee, Langston, and Ouellette 2011), and gene deletion (Ouameur et al. 2008), copy number variations (CNVs). Other modifications such as recombination and rearrangement of chromosomes, and aneuploidy, are also frequent (Rogers et al. 2011). Some of these changes result from drug exposure and are related with resistant phenotypes, whereby is essential to differentiate them from those alterations that appear stochastically as part of the adaptive mechanisms of *Leishmania* spp. to the environment (Ubeda et al. 2014).

1.5 Life cycle

The dixenous life cycle of *Leishmania* species is complex. The amastigote form is taken up by a sandfly during its blood meal and transforms into a flagellated stage called the promastigote which needs to survive and pass through various life cycle stages within the insect digestive tract before being reinoculated into a new mammalian host (Grimaldi and

Schottelius 2001). Section 0., provides a detailed description of the stages within the insect vector.

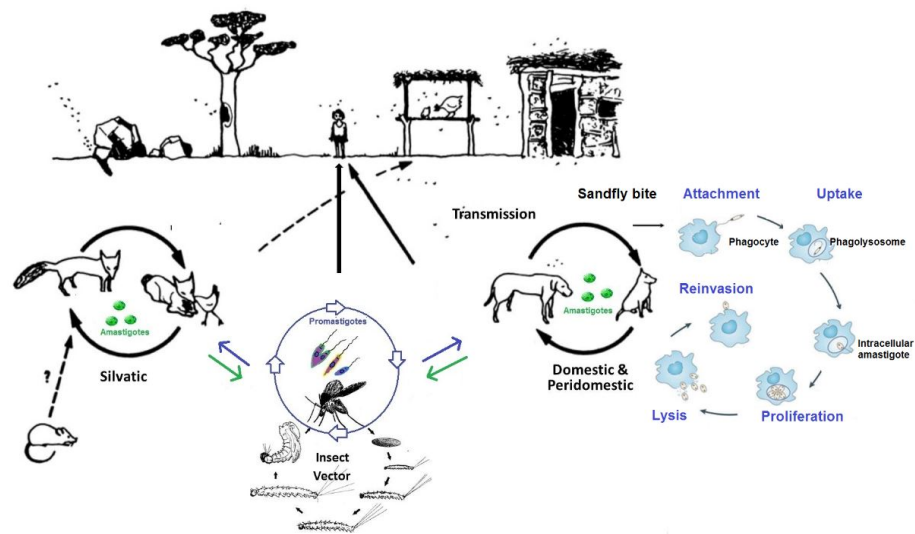


Figure 1-3. Life cycle of *Leishmania* spp.

Leishmania spp. are transmitted to different mammal hosts by adult female sand flies during blood meals. Sandflies inoculate infective metacyclic promastigotes into their hosts via the proboscis and they transform into amastigotes inside macrophages (mainly of lymphoid organs in species causing VL and dendritic cells of the skin in those species causing CL) and multiply by binary fission until the burst of the cell allows them to infect more cells until they are ingested again by the insect vector during the blood meal. Inside the sand fly, amastigotes differentiate into several intermediate stages before reaching the infective stage (metacyclic) and are taken up again by the sandfly in the next blood meal recommencing the life cycle. Sand flies also need to become adults in order to be competent vectors and their growth and development depends on the environment (Modified from: (Tesh 1995) and (Kaye and Scott 2011)).

After being inoculated into the mammalian host, the infective promastigotes attach to macrophages and are phagocytosed before transforming into amastigotes which replicate inside the parasitophorous vacuole, which is a modified phagolysosome. The cell body length of the intracellular amastigote is smaller (1-2 μm in all species except *L. mexicana* and *L. amazonensis*) than the promastigote (10-12 μm) and morphologically distinct (De Pablos, Ferreira, and Walrad 2016; Richard J Wheeler, Gluenz, and Gull 2011), characterised by the lack of a protruding flagellum (Kaye and Scott 2011).

Amastigogenesis is an important process during which parasites adapt their metabolism to the intracellular environment of the phagolysosome within the host macrophages. The amastigote is metabolically less active than the promastigote (Kloehn et al. 2015), and this metabolic plasticity confers some advantages for their survival and progression of transmission as well as protecting them against environmental stresses imposed by the

phagocytic cell in which they reside, the immune system and even drug exposure (Barisón et al. 2017; Sánchez-Valdéz et al. 2018).

1.5.1 The sandfly vector

Leishmaniasis is transmitted by the female sandflies of the family *Psychodidae*. Although not all the sandfly species are competent vectors, over 50 species of the genus *Phlebotomus* and *Lutzomyia* in the Old and New World, respectively, have been identified to transmit the disease. In some endemic regions (e.g. Mexico) up to four endemic species of sandflies are involved in the transmission of *L. mexicana* (Pech-May et al. 2010). Sandflies can travel from 300 to 2300 m (Ghazanfar and Malik 2016).

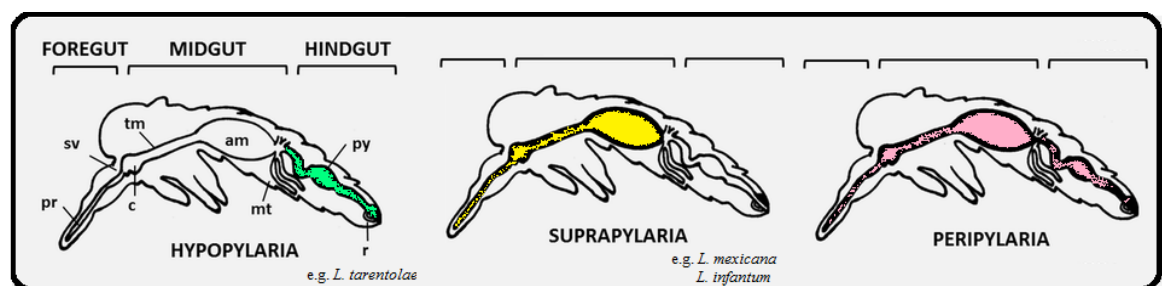


Figure 1-4. Tropism of *Leishmania* species within the sandfly vector. Most species of the subgenera *Leishmania* develops within the midgut and foregut (suprapylaria) and the species of the subgenera *Viannia* develop within the hindgut (peripylaria). Modified from: (Kaufer et al. 2017).

Generally, descriptions of the *Leishmania* spp. life cycle focus on the procyclic and metacyclic promastigotes as the main stages, nonetheless, the parasites undergo at least five different stages within the vector. *Leishmania* species possess certain level of tropism towards different portions of the insect gut, most species (e.g. *L. mexicana* and *L. infantum*) develop in the midgut (suprapylaria) before reaching the foregut and mouthparts in order to be regurgitated and transmitted, whereas species from the subgenera *Viannia* (e.g. *Leishmania braziliensis*) localise in the hindgut (peripylaria) before migrating towards the midgut and mouthparts of the vector (Dostálová and Volf 2012). Finally, species of the subgenus *Sauroleishmania* (e.g. *Leishmania tarentolae*) attach to the pyloric region at the posterior end of the hindgut (hypopylaria) during their development within *Lutzomyia longipalpis* and little is known about the fitness costs for the sand fly and to what extent this determines their pathogenicity and transmission to the lizard, some hypotheses suggest that the infection occurs orally and that the parasites are ingested during the insectivorous behaviour of the reptile (Gossage, Rogers, and Bates 2003; Kaufer et al. 2017).

1.5.1.1 The life stages of *Leishmania* within the sandfly

It is often assumed that *Leishmania* parasites live only as promastigotes within the sand fly, however, the parasites undergo a complex, multi-staged life cycle within the sandfly (Figure 1-5 and Figure 1-6). During the first 24-48 hours post blood meal, amastigotes (1) transform into procyclic promastigotes (2). Between 48-72 hours they replicate and elongate becoming long nectomonad promastigotes (3), which is a non-dividing stage. The digestion of the blood meal takes place in the abdominal midgut where promastigotes are surrounded by the peritrophic matrix (PM) which is eventually digested by the sand fly enzymes releasing the parasites.

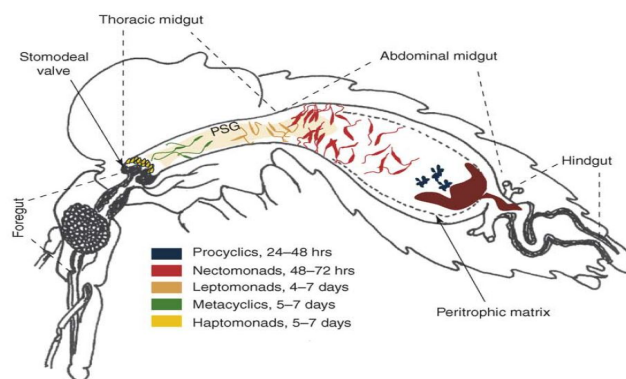


Figure 1-5. The life cycle of *Leishmania* within the sandfly vector. The different stages within the sandfly appear at different time points during the blood meal and the sugar phases. Source: (Kamhawi 2006).

The long nectomonads cross the posterior end of the PM and secrete a filamentous proteophosphoglycan (PSG) that obstructs the thoracic midgut, creating a plug, which needs to be removed together with the stomodeal valve for the reflux of infective stage to the foreparts of the sand fly. Nectomonads also attach to the midgut of the insect and transform between 4-7 days into the next stage which is shorter than the nectomonad and is known as the leptomonad (4). These replicate and transform between 5 to 7 days into two subpopulations: the haptomonad (5) that attaches to the chitin of the stomodeal valve, and the metacyclic promastigote (6) which is the infective stage that is regurgitated to the foregut and mouthparts before being regurgitated into the mammalian host, when infection occurs (Bates 2018; Dostálová and Volf 2012; Gossage et al. 2003; Kamhawi 2006; Serafim et al. 2018). Metacyclic promastigotes were long believed to be non-replicative and the terminally differentiated stage inside the vector. Recently, however, Serafim et al. showed in laboratory conditions that after a second uninfected blood meal in *Leishmania*-infected sandflies, metacyclic can enter a reverse metacyclogenesis and dedifferentiate into a new replicative stage called retroleptomonad promastigotes (7). Retroleptomonads reach

levels up to 125-fold higher than leptomonads from a classic infection and differentiate into two subpopulations: the haptomonads (8) and the infective metacyclic (9). Both are functionally similar to the first populations of haptomonads (5) and metacyclic promastigotes (6) but are amplified in number and with enhanced infectivity, resulting in, first, a larger haptomonad sphere in the stomodeal valve (Figure 1-6), and second, a 4-fold increase of the lesion frequency (Serafim et al. 2018).

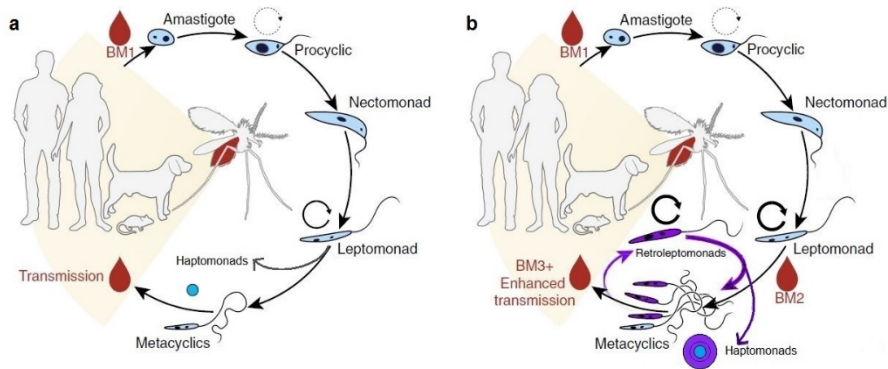


Figure 1-6. Old and new life cycle of *Leishmania* within the insect vector.

a) The old (classical) life cycle of *Leishmania* stages within the insect. Amastigotes are taken up from the infected host, transform into procyclic, Nectomonads, leptomonads which differentiate into two subpopulations: haptomonads which form the stomodeal plug and metacyclics, the infective stage which is transmitted in the next blood meal. b) the so-called New life cycle shows that metacyclic dedifferentiate through a reverse metacyclogenesis step into a new stage called retroleptomonads, which replicate in higher numbers than leptomonads forming a bigger plug in the stomodeal valve, metacyclics from retroleptomonads are also hyper infective. See text 0 for a more detailed explanation (modified from Serafim, 2018).

Interestingly, the question of how different functionally and biochemically these subpopulations are remains unanswered but is important as it may offer new options for the treatment and control of the disease (Bates 2018). Previous work has shown, for instance, that the metabolism of *L. mexicana* and *L. major* metacyclics is biochemically preadapted to survive as amastigotes within the intracellular acidic pH of the phagolysosome (Bates and Tetley 1993; Opperdoes and Coombs 2007). Analysis of the transcriptome revealed that procyclic promastigotes had amino acid transporters and other genes related to the glucose metabolism upregulated as compared with amastigotes (Inbar et al. 2017).

1.6 Use, mode of action and resistance to antileishmanial drugs

Current therapy relies on just a few Antileishmanials that have been used for decades and are inadequate for many reasons including toxicity, cost, course of administration and increasing drug resistance (Barrett and Croft 2012; Burza et al. 2018; Creek and Barrett

2014). Although little or no resistance has been reported in the field against paromomycin (Hendrickx et al. 2015), miltefosine and amphotericin B (AmB), these drugs have not, to date, been widely used for a substantial period of time (AmB has been for over 50 years to treat CL). PM resistant lines develop easily in laboratory conditions (Hendrickx et al. 2015; Jhingran et al. 2009; Rastrojo, et al. 2018), as does miltefosine (Seifert et al. 2003; Shaw et al. 2016) – and the first reports of miltefosine treatment failure are appearing in the field (Bhandari et al. 2012; Deep et al. 2017; Rijal et al. 2013; Sundar et al. 2012).

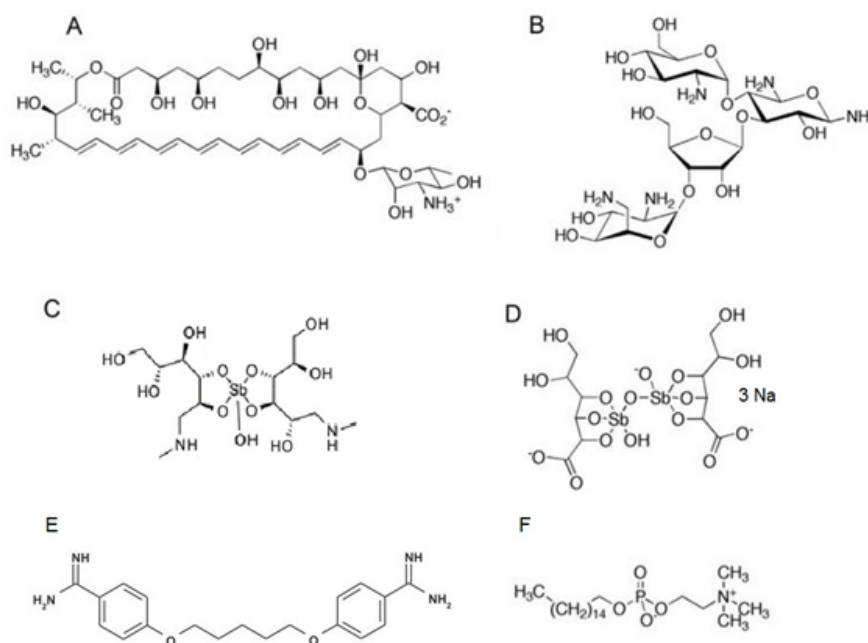


Figure 1-7. Compounds used for the therapy of leishmaniasis.
A. AmB B. paromomycin C. meglumine antimoniate D. sodium stibogluconate E. pentamidine and F. miltefosine. Modified from (Barrett and Croft 2012).

AmB is an antifungal that has replaced other compounds (e.g. antimonials) as the drug of choice (Fairlamb et al. 2016; Rastrojo, et al. 2018). The need for new compounds is pressing as there is no vaccine registered for use in humans (Burza et al. 2018; Dantas-Torres 2009). In dogs, a vaccine comprised of an attenuated *L. infantum* strain has shown good levels of protection and potential to control the disease in humans (Daneshvar et al. 2003, 2009, 2010, 2012; Daneshvar et al. 2014; Daneshvar et al. 2014). Several vaccines licensed for veterinary use contain excreted/secreted antigens of *L. infantum* and have an efficacy between 68.4 and 80% (Consulted on January 2019: <http://www.leishvet.org/wp-content/uploads/2018/07/EN-Guidelines.pdf>). Drug designing of an antileishmanial needs to consider the chemistry of the molecule (Figure 1-7) and the barriers that the drug needs to cross in order to reach the amastigote, which resides inside the parasitophorous vacuole within the macrophages, in many tissues. The pharmacokinetics differ between different

internal organs affected by leishmania species which compounds problems in seeking a pan-leishmaniasis drug.

1.6.1 Pentavalent antimonials

Pentavalent antimonials (Sb^{V}) have been used since 1940 to treat all forms of leishmaniasis (VL, CL, MCL), when often, albeit not always, were effective (Baker 1969) In patients infected with *L. mexicana*, Glucantime -15 series of IM QP (daily) injections 60-100 mg/kg BW and 10 days intervals- or Repodral -series of 3 IM injections of 1.5, 3.5 and 5ml (a 1/5 of this dose in paediatric patients per 10 kg BW) with 10 days intervals- were applied in series of three injections. Others like Camolar (cycloguanil pamoate -6-8 mg/kg BW IM at 38-40 C, use needle 18-calibre, painful c/2 months-) cured up to 70 percent of the cases with only one intramuscular injection and similar efficiency with oral metronidazole (Flagyl) and nimorazole - a water soluble, 5-nitroimidazole- (Naxogil) 15-20 mg/kg BW/day 15 days PO (Biagi 1974). Biagi and colleagues also observed that 420 mg of IM Camolar prevented ulcers development in susceptible patients (even when infected) every 4 months or 2-3 days before visiting endemic areas. Despite drug resistance in some regions (Matrangolo et al. 2013; Pund and Joshi 2017) and the severe adverse effects (e.g. cardiotoxicity, hepatotoxicity) (Sundar and Chakravarty 2013) these compounds are still the first choice in many countries (e.g. sub-Saharan Africa and Brazil), probably because they are more cost-effective than other compounds (Frézard, Demicheli, and Ribeiro 2009). Meglumine antimoniate (Glucantime®) and sodium stibogluconate (Pentostam®) contain different concentrations of Sb^{V} (85 mg/mL and 100 mg/mL, respectively (Robert N. Davidson, in Infectious Diseases (Fourth Edition), 2017). The trivalent antimony Sb^{III} is the active/toxic form with antileishmanial activity and is formed after the reduction of Sb^{V} by the parasite and human reductases. A third antimonial, Potassium Antimony (III) Tartrate trihydrate (PAT) is a metalloid salt in which the antimony is in the trivalent state, Sb^{III} , which is used as oxidative stress inducer in promastigotes (Ouellette M et al. 1998; Rojo et al. 2015; Tirmenstein et al. 1995), which can be selected for PAT resistance *in vitro* (Liarte and Murta 2010), too toxic for therapeutic use, but widely used in laboratory experimentation to test modes of action and resistance mechanisms.

Although it remains unclear exactly how antimonials are reduced by either the macrophage, the parasite or both (Kaur and Rajput 2014), it has been described that the reduction of Sb^{V} to Sb^{III} can occur within the host macrophages where the acidic pH and the slightly elevated temperature favour the reaction. Moreover, the ability of *Leishmania*

to reduce Sb^{V} to Sb^{III} is stage-specific (Pund and Joshi 2017), amastigotes being more able to perform this reaction rendering them more susceptible than promastigotes to antimony (Liarte and Murta 2010; Ouellette M et al. 1998; Tirmenstein et al. 1995).

In *Leishmania*, the uptake of Sb^{III} (generated within the macrophage) is modulated by the aquaglyceroporin AQP1 the expression of which affects parasite susceptibility to Sb^{III} , however, interpretation is complex as deletions of chromosome 31 have been reported in antimony-resistant lines (Kaur and Rajput 2014), in *Leishmania*, AQP1 is located in this chromosome which frequently presents polyploidy (Fairlamb et al. 2016). The transporter responsible for uptake of Sb^{V} is unknown, although inside the parasite it has been proposed that Sb^{V} is reduced to Sb^{III} by thiol-dependent reductase (TDR1) (Singh, Kumar, and Singh 2012). In addition, an arsenate reductase (*LmACR2*) in *L. donovani* and *L. infantum* has been proposed to be responsible for this reduction (Kaur and Rajput 2014).

Although the MoA of antimonials in *Leishmania* is not fully understood, it has been proposed to involve inhibition of glycolysis and β -oxidation of fatty acids (Wyllie, Cunningham, and Fairlamb 2004), phosphorylation of ADP (Singh et al. 2012), DNA fragmentation (Ouellette, Drummelsmith, and Papadopoulou 2004) and inhibition of trypanothione reductase (TRYR) (Wyllie et al. 2004). Antimony generates intracellular oxidative stress (Singh et al. 2012; Wyllie et al. 2004) and apoptosis (Moreira, Leprohon, and Ouellette 2011). Transcriptomics and metabolomics has shown that the polyamine-trypanothione pathway (PTP) (see 1.7.3) to be upregulated after treatment with antimonials and in resistant lines (Kaur and Rajput 2014; Wyllie et al. 2010), which protects *Leishmania* against reactive oxygen species (ROS) and nitric oxide (NO) (Mandal et al. 2017; Manta et al. 2013).

Resistance against antimonials is multifactorial (Figure 1-8) (Singh et al. 2012; Wyllie et al. 2010, 2004) and some of the molecular mechanisms known to be involved include: 1) lower reduction of Sb^{V} to Sb^{III} (Singh et al. 2012). 2) reduced uptake of Sb^{III} via the AQP1 transporter (Kaur and Rajput 2014). 3) increased efflux or sequestration of the complex Sb^{III} -thiol-mediated by the ATP-binding cassette (ABC) transporters e.g. that encoded by the multidrug resistance protein A (MRPA) gene (Fairlamb et al. 2016; Kaur and Rajput 2014; Singh et al. 2012). 4) upregulation of thiol metabolism producing increased abundance of trypanothione (TSH) is observed in antimony resistant lines and parasites under oxidative stress conditions induced by the intracellular Sb^{III} (Kaur and Rajput 2014; Singh et al. 2012; Wyllie et al. 2010, 2004). 5) overexpression of TDR1 and other enzymes such as arsenate reductase (ArsC-), ornithine decarboxylase (OCD), over-expression of the

intracellular meta-thiol PgpA transporter, and gamma-glutamylcysteine synthetase (*gshI*) which favour detoxifying the drug conferring a resistant phenotype (Wyllie et al. 2004; Wyllie, Vickers, and Fairlamb 2008).

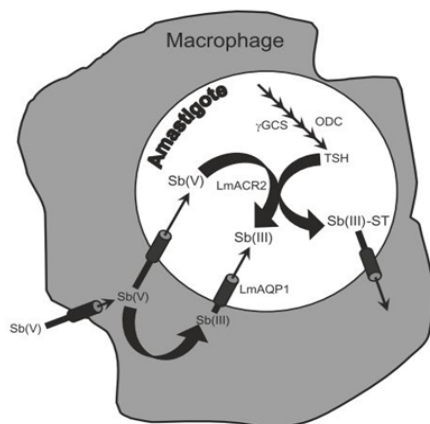


Figure 1-8. Model of the MoA and MoR of antimonials in *Leishmania*.

Sb^V enters the host macrophage and is reduced to Sb^{III} and uptake into the amastigote via AQP1, another portion enters as Sb^V and is reduced via the amastigote-specific TDR1 and other enzymes. Intracellular TSH concentrations increase and regulated by enzymes of the polyamine-trypanothione pathway (γ -GCS or ODC). Efflux or sequestration of the complex Sb^{III}-thiol. Source: (Mandal et al. 2017).

1.6.2 Pentamidine

Pentamidine (PENT) was developed in 1937 and has been used to treat the first stage of human African trypanosomiasis (HAT) caused by *T. brucei gambiense* as well as other infectious diseases. Like other diamidines, PENT targets the mitochondrion of trypanosomatids although its exact mode of action remains unclear (Bridges et al. 2007; Zhang et al. 2002). It binds to DNA, RNA and nucleotides and disrupts the mitochondrial genome (kinetoplast) (Wilson et al. 2008). In *T. brucei* PENT is transported into the cell through the P2 amino purine transporter as well as a low affinity pentamidine transporter and a high-affinity pentamidine transporter (HAPT1) (Munday, Settimo, and de Koning 2015). HAPT1 is encoded by the aquaglyceroporin *TbAQP2*, and drug resistance has been related with the loss of this gene, as well as the P2 amino purine transporter gene *TbAT1*. The expression of the wild type copy of *TbAQP2* in *TbAQP2* knockout cells restored HAPT1 activity and susceptibility. Interestingly, the wild type copy of the *AQP2* gene was absent or replaced by a chimeric protein containing part of the *TbAQP3* gene (which sits adjacent to *TbAQP2* in the trypanosome genome) in both lab strains and field isolates of PENT resistant trypanosomes. *L. mexicana* promastigotes expressing *TbAQP2* developed 40-fold hypersusceptibility to PENT (Munday et al. 2014). Recently, the accumulation of PENT in high concentrations inside the cells was shown to collapse the mitochondrial

membrane potential leading to selective inhibition of replication and progressive loss of kinetoplast DNA (Kaur and Rajput 2014; Thomas et al. 2018).

Twenty years ago, Basselin et al. showed that PENT affects the kDNA and that polyamine metabolism was altered in *Leishmania* lines resistant to PENT (Basselin et al. 1997). Efflux of PENT via plasma membrane pumps (PRP1) has also been shown to confer resistance (Coelho et al. 2007; Kaur and Rajput 2014). In *T. cruzi* in which PENT strongly inhibited the transport of putrescine and spermidine in epimastigotes and amastigotes (Díaz et al. 2014), however, although pentamidine also inhibits transport of polyamines in *Leishmania* (Díaz et al. 2014), uptake of radiolabelled pentamidine was not inhibited by polyamines, hence it does not enter on a polyamine transporter (Basselin et al. 2002). In *L. donovani* and *L. amazonensis*, polyamine biosynthesis showed differences between wild type and PENT resistant lines. Although spermidine was unaltered between lines, in wild type, putrescine, arginine and ornithine decreased, while in PENT resistant lines, the content of putrescine also decreased, however, an increase in arginine and ornithine was observed. In this work, interestingly, spermidine synthase showed increased affinity for spermidine and decreased affinity for PENT (Basselin et al. 1997). In summary, mechanisms of resistance proposed for PENT in *Leishmania* include 1) changes in kDNA sequence (Basselin et al. 1997) and loss of kDNA, 2) the efflux of the drug by the pentamidine resistance protein 1 (PRP1) pump (Coelho et al. 2007; Kaur and Rajput 2014), 3) changes in membrane potential (Basselin et al. 2002) and 4) alterations in polyamine and arginine metabolism (Kaur and Rajput 2014; Ouellette et al. 2004). Interestingly, some of these proposed mechanisms are similar to those described with antimonials (section 0 and Figure 1-8). Moreover, *L. mexicana* promastigotes selected for AmB resistance showed higher susceptibility to PENT (Mwenechanya et al., 2017; Pountain et al., 2019; PhD Thesis Raihana Binti, unpublished data), although mechanistic reasons for this are not yet understood. Similar results were also found in all AmBR and NysR lines in this study, and are discussed further (see chapter 3).

1.6.3 Paromomycin

Paromomycin (PAR) is an aminoglycoside, a group of antibiotics extensively used in human and veterinary medicine (Jhingran et al. 2009). Paromomycin, also known as aminosidine and monomycin, has been used to treat leishmaniasis for more than 50 years (Hailu et al. 2010). In India, a Phase III clinical trial showed 94% efficacy of parenterally-administered paromomycin in patients with VL (Sundar et al. 2007). A topical formulation with 15% PM has been approved for the treatment of CL (de Morais-Teixeira, et al, 2014;

Jhingran et al., 2009; Soto et al., 2018). In bacteria, PAR inhibits protein synthesis, but the specific MoA in *Leishmania* spp. is not fully understood. Shalev et al. showed the binding of PAR to an rRNA model using X-ray crystallography at 3.0 Å resolution, these models have been also used to explore interactions between aminoglycosides in prokaryotic and eukaryotic ribosomal A-sites (Shalev et al. 2015). PAR and other analogues inhibited translation and growth in *L. donovani*, *L. major* and *L. tarentolae* and the structural data presented by Shalev and colleagues, showed the binding of PAR to the ribosomal A-site, stressing the importance of the position 5' of ring III to determine the selectivity and enhanced binding for the leishmanial cytosolic ribosomes versus their prokaryotic counterpart. In *L. mexicana* the effects of PAR on translation were observed to be different than those on its mammalian host (Fernández, Malchiodi, and Algranati 2011). Other work in *L. donovani* and *L. mexicana* promastigotes also demonstrated that PAR inhibited protein synthesis with strong specific binding to rRNA of the parasite but little or no binding to mammalian ribosomes. A lower proliferation rate and reduction in mitochondrial membrane potential were also observed (Fernández et al. 2011; Jhingran et al. 2009). Although PAR has the advantage of low cost and that resistant clinical isolates have not been identified (Hendrickx et al. 2015; Rastrojo, et al. 2018), poor efficacy in VL was observed with parenteral PAR in Sudan (Hailu et al. 2010).

Experimentally, resistant lines have also been developed relatively easily and rapidly in both promastigotes and amastigotes (Hendrickx et al. 2015; Jhingran et al. 2009; Rastrojo, et al. 2018). A resistance mechanism may involve different efflux transporters (ABC-type efflux, MDR1) with reduced uptake and increased efflux of the drug (Jhingran et al. 2009). MDR1 has also been proposed to contribute to an efflux of AmB from *L. donovani* possibly contributing to resistance to this polyene (Purkait et al. 2012, 2014, 2015). Another interesting feature in PAR resistant lines selected *in vitro* is the lack of evidence related with cross-resistance against other Antileishmanials (Bhandari, et al., 2014; Jhingran et al., 2009). Genomics and transcriptomics recently showed two transcripts (LINF_270027300 and LINF_270027400), a D-lactate dehydrogenase-like protein (D-LDH) and an aminotransferase of branched-chain amino acids (BCAT) which transcripts were significantly overexpressed (56- and 32-fold, respectively) and both fall within a region in which the coverage of the genomic DNA was up-regulated by 150-fold in the PAR resistant line compared with the parental wild type, suggesting that these might be one of the mechanisms of action of this drug (Rastrojo, García-Hernández, Vargas, Camacho, Corvo, Imamura, J.-C. Dujardin, et al. 2018).

1.6.4 Miltefosine

Antileishmanials that target components of the membrane of the parasite such as MF is also known as hexadecylphosphocholine and is the only oral treatment available with antileishmanial activity. Initially, it was licenced for VL in India in 2002 but it is also used for other forms of leishmaniasis, particularly in regions where drug resistance against antimonials is a problem (Banerjee, Roychoudhury, and Ali 2008). After receiving orphan drug status, MF was also approved in 2015 by the FDA for leishmaniasis (Sunyoto et al. 2018). Initially investigated for its antitumor and anti-inflammatory properties, MF is an alkyl-phospholipid analogue of phosphocholine which mimics the structure of phospholipids found in cell membranes. Miltefosine interacts with phospholipids and sterols in the membrane. Apart from some side effects such as vomiting, diarrhoea and nausea, the issue of teratogenicity is a major concern for its use (Sunyoto et al. 2018).

Although resistance against MF is multifactorial, the long course of administration of more than 20 days, i.e. 100 mg/kg for 28 days (Abongomera, et al., 2019), as with the administration of parenteral antimonials or topical paromomycin, might lead to low compliance and lead to under-dosing, treatment failure and possibly, drug resistance (Burza et al. 2018). Although oral MF was initially a breakthrough, over the years some clinical cases have reported decreased efficiency and unresponsiveness to MF in endemic regions (Rijal et al. 2013) and relapse (Hendrickx et al. 2015). Clinical isolates refractory to treatment with MF were also resistant to other antileishmanials (e.g. antimonials). Importantly, in recent years, characterisation of the mechanisms underpinning resistance to MF in *Leishmania* has improved our understanding on the MoA of this phospholipid derivative, although it is still not fully understood (Barrett and Croft 2012). In *Leishmania* and *Trypanosoma cruzi*, it has been observed perturbation of the alkyl-lipid metabolism, phospholipids and membrane biosynthesis and apoptosis after treatment with MF and other alkyl-lysophospholipid analogues (Seifert et al. 2003; Varela-M et al. 2012).

As with PAR, generation of laboratory stable MF resistant lines has proven easy to achieve (Seifert et al. 2003; Shaw et al. 2016) although some studies in *L. donovani* found this to be very challenging (Hendrickx et al. 2015). In some studies, no cross-resistance to other antileishmanials was observed (AmB, sodium stibogluconate and PAR) (Fairlamb et al. 2016; Seifert et al. 2003). However, other studies found higher susceptibility (3-fold) against PENT (Turner et al. 2015), and more recently, reciprocal cross-resistance between two MF- and AmB resistant lines of *L. infantum*, was reported (Fernandez-Prada et al. 2016). In the latter of these studies, the resistance was determined by the effect of lipid

species caused by the mutations in the MF transporter during the selection with both compounds (Fernandez-Prada et al. 2016). In MF resistant lines of *L. donovani* selected *in vitro*, there was no evidence of amplification of the P-glycoprotein gene, which has been previously described to be resistant against ether lipids in *L. tropica* (Seifert et al. 2003). In another work, MF resistant *L. donovani* showed an altered composition of membrane lipids, including fatty acids, phospholipids and sterols. Interestingly, in wild type parasites, cholesterol was significantly higher in mitochondrial membranes without Ergosterol being detected. On the other hand, the content of ergostane-type (i.e. C-24 alkylation) intermediates was reduced in resistant parasites, although the susceptibility against MF was unaltered (Rakotomanga, et al., 2005). Changes in the content of sterols and phospholipids have been observed in tumour cells after treatment with MF (Geilen, et al., 1996).

The depletion of sterol was shown to decrease the susceptibility to MF by 40% in both wild type and MF resistant *L. donovani* promastigotes, moreover, resistant cells showed a more rigid membrane than wild type. Nuclear magnetic resonance (NMR) indicated that MF stimulates lipid trafficking across the parasite membrane (Saint-Pierre-Chazalet et al. 2009). Characterisation of MF resistant strains using genomic and transcriptomic approaches has confirmed that mutations (SNPs, indels) in the MF transporter gene (LINF_130020800) triggered a significant reduction of the uptake of the drug and a MF resistant phenotype (Mondelaers et al., 2016; Pérez-Victoria et al., 2006; Shaw et al., 2016; Srivastava, et al., 2017), and a mitochondrial heat shock protein HSP70 (LINF_300030100) which overexpression confers more susceptibility to MF but without increasing its uptake (Pérez-Victoria et al., 2006; Vacchina, et al., 2016). In clinical isolates from patients with VL refractory to treatment with MF, an MF resistant phenotype was caused by mutations in both genes (LINF_130020800-LINF_320010400) of the lipid transporting complex LiMT-LiRos3 (Ros3 is an accessory protein associated with function of MF (Mondelaers et al. 2016).

Shaw *et al.* showed disruption of the profile of lipids that are important for the stability of the membrane (e.g. phosphatidylcholines, lysophosphatidylcholines) and revealed that the Kennedy pathway may play a role in MF resistance (Shaw et al. 2016). Vincent *et al.*, using metabolomics, revealed many effects of MF on the biochemical pathways of *Leishmania*. For instance, after 3.5 hours of treatment, 10% of metabolites were significantly altered, including alkanes and decreased levels of sugars, thiols and polyamines, which are related to the production of ROS. Membrane phospholipids were normal, suggesting the integrity of the membrane. When cells were treated for 5 hours signs of membrane disintegration such as generalised depletion of many metabolites was observed suggesting a cell death

phenotype. Interestingly, these alterations observed in wild type cells were similar in Sb^{III} resistant parasites, but not in MF resistant lines, in which MF was not internalised (Vincent et al., 2014). Contrary to these findings, another study found a significant decrease in membrane phospholipids in *L. donovani* amastigotes treated with MF, while other lipids including sphingolipids and sterols increased. A possible role for sphingolipids in MF mode of action was implied since a knockout line of serine palmitoyl transferase gene (Δ LCB2) which cannot make sphingolipids de novo was 3-fold less sensitive to MF than wild-type (WT) parasites (Armitage et al. 2018). However, whole genome sequencing of the Δ LCB2 revealed an unexpected deletion in the MF transporter gene, possibly selected as a compensation during selection of the Δ LCB2 mutant, hence it is possible that the link between sphingolipids and MF mode of action is indirect and complex (Shaw et al. 2016). Recently a genome-wide association study (GWAS) looking for SNPs in isolates from patients refractory and sensitive to treatment with MF found a locus associated with the failure of MF against VL caused by *L. infantum*, the presence of this locus named Miltefosine Sensitivity Locus (MSL) is associated with response whereas the absence of MSL leads to an increased risk of treatment failure by 9.4-fold (Carnielli et al. 2018).

1.6.5 Polyene antifungals

Polyenes are natural metabolites produced by the soil Actinomycete genus *Streptomyces*. Although there are more than one hundred known polyenes, amphotericin B (AmB) and nystatin (Nys) have been widely used to treat fungal (Lopes and Castanho 2002) and protozoan infections for over fifty years (McCarthy et al 2009 revised by (Mayers 2017)). Polyenes are formed by a macrolide lactone ring and two chains, a hydrophobic chain composed by alternating conjugated carbon double bonds (C=C) joined to a mycosamine group, and an antagonist hydrophilic chain formed by a similar number of hydroxyl groups. The number of carbon double bonds is variable and determines the MoA, energy, stability and other properties of these compounds, including their classification into large and small polyenes (see Figure 1-9 and Figure 1-10).

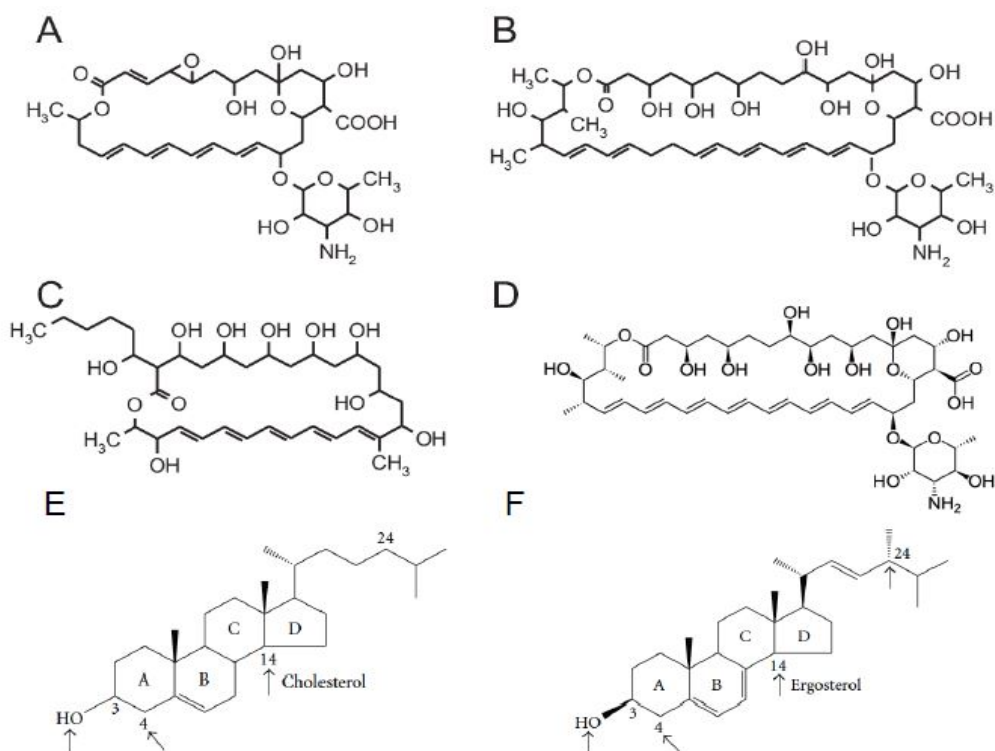


Figure 1-9. Chemical Structure and classification of polyenes and their target sterols. A, B, C and D show large (≥ 35) and small polyenes (< 30) carbon atoms. A. NMC (33) 26 carbons, B. Nys (47) 38 carbons, C. Filipin 35 carbons lacking the mycosamine and D. AmB (47) 37 carbons. E. Cholesterol (C27) and F. Ergosterol (C28). The structural differences are the presence of an extra double bond at C7 in the B-ring and at C22 of the side chain, and an extra methyl group at C24(C28) of the side chain (Welscher et al., 2008; Welscher et al. 2010; Tutaj, 2015).

Large polyenes are used as dyes due to the absorption of high energy/light from the ultraviolet (< 380 nm) or visible spectrum (380-760 nm) which is a property of the C=C bonds alternated in the hydrophobic chain, and this chain is indeed the side of the polyene molecule that binds to sterols (Boukari et al. 2016; Sokol-Anderson, Brajtburg, and Medoff 1986; Tutaj et al. 2015; Te Welscher et al. 2010). AmB owes its name to the amphoteric properties which is characteristic of the members of this group. Natamycin (NMC), also known as primaricin, is also amphiphilic (amphipathic), in its pure form both AmB and NMC have low solubility in water and poor absorption systemically, however, NMC is less toxic than AmB and is widely used in the food industry to prevent fungal contamination (te Welscher, 2010). NMC can also be administered intraocular (Lakhani, et al., 2019) at higher concentrations than AmB as to treat *Candida* spp. (O'Day & Head, 2006; O'day, et al., 1986; Te Welscher et al., 2010). The use of this route of administration (intraocular) remains unexplored in human and animal patients with leishmaniasis.

AmB and Nys are the most widely used antifungals, while Nys is mainly used to treat Candidiasis and AmB has a broader spectrum of action, is also active against yeast, mould,

and is the only effective drug against some mycoses, and is effective to treat parasitosis caused by protozoa (Yardley and Croft 1997) and some stages (sporocyst) of *Schistosoma mansoni* (Moné, et al., 2010). AmB is also the drug of choice for the treatment of other fatal infections such as the primary amoebic meningoencephalitis (PAM) caused by the amoeba *Naegleria fowleri* (Debnath et al. 2012) which has been successful for the treatment of PAM in combination with other antimicrobials (Vargas-Zepeda et al. 2005).

1.6.5.1 Mode of action of polyenes

The MoA of polyenes differs from other antifungals that interfere with the synthesis of essential components of the cell. Azoles and statins, for instance, disrupt the synthesis of sterols by targeting the enzymes C14-Lanosterol demethylase (C14DM) and 3-hydroxy-3-methylglutaryl-CoA reductase (HMGR), respectively. In some fungi, echinocandins inhibit the β -(1,3)-D-glycan synthase, necessary for the synthesis of the cell wall (Grover 2010), although this structure is not present in trypanosomatids. Polyenes on the other hand, bind to ergosterol and other sterols that are the final product of the Sterol Biosynthetic Pathway (SBP). The interaction between polyene and sterols is determined by the structure of the polyene itself and by the type and composition of the different sterols within the membrane. Given the structural differences between large and small polyenes (Figure 1-9), their MoA (Table 1-2), efficacy and toxicity present important differences (Ben-Ami, et al., 2008; Chiou, et al., 2000; de Souza & Rodrigues, 2009b; O'day et al., 1986).

Table 1-2. Modes of action (MoA) of large and small polyenes.

Polyene	MYC	Size	Mode of Action
AmB and Nystatin	Yes	Large ≥ 35 carbons	Disrupt and form pores (permeabilization) in plasma membranes, causing leaking and cell death. Binding to ergosterol and cholesterol
Filipin	No	Medium	Form complexes and loss of function of the membrane as barrier. Neutral polyene
Natamycin	Yes	Small < 30 carbons	Unique MoA does not disrupt or alter the permeability of the membrane. Instead, NMC accumulates in the membrane, form blisters, disrupts the cell wall and blocks growth (at least in fungi). Ergosterol specific binding

MYC: mycosamine group

Both AmB and Nys, have a hydrophobic chain of similar size joined to a mycosamine group, the latter is also present in NMC but joined to its shorter macrolide ring. Filipin on the other hand, lacks the mycosamine group, which is essential for the antifungal properties of these compounds. Gray et al. 2012 studied the functionality of the mycosamine and found that this group is essential for the orientation of the polyene within the membrane. The authors produced analogues of AmB and NMC, named

amphoteronolide B and natamycin aglycone, respectively, which lost their antifungal properties, particularly the ability to bind to sterols, after removing the mycosamine.

Electron microscopy revealed that large polyenes produced a more distinctive morphological change on fungal membranes than small polyenes (Kitajima, Sekiya, and Nozawa 1976). Large polyenes, AmB and Nys, bind to sterols found in the membrane of yeast (Serhan, et al., 2014), pathogenic fungi and *Leishmania*, forming transmembrane pores between 4-10 Å in diameter which leads to the loss of monovalent ions (e.g. Na⁺, K⁺, Cl⁻) and small organic particles. Filipin, of medium size, binds to cholesterol and ergosterol disrupting the membrane and forming pits or invaginations of 250-300 Å that allowed the leakage of both, small ions and large molecules (e.g. K⁺ and glucose-6-phosphate dehydrogenase). Finally, the small polyene NMC showed a unique mechanism of membrane disruption (Figure 1-10), producing aggregated areas of 800-1000 Å that appeared elevated and without formation of pores (Bolard, 1986; Kitajima et al., 1976; Te Welscher et al., 2010; te Welscher et al., 2008).

1.6.6 Amphotericin B

Initially used as a second-line treatment, AmB is now the drug of choice for leishmaniasis, particularly in endemic regions where resistance against some antileishmanials (e.g. antimonials) is prevalent (Mayers et al., 2009). AmB is also effective against CL but the self-healing nature of this form of the disease has limited its use (Yardley and Croft 1997, 2000), AmB has comparable efficacy *in vitro* against clinical isolates of *L. infantum* causing VL in dogs (Aït-Oudhia et al. 2012). Due to its poor solubility in aqueous solutions at physiological pH, AmB needs to be in complex with solubilising agents before administration. Sodium deoxycholate for instance, allows the administration of AmB intravenously, intra-lesionally and intra-articularly. The dissociation of AmB from deoxycholate (AmB-D) occurs in the blood, however, the use of AmB alone or in complex with deoxycholate (Fungizone®) presents some disadvantages; it requires hospitalization and special monitoring during the infusion and can cause acute and chronic toxicity with severe side effects including nausea, hypertension, myocarditis, hypokalaemia and nephrotoxicity. The use of lipid formulations lessens the toxicity associated with AmB significantly. The properties and uses of AmBisome are discussed further (see section 1.6.6.2).

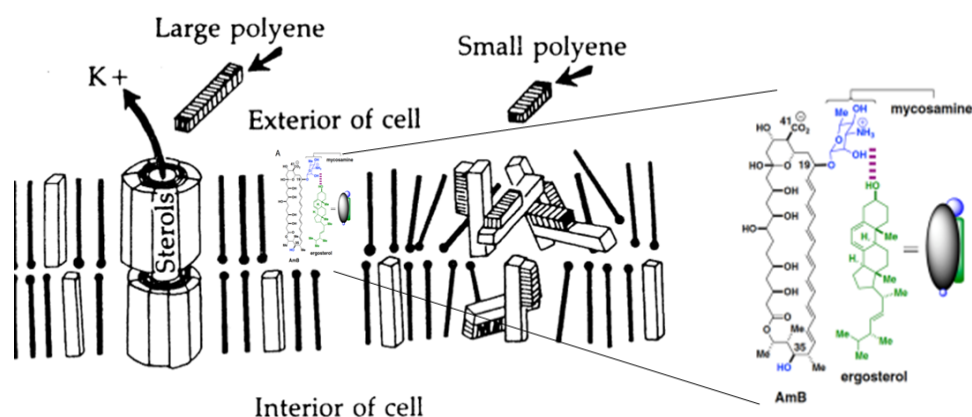


Figure 1-10. Model of the MoA of large and small polyenes in sterol-containing membranes. Large polyenes (AmB and Nys) bind sterols in the membrane and form pores that span the entire membrane. Small polyenes (NMC) only form complexes with the membrane sterols disrupting the structure and blocking the growth of the cell. Modified from: (Bolard, 1986; Denis and Head, 1987; Gray et al, 2012).

1.6.6.1 Mode of action of amphotericin B

The MoA of AmB is related to the impairment of stability and the permeability of the plasma membrane. The selectivity and toxicity of AmB are determined by the interaction with different types of sterols found in membranes of both the host and the pathogen, and other components such as phospholipids and in particular, lipid rafts, which contain high amounts of sterols, sphingolipids and proteins, which are involved in maintaining the integrity and signaling functions of the membrane (Anderson et al. 2014; Pike 2003). The molecule of AmB has a macrolide ring of about 24 Å in length that allows the formation of trans-membrane pores with a diameter of 8 Å. Each pore is composed of two complexes of eight molecules of AmB that together extend towards both sides of the membrane, reaching the intra and extracellular space and acting like aqueous channels (Figure 1-10 and Figure 1-11). These pores can transport monovalent ions, water and other intracellular components, leading to an alteration of the osmotic equilibrium and eventual cell lysis (Bolard 1986; Sokol-Anderson et al. 1986; Tutaj et al. 2015). Contrary to the dogma that the formation of the aqueous channels was responsible for the cidal effects of AmB, Gray *et al.* showed that the antifungal properties of AmB can also depend on the binding to ergosterol without forming pores, which is only a secondary effect independent of the presence of sterols. These aqueous channels tend to accumulate at higher concentrations of AmB and the permeability of the membrane seems to be involved (Gray et al. 2012). In accordance with this, Anderson, et al. proposed a new model called "the sponge model" in which AmB binds ergosterol without being internalised within the lipidic bilayer, instead, AmB aggregates in the outer surface of the membrane extracting ergosterol. This depletion of ergosterol then causes disruption and impairment of the functions of the plasma

membrane. Interestingly, this model resembles with the MoA of small polyenes which bind ergosterol without forming pores (Anderson et al. 2014; Te Welscher et al. 2008, 2010).

According to the sponge model, the interaction between AmB and ergosterol is essential. The binding of AmB to ergosterol and other sterols has been analysed in a series of molecular dynamic simulations and experimental models (Anderson et al., 2014; Baginski, et al., 2002; Boukari et al., 2016; Gray et al., 2012). The study of Anderson et al. in particular, characterised the nature of the binding of AmB to various membrane sterols, and minor structural differences were shown to cause differences in affinity (Lohner 2014). AmB bound to ergosterol in a strong manner whereas for cholesterol the binding was weak, and no binding was observed between AmB and lanosterol (Anderson et al. 2014), although in some reports, including 3D modelling (Boukari et al. 2016), the latter has been cited to act as a target of AmB (Adler-Moore, et al., 2016). In another study published over forty years ago, De Kruijff et al. incorporated sterols other than cholesterol into membranes and determined three components that are essential. Only those sterols with, 1) a 3β -OH group, 2) a planar molecule, and 3) a hydrophobic side chain in C17, were able to bind to a large polyenes and permeabilise the membrane (De Kruijff, et al., 1974). In 1973, Hsuchen and Feingold, described the importance of these structural components of the sterol molecule, highlighting that the distribution of the double bonds within the sterol nucleus is another structural feature that is key to determine the selectivity of AmB and other polyenes.

Briefly, sterols with two double bonds bind more strongly than those with only one double bond within the sterol ring (Hsuchen and Feingold 1973). Recently, the selective toxicity of AmB was reduced upon modification of some bulky substituents in the amino sugar moiety (mycosamine). All the derivatives obtained were significantly less toxic than AmB in several mammalian cell lines, and those with the best selectivity index, induced potassium release in *C. albicans*, but not in human cells (erythrocytes) at concentrations lower than 100 $\mu\text{g/mL}$ (108.2 μM) and are therefore considered as promising antifungals (Borowski et al. 2018). In *Leishmania* and fungi, the first of these double bonds is introduced by the C-8 sterol isomerase (C8SI) (ERG2 in fungi, LmxM.08_29.2140 in *L. mexicana*) that catalyses the isomerization of $\Delta 8$ double bond to $\Delta 7$ position, whereas the second double bond is introduced at the position $\Delta 5$ by the glycoprotein C5-sterol desaturase (C5DS) (ERG3 in fungi, LmxM.23.1300 and/or LmxM.30.0590 in *L. mexicana*). With regard to the lateral chain, in *Leishmania*, a double bond in the position 24 of the side chain is introduced by the enzyme C-24 sterol methyl-transferase (C24SMT) which has two copies (LmxM.36.2380 and LmxM.36.2390 in *L. mexicana*) arranged in

tandem (Jiménez-Jiménez et al. 2008; Mukherjee et al. 2018), and has no orthologue in mammals (Chawla and Madhubala 2010), making this enzyme an attractive target for drug development against Trypanosomatids (Gros et al. 2006; Magaraci et al. 2003). Evidence of defects in both enzymes, C5DS and C24SMT, have been implicated with AmB resistance in yeast, pathogenic fungi (Kelly et al. 1994), and more recently in *Leishmania* (Pountain et al. 2019). Details of the mechanistic of these changes are discussed further (see 1.6.6.3). Structural differences between ergosterol (*Leishmania* and fungi) and cholesterol (mammals), i.e. the extra double bonds at C7 and C22, in the A ring and the side chain, respectively, and an additional methyl group at C24(C28) of the side chain, are important for the selectivity and the binding to polyene antibiotics (Smith, Crowley, and Parks 1996; Veen and Lang 2005).

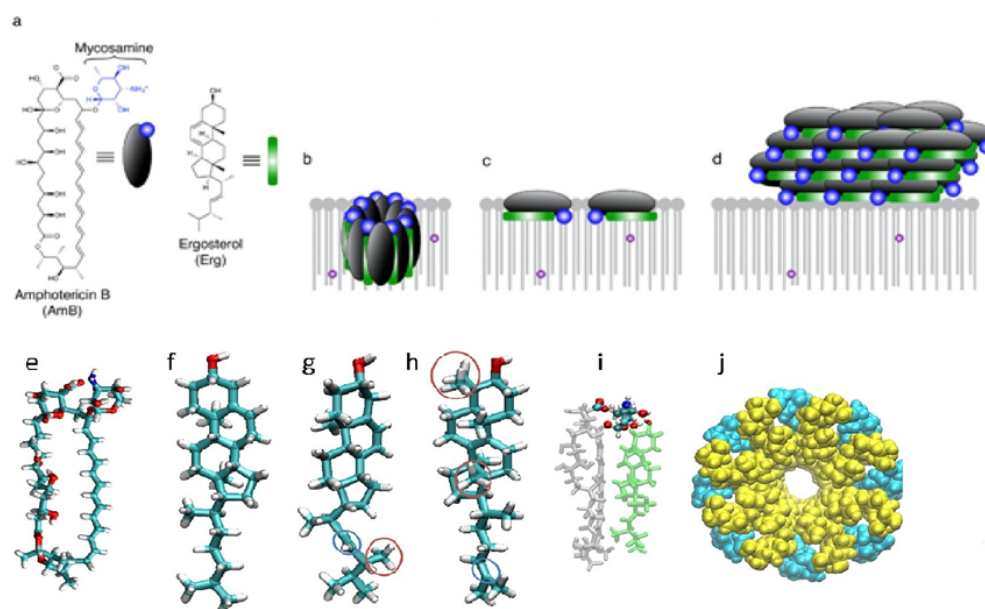


Figure 1-11. Model of structure and interaction of AmB and ergosterol-and phospholipid containing membranes.

a) Structure of AmB and Ergosterol (Erg). b) classic channel (pores) model, c) sequestering model, AmB positioned in the head group region of the membrane parallel-oriented and pulling out Erg to the surface. d) sponge model, AmB initially aggregates outside of the membrane and extracts Erg from the lipid bilayers. e) 3D structure of AmB, and other Ergostanes f) Cholesterol g) Ergosterol and h) Lanosterol i) 3D binding AmB-Cholesterol in aqueous solvent j) channel with 8 molecules of AmB (yellow) and 8 of Cholesterol (cyan). Polar head of AmB and Hydroxyl group of Cholesterol are coloured in CPK (red for oxygen, white for hydrogen, blue for nitrogen and cyan for carbon atoms, respectively). Source: Anderson et al, 2014; Boukari et al, 2015; Gray et al, 2012.

Gray et al. and Anderson et al., showed in their respective models, that AmB also induces oxidative stress (Anderson et al. 2014; Gray et al. 2012). In *Leishmania*, AmB has also been described to disrupt metabolic pathways other than the sterol biosynthetic pathway (SBP), such as the pentose phosphate pathway (PPP) (Fan et al. 2014), and the polyamine-trypanothione pathway (PTP) (see 1.7.2 and 1.7.3) (Mandal et al. 2017; Manta et al. 2013;

Purkait et al. 2012). In both pathways, some enzymes are unique of Trypanosomatids and therefore attractive drug targets. The use of antioxidants in fungi caused effects associated with changes in the susceptibility towards AmB, suggesting that oxidative stress is possibly another MoA (Mesa-Arango, Scorzoni, and Zaragoza 2012), however, the molecular basis of the generation of ROS by AmB and in *Leishmania* is unknown. Some studies have suggested a central role of the mitochondria in the protective against ROS. In this sense, Bonneau, *et al.* showed that after sequestering ergosterol from membranes of tobacco cells, filipin triggered a transient production of ROS dependent of NADPH oxidase (Bonneau et al. 2010). This enzyme and the mitochondrial metabolism are the primary source of ROS in immune cells, including macrophages, and ROS can contribute to killing intracellular pathogens (Abuaita, Schultz, and O’Riordan 2018).

Genome-wide studies (GWAS) showed that AmB caused upregulation of genes of both, the SBP, and oxidative stress pathways (Liu et al. 2005). Barker et al. also observed overexpression of several ergosterol and catalase genes after the treatment of *C. albicans* with sub lethal concentrations of the antifungal fluconazole, the adaptive process against the induced oxidative stress increasing the tolerance against AmB. In this study, the activity of mitochondrial enzymes (e.g. Acetyl Co-A synthetase) was reduced and resulted in low abundance of other ROS intermediates, suggesting that the MoA of AmB is related to the production of ROS (Barker et al. 2004). Oxidative stress seems to occur independently of the permeabilization of the membrane but to contribute to the lethal properties of AmB (Sokol-Anderson et al. 1986). In accordance to the models of Gray et al., and Anderson et al., both which establish that pores form independently of the content of ergosterol, peroxidation of lipids was observed in membranes of *Candida* (Bolard, 1986; Bolard, et al., 1991), and other pathogenic fungi that were resistant to AmB (Walsh et al. 1990). Interestingly, these membranes were permeable to polyenes regardless their complete lack of sterols (Walsh et al. 1990). AmB also induces the production of Nitric Oxide (NO) and ROS intermediates in both infected and uninfected macrophages, triggering an immuno-regulatory effect, particularly at sub-lethal concentrations (Bolard 1986), and a pro-inflammatory response, accelerating the elimination of the pathogen (Mesa-Arango et al. 2012).

AmB is known to induce a pro-inflammatory Th1 response with depletion of Th2 type cells, and to also bind to Toll-like receptors (TLR), releasing chemokines and cytokines (Mesa-Arango et al. 2012). Before the work of Abuaita, et al., it was unclear how ROS kill pathogens inside the phagosome, by inducing a stress response. On the one hand, the secretion of mitochondrial ROS (mROS) is elicited by the endoplasmic reticulum (ER),

and on the other side, mitochondrial-formed vesicles carry and deliver both, mROS and the mitochondrial enzyme superoxide dismutase-2 (Sod2) within the phagosome, this process involves TLR receptors and Sod2. If Sod2 is depleted, the production of mROS and the capacity to eliminate the pathogen are both reduced significantly (Abuaita et al. 2018).

The parenteral use of AmB creates a potential interaction with other components of the blood, particularly lipoproteins and sterol-containing cells, such as erythrocytes which also have cholesterol in their membranes. Such interactions affect the efficacy and toxicity of AmB (Brajtburg et al., 1984). Bekersky, et al. compared the amount of AmB that was bound to plasma lipoproteins between AmB-D and AmBisome. Even though both formulations showed similar mechanism of renal clearance of the unbound drug, AmB was highly bound (>95%) to plasma proteins such as albumin and glycoproteins whereas in AmBisome, most of the drug (97%) was in an unbound state (i.e. inside the liposomes), reducing significantly the total amount of drug cleared from the body (Bekersky et al. 2002). Lipoproteins are particularly important because they transport lipids within the body, including cholesterol bound to low density-lipoproteins (LDL) (up to 50%) (Estrada-Luna, et al. 2018). The binding of AmB to lipoproteins forms a complex which is internalized by endocytosis, possibly mediated by LDL receptors. The mechanism of delivery of AmB within the cell depends on the physicochemical properties (e.g. size <100 nm, content of cholesterol) of the LDL particles and the liposomes. Interestingly, both type of particles carry the molecule of AmB in a very similar manner inserted within the lipid bilayer (Brajtburg and Bolard 1996). Other aspects of the binding between AmB and lipoproteins are important to consider for studies *in vitro*, due the addition of serum into the culture medium, similarly, dosing and availability of AmB in studies *in vivo* need to consider the possibility of less drug available due to this binding.

1.6.6.2 MoA of liposomal amphotericin B

Liposomal AmB (AmBisome®) consists of unilamellar liposomes (Gilead Sciences Ltd, AmBisome®, 2018), Amphocil™ is a colloidal dispersion and Abelcet® contains AmB in a lipidic complex. The composition and physicochemical properties of these and other generic formulations available have been extensively tested against fungi and *Leishmania* spp., both *in vitro* and *in vivo* (Adler-Moore et al., 2016; Adler-Moore & Proffitt, 2008; Brajtburg & Bolard, 1996; Gangneux, et al., 1996; Gupta, et al., 2010; Tollemar, et al., 2001; Yardley & Croft, 1997, 2000). Although its cost is higher, AmBisome is the most widely used formulation of AmB and is currently effective as monotherapy (40 mg/kg) to treat VL (Sundar et al. 2011). This formulation is particularly valuable in patients that

require special care, such as populations co-infected with HIV (Abongomera et al. 2018; Banerjee et al. 2008; Sundar and Jaya 2010) and in the Indian Subcontinent where VL is endemic and drug resistance is an issue (Singh et al., 2012; Sundar & Chakravarty, 2013).

As combination therapy, liposomal AmB also represents a valuable alternative to be considered by health policy makers. A Phase III Trial showed that AmBisome (30 mg/kg) in combination with MF (100 mg/day for 28 days) was comparable to AmB monotherapy in VL patients co-infected with HIV (Abongomera et al. 2018; Diro et al. 2019).

AmBisome is characterized by a favourable therapeutic index with a significant reduction of the toxicity and lower dose required to achieve 90% cure in VL patients. The duration of the treatment was also reduced up to 15-30 fold, AmBisome (7-10 mg/kg) administered for 1-10 days was superior than doses up to 2-fold higher (11.25 to 20 mg/kg) over 15-30 days with AmB-deoxycholate complex (AmB-D) (Adler-Moore et al., 2016; Sharma et al., 2011; Singh et al., 2012). The MoA of AmBisome is different than the conventional AmB due to its physicochemical properties. AmBisome liposomes are composed of cholesterol that binds to AmB, a hydrogenated soy phosphatidylcholine (HSPC), and distearoyl phosphatidyl-glycerol (DSPG) which is negatively charged and interacts with the positive amine group of AmB to form a complex within the lipid bilayer of the liposome, which is stable at body temperature. In *Leishmania*, AmBisome allows the internalization of AmB inside specific intracellular compartments such as the phagolysosome, and therefore delivering higher concentrations of drug that can target the amastigotes inside the macrophages (Adler-Moore et al. 2016).

1.6.6.3 Drug resistance against polyenes

Resistance to AmB and other antileishmanials is multifactorial (Mesa-Arango et al. 2012), and difficult to detect given the diversity of the MoA of polyenes. One common feature however, seems to be the loss of the wild type sterol, ergosterol, which is replaced by different sterol intermediates, depending on the mutations in different enzymes of the sterol biosynthetic pathway (SBP). The main MoA, i.e. binding to ergosterol, and the higher selectivity to AmB in comparison to cholesterol, is of particular interest in *Leishmania*, because both the ergostane and stigmastane families, are key endogenous sterols in trypanosomatids and are absent in mammals (Choi, Podust, and Roush 2014). This selective binding has been observed in different species of *Leishmania* (Xu, et al., 2014). A study with ergosterol- and cholesterol-containing membranes, showed that the effect of AmB is concentration dependent. In cholesterol containing membranes, AmB showed no effects, and led to membrane permeability and leakage of K^+ at concentrations

lower and higher than 80 nM, respectively. On the other hand, ergosterol containing membranes were more sensitive to AmB and similar effects were observed with a concentration ten-fold lower (8 nM). This study highlights the fact that apart from the type of sterol in the membrane, the concentration of AmB is also key to determine the effects of AmB (Bolard et al. 1991).

In *Leishmania*, the lower abundance of ergosterol that is frequently observed in AmB resistant mutants created in laboratory conditions, is rare in clinical samples (Chakravarty and Sundar 2010; Fairlamb et al. 2016). Resistance to AmB has been, however, observed in clinical isolates of *L. donovani* with alterations of the membrane (and loss of ergosterol) (Purkait et al. 2012), in isolates from non-endemic areas (Srivastava, et al., 2011), and in other studies published before AmB became the first treatment for VL (Chakravarty and Sundar 2010; Durand et al. 1998; Giorgio 1999). Durand et al., 1998 could not detect a change in susceptibility in *L. infantum* promastigotes after the treatment with AmB in a patient co-infected with HIV. The effective dose (ED₅₀) before and after the treatment was 0.056- and 0.064 mg/kg body weight, respectively (Durand *et al.*, 1998). Giorgio et al, 1999 detected a reduction in the susceptibility (EC₉₀) of isolates in eleven patients infected with *L. infantum* and HIV, which were obtained at the time of repeated relapses after treatment. In this latter study, the susceptibility to AmB was determined using the EC₉₀ values, showing that in all cases, the lack of response after the treatment with intralipid AmB (intralipid 20% emulsion, Pharmacia SA, Paris, France) at 1–2 mg/kg per day, for 21 days, was associated with an increase of the EC₉₀ values. Moreover, promastigotes and amastigotes isolated from a patient after six relapses, were resistant to AmB (Giorgio 1999). The fact of the increasing use of AmB after it became the leading compound for the treatment of VL cannot be ignored. Particular interest needs to be addressed to the lipid formulation, AmBisome, which increases the half-life of AmB within the body (Chakravarty and Sundar, 2010).

Reports of clinical isolates resistant to AmB (and azoles) are now more frequent in fungi, particularly in emerging species (although it has been also reported in *C. albicans*), for instance, 50% or more of the resistant isolates are non-candida species (McCarthy et al. 2017). The low susceptibility to AmB reported in fungi with normal levels of ergosterol suggests that other mechanisms are, possibly, involved in resistance (McCarthy et al. 2017). In fungi, AmB resistance can be categorized into three main types: (1) primary or intrinsic, (2) acquired, and (3) clinical resistance (McCarthy et al. 2017). Some strains of *Trichosporon beigelii*, a pathogen that causes fatal disease, which have normal concentrations of ergosterol, are intrinsically resistant to AmB, and oxidative stress

defence has been proposed to be involved in this protection (Walsh et al. 1990). Another species naturally resistant to AmB is *Aspergillus terreus*, where high levels of catalase involved in protection against oxidative stress have been proposed to play a role (McCarthy et al. 2017). Recent work showed that cross resistance between azoles and polyenes (AmB and nystatin in this study), was also present among other emerging fungal species including *Candida auris* (de Cássia, et al., 2018).

The techniques and protocols employed to analyse resistance may also be related to the low frequency of reports about resistance to AmB. In fungi, the minimum inhibitory concentration (MIC) is normally used, while a minimum fungicidal concentration (MFC) would be better for the detection of *in vivo* and *in vitro* activity. The MIC, for instance, varies depending on many factors (e.g. strain, media, culture conditions), and cannot discriminate between susceptible and resistant strains because this technique is limited by the narrow concentrations of drug that are tested. Similarly, the great majority of studies in parasitology, report the half-maximum effective concentration (EC₅₀) and most of the time, the inhibitory growth curve (Hill slope) is not provided and could indicate non-standard inhibitory characteristics. Moreover, the EC₉₀ value is rarely published (McCarthy et al. 2017). As described in section 1.6.6.1, the binding of AmB and other polyenes for ergosterol and other membrane sterols is variable (Anderson et al. 2014) and various factors influence the degree of such affinity. That said, changes in the sterol pathway that interrupt the biosynthesis and reduce the abundance of those intermediates that bind drug with high affinity are expected to confer resistance. Of particular interest in *Leishmania*, are the number of double bonds in the lateral chain, and the number and distribution of the double bonds within the sterol ring (Hsuchen and Feingold 1973). Changes in sterols with loss of ergosterol relate with AmB resistance in both pathogenic fungi and *Leishmania*. Some enzymes involved in changes in the content of ergosterol and antifungal resistance are, HMGR (Brooks et al., 2012; Dinesh, et al., 2014; Dinesh, et al., 2015; Singh, et al., 2014; Young, et al., 2003b), C14DM (Kanafani & Perfect, 2010; Martel, et al., 2010; Mwenechanya et al., 2017), C24SMT (Pountain et al., 2019; Pourshafie et al., 2004; Purkait et al., 2012), C5DS (Geber *et al.*, 1995; Alcazar-Fuoli *et al.*, 2006; Morio *et al.*, 2012; Rastrojo, *et al.*, 2018; Pountain *et al.*, 2019), and C8SI (Kelly et al. 1994).

Defects in C24SMT in *Leishmania* spp., have similar effects as in fungi (Laura et al, 2003), in which AmB resistance is, in part, explained by the replacement of ergosterol and other ergostanes by cholestane-type intermediates, after the loss of expression of one transcript of C24SMT observed in *L. donovani* (Pourshafie et al. 2004; Purkait et al. 2012). The actual genome based mechanism of AmB resistance that operates due to changes in

this enzyme is, however, somewhat different than that observed with resistance associated with changes to C14DM or C5DS in *Leishmania*, and also in fungi, in which SNPs are frequently observed (Chakravarty and Sundar 2010).

The loss of the trans-methylation in C-24 is derived from the loss of the function of C24SMT, which is in turn related with the loss of the expression of one of the two transcripts of this gene in *L. donovani* promastigotes (Pourshafie et al. 2004), and in *L. mexicana* (Pountain et al. 2019a). In both species, this resulted in the replacement of the wild type sterol profile with the cholestane, cholesta-5,7,24-trien-3 β -ol, which leads to resistance to AmB. A detailed discussion of the changes in sterol intermediates, and the mechanism of resistance related with C24SMT are described further (see Chapter 5, and Chapters 4 and 6, respectively). The study of Purkait and colleagues, described the molecular mechanism of resistance to AmB, which was related to an alteration in the expression of the two transcripts coding for C24SMT, and resulted in a reduced binding affinity and less uptake of AmB (Purkait et al. 2012). In another study with four AmB resistant lines of *L. mexicana*, C24SMT was also involved in AmB resistance (Pountain et al. 2019a). C24SMT is a critical enzymatic step for the disruption of the biosynthesis of ergosterol and is also involved in the susceptibility/resistance to AmB in fungi (Konecna et al. 2018; Nes et al. 2009). Nystatin resistant mutants (yeast) showed defects in C24SMT (McCammon, et al., 1984). Mutations in other enzymes, i.e. C14DM (Mwenechanya et al., 2017), and C5DS (Pountain et al., 2019), also lead to AmB resistance in *L. mexicana* promastigotes, in both cases, the loss of the wild type sterol and the accumulation of other intermediates, was observed.

With regard to the role of the double bonds within the sterol ring, sterols with one double bond (Δ 5) in their sterol nucleus such as cholesterol (5-cholesten-3 β -ol) and stigmasterol (5,22-cholestadien-24 β -ethyl-3 β -ol) had less affinity for AmB (and Nys) in comparison with ergosterol (5,7,22-cholestatrien-24 β -3 β -ol or ergosta-5,7,22-trien-3 β -ol) and 7-dehydrocholesterol (5,7-cholestadien-3 β -ol) which have two double bonds (Δ 5,7). AmB did not bind to dihydrocholesterol (5 α -cholestan-3 β -ol) which lacks double bonds in the sterol nucleus (Hsuchen and Feingold 1973). This is of major relevance in *Leishmania* and fungi, in which C8SI catalyses the isomerization of the Δ 8 double bond to the Δ 7 position, while C5DS introduces a second double bond at the position Δ 5. The latter of these double bonds is essential for the synthesis of ergosterol and other ergostanes. C5DS converts episterol (ergosta-7,24(28)-dien-3-ol or ergosta-7,24(28)-dien-3 β -ol) which has one double bond (Δ 7), into ergosta-5,7,24(28)trienol. Null mutants of *S. cerevisiae* (Bard et al. 1993a) and clinical isolates of several species of *Candida* with defects and reduced expression of

C5DS (and other sterol enzymes such as C14DM and C22-sterol desaturase (C22DS) (ERG11 and ERG5 in fungi, respectively) (Martel, et al., 2010; Miyazaki et al., 1999; Young et al., 2003a), showed reduced fitness and were resistant to AmB and azoles (Joseph-home *et al.*, 1995; Martel, *et al.*, 2010; Branco *et al.*, 2017), and more susceptible to other antifungals (<https://www.yeastgenome.org/locus/S000004046>). Although there is no evidence of similar changes occurring in clinical isolates of *Leishmania*, a recent study in *L. mexicana* axenic promastigotes, demonstrated mutations in this enzyme associated with resistance (Pountain et al. 2019a). In my study, I identified five novel mutations in C5DS related with polyenes. Additional details related with the annotation of C5DS, and the implications of the recent evidence of the role of this enzyme with AmB resistance in *Leishmania*, are discussed further (see 1.6.6.3 and Chapter 4, section 4.1.5). Interestingly, no reports of the role of C8SI with resistance to AmB, have been described in *Leishmania*.

Another challenge for the detection of resistance to AmB is the ability of *Leishmania* to replace endogenous ergostanes, with exogenous cholesterol and other sterol intermediates that can be obtained from the culture medium or from the host, allowing the parasites to maintain the functionality of their membrane (Andrade-Neto et al. 2011; De Cicco et al. 2012; Ghosh et al. 2012a). A study in *Leishmania amazonensis* treated with two inhibitors of the enzymes HMGR and C14DM, showed that exogenous cholesterol was compensatory irrespective of which enzyme was inhibited (Andrade-Neto et al. 2011). Further confirmation on the role of exogenous cholesterol as a buffer mechanism, was also observed in mice with hypercholesterolemia (dietary and intrinsic), and in another group treated with statins after infection with *L. donovani*. Mice with hyper- and hypocholesterolaemia, were resistant and more susceptible to the infection with *L. donovani*, respectively, confirming that the parasites can uptake cholesterol from the host to their advantage. Moreover, amastigotes are able to extract cholesterol from the membrane of macrophages, leading to the disruption of the lipid rafts and to a lack of stimulation of T cells (Ghosh et al. 2012b). In mammals, the content of cholesterol in low density lipoproteins (LDL) is up to 50% (Estrada-Luna, et al. 2018), this concentration of cholesterol could, possibly, act as a sequestering mechanism of AmB.

Some of these ergostane-type intermediates accumulate and are related with resistance to AmB and with the virulence in *Leishmania* (Mwenechanya et al. 2017; Yao and Wilson, 2016; Vincent et al, 2013; Anderson et al., 2014; Mukherjee et al. 2018) and pathogenic fungi (Anderson et al., 2014). The use of other sterol intermediates to replace membrane sterols is also observed in fungi, in yeast for instance, lanosterol can support growth (Gachotte et al. 1997). However, systematic studies evaluating the selectivity and the

degree of the binding (affinity) of AmB towards other sterol intermediates in both *Leishmania* and fungi, are scarce.

Resistance to AmB (and other polyenes) due to other mechanisms than the content of ergosterol, and other membrane sterol intermediates, is also relevant. The over-expression of multidrug receptors ABCB (ABCB4, MDR1) has been described in *Leishmania* resistant to AmB, suggesting that the parasites are able to increase the efflux of this polyene (Purkait et al. 2012). Studies related with the cross-resistance between MF and AmB are contradictory, while in some reports cross-resistance was not identified (Fairlamb et al. 2016; Seifert et al. 2003), reciprocal cross-resistance between these two antileishmanials was reported in *L. infantum* (Fernandez-Prada et al. 2016). Similarly, the loss of the miltefosine transporter was observed in some AmB resistant lines of *L. mexicana* (Pountain et al. 2019a). More recently, upregulation of the Pentose Phosphate Pathway (PPP), was also identified in promastigotes treated with higher concentrations of AmB (5 x the EC₅₀) (PhD Thesis, Dr Raihana Binti, unpublished data). In *L. donovani* resistant to AmB, the upregulation of thiol metabolism and an increase of reduced-intracellular-thiols, were involved in AmB resistant parasites isolated from patients (Purkait et al. 2012). Further studies of this clinical isolate also identified a NAD⁺ dependent histone deacetylase (HDAC) to be directly involved in the resistance to AmB. This protein (named LmSIR2 in *L. major*), is involved in detoxification of ROS and the concurrent overexpression of the MDR1 transporter in resistant parasites, therefore confers protection against oxidative stress and increases the efflux of AmB (Purkait et al. 2014). Studies with the small polyene natamycin (NMC), which disrupts the stability of the membrane without forming pores, are also indicative that other mechanisms are involved in the leishmanicidal (and fungicidal) properties of polyenes (te Welscher et al., 2008).

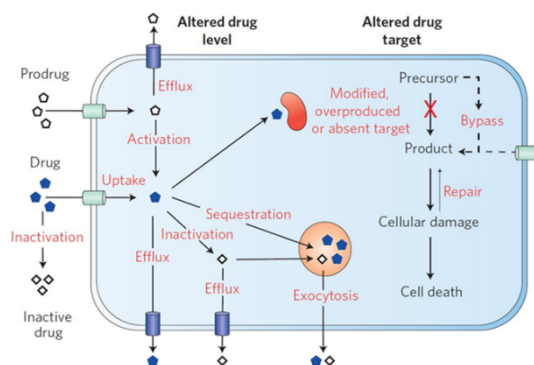
Although the loss of ergosterol seems to be the main mechanism associated with AmB resistance in *L. mexicana* (Mwenechanya et al. 2017; Pountain et al. 2019a), other lipids are also related with the MoA (and resistance) of polyenes (Bolard 1986). Some lipids such as inositol phosphorylceramide (IPC), which are unique in *Leishmania*, are known to interact with sterols in the membrane, therefore, the loss of any of these components can contribute to its destabilisation (Denny, et al., 2006). The nature of this interaction is, however, very complex. Interestingly, the loss of ergosterol can result from the exposure to other antileishmanials that target the membrane lipids. For instance, ergosterol (and 5-dehydroepisterol), was dramatically decreased in two lines of *L. infantum* that were selected for resistance to MF and AmB (Fernandez-Prada et al. 2016). Other sterols (C24-alkylated) were strongly reduced (43%) in MF-resistant, and in MF-treated *L. donovani*

promastigotes (Rakotomanga, et al., 2007; Rakotomanga et al., 2005), possibly because the substrate of C24SMT, zymosterol, is a membrane component that depends on sphingolipids (Veen and Lang 2005).

In another study with *L. donovani* axenic amastigotes, and *L. major* promastigotes, both ergosterol and sphingolipids, were involved in the susceptibility to both antileishmanials. After the treatment with MF, the content of membrane phospholipids and aminoacids was reduced, while the abundance of sterols and sphingolipids increased (Armitage et al. 2018). In contrast with this, a significant reduction in the content of ergosterol was observed in a *L. major* serine palmitoyl transferase null-mutant (Δ LCB2) that lacks sphingolipid biosynthesis. Interestingly, Δ LCB2 was 3-fold less susceptible to MF (Armitage et al. 2018), and 4.3-fold more susceptible to AmB (data not shown), irrespective of the lower abundance of ergosterol. In fungi, the higher susceptibility to AmB derived from the depletion of sphingolipids is associated with PMP3, a highly conserved small membrane protein that requires a functional sphingolipid pathway. No evidence of the presence of a similar protein to PMP3 is known in *Leishmania*. The overexpression and deletion of PMP3, resulted in increased resistance and susceptibility to AmB, respectively in fungi (Bari, et al., 2015). Moreover, the addition of phytosphingosine (an intermediate of the sphingolipid pathway), restored the susceptibility of the PMP3 deletion mutants, thus confirming that the interaction between the sterol and the sphingolipid pathways plays a key role in AmB resistance (Veen and Lang, 2005; Bari *et al.*, 2015). Recently, another study using RNAi in *T. brucei* confirmed that the MoA of AmB, and the transport and metabolism of membrane lipids (phospholipids) are related. The depletion of the MT (Tb927.11.3350 in *T. brucei*), and other flippases, led to an increase in the EC₅₀ of both, AmB and MF. Interestingly, a vesicle-associated membrane protein, TbVAMP7B, possibly with similar function to PMP3 in fungi, and other membrane associated hits, were identified to influence the activity of AmB and MF (Collett et al. 2019).

Another aspect that remains poorly studied, is whether the composition of the sterols in the membrane in amastigotes is similar to that described in the promastigote stage. Yao and Wilson, observed in *L. infantum*, that the sterol composition was variable between log- and stationary (including metacyclic) stages, and involved in the virulence of the parasite (Yao and Wilson 2016). Similarly, differences in the abundance of sterols between the insect- and the intracellular stages, have also been described in AmB resistant lines of *L. mexicana* (Mbongo, et al., 1998), but is still unknown in other species. A summary of some of the mechanisms of drug resistance, in *Leishmania* is shown in Figure 1-12.

PANEL A:



PANEL B:

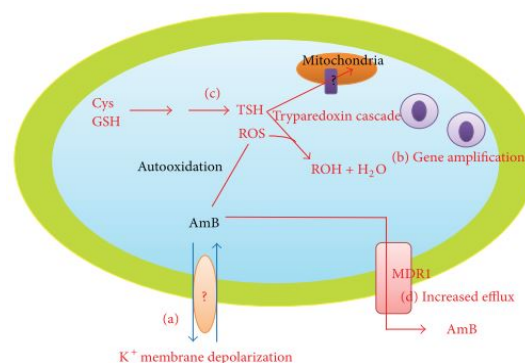


Figure 1-12. Molecular mechanisms of drug resistance in *Leishmania* spp.

PANELS A and B show the mechanisms of resistance that are general to different drugs, and to polyenes, respectively. PANEL A: 1) Reducing the total concentration of drug inside the cell (reduced uptake, increased efflux. 2) inactivating or non-activating the drug. 3) sequestration from the target, 4) reduced target-affinity via mutations or 5) reducing effects of drug by over expression of the target, 6) Pathways can be either 6.1) salvaged/bypassed to diminish the impact of the drug or 6.2) activated to repair/compensate damage. PANEL B: a) membrane alterations (e.g. depolarization, fluidity) occur after the binding of polyenes to ergosterol (and other membrane sterols). Other mechanisms that block the entry of the drug are still unknown. b) Changes (SNPs, indels, CNVs, gene amplification/duplication) at the level of genes in different pathways (e.g. sterols, polyamine-trypanothione, pentose phosphate pathway) are known to be related with AmB resistance. c) tryparedoxin is involved in resistance to several antileishmanials that cause oxidative stress. d) various membrane drugs transporters (e.g. MDR1) have been described to be related with AmB resistance. In this diagram, miltefosine transporter and other mechanisms are not included. See text (section 1.6.6.3) for a detailed description. Adapted from (Fairlamb et al. 2016; Kaur and Rajput 2014).

1.7 *Leishmania* metabolism

The metabolism of *Leishmania* is different from other trypanosomes. For instance, *L. major* is the only trypanosomatid that metabolizes disaccharides (Ginger, 2005). In this specie, there are four hundred genes coding for unique enzymes that compose the main metabolic pathways of the parasite, and some of these genes (8%) have no orthologue in mammals (Opperdoes and Coombs 2007). Some examples of these genes are the C24-sterol methyl transferase in *Leishmania* spp. (Jiménez-Jiménez et al. 2008), and the trypanothione reductase (TR), which are essential for the sterol- and the trypanothione-metabolism, respectively (Jain and Jain 2018; Mandal et al. 2017). Subramanian and colleagues, reconstructed the metabolic network in *L. infantum*, finding 142 genes encoding enzymes that perform 237 reactions which are localised in five different compartments of the parasite (Subramanian, et al., 2015).

Leishmania are essentially aerobic parasites (Brand 1966), however, the parasites are adapted to starvation, showing features of aerobic fermenters with production of organic

acids (e.g. succinate, acetate, pyruvate) in the presence of glucose and oxygen, suggesting that nutrients are not completely oxidised (Blum 1993; Brand 1966). Marchese et al. revised the uptake and the metabolism of amino acids in *Leishmania*. Apart from their function as building blocks for proteins, energy and carbon sources, amino acids are critical for other biological functions such as differentiation, regulation of the cell cycle, survival to adverse conditions, and for the establishment of the infection within the insect vector and the mammal hosts (Marchese et al. 2018).

The metabolism of *Leishmania* is moreover, adapted to the various conditions that the parasites encounter along their life cycle (Burchmore and Barrett 2001; Subramanian et al. 2015). Promastigotes, for instance, have their metabolism adapted to transform from the procyclic to the metacyclic stage within the different parts of the alimentary tract (e.g. midgut, foregut, mouth parts) of the sandfly (Dostálová and Volf 2012) and benefit from the sugar-rich nectar environment (Burchmore and Barrett 2001). It is unknown, however, if other metabolic differences between species are related to the development of certain species in specific compartments within the insect. For instance, *L. mexicana* and *L. infantum* (suprapylaria) live in the midgut, whereas *L. tarentolae* and *L. (Viannia) braziliensis* have tropism for the hindgut (Opperdoes and Coombs 2007; Rogers and Bates 2007). Ideally, the metabolism of both stages of *Leishmania* spp. should be studied in their respective “natural” niches (i.e. sandflies and macrophages) (Opperdoes and Coombs 2007). Both scenarios present, however, additional challenges. Some examples are: 1) facilities to rear and keep sandflies, 2) technical skills to maintain, infect and dissect sandflies, 3) type(s) of macrophages infected, 4) differences between species and lines, 5) recovery of *Leishmania* amastigotes from macrophages post-infection is challenging (Brand 1966), 6) dissecting the parasite-, from the host-cell metabolism is difficult. Axenic promastigotes are the most investigated model, given the easiness to handle and maintain this stage *in vitro*, although the interpretation of the biological value is still arguable (Barisón et al. 2017; Opperdoes and Coombs 2007).

Promastigotes uptake glucose, and other essential nutrients (e.g. amino acids and purines), from their host or from the culture medium (Creek, Anderson, et al. 2012; Creek and Barrett 2014; McConville et al. 2015). In *Leishmania*, glucose is stored as mannogen (Opperdoes and Coombs 2007), and both glycolysis and gluconeogenesis (also a source of glucose) are important sources of energy. Most of the glycolytic enzymes reside within the glycosomes (peroxisome like organelles) and present important structural and mechanistic differences in comparison with other organisms (including humans) in which they are cytosolic (Opperdoes and Michels 2010; Verlinde et al. 2001). Some enzymes, such as

pyruvate kinase (Rigden, et al., 1999) and fructose-1,6-biphosphatase (F-1,6BP) are key for the regulation of glycolysis and gluconeogenesis, respectively (Opperdoes and Michels 2010), the latter of these enzymes influences the virulence and is essential for replication of amastigotes in *L. major*, and promastigotes lacking this enzyme also exhibit a growth defect (Naderer et al. 2006). The expression of other enzymes is also stage-specific, for instance, alcohol dehydrogenase, enolase, and ATP synthase, are more highly expressed in promastigotes whereas hexokinase is preferentially expressed in amastigotes (Arjmand et al. 2016).

Amastigotes are adapted to survive inside the phagolysosome of mammalian macrophages where the levels of sugar are low (Naderer et al. 2006), the acidic environment activates their metabolism, optimising the uptake of glucose at pH 5 (the first transport activity studied in amastigotes), polyamines, nucleosides and amino acids (Burchmore and Barrett 2001). The latter seem to be the main source of carbon for amastigotes (McConville and Handman 2007) and the parasites scavenge them from the parasitophorous vacuole using specific permeases (McConville, et al., 2007). Some studies revealed that *Leishmania* avoids destruction by subverting macrophage functions (Handman and Bullen 2002), and disrupting metabolic and signalling pathways (Arango Duque & Descoteaux, 2015; Marr et al., 2014; Rosenzweig et al., 2008), including the central carbon metabolism (McConville 2016). Although the role of the carbon sources in the metabolism of amastigotes is less complete than in promastigotes (Arjmand et al. 2016), it is known that axenic amastigotes have the glycolytic pathways reduced and that the β -oxidation of fatty acids is increased (Creek, et al., 2012). Fatty acids are degraded using thiolases that remove an acetyl-CoA group from the acyl-CoA, this group of enzymes are also important for the biosynthesis of sterols (condensation reaction) and ketone bodies (McConville et al. 2007; Opperdoes and Michels 2010). Amastigotes develop a stringent metabolic response in which the major changes seem to be related with the central carbon metabolism, while promastigotes are highly glycolytic and can co-catabolize amino acids, and fatty acids, the much lower (up to 10-fold) uptake of glucose and amino acids is replaced by fatty acids that enter the tricarboxylic acid cycle (TCA) in amastigotes. Interestingly, differentiation also occurs *in vitro* and independently of the nutrients, suggesting that the down regulation of glucose and amino acids are controlled by the amastigotes (McConville 2016), which enters to a metabolically quiescent state with a lower growth rate (Kloehn et al. 2015).

1.7.1 The sterol biosynthetic pathway

The sterol biosynthetic pathway (SBP) is essential for the synthesis of molecules with the 1,2-cyclopenta-noperhydrophenanthrene ring system, such as cholesterol and ergosterol, which are the end products of the SBP, and the main sterol species in mammalian cell membranes, and in *Leishmania* and fungi, respectively (Nes, 2011a; Mesa-Arango, Scorzoni and Zaragoza, 2012). The structural differences between these two sterols are described in more detail later (see Chapter 5, Figure 5-1, Panel A, and Figure 1-9, Panels E and F) (Tutaj et al. 2015; Te Welscher et al. 2008, 2010). Cholesterol and ergosterol are also intermediates for the synthesis of vitamin D3 (cholecalciferol), and vitamin D2 (ergocalciferol), respectively (https://www.genome.jp/kegg-bin/show_pathway?map01100). In mammals, cholesterol is crucial for steroidogenesis, which is necessary for the synthesis of corticosteroids and other molecules with a wide range of physiological and regulatory functions (Miller and Auchus 2011; Mohammed 2012). The SBP is an attractive drug target for the treatment of leishmaniasis, several enzymes, e.g. HMGR, C14DM and C24SMT (see Table 1-3 for more details) being proposed as targets, while rational drug design studies with others enzymes of this pathway (e.g. C5DS and C8SI), remain unexplored. Most antifungals disrupt the biosynthesis of sterols by targeting different enzymes, e.g. statins, azoles, azasterols, of this pathway. On the other hand, polyenes AmB, nystatin and natamycin, bind to the end products of the SBP, ergosterol, and to a lesser extent, to cholesterol (Anderson et al. 2014). The SBP was first described in the budding yeast (Bard et al. 1993c; Mo and Bard 2005b), and studies in *Leishmania* spp., have shown differences between the protozoan and fungal SBP. Similarly, some differences in the SBP are also present between kinetoplastids (Cosentino and Agüero 2014; Yao and Wilson 2016). In *L. mexicana* promastigotes, for instance, leucine is favoured as a carbon source for the SBP, while in *T. cruzi*, acetate seems to be more important for sterols biosynthesis (Ginger et al. 2000, 2001; Ginger, Chance, and Goad 1999).

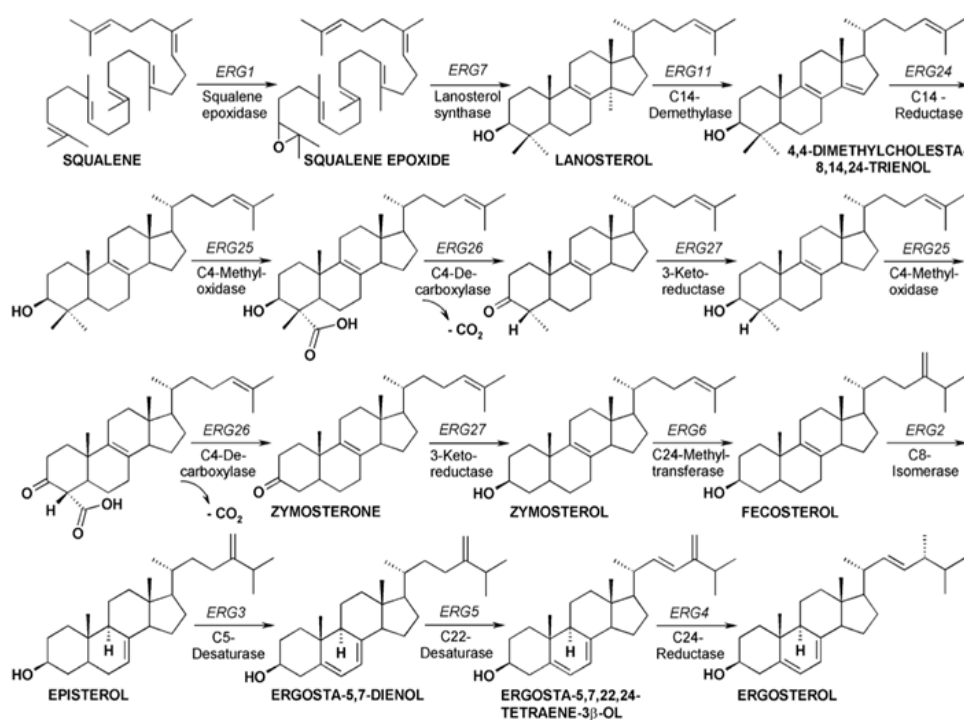


Figure 1-13. Enzymatic reactions of the Sterol biosynthetic pathway (SBP) in the budding yeast (*Saccharomyces cerevisiae*).

The SBP starts from lanosterol and ends at ergosterol, the final product in yeast and other fungi. This scheme shows the SBP (post squalene) and the names of the enzymes and their ID's in fungi, e.g. ERG1, ERG6, etc. A full description with the sequential order of the pathway and the type of reaction and product in each step, including the orthologues in *Leishmania* (including their ID, name, and E.C. and KEGG numbers), is detailed in Table 1-3. Modified from: (Kristan and Rižner 2012a; Veen and Lang 2005)

The enzymatic reactions of the SBP includes around 40 enzymes, from acetyl-CoA until the last reaction, i.e. the conversion of ergosta-5,7,22,24(28)tetraenol to ergosterol. The SBP and the localisation within the cell in *Leishmania* spp., is shown in Figure 1-13 and Figure 1-14 (Bansal, et al. 2019; Carrero-Lérida, et al. 2009; Cosentino & Agüero, 2014; Fügen et al., 2014; Jiménez-Jiménez et al., 2008; Nes, 2011; Yao & Wilson, 2016b; Zhou, et al. 2006). Another model, the yeast two-hybrid system (Y2H), developed by Stagljar, et al. 1998, showed that the SBP is a multi-enzymatic complex named, the ergosome, in which protein-protein interactions are essential for the correct function of the pathway (Mo & Bard, 2005b; Mo, Valachovic, & Bard, 2004; Stagljar, et al., 1998; Teske et al., 2008).

The presence of an ergosome-like structure in trypanosomatids has been previously suggested in *L. mexicana* (Mwenechanya, et al. 2017), but still not observed. While some of the enzymes are well identified within specific compartments, the topology and localisation of others remain unclear, in some cases, due to the lack of the structure of the protein. Current genome editing tools, such as CRISPR/Cas9, allow N- and C-terminal fluorescent tagging, which will help to determine the topology of all the enzymes of the

SBP in *Leishmania* spp. (Beneke, et al. 2017). Despite the lack of studies on the regulation of the SBP, some of the mechanisms are conserved in mammals and fungi, i.e. sterol regulatory element-binding proteins (SREBPs) (Quan-zhen, Yan, and Yuan-ying 2016), have also been identified in *Leishmania*. SREBPs modulate the transcription of LDL receptors and many of the sterol enzymes, e.g. 3-hydroxy-3-methylglutaryl-CoA synthase (HMGS), and are implicated in the synthesis of both, sterols and fatty acids (Horton and Shimomura 1999).

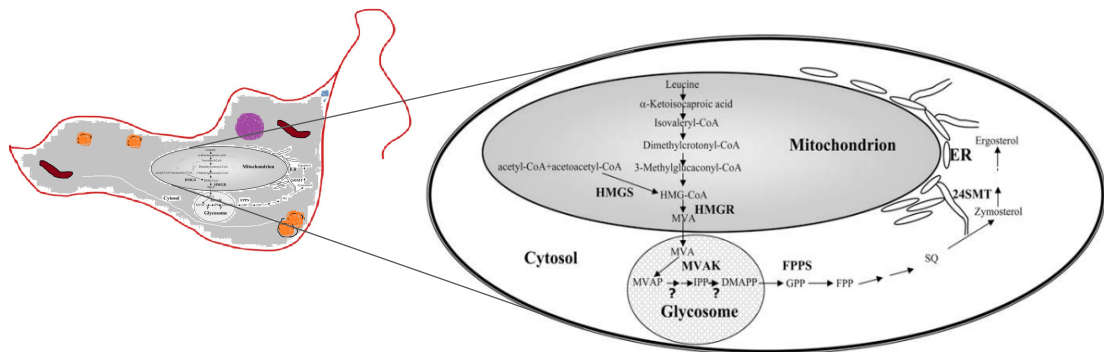


Figure 1-14. Localisation of the SBP enzymes in the trypanosomatids.

The scheme shows that the first part of the SBP from leucine to mevalonate (MVA) occurs within the protozoa mitochondrion, while the following steps up to the conversion of isopentenyl diphosphate (IPP) into dimethylallyl diphosphate (DMAPP) is performed within the glycosome. In the cytosol, geranyl diphosphate (GPP) is the substrate of farnesyl pyrophosphate synthase (FPPS) that synthesizes farnesyl pyrophosphate (FPP). Squalene (SQ) is the precursor of all plant, animal, fungi and kinetoplastid sterols, SQ is converted into lanosterol by lanosterol synthase, and the latter is the substrate of C14DM. The following enzymes are localised within the endoplasmic reticulum (ER). Conversion of zymosterol into fecosterol is a reaction exclusive of fungi and kinetoplastids, the enzyme C24SMT (24SMT in this diagram) is not present in mammals. Adapted from (Carrero-Lérida et al. 2009).

SREBPs are also involved in protection against oxidative stress. After infection with *L. donovani*, SREBP2 regulates the expression of a mitochondrial protein that suppresses the production of ROS in host mitochondria (Basu Ball et al. 2014), and the content of cholesterol in the macrophage (Mukherjee, Basu Ball, and Das 2014). Similar findings were found *in vitro*, cholesterol sequestration from the macrophage (between 72 and 96 hours) was correlated with the upregulation of SREBPs (HMGR, farnesyl pyrophosphate synthase, squalene epoxidase and the LDL-receptor) involved in the synthesis of cholesterol (the end product of the mammalian SBP), after infection with *L. mexicana* amastigotes (Semini et al. 2017).

Interestingly, SREBPs bind to specific repeats known as sterol response elements (SREs) which are located in the promoters of genes (Horton and Shimomura 1999). In *Leishmania* spp., repetitive sequences (small interspersed degenerate retrotransposon or SIDER) are

also linked to post transcriptional gene regulation. SIDER elements are known to be dispersed throughout the *Leishmania* spp. genome (Smith, Bringaud, and Papadopoulos 2009). Some SIDER elements were recently found to be related with the expression of some genes (C24SMT) of the SBP, and with AmB resistance (Pountain et al. 2019a). To the best of my knowledge, there is no evidence that suggests that these elements are related with the mode of action of SREBPs. As with other metabolic pathways that are stage specific, some enzymes of the SBP are expressed differently between amastigotes and promastigotes. For instance, all the enzymes of the SBP (except C24R), are downregulated in amastigotes (Fiebig, Kelly, and Gluenz 2015). Similar observations were found in amastigotes lacking C14DM, in which *de novo* sterol synthesis was downregulated (W Xu et al. 2014). In contrast, higher expression (mRNA, protein and the product stigmasterol) of the sterol gene, CYP710C1 (LmxM.29.3550 in *L. mexicana*), was found in the intracellular stage (Chang, et al., 2019).

The entire picture of the organisation, topology and functionality of the SBP in *Leishmania* spp., still presents some caveats related with the annotation, and characterisation of some genes (<https://tritrypdb.org>). For instance, according to previous studies, the last enzymatic reaction before ergosterol is performed by sterol C-24 reductase (C24R) (ERG4 in fungi). However, an additional enzymatic step after ergosterol was described in a 3-beta hydroxysteroid dehydrogenase (LmxM.18.0080 in *L. mexicana*), which according to this study, converts ergosterol into ergosta-7,22-dien-3 β -ol (Yao and Wilson, 2016). More recently, a plant-like gene, LmxM.29.3550 that is annotated as a cytochrome P450-like protein (<https://tritrypdb.org>), and which converts episterol into ergosta-5,7,22,24(28)tetraenol in fungi and *Leishmania*, was reported to encode a CYP710C1, an enzyme that converts stigmasterol from β -sitosterol and is related with AmB resistance in *L. donovani*, suggesting the presence of a hybrid SBP (Bansal et al. 2019). Other genes of the SBP in which I identified similar disparities in their annotation, are discussed in detail in chapter 4 (see section 4.1.5). Although there is some evidence that the SBP can be a non-linear pathway, the order (in sequence) of the enzymes identified in kinetoplastids, including their orthologues in fungi and *Leishmania* spp., is outlined in Table 1-3.

Table 1-3. Sterol Biosynthetic Pathway (SBP) genes and enzymes in *Leishmania* spp. and orthologues in *Saccharomyces cerevisiae*. This list includes the mevalonate pathway, here I used the yeast *S. cerevisiae* SBP that is the pathway of reference for the development of the kinetoplastids counterpart. Names are according to the Enzyme Commission (E.C.) and the Kyoto Encyclopaedia of Genes and Genomes (KEGG) identifier numbers. **Sources:** sterol genes E.C. were obtained from the Enzyme Nomenclature Database (<https://web.archive.org/web/20060218084611/http://www.expasy.org/enzyme/>) based on the analysis of the SBP described in parasites by (Fügi et al., 2014). Yeast orthologue names are from the Yeast Genome Database (<https://www.yeastgenome.org/>) and from Chempidier (<http://www.chemspider.com/>). *Leishmania* gene LmxM.18.0080 was described by (Yao and Wilson, 2016), and verified in the TriTrypDB (<http://tritrypdb.org/tritrypdb/app/record/gene/LmxM.18.0080>). Due to mismatches in the nomenclature, missing or unknown enzymes, or annotation discrepancies, some gene/enzyme(s) were not identified or not determined (ND) in *Leishmania* during this search. Their absence from this list is not a confirmation that they are not present or do not exist. Enzyme identity that have been described in the literature more recently are identified with stars as follows: ** Number was obtained from (W. David Nes 2011); *** Yao and Wilson, 2016; **** (Bansal et al., 2019).

Yeast Gene ID	# of reaction	E.C. / KEGG numbers	<i>Leishmania</i> Gene ID	<i>Leishmania</i> spp. enzyme name	Yeast enzyme name	Type of reaction	Product
MEVALONATE PATHWAY (Pre-Squalene)							
Erg 10	1	2.3.1.9 / K00626	LmxM.23.0690	3-ketoacyl-CoA thiolase-like protein	Acetyl-CoA C-acetyltransferase (acetoacetyl-CoA thiolase)	Transfers an acetyl group from one acetyl-CoA molecule to another, first step of the Mevalonate biosynthesis	Acetyl-CoA Acetoacetyl-CoA (acetoacetyl-S-CoA)
			LmxM.30.1640	thiolase protein-like protein			
Erg 13	2	2.3.3.10 / K01641	LmxM.24.2110	3-hydroxy-3-methylglutaryl-CoA synthase, putative (HMGS)	3-Hydroxy-3-methylglutaryl-CoA synthase	Catalyses the formation of HMG-CoA from acetyl-CoA and acetoacetyl-CoA	HMG-CoA ((S)-3-hydroxy-3-methylglutaryl-CoA, hydroxymethylglutaryl-CoA, 3-hydroxy-3-methylglutaryl-coenzyme A, 3-Hydroxy-3-methylglutaryl-CoA)
HMG1 &	3	1.1.1.34 / K00021	LmxM.29.3190	HMG-CoA reductase (NADPH) (HMGR)	3-Hydroxy-3-methylglutaryl-CoA reductase , putative	Converts HMG-CoA to mevalonate, this is a rate-limiting step in sterol biosynthesis	Mevalonate
HMG2	4	1.1.1.88 / K00054	ND	HMG-CoA reductase (HMGR)	Similar than HMG1	Similar than HMG1	
Erg 12	5	2.7.1.36 / K00869	LmxM.30.0560	mevalonate kinase, putative (MVAK)	Mevalonate kinase	Forms isoprenoids and sterols. (catalyzes the phosphorylation of mevalonic acid to form mevalonate 5-phosphate. Enzymes in <i>L. major</i> and <i>T. brucei</i> present the three highly conserved motifs typical of the galactokinase, homoserine kinase, mevalonate kinase and phospho-mevalonate kinase (GHMP) superfamily	Mevalonate phosphate (mevalonate-5P, mevalonate-5-phosphate, (R)-5-Phosphomevalonate, (R)-Mevalonic acid 5-phosphate, (R)-5-Phosphomevaloonic acid, mevalonate-P, P-mevalonate, 5-phosphomevalonate)

Erg 8	6	2.7.4.2 / K00938	LmxM.15.1460	Phospho-MEV-kinase-like protein	Phospho-MEV-kinase	Essential to form isoprenoids and sterols.	Mevalonate pyrophosphate (mevalonate 5-PP, mevalonate-diphosphate, (R)-5-Diphosphomevalonate)
ERG19 (MVD1)	7	4.1.1.33 / K01597	ND	ND	Mevalonate pyrophosphate decarboxylase	ND	isopentenyl pyrophosphate (Δ3-isopentenyl-PP Synonyms: isopentenyl-pp, isopentenyl diphosphate, IPP, delta(3)-isopentenyl-PP, isopentenyl pyrophosphate)
IDI1	15	5.3.3.2 / K01823	ND	(IPP isomerase)	Isopentenyl diphosphate:dimethylallyl diphosphate isomerase	Activates the essential step for the synthesis of isoprenoids.	dimethylallyl phosphate (dimethylallyl-pyrophosphate, DPP, dimethylallyl-diphosphate, di-CH3-allyl-PPi, dimethylallyl-PP, dimethylallyl-PPi, DMPP)
Erg 20	17	2.5.1.1 / K00787	LmxM.33.4030	Geranylgeranyl transferase, putative	Geranyltranstransferase (geranyl-diphosphate synthase, Prenyltransferase)	Has both functions (geranyl and farnesyl). Forms C15 farnesyl pyrophosphate units for isoprenoid and sterols	geranyl phosphate (geranyl-diphosphate, geranyl-pyrophosphate, 2 geranyl-PP, GPP)
	20	2.5.1.10 / K00787 (Farnesyl diphosphate synthase)	LmxM.22.1360	farnesyl pyrophosphate synthase, putative	Farnesyl pyrophosphate synthetase (FPP synthetase, farnesyl-diphosphate synthase, dimethylallyl-transtransferase)		farnesyl pyrophosphate (farnesyl-PP, farnesyl diphosphate)
Erg 9	21	2.5.1.21 / K00801 ND	LmxM.30.2940	farnesyltransferase, putative	Squalene synthase (farnesyltransferase) Pre-squalene diphosphate + NADPH	joins two farnesyl pyrophosphate moieties to form squalene	Pre-squalene diphosphate squalene
SQUALENE PATHWAY (Post-Squalene) OR STEROLS BIOSYNTHETIC PATHWAY							
Erg 1	22	1.14.13.132 / K00511	LmxM.13.1620	squalene monooxygenase-like protein	Squalene epoxidase (squalene monooxygenase)	Epoxidation reaction	2,3-oxidosqualene (Squalene 2,3-epoxide, Squalene 2,3-oxide, (S)-Squalene-2,3-epoxide)
Erg 7	23	5.4.99.7 / K01852	LmxM.06.0650	lanosterol synthase, putative	Lanosterol synthase (Squalene-2,3-oxide-lanosterol cyclase, oxidosqualene--lanosterol cyclase, 2,3-epoxysqualene--lanosterol cyclase)	Cyclization of squalene 2,3-epoxide	lanosterol
Erg 11	24 (1)***	1.14.13.70 / K05917	LmxM.11.1100	Lanosterol 14-alpha demethylase (C14DM)	C14-lanosterol demethylase (cytochrome P450 family 51 (CYP51; lanosterol 14-demethylase)	Catalyses C-14 demethylation of lanosterol, removing the CH3 from C14.	4,4-dimethyl-8,14,24-trienol (4,4-dimethyl-cholesta-8,14,24-trienol)
Erg 24	25 (2)***	1.3.1.70 / K00222 (Delta14-sterol reductase)	LmxM.31.2320	C-14 sterol reductase, putative	C14-sterol reductase		4,4-dimethylzymosterol (4,4-dimethyl-8,24-cholestadienol, 4,4"-dimethyl cholesta-8,14,24-triene-3-beta-ol)

Erg 25	26 (3)	1.14.13.72 / K07750	LmxM.36.2540	C-4 sterol methyl oxidase, putative (SMO)	C4-sterol methyl oxidase (C-4 demethylase) (methyl sterol monooxygenase)	First of three steps required to remove two C-4 methyl groups from Ergosterol intermediates	4α-hydroxymethyl-4β-methyl-5α-cholesta-8,24- dien-3β-ol 4 α -formyl-4 β -methyl-5 α -cholesta-8,24-dien-3 β -ol or 4 α -carboxy-4 β -methyl-5 α -cholesta-8,24-dien- 3 β -ol
Erg 26	27 (4)***	1.1.1.170 / K07748	LmxM.06.0350	NAD(P)-dependent steroid dehydrogenase protein, putative	sterol C-3 dehydrogenase (C-3 sterol dehydrogenase, C4- Sterol decarboxylase)	Second of three steps required to remove two C-4 methyl groups from Ergosterol intermediates	4-methyl zymosterol (3-keto-4-methylzymosterol, 4 α -methyl-5 α - cholesta-8,24-dien-3-one)
		ND	LmxM.34.1230	short chain dehydrogenases, putative			
		ND	LmxM.34.2150	short chain dehydrogenases, putative			
Erg 27	28 (5)	1.1.1.270 / K09827 (3-Keto steroid reductase)			C3-Sterol ketoreductase (3-keto sterol reductase)	Last of three steps required to remove two C-4 methyl groups from Ergosterol intermediates	4-α-methylzymosterol (4- α -methylzymosterol, 4-methyl-8,24- cholestadienol, 4- α -methyl-5 α -cholesta-8,24-dien- 3 β -ol)
Erg 25	26	Same than above	Same than above	Same than above	Same than above	Same than above	4α-hydroxymethyl-5α-cholesta-8,24-dien-3β-ol 4 α -formyl-5 α -cholesta-8,24-dien-3 β -ol 4 α -carboxy-5 α -cholesta-8,24-dien-3 β -ol
Erg 26	27	Same than above	Same than above	Same than above	Same than above	Same than above	5 α -cholesta-8,24-dien-3-one
Erg 27	28	Same than above	Same than above	Same than above	Same than above	Same than above	zymosterol (5- α -cholesta-8,24-dien-3- β -ol)
Erg 28	29 (6)	5.3.3.5 / K01824 (Cholestenol delta- isomerase)	Possibly LmxM.08_29.19 70	hypothetical protein, unknown function	Scaffold	In budding yeast facilitates protein- protein interactions (Erg26-Erg27) and tether the enzymes to the ER. Another interesting and relevant interaction is Erg28-Erg6.	None (Scaffold)
Erg 6	37 (7)***	2.1.1.41 / K00559	LmxM.36.2380 LmxM.36.2390	sterol 24-c- methyltransferase, putative (C24SMT1) sterol 24-c- methyltransferase, putative (C24SMT2)	C-24 Sterol methyl-transferase (SAM:C-24 sterol methyltransferase)	Methylation of position C-24 in the side chain is localized to lipid particles, plasma and mitochondrial membranes and ER.	fecosterol (Ergosta-8,24(28)-dien-3-ol) (5 α -ergosta-8,24(28)-dien-3 β -ol) (24-methylene-5- α -cholest-8-en-3- β -ol)
Erg 2	38 (8)***	5.-.-.- / K09829	LmxM.08_29.21 40	C-8 sterol isomerase-like protein (C8SI)	C8-Sterol isomerase	Isomerization of delta-8 double bond to delta-7 position.	episterol (lathosterol in human) ergosta-5,7,24(28)-trien-3-ol, (3 β - ((3 β ,5 α)-ergosta-7,24(28)-dien-3-ol)
Erg 3	31 (9)***	1.14.21.6 / K00227 (Lathosterol oxidase)	LmxM.23.1300	Lathosterol oxidase-like protein or 18 Erg 3 /14.1 Erg25 (LOX) (syn. C5DS)		Oxidizes Lathosterol in humans 5-DES is converted to 24- methylencholesterol by DHCR7. Is the C5DS, possibly, in <i>Leishmania</i> and catalyses the dehydrogenation of a C-5(6) bond.	Formed from episterol to 5-dehydroepisterol

Erg 3	ND (9)***	1.14.21.6 (5-SD) **	LmxM.30.0590	C-5 sterol desaturase, putative (C5DS)	C5-Sterol desaturase (Delta7-sterol Delta5- dehydrogenase, Delta7-sterol 5- desaturase, Delta7-sterol-C5(6)- desaturase, and 5-DES)	Introduces a C-5(6) double bond into Episterol.	ergosta-5,7,24(28) trienol 5-dehydroepisterol (5,7,24(28)-ergostatrienol)
Erg 5	ND (10)***	ND	LmxM.29.3550 and/or LmxM.33.3330	cytochrome p450-like protein (TriTrypDB), C22-sterol desaturase (C22DS) ****	cytochrome P450 subfamily, C22-sterol desaturase, CYP710C1 ****	A cytochrome P450 enzyme, forms of the C-22(23) double bond in the sterol side chain.	ergosta-5,7,22,24(28)tetraenol (5,7,22,24(28)-ergostatetraenol) and possibly, stigmasterol ****
Erg 4	39 (11)***	Possibly 1.3.1.71 / K00223 (Delta24[24 (1)]-sterol reductase)	LmxM.32.0680	sterol C-24 reductase, putative (C24R)	C24-sterol reductase	Catalyses the "last" step in ergosterol biosynthesis. Mutants lack ergosterol but are viable.	ergosterol
ND	ND (12)***		LmxM.18.0080	3-beta hydroxysteroid dehydrogenase/isomerase family, putative		ND	ergosta-7,22-dien-3β-ol

1.7.2 The Pentose phosphate pathway

The pentose phosphate pathway (PPP) provides the parasite with precursors of nucleotides (e.g. ribose 5-phosphate). In other organisms erythrose 4-phosphate from the PPP can be a precursor to aromatic amino acids, although *Leishmania* seem to require pre-formed aromatic amino acids rather than to synthesise them. Moreover, PPP is the main source of the reduced cofactor NADPH (other sources are pyruvate and malate). The pathway is composed by two branches. First, the oxidative branch generates NADPH and ribulose 5-phosphate from glucose 6-phosphate (an intermediate of glycolysis). These NADPH generating reactions are catalysed by glucose-6-phosphate dehydrogenase (G6PDH), the first enzyme of this pathway, and 6-phosphogluconate dehydrogenase (6PGDH). The former of these enzymes was inhibited with steroids, causing arrest of cell growth and death in trypanosomes, but not in *Leishmania* (Kovářová and Barrett 2016; Opperdoes and Michels 2010).

Second, the non-oxidative branch converts the product of the oxidative branch (i.e. ribulose 5-phosphate), into either ribose 5-phosphate or xylulose 5-phosphate, which are substrates of transketolase. These two reactions are catalysed by ribose-5-phosphate isomerase (RPI) and ribulose 5-phosphate epimerase (RuPE), respectively (Opperdoes and Michels 2010). During the non-oxidative branch various sugar phosphate intermediates are interconverted by transketolase (TKT) and transaldolase (TAL), thus providing an important metabolic flexibility for the parasite. As mentioned above, two of these substrates result from the oxidative branch (i.e. ribulose-5-phosphate), whereas other intermediates, i.e. sedoheptulose 7P, fructose 6P and glyceraldehyde 3P, are related with the non-oxidative branch (the latter two from glycolysis) (Kovářová and Barrett 2016). The names of all the enzymes of the PPP are shown in Figure 1-15.

The PPP is important for cellular functions other than the biosynthesis of molecules; for example, this pathway is a key mechanism of protection against ROS through generation of NADPH (Opperdoes and Michels 2010). The shift in the flux of metabolites from glycolysis towards the PPP (Ghosh et al. 2015), and the activity of some enzymes of the PPP is increased when *Leishmania* spp., and other trypanosomatids (e.g. *T. cruzi*) are exposed to oxidative stress (Kovářová and Barrett 2016). Similar upregulation of the PPP has been observed in AmB resistant promastigotes of *L. mexicana* (PhD Theses Dr Andrew Pountain, and Dr R Binti, University of Glasgow).

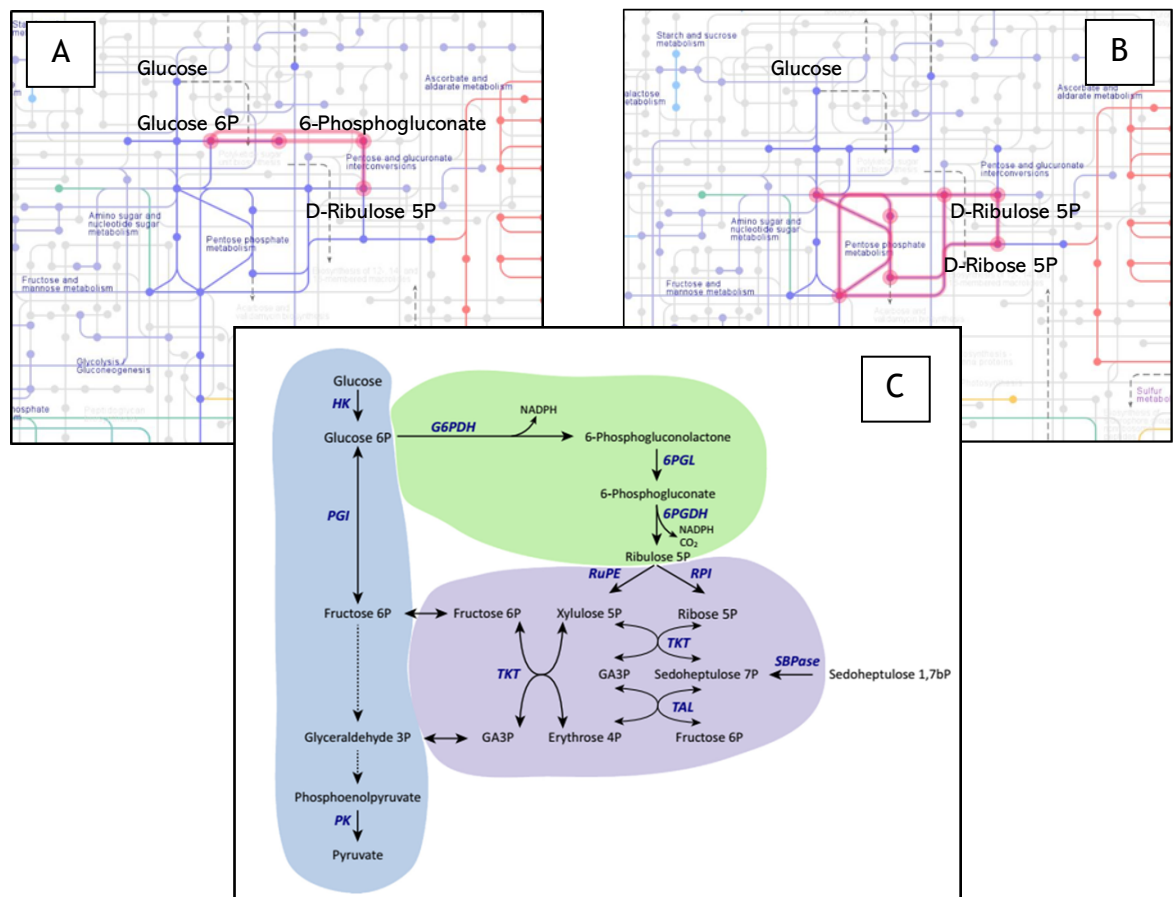


Figure 1-15. The Pentose Phosphate Pathway in *Leishmania*.

Panel A (oxidative branch) and panel B (non-oxidative branch) show the PPP (highlighted in carnation lines) as they look in the general metabolism. Panel C shows a detailed breakdown of the enzymes of both branches. The enzymes of the oxidative branch (green): glucose 6-phosphate dehydrogenase (G6PDH), 6-phosphogluconolactonase (6PGL), 6-phosphogluconate dehydrogenase (6PGDH) produce NADPH and ribulose 5P. The latter enters to the non-oxidative branch (purple) and is catalysed by either ribose 5-phosphate isomerase (RPI) or ribulose 5-phosphate epimerase (RuPE). Glycolysis (blue) is tightly connected to both branches of the PPP. First, glucose 6P enters the oxidative branch. On the other hand, fructose 6P and glyceraldehyde 3P are linked to the non-oxidative branch and are interconverted into other sugars by transketolase (TKT) and transaldolase (TAL). Another enzyme, sedoheptulose-1,7-bisphosphatase (SBPase) provides an additional intermediate. Only three enzymes of the glycolysis are shown here: hexokinase (HK), phosphoglucose isomerase (PGI) and pyruvate kinase (PK). Sources: Panels A and B were constructed from KEGG Pathways in *Leishmania* (https://www.genome.jp/kegg-bin/show_pathway?map01100), panel C is from Kovářová & Barrett 2016.

1.7.3 Polyamine-trypanothione pathway

The polyamine-trypanothione pathway (PTP) contains several enzymes that are essential for the growth, survival and infectivity of the parasite. One of the key functions of the PTP is in the production of particular thiols, which act as reductants to protect *Leishmania* against reactive oxygen species (ROS) and nitric oxide (NO) (Colotti and Ilari 2011; Mandal et al. 2017; Manta et al. 2013; Dos Santos Ferreira et al. 2003; Singh et al. 2012). Polyamines (putrescine, spermidine and spermine) can be synthesized and interconverted

within human cells (Birkholtz et al. 2011). On the other hand, trypanothione (TSH), the major redox active thiol in *Leishmania*, is found only in trypanosomatids (Vijayakumar and Das 2018), and is different from its mammalian counterpart, the disulphide glutathione (GSH). (Colotti and Ilari 2011; Fairlamb and Cerami 1992). For this reason, some proteins involved in the metabolism of TSH are attractive drug targets (Birkholtz et al. 2011; Rajasekaran and Chen 2015).

The PTP is a complex pathway and can be divided in various steps outlined in Figure 1-16. The first two steps (1, 2) are the biosynthesis of the thiol, cysteine (Cys), followed by the synthesis of GSH (3). Cysteine can be obtained either from *de novo* synthesis from serine, or from reverse trans-sulfuration of methionine. GSH- and the spermidine are produced *via* two separate pathways. The synthesis of one molecule of GSH requires ATP for the ligation of glutamine and glycine to cysteine. Another separate step (4) is the uptake and biosynthesis of polyamines, which requires the conversion of arginine to ornithine and then on to putrescine by the enzymes arginase (ARG) and ornithine decarboxylase (ODC), which occur within the glycosomes and the cytosol, respectively (Marchese et al. 2018). The next-product of the polyamine synthesis, spermidine, is created by spermidine synthase (SpS) from putrescine and decarboxylated AdoMet, the product of AdoMet from S-adenosylmethionine decarboxylase (AdoMetDC). In the following step (5), spermidine is ligated with two molecules of GSH. This ligation requires ATP and is performed by glutathionyl spermidine synthetase and trypanothione synthetase (TRYs), resulting in one molecule of TSH in its reduced form T(SH)₂ (Manta et al. 2013). T(SH)₂ is regenerated from oxidised TS₂ by the NADPH dependent trypanothione reductase (TRYr). The last step (7) is the use of T(SH)₂ for the reduction of tryparedoxin (TRYx), a unique type of protein only found in kinetoplastids (Colotti and Ilari 2011), which serves as electron source for the complex of peroxidases form by tryparedoxin peroxidase (TRYP1 or type I), and tryparedoxin dependent peroxidases (TDPX or type II) (Colotti and Ilari 2011; Mandal et al. 2017; Manta et al. 2013). TRYP1/TDPX replaces the catalase and other peroxidases (Colotti and Ilari 2011) that are abundant in mammals and other organisms, e.g. *M. tuberculosis* (Spies and Steenkamp 1994), and are also present in some fungi (Mayers, Ouellette, J.D., Sobel, and Marchaim, K.S., Kaye 2017), but absent in *Leishmania* spp. (Colotti and Ilari 2011; Spies and Steenkamp 1994). Some studies with amastigotes have detected catalases in trace amounts, however, these are believed to be contaminants from the host cell (Fairlamb and Cerami 1992). The metabolism of ascorbate is another defence against ROS in some trypanosomatids, particularly in *T. cruzi*, although the biosynthesis of ascorbate is less clear in some *Leishmania* spp. (*L. major* and *L. braziliensis*) and in *T.*

brucei, due to the loss of some genes, ascorbate-dependent peroxidases are present in *T. cruzi* and *L. major* (Oppendoes and Coombs 2007).

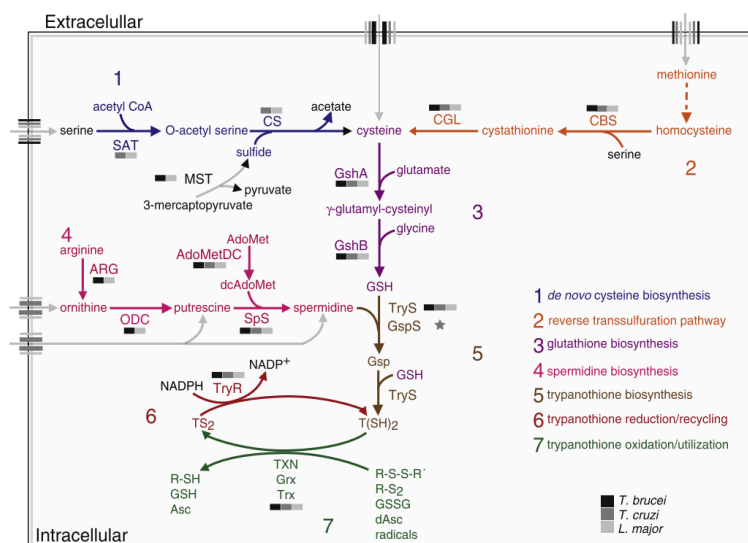


Figure 1-16. The polyamine-trypanothione pathway in trypanosomatids. 1. *de novo* cysteine biosynthesis; 2. reverse transsulfuration pathway; 3. glutathione biosynthesis; 4. spermidine biosynthesis; 5. trypanothione biosynthesis; 6 and 7. trypanothione reduction/recycling, and oxidation/utilization. Tryparedoxin (TXN in this scheme) is referred in the text as TRYX. Some abbreviations shown in this diagram are not mentioned in the text. Modified from: Manta et al., 2013.

Ovothiol A, also known as (N⁷-methyl-4-mercaptohistidine), is an unusual thiol (Tetaud and Fairlamb 1998) that is also involved in detoxifying hydro-peroxide (H₂O₂) and other oxidants in trypanosomatids, e.g. *L. donovani* (Spies and Steenkamp 1994), and *T. cruzi* (Trochine, et al., 2014). Metabolomics studies have found an increase (2.79-fold) in ovothiol A, in AmB-Sb^{III} resistant *L. donovani* promastigotes (Berg et al. 2015). A similar augmentation (3-fold) of ovothiol A disulfide was observed in a mutant of *L. mexicana* (Δ LmGT) deficient in glucose transport and more susceptible to oxidative stress (Akpunarlieva et al. 2017). In another study, the reduction (7%) of ovothiol A disulfide was correlated with the production of ROS after 1.2 hours of treatment with MF (EC₉₀) in *L. infantum* (Vincent et al. 2014), confirming the role of this thiol in maintaining the redox equilibrium within the cell. Other antileishmanials in which the PTP and thiols have been shown to be involved (Kaur and Rajput 2014) are, AmB (thiols were alerted during AmB selection for resistance)(Brotherton et al., 2014; Mbongo, et al., 1998), pentamidine (Basselin et al. 1997; Díaz et al. 2014; Kaur and Rajput 2014; Ouellette et al. 2004), and antimonials (Singh et al., 2012; Wyllie et al., 2004).

1.8 Omics technologies, gene editing and drug discovery

Omics technologies have accelerated our understanding of the MoA of antileishmanials within a biological context (Kaur and Rajput 2014). While the number of omics tools comprises over 30 fields, the most studied are genomics, transcriptomics, proteomics and metabolomics. These technologies, however, present various challenges such as the reduction of dimensionality of large-scale datasets, data integration and interpretation, reproducibility and statistical analysis, among others (Misra, et al., 2018).

The use of metabolomics integrated with other approaches, i.e. genomics, proteomics and transcriptomics, enables for the identification of the molecular mechanisms related with specific phenotypes in *Leishmania* mutants (Akpunarlieva et al. 2017), and drug resistant parasites (Mwenechanya et al., 2017; Pountain et al., 2019), in a manner that is not possible to achieve using these tools separately et al., 2018; Barrett & Croft, 2012; Creek & Barrett, 2014; Kaur & Rajput, 2014). Recently, genomics coupled with metabolomics was applied in a field isolate that caused an outbreak of VL in the Indian subcontinent, identifying changes in various genes (i.e. SNPs, CNVs, indels), and metabolic pathways involved in the production of virulence factors, and that are essential for the interaction of *Leishmania* with the host (Cuypers et al. 2018).

1.8.1 Whole genome sequencing and transcriptomics in *Leishmania*

New sequencing tools allow for the identification of genomic- and other structural changes such as, single nucleotide polymorphisms (SNPs), copy number variants (CNVs), loss of heterozygosity variants, genomic rearrangements, and rare variants associated with drug resistance in *Leishmania* spp. (Misra et al. 2018). Sanger sequencing, whole genome (shotgun) sequencing (WGS), and next generation sequencing (NGS) tools, allow the high-throughput sequencing and analysis of large-genomic datasets. These approaches are nowadays applied in either field isolated or laboratory generated resistant mutants, the latter can be generated *in vitro* by serial passage of *Leishmania* spp., with increasing concentrations of different anti-leishmanials in a step-wise manner (Leprohon, et al., 2015). Generating resistant mutants of *Leishmania* can take months (as with AmB), and therefore the use of accurate NGS methods in these valuable samples is needed.

NGS technologies are around 10 million times more powerful (4×10^9 versus <400 sequence reads) than Sanger sequencing for the analysis of WGS. Another advantage of the higher base call accuracy, i.e. 99.99% and 99.4% for Illumina and Sanger, respectively.

The base call accuracy is the probability of calling the correct base and is measured using the so called, Phred quality score (Q). Phred scores values are Q10 (90%), Q20 (99%), Q30 (99.9%), Q40 (99.99%) and Q50 (99.999%), which determine the probability of an incorrect base call of 1/100 and 1/1000 for a Q20 and Q30 (as in Illumina), respectively. A Q30 is considered benchmark for NGS, a high Q score reduces the number of false positive variant calls (https://www.illumina.com/documents/products/technotes/technote_Q-Scores.pdf). Sanger sequencing is the gold standard in clinical research and for NGS confirmation, however, it can read only short sequences (<1000 bp), and in some studies has been unable to provide insight about the gene copy number (Kaur and Rajput 2014), and it can be time consuming and more costly for the analysis of millions of fragments that can be sequenced in parallel using NGS.

Library preparation is a key step of the NGS process and requires high quality DNA. Preparing DNA for sequencing requires breaking the DNA (using ultrasound, sonication or other methods) into fragments between 150 and 1000 bp (average of 350-500 bp). Based on their size, a minimum number of copies of each fragment is expected. Then adaptors (oligonucleotides that function as primers or linkers) are added to the DNA fragments binding to their 5'- and 3' ends where they serve as reference (barcodes or tags) of the position where the sequencing process should start. Adaptors have multiple components (sequences) that have different functions such as, binding to the oligonucleotides in the flow cell (as with Illumina), PCR amplification, sequencing, sample indexing, barcoding of specific libraries, and inserts that are target DNA or RNA in specific libraries, and are also essential for multiplexing sequencing (<https://www.idtdna.com>). The following steps then resemble a PCR reaction (hybridization, extension, denaturation, annealing), several cycles produce the extension of complementary strands, resulting in the formation of bridges and millions of clusters. In the final step, the process is finished by a denaturation step, resulting in single strands which serve as templates. The binding of the sequencing primers to the adaptor in the strand initiates the synthesis in which nucleotides with different fluorophore are added and identified with an instrument. One advantage of Illumina is that allows paired-end sequencing, which produces a higher volume of sequencing information, which are moreover, useful for accurate mapping of the reads during the analysis.

The use of NGS in *Leishmania* spp. is challenging given the organisation of their genome, and the complexity of some of the changes of their genome, such as, chromosome- and copy number variations and genes arrayed in tandem (Rogers et al., 2011). Identification of some of these genomic alterations is particularly challenging with Illumina, due to the size of the reads produced by this platform. The first kinetoplastid genomes were published

over a decade ago (El-Sayed et al. 2005; Ivens et al. 2005a). These studies have contributed to understand the architecture and identified different elements that are unique in these parasites, such as, pseudogene formation and species-specific genes (Peacock et al. 2007), the presence of retrotransposons and a putative RNAi machinery (in *L. braziliensis*) (Peacock, & Cruz, 2007), and Short Interspersed Degenerated Retroposons (SIDER) (Pountain et al., 2019; Smith et al., 2009). The presence of several genes that code for demethylases and methyltransferases has been also noted in *Leishmania* (Ivens et al. 2005a). Interestingly, both types of enzymes are part of the SBP and are involved in polyene resistance (Mwenechanya et al., 2017; Pountain et al., 2019). A detailed explanation of the role of these two genes in the SBP of fungi and *Leishmania* is discussed further (see section 1.6.6.3, and chapter 3). Gene expression is also unique in *Leishmania*: many genes, often functionally unrelated, are arranged in polycistronic transcription units (El-Sayed et al. 2005; Peacock et al. 2007). These polycistrons, however, are different than in bacteria where gene regulation usually occurs at the transcription level, and a transcription promoter controls clusters of functionally related genes (Ginger, 2005). A compilation of all the previous and current releases of the kinetoplastid genomes, is available in TriTrypDB (<https://tritrypdb.org/tritrypdb/>). Although some caveats can be found in the annotation of some genes, the genome versions, and the platform are constantly updated and refined.

NGS analysis uses these reference genomes to align short reads (as with Illumina) in combination with various tools such as MAQ and BWA (Burrows-Wheeler Alignment). The latter is particularly efficient to align short read to a reference genome (Li and Durbin 2009). Another advantage of BWA is that it produces an output file with a SAM (Sequence Alignment/Map) format, which is the standard for the use of other applications, e.g. variant calling with SAMtools, are commonly used in the following steps of the analysis (Li and Durbin 2009). Interpretation of the increasing amount of NGS data makes necessary the use of bioinformatics tools that are often complex. Different platforms, such as the Genome Analysis Toolkit (GATK) (McKenna et al. 2010) and the Galaxy Project, a web browser-based platform (Blankenberg et al. 2010), have improved the development and use of different tools for the analysis of NGS data, and enabled access to data integration and data analysis using bioinformatics tools without the need of programming skills, command line tools or scripting (as with Linux). The workflow with all the steps used in this study for both, genomics and transcriptomics (RNAseq) analysis, is described in detail in the materials and methods section (see chapter 2).

1.8.2 Gene editing of *Leishmania* spp. as a tool for drug discovery

NGS allows the identification of changes in one, or a set of genes that are responsible for a particular phenotype (forward genetics). Generating mutants using gene editing tools (reverse genetics) enables scientists to reverse this process by first disrupting a gene candidate, or several genes of the same pathway (as with the SBP), followed by the characterisation of their phenotype. Over the past decade, the genetic tools available for genetic manipulation in *Leishmania* has increased dramatically (Jones, et al., 2018; Santos et al., 2017). Some of these tools, such as RNA interference (RNAi) target sequencing (RIT-Seq), allowed for genome-scale loss-of-function (in *T. brucei*) screening and have contributed to our understanding on the MoA of drugs, including the antileishmanials AmB and MF (Collett et al. 2019). RNAi machinery does not exist in *Leishmania*, other than in *L. (Viannia) braziliensis* (Lye, et al., 2010) which has hindered progress, but CRISPR Cas9 as technology (Beneke et al., 2017) offers a means to improve research. Other methods like homologous recombination (HR) can incorporate targeted mutations into primers that are then PCR-amplified, however, long homology arms (~300 bp) are needed for accurate and efficient integration in *Leishmania* (Dean et al. 2015).

Recently, clustered regularly interspaced short palindromic repeats (CRISPR) combined with Cas9 (an RNA-guided DNA endonuclease) genome editing methods (CRISPR-Cas9), have been developed for use in kinetoplastids (Beneke et al., 2017; Dean et al., 2015; Ishemgulova et al., 2018; Sollelis et al., 2015; Zhang & Matlashewski, 2015), including some inducible systems (in *T. brucei*) (Rico, et al., 2018). These systems have additional applications such as N- and C-terminal fluorescent and bioluminescent tagging of proteins, that can be further analysed for localisation, and for the assessment of the infection in other models where parasites can be visualised within the animal or insect tissues (Costa et al. 2018). The first CRISPR system in *Leishmania*, simplified the generation of null mutant knockouts of genes arrayed in tandem in a single round of transfection and without producing off-targets (Sollelis et al. 2015). More recently, high-throughput methods have facilitated the generation of mutants in a scalable manner. The most notable of these systems, for instance, generates mutants in a single round of transfections, and without needing additional cloning or selection of individual clones (Beneke et al. 2017). Other systems like DiCRE (dimerizable Cre recombinase), allow for the study of gene expression of specific genes in a dose/time dependent manner (Santos et al. 2017). Importantly, due to possible caveats with these CRISPR-Cas9 editing systems in *Leishmania*, WGS of independent clones is still necessary to confirm their efficiency and accuracy. In my study,

I have used the system developed by Beneke et al., in *L. mexicana*, to generate a knockout of the C24SMT. Details of all the steps, and the characterisation (drug screening and sterol profiling with GC-MS) of this KO, are described further (see chapter 2, and chapter 6).

1.8.3 Untargeted and targeted metabolomics

Targeted and untargeted metabolomics allow for the detection and quantification of hundreds of molecules, e.g. lipids, carbohydrates, amino acids, organic acids, and others with low molecular weight (<1500 Da) (Atan et al. 2018). The study of the whole metabolome can be performed in a broad range of biological samples, in response to different environmental or external conditions (Subramanian et al. 2015). The identification and characterisation of biochemical and enzymatic pathways can be improved using a stable isotope that can be traced, thus confirming or describing unknown features of some pathways (Creek, et al., 2012). Metabolomics can also detect perturbations induced by drugs used for the treatment of diseases caused by kinetoplastids, and which MoA is still unknown (Atan et al., 2018; Creek & Barrett, 2014; Vincent & Barrett, 2015; Vincent et al., 2012). Some examples of compounds analysed in these studies are, AmB (Mwenechanya et al. 2017), eflornithine (Vincent et al., 2010), and MF (Vincent et al., 2014).

Other relevant uses of metabolomics include the identification of essential metabolites present in different formulations of culture media. Recently, a study devised six essential amino acids that support axenic growth of *L. mexicana* without the supplementation of serum. This medium, named, Nayak medium (NM), reduced both, cost, and the interference of other exogenous contaminants and unknown components from the serum (Nayak, et al., 2018).

No universal method can detect all the metabolites present in a biological sample, therefore, combining different approaches increases the coverage. Mass spectrometry (MS) offers higher susceptibility than nuclear magnetic resonance (NMR), particularly for the analysis of the global metabolome (Creek, et al., 2012). MS measures the mass-to-charge ratio (m/z) of ions, which is calculated based on, the ionisation- and abundance of individual mass, of the metabolites present in the sample (Creek, et al., 2012). Metabolite detection with MS is improved by combining MS with other chromatographic methods such as gas chromatography (GC-MS), liquid chromatography (LC-MS), and capillary electrophoresis (CE), which are often used for the study of the effects of drugs on the metabolome of trypanosomatids (Armitage et al., 2018; Kloehn et al., 2016). These

methods can be used for both targeted and untargeted approaches and their main differences are related to sample preparation, and the number- and quantification of metabolites that can be detected.

Some of the limitations of metabolomics are, the complexity and slow preparation of samples, the presence of similar isomers of the same metabolite, the inability of measuring every metabolite, including large molecules like proteins, creating gaps in various metabolic pathways, and the high costs of apparatuses, which can be found only in large institutions (Atan et al., 2018; Creek, et al., 2012; Kaur & Rajput, 2014). Data analysis is also slow and very complex, it requires complex bioinformatics tools (Kaur and Rajput, 2014), and the synergy between bioinformaticians and biologists for the adequate interpretation of the data into a biological context. In this study, I focus on the use of untargeted (LC-MS), and targeted (GC-MS) metabolomics for the detection of perturbations in the global metabolome (see chapter 7), and the content of lipids (sterols) (see chapter 5), in AmB resistant *L. mexicana* promastigotes.

1.8.3.1 Liquid Chromatography-Mass Spectrometry (LC-MS)

LC-MS exploits the charge and the lipophilicity of metabolites for separation (Creek, Anderson, et al. 2012). LC-MS has the advantage of high coverage of mass range without derivatization and can also measure both lipid and aqueous samples (Atan et al. 2018). Hydrophilic interaction chromatography (HILIC) columns are frequently used with LC-MS to overcome the loss of polar or charged metabolites with reverse columns. Another feature of LC-MS is the use of electrospray ionisation (ESI) in either positive or negative modes. Metabolites are identified based on their ability to gain or lose (positive and negative, respectively) protons, therefore the analysis of both modes increases coverage.

LC-MS presents some challenges such as the lack of a standard library of metabolites and higher variability (Atan et al. 2018), the adequate comparison of methods between laboratories that differ in several conditions, e.g. solvents, sample preparation, extraction- and analytical methods (Creek, et al., 2012). Another consideration is the different resolution between mass spectrometers. Orbitrap devices for instance, have increased their detection considerably, ultra-high-resolution mass accuracy (<1 ppm with resolution higher than 100,000) can now be achieved with this devices. One of the most notable disadvantages of LC-MS is that HILIC-based analysis poorly detect lipids due to their hydrophobicity, giving several isomers with similar mass which are difficult to discriminate given the limited number of standards. Reverse phase chromatography with MS can improve resolution of hydrophobic compounds. A more powerful approach in this

case is the use of GC-MS (for sterols), or for other lipids including fatty acids and other saponifiable lipids (sphingolipids and glycerophospholipids), is necessary to perform either biphasic extraction (lipid extracts are analysed from the organic phase) with further analysis using electrospray-mass spectrometry (ES-MS) for phospholipids, or using GC-MS for further fatty acid derivation (T. K. Smith's Lab, personal communication). Another method can also resolve for both, metabolomics and lipidomics samples using a single extraction and combining HILIC- and reverse phase (RP) chromatography for separate analysis of polar- and non-polar lipids, respectively (Fauland et al. 2011; Rampler et al. 2018). Similar protocols have been adapted to optimise the analysis of the global metabolome of parasites, using the same instrument (e.g. Q-extractive or Fusion) (<http://polyomics.mvls.gla.ac.uk/>).

Previous studies using metabolomics in kinetoplastids have developed and improved the methodology for sample preparation and analysis of the metabolome specific for *Leishmania* spp. These methods have determined, for instance, the minimum biomass needed for each method, i.e. 10^8 for LC-MS, and improved the freezing and quenching methods avoiding the lysis of the membrane caused by other protocols (Vincent & Barrett, 2015; Vincent et al., 2012). Details on sample preparation, solvents and extraction methods used in this study, are described further (see chapter 2).

1.8.3.2 Gas Chromatography-Mass Spectrometry (GC-MS)

GC-MS can detect a broad range (hundreds) of metabolites (e.g. amino acids, sugars, lipids), with good reproducibility and precision (Creek, et al., 2012; Kaur & Rajput, 2014; Vincent & Barrett, 2015). In this study, however, I used GC-MS for the detection of sterol lipids in whole cell extracts. A detailed explanation of the methodology used here for GC-MS, and the advantages of this approach over other methods that can also detect sterols, is discussed further (see Chapter 2, section 2.8, and Chapter 5, section 5.2, respectively).

1.9 Aims of the study

The aim of this Thesis is to apply a polyomic approach to characterise laboratory generated polyene (AmB and NyS) resistance lines of *Leishmania* spp. to identify new drug targets and to understand the mode of action of polyenes, as well as the implications of resistance against AmB in *Leishmania* spp. Previous work has characterised multiple lines against AmB in both, amastigotes and promastigotes (Al-Mohammed, et al., 2005; Pountain et al., 2019), and others have identified several genomic changes associated with resistance to AmB in *L. mexicana* (Mwenechanya et al., 2017; Pountain et al., 2019; PhD Thesis

Raihana Binti, University of Glasgow, unpublished). A common feature observed in all these studies, is the loss of the wild type ergosterol, which leads to AmB resistance.

Here, I intended to use genomics coupled with untargeted and targeted metabolomics, to identify molecular changes that arise as an effect of drug pressure and to differentiate these changes from other stochastic alterations. Additionally, identifying mutations that are conserved across AmB resistant lines and to correlate these genomic changes with their sterol profiling and with their phenotype *in vivo* can help to identify potential new drug targets. Assessing the retention of resistance and the fitness cost of these mutants within the host and the insect vector, are both an essential objective of this project. Moreover, I will analyse the grounds of cross-resistance of these polyene-resistant lines against a series of compounds, including the antileishmanials, and also against a new library of sterol inhibitors. Therefore, the aims of this study were:

- To select eight independent polyene-resistant *L. mexicana* lines and to characterise their phenotype, e.g. drug sensitivity, sterols profile, metabolome, growth, cross resistance.
- Use NGS to identify mutations related with polyene-resistance, in particular in the sterol biosynthetic pathway
- Characterise the infectivity and response to treatment of four AmBR-lines *in vivo*.
- To determine the susceptibility of these polyene-resistant lines to a new series of sterol inhibitors.

2 Materials and methods

2.1 Culture of *Leishmania* spp. cells in vitro

L. mexicana wild type promastigotes (reference strain WHO MNYC/BZ/62/M379 or simply M379) were cultured at 25°C in complete haemoflagellate-modified minimal essential medium named HOMEM (from GE Healthcare or Gibco®), described elsewhere (Berens et al. 1976), supplemented with 10% (vol/vol) heat-inactivated foetal bovine serum (HI-FBS) (Labtech International) and 1% (vol/vol) of penicillin-streptomycin (10,000 IU and 10 mg/ml in 0.9% NaCl, respectively) (Sigma®). HOMEM is a culture medium adapted from the Eagle's minimal essential medium (MEM), and the defined medium (DM) used in this study is a modified version from previous studies (Merlen et al. 1999; Nayak et al. 2018), adapted by a former member of the Barrett Lab (PhD Thesis Raihana Binti, University of Glasgow, unpublished data) (see Supplementary file 1, composition of media; see page 8). *L. tarentolae* (strain Parrot-TarII), and *L. infantum* JPCM5 (MCAN/ES/98/LIM-877) were grown only in HOMEM.

Promastigotes were maintained in culture by passaging cells weekly with a starting density between 1 to 5 x 10⁵ cells per ml in HOMEM medium. Growth rate and assessment of morphology (including body size) of all the parental- and resistant lines, were determined by counting (in duplicates then the average count was reported) parasites density every 24 hours during seven- or ten days, and compared with previous reports (Bates & Tetley, 1993; Vermeersch et al., 2009). Cell density was determined in triplicate in parental wild type and polyene resistant lines (see chapter 3, Figure 3-4), and also CRISPR/Cas9 wild type (constitutive expression of Cas9) and knockout lines generated with this system (see chapter 6). Cultures were evaluated weekly using an inverted microscope to observe cell growth and motility of the promastigotes and morphological changes, i.e. mid- to late-logarithmic, and stationary phases, respectively. A Neubauer chamber (haemocytometer) was used to assess cell density (for downstream experiments), and to determine growth rate of all clones (four AmB- and four from Nys-resistant from *L. mexicana*, and one AmB-resistant from *L. infantum*), selected from each independent line (chapter 3, section 3.2.2, Figure 3-4). A list of the clones selected for each line and their EC₅₀ (for AmB or nystatin) is shown in chapter 3 (see section 3.2.1, Table 3-1).

Amastigotes derived from footpad lesions and lymph nodes tissue (macerates) of infected BALB/c mice (see section 2.6 and chapter 5, section 5.2.3), were transferred into HOMEM medium, whereupon they differentiated into promastigotes over 48-72 hours, and were

sub-cultured as described before for promastigotes. For those lines in which amastigogenesis was assessed, transformation was performed using *Leishmania* spp. late-log stage (i.e. stationary phase) promastigotes, following the method described elsewhere (Bates, et al., 1992). Amastigotes, either from mice lesions or from axenic promastigotes, were maintained in culture using Schneider's medium (SDM) with HI-FCS (10% v/v) and 1.5 mL of hemin (2.5 mg per mL in 50 mM NaOH, 0.003% v/v), with a pH 5.5, and incubated at 32.5 °C with 5% CO₂ in vented cap 25 mL flasks, and sub-cultured weekly.

2.2 Selection of polyene resistant *Leishmania* spp.

Leishmania mexicana, *L. infantum* and *L. tarentolae* axenic promastigotes were selected for resistance by exposure to increasing concentrations of polyenes, starting with a sub-lethal concentration based on the EC₅₀ of their respective parental wild type (between 20 to 80 nM). The concentration of either AmB or nystatin, were increased in a stepwise manner following the method described elsewhere with some modifications (Al-Mohammed, et al. 2005). All independent cell lines were cultured in parallel with their respective parental line that was cultured in absence of drug, to confirm that resistance and other changes were not the result of long-term cultivation or other stochastic changes. A detailed explanation of the duration and concentrations added into the medium during the resistance selection is detailed in Chapter 3 (section 3.2.1, Figures 3-1 and 3-3). Aliquots of both, AmB and nystatin, were stored in 0.5 mL Eppendorf's at -20°C and protected from light until use. Assessment of the increase in resistance was performed with the Alamar Blue assay (section 2.4.) at least every month or when the growth rate of cells exposed to drugs was similar to that of the parental wild type cultured without drug pressure. The maximum concentration of drug added into the culture and the EC₅₀ values of all lines are described in detail in chapter 3 (section 3.2.3). All cell lines were preserved in culture medium with 15% DMSO (v/v) and stored in cryovials in liquid nitrogen (-80°C).

2.3 Clonal populations by limiting dilution cloning

After polyene resistant populations of *L. mexicana* and *L. infantum* were obtained, individual clones were isolated from each independent resistant line by limiting dilution, for further genotypic and phenotypic characterization. Briefly, selection of Individual clones involved diluting promastigotes to a concentration of 1 x 10⁴ cell per mL, followed by further dilution of 5 x 10² cells per mL that was then adjusted to the final desired number of clones expected. In this study, I adjusted my protocol to a final concentration of approximately five cells per 5 mL (10 cells per 10 mL) as follows. Adding 50 ul to 4,950

ul (dilution factor (df) 1:100), or 50 ul cells into 9,950 ul (df 1:200) of HOMEM (final volume of 5 or 10 mL) that were plated out into 48 wells (100 ul per well) (Hu et al. 2016) (<https://www.addgene.org/protocols/limiting-dilution/>).

2.4 Drug screening assays

The Alamar Blue® assay is a rapid method to measure quantitatively the inhibitory concentration (EC_{50}) and to determine the toxicity and proliferation (viability) of compounds and cells, respectively. This assay measures the reducing activity of viable cells by correlating their proliferation with the intensity of fluorescence (Invitrogen™; Promega). In this study, this assay was used to measure the viability-toxicity of *Leishmania* spp. promastigotes (*L. mexicana*, *L. infantum* and *L. tarentolae*), exposed to more than twenty compounds, as described previously (Mikus and Steverding 2000; Pan 1984; Shimony and Jaffe 2008). All of the compounds tested were purchased from Sigma unless otherwise stated. A stock solution of the following compounds was prepared using filter sterilised (0.22 μ M filter) distilled water (dH_2O): AmB, nystatin, natamycin, methylene blue, miltefosine hydrate, potassium antimonyl tartrate, paromomycin sulphate, pentamidine isethionate, mianserin and clomipramine. Ketoconazole and fenarimol stocks were dissolved in methanol, and the compounds from the library from Argentina (see below), were diluted in dimethyl sulfoxide (DMSO). Imipramine, a tricyclic antidepressant (TCA), was dissolved in either dH_2O or DMSO. Other TCAs, desipramine and trimipramine (both at 1.0 mg/mL in methanol), were dissolved directly in HOMEM before use. For the drug screening assay, each drug was prepared the stock solution on the day of the assay by dissolving the stock solution in fresh medium (HOMEM) at a concentration two times higher than the desired starting concentration, maintaining the volume of the solvent below 1% of the final volume. A control with a similar volume of solvent without drug was included. Drugs were serially diluted in a two-fold stepwise fashion in 96-well plates with a final volume of 100 μ l per well. The last well was always maintained without drug as negative control. Then a similar volume (100 ul) of either wild type or polyene-resistant parasites was added to each well at a final density of 1×10^6 cells per mL and further incubated for 72 hours with drugs. Resazurin dye (0.49 mM dissolved in 1x phosphate-buffered saline (PBS), pH 7.4) was added (20 μ L) into each well and incubated for another 48 hours. Resazurin (blue) is reduced to resorufin (fluorescent) by metabolically active cells and the absorbance (fluorescence) was measured using a BMG LabTech Fluostar Optima fluorometer. Intensity was read at λ_{EX} 530 nm and λ_{EM} 590 nm and analysed with Prism 8.0 software to obtain the 50% inhibitory concentration (EC_{50}) for each compound using regression analysis.

I also screened a new library of heterocyclic steroid inhibitors, named 1,2,3-triazolyl sterols (TAZ), with expected activity against the C14DM and C24SMT enzymes. Stock solutions of these compounds were prepared in DMSO. A detailed description of their chemical structures is provided in Chapter 6 (see Table 6-1). Except for 2DR, 2DS and 2ES that were synthesised by Yazmin Santos (Degree Thesis, Universidad Nacional del Rosario, unpublished), all of the other sterol inhibitors were synthesised by Dr Exequiel Porta, both members from Guillermo Labadie Lab, at The National University of Rosario, Argentina. All TAZ compounds were prepared from pregnenolone by adding a propargylamine to the side-chain following a method described previously (Porta et al. 2014). Another library of twenty compounds (thiosemicarbazones), synthesised by Cristina Soares (Univ. of Argentina) was tested in some lines (not included in this Thesis, due to time constraints). Another AmBR clone, named AmB 0.27 μ M hereon, with a mutation (N176I) in C14DM (Mwenechanya et al. 2017), and developed by a former member within the Barrett Lab, was also included in the screening of this library (chapter 6). In this study, I tested a total of thirty five compounds (chapter 3, section 3.2.3 and chapter 6, section 6.2). Unless stated otherwise, all experiments were performed in three biological replicates. One-way ANOVA was performed independently for each compound to determine differences of the mean between groups, and a Tukey's multiple pairwise comparison was also performed to assess differences between polyene-resistant lines with respect to their parental wild type.

2.5 Time-to-kill and dose-to-kill in wild type and two resistant cell lines

A time to kill assay was performed to determine cell viability of wild type and two AmBR lines (AmBRcl.14 and AmBRcl.8) of *L. mexicana* after the treatment with AmB (chapter 7), and with the two most potent compounds (156.A and 156.D) from the library of 1,2,3-triazolylsterol inhibitors (chapter 6). The stocks of the three compounds were prepared as described in section 2.4. Assessment of cell viability after drug exposure was performed using light microscopy (Zeiss Axiovert A1). Parasites were treated with AmB (5 x the EC_{50}), and compounds 156.A and 156.D, were used at three doses, 1) 5 x EC_{50} (22.5 μ M and 17.5 μ M), 2) EC_{50} (4.5 μ M and 3.5 μ M) and 3) the minimum inhibitory concentration (MIC) (2.8 μ M and 1.6 μ M), and further incubated for 2, 6, 8, 16 and 24 hours. Treated cells were then cultured as described before (section 2.1). Considering the presence alterations in morphology, growth, motility and integrity (some death cells) at longer time of exposure, a time point and concentration of 15 minutes for AmB (Ms Alison Reilly, former student within the Barrett Lab, unpublished), and of 12 hours for the two

compounds 156.A and 156.D, were selected, respectively. Three separate sets of experiments, the first two for LC-MS and the third one for GC-MS, were then performed as follows:

1. *L. mexicana* wild type, and two resistant lines, AmBR- cl.14 and cl.8, were treated with AmB at 5 x their respective EC_{50} (50 nM for wild type and 3 μ M for both resistant lines), before samples were processed for LC-MS (see section 2.7. and chapter 7).
2. Another *L. mexicana* line lacking the transketolase gene (including the parental line and the add-back), developed by a former member within the Barrett Lab (Kovářová et al. 2018), were also treated with 5 x their respective AmB EC_{50} , as follows: a transketolase gene (Δ TKT) (EC_{50} 52 \pm 4.3 nM), the parental wild type (wtTKT) (EC_{50} 67.5 \pm 0.70 nM), and the add-back (+TKT) (EC_{50} 52 \pm 2.8 nM), final doses of AmB added in the culture (15 mins) were, 250 nM for both, the wild type and the add-back lines, and 338 nM for the Δ TKT, followed by the extraction of the metabolome for LC-MS as described in the previous step (see number one of this section).
3. The effect of TAZ compounds, upon the content of sterols was assessed using GC-MS. Considering the volume of drug available, and the cost of the sterol analysis, I selected only one compound (156.D) to treat wild type and two AmBR lines with the same two concentrations of 156.D, i.e. 3.5 μ M (1 x EC_{50}), and 1.6 μ M (MIC). Note that wild type and AmBRcl.14 were treated with both the EC_{50} and MIC, while AmBRcl.8 was treated only with the MIC, due to the lack of sufficient compound. After treatment, sterols were extracted as described in section 2.8. Parasite pellets (3 x 10⁸ parasites) were weighed to estimate the content of sterols per parasite before samples were processed for GC-MS as described below (see section 2.8). Controls were included using the same volume of DMSO added with each treatment.

2.6 Infectivity of *Leishmania mexicana* in a murine model

All animal experiments were performed by a certified technician, i.e. Ms Anne Marie Donachie, and Mr Ryan Ritchie. All mice were from Harlan UK Ltd, and kept at the Central Research Facilities of the University of Glasgow, Glasgow U.K, and were randomly assigned to either of the treatment groups (wild type versus AmB resistant lines). Infection of BALB/c female mice (two-months at the time of inoculation) was performed by inoculating *L. mexicana* (2 x 10⁶) stationary promastigotes in 100-200 μ l of filter sterilised PBS in the left footpad. Progress of the footpad lesions was assessed weekly during the entire duration of the experiment (thirteen weeks) and all infections were stopped before any of the lesions reached a size of 5 mm, following the Animals (Scientific

Procedures) Act, 1986 (ASPA) <https://www.gov.uk/government/publications/consolidated-version-of-aspa-1986>). Amastigotes were recovered post infection, from all mice by sub-culturing tissue from footpad lesions and lymph nodes after animals were euthanized, then amastigotes were transformed into promastigotes for downstream analysis (e.g. retention of resistance). A detailed explanation of all the wild type and all the four AmBR lines used for infection of mice is detailed in Chapter 5 (see section 5.2.3). Briefly, three BALB/c mice (one mouse for each line) were infected with two resistant lines (AmBRcl.14 and AmBRcl.8) and wild type (first infection experiment). A second experiment included four resistant lines (AmBRcl.14, AmBRcl.8, AmBRcl.6 and AmBRcl.3) and wild type, and mice were treated with AmBisome (see details in Figure 5-6) (second infection experiment). A third experiment was performed to test the activity of AmB in liposomes (AmBisome®). In this experiment, another AmB resistant line selected for resistance to AmB by a former student in the Barrett Lab (Dr Andrew Pountain), was used (see details in chapter 5, section 5.2.5).

After all animals were euthanised, tissue from footpad lesions and lymph nodes were recovered and preserved in either neutral buffered formalin (10%) or paraformaldehyde (4%) in PBS and fixed during 24 hours. Tissue specimens were then placed and stored in ethanol (70%) until they were processed for histology at the Beatson Institute (Garscube campus, University of Glasgow, histology services from, head Colin Nixon). Samples were stained with haematoxylin and eosin (H&E), for their analysis with light microscopy. Note that tissue samples from the third experiment also included whole organs (liver, kidney, spleen), left hind footpad and popliteal lymph node from all mice (see section 5.2.5 and 5.2.7.1).

2.7 Liquid Chromatography/Mass spectrometry (LC/MS) based metabolomics analysis

The global effect of the treatment with AmB (as deoxycholate) was tested in *L. mexicana* wild type strain M379, and in two resistant lines (AmBRcl.14 and AmBRcl.8) to study the effects of AmB treatment on the metabolome of the parasites after 15 mins (the time point was determined previously, see section 2.5). To extract both polar and nonpolar metabolite species, 1×10^8 mid Log promastigotes were quenched by rapid cooling at 10°C in dry ice/ethanol bath, culture medium was removed by centrifugation at 1,250 g for 10 minutes at 4°C, then transferred centrifuged twice at 4,500 rpm for 10 minutes at 4°C with a wash in 1ml of cold PBS in between and the pellet was resuspended in 200 ul of monophasic chloroform/methanol/water (CMW 1:3:1) followed by 1 hour shaking (max speed) at 4°C

and a final spin at 13,000 rpm for 10 minutes at 4°C. Pooled sample was made by taking 10ul from each sample and blanks were also included. Samples were sealed after adding argon and stored at -80°C until analysis with LC-MS. Identification of metabolites for LC-MS was performed with a ZIC pHILIC column (150 mm × 4.6 mm, 5 µm column, Merck Sequant) coupled to high-resolution Thermo Orbitrap QExactive (Thermo Fisher Scientific) mass spectrometry in both positive and negative ionization modes.

Samples were analysed in four replicates and data were processed in Glasgow Polyomics and provided as raw data. Identification of Liquid Chromatography-Mass Spectrometry (LC-MS) was done with IDEOM workflow which requires data processing using XCMS, mzmatch, R tools, filtering and storage of data in peakML files, according to a method described elsewhere (Creek et al., 2012; and Creek et al. 2012b). A similar analysis was performed in parallel using PiMP, an in-house software developed by Glasgow Polyomics to standardize and automate metabolomics analysis (Gloaguen et al. 2017). PiMP is a user-friendly platform that integrates all steps of a metabolomics study and allows users to share experimental designs and results online (<http://polyomics.mvls.gla.ac.uk/>).

2.8 Gas Chromatography/Mass spectrometry (GC/MS)

GC-MS is the standard method for the identification and quantification of sterols (Goad and Akihisa 1997). Sterols were extracted for analysis with Gas chromatography-mass spectrometry (GC-MS) using a protocol developed within Glasgow Polyomics. Briefly, a total of 3×10^8 mid-log phase promastigotes (between 5 to 10×10^6 per mL) were resuspended and washed twice in PBS by spinning cells down at 1,250 – 1,300 g for 5 to 10 minutes. Pellets were stored at -80°C until used. Before extraction, parasite pellets were thawed at room temperature and 500 ul of fresh KOH-ethanol (KO-EtOH) (20 ml dH₂O, 30 ml EtOH, 12.5 g KOH) was added to each sample (including a blank without cells), and incubating at 85°C for 1 hour in Pyrex glass tubes. After heating, a similar volume of n-heptane was added and samples were mixed by vortexing for 30 seconds. Samples were left over 20 – 30 minutes to allow for separation of the organic and the aqueous layers. The supernatant (the organic layer at the top containing the sterols) was separated using a glass Pasteur pipette, transferred to glass borosilicate vials with Teflon cap (Thermo Fisher®), and stored at -80°C until they were analysed with GC-MS. All samples were prepared in triplicate, and a pooled sample was also made by adding between 10 to 20 ul of each sample in one. Further sample processing for GC-MS and data analysis were done at Glasgow Polyomics (<https://www.polyomics.gla.ac.uk>) by Dr Stefan Weidt.

Analysis of sterols used standards and derivatization with a silylation agent, (Koek et al. 2011; Zarate et al. 2016), here trimethyl silane (TMS) was used. Sterols were then detected as their TMS ester derivatives but are reported as their underivatized form, and expressed as a percentage of the total sterol content after normalisation, and comparison with the pool of the reference standards. The stability and reproducibility of the instrument were assessed using external QC samples along with the pool samples (this is the mix of the *Leishmania* samples) followed by the addition of a mix of sterol standards and a blank (solvent only). Samples and standard mix were dried into amber with N₂ flow at 60 °C glass vials, then 50 µl of N-methyl-n-trimethylsilyltrifluoroacetamide with 1% 2,2,2-trifluoro-N-methyl-N-(trimethylsilyl)-acetamide, chlorotrimethylsilane (Thermo Scientific) were added and samples were vortexed for approximately 10 secs followed by incubation at 80 °C for 15 mins. Samples were cooled down at RT. After this, 50 µl of pyridine was added, together with 1 µl of the retention index solution, and samples were vortexed for another 10 secs. The retention mix consists of an *n*-alkane mixture of C12, C15, C19, C22, C25 and C29. Analysis in gas chromatography was performed in a TraceGOLD TG-5SILMS column with 30 m length, 0.25 mm inner diameter and 0.25 µm film thickness (Thermo Scientific) installed in a Trace Ultra gas chromatograph (Thermo Scientific). Carrier gas used was helium at a flow rate of 1.0 ml/min, then 1 µl of TMS-derivatised sample was injected into a split/splitless (SSL) injector at 250 °C using a surged splitless injection, a splitless time of 30 secs and a surge pressure of 167 kPa. Initial oven temperature was 70 °C and this was increased up to 250 °C at a ramp rate of 50 °C/min followed by a ramp rate reduction of 10 °C/min reaching a final temperature of 330 °C that was maintained for 3.5 min. Eluting peaks were transferred at an auxiliary transfer temperature of 250 °C to a ITQ900-GC mass spectrometer (Thermo Scientific), with a filament delay of 5 min. Electron ionisation (70 V) was used with an emission current of 50 µA and an ion source that was held at 230 °C. The full scan mass range was 50-700 m/z with an AGC (automatic gain control) of 50%, and maximum ion time of 50 ms. Then the *Leishmania* samples, QCs and standards were loaded into the instrument (Dr Stefan Weidt). Identification of sterols peaks detected in any of the *Leishmania* samples that matched the standards (see chapter 5, section 5.2 and Figure 5-2), was performed with a TraceFinder v3.3 (Thermo Scientific). Identification of peaks to which standards did not match was conducted by comparison to the NIST library, also using TraceFinder (Glasgow Polyomics, Metabolomics analysis Report by Stefan Weidt).

2.9 DNA and RNA sample preparation

Extraction of genomic DNA (gDNA) and RNA (total) from promastigotes (5×10^7) were performed using the Nucleospin Tissue and Nucleospin RNA kits (both from Macherey-Nagel), respectively. Concentration (ng/ μ L) and purity (absorption ratios A260/A230 and A260/280 ≥ 2.0) of gDNA and RNA were determined using a Nano Drop machine (Thermo Scientific) and stored at -80°C until further processing and analysis. Both, preparation of library and sequencing, were performed by staff Dr David McGuinness, from Glasgow Polyomics (https://www.polyomics.gla.ac.uk/ngs_omics.html). Samples for Whole Genome Sequencing (WGS) were prepared using a TruSeq Nano DNA library preparation Illumina Kit. The cDNA libraries (for RNA seq) were generated using the Illumina TruSeq stranded mRNA library preparation kit, also from Illumina. Genomic DNA was obtained from the parental wild type, and all four independent AmBR lines (AmBcl.14, AmBcl.3, AmBcl.8 and AmBcl.6). A second clone (Lm8E12_S221) of the same line AmBcl.8 was included for comparison. After being sequenced, all files were provided as raw files, and transformed into, fasta and fastq files that were used for alignment to the reference genome (section 2.9.1).

2.10 Generation of *Leishmania* overexpression line of C24SMT

L. mexicana promastigotes were transfected using the episomal vector pGL1132 that has been used in *Leishmania* spp. before (Diaz-albiter et al. 2018; Pountain et al. 2019b). Construction, transformation, PCR colony screening and amplification of positive colonies (including Sanger sequencing confirmation) of this plasmid (pGL1132-C24SMT) containing a wild type copy of the C24SMT (LmxM.36.2380) was previously performed by Dr A Pountain (Dr Andrew Pountain PhD Thesis, University of Glasgow). Briefly, pGL1132 is a construct made from the pNUS vector (<http://www.pnus.cnrs.fr/tools.html>) encoding the neomycin gene, elements for expression of inserted genes in *Leishmania* are mediated by the phosphoglycerate kinase B (5'UTR) and A (3'UTR). I amplified and purified this plasmid from *E. coli* grown in Luria-Bertani (LB) medium (100 μ g per mL ampicillin), and using the Nucleospin plasmid kit (Macherey Nagel), followed by ethanol precipitation. Briefly, the pGL1132-C24SMT vector was resuspended in sodium acetate (NaOAc 0.3 M, pH 5.2) at a ratio 1:10 (v/v) NaOAc: pGL1132-C24SMT, followed by the addition of ice cold ethanol at a ratio 2:1 (v/v) EtOH: pGL1132-C24SMT.

Samples were washed once with 70% ethanol, centrifuged at 17,000 x g, 10 min and supernatant removed. Samples were allowed to dry before resuspension in sterile water (dH₂O) followed by determination of DNA concentration using a nanodrop spectrophotometer (Thermo Fisher). Parasites (1×10^7) were harvested, pelleted (1200 x g, per 10 min) and washed with ice-cold PBS before being resuspended in 100 μ l transfection buffer (90 mM NaPO₄, 5mM KCl, 50 mM HEPES, 0.15 mM, CaCl₂, pH 7.3). Plasmid DNA (10 μ g) was added into a cuvette and transfection was performed using the Amaxa protocol U-033 (NucleofectorII, Lonza). Transfected parasites were then transferred into 5 mL of HOMEM medium and left to recover for 24-48 hours before positive selection of transfectants, the latter was performed with further passages over 1-2 weeks with G418 disulfate salt (Sigma Aldrich) at 50 μ g/ml in the medium, culture conditions were as described in section 2.1. G418 is an aminoglycoside structurally similar to gentamicin that inhibits elongation by interfering with the function of 80s ribosomes and protein synthesis in eukaryotes, this mechanism is analogue to neomycin. Resistance to G418 is conferred by neo gene which encodes an aminoglycoside 3'-phosphotransferase (ATP 3' II).

2.11 Quantitative PCR

Reverse transcription (RT) is performed by RNA reverse transcriptase to produce complementary DNA (cDNA). Here, the RT reaction was performed using Superscript III reverse transcriptase (Invitrogen) following the manufacturer's instructions. Primers (0.3 μ g/ μ L), RNA (1 mg) and dNTPs (10 mM) were added into a nuclease-free eppendorf tube with RNase free water (final volume 14 μ L), followed by heating (65°C for 5 minutes) in a PCR machine (G-Storm). The mixture was kept on ice (60 secs). First-Strand Buffer (5x) was added (4 μ l), DTT (0.1 M) and Superscript III reverse transcriptase (1 μ l) were added to the reaction tube and further incubated at 25°C for 5 minutes, and at 50°C for 60 min in a PCR machine. The reaction was inactivated at 70°C (15 min) and the remaining RNA was removed with *E. coli* RNase H (1 μ l) and incubation at 37°C (20 min). The single stranded cDNA product was resuspended in nuclease free water stored at -20°C. A control without enzyme (RNAase free water was added instead) was included to detect gDNA contamination.

Levels of expression of C24SMT (LmxM.36.2380) were measured using quantitative reverse transcription PCR (qRT-PCR), C24SMT expression was normalised using the housekeeping gene, glyceraldehyde-3-phosphate dehydrogenase (GAPDH) (LmxM.36.2350 in *L. mexicana*). Pairs of primers: FP2 and RP2, and FP5 and RP5 (see Table 2-1) were previously designed (Primer Express v3 software (Applied Biosystem)

and optimized by a former member within the Barrett Lab (Dr. Andrew Pountain). GAPDH is a cytosolic single copy (Zhang, et al., 2013) that has been previously used as internal control reference gene in other expression analysis, and has the advantage of being located in the same chromosome (Chr20) than the two copies of C24SMT (Pountain et al. 2019b; Vacchina, Norris-Mullins, Abengózar, et al. 2016). The reaction (Applied Biosystems) was prepared adding 2.5 μ l of cDNA template and a similar volume of each of the primers (FP2 and RP2 or FP4 and RP4), 5 μ l of RNAase free water and 12.5 μ l of SYBR Green Master Mix to give a final volume of 25 μ l. The reaction was plated out into a 96-well MicroAmp® optical qPCR reaction plate (Applied Biosystem), sealed with MicroAmp Optical Adhesive Film (Applied Biosystem) and placed in a RT-PCR system (Applied Biosystem 7500). Reaction steps were as follows: 2 min at 50 °C, and 10 min at 95 °C, followed by 40 cycles at 95 °C during 15 secs and a final step at 60 °C during 60 secs, fluorescence was measured in the latter of these steps. Passive reference dye used was ROX. All experimental reactions, and control (without RT enzyme) and blank (water-only), were performed in three and two replicates, respectively. Delta Ct threshold (δ Ct) of 6 value was used as a difference between experimental (RT-included) and control (RT-free) samples. Although the threshold obtained with C24SMT was lower (-4.13), this was equivalent to a 17.5-fold difference in DNA abundance.

2.12 CRISPR Cas9 system

In this study, I used the genome editing CRISPR-Cas9 system in *L. mexicana* promastigotes following the protocols designed by Beneke et al. 2017. An overview of the system, and the plasmids maps (the latter were provided by Dr Eva Gluenz Lab) used in this project is depicted in Figure 2-1 and Figure 2-2. Briefly, 5' and 3' sgRNA templates were PCR amplified using the following steps: 0.2 mM dNTPs, 2 μ M of each, reverse (G00R), and 2 μ M gene-specific forward primers (G00F), and 1 unit of HiFi Polymerase (Roche) were mixed in 1x HiFi reaction buffer with MgCl₂ (Roche), adjusting to a final volume of 20 μ l total per reaction. PCR steps were as follows: 30 seconds at 98°C, followed by 35 cycles of 10 seconds at 98°C, 30 seconds at 60°C, and 15 seconds at 72°C. The presence of the expected product (126 bp for both 5' and 3' sgRNAs) was verified adding 2-5 μ l of each reaction to Gel Loading Dye (NEB®) Purple (6X) and run in a 2% agarose gel with SYBR® Safe (10 mg per mL) at 100 volts for 45-60 minutes in TAE (Tris-acetate-EDTA) running buffer. The remainder of each reaction was heat-sterilised at 94°C for 5 minutes and maintained at 4°C and used for transfection of *L. mexicana* promastigotes without further purification (i.e. ethanol precipitation). Transformation of each plasmid was performed by mixing 5 ng (pre-diluted into 50 μ l of dH₂O), with 50 μ l (1:10 v/v) of kit supplied *E. coli* DH5 α thermo-competent cells that were kept on ice for 15-20 mins followed by heat shock at 42 °C for 30- to 60 secs, and maintained on ice for another 2 mins. Cells were resuspended into 1 mL of LB broth and incubated for 30-60 mins at 37 °C and plated on agar plates with ampicillin (100 μ g per mL) for further incubation overnight at 37 °C. Positive colonies were obtained after 12 hours and one colony for each plasmid was selected and amplified in 30 mL of LB-ampicillin (100 μ g/ml), followed by: 1) concentration in LB broth with glycerol (15%) for long term storage at -80 °C (glycerol stocks), and 2) isolation of purified plasmids using the Nucleospin plasmid kit (Macherey Nagel), that were also stored at -80 °C.

PCR amplification of targeting fragments was performed by mixing 30 ng of each pT plasmid (circular), 0.2 mM of dNTPs, 2 μ M of each gene specific forward, upstream forward (UF) and downstream forward (DR), and reverse, upstream reverse (UR) and downstream reverse (DR) primers, and 1 unit of HiFi Polymerase (Roche), then adding 1x HiFi reaction buffer (Roche), adjusted to a final 3.375 mM of MgCl₂, and 3% (v/v) of DMSO, giving a final volume of 40 μ l per reaction. PCR steps were as follows: 5 minutes at 94°C followed by 40 cycles of 30 seconds at 94°C, 30 sec at 65°C, 2 min 15 sec at 72°C, followed by a final elongation step for 7 min at 30 sec at 72°C. A volume of 2-5 μ l of each reaction was mixed with Gel Loading Dye (NEB®) Purple (6X) and run in a 1% agarose

gel with SYBR® Safe (10 mg per mL) and TAE buffer to check for the presence of the expected products (see Table 2-1 section C, for the size of each plasmid). The remainder of each PCR reaction was heat sterilised at 94°C for 5 minutes and kept at 4°C until use for transfection without further purification. Sequences of all the primers used in this study are detailed in Table 2-1. All primers were synthesised by Eurofins® (<https://www.eurofinsgenomics.eu>).

Transfection buffers (for knockouts) were as follows: a stock solution of buffer named 3x Tb-BSF (200 mM Na₂HPO₄, 70 mM NaH₂PO₄, 15 mM KCl, 150 mM HEPES pH 7.3), and a stock solution of CaCl₂ (1.5 mM CaCl₂ in dH₂O) were prepared and stored at 4°C until used. Note that transfection buffer for tagging (not used in this thesis) is different (Beneke et al. 2017). Before transfection, cells were washed twice in cold PBS and resuspended in 150 µl KO transfection buffer that was freshly prepared by mixing 25 µl of CaCl₂ with 83 µl of 3x Tb-BSF buffer and 42 µl of water. PCR amplicons were mixed directly from the PCR tube by adding 100 µl of the PCR reaction, giving a final transfection volume of 250 µl.

Log phase *L. mexicana* M379 promastigotes expressing Cas9 (humanised *S. pyogenes* nuclease gene; *hSPCas9*), and T7 RNA polymerase (T7RNAP), as a driving mechanism of sgRNA transcription from DNA templates (Cas9 and T7RNAP were integrated in the β -tubulin locus of *L. mexicana*). This Cas9-wild type cell line provided by Dr Eva Gluenz Lab, and cells were cultured with selection drugs in the Cas9 and T7RNAP construct, i.e. hygromycin (32 µg per mL) for a minimum of 4 passages. Before transfection, parasites were centrifuged at 800 g for 5 min and a total of 1×10^7 cells per transfection were resuspended in pre-chilled electroporation cuvettes, and transfected with one pulse using the X-001 protocol (Amaza Nucleofector 2b) in sterile conditions. After transfection, cells were immediately transferred into 5 ml of pre-warmed (26°C) HOMEM medium (10% FCS) without antibiotics, in 25 cm² flasks, and allowed to recover (8-16 hours) before further subculture with selection drugs of the repairing cassettes, pTb (5 µg per mL) and pTp (20 µg per mL), used in this study, and cultured until resistant populations were obtained. Transfections for double KOs were performed using two sgRNA templates (5' and 3' sgRNA), and two KO repairing cassettes (donor DNA), the latter two are necessary to ensure elimination of any heterozygous cells that may carry one copy of the gene of interest. Note that this is, possibly, more complex with genes that have two copies in tandem (as with C24SMT). According to the protocol developed by Beneke, et al. 2017, clonal selection to find null mutants can be necessary, if remaining copies of the target genes are identified and parasites do not survive the drug selection *in vitro* (Dr Eva Gluenz,

personal communication), here, positive selection of knockouts after transfection was performed by adding puromycin (20 µg/ml) and blasticidin (5 µg/ml) antibiotics without selection of clones by limiting dilution. Further characterisation of the phenotype of this mutant was performed by means of assessing growth rate, morphological alterations, and amastigogenesis *in vitro*.

PCR diagnostic reactions were performed to test deletion of the gene of interest (GOI) and integration of the donor DNA cassette (plasmid) using a combination of primers (Table 2-1). Three strategies can be used here, 1) a pair of primers that bind outside the ORF of the GOI or plasmid, 2) primers that both bind within the ORF/plasmid, and 3) one primer that binds outside (upstream of downstream) with another primer that binds inside of either the ORF or the plasmid. PCR reaction was prepared adding, template DNA (gDNA) (<500 ng), reverse and forward primers (400 nM of each), 1 unit of HiFi Polymerase (Roche) mixed in 1x HiFi reaction buffer with MgCl₂ (3 mM), dNTPs (1 mM) adjusted with nuclease free dH₂O into a final volume of 50 µl total per reaction. PCR steps were as follows: 2 mins at 98°C initial denaturation, followed by 40 cycles of 15 seconds at 95°C, 15 seconds at 55-65°C, and 50 seconds/Kb at 72°C. A final extension step of 10 mins at 72°C and final hold at 4°C. The expected product(s) were verified by adding 2-5 µl of each reaction was mixed with Gel Loading Dye (NEB®) Purple (6X) and run in a 2% agarose gel at 80-100 volts for 45-60 minutes in TAE (Tris-acetate-EDTA) running buffer, using a 1 Kb ladder as control (Promega). Further characterisation was also performed using drug susceptibility assays against a series of compounds, including AmB and other antileishmanials, and a new library of sterol inhibitors, potentially targeting C24SMT. Finally, sterol profiling using GC-MS (see section 2.8 and Chapter 5 for GC-MS details) was also performed in this mutant (see Chapter 6). Further characterisation of this mutant (e.g. Southern blot, qPCR, RNA-seq and Sanger sequencing) is essential to confirm the deletion of both copies of C24SMT, and could not be carried out due to time limitations in this thesis.

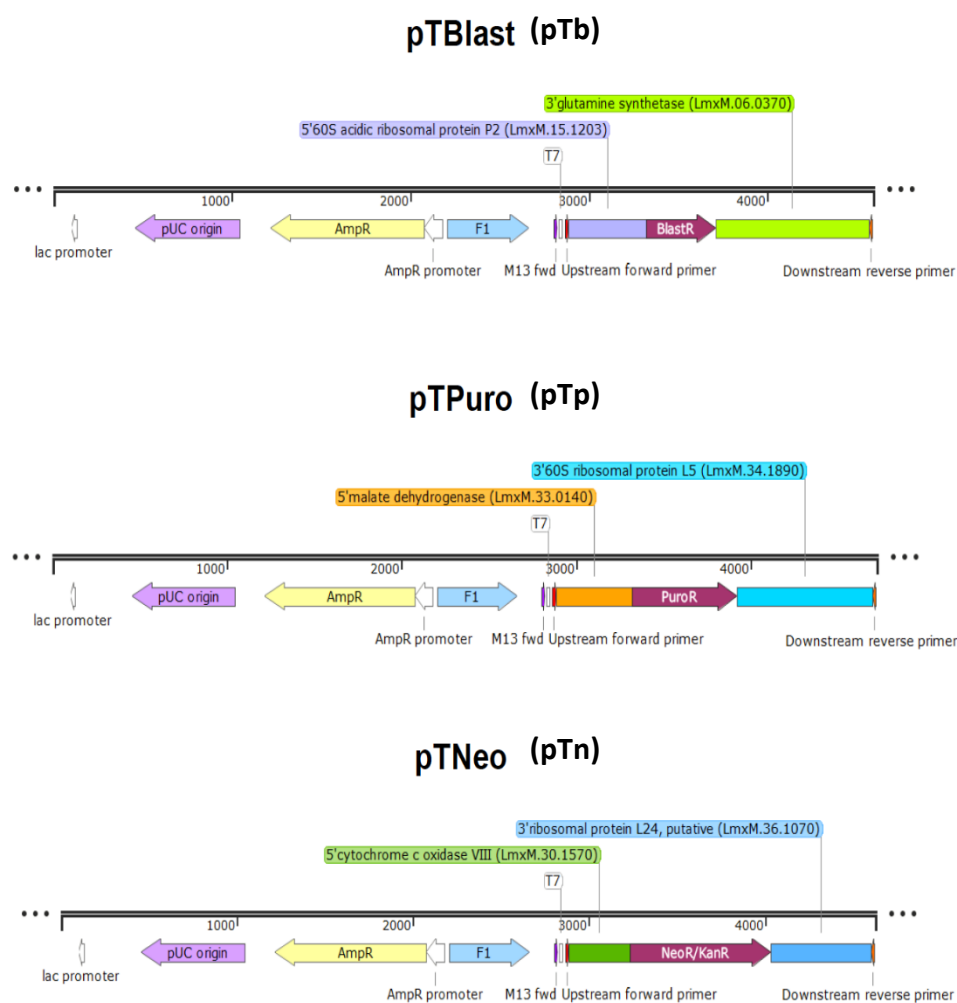


Figure 2-1. Detailed maps of pT plasmids of CRISPR-Cas9 used for generation of single and double knockouts of target genes in *Leishmania* spp. Here the plasmids maps show the different selection markers that need to be added in the culture medium for the selection of single (one plasmid only) or double (any combination of two plasmids) knockouts, after transfection (see section 2.12 for details). In this study, I used a combination of plasmids containing blasticidin (pTb) and puromycin (pTp). Details of the full strategy are described in Figure 2-1. Source: Beneke, et al. 2017.

Table 2-1. Primers sequences for PCR amplification of, sgRNA templates, and targeting fragments (plasmids with resistance cassettes) used to knockout *L. mexicana* C24SMT. A) sgRNA primers (5' and 3'): Low case indicates the T7RNAP (left) and Cas9-backbone start (right), respectively, UPPER CASE (centre of the primer) indicates the 5' or 3' 20 nucleotides of the sgRNA-target sites that are gene specific. B) UPPER CASE indicates the 30 nucleotides homology arms for recombination. Lower case indicates the Primer Binding Site (PBS) that is located in both, the primer, and the plasmid repairing cassettes. C) Plasmid repairing cassettes of pT plasmids to generate knockouts (KO), plasmids size and selection markers are shown. D) PCR primers for diagnostic of C24SMT KOs. Modified from: Beneke, et al. 2017. * Pountain et al. 2019. ** Designed and provided by Dr Emily Dickie. All sequences are written from 5' to 3' orientation.

A) sgRNA transcription primers			
	Upstream 5' sgRNA (126 bp)	Downstream 3' sgRNA (126 bp)	
G00F (forward) gene specific	gaaattaatacgcactcactataggGTGTAGGTGTGG GGGTAAGTgttttagagctagaaatagc	gaaattaatacgcactcactataggAAGAACGCTGAA CGCACTGGgttttagagctagaaatagc	
G00R (reverse) (size 80 bp)	AAAAGCACCGACTCGGTGCCACTTTTTCAAGTTGATAACGGACTAGCCTTATTTAACTTGCTATTT CTAGCTCTAAAAC		
B) Forward and Reverse Primers of plasmids repairing cassettes (donor DNA)			
	Upstream (UF)	Downstream (DF)	
Forward	TGCGCACTACCTCTTCGCTTGTTCCTGtataa tgagacctgctgc	ATCCGCGCTCGCAAGCCGTCCAAGGAGGTGggttctg gtagtggttccgg	
	Upstream (UR)	Downstream (DR)	
Reverse	CGGCGCGGTCTCACGGCCACCGCGGACATact accgatcctgatccag	GCCAAGTATGGCGGAGGTTAGACGTAGCCGccaatt tgagacctgtgc	
C) Plasmids repairing cassettes (KO cassettes)			
Plasmid name	Resistance marker	Cassette size (kb)	
pTBlast (pTb)	blasticidin	1.7	
pTPuro (pTp)	puromycin	1.8	
pTNeo (pTn)	neomycin	1.75	
D) Plasmids for PCR diagnostic of true C24SMT KOs			
	Forward	Reverse	Size
CDS (both)	ATGTCCGCCGGTGGCCGT (FP1)	CTACACCTCCTTGACGGCTTGC (RP1)	1,062 bp
Intergenic region (both)	TGCCACGCGAAGGACAA (FP2)*	CGGGCTTGATGACACGAAA (RP2)*	58 bp
	FP1	TTCACCATCGTCGTGGTAGC (RP3)*	161 bp
	ACCGAAGGGCACGTATAAGG (FP3)*	RP1	130 bp
	FP3 *	RP3 *	2991 bp
3 UTR (2390)	TCCCTCCCTCAAAGACATG (FP4) *	CTCTGTTACGAAAGTTGTCATATTCT (RP4) *	78 bp
GAPDH	TCAACGACCTGCTGGATGTC (FP5)	GCCATGCGTGGAGTCGTA (RP5)	
E) Plasmids for checking integration of repairing cassettes			
Plasmid name	Resistance marker	Primers	Expected size
pTBlast (pTb)	blasticidin	Forward: CACCCTATTGAAAGAGCAACGG Reverse: CACTATCGCTTTGATCCCAGGA	295 bp
pTPuro (pTp)	puromycin **	Forward: AGAACTTCAAGAGTTATTCTTAACACGG Reverse: CAAGGAACGCCGGCACAC	341 bp
pPLOTp	puromycin	(included for comparison)	2-3 kb

2.13 Data analysis of genomics and transcriptomics

2.13.1 Next generation sequencing

Design and analysis of tailored tools for WGS was performed by Dr. Andrew Pountain. Tools used here are underlined. NGS was performed using Illumina sequencers, NextSeq 500 and HiSeq 4000, to obtain reads of 2 x 75 bp paired-ends at Glasgow Polyomics. Data analysis was performed using two platforms, coding lines (Python, Linux) and Galaxy server (Afgan et al. 2018). Tools included in the workflow were as follows: Trim Galore v0.4.4_dev, was used to remove adaptors and for quality trimming, using a quality score cut-off of 20 and a minimum read length after trimming of 20 (<https://www.bioinformatics.babraham.ac.uk/>). Reads were aligned to the version of the reference genome of *L. mexicana* MHOM/GT/2001/U1103 release 36, downloaded from the database TriTrypDB (<http://tritrypdb.org>). Fastq files were aligned with the reference genome and SAM/BAM files were produced (SAM files are very large and BAM (Binary Alignment/Map) files are their binary equivalent in a compressed size). Mapping was performed in BAM files using Burrows-Wheeler Alignment (BWA), which is a software package used for mapping low-divergent sequences against a large reference genome (<http://bio-bwa.sourceforge.net>) (Li and Durbin 2009). BWA-MEM algorithm was used with default settings. BWA-MEM is the latest of three algorithms of BWA for sequences from 70bp to 1Mbp (therefore specific for these samples) which is suggested for high-quality queries and is faster and rendering more accurate alignments (<http://bio-bwa.sourceforge.net>). SAMtools v.1.7 was used for storing the reads post-processing (Li et al. 2009), and Picard Tools v2.18.0-0 was used to remove PCR duplicates and adding read-group names (<http://broadinstitute.github.io/picard/>). HTseq-count v0.6.1, was used to quantify mapped counts per-gene (Anders, et al., 2015). Python scripts adapted to the new genome release were used to calculate ploidy and haploid ratios (median length of individual chromosomes was compared with the median of all chromosomes) and customised by Dr Andrew Pountain. Freebayes v1.1.0-dirty was used to call variants on a BAM file (<https://github.com/ekg/freebayes>), and to generate genotypes (by merging outputs of previous step) that were annotated and filtered with SnpEff v4.3.1 (minimum quality score of 30, a minimum number of alternative counts across all samples of 5, and a minimum number of mapped reads (from the reference or alternative) across all samples of 31). SnpSift v4.3.1 was used to convert variants obtained from VCF (variant call format) into a tabulated format. Other changes (e.g. non-coding changes, intergenic SNPs) were removed by filtering for “moderate” or “high” effects. Finally, a custom (in house) Python script (Dr Andrew Pountain PhD Thesis, University of Glasgow, 2018) was used to obtain

only those genotypes that were different between lines. Those genotypes that varied between different heterozygous genotypes only (e.g. 0/1 vs 0/0/1, 0/1/1 vs 0/0/1 etc.) were not included. SNPs, insertions and deletions (InDels) were called using FreeBayes (<http://clavius.bc.edu/~erik/CSHL-advanced-sequencing/freebayes-tutorial.html>). Freebayes (and most of the other tools used here), is available for use in the Galaxy server (https://toolshed.g2.bx.psu.edu/repository/display_tool?repository_id=491b7a3fddf9366f&render_repository_actions_for=tool_shed&tool_config=%2Fsrv%2Ftoolshed%2Fmain%2Fvar%2Fdata%2Frepos%2F000%2Frepo_226%2Ffreebayes.xml&changeset_revision=156b60c1530f). A full script of the WGS workflow is provided (Supplementary file 2) (see page 8).

2.14 RNA-seq analysis

RNA-seq (RNA sequencing) analysis was performed in *L. mexicana* wild type promastigotes transfected with the wild type copy of the C24SMT gene (LmxM.36.2380) (see section 2.10). After preparation of the cDNA library, RNA sequencing was performed in the NextSeq 500 system (Glasgow Polyomics) to generate a sequence size of 2 x 75 bp paired-end reads. Raw data generated were aligned to the reference genome similarly to that described above for NGS analysis, with the difference of the genome version of reference (here release 32 was used). Differentially expressed genes were identified using the Galaxy server (<http://heighliner.cvr.gla.ac.uk/root/login?redirect=%2F>). The RNA-seq analysis workflow used here was published in the Galaxy server for public use at (<http://heighliner.cvr.gla.ac.uk/workflow/editor?id=b06694bc6c2663c4>), and is provided (Supplementary file 3) (see page 8). RNA-seq analysis with Linux (performed by Dr Andrew Pountain) using a similar workflow to that described below (with some differences indicated with stars **) was run in parallel to validate the usefulness of Galaxy tools. Briefly, FastQC (<http://www.bioinformatics.babraham.ac.uk/projects/fastqc/>) and Trimmomatic (<http://www.usadellab.org/cms/?page=trimmomatic>) (**Trim Galore), were used to assess and improve the quality of the data. HISAT2 (**BWA) for splicing-alignment and mapping of RNA-seq reads. SAMtools was used to sort out BAM outputs. HTseq-count for counting of aligned reads, and DESeq2 to determine differentially expressed genes based on relative abundance of reads mapped to a reference genome (Love, Huber, and Anders 2014; Trapnell et al. 2012).

2.15 Bioinformatics and other computational tools

In silico modelling of the sterol biosynthetic pathway (SBP) was performed in *S. cerevisiae*, *L. donovani*, *L. infantum*, *L. mexicana*, and *T. cruzi*, following the model of the ergosome described by (Mo and Bard 2005b). Protein-protein Interactions (PPIs) were

called using the STRING database (<https://string-db.org/>). BLAST search was performed against the National Center for Biotechnology Information (NCBI) database using default settings. ClustalW Omega was used to identify and align sequences with output format (<https://www.ebi.ac.uk/Tools/msa/clustalo/>). Nucleotide and amino acids sequences were submitted to Expassy (<https://www.expasy.org/>) or the Protein Data Bank (PDB) (<https://www.rcsb.org>) from which protein queries were obtained. *Leishmania* spp sequences (genomic, CDS or protein) were obtained from the TriTrypDB database (<https://tritrypdb.org/tritrypdb/>) or from Uniprot (<https://www.uniprot.org/>). Protein alignment viewers used were Clustal X2 (Thompson, et al., 1994) (<https://www.ebi.ac.uk/Tools/msa/clustalo/>), PyMOL (<https://pymol.org/2/>), Cytoscape, and the software UCSF Chimera (Pettersen et al. 2004) (<https://www.cgl.ucsf.edu/chimera/>). Modelling and localisation of SNPs and protein topology were optimised by means of the PDB databank (<https://www.rcsb.org/>) and the OPM database (<https://opm.phar.umich.edu/>).

2.16 Infectivity in the sandfly vector

I intended to analyse the phenotype of AmBR resistant lines (as promastigotes) within the insect vector. For this, we developed a model using fluorescent *Leishmania tarentolae* parasites (Diaz-albiter et al. 2018). This non-invasive technique for detection of infection in sand flies, developed within the Barrett Lab, allowed us to perform infections of sand flies using *L. tarentolae* or *L. mexicana*. Parasites (2×10^6 per mL) were resuspended in a 1 ml of heat inactivated (56 °C for 60 minutes) sheep blood serum, followed by blood feeding of colonies of sand flies *Lutzomyia longipalpis*. Female sand flies were dissected and analysed between 3 to 5 days post infection, and cold anaesthetized before fluorescent microscopy analysis (GFP channel (at λ_{EX} 488 nm and λ_{EM} 509 nm). Sand flies infected with wild type and AmBR *L. mexicana* parasites were also performed, however, the low infection rates observed with both groups deemed for insufficient experimental controls. For this reason, the analysis of the phenotype of AmBR lines *ex vivo* within the insect vector were not included in this thesis. Infections with both species were performed following the methods described elsewhere (Díaz-Albiter et al. 2016).

3 Drugs screening in polyene resistant lines of *L. mexicana*

3.1 Introduction

The emergence of resistance against the existing drugs for the treatment of leishmaniasis is one of the main challenges related with their use in clinical settings (Jain and Jain 2018). Other issues related to the antileishmanials are their toxicity, modes of administration and cost (Barrett and Croft, 2012, Creek and Barrett, 2014; Burza, Croft and Boelaert, 2018). For some antileishmanials (e.g. antimonials), resistance has spread across various regions (Matrangolo et al. 2013; Pund and Joshi 2017). Clinical resistance to antimonials has been recorded in up to 60% of patients that never received previous treatment with these compounds (Rojo et al. 2015; Sundar 2001). Reports of resistance to other antileishmanials such as paromomycin (PAR) (Hendrickx et al. 2015), miltefosine (MF), and AmB, in the field are less common. One of the reasons for the little resistance found to AmB in the field is, possibly, the high initial cure rate (up to 99.3%) (Burza, Prabhat Kumar Sinha, et al. 2014), and in the long term (98% at 6 months) (Burza, Prabhat K Sinha, et al. 2014) in patients treated with this polyene in its liposomal formulation, AmBisome (Burza, Prabhat K Sinha, et al. 2014; Burza, Prabhat Kumar Sinha, et al. 2014), and a belief that resistance mechanisms may carry a fitness cost for the pathogens, e.g. *Leishmania* parasites and fungi (Vincent et al. 2013).

Clinical resistance and treatment failure with AmB and MF are, nonetheless, possible in *Leishmania*. Reports of the loss of efficacy (Bhandari et al. 2012; Deep et al. 2017; Rijal et al. 2013; Sundar et al. 2012), and treatment failure with MF (Carnielli et al. 2018), as well as high (8-fold) AmB resistance (Purkait et al. 2012), have also been reported in patients. AmB resistance is complex and can result from causes other than selection with AmB. For example, in fungi selection with other antifungals (e.g. azoles and echinocandins) (Marr 2004; Yoon et al. 1999) has yielded cross-resistance to AmB. This cross resistance to AmB has been also observed in patients with leishmaniasis treated with the antileishmanials, antimonials and miltefosine. The possibility that AmB resistance may emerge is of considerable concern, given the drug has been used increasingly for VL both as monotherapy (Fairlamb et al. 2016; Mudavath et al. 2014; Rastrojo, García-Hernández, Vargas, Camacho, Corvo, Imamura, J.-C. Dujardin, et al. 2018) and is being considered as a partner drug in combination therapy, e.g. with MF, in VL patients co-infected with HIV (Diro et al. 2019). Combined therapy can be an alternative to the problem of drug resistance with some advantages (e.g. cost-effective, less duration of treatment), however,

whether the use of two antileishmanials can contribute to prevent resistance are still unknown (van Griensven et al. 2010). Risks of cross-resistance between these two compounds, however, needs consideration too, since selection of resistance to AmB has, on occasion, been associated with cross-resistance to MF (Fernandez-Prada et al. 2016; Pountain et al. 2019a), due to mutations to the miltefosine transporter appearing during selection of AmB resistance. Other causes of resistance to miltefosine were recently related to the loss of a particular genetic locus, not involving the miltefosine transporter, LMT, increased the risk of treatment failure by 9.4-fold (Carnielli et al. 2018).

Other examples of cross resistance are, paromomycin (García-Hernández et al. 2012; Pountain et al. 2019a), and azoles. Although in other studies, some AmBR lines (AmBRA/cl1 in the study of Pountain) have been also found to be more susceptible to this aminoglycoside (Mbongo et al., 1998; Mwenechanya, R. PhD Thesis University of Glasgow, 2014), possibly, due to mutations in different enzymes of the sterol pathway. With regard to azoles, point mutations in the enzyme Lanosterol 14- α demethylase (C14DM), the target of azoles, have been shown to cause AmB resistance in *Leishmania* (Mwenechanya et al. 2017) and fungi (Sagatova et al. 2015), because ergosterol, the target of the drug is no longer produced when the enzyme is mutated. Kelly and colleagues observed cross-resistance to AmB in two fluconazole resistant strains of *C. albicans* isolated from humans with HIV/AIDS (Kelly et al. 1997). Another clinical isolate of *C. albicans* with mutations in ERG11 (C14DM in *Leishmania*) and ERG5 (C22-sterol desaturase), was cross-resistant to AmB and azoles (Martel, Parker, Bader, Weig, Gross, Warrilow, Kelly, et al. 2010).

Laboratory-selected AmB resistant *L. mexicana* lines were more susceptible to pentamidine (PENT) (Mbongo et al. 1998a; Pountain et al. 2019a), an oxidative stress-inducing agent (Mehta and Shaha 2004), and to other oxidising agents e.g. methylene blue (Buchholz et al. 2008; Farjami et al. 2010) and hydrogen peroxide (Mwenechanya et al. 2017). Previous work of Mwenechanya, also found an increase in the abundance of trypanothione in the AmB resistant lines. This was linked to a duplication of chromosome five (Chr5) in which trypanothione reductase (LmxM.05.0350) is located, and to an increase in the CNV of this gene (PhD Thesis Mwenechanya, R. University of Glasgow, 2014). Proteins involved in stress-responses have also been found to be increased in other AmB resistant lines (Brotherton et al. 2014).

The scarcity of field isolates of *Leishmania* demonstrating AmB resistance has necessitated the creation of laboratory induced resistance, which has the advantage of allowing

comparison between isogenic lines. However, to do this, selection of individual lines in parallel is necessary, given the genome instability of *Leishmania* parasites grown in culture (Laffitte et al. 2016; Pountain et al. 2019a; Ubeda et al. 2008). A full description of all the enzymes related with polyene drug resistance in *Leishmania* spp., with special focus in AmB resistance *in vitro* (Al-Mohammed, et al., 2005; Mwenechanya et al., 2017; Pountain et al., 2019) and in clinical isolates (Durand et al. 1998; Giorgio 1999; Purkait et al. 2012), is discussed in chapter 1 (section 1.6.6.3). Lines resistant to various antileishmanials, including AmB, antimonials (PAT and Sb^{III}) (Berg et al. 2015; Parmar et al. 2011), PAR (Hendrickx et al. 2015; Jhingran et al. 2009; Rastrojo, et al. 2018), Ketoconazole (Andrade-Neto et al. 2012), MF (Canuto et al. 2014; Seifert et al. 2003; Shaw et al. 2016; Turner et al. 2015), as well as different combinations of these drugs (Berg et al. 2015; García-Hernández et al. 2012) have all been studied. Comparing results between non-isogenic strains, and parasites selected under different experimental conditions (Fernandez-Prada et al. 2016; Mbongo et al. 1998a; Mwenechanya et al. 2017; Purkait et al. 2012) can confound comparisons. Several studies have characterised multiple lines selected in parallel (Al-Mohammed et al. 2005; Pountain et al. 2019a). Al-Mohammed et al., selected for AmB resistance in both amastigotes and promastigotes, whereas Pountain et al. simultaneously selected four AmB resistant lines and profiled their sterol content as well as genome sequence, which revealed multiple different genetic changes, all of which lead to a reduction in ergosterol in the resistant parasites. Another advantage of generating clearly defined resistant lines *in vitro* is the ability it offers to analyse cross-resistance between antileishmanials, and to other compounds, including libraries that have never been explored previously.

Given the minor structural differences between the two large polyenes AmB and nystatin (Nys) (see Figure 1-10, E and F), here we selected several independent lines for resistance to both polyenes, and assessed whether cross-resistance is reciprocal between these two, and to the small polyene, Natamycin (NMC), as well as to other compounds with different mode of action. One common change across AmB resistant lines (in *Leishmania* and in fungi) is the alteration of the composition of sterols, with ergosterol or closer relatives, that bind AmB replaced by various intermediates depending on the defects in different enzymes of the sterol pathway. For this reason, we used a more integrative approach combining genomics and other bioinformatics tools (chapter 4), and metabolomics (chapter 7), to characterise these polyene-resistant lines. Gas chromatography–mass spectrometry (GC-MS) was employed to determine if changes in the sterol profile are associated in AmBR lines (chapter 5). Broader changes in the metabolism were also investigated using untargeted metabolomics (LC-MS) (chapter 7). Additionally, we explored the relationship

between these alterations in sterols in the AmB resistant lines and their infectivity *in vivo*, as well as the response to different formulations of AmB (i.e. AmB-D and AmBisome) in a mouse model. Finally, I present some evidence of the role of protein-protein interaction (PPIs) in the sterol biosynthetic pathway in *Leishmania*, and how this multi-enzymatic complex, initially described in the budding yeast (Mo and Bard 2005a), related to the mutations that were identified in this study, and in other reports, with AmBR lines of *Leishmania* spp.

3.2 Results

3.2.1 Selection of polyene resistance in *Leishmania* spp.

Leishmania mexicana M379 promastigotes were selected for resistance to the polyenes amphotericin B (AmB) and nystatin (Nys). The first step was to determine the EC₅₀ for each of these compounds in the parental wild type. Subsequently, drug selection was done by adding a concentration of each drug similar to the EC₅₀ for each polyene to the culture medium. Parasites growth and morphology were assessed by light microscopy. The concentration of AmB or Nys in the culture was increased in a stepwise-manner following the method described elsewhere (Mbongo et al. 1998a; Phelouzat, Lawrence, and Robert-Gero 1993), with some differences for each of these polyenes, outlined below.

3.2.1.1 Amphotericin B resistant lines

Four independent lines of *L. mexicana* were selected for resistance against AmB. The starting concentration of AmB was between 50 to 60 nM, which corresponds to the EC₅₀ of the parental wild type. Parasite growth was monitored weekly and compared with the parental line which was cultured in parallel for the same number of passages without adding drug. Drug assays (i.e. Alamar Blue assay) were performed approximately each four weeks to detect increases in the EC₅₀. When parasites under drug pressure attained growth comparable to the parental line, or no inhibition of growth was observed between 18 to 48 hours after adding the drug, the EC₅₀ was measured and the concentration of drug added in the sample (culture medium) was doubled, adjusting based on the EC₅₀ of each line. In some cases, this concentration was reduced by 25% after identifying a high percentage of cell death (over 50%) between 24 to 48 hours after increasing the concentration (i.e. if the new concentration had been increased from 50 to 100 nM, it was readjusted to 75 nM). Development of resistance against AmB showed variation between lines. The increase in resistance was more abrupt and occurred earlier in some lines (i.e. AmBRcl.14) whereas in others (e.g. AmBRcl.8) it appeared more gradually. After ceasing

the drug selection, and before selecting individual clones, the four AmBR lines were between 6 and 10-fold less sensitive to AmB in comparison to the parental line (Figure 3-1). Although the fold change in resistance was marginally lower after selecting individual clones (Table 3-1), values in the order of 8 to 10-fold or above were observed in most of the experiments (Figure 3-5).

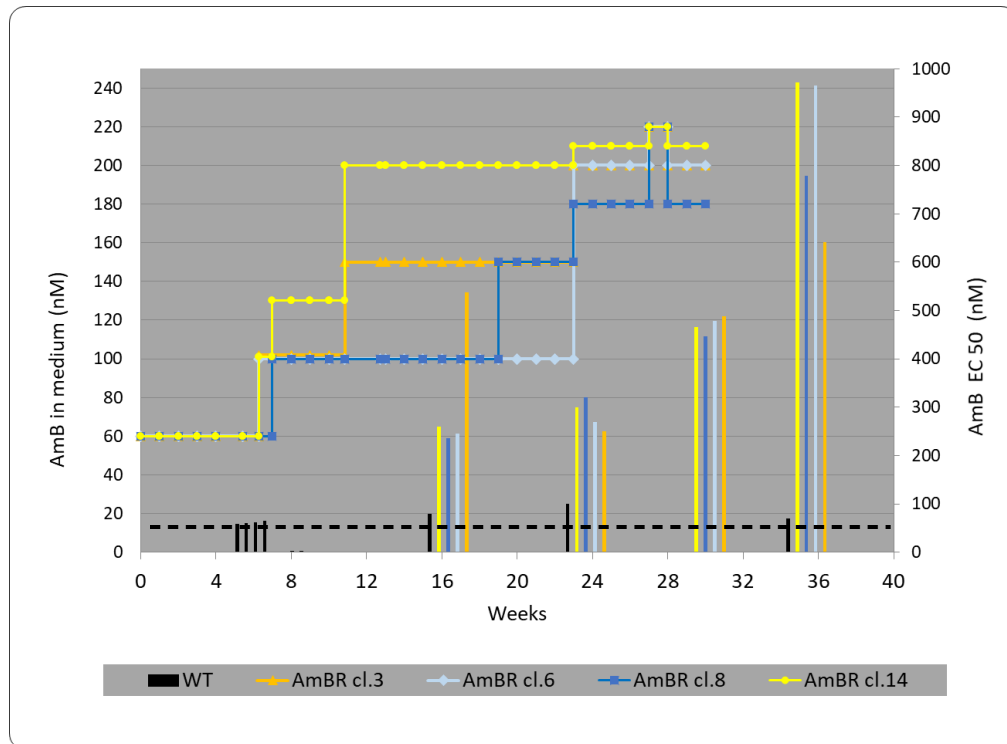


Figure 3-1. Selection of AmB resistance in *L. mexicana* promastigotes. The concentration of AmB in the culture medium was increased in a stepwise-manner with a starting density of 5×10^5 parasites per ml. The pipelines-like and left-hand y axis indicate the concentration of AmB (nM) added in the culture medium. The bars and right-hand y axis refer to the EC₅₀ values (mean of triplicates) of AmB attained by the four resistant lines at different times during the drug selection process as indicated by the x axis. The horizontal dotted line (black) indicates the mean EC₅₀ value of the parental wild type. Bars: Wild type (black). AmBRcl.14 (yellow). AmBRcl.3 (orange). AmBRcl.8 (dark blue). AmBRcl.6 (light blue).

Comparable fold changes to those found here have been reported in other AmB resistant *Leishmania* spp., including a clinical isolate of *L. donovani* that was 8-fold-higher (Purkait et al. 2012). Another strain of *L. tropica* attained a 16-fold resistance after only four months (Khan et al. 2016). In this study, the maximum fold change in all the AmBR lines of *L. mexicana* was between 11- to 12.7-fold change (see section 3.2.3.1) in resistance after eight months (Figure 3-1). Interestingly, the maximum concentration of AmB tolerated (i.e. added in the culture) by the resistant line of *L. tropica*, was 0.1 μg , which is comparable to the concentration added here ($\sim 1 \mu\text{M}$) in all AmBR lines of *L. mexicana*. The difference in the final fold change observed between these two species, is probably,

due to the difference in their initial EC₅₀ values for AmB (30 nM in *L. tropica* versus ~60 nM in *L. mexicana*). However, while concentrations of 0.2 µg per ml were not tolerated by the AmBR of *L. tropica* (Khan et al. 2016), concentrations as high as 0.2 µg, were added in the culture in all the AmBR of *L. mexicana*. In some lines (e.g. AmBRcl.14) these concentrations were well tolerated for a period of up to four months.

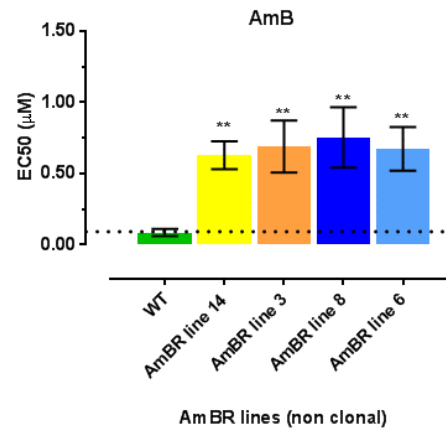


Figure 3-2. Susceptibility of AmBR lines before the selection of individual clones. Mean EC₅₀ values are shown in µM with their standard deviation (bars). Tukey's multiple comparison test measured pairwise differences between each resistant line compared with wild type. Statistically significant values ($P < 0.05$, 95% Confidence Interval) are shown with stars: * $P \leq 0.05$, ** $P \leq 0.01$, *** $P \leq 0.001$, **** $P \leq 0.0001$).

Individual clones were obtained from each independent line by limiting dilution (see chapter 2, section 2.3) and the EC₅₀ was measured in at least two clones per line. One clone (the highest EC₅₀) was selected from each line for downstream analysis (named AmBR cl.14, AmBR cl.8, AmBR cl.6 and AmBR cl.3). Retention of resistance was confirmed after sub-culturing all the selected clones for an additional 5 to 10 passages without drug pressure. Except for one clone of line 3 (cl.3E12), the mean EC₅₀ was very similar between clones obtained from the same line (see Table 3-1). As with the mean EC₅₀ observed in the four lines before the selection of clones, there was some variability in the mean EC₅₀ values between the four AmBR clones selected. However, the difference of the mean EC₅₀ between resistant lines and the parental wild-type was statistically significant either before (Figure 3-2) and after the selection of individual clones (Figure 3-5 and Table 3-2).

Table 3-1. Susceptibility to AmB and Nys of individual clones selected for resistance. AmBR and NysR individual clones from each independent line were selected by limiting dilution and those with the highest fold change (highlighted in bold and red) with respect their respective parental wild type (WT) were selected for further experiments. AmB clones are all from the same WT. NysR clones are from two wild types. Clones cl.B2 and cl.C1 are from WT HP, and clones cl.E1 and cl.F2 are from WT P0 (all WT are highlighted in grey). Except in those clones marked with star (*) which are from a single test, the EC₅₀ values show the mean \pm standard deviation (SD) of at least two biological replicates. I decided to include the SD from duplicates to indicate the variation from the mean, although this value of SD from duplicates is nonetheless, less powerful than with samples with a larger *N* size (e.g. this is considering 95% confidence level, Student *t* distribution with *n*-1 degree of freedom, and assuming normal distribution of the sample, in which the multiplicative factor is 12.71 when *n* = 2, instead of 1.96 when *n* = infinite). AmBR and NysR clones were tested for AmB and Nys, respectively. In the rest of this thesis, AmBR clones cl.14G4, cl.8A11, cl.6E10 and cl.3B12 correspond to names AmBR -cl.14, -cl.8, -cl.6 and -cl.3, respectively.

AmBR lines				NysR lines			
Clone	AmB EC ₅₀ (μM)	±SD	Fold Change	Clone	Nys EC ₅₀ (μM)	±SD	Fold Change
WT	6.24E-02	3.87E-03	-	WT HP	2.463	1.61E-06	-
cl.14B3	5.19E-01	2.30E-02	8.3	cl.B1 *	48.69	0.00E+00	19.7
cl.14G4	5.48E-01	7.79E-02	8.8	cl.B2 *	49.58	0.00E+00	20.1
cl.8A11	4.37E-01	7.07E-04	7	cl.C1 *	22.95	0.00E+00	9.3
cl.8E12	4.38E-01	9.83E-03	7	cl.C2 *	13.26	0.00E+00	5.3
cl.6E10	4.19E-01	1.67E-01	6.7	WT P0	1.909	7.27E-07	-
cl.6C3	3.57E-01	9.57E-02	5.7	cl.E1 *	23.08	0.00E+00	12.3
cl.3B12	3.78E-01	5.95E-02	6.1	cl.E2 *	22.54	0.00E+00	11.8
cl.3E12	2.19E-01	9.57E-02	3.51	cl.E3 *	22.96	0.00E+00	12
				cl.FA3 (F1)	11.93	1.19E-05	6.2
				cl.F F11 (F2)	13.72	1.38E-05	7.2
				cl.F H6 (F3)	12.88	1.31E-05	6.7

3.2.1.2 Nystatin resistant lines

Selection for resistance of four independent lines against nystatin (NysR) was also performed in *L. mexicana* M379 promastigotes using the same method described with AmBR lines (see 3.2.1.1). However, unlike the selection with AmB in which four lines were selected from a single parental wild type, two parental wild types were used to select resistance for nystatin. The first wild type was a low passage (named WT P0) recently recovered from mice infection and subculture *in vitro* for one or two passages. The other wild type was a high passage wild type (named WT HP) from axenic culture which had been previously maintained *in vitro* for at least 50 passages. Each wild type was selected with two different concentrations of drug (named low and high), thus resulting in a total of four Nystatin resistant lines.

The first concentration (high) was determined by the EC₅₀ and a stable growth comparable to the parental line cultured in parallel without drug, as described with AmBR. On the other hand, the second concentration (low) was between 25 to 50% lower than the high

concentration. NysR-B and NysR-C were from the high passage wild type (WT HP), and NysR-E and NysR-F were selected from the low passage wild type (WT P0). Regarding the drug concentration, NysR-B and NysR-E were maintained with high concentration of Nys, whereas NysR-C and NysR-F were selected with lower concentration of drug. The starting EC_{50} of Nys in the parental wild types was between 1.5 to 1.7 μM . All four NysR lines, including both wild types, which were cultured in parallel without drug, were maintained for the same number of passages (Figure 3-3).

In some assays, the level of resistance was correlated with the concentration of drug added in the culture. For instance, clones from lines NysR-C and NysR-F, which were maintained with lower concentration of Nys, attained a lower level of resistance than those from lines NysR-B and NysR-E (see Table 3-1). However, in subsequent tests, clones from line NysR-F showed comparable EC_{50} values to Nys as those lines selected with a higher concentration of drug, suggesting that other factors are involved in the development of resistance. This partial correlation between the concentration of drug and the degree of resistance was also observed in the cross-resistance to AmB in the same line NysR-F, and NysR-C (Figure 3-3, panels C and D). The highest concentration of Nys that was added to the culture medium at the time when drug selection was stopped, was around 12 μM . After one or two passages at this concentration, the amount of drug was reduced slightly in some lines (Figure 3-3, panel B) that showed signs of death cell (e.g. swollen or dark cells).

As the main interest of investigating Nys was to gain insight with regard the MoA of AmB as one of the main treatments for leishmaniasis, the development of cross-resistance against both polyenes was also monitored in parallel during the drug selection (Figure 3-3 Panels C and D). After 4 to 5 months selecting for Nys-resistance, lines attained comparable EC_{50} values of cross-resistance to AmB as those observed in the AmBR lines after 7 to 8 months. While the difference in the mean EC_{50} to AmB was significantly different than the parental wild type only in three lines (i.e. NysR-B, -C and -F), the difference in resistance developed to Nys was significant in all NysR lines (Table 3-3 and Figure 3-7).

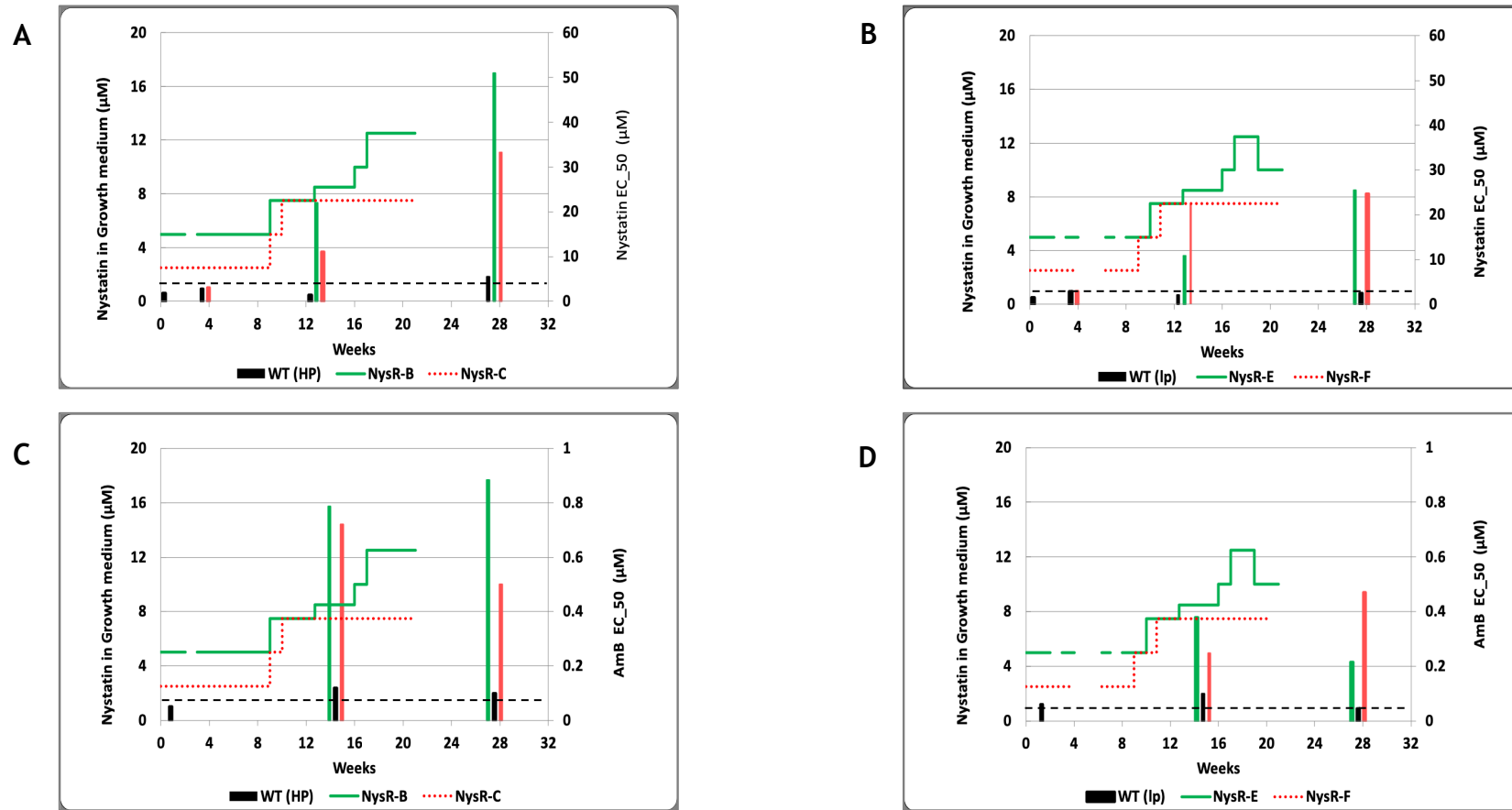


Figure 3-3 Selection of resistance to nystatin (NysR) in *L. mexicana* promastigotes and cross-resistance with AmB.

Left hand Y axis shows the concentration (µM) of drug added in the culture. Right hand Y axis shows the Nys EC₅₀ in µM (Panels A and B), and AmB EC₅₀ in nM (Panels C and D). Lines NysR-B and NysR-C were selected from a high passage wild type (WT HP), and lines NysR-E and NysR-F were selected from a low passage wild type (WT P0). The horizontal dotted lines (black) indicate the mean EC₅₀ values of the parental wild types.

As with AmBR lines, individual clones were also selected following the same protocol (limited dilution) described with AmBR lines. Similarly, the retention of the resistant phenotype *in vitro* was confirmed after an additional 5 to 10 passages without drug. Unlike AmBR clones, in which little variation between clones from the same line was observed, higher differences were observed between some clones obtained from the same line, possibly because the concentration of drug added to the culture medium attained during the drug selection was also more heterogeneous (to analyse the effect between high and low concentrations, as described before) than with the AmBR lines. Finally, the four most resistant clones (one from each line) were selected for further analysis (named NysRcl.B2 NysRcl.C1 NysRcl.E1 and NysRcl.F2). The fold change in EC₅₀ of the selected clones in comparison with their respective wild type was between 5- to 20-fold at the time of being selected by limiting dilution (Table 3-1). However, the maximum fold change observed in subsequent tests was between 7- to 11-fold (Figure 3-8).

3.2.2 Growth rate of polyene resistant promastigotes.

The growth of the polyene resistant lines was assessed and the presence of the different stages was assessed as described for *L. mexicana* wild-type promastigote (Bates and Tetley 1993) and in chapter 2 (section 2.1). In general, no changes were observed in Haemoflagellate-modified minimal essential medium (HOMEM) medium (<https://www.bioz.com/Gibco>). Parasites of both, AmBR and NysR lines showed growth with a typical S-shape curve consisting of a log-phase during the first 72 hours, and a stationary phase from day four, and onwards. As shown in Figure 3-4 (Panels A and C), during the stationary phase, all AmBR and NysR clones achieved densities of 1.0 - 1.5 x 10⁷ comparable to their respective wild types, no-significant difference between their means (ANOVA, P= 0.9983). However, NysRcl.B2 and NysR.cl.C1 (Figure 3-4 Panel B) showed a reduced growth during log phase (between 48- and 72 hours) which was statistically different than in the parental wild type WT HP (Two-way ANOVA, P=0.0005 and P<0.0001, respectively). As parasites were selected for resistance in this medium (HOMEM), therefore, the selection for resistance against both polyenes showed no significant effects on the growth of the resistant lines. Growth of AmBR clones was assessed in parallel in Defined Medium (DM) (see Chapter 2; PhD Thesis Raihana Binti, unpublished), a medium without foetal bovine serum (FBS) and lacking other macromolecules, which was engineered to grow *Leishmania* and avoiding variations due to the serum components between batches, among other additional advantages, such as reducing costs of medium (Ali, Ahmad, and Masoom 1998; Merlen et al. 1999).

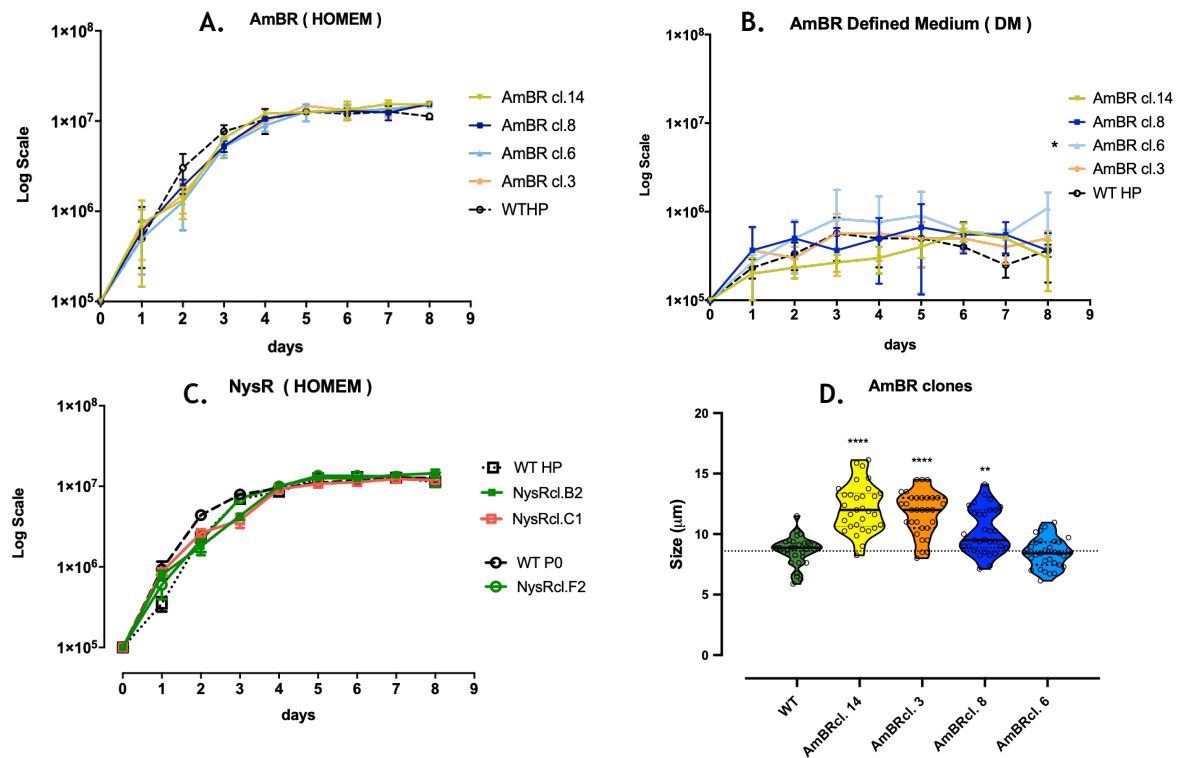


Figure 3-4. Culture and growth rate and size of polyene resistant lines of *L. mexicana* promastigotes in HOMEM and Defined Medium (DM). Cell density of the procyclic promastigote stage was measured every 24 hours for 8 days using the haemocytometer. Starting density of 1×10^5 cells/ml. Panel A. AmBR in HOMEM, Panel B. AmBR in Defined Medium (DM) and Panel C. NysR in HOMEM. Measurements are the median of three biological replicate, bars represent standard deviation. Panel D. Violin plot of the mean size of the resistant lines is shown in μm . The central continuous line within each coloured plot represents the median value of each group. The cell body length was measured from the base of the flagellum until the posterior endpoint of the cell body of promastigotes in the stationary phase. Data were processed with ImageJ software and represent the measurements of at least 30 cells (empty circles). In all Panels, mean values are shown with their standard deviation (bars). Tukey's multiple comparison test was used to find pairwise differences between resistant lines and parental wild type. Statistically significant values ($P < 0.05$, 95% Confidence Interval) are indicated with stars as follows: * $P \leq 0.05$, ** $P \leq 0.01$, *** $P \leq 0.001$, **** $P \leq 0.0001$).

In DM, all of the AmBR lines tested, including the parental wild type, no log phase was observed, and the highest density attained remained below 1.5×10^6 until day 8. However, in line AmBRcl.6, the mean value of growth was significantly higher than in the wild type (Tukey's Test, $P=0.0191$). The distributions of cell body length are shown in Figure 3-4 Panel D. Overall, the range of the cell body length was very similar to those values (6 - 12 μm) described by Wheeler, Gluenz and Gull, 2011. Interestingly, while AmBRcl.6 was the only resistant line with similar cell body length as wild type with mean values of 8.4 μm and 8.6 μm , respectively ($P=0.9814$), AmBRcl.14, AmBRcl.8 and AmBRcl.3 showed a wider distribution of size (7 to 16 μm) with significant difference in comparison with wild type ($P < 0.001$). Similarly, the mean values (8.4 - 12 μm) of the flagellum length in all

resistant lines and wild type, were between the range (5 – 13 μm) reported before in *Leishmania mexicana* promastigotes (Richard J. Wheeler, Gluenz, and Gull 2011).

3.2.3 Drug screening of polyene-resistant lines

After confirmation of resistance, a total of eight polyene-resistant lines of *L. mexicana* (four AmBR and four NysR) were screened for the presence of cross-resistance against a broad range of compounds, including anti-leishmanials, some inhibitors of the synthesis of sterols, such as imipramine (Andrade-Neto, Pereira, Do Canto-Cavalheiro, et al. 2016), and other tricyclic antidepressants (TCA). A full list of the mean EC_{50} values of all the compounds screened in both, AmBR and NysR lines, is shown in Table 3-2 and Table 3-3, respectively. Similarly, fold-changes with respect to their parental wild types is shown for all compounds in Figure 3-6 and Figure 3-8. Additionally, two clones from each polyene (AmBRcl.14 and AmBRcl.8, and NysRcl.B2 and NysRcl.E1) were tested against a library of a new class of inhibitors active in *Leishmania* spp. (chapter 6).

3.2.3.1 Cross-resistance between polyenes

While cross-resistance to other compounds was heterogeneous, all AmBR and NysR clones were cross-resistant to AmB, Nys, and to a lesser extent, to the small polyene Natamycin (NMC). Cross-resistance between polyenes was expected, as polyene antifungals possess a similar MoA, with minor differences (Serhan et al. 2014), for instance, NMC has been reported to have the advantage of the lack of resistance (Welscher, et al. 2008; 2010). In general, AmBR clones were between 11- to 12.7-fold resistant to AmB. Similarly, NysR lines were between 7- to 11-fold resistant to Nys, although in the latter, resistance developed in less time. While no difference in resistance to AmB ($P > 0.9999$), and Nys ($P > 0.997$), was observed between the high passage (WT HP) and the low passage (WT P0) wild types, clones NysRcl.E1 and NysRcl.F2, selected from the latter, attained lower fold change (6.6- to 7.7-fold) in comparison with those from the WT HP (7.4- to 11-fold). This difference was significant when compared with the clone NysR.cl.B2 ($P < 0.01$). Interestingly, cross-resistance between AmB and Nys increased in a similar fashion (between 10- to 20-fold). In contrast with this, cross-resistance to NMC was around ten times lower (i.e. 1.7- to 2-fold) in AmBR lines (NMC was not tested in NysR lines), possibly due to the structural differences between this small polyene in comparison with AmB and Nys (de Souza and Rodrigues 2009b), which are both large polyenes (Te Welscher et al. 2010).

3.2.3.2 Susceptibility to other anti-leishmanials

For MF, NysRcl.B2 was the only line with mild increase in susceptibility, by contrast, all the other polyene resistant lines were cross resistant to MF, with a fold change up to three times higher in the AmBR lines than in the NysR lines (5- to 10-fold versus 2- to 3.7-fold, respectively). Moreover, AmBRcl.8 and AmBRcl.6 lines were twice less sensitive than the other two AmBR lines, AmBRcl.14 and AmBRcl.3. Although the uptake of MF was not determined in this study, the changes found in the MF transporter (MT) gene (LmxM.13.1530) in AmBRcl.8 and AmBRcl.6, can account for this difference in susceptibility (see chapter 4, section 4.1.2, Figure 4-3). On the other hand, no change (deletion or mutations) in the MT, was identified in AmBRcl.14 and AmBRcl.3, which were between 5.37- to 5.48-fold cross resistant to MF, possibly, derived from the alteration of the sterols, i.e. increase of ergosta-7,22-dien-3-ol (96.7%), in these two lines (see chapter 5, Table 5-1). Interestingly, a comparable increase in cross resistant to MF (2.2- to 3.7-fold), was also observed in the two NysR clones, NysR.cl.E1 and NysR.cl.F2, which sterols profile resembled that observed in AmBR lines 14 and 3 (chapter 5, Table 5-3). The other two clones, NysR.cl.B2 and NysR.cl.C1, were between 3 to 4 times less resistant to MF, however, the difference in the EC₅₀ with their respective wild type lines, was statistically significant for MF (P=0.0004). Changes at the gene level were not analysed in none of the NysR lines, as time did not permit.

Comparable increase in resistance to MF (~3.8-fold) was reported in a line of *L. infantum*, selected for resistant to AmB, with a SNP in the MT (Fernandez-Prada et al. 2016). In the study of Pountain et al., in which four lines were selected in parallel for AmB, only one line, AmBRB/cl2, showed cross resistance to MF (2.3-fold), while the other three lines were MF-hypersusceptible. The low increase in MF resistance in the former, is somehow surprising, given that this line showed a complete deletion of the MT (Pountain et al. 2019a). Contrary to the study of Pountain et al., the study of Fernandez and colleagues, and another study in *L. donovani*, showed a 13.2- and 13.7-fold increase, respectively, in resistance to MF (Fernandez-Prada et al. 2016; Pérez-Victoria et al. 2006), this increase is in agreement with the fold change observed in my study with lines AmBRcl.8 and AmBRcl.6. Altogether, these studies show that MF resistance is associated with both, mutations (SNPs), and with the complete deletion of the MT, which derived from selection in vitro to either, MF or AmB.

For PAT, significant increase in susceptibility was observed for NysRcl.B2, with no change in any other line. The only change observed with any of the anti-leishmanials

tested, that was consistent across all polyene resistant lines was the significant higher susceptibility to PAR and to PENT. The greatest degree of susceptibility was observed in AmBR lines in comparison to the NysR lines. Moreover, some AmBR lines with the highest levels of resistance to AmB and Nys, were also more susceptible to PENT and to PAR. This negative correlation between AmB resistance and increase susceptibility to PENT seems to be universal. For instance, a line of *L. mexicana* was 23-fold resistant to AmB and decreased its EC₅₀ values to PENT by 13.3-fold (Mwenechanya et al. 2017).

Another resistant line of *L. donovani* showed 18.9- and 0.52-fold change for AmB and PENT, respectively (Mbongo et al. 1998a). Equally, in four AmBR clones, those with the highest fold change to AmB (between 8 to 10-fold) were also the most sensitive to PENT (from 0.2 to 0.10-fold change) whereas the two lines with lower resistance levels (3 to 5-fold) showed a decrease in their EC₅₀ to 0.24-fold (Pountain et al. 2019a). Although the differences in EC₅₀ values in the NysR lines were smaller, in all cases the difference with respect their parental wild type was significant. However, while there was no difference in the mean EC₅₀ between wild types (low and high passage) for PAT (P=0.8799), EC₅₀ values between both wild types were significantly different for PAR (P=0.0488) and PENT (P=0.0007). This increased susceptibility to PENT was also observed in all the NysR lines (between 1.7- to 2-fold, P= 0.0041 and 0.0168), and 3- to 3.8-fold (P<0.0001) for the resistant lines derived from the high and low passage wild types, respectively (Table 3-3).

3.2.3.3 Susceptibility to other sterol inhibitors

We assessed the susceptibility to inhibitors of other enzymes in the sterol pathway. Azoles (ketoconazole) inhibit the enzyme lanosterol 14- α demethylase (C14DM, LmxM.11.1100) (Emami, Tavangar, and Keighobadi 2017; De Macedo-Silva et al. 2013; W Xu et al. 2014) and fenarimol, has also been shown to interfere with the sterol synthesis by inhibiting C14DM (Choi et al. 2014; Zeiman et al. 2008). No significant changes were observed in susceptibility to ketoconazole (Keto) or fenarimol, although lines AmBR.cl14 and AmBR.cl.3 were slightly more sensitive to these two compounds than AmBR.cl8 and AmBR.cl.6.

Other compounds included in the screening were the tricyclic antidepressants (TCA) imipramine (IMI), clomipramine, mianserin and ketanserin. TCAs have been found to inhibit the synthesis of sterols, targeting the C-24-sterol methyltransferase (C24SMT, LmxM.36.2380 and LmxM.36.2390) (Andrade-Neto, Pereira, Do Canto-Cavalheiro, et al. 2016) and the 3-hydroxy-3-methylglutaryl-CoA synthase (HMG-CoA, LmxM.24.2110) (Brooks et al. 2012; Singh et al. 2014). In general, all lines showed mild resistance against

all these compounds. Mianserin was the only TCA with higher susceptibility in AmBRcl.14 and AmBRcl.3, but no statistical difference was observed. Susceptibility against a series of sterol inhibitors from a new library, 1,2,3-triazolyl sterols (TAZ), in AmBR lines (Figure 3-5) is discussed in more detail in chapter 6.

3.2.3.4 Agents inducing oxidative stress

AmB is known to induce oxidative stress (Anderson et al. 2014; Gray et al. 2012), for this reason, we tested the susceptibility of all the AmBR lines to methylene blue (MB). MB, also known as methylthionine hydrochloride or 3,7-bis(dimethylamino)phenothiazin-5-ium chloride (Buchholz et al. 2008), induces oxidative stress inside the cell by producing oxidised NADP⁺ from NADPH, thus stimulating the oxidation of glutathione (Kelner and Alexander 1985) and therefore can be utilised as REDOX indicator (Farjami et al. 2010). Interestingly, as with the antileishmanials PAR and PENT, MB also showed a significant increase in susceptibility which was consistent across all AmBR lines, with fold changes between 3- to 6.7-fold with respect the parental line. This higher susceptibility to oxidative stress inducing agents suggests that the reducing capacity is altered in AmBR *Leishmania*. MB susceptibility was not determined in none of the NysR lines neither in their parental wild types.

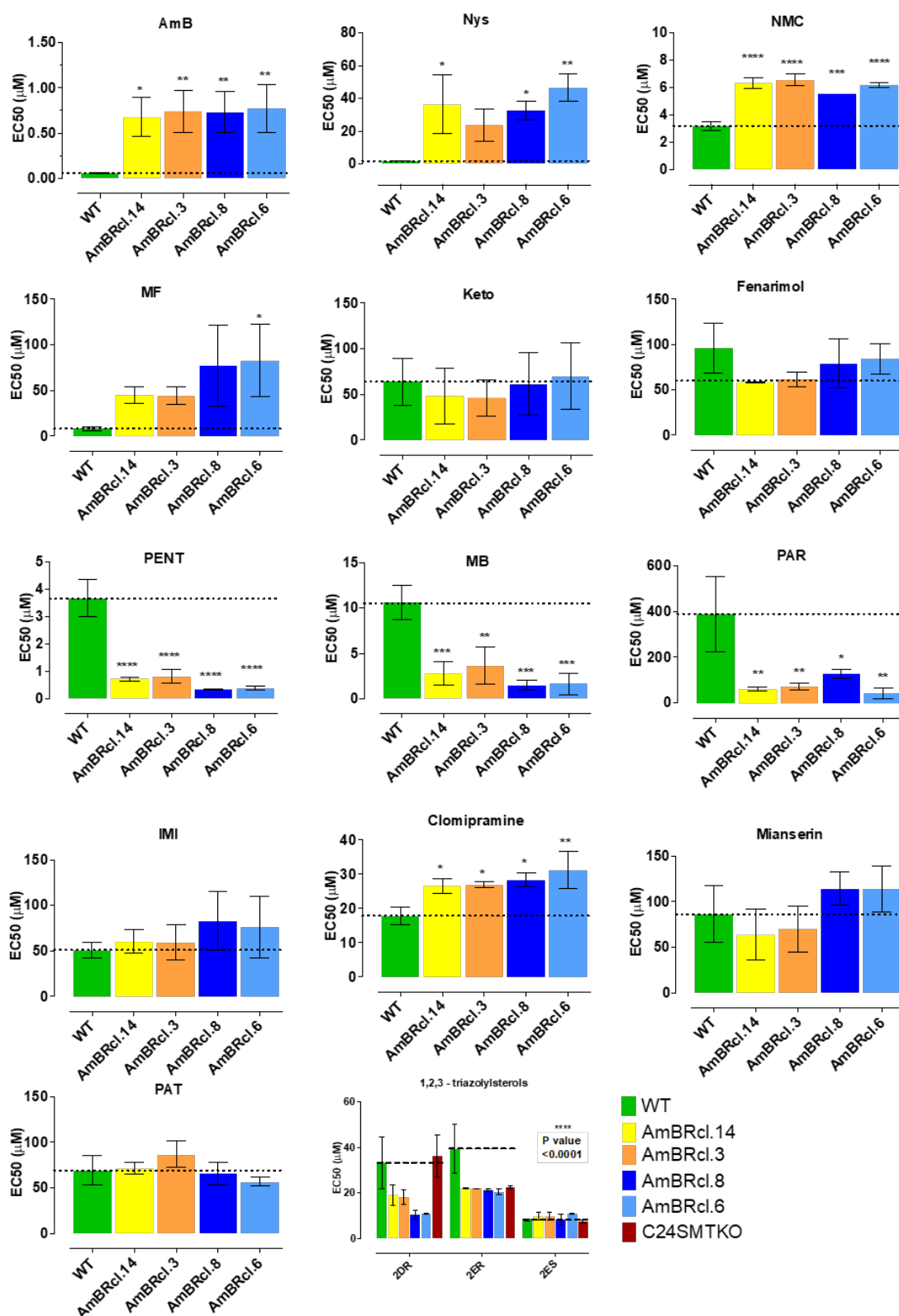


Figure 3-5. Susceptibility of AmBR lines of *L. mexicana* against different inhibitors. Mean EC₅₀ values are shown in µM with their standard deviation (bars). Tukey's multiple comparison test was used to find pairwise differences between resistant lines compared with the parental wild type. Statistically significant values ($P < 0.05$, 95% Confidence Interval) are shown with stars: * $P \leq 0.05$, ** $P \leq 0.01$, *** $P \leq 0.001$, **** $P \leq 0.0001$). Abbreviations of AmBR lines and compounds is similar to that written in the text. C24SMTKO: C24-sterol methyl transferase knockout (see section 2.8.4, and Chapter 6 for a full description / screening of this line).

Table 3-2. Susceptibility of AmBR lines and clones (*L. mexicana*) to a series of compounds. Values in μM , Mean \pm Standard Deviation (SD). One-way ANOVA was performed independently for each compound to determine differences of the mean between groups. Tukey's multiple compared pairwise differences of resistant lines with respect the parental wild type. Except for NMC tested in AmBRcl.8, values are from at least three biological replicates. Statistical difference ($P < 0.05$, 95% Confidence Interval) is shown with stars as follows: ns non-significant or $P > 0.05$; * $P \leq 0.05$; ** $P \leq 0.01$; * $P \leq 0.001$; **** $P \leq 0.0001$. Abbreviations of compounds are as in the rest of the text. MB: methylene blue.**

AmBR non-clonal		WT	AmBR line 14	AmBR line 3	AmBR line 8	AmBR line 6	ANOVA P value
AmB	Mean \pm SD P value	0.085 \pm 0.0246	0.6283 \pm 0.0982 0.0087 **	0.6893 \pm 0.183 0.0042 **	0.7536 \pm 0.212 0.0020 **	0.6731 \pm 0.153 0.0051 **	0.0017 **
AmBR clones		WT	AmBRcl.14	AmBRcl.3	AmBRcl.8	AmBRcl.6	ANOVA P value
AmB	Mean \pm SD P value	0.06 \pm 0.004	0.6747 \pm 0.216 0.0327 *	0.7402 \pm 0.234 0.0182 *	0.7297 \pm 0.228 0.02 *	0.7682 \pm 0.264 0.0142 *	0.0095 **
NMC	Mean \pm SD P value	3.161 \pm 0.328	6.454 \pm 0.496 <0.0001 ****	6.585 \pm 0.414 <0.0001 ****	5.524 \pm 0 0.0002 ***	6.167 \pm 0.161 <0.0001 ****	<0.0001 ****
Nys	Mean \pm SD P value	1.829 \pm 0.101	36.49 \pm 17.77 0.0124 *	23.75 \pm 9.609 0.1326 ns	32.68 \pm 5.809 0.0251 *	46.36 \pm 8.366 0.0022 **	0.0032 **
Ketoconazole	Mean \pm SD P value	64.01 \pm 25.58	48.49 \pm 30.79 0.9652 ns	46.05 \pm 19.9 0.9424 ns	61.53 \pm 33.79 >0.9999 ns	70.2 \pm 36.09 0.9989 ns	0.8292 ns
Fenarimol	Mean \pm SD P value	96.12 \pm 27.49	58.22 \pm 0.227 0.1852 ns	61.83 \pm 7.84 0.2561 ns	79.05 \pm 27.15 0.8065 ns	84.34 \pm 16.59 0.9381 ns	0.1629 ns
MF	Mean \pm SD P value	8.29 \pm 2.13	45.43 \pm 9.292 0.4912 ns	44.55 \pm 10.01 0.5126 ns	76.87 \pm 44.46 0.069 ns	83.13 \pm 39.29 0.0446 *	0.0446 *
PAR	Mean \pm SD P value	390.2 \pm 164.7	61.12 \pm 7.888 0.0023 **	71.91 \pm 16.61 0.003 **	126.5 \pm 19.87 0.0108 *	41.11 \pm 23.14 0.0015 **	0.0011 **
PAT	Mean \pm SD P value	69.14 \pm 15.95	71 \pm 6.371 0.9996 ns	86.6 \pm 14.43 0.4001 ns	65.78 \pm 11.9 0.996 ns	56.6 \pm 4.912 0.6818 ns	0.0955 ns
PENT	Mean \pm SD P value	3.659 \pm 0.681	0.7203 \pm 0.08 <0.0001 ****	0.8212 \pm 0.261 <0.0001 ****	0.3363 \pm 0.016 <0.0001 ****	0.3826 \pm 0.079 <0.0001 ****	<0.0001 ****
IMI	Mean \pm SD P value	51.09 \pm 8.701	60.36 \pm 13.26 0.9875 ns	59.47 \pm 19.64 0.9914 ns	83.01 \pm 31.77 0.5004 ns	76.24 \pm 33.94 0.6961 ns	0.4867 ns
Mianserin	Mean \pm SD P value	86.2 \pm 31.06	63.95 \pm 28.13 0.8275 ns	70.14 \pm 25.05 0.9372 ns	114.6 \pm 18.56 0.6764 ns	113.8 \pm 25.42 0.6959 ns	0.1084 ns
Clomipramine	Mean \pm SD P value	17.81 \pm 2.586	26.46 \pm 2.098 0.0372 *	26.87 \pm 0.86 0.0288 *	28.37 \pm 2.062 0.0114 *	31.17 \pm 5.496 0.0022 **	0.0035 **
MB	Mean \pm SD P value	10.58 \pm 1.881	2.815 \pm 1.312 0.0006 ***	3.639 \pm 2.024 0.0014 **	1.469 \pm 0.564 0.0002 ***	1.619 \pm 1.199 0.0002 ***	0.0001 ***

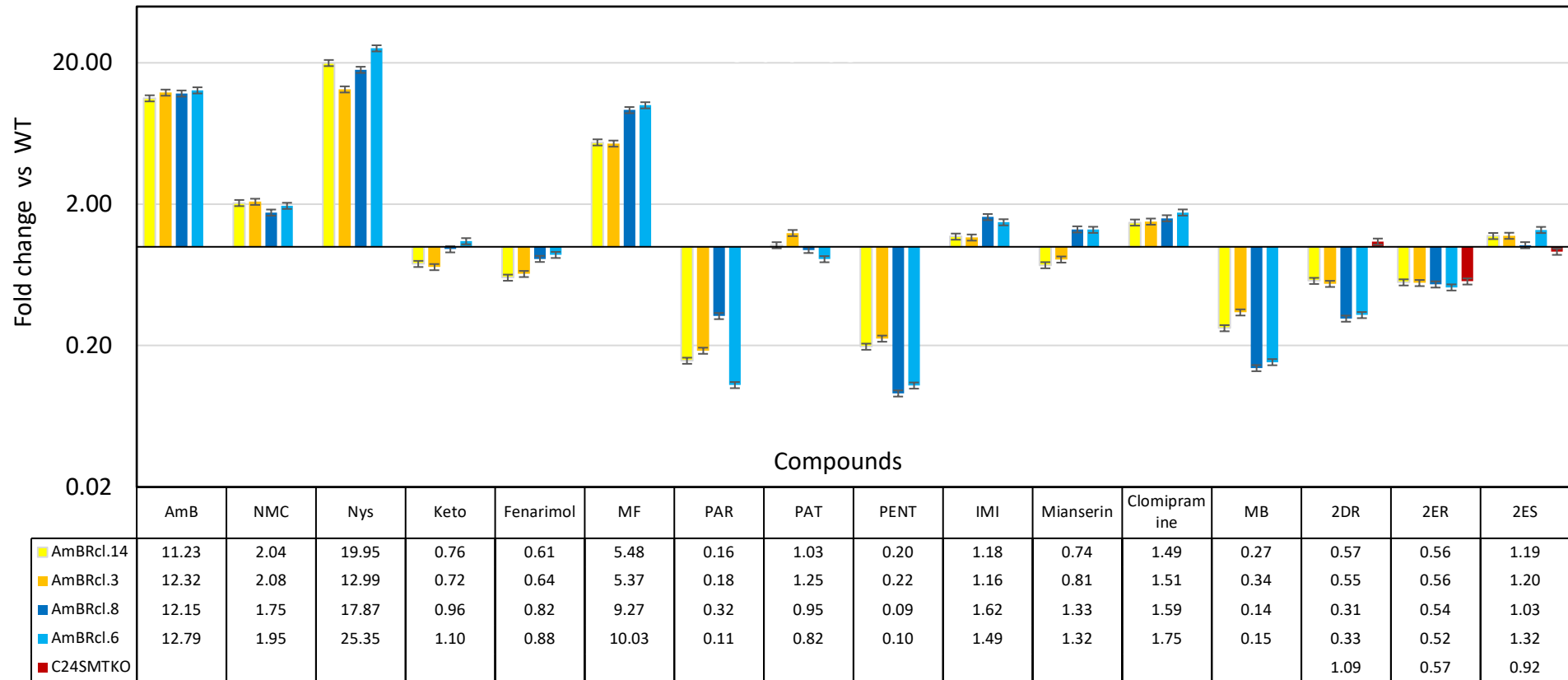


Figure 3-6. Fold changes to a series of compounds of AmBR clones compared with the parental wild type. Fold changes in EC_{50} in comparison with the parental wild type cultured in parallel without drug. Bars indicate the standard deviation expressed as percentage (5%) of the fold change. Compounds abbreviations are as in the rest of the text, except for MB-methylene blue, keto-ketoconazole, and 2DR, 2ER and 2ES are 1,2,3-triazolyl sterols (see chapter 6). C24SMTKO – C24-sterol methyl transferase double KO. Statistical differences are shown in Table 3-2. Values higher and lower than 1, indicate resistance and higher susceptibility, respectively.

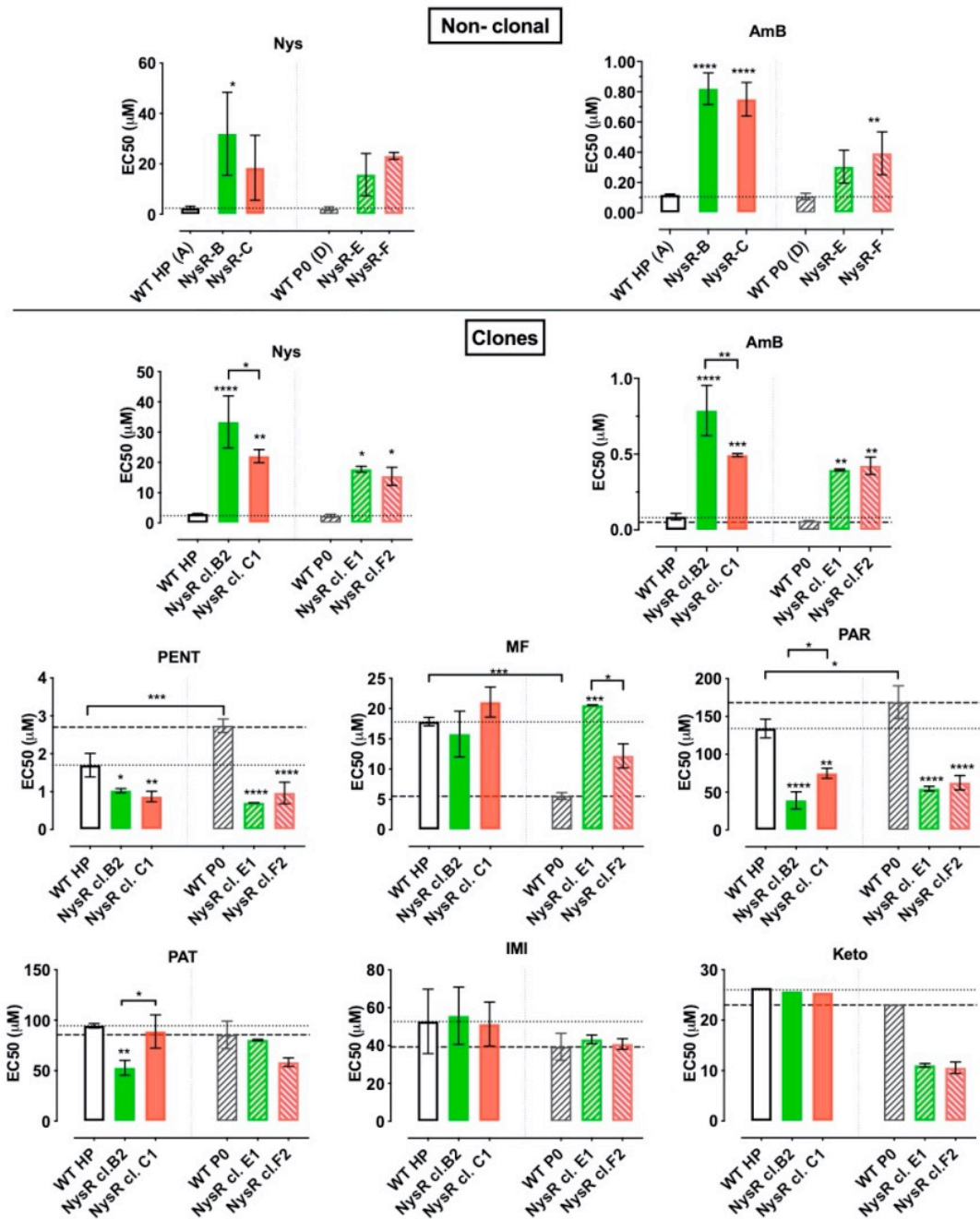


Figure 3-7. Susceptibility of NysR lines of *L. mexicana* to different inhibitors. Mean EC₅₀ values (µM) are shown with their standard deviation (bars). Vertical dotted black lines denote groups of clones related with their respective parental wild type as follows: Clones cl.B2 and cl.C1 are grouped with the parental wild type WT HP (wild type high passage). Clones cl.E1 and cl.F2 are grouped with the parental wild type WT P0 (low passage). Horizontal dotted black lines denote the mean of each wild type. Tukey's multiple comparisons test was used to identify pairwise differences of resistant lines in relation with their respective parental line. Statistically significant values ($P < 0.05$, 95% Confidence Interval) are shown with stars: * $P \leq 0.05$, ** $P \leq 0.01$, *** $P \leq 0.001$, **** $P \leq 0.0001$). Abbreviations of AmBR lines and compounds is similar than in the text.

Table 3-3. Selectivity of NysR lines (*L. mexicana*) to antileishmanials, and other compounds.

Values are shown in μM , Mean \pm Standard Deviation (SD). One-way ANOVA test was performed independently for each compound to determine the difference of the mean between groups. Tukey's multiple comparison was used to identify pairwise differences with respect the parental wild type (WT). Lines B and C, and clones cl.B2, cl.C1 were compared with the parental WT HP. Lines E and F, and clones cl.E1 and cl.F2 are compared with the parental WT P0. Values are from at least three biological replicates. Statistically significant difference ($P < 0.05$, 95% Confidence Interval) is shown with stars as follows: ns non-significant or $P > 0.05$; * $P \leq 0.05$; ** $P \leq 0.01$; *** $P \leq 0.001$ and **** $P \leq 0.0001$. Abbreviations of compounds are as in the rest of the text.

NysR Non-clonal		WT HP (A)		NysR- B		NysR- C		WT P0 (D)		NysR- E		NysR- F		ANOVA P value
Nys	Mean \pm SD	2.492	\pm 0.687	31.94	\pm 16.48	18.45	\pm 12.88	2.205	\pm 0.713	15.77	\pm 8.386	23.13	\pm 1.389	0.0120 *
	P value			0.0198	*	0.3398	ns			0.5001	ns	0.1296	ns	
AmB	Mean \pm SD	0.118	\pm 0.0048	0.82	\pm 0.1049	0.7505	\pm 0.1114	0.1081	\pm 0.0215	0.304	\pm 0.1089	0.3928	\pm 0.1419	<0.0001 ****
	P value			<0.0001	****	<0.0001	****			0.089	ns	0.0064	**	
Nys R Clones		WT HP		NysR cl. B2		NysR cl. C1		WT P0		NysR cl. E1		NysR cl. F2		ANOVA P value
Nys	Mean \pm SD	2.973	\pm 0.156	33.37	\pm 8.624	22.09	\pm 2.157	2.338	\pm 0.5292	17.77	\pm 0.9717	15.42	\pm 2.975	<0.0001 ****
	P value			<0.0001	****	0.0026	**			0.0316	*	0.0449	*	
AmB	Mean \pm SD	0.087	\pm 0.021	0.7878	\pm 0.1662	0.494	\pm 0.0106	0.058	\pm 0.0017	0.3962	\pm 0.0062	0.4231	\pm 0.058	<0.0001 ****
	P value			<0.0001	****	0.0003	***			0.0017	**	0.0022	**	
Ketoconazole	Mean \pm SD	26.39	\pm 0	25.72	\pm 0	25.48	\pm 0	23.12	\pm 0	11.07	\pm 0.3465	10.56	\pm 1.143	0.0085 **
	P value			0.9849	ns	0.9522	ns			0.025	*	0.0237	*	
MF	Mean \pm SD	17.85	\pm 0.704	15.79	\pm 3.787	21.08	\pm 2.483	5.564	\pm 0.565	20.58	\pm 0.0636	12.2	\pm 1.987	<0.0001 ****
	P value			0.8434	ns	0.4885	ns			0.0002	***	0.059	ns	
PAR	Mean \pm SD	134.1	\pm 12.3	39.19	\pm 11.31	74.84	\pm 6.668	168.8	\pm 21.65	54.49	\pm 3.159	62.49	\pm 9.397	<0.0001 ****
	P value			<0.0001	****	0.0012	**			<0.0001	****	<0.0001	****	
PAT	Mean \pm SD	94.52	\pm 2.275	52.9	\pm 7.327	88.93	\pm 16.48	85.5	\pm 13.65	80.44	\pm 0.6505	58.36	\pm 4.299	0.0034 **
	P value			0.0054	**	0.9818	ns			0.9929	ns	0.1191	ns	
PENT	Mean \pm SD	1.698	\pm 0.312	1.026	\pm 0.0546	0.8697	\pm 0.138	2.739	\pm 0.179	0.7059	\pm 0.0042	0.965	\pm 0.285	<0.0001 ****
	P value			0.0168	*	0.0041	**			<0.0001	****	<0.0001	****	0.0007 ***
IMI	Mean \pm SD	52.79	\pm 17	55.78	\pm 15.18	51.35	\pm 11.63	39.36	\pm 7.125	43.28	\pm 2.284	40.86	\pm 2.835	0.4425 Ns
	P value			0.9994	ns	>0.9999	ns			0.9978	ns	>0.9999	ns	

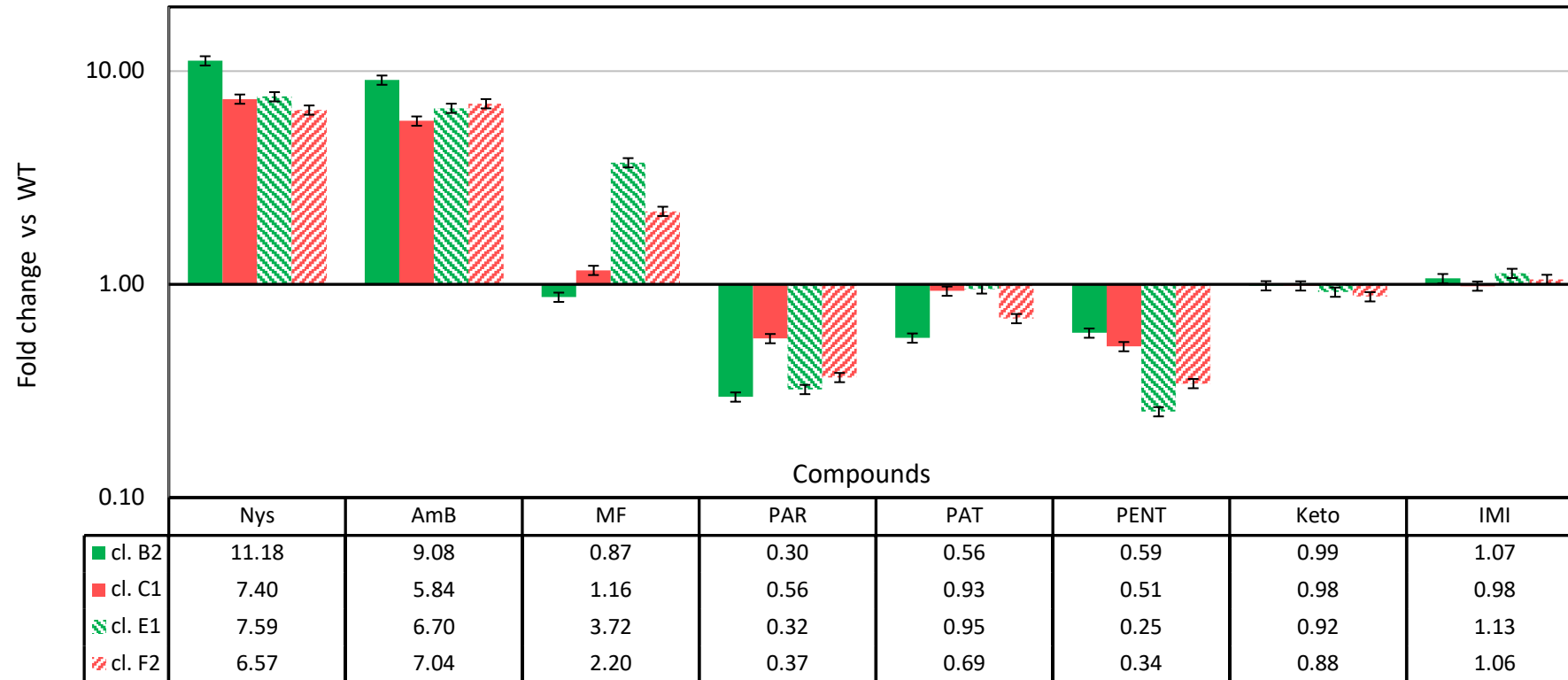


Figure 3-8. Fold changes of NysR clones to a series of compounds.

Fold change in EC_{50} in comparison with their parental wild type cultured in parallel without drug. Lines B and C, and clones cl.B2, cl.C1 were compared with the parental WT HP. Lines E and F, and clones cl.E1 and cl.F2 are compared with the parental WT P0. Bars indicate the standard deviation expressed as percentage (5%) of the fold change. Compounds abbreviations are as in the rest of the text, except for keto-ketoconazole, and IMI-imipramine. Statistical differences are shown in Table 3-3. Values higher and lower than 1, indicate resistance and susceptibility, respectively.

3.3 Discussion

Profiling cross-resistance in either field isolates or laboratory generated resistant lines, has been proven to be an informative tool towards the understanding on the molecular MoA and resistance in *Leishmania*, moreover, screening a diverse number of molecules with similar structures, can help to differentiate the importance of other chemical groups related with their potency. Here, I have identified reciprocal cross resistance between AmB- and Nys resistant mutants selected in vitro. First, both methods of drugs selection were performed during comparable period of time between 6 and 9 months. Selection for resistance using nystatin, resulted in comparable EC₅₀- and fold change final values, irrespective of the EC₅₀ (micromolar range in wild type) of this polyene, is higher than its counterpart AmB, which is in the sub-micromolar or nanomolar order. Contrary to this, natamycin (a small polyene), which chemical structure and MoA is more different than that of these two polyenes, the highest increase observed was around 2-fold in AmBR lines (note that I could not get reliable numbers of EC₅₀ with NMC in NysR lines). With the exception of NysRcl.B2, all polyene resistant lines were MF resistant, with a higher increase in those two lines (AmBRcl.8- and 6), in which the loss of the MT was identified using NGS analysis. Interestingly, two antileishmanials, PAR and PENT, were more potent in all resistant lines. While the mechanism of this in PAR is unclear, the increased susceptibility observed with PENT is more probably related with the oxidative stress induced by this compound, as confirmed with MB, another oxidative stress inducer. The oxidative stress induced by AmB has been previously reported in *Leishmania*, in my study, I have identified changes in metabolites such as upregulation of the PPP and other metabolites of the PTP, both which are related with the ability of *Leishmania* to detoxify ROS. Interestingly, both lines with the loss of the MT (and other changes in C24SMT), were more sensitive to the both PENT and MB, and another sterol inhibitor (2DR) that has never been studied (a more detailed analysis of the complete library of these new sterol inhibitors is discussed in chapter 6), than the other two AmBR lines. On the other hand, these two lines were more resistant (than AmBRcl.14 and 3) to IMI, a tricyclic antidepressant that has been reported to inhibit C24SMT, although these differences were marginal. The increased susceptibility towards PENT and MB, is in agreement with previous studies in another eight independent AmBR lines, previously characterised within the Barrett Lab, and are strong evidence of the usefulness of PENT (and other oxidative stress drugs) should the emergence of resistance against AmB emerge in the field, however, further studies on this are necessary. To further support this, a similar increase in susceptibility was observed in all four NysR lines characterised in this study.

4 Characterization of polyene resistant lines of *Leishmania mexicana*: whole genome sequencing

4.1 Results

Enzymes of the sterol pathway that have been found to be related with AmB resistance in fungi are C14DM (Martel, *et al.*, 2010 a; Xiang *et al.*, 2013), C-8 sterol isomerase (C8SI) in *S. cerevisiae* and *C. albicans* (Kelly *et al.*, 1994), and C5-sterol desaturase (C5DS) (Martel, *et al.*, 2010 b) and C-22 sterol desaturase in *C. albicans* (Martel, *et al.*, 2010 a; Sun *et al.*, 2013). Similarly, in *Leishmania* spp., examples of enzymes related with AmB resistance are, the 3-hydroxy-3-methylglutaryl-CoA synthase (Brooks *et al.* 2012), C14DM (Mwenechanya *et al.* 2017), C-24-sterol methyltransferase (C24CSMT) (Jiménez-Jiménez *et al.*, 2008; Cosentino and Agüero, 2014; Viana Andrade-Neto *et al.*, 2016; Rastrojo, *et al.*, 2018; Pountain *et al.*, 2019), and C5DS (Pountain *et al.* 2019). In this chapter, I describe mutations, and other genomic alterations, identified in four AmBR clones. Moreover, these mutations were correlated with alterations in the sterol profile in these mutants similar to those described in other lines with an AmB resistant phenotype (Al-Mohammed *et al.* 2005; Mbongo *et al.* 1998; Purkait *et al.* 2014), and their virulence *in vivo* (see chapter 5), and changes in other metabolites (chapter 7).

The library and sequencing were performed at Glasgow Polyomics facility (<https://www.polyomics.gla.ac.uk/>). Whole Genome Sequencing and preparation of libraries of DNA were performed by Dr David McGuinness and run as paired ends with a length of 75bp with an average of over 12 million reads. Analysis was performed following the workflow described before using two platforms, Galaxy and Linux (see Chapter 2, section 2.12). Results are from samples processed from at least two biological replicates (Table 4-1). Genomic DNA was obtained from a wild type (LmWT) and four independent AmBR lines (AmBcl.14, AmBcl.3, AmBcl.8 and AmBcl.6). A second clone (Lm8E12) of line AmBcl.8 was included for comparison. The quality of reads (FastQC) in all of these samples was high, however, lower quality was observed in the reverse reads of LmWT3, Lm14G4-B, Lm3G4-B, Lm8A11-B and Lm6G7-B (Table 4-1, highlighted in red), was of lower quality, therefore these readings were not included in the analysis, which reduced their coverage in some samples. Forward readings from LmWT3 have higher quality and can be included to increase the coverage. Read number output are as follows: LmWT1: 12,114,797, AmBRcl.14: 8,099,926, AmBRcl.3: 8,725,643, AmBRcl.8:

8,942,188, AmBRcl.6: 10,840,973, and from project 3, LmWT2: 22,025,445. Overall, the percentage of reads mapped (BAM files) was high (94.23% to 97.68%).

Table 4-1. Samples for WGS of AmB resistant *Leishmania mexicana* promastigotes. Genomic DNA was obtained from wild type and four AmBR individual clones, in duplicates. Samples in red were not included due to low quality (see text). Samples and library were processed at Glasgow Polyomics <https://www.polyomics.gla.ac.uk/>.

Illumina Sequencer			
	NextSeq 500 and HiSeq 4000 *	HiSeq 4000	HiSeq 4000
Lines	Samples names		
LmWT1	LmWT1	LmWT3	
LmWT2			LmWT2
AmBcl.14	Lm14G4	Lm14G4-B	
AmBcl.3	Lm3G4	Lm3G4-B	
AmBcl.8	Lm8A11	Lm8A11-B	Lm8E12
AmBcl.6	Lm6G7	Lm6G7-B	

*Due to insufficient read numbers, these samples were rerun in HiSeq 4000

4.1.1 Chromosome changes

Changes at the chromosome (Chr) level showed that ploidy was variable. Ploidy ratio was calculated as described before (Chapter 2, section 2.12). After the alignment with the reference genome (*L. mexicana* MHOM/GT/2001/U1103 release 9.0), obtained from the TriTrypDB database (<http://tritrypdb.org/tritrypdb/>), the majority of the chromosomes appeared without shifts in all lines, ploidy shifts were evident in eight chromosomes across the different resistant lines, and in ten chromosomes between wild types. All changes observed were an increase in copy number. No decrease in copy number or any universal change were observed in any resistant lines or the two wild types (Figure 4-1). There were more ploidy increases in Lm WT1 chromosomes than in WT2. Similarly, in many chromosomes (Chr4, Chr6, Chr11, Chr13, Chr15, Chr20 and Chr32), Lm WT1 decreased from triploidy or tetraploidy to diploidy in AmBR lines.

AmBRcl.8 (A11) showed an increase in Chr3, Chr6 and Chr17, and lines AmBRcl.14 and AmBRcl.3, both showed an increase in Chr7, Chr16, Chr18 and Chr24. Only two chromosomes, Chr16 and Chr30, showed polyploidy in all four AmBR lines, and in both wild types. Interestingly, while a similar increase in Chr30 was also observed in another study on AmBR lines (Pountain et al. 2019), increase in these two chromosomes (Chr16 and Chr30), has also been reported in two strains (M379 and U1103) of *L. mexicana* irrespective of drug pressure (Rogers et al. 2011). The work of Pountain observed between three to four copies in both Chr16 and Chr30, which is similar to our findings here, where

chromosome 30 increased to four copies in all AmBR lines, and in the wild type Lm WT2, and to three copies in AmBRcl.8 (A11), and wild type Lm WT1. Chr16 showed triploidy in most lines, and two lines (AmBRcl.14 and AmBRcl.3) were tetraploid (Figure 4-2).

In *L. major*, the equivalent homologous Chr31, numbered differently due to two fusion events in *L. mexicana* between Chr8 and Chr29, and between Chr20 and Chr36, which merged into Chr8 and Chr20, respectively (Valdivia et al. 2017), was the only supernumerary chromosome in all species (*L. major*, *L. infantum*, *L. donovani* and *L. braziliensis*) (Rogers et al. 2011). A similar observation was found in isolates of *L. (L.) amazonensis*, in which Chr30 (as in *L. mexicana*, and assuming a similar organisation, this is the homologue of Chr31 of the Old World *Leishmania* and New World *Viannia* species), was the only one showing a large increase in copy number. Interestingly, the read depth (Chr30) in both isolates was distributed homogeneously, suggesting the amplification of the whole chromosome rather than duplication of a sub-region (Valdivia et al. 2017). The authors found that these results are contradictory given the diversity in aneuploidy that is characteristic across species, between different isolates or even within a single population. Rogers and colleagues, analysing the copy number of chromosomes in *Leishmania*, state that significant differences are present between some species and strains, in all of the species analysed (*L. infantum*, *L. mexicana*, *L. braziliensis*, *L. major*). This increase in the number of some chromosomes can also increase gene copy numbers and gene expression, and is related to the genetic basis of tropism of parasites as a response to external stressors (Rogers et al. 2011). In this study, the presence of changes observed in Chr30, for instance, suggests that these alterations may be related to events other than drug pressure, given that these changes were also observed in both wild type parasites that were included in the alignment. Increases between 2-20 fold in copy numbers in regions of genes involved in drug resistance have been observed before (Kazemi 2011). With regard to Chr30, many reports have found that this chromosome is polysomic in all *Leishmania* isolates that have been sequenced to date (Valdivia et al. 2017), suggesting that the polyploidy observed here, might not be a direct effect of drug pressure with AmB.

4.1.2 Gene copy number and changes in chromosome ploidy

Analysis of ploidy (number of copies of whole chromosomes) was performed for each sequenced line as described before (Chapter 2, section 2.12). The plasticity of the *Leishmania* genome can often lead to copy number variation (CNV) of genes, as a response to environmental stressors, including drug pressure and number of passages among others (Bussotti et al. 2018). As a result of this, the loss of specific regions or whole

chromosomes (aneuploidy) can be observed (Laffitte et al. 2016). Analysis of coverage per gene showed changes in two genes that may be functionally relevant to AmB resistance based on our understanding of the process to date. In both cases, secondary alterations were associated with genes proximal to what are considered genes of primary interest. In the first case, two lines: AmBRcl.6 and two clones from the same line, AmBRcl.8(A11) and AmBRcl.8(E12) showed lack of coverage of the gene *LmxM.13.1530* encoding the miltefosine transporter (MT), and its neighbouring gene *LmxM.13.1540* (see Figure 4-4), the latter which has unknown function (<https://tritrypdb.org/tritrypdb/app/record/gene/LmxM.13.1540>). This is interesting given the similarity of these changes with that reported in another AmBR line (AmBRB/cl2) of *L. mexicana*, in which a deletion of the 8 kb region spanning the loci of these two genes was also described (Pountain et al. 2019). Similar changes (i.e. the absence of a locus named Miltefosine Sensitivity Locus or MSL), have been observed in patients refractory to miltefosine treatment (Carnielli et al. 2018). Other types of alterations (SNPs, indels) in the MT, LINF_130020800 (Pérez-Victoria et al. 2006; Shaw et al. 2016; Srivastava et al. 2017), are associated with reciprocal resistance between AmB and MF (Fernandez-Prada et al. 2016), and were confirmed by means of genomic and transcriptomic approaches (Mondelaers et al. 2016).

Loss of expression in C24SMT was described in *L. infantum* and *L. donovani* resistant to AmB, and from a patient refractory to treatment with AmB. C24SMT has been related with AmB resistance, in several studies, due to the loss of the methylation in carbon 24, which is introduced by this enzyme. Some of these alterations resulted in the loss of ergostanes that were replaced by cholesta-5,7,24-trienol. The similarities between our findings and those reported by Pountain and colleagues, suggest a role for specific repetitive sequences (i.e. SIDER motifs), and that the homologous recombination model proposed by these authors, i.e. a fusion of the 5'-region including its UTR of *LmxM.36.2380* and the 3'-region including the UTR of *LmxM.36.2390* that resulted in a chimeric version of C24SMT, can be responsible of these changes. Other similarities, i.e. loss of ergosterol and other ergostane intermediates that were replaced with cholestanes, found in this study, are discussed further (see Chapter 5).

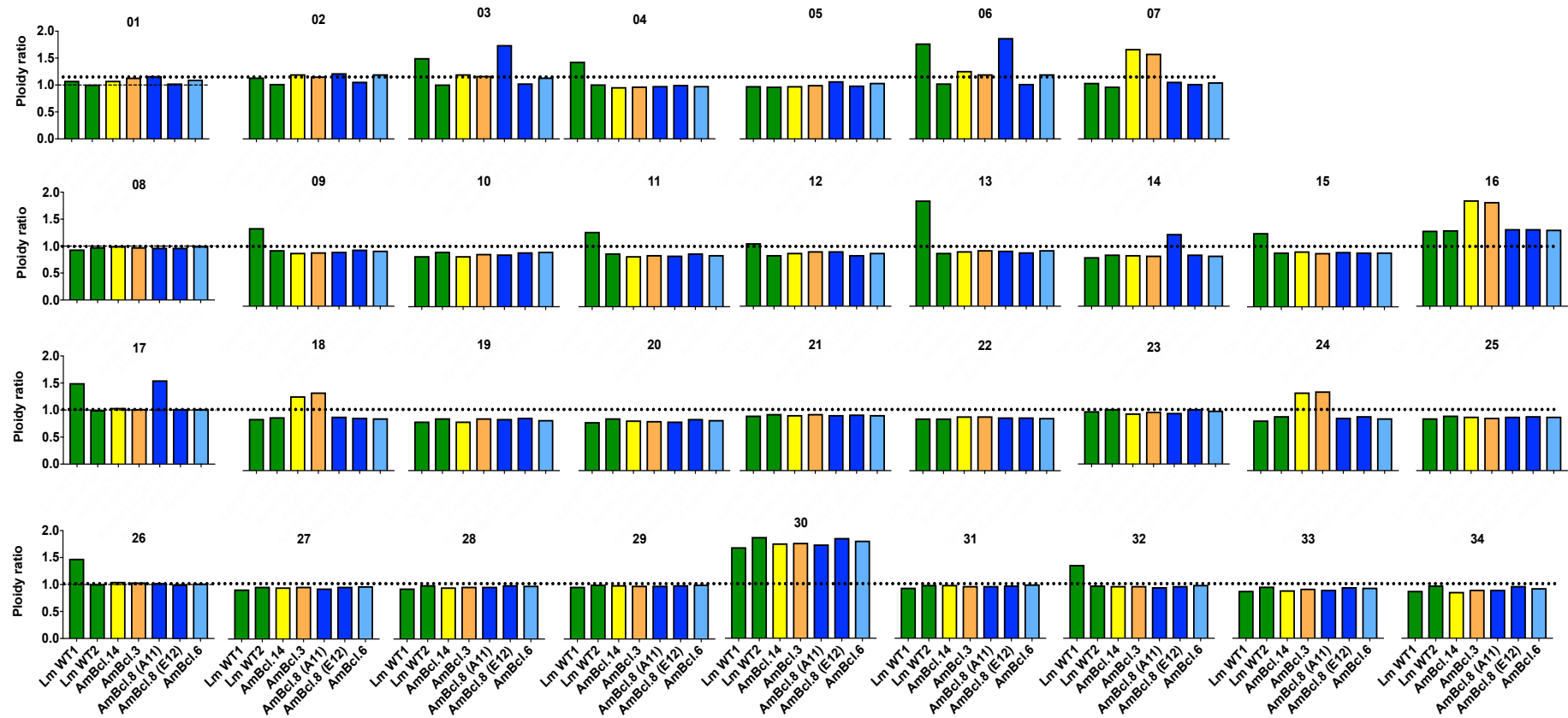


Figure 4-1. Ploidy changes derived from WGS data in AmBR lines and wild type *Leishmania mexicana*.

Ploidy ratios shown per each chromosome (numbered from 01 to 34) in *Leishmania* are the median length (normalised) per-gene coverage of each individual chromosome over the median of every chromosome altogether. Wild type (green), AmBRcl.14 (yellow), AmBRcl.3 (orange), AmBRcl.8 (dark blue) and AmBRcl.6 (light blue). This graph is based on raw data provided by Dr Andrew Pountain, as indicated in section 2.12.

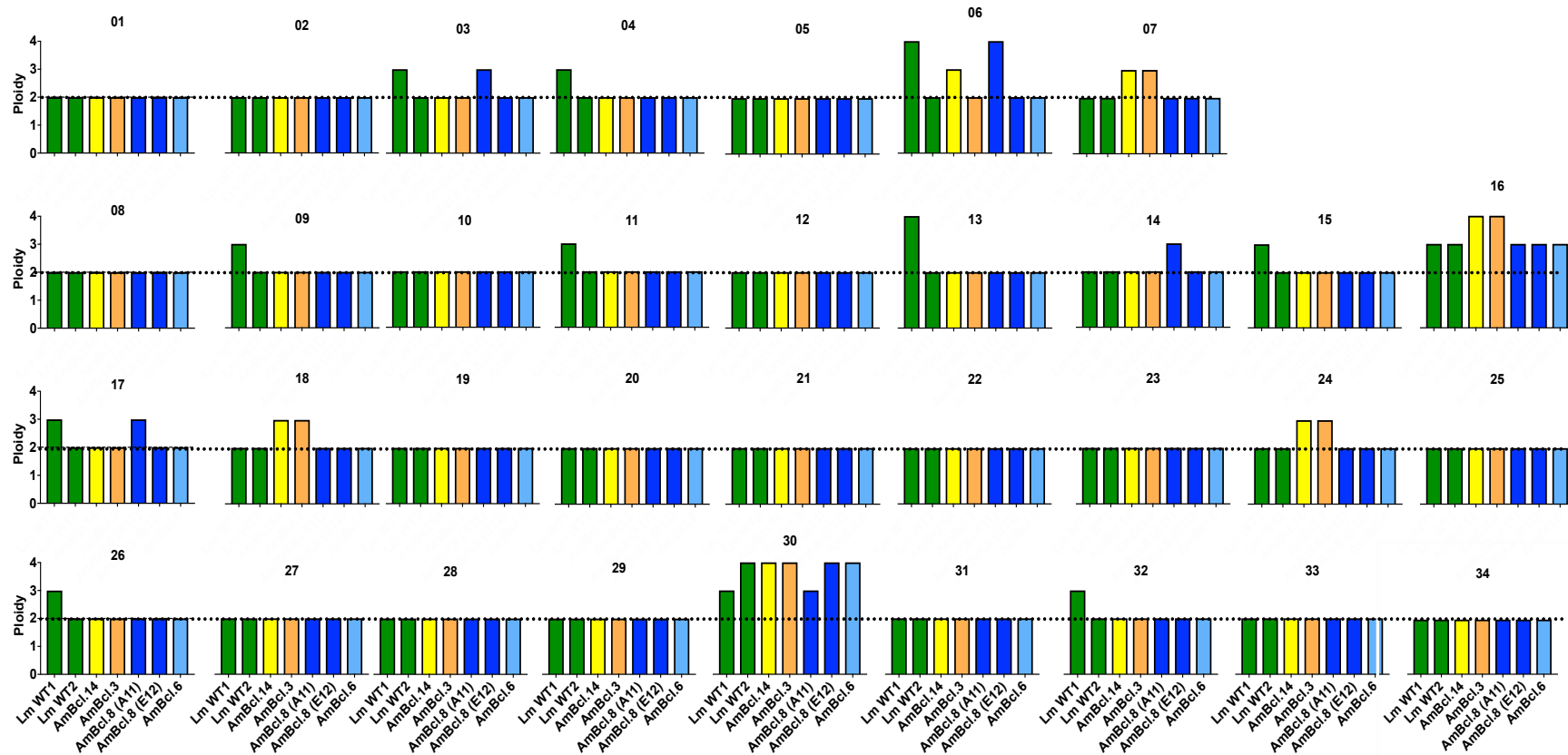


Figure 4-2. Ploidy (absolute) changes of *Leishmania mexicana* derived from WGS data.

Ploidy ratios were converted into “absolute” ploidy by multiplying ratio values by two, assuming that default basal diploidy. Then values were rounded to the nearest integer value. Freebayes assumes diploidy for all samples by default and may be set to any level (-p)

(<https://github.com/ekg/freebayes>). Wild type (green), AmBRcl.14 (yellow), AmBRcl.3 (orange), AmBRcl.8 (dark blue) and AmBRcl.6 (light blue). This graph is based on raw data provided by Dr Andrew Pountain, as indicated in section 2.12. Chromosomes are numbered from 01 to 34.

4.1.3 Mutations triggering coding changes

Using Whole Genome Sequencing (WGS), mutations in two genes, C24SMT and C5DS, of the sterol biosynthetic pathway (SBP) were identified. The nature of these changes varied between lines. Moreover, the sterol profiles derived provide strong evidence of the genetic basis of these alterations in AmBR *L. mexicana* promastigotes. First, two lines, AmBRcl.8 and AmBRcl.6 (including a second clone from line AmBcl.8), showed a lack of coverage of C24SMT (Figure 4-3 and Figure 4-5), which was associated with an additional total loss of the miltefosine transporter (MT) and its neighbouring downstream gene (Figure 4-4). C24SMT has two copies arranged in tandem. Haploid ratio (HR) is the ratio of length-normalised coverage for an individual gene to the median length-normalised coverage across all genes the parental chromosome. In two lines, AmBRcl.6 and AmBRcl.8 (including two clones, A11 and E12, both from line AmBRcl.8), HR showed little variation for the first copy (LmxM.36.2380). However, in the second copy (LmxM.36.2390), a decrease in HR between 0.26 to 0.4-fold in comparison to the parental wild types (LmWT1 and LmWT2) was observed, suggesting copy number variation (Figure 4-3, panels A and B). The other two lines, AmBRcl.14 and AmBRcl.3, showed mutations in the sterol-C5-desaturase gene (C5DS), a detailed description of these changes is discussed further (section 4.1.5).

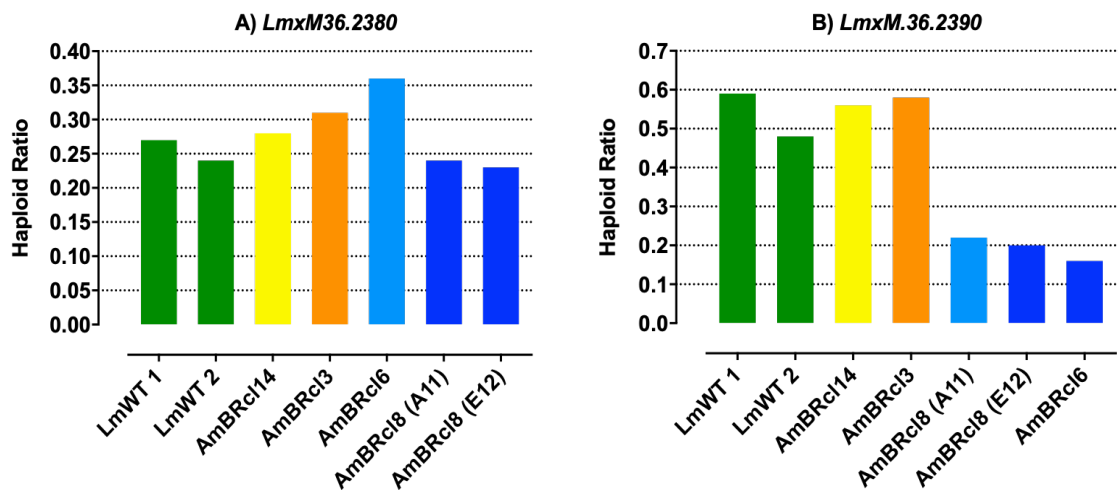


Figure 4-3. WGS data showing coverage of the two copies of the C24SMT gene. Per-gene coverage of the two copies of the C24SMT gene (*LmxM.36.2380* and *LmxM.36.2390*). Raw data was provided by Dr Andrew Pountain, as indicated in section 2.12. Lm14G4, Lm3G4, Lm6G7, Lm8A11 and Lm8E12, correspond to lines AmBRcl.14, AmBRcl.3, AmBRcl.6, AmBRcl.8 (A11) and AmBRcl.8 (E12), respectively.

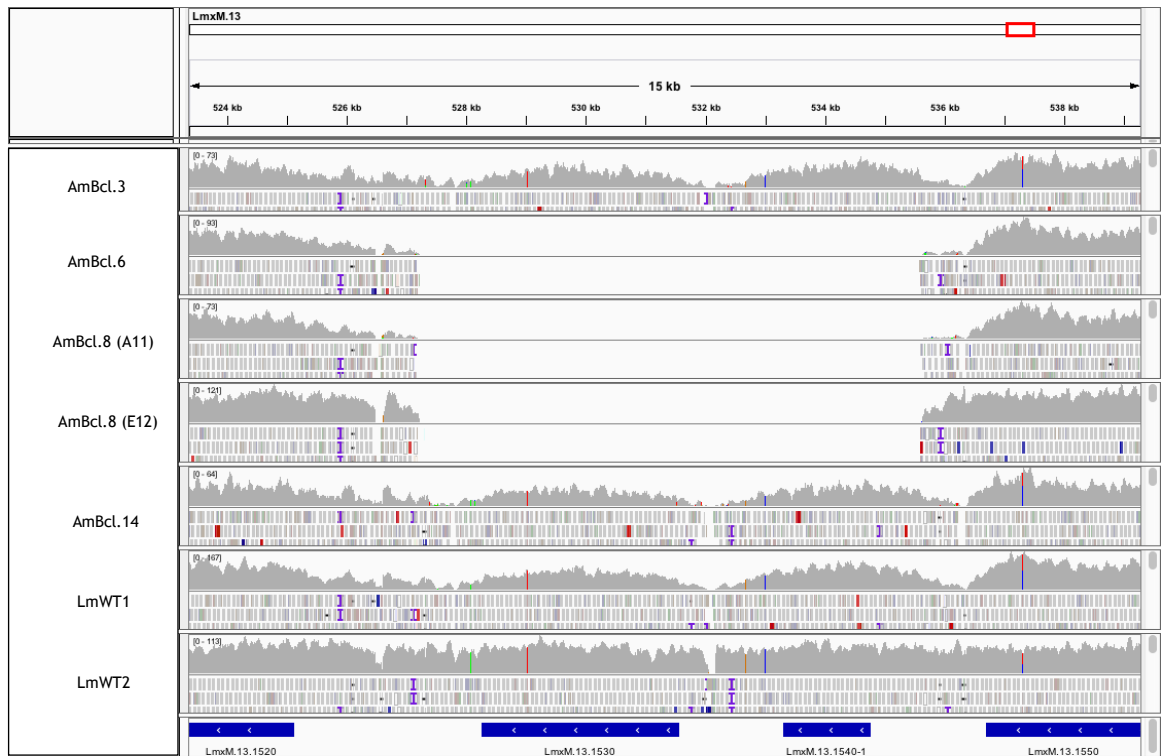


Figure 4-4. Visualization of the genomic region of LmxM.13.1530 (miltefosine transporter) and LmxM.13.1540: (unknown function).

At the bottom is shown (blue) the locus or position of the genes. The bar on the left is the list of the different lines. At the top is shown a region spanning 15 kb of Chr13 from left to right and containing the coordinates of the genes. In grey areas of different height, showing the coverage or total read depth. The reads are arranged in read pairs. Red lines indicate read pairs, which map did not match bases on the reference genome. Note that at the centre in the line at the top (AmBcl.3) and at the bottom in line AmBcl.14 and LmWT1 and LmWT2, there is a small region (blank space) of low or complete absence of coverage. The intergenic region of the other three lines is described in the text. The image was created using the Integrative Genomics Viewer IGV (<http://software.broadinstitute.org/software/igv/>), including the experimental strains and the reference genome strains, and provided by Dr Andrew Pountain as indicated in section 2.12.

4.1.4 Changes in the C-24 sterol methyltransferase gene

Previous studies (Mbongo et al. 1998; Mukherjee et al. 2018; Nakagawa et al. 2014; Pountain et al. 2019; Purkait et al. 2012; Rastrojo, et al. 2018) have demonstrated the role of C24SMT in *Leishmania* and in AmB resistance (loss of C24 methylated sterols, altered sterols profiling) and virulence *in vitro* (Mukherjee et al. 2018). In these studies, the loss of expression of one of the transcripts of C24SMT (LmxM.36.2380) has been observed in several species, such as *L. donovani* (Pourshafie et al. 2004; Purkait et al. 2012), *L. infantum* (Rastrojo, et al., 2018) and *L. mexicana* (Pountain et al. 2019b). While the study of Rastrojo and colleagues found a deletion of one of the copies of this gene (LINF_360031200) in *L. infantum* and suggested that homologous recombination (HR) between the coding regions was a possible mechanism of this loss of expression, the study of Pountain showed clear evidence of the loss of the 3'UTR in one of the transcripts of the

gene (LmxM.36.2380), and proposed a model of the role of the HR event in AmBR lines. Moreover, this study proved that both copies of C24SMT have different expression levels in wild type compared to AmBR lines.

The loss of the first copy of the C24SMT gene, LmxM.36.2380, suggests that homozygous genotypes are present. For instance, line AmBRcl.3 was the only line that was called homozygous but did not show any changes in haploid ratio (Figure 4-3 panel A). Moreover, the low coverage of this line indicates that some of the reads with genotype G961, were, possibly, mis-mapped with the other copy, LmxM.36.2390, which genotype is A961, and consequently, these heterozygous genotypes are, possibly, not real heterozygous sites. This is shown in Figure 4-5, panel A, where the region between the two copies of C24SMT is missed. In the same figure (panel B), analysis using a mapping quality threshold of 1, removed reads with a similar probability to align with the sequence of either of the copies, resulting in a greater area miss-mapped. The downstream end (3'-UTR) of the copy C24SMT (LmxM.36.2380), and the upstream end (5'-UTR) of the copy C24SMT (LmxM.36.2390) are absent in lines AmBRcl.8 (in both clones A11, and E12), and AmBRcl.6.

Similar alterations in C24SMT were described by Pountain and colleagues, in their study, loss of expression of C24SMT was observed in three lines (AmBRB/cl2, AmBRC/cl3 and AmBRD/cl2), and in some cases, loss of fitness, and in another three AmBR lines, selected by a former student in the Barrett Lab (PhD Thesis Raihana Binti Ithnin, unpublished). A concomitant loss of the MT was identified only in one line (AmBRB/cl2) of the study of Pountain and colleagues, and in one line with a novel mutation, A325V (C974T) described in the study of Dr Raihana Binti Ithnin. I analysed the ORF of this new SNP and observed that the mutation corresponds to the second base of the codon (GCT/GTT) resulting in a non-silent mutation (substitution from Alanine to Valine, both non-polar residues). The localisation of all these SNPs is shown in a 3D model constructed using PyMOL and Chimera (Figure 4-10). The presence of two copies of a particular gene allows the parasite to use HR. This can result in other changes such as deletions, extrachromosomal amplifications (linear and circular), aneuploidy, and eventually drug resistance (Genois et al. 2014; Ubeda et al. 2008). The advantages of HR have been previously observed in mutants of *L. infantum* and *L. major* highly resistant to methotrexate (Ubeda et al. 2008) and AmB (Pountain et al. 2019b). The latter of these studies showed that *Leishmania* used HR with two copies of the gene C24SMT to become resistant against AmB.

Table 4-2. Summary of genomic changes identified with WGS in AmBR and NysR lines of *L. mexicana* promastigotes.

Hom: homozygous, Het: heterozygous. The homologous genotype that is possibly mismatched due to the alignment with the copy LmxM.26.2390 of the C24-sterol methyl transferase (C24SMT) gene, is shown in red. MT: miltefosine transporter. C5DS: C-5 desaturase, LOX: lathosterol oxidase.

Lines	Gene and mutations			
	LmxM.23.1300 (LOX syn. C5DS)		LmxM.36.2390 (C24SMT)	LmxM.13.1530 (MT)
	V74E (T221A)	M93del (277- 279delATG)	R244L (G731T)	V321I (G961A)
LmWT1				Het. 0/1
LmWT2				Het. 0/1
AmBRcl.14		Hom.	Hom.	Het. 0/1
AmBRcl.3	Het.		Hom.	Hom. 1/1
AmBRcl.8 (A11)				Hom. 1/1 Deletion
AmBRcl.8 (E12)				Hom. 1/1 Deletion
AmBRcl.6				Hom. 1/1 Deletion
NysRcl.B2		A95del (hom)		

In this study, the evidence of structural variations at the C24SMT locus was notable in lines AmBRcl.6 and AmBRcl.8 (clones A11 and E12), however some gaps in the assembly and the similarity of the sequences suggest the possibility of potential errors in these results, regardless the variation observed in the HR. Sanger sequencing and qRT-PCR would be necessary to confirm CNV, loss of expression of C24SMT, and genotype (possibly G391/A961). Sanger sequencing was previously used to prove that the G961 and A961 genotypes belong to LmxM.36.2380 and LmxM.36.2390, respectively (Pountain et al. 2019b).

Genomic changes in C24SMT (ERG6 in fungi) in pathogenic fungi, result in the substitution of ergosterol and other ergostanes by cholestane intermediates characterised by lacking the C-24 methylation (Young et al. 2003). The accumulation of cholestane intermediates was also observed in C24SMT-null mutants of *L. major* promastigotes. In addition to the loss of ergosterol, these changes lead to AmBR resistance and an increase in susceptibility to other lipid inhibitors (Mukherjee et al. 2018). Similar observations in the substitution of the wild type sterol with an increase in cholestane-type intermediates, have been reported in *L. donovani* selected *in vitro* to AmB (Pourshafie et al. 2004), and in *L. infantum* after the loss of expression of C24SMT (LINF_360031200 in *L. infantum*) (Rastrojo, et al. 2018). These findings are in agreement with the increase of cholestane-based sterols observed two AmBR lines, AmBR.c18 and AmBRcl.6. This increase in cholestanes was more pronounced (90.8 to 91.2%) in a C24SMT knockout created using CRISPR-Cas9 (Beneke et al. 2017) and discussed further (chapter 6).

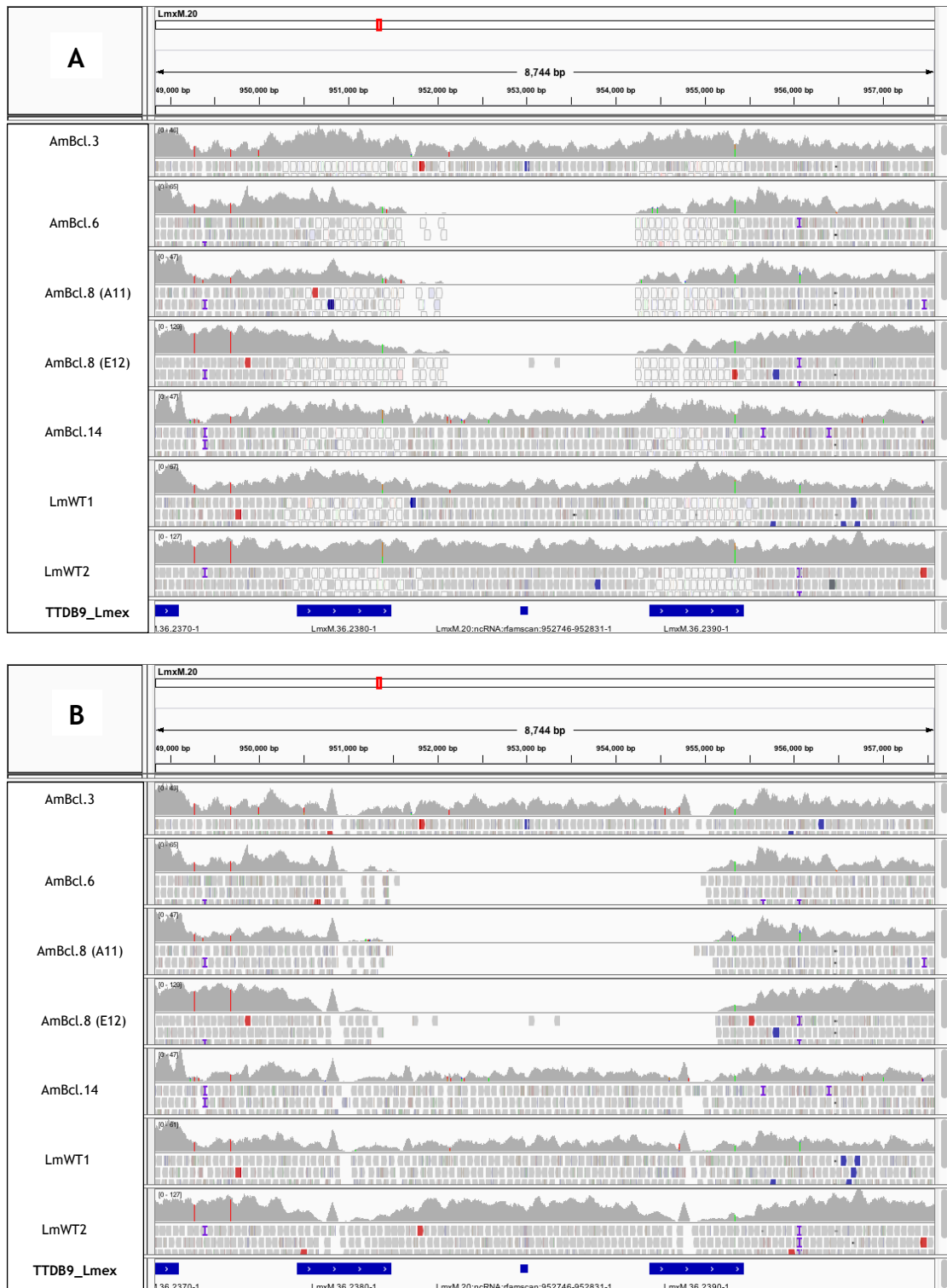


Figure 4-5. Visualization of the genomic region of LmxM.36.2380 and LmxM.36.2390. The lack of coverage in the intergenic region is clear in lines AmBRcl.6, AmBRcl.8A11 and AmBRcl.8E12. C24SMT (panel A) – no mapping quality threshold; (panel B) mapping quality threshold of 1 (as in Pountain, A. PhD Thesis). Image was created using the Integrative Genomics Viewer IGV (<http://software.broadinstitute.org/software/igv/>), including the experimental strains and the reference genome strains, and provided by Dr. Andrew Pountain as indicated in section 2.12. See Figure 4-4 for a full description of the panel features.

4.1.5 Changes in sterol C-5 desaturase

Another enzyme in which mutations were found was LmxM.23.1300, this is annotated as lathosterol oxidase (LOX) (<https://tritypdb.org/tritypdb/>), which is a synonym of the glycoprotein C5-Sterol desaturase (C5DS). The functional role of LmxM.23.1300 as C5DS in *Leishmania mexicana*, was demonstrated for the first time in an AmBR mutant (AmBRA/cl1) of *L. mexicana* with defects in this enzyme, which was unable to produce sterols with the double bond ($\Delta 5$) in the sterol nucleus (Pountain et al. 2019). In this work, Pountain and colleagues were the first in identifying the role of LmxM.23.1300 in AmB resistance. However, the annotation of another gene (LmxM.30.0590) as the putative C5DS in *Leishmania* spp., raised the question of the existence of another copy of this gene. The role of LOX (or C5DS) is essential for the synthesis of ergosterol and other ergostanes. These enzymes convert episterol (ergosta-7,24(28)-dien-3-ol or ergosta-7,24(28)-dien-3 β -ol) that has one double bond ($\Delta 7$), into ergosta-5,7,24(28)trienol, with two double bonds ($\Delta 5,7$). In null mutants of *Saccharomyces cerevisiae* (Bard et al. 1993b), and clinical isolates of several species of *Candida* spp., with defects and reduced expression of C5DS (ERG3 in fungi) (Miyazaki et al. 1999; Young et al. 2003), the increase in resistance to AmB and azoles (Branco et al. 2017; Joseph-home et al. 1995), and reduced fitness and higher susceptibility to some antifungals was noted (<https://www.yeastgenome.org/locus/S000004046>).

In the present study, five novel mutations (3 and 2 in AmBR- and NysR lines) were identified in LmxM.23.1300 and resulted in three variants (Figure 4-6 and Figure 4-7). Unlike the only mutation, G139R, that has been reported to date in this enzyme in *L. mexicana* (and in any other species), and which changed the functionality of the residue from a non-polar with a single hydrogen (glycine) into a positively charged side chain (arginine), and is moreover, located between two His-rich regions (Pountain et al. 2019), none of the three SNPs found in this study, is localised between highly conserved clusters of His residues (Figure 4-7). These His clusters have been found to be functionally important for the binding of substrates in other fatty acid desaturases (as with LOX and C5DS) in the budding yeast (Taton and Rahier 1996) and in *A. thaliana* (Nes 2011), and also in other enzymes (e.g. ERG25) of this pathway (Kristan and Rižner 2012). The first of the three mutations identified in AmBR lines, was found only in one line (AmBRcl.3); a heterozygous substitution (T221A) causing an amino acid change from valine into glutamate (V74E). This change from a residue with a non-polar side chain to a negatively charged side chain could represent a change in functionality in this position.

The alignment with other orthologues in kinetoplastids, and other eukaryotes, revealed that the V74 residue is conserved across all *Leishmania* species (see Figure 4-7). Another mutation was found only in one line (AmBcl.14), this was a homozygous in frame codon deletion (277_279del ATG), which resulted in the loss of one methionine (M93del). The deleted methionine is one of a pair of methionines in positions M92-M93. While the former is conserved across all kinetoplastids, the latter is only conserved across all *Leishmania* species (Figure 4-7). The last of the three bp mutations observed here in C5DS, was found in two lines, AmBRcl.3 and AmBRcl.14. This was a homozygous substitution (G731T) that caused a change in from arginine to leucine (R244L). As with the other mutations, the functionality of the side chain was altered, in this case from a polar (positively charged) side chain (arginine) into a non-polar side chain (leucine). Given that this is conserved across all kinetoplastids, the budding yeast, and humans, the functional role of this residue could be relevant.

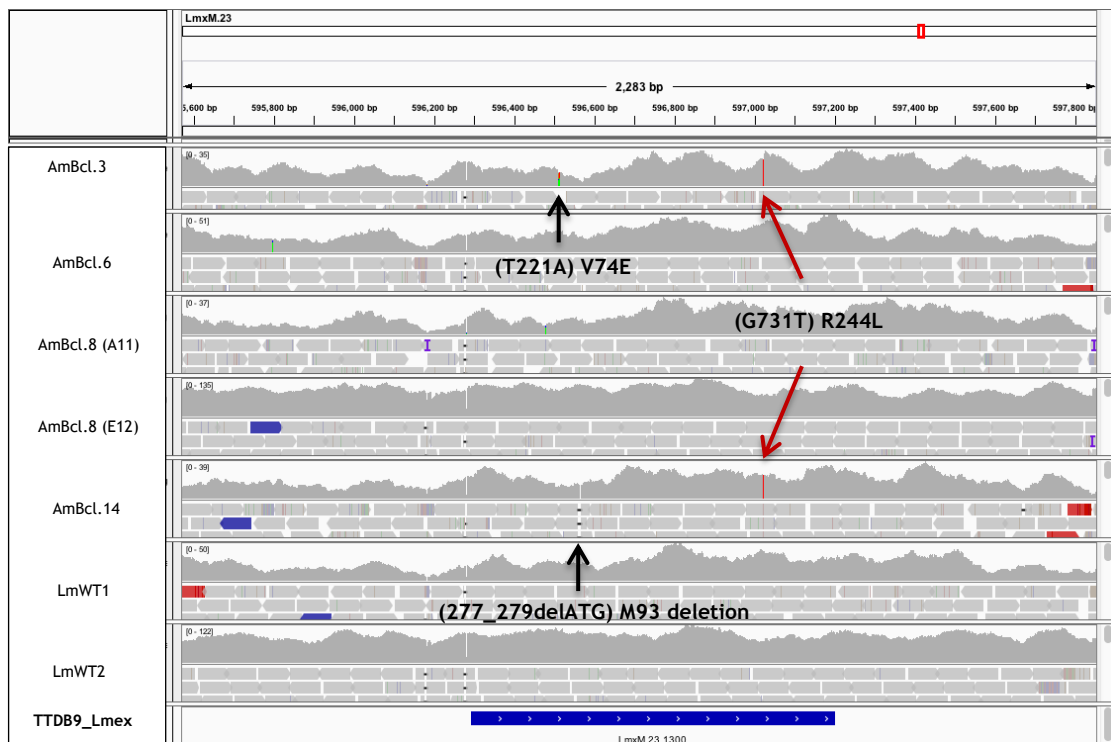


Figure 4-6. Visualization of the genomic region of LmxM.23.1300 (LOX) (syn. of C5DS). The black arrows denote a substitution and an in-frame deletion. Red arrows highlight another mutation observed in two independent lines. The image was created using the Integrative Genomics Viewer IGV (including the experimental strains and the reference genome strains and provided by Dr Andrew Pountain as indicated in section 2.12. See Figure 4-4 for a full description of the panel features.

The fact that these two lines were selected for resistance independently, the presence of an identical SNP is striking, and raises the possibility of cross contamination, either earlier in the course of cell culture or during the processing of the DNA samples. A further analysis

of other SNPs could help to identify this (Supplementary file 4) (see page 8). A full list of the genotypic changes identified in C24SMT (and in other enzymes) in this study, are shown in Table 4-2. Similarly, a complete summary of these mutations related to their sterol profile (GC-MS), and their phenotype in a mouse model, is detailed further (see Chapter 5).

I identified several discrepancies related to the annotation of C5DS in *Leishmania*. First, there is another gene, LmxM.30.0590 (NCBI Reference Sequence: XP_003877581.1) annotated as putative C5DS in kinetoplastids (<http://tritrypdb.org>), whereas the gene LmxM.23.1300 (NCBI Reference Sequence: XP_003875772.1), is annotated in both databases, NCBI and Uniprot, as lathosterol oxidase-like protein (LOX). As mentioned at the beginning of this section, LOX is a synonym of the C5DS in humans (O75845 SC5D_HUMAN) (<https://www.uniprot.org/uniprot/O75845>), and in other organisms (Altschul et al. 2005). Intriguingly, both genes, LmxM.30.0590 and LmxM.23.1300 correspond to the ERG3 family (the orthologue of C5DS in yeast and other fungi), a sterol desaturase/sphingolipid hydroxylase, fatty acid hydroxylase superfamily (<https://www.ncbi.nlm.nih.gov/Structure/cdd/cddsrv.cgi>) that is involved in the transport and metabolism of lipids. Although LmxM.30.0590 is also annotated as C5DS in *T. brucei* and has some relatedness with LmxM.23.1300 and with ERG3 in fungi (Figure 4-8 panel A), its identity remains unclear. Both genes are syntenic with respect to other orthologues in *Leishmania* and in trypanosomes, including *T. brucei brucei* and *T. cruzi* (<https://tritrypdb.org/tritrypdb/>) (Figure 4-8 panel B and C).

Interestingly, LmxM.23.1300 has two copies in tandem, CFAC1_150028200 (CfaC1_15: 670365 – 671270), and CFAC1_150028300 (CfaC1_15: 673651– 674604) in *Crithidia fasciculata* (Figure 4-8 panel C), a non-human infective trypanosomatid parasite related to *Leishmania* and *T. brucei*, in which is located in Chr15. Similarly, various copies of the ERG3 lathosterol oxidase-like (LOX) gene, have been described in other fungi. For instance, in some studies, two copies of ERG3 are described in *Aspergillus fumigatus* (Alcazar-Fuoli and Mellado 2012), *Candida albicans* (Vale-Silva et al. 2012), and *Schizosaccharomyces pombe* (*Sp*). Contrary to this, the study of Iwaki and colleagues, highlights that only one copy of ERG3 is present in *Saccharomyces cerevisiae* (*Sc*) and *Candida* spp., while three copies exists in *Aspergillus fumigatus* (Iwaki et al. 2008).

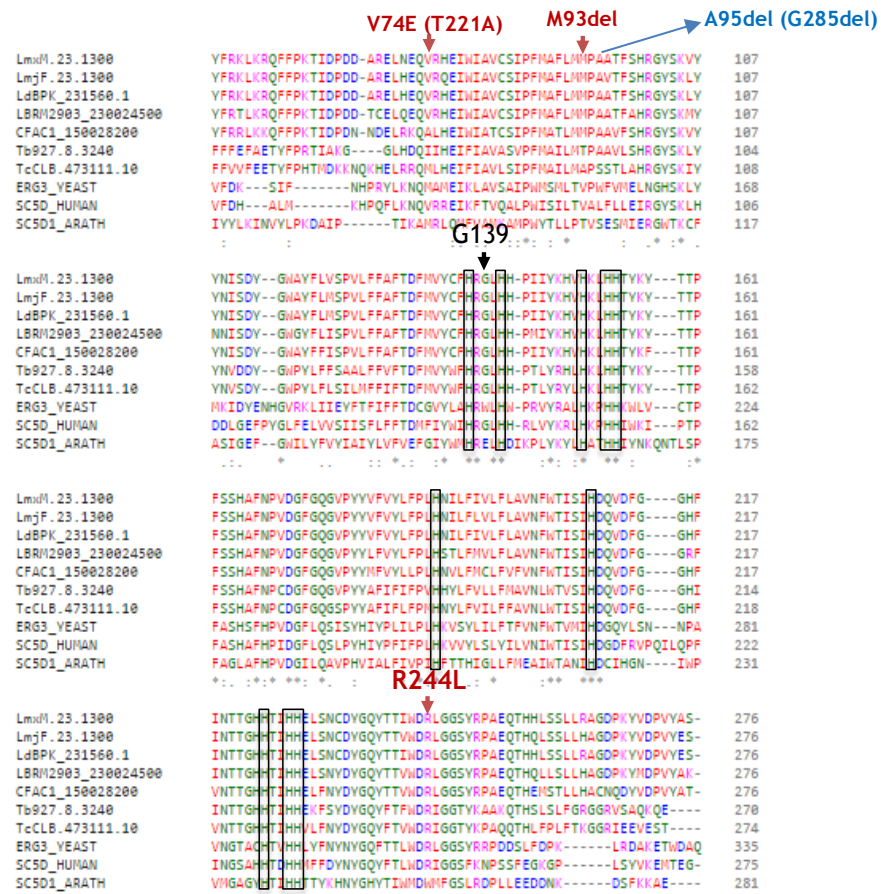


Figure 4-7. Alignment of lathosterol oxidase LmxM.23.1300 (LOX) with orthologues (C5-desaturase) from kinetoplastids and other eukaryotes. His residues that are conserved across species are marked by black boxes. A black arrow denotes the G139R substitution in LmxM.23.1300 reported by Pountain et al. 2019. Red arrows highlight other novel mutations. A deletion (A95del) in LmxNysR cl.B2 (see Chapter 3) is also shown (blue arrow). Kinetoplastids species are: *L. mexicana* (top), *L. major*, *L. donovani*, *L. braziliensis*, *Crithidia fasciculata*, *T. brucei* and *T. cruzi*. Also included *ERG3* (*S. cerevisiae*), and *SC5D* (*Homo sapiens*) and from plants (bottom) *Arabidopsis thaliana*. Sequences were obtained from the databases TriTrypDB (<https://tritrypdb.org/tritrypdb/>) or from Uniprot (<https://www.uniprot.org/>). Alignment was performed with Clustal Omega (<https://www.ebi.ac.uk/Tools/msa/clustalo/>), provided and modified from (Pountain et al. 2019), as indicated in section 2.12.

Another noteworthy observation is that LmxM.30.0590 is annotated as C5DS or ERG3 in *Sc* and in *Candida spp.*, whereas in *Sp* is differentiated into C5DS-Erg31 or C5DS-Erg32, which correspond to two copies with overlapping function (Iwaki et al. 2008). Studies of ergosterol in *Sc*, revealed that mutants lacking some enzymes of the SBP, e.g. C24SMT and C8SI (ERG6 and ERG2 in fungi, respectively), were unable to produce ergosterol and developed resistance to both polyenes studied in this thesis, i.e. AmB and nystatin, which resembles the resistant phenotype observed in the present, and other studies with AmBR lines of *Leishmania spp.* While single knockouts of the two ERG3 homologues in *Sp*, named Erg31p and Erg32p, respectively, showed unaltered synthesis of ergosterol and no change in resistance to polyenes, no ergosterol was observed in the ERG3-double

knockout, thus confirming that both orthologues have analogous function (Iwaki et al. 2008). In *Leishmania* spp., however, there is no experimental data to support the presence of another copy of C5DS and to confirm the annotation of LmxM.30.0590, which is annotated as C5DS in the TriTrypDB, this gene has, possibly, a distinct function or is probably wrongly annotated as C5DS and is therefore, not a real C5DS. In agreement with these results, low identity (<35%) between the amino acid sequences of C5DS (ERG3) has been observed in various species, which suggests that these two orthologues have a low degree of relatedness (Nes 2011) and are possibly different genes (Figure 4-8, panel A).

I also looked into another study in which the genome profiling of the sterol biosynthetic pathway was analysed in *L. donovani*, *T. brucei*, and *T. cruzi* (and other apicomplexan parasites), without further evidence supporting the role of LmxM.30.0590 as C5DS, as part of this pathway (Fügi et al. 2014). Further investigation in the AmBR line from Pountain et al. 2019, which has a mutation in LmxM.23.1300, also revealed the absence of SNPs in LmxM.30.0590, with respect to RNA expression, the latter showed a decrease of 15-20% relative to LmxM.23.1300, in two lines, AmBRB and AmBRC, however, the biological meaning of this is unknown (personal communication, Dr Andrew Pountain). Experimental characterisation of the phenotype of this gene in *Leishmania*, is needed, the use of genome editing tools, i.e. CRISPR-Cas9, DiCre (Beneke et al. 2017; Damasceno et al. 2018; Duncan et al. 2016; Jones et al. 2018), can contribute to characterise individual genes, however, the interpretation of changes in sterols in *Leishmania* spp. still represents a challenge.

A summary of the mutations identified in this study in C5DS and C24SMT, and other changes related with the MoA of antileishmanials, e.g. deletion of the MT, is shown in Table 4-2. The results obtained in this study, are comparable to previous findings reported recently (Pountain et al. 2019), in eight AmBR lines of *L. mexicana*, which were selected independently by a former member of the Barrett Lab (PhD Thesis Raihana Binti Ithnin, unpublished).

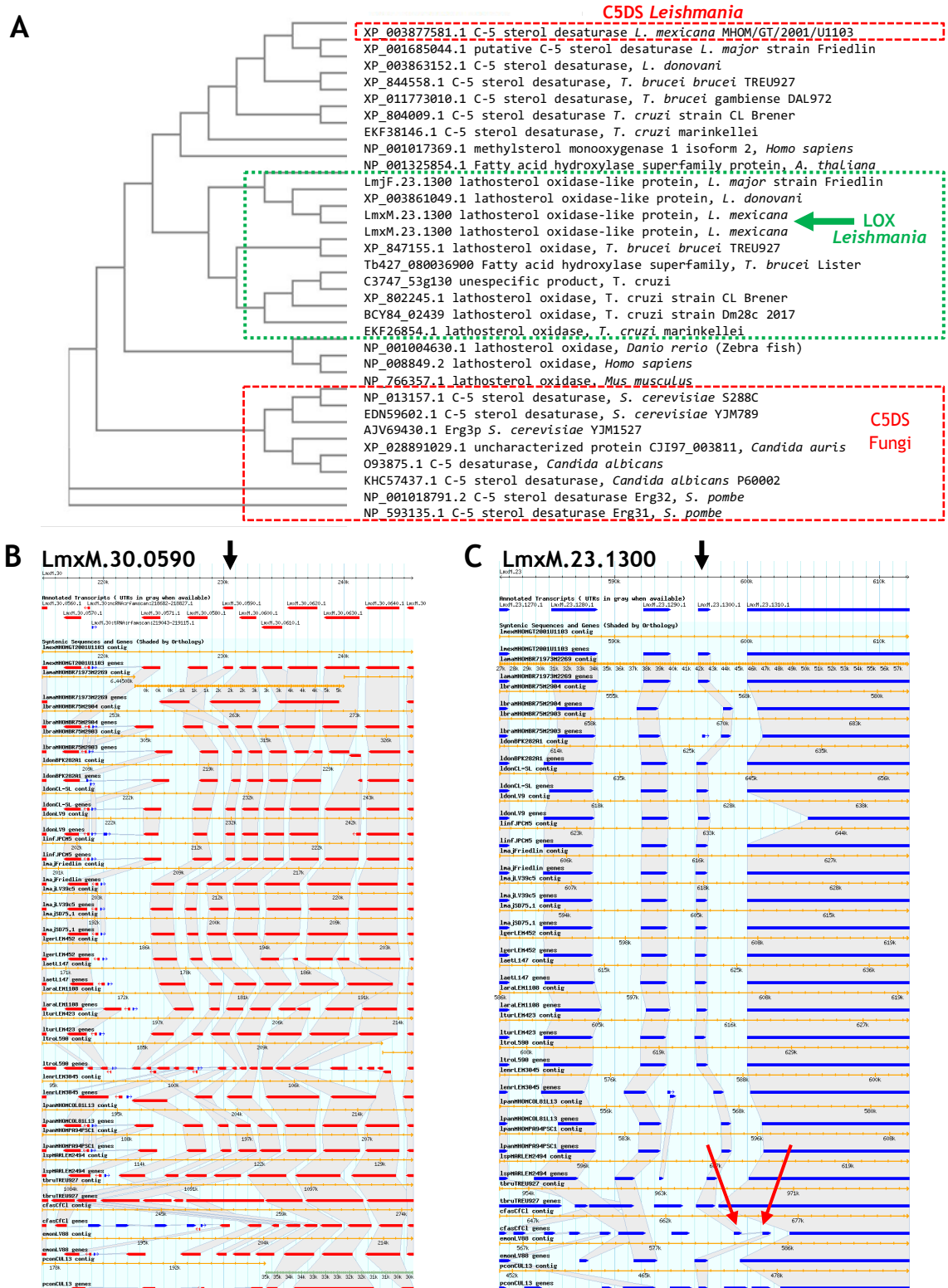


Figure 4-8. Cladogram and synteny of *L. mexicana* C5DS and LOX genes.
Panel A: cladogram with C5DS (red dotted boxes) and LOX (green dotted box). *L. mexicana* LOX, in which three novel mutations were found in this study is highlighted (green arrow). Source: Clustal Ω (<https://www.ebi.ac.uk/Tools/msa/clustalo/>). **Panel C:** synteny of (C5DS) LmxM.30.0590 and (LOX) LmxM.23.1300 (black arrows), with respect to other kinetoplastids. The two copies of LOX in *C. fasciculata* are highlighted (red arrows). Source: TriTrypDB (<https://tritrypdb.org/tritrypdb/>).

4.1.6 Predicted protein-protein interactions in the ergosterol biosynthetic pathway in *Leishmania*.

Computational and bioinformatics tools are an essential part of an integrative approach to large amounts of high-throughput biological data (e.g. genomics, proteomics, etc.) in the search of new drug targets (Rezende et al. 2012). Identification of protein-protein interaction (PPI) networks is part of these approaches that can provide a better understanding of complex protein interactions in biological systems, including in *Leishmania major* (Dashatan et al. 2018). Interactomes have also been predicted in other species, such as, *L. braziliensis*, *L. infantum* (Rezende et al. 2012) and *L. major* (Flórez et al. 2010; Rezende et al. 2012). The use of PPIs networks in *Leishmania* spp., has contributed to the understanding of the functionality of many hypothetical proteins present in such networks. If we consider that around 60% of the proteins lack a predicted function, the use of this approach, i.e. PPI, has provided a framework to better understand their organization in *Leishmania* spp. (Dashatan et al. 2018; Rezende et al. 2012). Moreover, interactomes can help to predict biological processes and to find potential drugs. For instance, Flórez et al. used enrichment analysis of clusters from 1,366 nodes and over 30,000 interactions and predicted 263 interacting proteins and 142 drug targets. Importantly, in this work, PPI networks allowed to discriminate between those targets that are essential for the parasite and those that have no orthologue in human (Flórez et al. 2010).

The ergosome is a multi-protein complex proposed based on a study using a yeast-two-hybrid system in the budding yeast (Mo and Bard 2005a). The ergosome model suggests that the PPI is key for the proper function of the SBP, and therefore for the synthesis of ergosterol, thus suggesting the feasibility of the presence of an ergosome in *Leishmania* spp. (and other species). Here, I modelled the PPI of the sterol biosynthetic pathway (SBP) in *Leishmania major* and *L. infantum* using the string database (<http://string-db.org>) (Szkarczyk et al. 2011, 2015). First, I obtained the 3D models of C14DM (Figure 4-9) and C24SMT (Figure 4-10), both of which are known to play a key role in AmB resistance (and to other antifungals). Second, using PyMOL and Chimera, I localised in these enzymes, those mutations that have been identified in AmBR lines of *L. mexicana*, including those found here. Finally, I discuss the ergosome in *Leishmania* spp. and how this might be related to these mutations (Figure 4-11). The PPI network was also predicted in *T. cruzi* and *C. albicans*, and then compared with the interactome (named the ergosome herein) which was originally described in the budding yeast (Mo and Bard 2005a) (Figure 4-11, panels D to F).

Some examples of previous evidence of disruption of the SBP (and of ergosterol synthesis) due to various defects in several enzymes that support the hypothesis of the ergosome in *Leishmania* are, first, a SNP (N176I) described in the C14DM (Figure 4-9) (Mwenechanya et al. 2017), second, another SNP found in C5DS (G139R), and finally, a mutation (F72C) found in C24SMT (an exhaustive list is discussed below) (Pountain et al. 2019). The first of these SNPs (N176I) is localised out of the active site of the enzyme C14DM. Moreover, this residue seems to be functionally important across the Kinetoplastids, and is possibly relevant for protein-protein interactions (Mwenechanya et al. 2017). As shown by the authors, N176I caused the disruption of ergosterol synthesis with accumulation of various sterol intermediates. Another example that is, possibly, related with the presence of an ergosome in *Leishmania*, are the mutations identified here in C5DS (LmxM.23.1300) in two AmBR lines. Contrary to another mutation (G139R) detected in this enzyme, which is within a His-rich region that was predicted to be relevant for enzymatic activity after the alignment with orthologues in other eukaryotes (Pountain et al. 2019). In my study, the five mutations identified in LmxM.23.1300 are, possibly, localised out of the active site, given that the mutated residues are situated in the extremes of the protein sequence (see Figure 4-7, red arrows). However, this cannot be assumed since no structure of C5DS is available. The substrates of the enzyme C5DS (E.C. 1.14.21.6), are specific between different organisms, while cholest-7-enol, and campest-7-enol or stigmast-7-enol, are specific for animals and plants, respectively, ergosta-7,22-dienol is the counterpart, in fungi (Nes 2011), and possibly in kinetoplastids. A common feature in all these substrates is, however, the lack of the double bond system ($\Delta 5,7$).

In this study, the latter of these intermediates (i.e. the enzyme's substrate) was the most abundant in two AmBR- and all four NysR-lines with SNPs in LmxM.23.1300, thus suggesting that these mutations, possibly, interfere with the activity of the enzyme (Table 4-2) irrespective of their position with the amino acids sequence. However, other intermediates with two double bonds ($\Delta 5,7$), including the product of the enzyme, i.e. ergosta-5,7,24(28)-trien-3 β -ol, were also detected in low abundance (<1%) in AmBRcl.3, in which the mutation (V74E) was present, suggesting a partial activity of this enzyme in this line. Contrary to this, in AmBRcl.14, which has a different mutation (M93del), the substrate, ergosta-7,22-dien-3-ol, increased its abundance significantly (up to 96.73%), whereas the product of the enzyme C5DS was completely absent. As mentioned before, the lack of a structure in any specie, limits the prediction of the topology of C5DS, and further analysis of the potential effects of these mutations. Moreover, the presence of a common mutation in both lines (R244L), further complicates this picture, and the analysis of the individual effect of each of these mutations is also restricted.

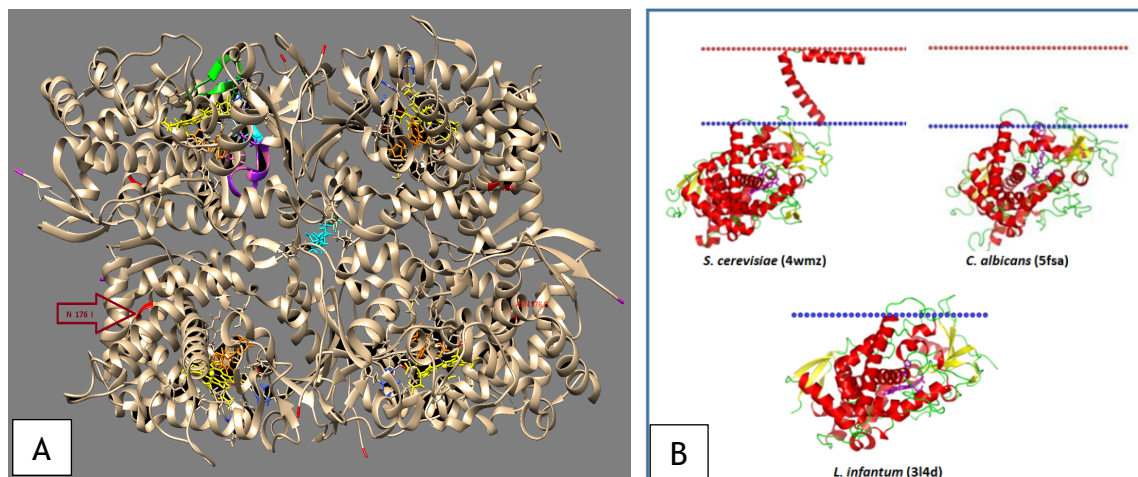


Figure 4-9. Structural 3D models of C14DM (ERG11 in yeast and fungi) in *Leishmania* spp. **A)** model of the structure of CYP51 in *L. infantum* (LINF_110017200), PDB ID 3L4D, 97% amino acid sequence identity with the orthologue in *L. mexicana* (LmxM.11.1100) in which the non-synonymous mutation N176I (red arrow) localised out of the active site of the enzyme is shown (Mwenechanya et al. 2017). The stick model is the heme (yellow) and binding pocket for azoles (orange). The protein ribbon is coloured red (N-terminus), and purple (C-terminus). The first 27 amino acids were removed. Protein structure was processed using the software UCSF Chimera (Pettersen et al. 2004) (<https://www.cgl.ucsf.edu/chimera/>) Chimera. **B)** 3D models showing the orientation of membrane proteins ERG11 (C14DM) of *S. cerevisiae*, *C. albicans*, and *L. infantum*. **Source:** Protein query from panel A, is from the PDB databank (<https://www.rcsb.org/>) and modified from the 3L4D model (W Xu et al. 2014) using Chimera. Images from panel B are from the OPM Database (<https://opm.phar.umich.edu/>).

The last of the three enzymes in which we identified mutations is C24SMT. As mentioned before, changes in this enzyme have been studied extensively in *Leishmania* spp. (section 4.1.4). For this reason, I localised these mutations, along with those reported before by former members in the Barrett Lab, using a predicted model developed in *S. cerevisiae* (Figure 4-10). According to this model, C24SMT performs two types of activity, named C24SMT1 and C24SMT2, which form ergostanes and stigmastanes, respectively. The C24SMT1 type operates in fungi forming a single product, whereas type C24SMT2 is characteristic of protozoa. The above mentioned model was proposed after elucidation of the functional differences that were investigated using different substrates and site-directed mutagenesis to modify several residues (Nes et al. 2002; Ganapathy et al. 2008).

According to the predicted secondary structure of C24SMT (ERG6 in the budding yeast), there are four regions which are formed by residues that are conserved between species: region I (residues 78-98), region II (121-133), region III (188-199) and region IV (215-226). Region I, is an aromatic-rich signature motif relevant for the binding to sterols (Ganapathy et al. 2008). Interestingly, a mutation (F72C) in this region was identified in an AmBR line (AmBRC/c13) of *L. mexicana* in which this mutation influenced the susceptibility (EC_{50}) to AmB and the restoration of the wild type sterols (Pountain et al. 2019). Previous work in *Sc*, had also confirmed that region I is the active site of C24SMT,

related with the catalysis and binding to sterols, and that this region is moreover, involved in substrate binding (i.e. zymosterol) and product formation (Nes et al. 2002; Marshall and Nes 1999). Due to similarities in the alignment between *L. mexicana* and Sc, Pountain and colleagues suggested that this SNP could also be relevant in the interruption of enzymatic activity in the parasite.

Additional substitutions, V131I and V321I, in C24SMT (in LmxM.36.2380 and LmxM.36.2390, respectively) were also reported by Pountain and colleagues in three AmBR lines of *L. mexicana*. The former of these two mutations is localised in region II (as per the model of Ganapathy) (Figure 4-10, panels A to C), whereas the latter is, possibly, the most frequent change reported to date in C24SMT in AmBR lines of *L. mexicana* (Figure 4-10, panel D). Pountain and colleagues described its presence (V321I) in three lines (AmBRB/cl2, AmBRC/cl3 and AmBRD/cl2) and elucidated the mechanism of how this change occurred. Here, this SNP was also found in two individual lines, AmBRcl.8 (two clones) and AmBRcl.6 (one clone). Interestingly, another neighbouring SNP (A325V) (Figure 4-10, panel E) was recently found in another line selected for AmB resistance (PhD Thesis Raihana Binti, unpublished). While both, V131I and V321I, are pre-existing differences between the two copies of C24SMT, there is no evidence suggesting that any of these three SNPs are related with drug resistance. In fact, these alterations in C24SMT seem to be localised out of the active site of the enzyme, notably, these residues are sitting in the extremes of the protein sequence. According to the model of Ganapathy, however, V321I and A325V, are located in a region that is, possibly, in contact with region I, in which case their role with the enzymatic activity of C24SMT, is an interesting observation to be further interrogated (Figure 4-10, panel E and F) (Ganapathy et al. 2008). Furthermore, the product of C24SMT, fecosterol, was undetected in these mutants. If this is the case, then the ergosome model is not supported by the effects derived from these changes, which affect the function of the enzyme along with a significant increase of its substrate. Interestingly, ergosterol (which is C-24 methylated), was detected in low abundance in both these mutants (see Table 5-1). This, as in the case of C5DS mentioned above, suggest that the ergosome is present and that the products of the enzymes are not being channelled adequately. Based on these data, the presence of a *Leishmania* the ergosome remains uncertain, given the fragmented nature of this evidence.

As it is shown in the ergosome models obtained from the STRING database in several species, some of the enzymes (and interactions) of the SBP were absent (Figure 4-11, panels A and B). After comparing with the model of reference in yeast proposed by Mo and Bard (Figure 4-11-A), I identified eight enzymes of the SBP that were absent in

Leishmania (Figure 4-11-D, red and green circles). This is, in part, due to mismatches in the annotation of five enzymes which have two putative homologues (Figure 4-11-D, white dotted circles). Further analysis is needed to identify which of these enzymes are true orthologues of the yeast SBP enzymes. However, by revising previous evidence of the SBP in Kinetoplastids (Cosentino and Agüero 2014; Liendo et al. 1999; Viana Andrade-Neto et al. 2016a; Wei Xu et al. 2014; Yao and Wilson 2016), the presence of these enzymes in Kinetoplastids was corroborated. This was also revised using the Kinetoplastids database (<http://tritrypdb.org>), confirming that the interactomes obtained with the STRING database were incomplete in this database.

A similar situation was observed in *T. cruzi*. Cosentino and colleagues, used a number of bioinformatics strategies and identified several genes of the isoprenoid, and the sterol pathway that were missing or truncated in the genome of *T. cruzi* (Cosentino and Agüero 2014). This work also completed the sequence of another ERG26 gene (LmxM.06.0350) which has a non-orthologous homologue in yeast ERG25 (LmxM.36.2540), suggesting that this enzyme has been lost in trypanosomes, but not in *Leishmania* (Figure 4-11-D, red circles). Another interesting finding of the work of Cosentino and colleagues, is that two enzymes, ERG3 (LmxM.23.1300 in *Leishmania*) and ERG5, which are present in the interactomes of yeast and *Leishmania*, seem to be stage-specific in trypanosomes, appearing only in the epimastigote form, and being absent in amastigotes. The absence of some enzymes of the SBP has been also reported in *Leishmania*. Recently, a “new” tentative SBP was proposed. In this work, the authors highlight that the identification and organization of all the enzymes of this pathway in *Leishmania* spp. is still unclear (Yao and Wilson 2016).

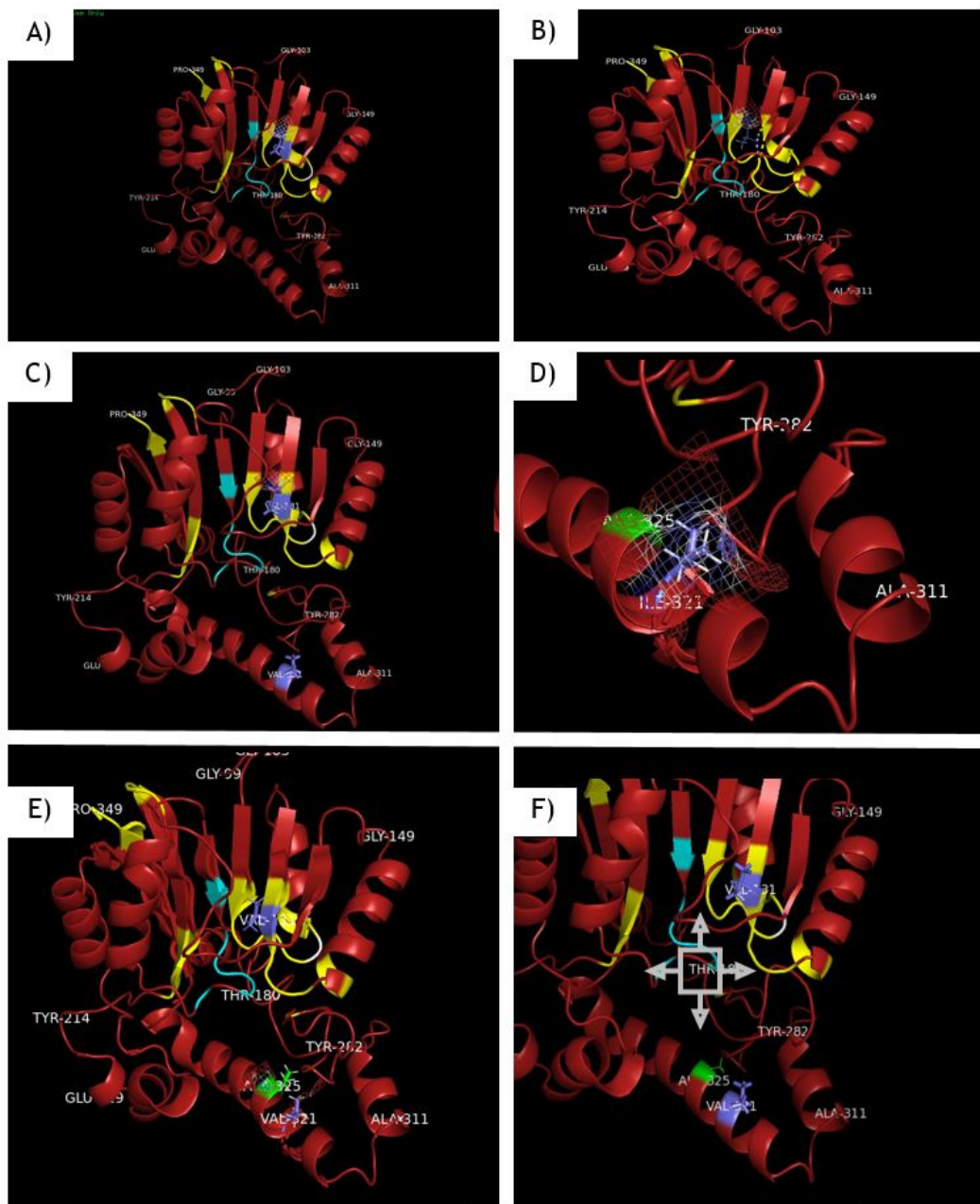


Figure 4-10. Docking of the predicted secondary structure of C24SMT LmxM.36.2380 (XP_003874589.1) of *L. mexicana*.

The Model shows alpha-helices, B-sheets and loops from amino acid 103 (glycine) to amino acid 349, the first 102 and last 4 amino acids, from N- and C-terminal ends, respectively, were removed. Conserved amino acids between species (see S5 Fig. in Pountain et al. 2019) are shown in yellow and cyan. A) Valine V131 (in slate). The SNP V131I has five rotamers with different probabilities to occur, changing the interaction with the neighbour residues. B) The two most probable (74.5%) rotamers in V131I. C) Valine V321 (also in slate). D) Closer view of the most probable (79%) rotamer after the V321I mutation. E) A novel SNP, A325V (green), in LmxM.36.2390 (XP_003874590.1) in an AmBR line of *L. mexicana* (PhD Thesis Raihana Binti, unpublished). F) Zoom in of the area (grey quad arrow) spanning the contour region of residues possibly involved in catalysis (see text). Sequences were obtained from the databases TriTrypDB (<https://tritrypdb.org/tritrypdb/>) or from Uniprot (<https://www.uniprot.org/>). Modelling, mutagenesis and localisation of SNPs were made using PyMOL (<https://pymol.org/2/>).

Following the results of the study of Cosentino et al., and Yao and Wilson, I revisited the string database after two years when the interactome was called for the first time (Figure 4-11, panels B to D). Surprisingly, in this second run, most of the enzymes were already present in the interactomes (Figure 4-11, panels E and F), reflecting that their initial absence was due to a lack of annotation or adequate update of the String database. The possibility of a *Leishmania* ergosome was proposed before based on the analogy of the yeast pathway (Mwenechanya et al. 2017). The yeast ergosome showed that the core of this multi-enzyme complex is formed by the following four enzymes: ERG11 (LmxM.11.1100), ERG25 (LmxM.36.2540), ERG27 and ERG28, the latter two are unknown in *Leishmania* spp., ERG28 is the scaffold of the complex with a strong interaction with four enzymes of the pathway: ERG6 (LmxM.36.2380 and LmxM.36.2390), and with the three C-4 demethylation enzymes, ERG25, ERG26 (LmxM.06.0350) and ERG27 (Mo and Bard 2005c; Mo et al. 2004), a full list with all the names of the orthologues of the SBP in *Leishmania* spp. and yeast, is shown in Table 1.3.

Interestingly, in *Leishmania*, three orthologues of components of the yeast ergosome, ERG11, ERG3 (LmxM.23.1300) and ERG6 in yeast, respectively, have been found with mutations, some, possibly, located out of the binding pocket. Based on the yeast ergosome, ERG2 (LmxM.08_29.2140) and ERG3, have different interaction partners. While ERG2 has a strong interaction with ERG24 (LmxM.31.2320) and ERG28, ERG3 strongly interacts with ERG25 (LmxM.36.2540) and ERG28. Importantly, these two enzymes, ERG2 and ERG3, perform two sequential reactions in the pathway, which are key for the presence of the two double bonds in positions $\Delta 5,7$, and for the binding to polyenes. Interestingly, ERG3 also interacts with ERG11 and ERG6. The protein-protein interactions between ERG3, ERG11 and ERG6 are of particular interest (<https://www.yeastgenome.org>). Similarly, the central role of ERG25 is intriguing, given that in AmBRB lines from Pountain (PhD. Thesis), a strong (3.9-fold) increase in RNA expression was observed in this gene, along with the significant decreases observed in both copies of the orthologue of ERG6 (Pountain et al. 2019b), in which mutations in the dominant transcript were identified (section 4.1.4 and Figure 4-30).

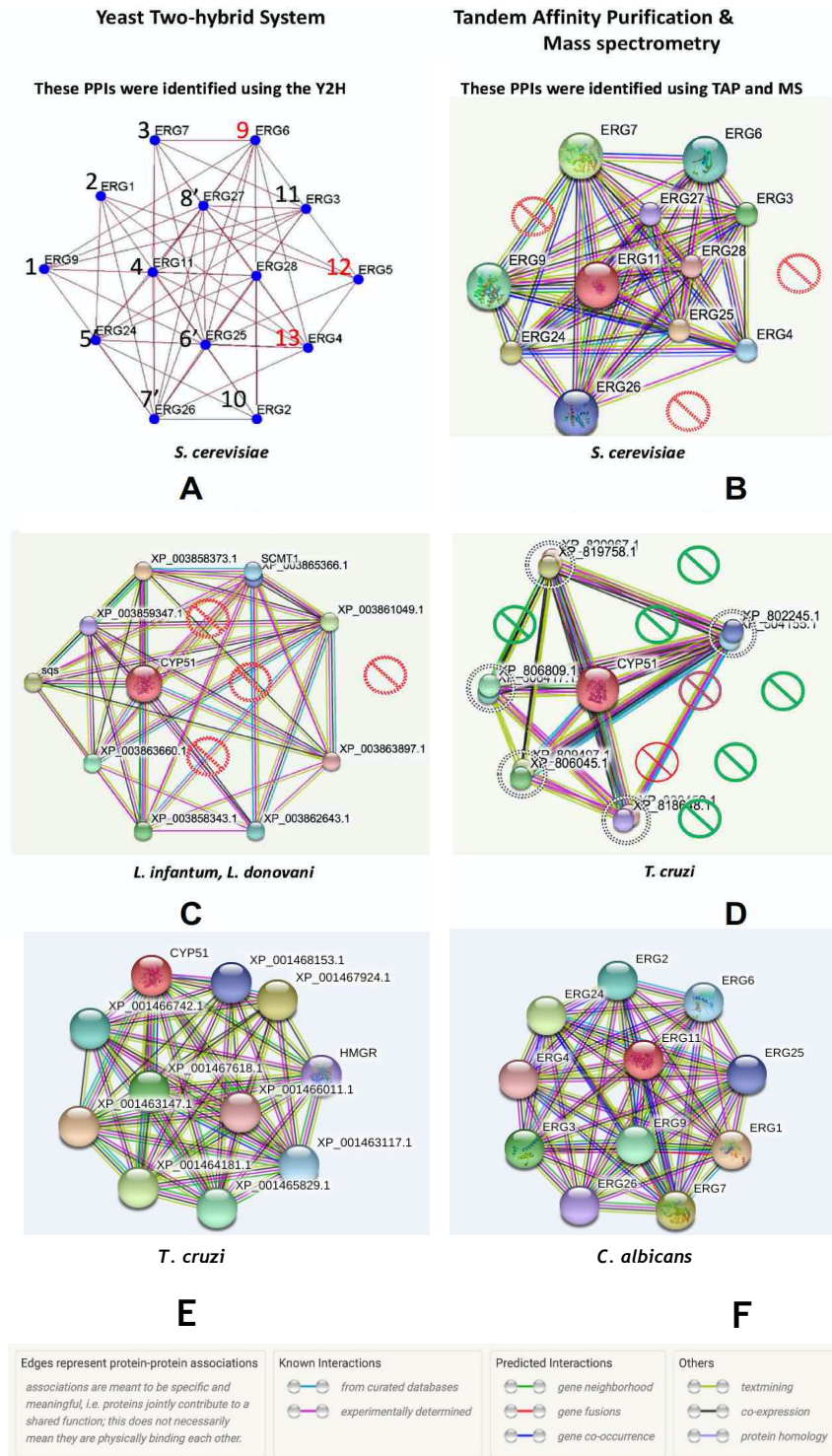


Figure 4-11. Protein-protein interaction (PPI) network in yeast and trypanosomatids. Source: A) from Mo and Bard, 2005 using the Yeast two-hybrid system (Y2H); B) *S. cerevisiae*, C) *L. donovani*, *L. infantum* and D) *T. cruzi* were called from the String database (<http://string-db.org>) from experimental data using Tandem Affinity Purification (TAP) and Mass Spectrometry (MS). Network nodes represent proteins. Coloured nodes represent primary interactions. Empty nodes represent proteins of unknown 3D structure. Filled nodes represent enzymes where 3D structure is known or predicted. A full list with orthologue names in yeast (ERG-) and *Leishmania*, is provided in Table 1-3.

4.2 Discussion

In this study, the evidence of structural variations at the C24SMT locus was notable in two lines, AmBRcl.6 and AmBRcl.8 (clones A11 and E12). These changes were accompanied by alterations in their sterol content. The accumulation of of cholesta-5,7,22-trienol, observed in both these mutants, is in agreement with previous reports, in which other species of *Leishmania* with loss of expression of C24SMT has shown the increase of similar intermediates. The five novel mutations identified in LmxM.23.1300 in three lines (i.e. AmBRcl.3, AmBRcl.14 and NysRcl.B2), produced changes in the sterol profile in both these mutants. Defects in C5DS lead to a loss of ergosterol with an increase in the abundance of sterol intermediates without the 5,6-double bond within the sterol ring, which is characteristic of the loss of functionality of the enzyme (Figure 5-3 lines AmBRcl.14 and AmBRcl.3). Such alterations are expected from mutants with redundant C5DS, and resemble the effects of mutations previously observed in fungi (Alcazar-Fuoli et al. 2006; Geber et al. 1995; Morio et al. 2012), and in *Leishmania* (Pountain et al. 2019), thus confirming the functionality of this enzyme as C5DS. In the study of Pountain et al., a mutation (G415C) in LmxM.23.1300, which was observed in one line, AmBRA/cl1, of *L. mexicana*, resulted in an amino acid substitution (G139R) with a complete loss of ergosterol which, as in two of my lines, AmBRcl.14 and AmBRcl.3, was substituted by ergosta-7,22-dienol (changes in sterols are discussed further (see Chapter 5)). As mentioned before, the presence of the two double bonds in carbons $\Delta 5,7$ is one of the structural components of the sterol molecule (see Chapter 1, Figure 1-9 for a complete list), which determines their selectivity to polyenes (Hsuchen and Feingold, 1973). Polyenes Nys and AmB, have partial or total loss of binding (resistance) for those intermediates with only one double bond ($\Delta 5$, such as cholesterol, stigmasterol, and dihydrocholesterol (Geber et al. 1995; Kontoyiannis and Lewis 2002)). Given the relevance of these double bonds, the correct identification of the C5DS in *Leishmania* spp., is fundamental for downstream analysis. For instance, in the study of Cosentino et al. (and others), is not possible to differentiate if the authors refers to LmxM.23.1300 or LmxM.30.0590, when they compare with the ERG3 orthologue. Although most probably, they refer to the latter, which is annotated as C5DS in the TriTrypDB (and considering that the former was found to have C5DS activity after the publication of the study of Cosentino). Moreover, this is further complicated by the fact that ERG3, like other enzymes, are stage specific or have no orthologue between different species of kinetoplastids. In support of this, the fact that all the enzymes, and the organization of the SBP is still unknown (Yao and Wilson 2016), makes their correct annotation essential.

Similarly, other sterol inhibitors, i.e. azoles, are also less effective in fungi with mutations in this enzyme (Vale-Silva et al. 2012). In my study, I present additional characterization of these two mutations (and others), such as their susceptibility to polyenes AmB and Nystatin and to various antileishmanials, their sterol profiling, and their phenotype in a mouse model. These analyses were also complemented with a characterisation of the histological alterations, which is an aspect that has never been described in AmBR lines of *Leishmania* spp. (Chapter 5, section 5.2.1 (sterols in AmBR lines) and section 5.2.7 (histology of mice infected with AmBR lines). Contrary to those changes in C24SMT, which were always associated with the loss of the miltefosine transporter (MT), none of the mutations in C5DS observed in this study, were related with additional changes in this gene. In another AmB resistant line selected by a former student in the Barrett Lab, a novel mutation (C974T) in C24SMT and the loss of the MT were also identified (PhD Thesis Raihana Binti Ithinin, Barrett Lab, unpublished). Alterations in the MT are, possibly, incompatible (e.g. deleterious) with certain types of sterols (in particular sterols without the two double bonds 5,6), which are lost (ergostanes) to give place to the accumulation of cholestanes as a results of mutations in C5DS. However, in the study of Pountain, AmBR/cl.2, showed mutations in C5DS and C24SMT along with the loss of the MT (Pountain et al. 2019).

In addition to the findings described here, which are consistent with the work of Dr Andrew Pountain and Raihana Binti Ithinin, in my study, I have identified an association between some of these mutations, their sterol profiling, and their phenotype in a mouse model. Moreover, I further characterised these phenotypes, using histology, and confirmed the presence (and virulence), and the retention of resistance of all these lines, including the two attenuated lines, after infection *in vivo*. Additionally, I screened a library of new sterol inhibitors (Chapter 6), which showed activity both *in vitro* in several species of wild type *Leishmania*, four polyene resistant mutants and a C24SMT KO (see chapter 6), and were also active against the *L. mexicana* C24SMT, with substrate specific assays (performed by Boden Vanderloop, from David Nes Lab, Texas Tech University). A summary of all the mutations in genes of the SBP in all four AmBR lines, and their phenotype (sterols, infectivity *in vivo*, and histology), is discussed further (Table 5-6, section 5.2.3 (infection *in vivo*), 5.2.7 (histological changes), and Chapter 7 (metabolomics), respectively.

5 Sterol profiling and infectivity of polyene resistant lines of *Leishmania mexicana*

5.1 Introduction

Leishmania spp. generally contain ergosterol or closely related ergostane sterols, in their membrane as the primary sterol. However, they can survive with an altered composition of sterols that derives from the loss of ergosterol as a result of defective enzymes in the sterol biosynthetic pathway (SBP). For example, exogenous cholesterol and other lipids, can be scavenged from the host or from culture medium (Andrade-Neto et al. 2011; Bastin et al. 1996; Yao et al. 2013; Zhang and Beverley 2010). Cholesterol is abundant in the host and also has structural similarities to ergosterol (section 1.6.5, Figure 1-9). While the former is the main sterol in mammalian cell membranes, the latter is the most abundant in *Leishmania* and also in fungi. Briefly, these two sterols differ in the number of carbons they possess, cholesterol having 27, while ergosterol has 28. Other structural differences include the extra double bonds at carbons C7 and C22, and the methyl group at carbon C24(C28) (Tutaj et al. 2015; Te Welscher et al. 2008, 2010) of ergosterol. Other properties, e.g. chromatography retention time (RT), of these two sterols, and others, are discussed in more detail in this chapter.

Ergosterol, along with sphingolipids, comprise core components of the lipid rafts in the membrane of *Leishmania*. The sterol ring physically contacts the acyl chains of the sphingolipids. Sterols and sphingolipids also contribute to cellular response to the environment and regulation of multiple cellular events (Gulati et al. 2010). Moreover, *Leishmania* parasites possess a unique sphingolipid, inositol phosphorylceramide (IPC), which, like ergosterol, is an attractive antileishmanial target (Denny et al. 2006), along with the enzymes involved in their synthesis. The loss of ergosterol observed in AmBR lines of *Leishmania* is, therefore, thought to alter the interaction between sterols and sphingolipids in the membrane and thus contribute to membrane destabilisation, albeit with no understanding of the mechanism of such events. Similarly, no studies have linked loss of sterol and IPC status in amphotericin B resistant lines that have lost ergosterol.

Defects in several enzymes of the *Leishmania* SBP give rise to AmB resistance, and to a range of different intermediates that replace the main sterol, ergosterol (or close isomers of the ergostane sterol type) (Andrade-Neto et al. 2011; Croft, et al. 2006; Pourshafie et al. 2004; Purkait et al. 2012), and in fungi (Kelly et al. 1994; Laura Y. Young et al. 2003). Similar alterations in sterols can also be observed after the treatment with antifungals. Despite the significant progress in understanding the mechanism of resistance of AmB in *Leishmania* (Pountain et al. 2019), little is known with regard to how the parasite uses cholesterol, or other intermediates, to enable replacement of ergosterol in resistant lines. Some enzymes related with the synthesis of ergosterol, 3-hydroxy-3-methylglutaryl-CoA synthase (HMGS)(LmxM.24.2110) (Carrero-Lérida et al. 2009; Cosentino and Agüero 2014), 3-hydroxy-3-methylglutaryl-CoA reductase (HMGR)(LmxM.29.3190) (Brooks et al. 2012; Dinesh et al. 2014, 2015; Ginger et al. 2001; Singh et al. 2014), and mevalonate kinase (MVAK) (LmxM.30.0560) have also been studied as drug targets in kinetoplastids (de Souza and Rodrigues 2009a). While the role of other enzymes that are essential in fungi, such as C-4 sterol methyl oxidase (SMO) (LmxM.36.2540) (Cosentino and Agüero 2014; Gachotte et al. 1997; Mo and Bard 2005a; Taramino et al. 2010), and C-5 sterol desaturase (C5DS)(see chapter 4, section 4.1.5), is however, poorly understood in these parasites. Similarly, other genes, i.e. C8-sterol isomerase (C8SI) (LmxM.08_29.2140), have never been characterized in *Leishmania* spp.

In the present study, I explored whether changes in sterols in lines I selected, resemble those reported previously in *Leishmania* spp. (Andrade-Neto, et al. 2016; Brooks et al. 2012; Pountain et al. 2019). While previous work with AmB resistance had identified changes to sterol C-14 demethylase (C14DM), sterol C-24-methyltransferase (C24SMT) and sterol C-5 desaturase (C5DS), no studies around changes in parasites selected for resistance to another polyene, nystatin (Nys), in *Leishmania* spp., have been performed.

Sterol and sphingolipid composition in the plasma membrane have been related with the infectivity in *Leishmania* previously, the latter, for instance, being important for the differentiation into the infective metacyclic promastigote form (Denny, Goulding, Michael A. J. Ferguson, et al. 2004; Yao et al. 2013). I therefore investigated possible associations of the sterol composition in AmBR lines with their phenotypes, including pathogenesis, response to treatment, and retention of resistance, during and after infection in BALB/c mice.

5.2 Results

Given the complexity of the Sterol Biosynthetic Pathway (SBP), understanding the structure and nomenclature of the different types of sterols is essential. Cholestanes are a group tetracyclic triterpenes with 27 saturated carbons. Sterols that contain one- or two double bonds, within the ring system are known as cholestene (e.g. cholesterol) and cholestadienes (e.g. ergosterol), respectively. Both cholesterol and ergosterol are also sterols, because they contain an alcohol group. Other examples of cholestane derivatives are lanosterol and stigmasterol. Other types of tetracyclic triterpenes are ergostanes (e.g. campestanol), and stigmastanes, which contain 28- and 29-carbons, respectively (Figure 5-1, Panel A). The sterol nucleus is formed by four domains or rings (named A, B, C and D). In the first domain A, the hydroxyl group located in the carbon 3, gives some polarity to the molecule (De Kruijff et al. 1974). In domains B and C, the number and position of double bonds affect the shape of the molecule, and the binding to polyenes (Hsuchen and Feingold 1973). Finally, domains C and D determine the orientation and length of the side chain, which is a unique substituent of ergostanes. Altogether, these features determine the functionality and other properties of the sterols. Importantly, these features can also be exploited for their identification (Nes 2011; Nes and Parish 1989a). Some of the first methods used for the identification of sterols were NMR and X-ray diffraction. These methods can differentiate ergosterol from cholesterol based on differences between their structures and their abundance in the cell. For instance, in plants and animals, the content of sterols is up to 50-fold (3000 fg/cell) higher than in yeast (20 fg per cell) (Nes 2011).

Other approaches commonly used for the identification of sterols are high-pressure liquid chromatography (HPLC) and UV-vis spectroscopy; the former can detect small amounts (up to 0.04 μg per gram), and the latter, identifies sterols based on the number and distribution of the double bonds within their ring. While the number of possible combinations of double bonds in the molecule is numerous (more than 10 combinations), each combination gives a unique absorption spectrum (Qiao et al. 2015).

Sterols with a pair of double bonds absorb energy between 240-300 nm. Ergosterol, for instance, has a $\Delta^{5,7}$ double bond system and a distinctive absorbance spectrum at 282-283 nm (Dorfman 1953; Seitz et al. 1979; Sokol-Anderson et al. 1986). By contrast, cholesterol and other plant sterols (e.g. sitosterol, stigmasterol) only have one Δ^5 double bond, and therefore absorb light at <240 nm (Seitz et al. 1977, 1979). In another study, 50 triterpenoids were characterised and compared with 31 standards, using ultra-high-performance liquid chromatography coupled with diode-array detection and quadrupole

time-of-flight mass spectrometry (UHPLC/DAD/qTOF-MS). Despite lacking the $\Delta 5,7$ double bond, some sterols produced peaks between 198 - 274 nm (Figure 5-1 Panels B and C)(Qiao et al. 2015), however, those sterols with at least two double bonds located in other carbons, produced peaks more similar to those observed with ergosterol. While UV-vis is useful for the detection of ergosterol (Gutarowska and Zakowska 2010), its use for the accurate identification of other sterols is more limited. In another interesting method, ergosterol was combined with iodine, forming a highly stable fluorescent product that absorbs at 271 nm (and is even more stable than ergosterol alone which auto-oxidises). With this method, ergosterol was differentiated from other sterols, none of which produced a fluorescent product after the addition of iodine (Rao et al. 1989). UV-vis is also useful to determine the orientation of polyenes (i.e. AmB and Nys) within membranes (Castanho, Lopes, and Fernandes 2003; Lopes and Castanho 2002).

In *Leishmania*, UV-vis identified the ergosterol spectrum, with a first peak at 281 nm, a second peak at 271 nm, and finally, a shoulder at 293 nm (Mwenechanya et al. 2017; Pountain et al. 2019a). In their work, Pountain and colleagues characterised various AmBR lines with defects in different sterol pathway enzymes (e.g. C14DM, C24SMT and C5DS), showing that those mutants with defects in the enzyme C5DS were lacking the characteristic spectra of ergosterol due to the absence of the $\Delta 7$ double bond within the sterol ring. Similarly, Mwenechanya *et al.* reported the absence of the ergosterol peak in AmBR lines of *L. mexicana* with a mutation in the enzyme C14DM. In another study in *L. major*, Xu and colleagues further confirmed this finding, using GC-MS. After the deletion of C14DM, a complete loss of various sterols with the $\Delta 5,7$ double bond system was found with GC-MS, including ergostane-based (i.e. 5-dehydroepisterol, ergosterol, and episterol), and a cholestane type (cholesta-5,7,24-trienol), suggesting a link between this enzyme and the production of sterols with two double bonds (Xu et al. 2014). UV-vis and GC-MS have been used previously in *Leishmania* spp. (Al-Mohammed et al. 2005; Pountain et al. 2019; Andrade-Neto et al. 2016b; Xu et al. 2014) and in *T. brucei* (de Souza and Rodrigues 2009a).

GC-MS offers a number of advantages and allows for the detection of a broad range of metabolites in any sample (e.g. amino acids, carbohydrates, fatty acids) and with good coverage (Zarate et al. 2016). GC-MS also has higher selectivity and susceptibility for the identification of different types of sterols (Varga, Bartók, and Mesterházy 2006). This method became the standard for the identification and quantification of sterols (Goad and Akihisa 1997) since the separation of sterols in gas-liquid systems (GLC) (such as GC-MS) depends on the polarity and molecular weight of the sterol molecule (Heupel, cited in

(Nes and Parish 1989a). As with the UV-vis spectra, each one of the substituents within the sterol ring and the side chain determines the retention time (RT) of sterols in GC-MS (Goad and Akihisa 1997). For instance, the single addition of an alkyl group, the number and distribution of double bonds within the sterol ring or in the side chain, will give a unique RT.

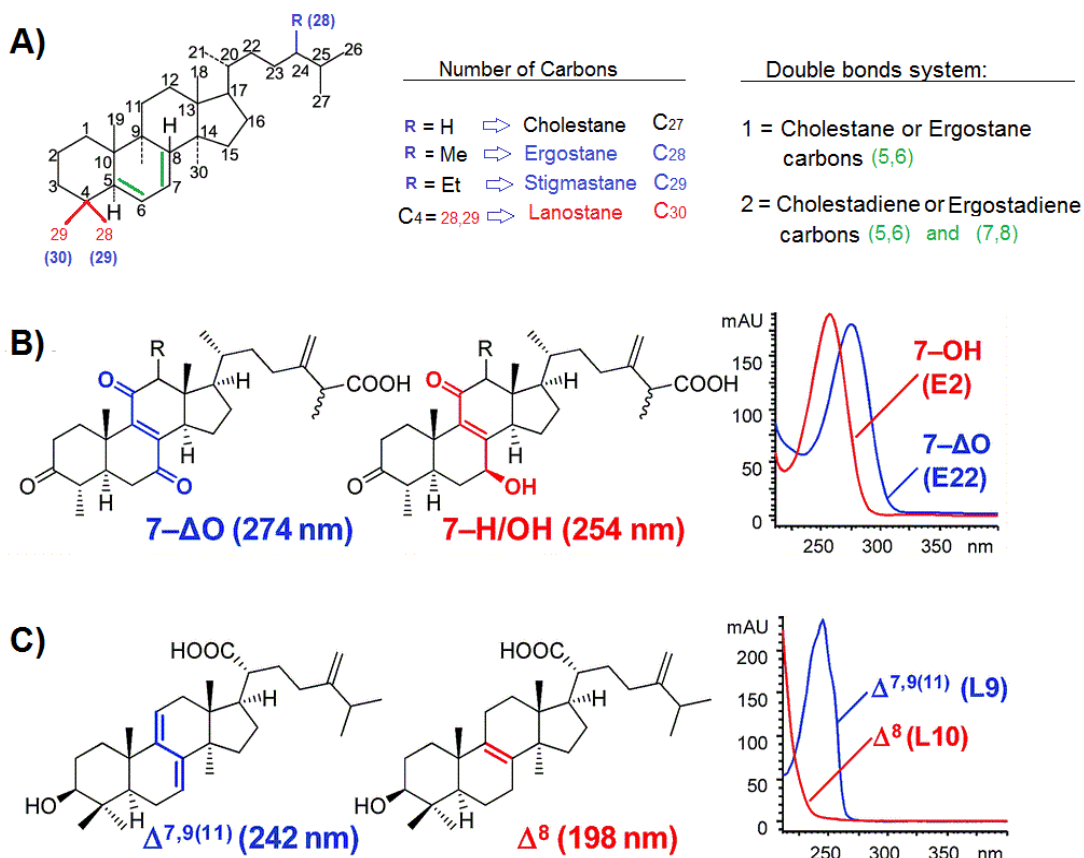


Figure 5-1. Nomenclature of Sterols and the double bond system.

The numbers of the carbon atoms of the sterol molecule. Group R (in blue) is replaced by different substituents to form cholestanes (27 carbons), ergostanes (28 carbons), and stigmastanes (29 carbons), lanostanes can have 29 or 30 carbons (red). Double bonds (in green) system: cholestanes or ergostanes have one double bond (Δ^5), cholestadienes or ergostadienes have a pair of double bonds ($\Delta^5,7$). More than two double bonds the suffix (-triene for 3, -tetraene for 4) allows for the identification (Panel A). The maximum UV absorption for ergostanes (Panel B) and lanostanes (Panel C) of *A. cinnamomea* (as example) show the changes of the absorbance after incorporating different substituents. Sources: Panel A modified from (Nes and Parish 1989a); Panels B and C (Qiao et al. 2015).

Another example is the C-24 methyl substituent, introduced by the enzyme C24SMT, which increases the elution time from 1.28 min to 1.31 min (Relative Retention Time (RRT), i.e. relative to cholesterol which has a RT of 1.000) independently of the gas liquid chromatography (GLC) system used, GLC is often referred only as gas chromatography (Patterson G. 1971). Given the relevance that these substituents also have in the MoA (Anderson et al. 2014; De Kruijff et al. 1974), and resistance (Mwenechanya et al. 2017; Pountain et al. 2019a) to polyenes, the employment of methods for the correct identification of sterols is essential. This is particularly relevant with triterpenoids, which can be considered as one single compound with other less specific approaches, due to the high similarity between their structures (Qiao et al. 2015). However, the annotations of peaks sometimes can be problematic when adequate standards are not available. Particularly, for those molecules with a number of isomers and with very similar structure and related ion patterns. In these cases, the use of derivatization (chemical alteration of sterols to produce a more amenable molecule for the analysis) is essential, as this method provides a more reliable identification based on the differential RT values of the sterols.

Although derivatization is an essential step for the accurate identification of sterols in GC-MS, it has some disadvantages that can perturb analysis of a given sample (Goad and Akihisa 1997). In a recent approach, GC-MS was performed without derivatization, where fragmentation was sufficient to allow detection of ergosterol accurately, and with excellent correlation ($R^2 > 0.96$) with HPLC (Zakir Hossain and Goto 2015).

Other disadvantages of GC-MS include a need to include reference standards which are expensive and can vary from one laboratory to another, the lack of uniformity between methods (Patterson G. 1971), and the requirement of heating or vaporisation of the sample, which can interfere with the identification of volatile metabolites. This can be improved using trimethylsilyl (TMS) (a silylation agent) and using derivatization (Koek et al. 2011; Zarate et al. 2016). Finally, the nomenclature of sterols is rather complex and the identification of similar compounds can be difficult. Here, we use the IUPAC-IUB nomenclature recommended by Nes (IUPAC-IUB Comm. on Biochem. Nomencl 1970; Nes and Parish 1989b).

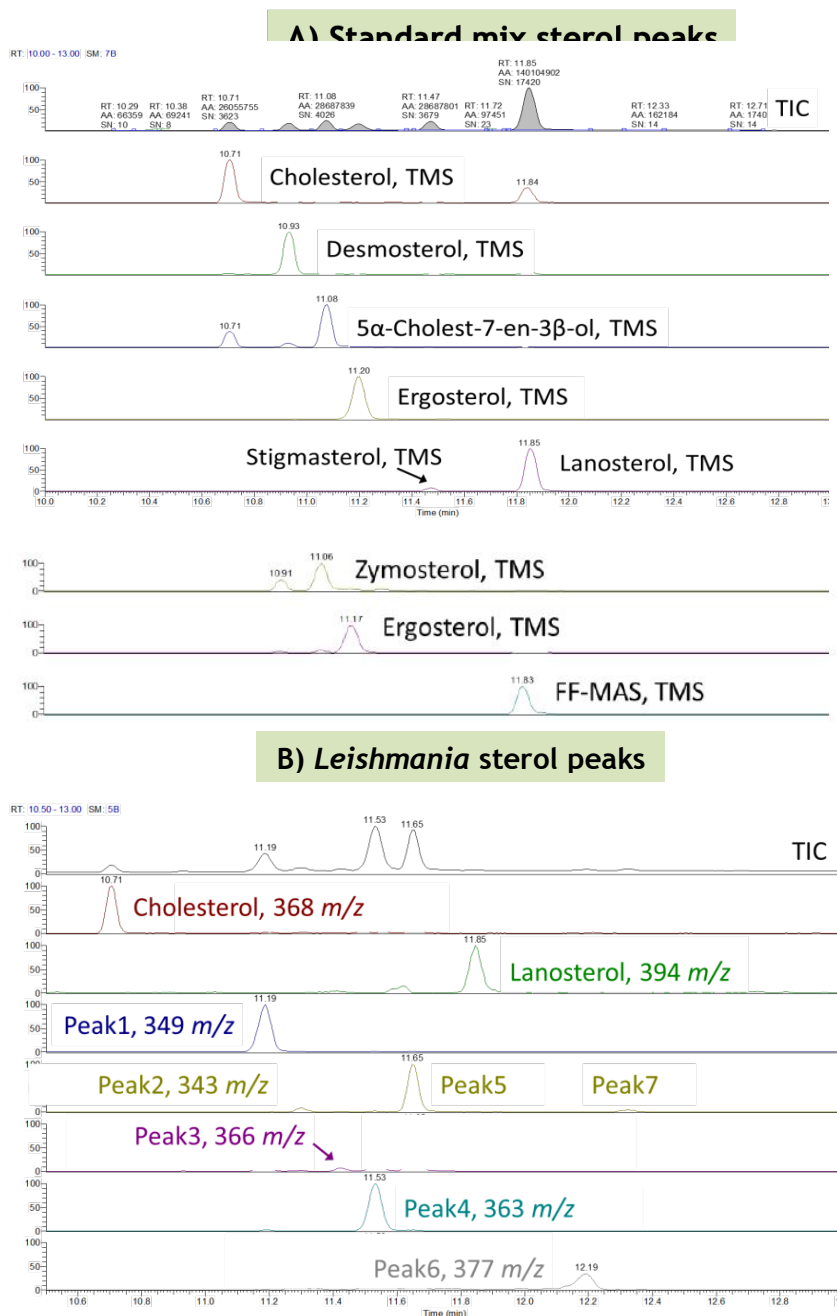


Figure 5-2. Ion chromatogram for the mass of the fragment ion for the standard mix- and the *Leishmania*-sterol peaks.

Sterol standard mix from Glasgow Polyomics* (communication from Stefan Weidt). The upper frame depicts the total ion chromatogram (TIC) of TMS derivatives of fraction of sterols from the standards (Panel A - top) and *Leishmania* sterol samples (Panel B - bottom). The mixture of standards was run with a blank, and the samples, to provide a reference spectrum and retention times (RT) for matching the experimental samples. The proposed annotations of the TMS derivatives are shown as the underivatized form in Table 5-1. * <https://www.polyomics.gla.ac.uk/>

5.2.1 The sterol signature of AmB resistant lines

5.2.1.1 Sterol signatures of AmBR promastigotes

Sterol profiling using GC-MS was performed on all of the polyene resistant lines of *Leishmania mexicana*. First, all sterols were detected as their trimethylsilyl (TMS) ester derivatives (but reported here in their underivatized form). Individual sterols are expressed as a percentage of the total sterol content following normalisation. After comparison with a pool of the reference standards, only three of the standards (cholesterol, lanosterol and zymosterol) matched any of the *Leishmania* samples. Sterol peaks are presented in a sequential order, starting from lanosterol (upstream) and with ergosterol at the end (downstream) of the pathway (see Table 1-3, for a full list of the genes and orthologues of the Sterol pathway). Other intermediates (e.g. cholesterol, desmosterol) which are not part of the *Leishmania* pathway, or for which identification was unclear or contradictory, are listed after ergosterol. A complete list of all of the sterols identified with GC-MS and their differences between wild type and all AmBR and NysR lines is shown in Table 5-1 to Table 5-3, and Figure 5-3 to Figure 5-5.

In this study, ergosta-5,7,24(28)-trien-3 β -ol, was the most abundant sterol (72 - 82 %) in wild type promastigotes of *L. mexicana*. This sterol is an isomer of ergosterol (C₂₈H₄₄O) also known as 5-dehydroepisterol. These two isomers differ in the position of the double bond of their side chain, which is located in carbon 22, and carbon 24, in ergosterol and 5-dehydroepisterol, respectively. The fragmentation pattern of both isomers is very similar, nonetheless, the corresponding peak for ergosterol in the *Leishmania* samples was very weak. In turn, the peak of 5-dehydroepisterol showed a strong signal. Moreover, the latter exhibited a different RT (11.61 to 11.67) than the reference standard of ergosterol (RT of 11.37).

A similar spectrum and RT in these two isomers was observed previously (Xu et al. 2014; Yao and Wilson 2016b). In the latter of these studies, two isomers of ergosterol (named type- I and II) with comparable values were reported in *L. infantum chagasi* (Yao et al. 2013; Yao and Wilson 2016). In *T. brucei*, four structural isomers, 1) ergosta-5,7,22-trien-3 β -ol, 2) ergosta-5,7,25(27)-trien-3 β -ol, 3) ergosta-5,7,24(28)-trien-3 β -ol, and 4) ergosta-5,7,24(25)-trien-3 β -ol, displayed a similar UV light spectra similar to that of ergosterol (Zhou, Cross, and Nes 2007). However, none of these four isomers showed a match with the internal ergosterol standard or the *Leishmania* isomer, possibly, because these isomers are from *T. brucei*.

Another abundant sterol (based on the comparison with NIST libraries) identified in wild type parasites in this study was, ergosta-7,22-dien-3-ol (11%). Other less abundant sterols were also found and are shown in Table 5-1. The relative abundance of cholesterol was between 2 to 7% and was similar across all samples. Cholesterol is probably from an exogenous source, e.g. foetal bovine serum (FBS) which is added to the culture medium. Although in lower abundance (0.2 – 0.4%), the presence of traces of lanosterol in all samples, suggests that the enzyme C14DM was functional. The abundance of ergostanes, i.e. ergosterol, found in this study, is in agreement with previous reports in which this class of sterol has been reported as the most abundant in both, promastigotes (between 60- to 80%), and amastigotes of *Leishmania* spp. (Roberts et al. 2003).

The GC-MS profile of all the polyene resistant lines showed significant changes in relation to their respective parental wild type. The most notable change that was observed across all AmBR lines, was the total or partial loss of the wild type sterol ergosterol (or any of its isomers). Overall, the four AmBR lines displayed two main patterns of alterations. Two lines, AmBRcl.14 and AmBRcl.3, had the wild type ergosterol replaced by ergosta-7,22-dien-3-ol (96 - 97%), the latter which is an intermediate lacking the 5(6) saturation. The presence of this intermediate suggests that defects in the enzyme C5-desaturase (C5DS) were, possibly, present or that the enzyme was redundant. In this study, five novel mutations were confirmed in this enzyme (discussed in detail in chapter 4) in resistant lines selected for resistance against AmB and Nys.

Interestingly, this intermediate, ergosta-7,22-dien-3-ol, also showed a two-fold increase with respect to wild type (18 to 20%), in a line overexpressing an episomal wild type-copy of the C24SMT. LmxM.36.2380, named C24SMT herein, measured using RNA-seq and qPCR (sections 2.14 and 2.11, respectively). RNA-seq data is shown in Figure 6-7 and is also provided as Supplementary 8 excel file (see page 8). The sterol profile (GC-MS), and susceptibility against a new library of sterol inhibitors of this line, is discussed further (Chapter 6, section 6.2). The negative controls, i.e. solvent without parasites pellet, used were as described in chapter 2 (see section 2.8).

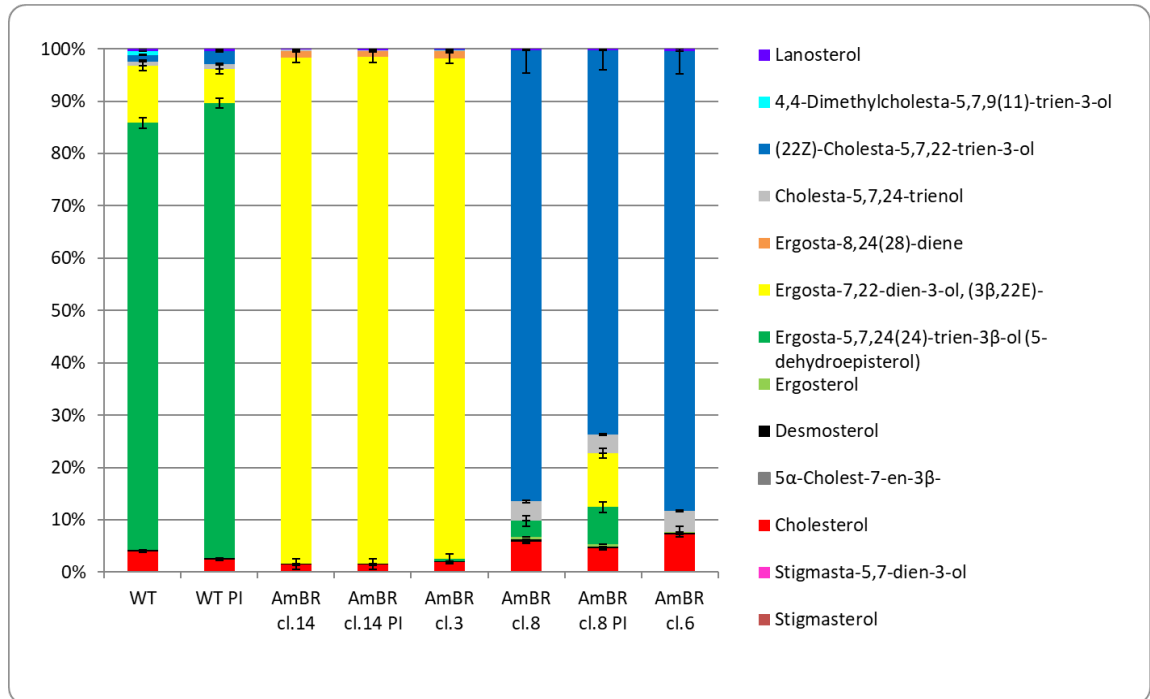


Figure 5-3. Metabolite profiling by GC-MS in AmBR lines of *L. mexicana* promastigotes. Content of sterols is shown as a percentage of the total of sterol identified, as determined by GC-MS. Error bars represent standard deviation of the mean of three biological replicates. AmBR resistant lines. Sterol profile of AmBR lines recovered post infection (PI) are included for comparison with the axenic lines (high passage).

The other two lines, AmBRcl.8 and AmBRcl.6, showed a different set of alterations. In these, the most abundant intermediate that replaced the wild type sterol was cholesta-5,7,22-trienol, the abundance of which rose from 1.2% in the wild type, up to 86% and 88% in both resistant lines, respectively. Another intermediate that increased moderately in AmBRcl.8 and AmBRcl.6, was cholesta-5,7,24-trienol (3.7 to 4%). These two intermediates have two double bonds and were absent or in very low abundance (0.2 and 0.6%) in lines AmBRcl.14 and AmBRcl.3. With respect to the isomer of ergosterol, 5-dehydroepisterol, it was absent from AmBRcl.6 and in low abundance (6 - 11%), in AmBRcl.8. In agreement with these findings, cholesta-5,7,24-trien-3-ol was also the most abundant membrane sterol in an AmBR-clinical isolate of *L. donovani* promastigotes, showing that this sterol showed a reduced affinity to AmB (Purkait et al. 2012). Similarly, cholestane-based intermediates, were the most abundant after the loss ergosterol and C24-methylated intermediates in a C24SMT null mutant of *L. major*. In my study, I further confirmed this effect in a C24SMT knockout (named C24SMTKO hereon), created using CRISPR-cas9 (Beneke et al. 2017), in which the increase of cholesta-5,7,24-trien-3-ol and cholesta-5-7-dienol, was more pronounced (90.8 to 91.2%) (see chapter 6 for details). The increase of cholesta-5,7,22-trienol (from 3.0 to 64.0%) and cholesta-5,7,24-trienol (from 3.0 to 64%), was also observed in wild type and one AmBR line of *L. infantum*

(Supplementary file 5) (see page 8) that I selected using a similar approach than with *L. mexicana* (see chapter 3, Figure 3-1). As with *L. mexicana*, this resistant line also showed a dramatic reduction of the wild type ergosterol (from 68 to 4%), and other ergostanes, i.e. ergosta-7,22-dien-3-ol (17 to 0%). Contrary to the samples of promastigotes and amastigotes of *L. mexicana*, in which only the isomer of ergosterol was detected, in this resistant line, both the isomer and ergosterol were present with similar abundance (4%).

Resistance to the antileishmanials MF, PAR (Hendrickx et al. 2015, 2016; Mondelaers et al. 2016), and antimonials (Fadili et al. 2005; Leprohon et al. 2009) have been reported in *L. infantum*, two studies with AmB in this specie were found, the first one used flow cytometry to analyse the effect of catalase, ascorbic acid and ketoconazole, on the permeability and potential of the membrane (Azas et al. 2001), whereas the second study, analysed the proteome of AmB resistant promastigotes (Brotherton et al. 2014). None of these two studies, however, analysed sterol changes. Two studies in *L. donovani* (both species are in the *L. donovani* complex), and another in *L. major* (Mukherjee et al. 2018), also found cholesta-5,7,22-trienol replacing the wild type ergosterol (Mbongo et al. 1998b; Purkait et al. 2012), and the only study in which both, sterols and AmB, are studied in *L. infantum*, found an increase in ergostane intermediates but not in cholestanes (Yao and Wilson 2016). A summary of these changes is showed in Table 5-5.

Cholesterol was present (between 4.5 to 7%) in wild type and in all of the AmBR resistant lines from all species analysed, i.e. *L. mexicana*, *L. infantum* and *L. tarentolae* (the latter not included in this thesis). Interestingly, the abundance of cholesterol in AmBR lines, AmBRcl.14 and AmBRcl.3, with mutations in enzymes C5DS, was notably lower, 2.0 - 2.8-fold, while in lines, AmBRcl.8 and AmBRcl.6, which have defects in C24SMT, in which cholesterol increased between 2.3 - 3.7-fold. Note that these fold changes are relative to the parental wild type. If the type of defects (and intermediates replacing ergosterol) are related with the ability of the AmBR mutants to uptake cholesterol is, however, unknown. This difference in the abundance of cholesterol in AmBR lines, indicates that in those lines with defects in C5DS there may be an altered association between sterols and sphingolipids, which caused a more fluid membrane (Xu et al. 2014).

5.2.1.2 Sterol signature of AmBR amastigotes

The extracts from amastigotes showed more sterols than promastigotes (Figure 5-4 and Table 5-2). Sterols were determined in amastigotes that were recovered from primary lesions or from lymph nodes and sub-cultured *in vitro* (only one passage), until a density of 1×10^8 cells was attained. While resistant promastigotes had a partial or total loss of the

wild type sterol, 5-dehydroepisterol, in amastigotes this sterol was the most abundant in both, wild type (41.4%) and in the resistant line AmBRcl.8 (48.6%). The sterol intermediates of the latter, suggest that, as in promastigotes, this line has a functional C5DS. The increase in the abundance of ergosterol observed in amastigotes of AmBRcl.8, was not observed in amastigotes of the other resistant line, AmBRcl.14, possibly due to the mutations present in the latter, i.e. a deletion of a methionine (M93del), and a substitution R244L (G731T), in C5DS (LmxM.23.1300), which inactivates the enzyme (Note that gDNA for sequencing analysis was obtained from promastigotes in all AmBR lines, but not from amastigotes). A full description of the changes in different genes is discussed further (chapter 4, section 4.1.3).

A secondary sterol, 4,4-Dimethylcholesta-5,7,24-trien-3-ol, was also abundant in wild type (11.6%) and AmBRcl.8 (12.9%) but absent in AmBRcl.14, and other less abundant sterols were also identified. For instance, lanosterol (0.3%) was only found in wild type amastigotes, whereas cholesta-5,7,22-trienol (2.7%), and cholesta-5,7,24-trienol (1.2%) were only present in AmBRcl.8. On the other hand, the resistant line AmBRcl.14, has two major sterols, ergosta-7,22-dien-3-ol (43%), and a new stigmastane-type sterol, which was annotated as stigmasta-5,7-dien-3 β -ol (50%). Although of lower abundance, both intermediates were also detected in wild type and AmBRcl.8 amastigotes. While the abundance of ergosta-7,22-dien-3-ol was 25.8% and 18.5%, that of stigmasta-5,7-dien-3 β -ol was 8% and 6%, in wild type and AmBRcl.8, respectively (Figure 5-4 and Table 5-2). Amastigotes contain a comparable abundance of cholesterol as promastigotes, (7-10% of total sterol in all AmBR lines, and 8.1% in wild type). Although the concentration of cholesterol in the culture medium was not measured with GC-MS, some variation can be expected between batches. However, its relatively homogenous abundance observed with GC-MS between promastigotes and amastigotes is explained, at least in part, by the similar concentration (10%) of FBS added in their respective culture media.

Overall, the identification of sterols is challenging given the nature of their complexity and that of the pathway. In *Leishmania*, this is more challenging as we need to consider that some genes have two copies (as in C24SMT), and that the amastigote stage also interacts and can uptake sterols from the host cell macrophages, e.g. cholesterol (Andrade-Neto et al. 2011; Bastin et al. 1996; Ginger et al. 1999; Yao et al. 2013a; Zhang and Beverley 2010). In amastigotes, the increase of two intermediates, both with two double bonds, and which were absent in promastigotes is not well understood. An explanation for this can be the presence of another enzyme with similar function, i.e. C5DS, in the intracellular stage. Interestingly, another enzyme is annotated as the putative C5DS in *Leishmania* spp.

(LmxM.30.0590 in *L. mexicana*). A detailed discussion of the annotation between these enzymes and their identity with respect to other orthologues, was presented in chapter 4 (see section 4.1.5). Alternative explanations to the increase of these intermediates with two double bonds in this line are, for instance, the presence of other host-desaturases, which could, possibly, convert other intermediates into ergosterol or stigmastane-type intermediates. This needs further investigations.

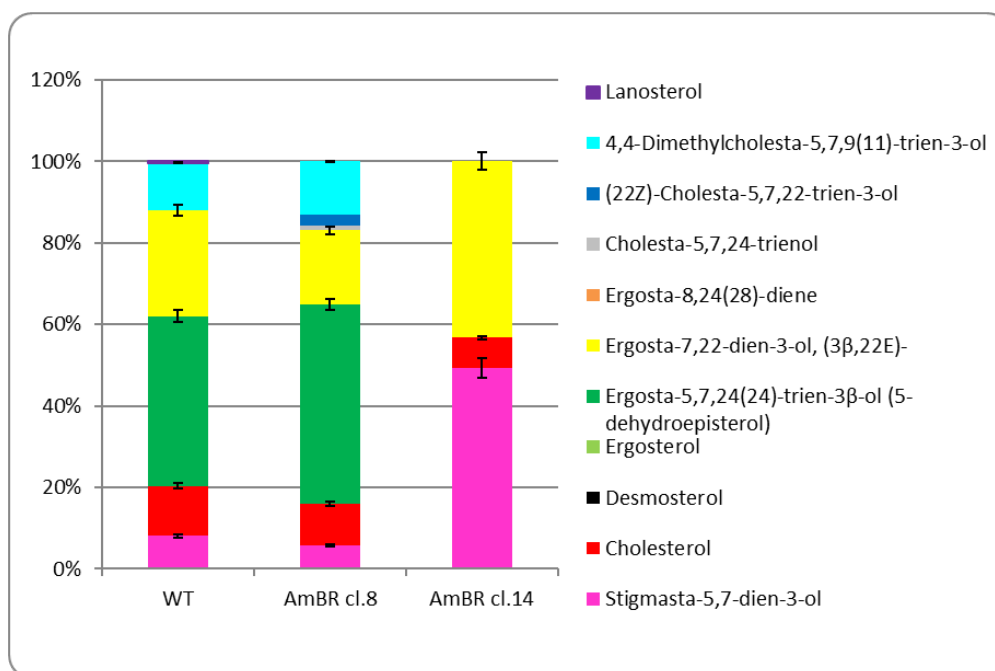


Figure 5-4. Metabolite profiling by GC-MS in AmBR lines of *L. mexicana* amastigotes. Content of sterols is shown in percentage of the total of sterol identified, as determined by GC-MS. Error bars represent standard deviation of the mean of three biological replicate.

The partial retention of activity of the enzyme is also feasible and could explain the increase of these intermediates. The presence of both, cholesta-5,7,22-trien-3-ol and stigmasta-5,7-dien-3-ol (both with Δ 5,7 double bonds), in amastigotes from both lines, AmBRcl.14 and AmBRcl.8, also supports the idea of partial C5DS activity. Interestingly, in their study, Al-Mohammed and colleagues, showed that both intermediates (both which are alkylated at C-24 in the side chain), were totally absent from both amastigote and promastigote forms that were highly resistant to AmB. Instead, the most abundant sterol was a cholestane-type, 4,14,dimethyl-cholesta-8,24-dienol, which increased significantly from 62.4% in promastigotes, to 97,3% in amastigotes (Al-Mohammed et al. 2005). Previous studies have also reported some stigmastane type sterols, e.g. stigmasterol, stigmasta-5,22-dienol, and stigmasta-5-en-3-ol, in *Leishmania* (Goad, Holz, and Beach 1984; Pomel, Cojean, and Loiseau 2015; Roberts et al. 2003; Yao and Wilson 2016). The study of Al-Mohammed et al., a stigmastane-type sterol, stigmasta-5,7,24(24)-

trienol, was identified in wild type promastigotes (10.6%) and at significantly higher concentration (47.2%) in the wild type amastigote stage.

Another notable difference between promastigotes and amastigotes was also observed with ergosterol (or its isomer ergosta-5,7,24(241)-trienol), the abundance of which decreased from 85.1% in the former to 40.9% in the latter. These values are comparable to those reported here in wild type promastigotes (81.63%) and amastigotes (41.4%), however, the isomer of ergosterol identified in this study was different, i.e. ergosta-5,7,24(28)-trien-3 β -ol (Table 5-1 and Table 5-2). Contrary to the study of Al-Mohammed, here, no stigmastane-type sterol was identified in any of the samples from wild type and from AmB resistant promastigotes. However, this sterol was detected in all of the amastigote samples analysed, i.e. wild type, AmBRcl.14 and AmBRcl.8 (Figure 5-4 and Table 5-2). Moreover, a stigmastane-type sterol was also detected in all four samples of promastigotes resistant to nystatin, discussed in the following section. In agreement to this, other studies have also reported low abundance (5%) of stigmastanes in promastigotes, which increased up to 20%, in amastigotes of some *Leishmania* spp., suggesting that these C-29 intermediates, possibly, confer some advantage to this stage of the parasite within the macrophage (Roberts et al. 2003).

5.2.2 Sterol signatures of nystatin resistant lines

As in all the other wild types, the isomer 5-dehydroepisterol was the most abundant sterol (77.8-81.6%) in both the low and high passage wild type cell lines used in selecting nystatin resistance. Another abundant sterol was ergosta-7,22-dien-3-ol (10.9-12.1%), followed by 4,4-dimethylcholesta-5,7,24-trien-3-ol (1.4-2.2%), and other less abundant sterols (0.5-1.2%) were also detected (e.g. cholesta-5,7,24-trien-3-ol, cholesta-5,7,22-trienol and ergosta-8,24(28)-diene). Unlike the two main patterns of alterations observed in AmBR lines, all four clones of NysR lines showed a similar profile. The most abundant intermediate replacing ergosterol was ergosta-7,22-dien-3-ol (80.2-89.1%), an intermediate lacking the C-5 desaturation. Interestingly, all four lines had a secondary sterol, stigmasta-5,7-dien-3-ol, which was more abundant in lines NysRcl.B2 and NysRcl.C1 (9.9 and 14.2%, respectively), than in NysRcl.E1 and NysRcl.F2 (6.1 and 7.0%, respectively). As described in chapter 4 (4.1.5), accumulation of ergostanes in these NysR mutants derived from lesions (A95del) in C5DS identified in NysRcl.B2 (the other three clones were not NGS-analysed due to costs limitations), which has never been reported in *Leishmania* spp.

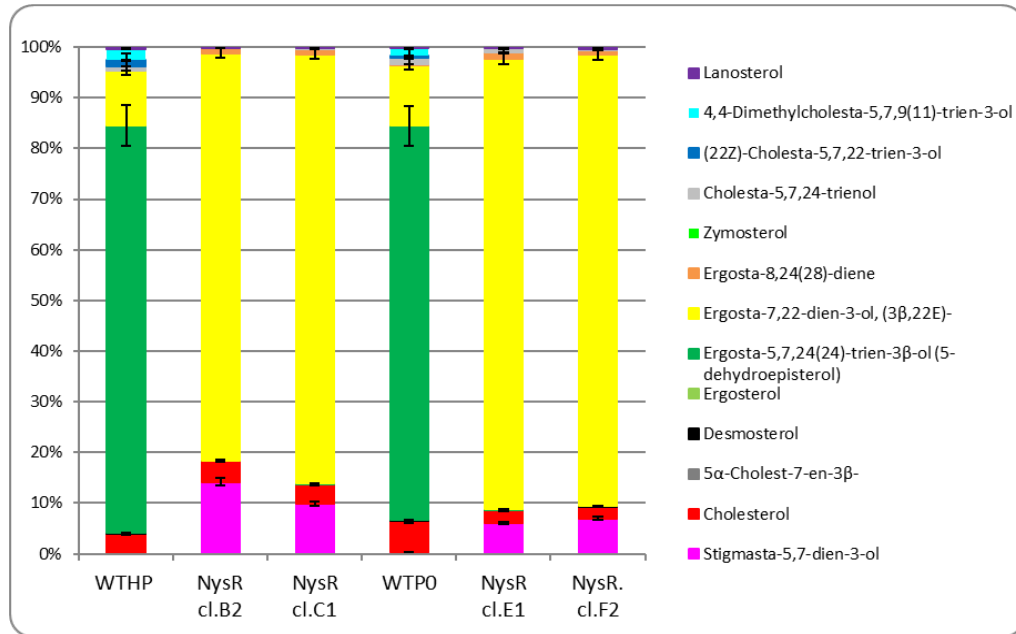


Figure 5-5. Metabolite profiling by GC-MS in NysR lines of *L. mexicana* promastigotes. Content of sterols is shown as a percentage of the total of sterol identified, as determined by GC-MS. Error bars represent standard deviation of the mean of three biological replicates. Names of WTHP and WTP0, and NysR lines are described here in the text (5.2.2), and in Chapter 3 (see 3.2.1.2).

As with all the other promastigote and amastigote AmBR lines, cholesterol was also present in all samples, being more abundant in WTHP (3.9-4.1%) than in WTP0 (2.3-2.5%) (Figure 5-5 and Table 5-3). A summary with the mutations in genes of the SBP in all four AmBR lines, and their phenotype, is shown in Table 5-5, and discussed in more detail in sections 5.2.3 (infection *in vivo*, histology), and Chapter 7 (metabolomics). Based on the GC-MS profile of sterols observed with the four NysR lines (Figure 5-5 and Table 5-3) was totally different than that for the AmBR lines, the analysis of the genotype using NGS, and phenotype *in vivo* of these lines, is important, but could not be carried out due to time constraints in this thesis.

Table 5-1. Metabolite profiling by GC-MS (derivatization with trimethylsilyl, TMS) in AmBR lines of *L. mexicana* promastigotes. Content of each sterol is the percentage of the total of the raw peak area detected per line \pm Standard deviation of three independent biological replicates. Standards used were: Cholesterol, TMS. Desmosterol, TMS. 5 α -Cholest-7-en-3 β -ol, TMS. Ergosterol, TMS. Stigmasterol, TMS. β -sitosterol, TMS. Lanosterol, TMS. FF-MAS (4,4-dimethyl-5 α -cholesta-8,14,24-trien-3 β -ol), and zymosterol (Source: Glasgow Polyomics). FF-MAS: Follicular fluid meiosis-activating sterol, is an intermediate in the cholesterol biosynthetic pathway present in all cells. Those peaks that did not match any standard were determined by comparing with the NIST spectral libraries with the ion trap mass spectrometer and Peak 4 was identified based on previous work (see text 5.1). SBP: Sterols Biosynthetic Pathway. RT: retention time.

SBP number	Peak and/or Putative Annotation	Major frag mass <i>m/z</i>	Molecular ion* <i>m/z</i>	-TMS <i>m/z</i>	Formula -TMS	RT /min	Evidence and Confidence	WT	WT PI	AmBR cl.14	AmBR cl.14 PI	AmBR cl.3	AmBR cl.8	AmBR cl.8 PI	AmBR cl.6
1	Lanosterol, TMS	394	499	426	C ₃₀ H ₅₀ O	11.85 - 12.01	Match both RT and <i>m/z</i> to standard	0.41 \pm 0.13	0.38 \pm 0.01	0.18 \pm 0.02	0.22 \pm 0.05	0.18 \pm 0.21	0.24 \pm 0.04	0.32 \pm 0.13	0.37 \pm 0.10
	Peak 6 - FF-MAS (aka 4,4-Dimethylcholesta-5,7,24-trien-3-ol), TMS or to 4,4-Dimethylcholesta-5,7,9(11)-trien-3-ol.	377	483	410	C ₂₉ H ₄₆ O	12.19 - 12.38	NIST Score 608 to 4,4-Dimethylcholesta-5,7,9(11)-trien-3-ol. Reported as FF-MAS based on previous data and literature.	0.73 \pm 1.27							
	Peak 1 - (22Z)-Cholesta-5,7,22-trien-3-ol, TMS	349	455	382	C ₂₇ H ₄₂ O	11.19 - 11.36	NIST Score 678	1.28 \pm 0.66	2.57 \pm 0.47			0.06 \pm 0.11	86.23 \pm 4.25	73.35 \pm 8.74	87.91 \pm 2.91
	Peak 2 - Cholesta-5,7,24-trienol	343	456	383	C ₂₇ H ₄₄ O	11.30 - 11.47	Desmosterol NIST match 699, wrong RT	0.77 \pm 0.35	0.88 \pm 0.18	0.23 \pm 0.10	0.16 \pm 0.04	0.19 \pm 0.33	3.72 \pm 0.25	3.61 \pm 1.9	4.04 \pm 0.60
5	Zymosterol, TMS	369.4	456.4	383.3	C ₂₇ H ₄₄ O	10.98	Match to standard								
6	Peak 3 - Ergosta-8,24(28)-diene, TMS (or Fecosterol)	366	470	397	C ₂₈ H ₄₆ O	11.43 - 11.6	NIST Score 552			1.24 \pm 0.08	1.11 \pm 0.11	1.33 \pm 0.14			
	Peak 5 - Ergosta-7,22-dien-3-ol, (3 β ,22E), TMS	343	470	397	C ₂₈ H ₄₆ O	11.65 - 11.82	NIST Score 701	10.95 \pm 1.93	6.53 \pm 0.24	96.73 \pm 0.23	96.88 \pm 0.18	96.01 \pm 1.08		10.27 \pm 14.77	
8	Peak 4 - Ergosta-5,7,24(28)-trien-3 β -ol (a.k.a. 5-dehydroepisterol)	363	469	396	C ₂₈ H ₄₄ O	11.61 - 11.7	Ergosterol NIST Match score 804, wrong RT	81.63 \pm 2.34	86.91 \pm 0.43			0.52 \pm 0.11	3.04 \pm 5.27	7.09 \pm 6.15	
10	Ergosterol, TMS	364			C ₂₈ H ₄₄ O	11.37							0.5 \pm 0.18	0.52 \pm 0.25	0.23 \pm 0.21
	Peak 7 - Stigmasta-5,7-dien-3-ol	343	485	412	C ₂₉ H ₄₈ O	12.33 - 12.42	NIST score 628 to Stigmasta-7,24(28)-dien-3-ol-TMS.								
	Cholesterol, TMS	368	459	386	C ₂₇ H ₄₆ O	10.71 - 10.87	Match both RT and <i>m/z</i> to standard	3.90 \pm 1.26	2.42 \pm 0.33	1.41 \pm 0.26	1.42 \pm 0.06	1.89 \pm 0.59	5.8 \pm 0.7	4.5 \pm 1.85	7.13 \pm 2.96
	Desmosterol, TMS	441	456	383	C ₂₇ H ₄₄ O	10.93 - 11.09	Partial match to standard	0.33 \pm 0.07	0.29 \pm 0.07	0.14 \pm 0.01	0.14 \pm 0.02	0.14 \pm 0.01	0.36 \pm 0.03	0.35 \pm 0.10	0.32 \pm 0.28

Table 5-2. Metabolite profiling by GC-MS (derivatization with trimethylsilyl, TMS) in AmBR lines of *L. mexicana* amastigotes. Content of each sterol is the percentage of the total of the raw peak area detected per line \pm Standard deviation of three independent biological replicates. Standards are as in Table 5-1. Those peaks that did not match any standard were determined by comparing with the NIST spectral libraries with the ion trap mass spectrometer (see text). Peak 4 was identified based on previous work (see text 5.2.1). SBP: Sterols Biosynthetic Pathway. RT: retention time.

SBP Number	Peak and/or Putative Annotation	Major frag mass <i>m/z</i>	Molecular ion* <i>m/z</i>	-TMS <i>m/z</i>	Formula -TMS	RT /min	Evidence and Confidence	WT	AmBR cl.14	AmBR cl.8
1	Lanosterol, TMS	394	499	426	C ₃₀ H ₅₀ O	11.95 - 12.01	Match both RT and <i>m/z</i> to standard	0.3 \pm 0.6		
	Peak 6 - FF-MAS (aka 4,4-Dimethylcholesta-5,7,24-trien-3-ol), TMS (4,4-dimethyl-5 α -cholesta-8,14,24-trien-3 β -ol)	377	483	410	C ₂₉ H ₄₆ O	12.28 - 12.38	NIST Score 608 to 4,4-Dimethylcholesta-5,7,9(11)-trien-3-ol. Reported as FF-MAS based on previous data and literature.	11.6 \pm 1.0		12.9 \pm 0.5
	Peak 1 - (22Z)-Cholesta-5,7,22-trien-3-ol, TMS	349	455	382	C ₂₇ H ₄₂ O	11.26 - 11.36	NIST Score 678			2.7 \pm 0.8
	Peak 2 - Cholesta-5,7,24-trienol	343	456	383	C ₂₇ H ₄₄ O	11.38 - 11.47	Desmosterol NIST match 699, wrong RT			1.2 \pm 0.2
5	Zymosterol, TMS	369.4	456.4	383.3	C ₂₇ H ₄₄ O	10.98	Match to standard			
6	Peak 3 - Ergosta-8,24(28)-diene, TMS or Fecosterol	366	470	397	C ₂₈ H ₄₆ O	11.5 - 11.6	NIST Score 552			
	Peak 5 - Ergosta-7,22-dien-3-ol, (3 β ,22E), TMS	343	470	397	C ₂₈ H ₄₆ O	11.74 - 11.82	NIST Score 701	25.8 \pm 3.3	43.0 \pm 1.5	18.5 \pm 0.5
8	Peak 4 - Ergosta-5,7,24(28)-trien-3 β -ol (a.k.a. 5-dehydroepisterol)	363 (changed to 337)	469	396	C ₂₈ H ₄₄ O	11.61 - 11.7	Ergosterol NIST Match score 804, wrong RT	41.4 \pm 4.8		48.6 \pm 1.8
	Peak 7 - Stigmasta-5,7-dien-3-ol	343	485	412	C ₂₉ H ₄₈ O	12.42		8.1 \pm 1.0	49.1 \pm 0.9	5.8 \pm 0.3
	Cholesterol, TMS	368	459	386	C ₂₇ H ₄₆ O	10.78 - 10.87	Match both RT and <i>m/z</i> to standard	12.2 \pm 0.9	7.3 \pm 0.4	10.2 \pm 0.7
	Desmosterol, TMS	441	456	383	C ₂₇ H ₄₄ O	11.02 - 11.09	Partial match to standard	0.33 \pm 0.07		

Table 5-3. Metabolite profiling by GC-MS (derivatization with trimethylsilyl, TMS) in NysR lines of *L. mexicana* promastigotes. Content of each sterol is the percentage of the total of the raw a peak rea detected per line \pm Standard deviation of three independent biological replicates. Standards are as in in Table 5-1. Those peaks that did not match any standard were determined by comparing with the NIST spectral libraries with the ion trap mass spectrometer (see text). Peak 4 was identified based on previous work (see text 5.2.1). SBP: Sterols Biosynthetic Pathway. RT: retention time.

SBP Number	Peak and/or Putative Annotation	Major frag mass <i>m/z</i>	Molecular ion* <i>m/z</i>	-TMS <i>m/z</i>	Formula -TMS	RT /min	Evidence and Confidence	WT HP	NysR cl.B2	NysR cl.C1	WT P0	NysR cl.E1	NysR cl.F2
1	Lanosterol, TMS	393.4	498.4	426.4	C ₃₀ H ₅₀ O	11.83	Match both RT and <i>m/z</i> to standard	0.41 \pm 0.13	0.1 \pm 0.0	0.1 \pm 0.00	0.3 \pm 0.00	0.3 \pm 0.10	0.3 \pm 0.10
	Peak 6 - to 4,4-Dimethylcholesta-5,7,9(11)-trien-3-ol, TMS	377.3	482.3	410.3	C ₂₉ H ₄₆ O	12.17	NIST Score 608.	2.20 \pm 0.44			1.4 \pm 0.5		3.0 \pm 3.0
	Peak 1 - (22Z)-Cholesta-5,7,22-trien-3-ol, TMS	349	454.2	382.2	C ₂₇ H ₄₂ O	11.17	NIST Score 678	1.28 \pm 0.66			0.5 \pm 0.6		
	Peak 2 - C27 dienol. Cholesta-5,7-dienol	343.3	456.3	384.3	C ₂₇ H ₄₄ O	11.28	Desmosterol NIST match 699, wrong RT	0.77 \pm 0.35		0.3 \pm 0.0	1.2 \pm 0.2	0.8 \pm 0.9	0.2 \pm 0.1
5	Zymosterol, TMS	369.4	456.4	383.3	C ₂₇ H ₄₄ O	10.98							
6	Peak 3 - Ergosta-8,24(28)-diene, TMS or Fecosterol	365.6	470.7	398.7	C ₂₈ H ₄₆ O	11.41	NIST Score 552		1.1 \pm 0.03	0.9 \pm 0.1	0.1 \pm 0.00	0.1 \pm 0.2	0.9 \pm 0.1
	Peak 5 - Ergosta-7,22-dien-3-ol, (3 β ,22E), TMS	343.2	470.3	398.3	C ₂₈ H ₄₆ O	11.63	NIST Score 701	10.95 \pm 1.93	80.2 \pm 0.7	84.7 \pm 0.2	12.1 \pm 2.7	88.8 \pm 3.4	89.1 \pm 0.3
8	Peak 4 - Ergosta-5,7,24(28)-trien-3 β -ol (a.k.a. 5-dehydroepisterol)	363.3 (changed to 337)	468.3	396.3	C ₂₈ H ₄₄ O	11.52	Ergosterol NIST Match score 804, wrong RT	81.63 \pm 2.34		0.3 \pm 0.7	77.8 \pm 5.0	0.2 \pm 0.00	
	Peak 7 - Stigmasta-5,7-dien-3-ol	343	485	412	C ₂₉ H ₄₈ O	12.42	NIST score 628 to Stigmasta-7,24(28)-dien-3-ol-TMS		14.2 \pm 1.1	9.9 \pm 0.2	0.3 \pm 0.1	6.1 \pm 3.5	7.0 \pm 0.8
	Cholesterol, TMS	368.3	458.3	386.2	C ₂₇ H ₄₆ O	10.68	Match both RT and <i>m/z</i> to standard	3.90 \pm 1.26	4.1 \pm 1.0	3.9 \pm 0.3	6.1 \pm 2.3	2.5 \pm 0.9	2.3 \pm 0.8
	Desmosterol, TMS	441.3	456.3	383.3	C ₂₇ H ₄₄ O	10.90	Partial match to standard	0.33 \pm 0.07	0.1 \pm 0.00		0.3 \pm 0.00	0.1 \pm 0.00	0.1 \pm 0.00

5.2.3 Infectivity of the AmBR lines in vivo

Characterization of anatomical and histological changes caused within the host combined with the identification of biochemical alterations of the metabolome of the parasite, can pinpoint important information towards the search of new drug targets. While the anatomical description of the infection with different *Leishmania* spp., is important to identify some macroscopic features of the disease, histology is necessary to confirm the presence of the parasite and can help to characterise the nature of the inflammatory process, respectively. Here, I assessed the infectivity of four AmBR lines in a mouse model and identified differences with respect to their parental wild type using histology. I also compared whether the virulence of these lines was related to their sterol composition. Broader changes in the metabolism and the MoA of AmB was also analysed in two of these resistant lines, AmBRcl.14 and AmBRcl.8, and is discussed further (see Chapter 7).

All mice were from Harlan UK Ltd, and kept at the Central Research Facilities of the University of Glasgow, Glasgow U.K. All the experiments were performed by a certified technician, i.e. Ms Anne Marie Donachie, and Mr Ryan Ritchie. Initially, three BALB/c mice (one mouse for each line) were infected with resistant lines AmBRcl.14 and AmBRcl.8, and wild type (first experiment). Progression of the infection was monitored weekly by assessing the growth of the lesion after subcutaneous inoculation with 2×10^6 metacyclic promastigotes, in the left footpad. Infections were stopped before any of the lesions reached a size of 5 mm, according to the Animals (Scientific Procedures) Act, 1986 (ASPA) <https://www.gov.uk/government/publications/consolidated-version-of-aspa-1986>). In this first infection, only AmBcl.14 and wild type produced an increase in footpad size of the mouse, whereas the footpad infected with AmBcl.8 retained normal size (as compared with the right footpad) and without any macroscopic alterations identified at physical exploration over the duration of the experiment (thirteen weeks).

Interestingly, viable parasites were recovered from all three mice. Although the density of parasites recovered from the mouse infected with AmBRcl.8 was lower, as indicated by the longer time (around two weeks) to reach a density of at least 1×10^5 which is the minimum that can be detected by microscopy. Next, additional mice were infected with all four AmBR lines (AmBcl.14, AmBcl.3, AmBcl.8, AmBcl.6). In this second experiment (also performed by Anne Marie Donachie), the wild type and the AmBRcl.14 (termed WTP0-low passage- and AmBRcl.14 PI -post infection- hereon) that were recovered after the first infection, were also included. While AmBRcl.8 was also recovered from the first infection, this clone was not included, as by the time of starting the second infection, the density of

parasites from this line was still insufficient, i.e. lower than 1×10^6 . In these experiments, mice were treated with AmB and AmBisome (see section 5.2.4 and 5.2.5). Primary lesion kinetics (from the second infection), showed a progressive increase in the size of footpad lesions in BALB/c mice. While mice infected with wild type parasites presented a lesion between 2 to 2.5 mm in size at the end of the experiment (13 weeks in total), the lesion size of primary lesions observed in the resistant lines was more heterogeneous showing to phenotypes (Figure 5-6). First, footpad lesions from mice infected with lines AmBRcl.14 (including AmBRcl.14 PI) and AmBRcl.3, were larger than in wild type. Lesions of mice infected with AmBRcl.14, started increasing in size around the second week, whereas in all the other lines, the growth of the lesion was not observed until week three or four. However, two resistant lines (AmBRcl.8 and AmBRcl.6) caused no increase in the size or any other sign of inflammatory reaction at the site of inoculation during the thirteen weeks of duration of the experiment, thus confirming that the observations from the preliminary infection with line AmBRcl.8, were, possibly, related with to a stable, attenuated phenotype.

The attenuated phenotype observed in lines AmBRcl.8 and AmBRcl.6, suggests that some of the sterol changes (or other genetic alterations) identified in these two lines, are related with this loss of virulence, possibly due to a loss or reduced capacity to induce an inflammatory response, or by affecting other features of the parasite, such as its internalisation, amastigogenesis, and replication within the host macrophage. Remarkably, viable parasites were recovered from both primary lesions (footpads) and lymph nodes from all mice infected with these two attenuated lines. This was further confirmed with histological analysis of footpads and lymph nodes and is discussed further (section 5.2.7). However, one cannot rule out other changes not determined here, can also arise during long culture (Nolan and Herman 1985), and can be different between independent lines. Examples of other virulence factors that can be lost along long-term subculture are, leishmanolysin (also known as GP63) and lipophosphoglycan (LPG) (Denny et al., 2004). Others related with the energy metabolism (Kovářová et al. 2018; Saunders et al. 2018), and the genetics of the host (Ribeiro et al. 2018), are also relevant and cannot be excluded.

In spite of the possibility that AmBRcl.8 and AmBRcl.6 clones could have evolved avirulence during *in vitro* cultivation separately from other strains, it is noteworthy that these two lines had a common feature with regards to their sterol profile, i.e. both showed elevated (22Z)-cholesta-5,7,22-trien-3-ol, and cholesta-5,7,24-trienol (Table 5-1), suggesting that the presence of these particular intermediates could play an important role in allowing the parasite to survive within mice without causing severe inflammatory

response (attenuated phenotype). As outlined in section 5.2.3, infection of mice was performed with axenic promastigotes that were selected for resistance *in vitro*, for 7 to 8 months (long passage) (Figure 3-1). In my study, I confirmed their transformation into amastigotes by histology, and by recovering amastigotes after infection. The absence of lesion and the fact that amastigotes of these two lines were not identified by microscopy, suggests that the two attenuated lines, did not replicate *in vivo*. This was also compared with tissue of mice infected with wild type and with the other two virulent lines, in which the numbers of amastigotes was estimated (see histology section 5.2.7.1 and Figure 5-9). However, the presence of these two intermediates (both cholestanes) alone, does not solely explain the lack of virulence, which can be instead, due to other factors that are related with the virulence of the parasite, such as the absence of ergostanes itself (Yao and Wilson 2016) and others that were not analysed in this study. Attenuation *in vivo* and *in vitro* was also observed in MF-resistant *L. major* promastigotes without altering the survival of the parasite within the insect vector (Turner et al. 2015).

In another study, Al-Mohammed and colleagues also observed an attenuated phenotype in BALB/c mice infected with AmB resistant promastigotes of *L. mexicana* that were cultured for 110 passages. This AmBR line showed an attenuated phenotype, with lesions that grew, although developed slower than those observed with wild type parasites. Interestingly, the most abundant sterols in promastigotes in these attenuated parasites were 4,14, dimethyl-cholesta-8,24-dienol (62.4%), 4,14, dimethyl-cholesta-7,24-dienol (6.5%), and lanosta-8,24-dienol (31.1%). The same three sterol intermediates were present in the intracellular form, with a relative abundance of 97.3%, 1.4% and 1.3%, respectively (Al-Mohammed et al. 2005). Although in their study, Al-Mohammed et al. did not measure short passage promastigotes, here I found an increase in two ergostanes, ergosta-5,7,24(28)-trien-3 β -ol and ergosta-7,22-dien-3-ol, (3 β ,22E), in line AmBRcl.8, after infection in mice (low passage). The presence of these two sterol intermediates in both attenuated promastigotes and the amastigotes, can be of clinical and epidemiological implications.

While these intermediates seem to be related to some fitness cost within the mammalian host, it would be interesting to determine if this occurs also within the sand fly. Considering that insects lack *de novo* synthesis of sterols (Janson et al. 2009), and parasites deficient in the synthesis of specific intermediates have, possibly, an altered capacity to survive (or replicate) within the insect, further studies on the effect of sterol composition in *Leishmania* are essential. This could be considered when developing new vector control strategies. In my research, I attempted to study the phenotype of AmBR resistant lines

within the sand fly, however, numbers of infected sandflies that survived deemed for insufficient experimental controls, i.e. low number of survivors (infected sand flies) in both, AmBR- and wild type (control) arms, therefore, infection rates could not be determined (data not shown).

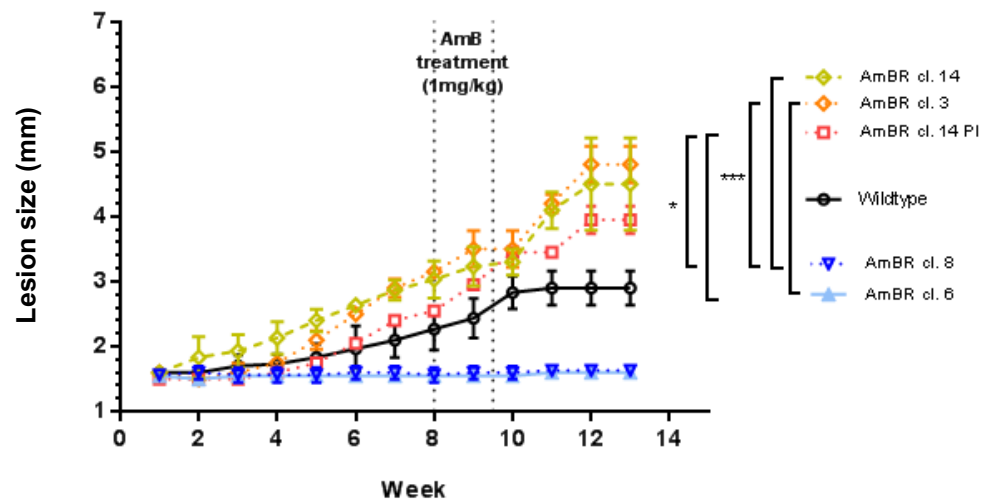


Figure 5-6. BALB/c mice inoculated with *L. mexicana* and treated with AmB. Parasites were inoculated at 2×10^6 into 500 μ l of PBS. Evolution of lesion was followed for three months and measured weekly. BALB/c female mice were two-months old at the time of inoculation. Treatment: 1 mg per kg IV every other day in the tail vein. A total of six injections ($\sim 120 \mu$ l) of AmB deoxycholate (AmB-D) diluted in PBS were administered. Tukey's multiple comparison test was used to find pairwise differences between resistant lines and parental wild type. Statistically significant values ($P < 0.05$, 95% Confidence Interval) are indicated with stars as follows: * $P \leq 0.05$, ** $P \leq 0.01$, *** $P \leq 0.001$, **** $P \leq 0.0001$).

The findings of the study of Al-Mohammed et al., are indicative that the loss of the wild type ergostanes, i.e. ergosterol and stigmastanes, can be related to the loss of virulence. Based on the slower development of the footpad lesions, the authors suggested that the acquisition of the resistant phenotype carries, possibly, some fitness cost that reduced the ability of amastigotes to replicate within the mice (Al-Mohammed et al. 2005). One difference between the attenuated lines in my study and that of Al-Mohammed et al., is that in the latter, the attenuated line produced lesions in mice, albeit at slower rate than the wild type, whereas in my study, the attenuation was more pronounced without increase in the lesion size (and other features such as amastigote replication rate). As with my study, another work with *L. mexicana* also reported the total absence of lesions in mice infected with attenuated parasites. In this study, parasites were attenuated after 20 passages *in vitro* and failed to transform into amastigotes in infected host cells (Ali et al. 2013). The authors concluded that attenuated parasites downregulated several virulence factors (e.g. Th2-associated cytokines), which were up-regulated in virulent parasites that were passaged between 1 to 7 times (Ali et al. 2013).

It is not certain that the loss of ergostane-type sterols is the sole mechanism responsible of the attenuated phenotype observed with lines AmBRcl.8 and AmBRcl.6, given that a combination of changes are present in these two lines, i.e. alterations in the C24SMT gene concomitant with the loss of the miltefosine transporter and its neighbouring downstream gene (see Chapter 4, section 4.2.2 and 4.2.4). The imbalance of these ergostanes could, however, provide a mechanism that facilitates a concomitant loss or reduction of other structural components of the membrane, e.g. sphingolipids, leading to an altered content of lipid rafts and other associated molecules associated with the stability of the membrane and involved in the virulence of *Leishmania* spp., such as, GP63, lipophosphoglycan (LPG) and LPS (Denny *et al.*, 2004), the latter is absent in *L. mexicana* (Torres-Guerrero *et al.* 2017).

The loss of these components can also derive from long-term subculture. However, since the hypothesis of my project was aiming to determine the role of sterols, I did not directly determine the role of other virulent factors (some data analysed the difference in drug susceptibility *in vitro* between long- and short-term passage in NysR lines, and in the content of sterols in these mutants, and in two of the AmBR lines). Interestingly, LC-MS found significant changes in lipids (including glycerol-phospholipids, sphingolipids, glycerol-3-phosphocholine, phosphoinositol and ceramides) in two AmBR lines, which were treated at high concentration of AmB (5 x EC₅₀). A detailed analysis of these changes is discussed further (see chapter 7). Attenuation has been reported frequently in *Leishmania* promastigotes after passaging cells long term (as during selection for drug resistance with AmB and Nys). This attenuation can also occur with several passages and regardless of the addition of drug to the medium (Nolan and Herman 1985). An example of this is an AmB-resistant line of *L. tropica* that was developed from a previously attenuated wild type. The attenuation of the latter was achieved through 20 serial passages without drug. After being attenuated, drug selection was performed using a stepwise increase of drug pressure (Khan *et al.* 2016), similarly to the method used here (section 3.2.1).

In the present work, all AmBR lines and wild type were maintained as promastigotes in axenic culture for a period between eight and nine months, therefore, an attenuated phenotype was expected irrespective of drug treatment. Interestingly, attenuation has been reported previously in *Leishmania* promastigotes with depletion or alteration of the main endogenous sterols, such as ergosterol and stigmasterol (Singh *et al.* 2012; Wei Xu *et al.* 2014; Yao *et al.* 2013). A mutant lacking the sterol enzyme C14DM, showed a dramatic attenuation of virulence in comparison with wild type and add-back parasites (both metacyclic promastigotes and lesion-recovered amastigotes), which caused a severe increase of the footpad lesion in BALB/c mice (Wei Xu *et al.* 2014). While attenuation can

take weeks or months in axenic conditions, it can also be attained in only 1 hour after the treatment (10 to 50 mM) of stationary and metacyclic promastigotes with methyl-beta-cyclodextrin (M β CD), a sterol-chelating reagent that depletes ergosterol (or some of its isoform stereoisomers), cholesterol, ergosta-7,22-dien-3 β -ol, and stigmasta-7-24(28)-dien-3 β -ol, without interfering with the ergosterol biosynthesis (Yao et al. 2013).

Other examples of physiological changes that can influence the virulence of *Leishmania major*, include some enzymes related with the metabolism of glucose, such as the major glucose transporters (LmxGT1-3 in *L. mexicana*) (Saunders et al. 2018), the gluconeogenic enzyme, fructose-1,6-bisphosphatase (FBP) that is expressed in both the extra- and intracellular forms of the parasite and being essential in the latter (Naderer et al. 2006), and transketolase (TKT), which is part of the non-oxidative branch of the pentose phosphate pathway (PPP) and plays a key role in the metabolism of glucose (Kovářová et al. 2018). In *L. mexicana* mutant amastigotes lacking the former of these enzymes, LmxGT1-3 transporters, showed a limited capacity to switch to using carbon sources other than glucose, and failed to induce lesions *in vivo* (Saunders et al. 2018). Similarly, a *L. major* FBP-null mutant was unable to grow *in vitro*, in the absence of an exogenous source of hexoses and were unable to metabolise glycerol and restoring growth (Naderer et al. 2006). When parasites were grown in a glycerol-containing medium, only wild type and FBP-complemented parasites were able to grow (similar than in glucose-containing medium), although a depletion of internal sources of carbohydrates, i.e. intracellular β 1,2-mannan oligosaccharides, was observed.

As with the two attenuated lines, AmBRcl.8 and AmBRcl.6, the FBP-null mutant persisted in mice but failed to generate normal lesions. Moreover, FBP-null mutant promastigotes, were internalised and differentiated into amastigotes inside the macrophages, however, replication was suppressed. In my study, I did not determine if these two attenuated lines had either a reduced capacity to transform into amastigotes, or if after transformation, amastigotes did not replicate. Irrespective of the absence of the intracellular form at the histological analysis (using light microscopy), in both these lines, viable parasites were recovered after thirteen weeks of infection (from both FP and LN), suggesting that amastigogenesis did occur (see section 5.2.7.1 and Figure 5-9). In their work, Naderer and colleagues, concluded that given that the amastigote resides in an environment that is poor in glucose, this stage is highly dependent on gluconeogenesis and carbon sources other than glucose such as amino acids (fatty acids were proven as a poor carbon source in amastigotes) (Naderer et al. 2006).

A role of gluconeogenesis as a source of carbon has also been demonstrated in *T. brucei* (bloodstream form) using a Cas9-mediated gene FBP-knockout (Tb927.9.8720 in *T. brucei*) which was able to metabolise glycerol as an alternative substrate for gluconeogenesis and the production of ATP and sugars, by converting fructose 1,6-bisphosphate into fructose 6-phosphate. The activity of FBPase is increased when gluconeogenesis is activated, this function is, however, FBPase-independent. Moreover, gluconeogenesis activity was also observed in wild type parasites cultured in the presence of glucose and glycerol (Kovářová et al., 2018a). With regard to TKT, the loss of virulence observed in a *L. mexicana* TKT-knockout, was attributed to the depletion of the amastigote-specific polymer, mannogen. Mannogen, a major energy reserve source in *L. mexicana* that was known as mannan, is catabolized when the sources of glucose are depleted (Ralton et al. 2003). Interestingly, the addition (and re-expression) of TKT back into the TKT-knockout, recovered virulence but without restoring the synthesis of this polysaccharide (Kovářová et al., 2018b). The role of TKT with the MoA of AmB and the effects of the treatment with AmB on the metabolome of this TKT-knockout (along with two AmBR lines) are discussed further (see Chapter 7).

Da Silva and Sacks (1987) observed that after repeated passages *in vitro*, attenuated promastigotes of *L. major*, recovered their virulence by a single *in vivo* passage in BALB/c mice, while avirulent parasites had a delayed metacyclogenesis, the authors related the virulence with the ability of the parasites to agglutinate with lecithin peanut agglutinin (PNA). For instance, log-phase parasites were 100% PNA-agglutinated and avirulent in mice, whereas in stationary parasites, only those with a non-agglutinable phenotype, PNA, were virulent. Moreover, clones derived from the PNA- population were the most virulent.

To confirm the role of the PNA marker, a virulent clone that produced 90% of PNA-promastigotes, was maintained for 94 passages and the amount of PNA- parasites was reduced to 10%, rendering an attenuated population, which was further sub-cloned, from which the authors could not isolate an infective population (Da Silva and Sacks 1987). Similar observations of recovery of virulence *in vivo*, were also observed in attenuated parasites after serial passages through sand flies (Sadlova et al. 2006) and in strains of *Leishmania infantum chagasi*, in which virulence is maintained by routinely inoculating into golden hamsters (Yao et al. 2013). For this reason, I expected a possible increase in virulence in both the wild type (WTP0) and the resistant line (AmBRcl.14.PI) that were recovered after the first infection in mice. Intriguingly, while no increase in virulence was evident in the wild type, an opposite effect was observed with AmBRcl.14 PI, in which the lesion size was slightly smaller than with AmBRcl.14 (although this difference in the

lesion size was non-significant ($P=0.7325$). The reason of this possible slight reversal in virulence in the former was unclear.

In contrast to the attenuated phenotype observed in lines AmBRcl.8 and AmBRcl.6, a slightly more virulent phenotype (relative to wild type) was present in two lines, AmBR.cl14 and AmBR.cl.3, and associated with significant changes in ergostanes, suggesting that these intermediates contribute, to some extent, to the fitness advantage observed in mice infected with these lines (see and Table 5-1). The most abundant intermediate in AmBRcl.14 and AmBRcl.3, was ergosta-7,22-dien-3-ol (96-96.7%). The presence of this ergostane might trigger an increased capacity for the parasite to replicate *in vivo*, or exacerbate and inflammatory response, or both. Histological analysis revealed that the number of parasites and inflammatory cells in footpads and lymph nodes was increased with these lines compared with WT (Figure 5-9). The presence of this sterol intermediate was also associated with an increase in virulence in *L. infantum* in which ergosta-7,22-dien-3-ol, increased significantly in virulent stationary parasites (Yao and Wilson 2016). In their study, Yao et al., did not measure ergosterol directly, due to the lack of deuterated standards. Instead, they extrapolated ergosterol (and the other sterols) based on the peak areas of the total- and relative amounts of cholesterol, and other sterols, in each sample, using deuterated H²-cholesterol as internal standard ($R^2 > 0.99$). The two stereoisomers of ergosterol only differed in their RT (11.61 and 11.67), and in relation to the reference standard of ergosterol (RT of 11.37). Similarly, two isomers of ergosta-7,22-dien-3-ol, named type I and II, showed a relative RT (RRT) of 1.078 and 1.131, respectively. In this case, RT was measured relative to cholesterol, which has a RT of 1.000 (Yao et al. 2013; Yao and Wilson 2016).

The variability in virulence between AmBR lines in mice needs to take into consideration other factors that also determine the pathogenicity and the course of the infection, and which were not measured here. Various examples of the role of the genetics of the host (Ribeiro et al. 2018), and of the immune system, have been described in different animal species. The former has been implicated in infections in hunting Foxhound dogs (Boggiatto et al. 2011; Petersen and Barr 2009). In another study, in hamsters, the individual immune response was found to be redundant for the resolution of the lesions caused by the infection with *Leishmania mexicana* (Parreira De Arruda et al. 2002). Similarly, the importance of the genetics of the host in the animal model studied here, i.e. BALB/c mice, has been confirmed experimentally in mice with different genetic backgrounds infected with *L. amazonensis*. While strains BALB/c, C57BL/6 and C57BL/10 were very susceptible to infection, strains CBA and DBA/2 developed mild to

severe late lesions, whereas the strain, C3H/He, showed no lesion and with a low or total absence of parasite load. Additionally, C3H/He, unlike all the other strains, showed no signs of visceralization, confirming that the genetic background of the host plays a key role in the pathogenesis of leishmaniasis (de Souza et al., 2018).

Similarly, another study showed that BALB/c mice were more susceptible to infection than the strain C57BL/6. While in the former a higher index of infected peritoneal macrophages and lower nitric oxide (NO) levels were observed in the latter, the histopathological alterations were less severe and accompanied by a lower number of parasites found in the skin (Passero et al. 2009). In this study, the role of the genetics and the immune system were, however, not considered to be a determinant factor of the differences in the pathogenicity observed across different animals, given that all mice were from the same strain, i.e. BALB/c, this factor can be ruled out. Other factors are also described at the end of this section (see 5.3).

Despite the fact that the content of sterols between wild type and AmBR lines of promastigotes was significantly different, it cannot be concluded that the attenuated and infective (virulent) phenotypes observed *in vivo*, are a direct effect of these changes in the promastigote stage. Although these changes in sterols in the promastigote form were correlated with defects in several enzymes (see chapter 4, section 4.1.3) which explain their nature, however, some enzymes of the SBP in kinetoplastids have been shown to be stage specific (Cosentino and Agüero 2014). A summary of the mutations identified in this study (see chapter 4, section 4.1.3, Table 4-2) in relation with the sterols derived, is included at the end of this chapter (Table 5-5).

Moreover, significant variations in sterols, including those related with the virulence of the parasite, i.e. ergosta-7,22-dien-3-ol, were observed between different stages (i.e. logarithmic, stationary and metacyclic) in *L. infantum* (MHOM/BR/00/1669), previously called *L. chagasi*, promastigotes (Yao and Wilson 2016). In this study, I measured the content of sterols only in *L. mexicana* promastigotes in logarithmic phase. Further analysis at later stages can provide useful information related to the sterol dynamics in these AmBR lines, particularly during the metacyclic stage. This is an important consideration given that, in this study, the metacyclic stage (instead of the logarithmic) was used to inoculate BALB/c mice (see section 5.2.3), which is the stage that is inoculated by the sand fly, thus mimicking the natural life cycle of the disease. Moreover, the metacyclic promastigotes have to undergo amastigogenesis within the mammalian host, and therefore, the content of

sterols in the intracellular stage is, possibly, an alternative explanation with regard to the relationship between sterols and the virulence of *Leishmania* spp. *in vivo*.

In the amastigote form, the content of sterols showed significant differences with respect to the promastigote stage (section 5.2.1.2, Table 5-2 and Figure 5-4). This was notable in both, wild type and resistant lines (only AmBRcl.14 and AmBRcl.8 were analysed as amastigotes). Interestingly, one of the resistant lines, AmBRcl.8, amastigotes showed a similar profile of sterols as wild type amastigotes, whereas in the other resistant line, AmBRcl.14, the difference with respect wild type was remarkable. In agreement with this, these two intermediates, cholesta-5,7,24-trienol (5.6 to 5.8%), and another cholestane, cholesta-5,7,22-trienol (80 to 68.5%), were the most abundant in two AmBR lines that had a relative low infectivity in primary macrophages and in mice (lesions grew from 1.8 to 2.1 mm) (Pountain et al. 2019a). It is unclear if the marginal increase observed in the former of these lines, in two cholestane-type intermediates, can explain the attenuated phenotype. With regard to the virulent phenotype shown with AmBRcl.14, this may be linked to two separate sets of changes in amastigotes. First, the total loss of ergosterol and of 4,4-dimethylcholesta-5,7,24-trien-3-ol. On the other hand, the significant increase of ergosta-7,22-dien-3-ol (1.7-fold), and a more dramatic increase of stigmasta-5,7-dien-3-ol (6.1-fold), with respect to the parental wild type (see Table 5-2). Interestingly, ergosta-7,22-dien-3-ol, was also the most abundant (69.7%) in AmBRcl.14 (and also in AmBRcl.3) in the promastigote form, in which the difference with respect the parental wild type was even higher (9.6-fold). Furthermore, the abundance of these two intermediates in virulent strains was significantly higher than in attenuated *L. infantum* metacyclic promastigotes (Yao and Wilson 2016). A comparison between the content of sterols in both the virulent and attenuated phenotypes, with other virulent/avirulent (Yao, et al. 2013; Yao and Wilson 2016a), wild type and AmBR promastigotes and amastigotes (Al-Mohammed et al. 2005), is outlined in Table 5-6.

The ergostane and stigmastane sterols are the main endogenous sterols in trypanosomatids and both are absent in mammals (Choi et al. 2014). These sterols also confer a selective binding to AmB (and possibly to other polyenes like nystatin) in different species of *Leishmania* (Xu et al. 2014). The effects in selectivity to AmB in the AmBR lines is discussed in more detail in the following section. As mentioned before, other virulence factors, including those that cannot be detected with the approaches used in this study, such as sphingolipids (Denny et al. 2006), and several enzymes of the energy metabolism (Kovářová et al. 2018; Saunders et al. 2018), and the number of passages in culture (Nolan

and Herman 1985), the host genetics (Ribeiro et al. 2018), and others not determined in this study, also influence the virulence of the parasite and cannot be excluded.

5.2.4 Response to treatment with AmB *in vivo*

Several alterations of sterols are related with AmB resistance in fungi (Kelly et al. 1994) and in *Leishmania* spp. (Andrade-Neto, et al. 2016; Cosentino and Agüero 2014; Mbongo et al. 1998; Mwenechanya et al. 2017; Pountain et al. 2019; Sagatova et al. 2015). After the identification of mutations in different genes of the SBP, which were associated with the presence of different sterol intermediates, and with remarkable differences in the size of lesions induced in mice, I sought to determine whether these resistant AmBR lines retained their resistant phenotype *in vivo*, and post infection. In a first experiment, mice were infected with WT and all four AmBR lines and treatment with a dose of 1 mg/kg AmB deoxycholate, AmB-D was administered at week eight (Figure 5-6). First, AmBRcl.14 and AmBRcl.3, showed a fitness advantage even before treatment, and resistance *in vivo*. Conversely, lesions from WT parasites showed a slight increase a few days after AmB was given, however, one week after the treatment was finished, WT reached a plateau by the end of the experiment (i.e. thirteen weeks), suggesting higher susceptibility to treatment in the parental line in comparison with AmBR- cl.14 and -cl.3 (Figure 5-6). To further confirm if the response to treatment was related with the retention of resistance within mice, viable parasites from all lines were recovered from footpad lesions, and from lymph nodes, at the end of the experiment, and their EC₅₀ was measured (section 5.2.6, Figure 5-8). These results showed that different sterol intermediates with the concomitant loss of ergosterol, are related to a differential in susceptibility towards AmB *in vivo*, and that the difference in their EC₅₀ values *in vitro*, was significant ($P \leq 0.01-0.05$) in comparison with the parental wild type (chapter 3, Table 3-2). Arguably, a curative dose to cure infected mice could not be determined with the BALB/c mouse model used in this study. The persistence of all AmBR *L. mexicana* lines within mice regardless of the treatment, indicates that the maximum dose of AmB-D used here, was not sufficient to clear *L. mexicana* in BALB/c mice. In the study of Al-Mohammed and colleagues, mice infected with the AmB resistant, developed lesions more slowly than those infected with wild type. Chemotherapy with AmB was similar (1 mg/kg over a period of two weeks), than that used in my study, with the difference that Al-Mohammed et al. treated WT and AmBR lines, at week 8 and 18, respectively. In my study, however, all groups of mice infected with WT and all four AmBR lines, were treated at the same time, i.e week 8, and irrespective of the difference of the lesion size. Although Al-Mohammed et al. reported a response to the treatment with AmB in both groups, being this effect higher in wild type than in the AmBR

line, this reduction of the size was only partial and temporary. The lesions restarted growing one week after the cessation of the treatment, attaining a comparable size to that observed in untreated mice, and suggesting that the emergence of resistant *Leishmania* is feasible. In their study, the authors did not provide additional information on the retention of resistance of these lines post infection. The recrudescence of lesions post treatment with AmB has also been observed in mice infected with *L. amazonensis* (Monzote et al. 2014). Other models for the assessment of the effect of AmB and AmBisome have been developed and are discussed further (see 5.3).

The response to treatment can be addressed by increasing the concentration of the dose, however, the use of higher doses of AmB deoxycholate is limited due to toxicity in mice. The issue of toxicity can be partially addressed by the administration of lipid-based formulations of AmB, such as AmBisome, which allows increasing the dose, diminishing the risk of toxicity, and administering multiple doses (Abongomera et al. 2018; Adler-Moore et al. 2016; Khalil et al. 2014). If other factors, such as the deactivation or sequestration of the drug within the animal tissues, contributed to the loss of the activity of AmB observed here, was not determined. However, I used the same AmB-D that was administered in mice, to test its activity and to determine if this stock had lost potency. By doing this, I could confirm that the AmB-D had comparable activity to that observed *in vitro* before the animal infections.

5.2.5 Response to liposomal AmB (AmBisome®) in vivo

In a recent publication, a clinical case of visceral leishmaniasis in a gorilla was confirmed (PCR positive for *Leishmania* sp. (donovani complex) in a zoo in Brazil and successfully treated with a single dose (1 mg/kg) of AmBisome (Tinoco et al. 2018). Similar and higher therapeutic doses have been tested against *Leishmania* spp. *in vitro* (O’Keeffe et al. 2019) and in other animal models (Forrester et al. 2019; Wijnant et al. 2018; Wijnant et al. 2018; Yardley and Croft 1997; Voak et al. 2018) including AmB resistant lines (Mohamed-Ahmed et al. 2013). The study of Forrester et al., (in VL) for instance showed parasite elimination from liver and splee, after 7 days of treatment at 8mg/kg (Forrester et al. 2019). I therefore proposed to analyse the response to treatment using this formulation, instead of AmB in complex with deoxycholate (AmB-D) which was used in all the other experiments *in vivo*. As mentioned before, one of the main advantages of this formulation is the reduction of toxicity, thus allowing to increase the dose of AmB. Other benefits are the delivery of more drug at the target site (i.e. the phagolysosome within the macrophage).

To test the effect of AmBisome in lines resistant to AmB, a third experiment with infected mice was performed using another AmB resistant line, named AmBRcl.3 herein, which was selected for resistance to AmB by Dr Andrew Pountain (a former student in the Barrett Lab), was used. AmBRcl.3 had an infectivity comparable to wild type, in murine macrophages and in mice and was 3.9-fold resistant to amB with respect to the parental line, and the main sterol intermediate that replaced ergosterol in this line was cholesta-5,7,22-trien-3-ol, with an abundance of 86.5% (PhD Thesis, Dr Andrew Pountain, Pountain *et al.*, 2019). Additionally, I determined the EC_{50} of AmBisome *in vitro* in this line (data not shown here) and all the four AmBR lines, recovered post-infection. These experiments helped me to determine, on the one hand, if AmBisome was active, regardless the lack of response observed *in vivo*, and on the other side, provided me with information related to the retention of resistance post infection in AmBR lines (Figure 5-8, Table 5-4).

Treatment with AmBisome® at doses between eight and fifteen times higher (8 and 15 mg/kg) than in the previous experiment (1 mg/kg), showed no effect in the reduction of the lesion size in both, wild type and AmBRcl.3, in comparison with the untreated group that was treated with dextrose (5%) (See Figure 5-7, panel A). AmBisome can be used in doses up to 40 mg/kg to treat VL (Banerjee *et al.* 2008; Sundar and Jaya 2010). At concentrations of 25 mg/kg, AmBisome was more effective than other formulations or AmB to reduce the lesion size in mice infected with *L. donovani* (Yardley & Croft, 2000). In other works, concentrations of 50 mg/kg have also proved to be efficacious and without causing toxicity in mice (Adler-Moore *et al.* 2016; Yardley and Croft 2000). In other works, lower concentrations, i.e. 20 mg/kg, have been tested as prophylactic (administered before the infection) for the prevention of systemic fungal diseases (Garcia, Adler-Moore, and Proffitt 2000). This prophylactic approach can be considered for future experiments with AmBR strains of *Leishmania* spp., in which doses of AmBisome up to 50 mg/kg of body weight, have been well-tolerated and showing total clearance of parasites from the animal tissues (Gangneux *et al.* 1996). I could not use higher doses, since we had only a limited quantity of AmBisome available for these experiments.

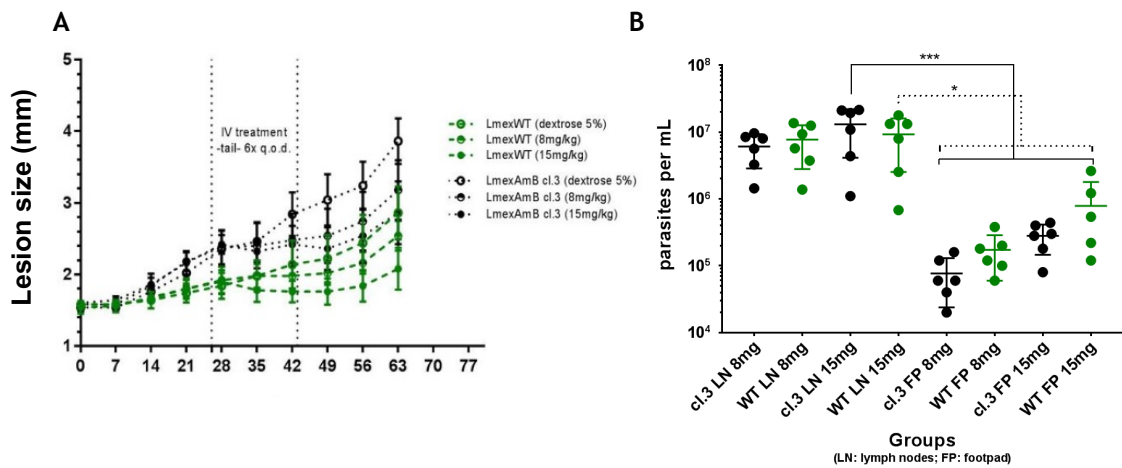


Figure 5-7. Susceptibility to AmBisome of *L. mexicana* in BALB/c mice.

Parasites were inoculated (2×10^6) in 500 μ l of PBS. Evolution of lesion was followed for three months and measured weekly. BALB/c female mice were two-months old at the time of inoculation. Treatment: 1 mg per kg IV every other day in the tail vein. A total of six injections (~ 120 μ l each) of AmBisome in PBS were administered. Tukey's multiple comparison test was used to find pairwise differences between resistant lines and parental wild type. Statistically significant values ($P < 0.05$, 95% Confidence Interval) are indicated with stars as follows: * $P \leq 0.05$, ** $P \leq 0.01$, *** $P \leq 0.001$, **** $P \leq 0.0001$). These data were collected by a certified animal handling technician, Ryan Ritchie, and analysed with Prism as indicated in chapter 2.

To confirm if the lack of response to AmBisome observed in mice related to retention of viable parasites, I recovered parasites from both primary lesions (footpad) and lymph nodes, from all mice (both groups, wild type and AmBRcl.3 were recovered). Interestingly, the number of parasites recovered from primary lesions (footpads), was significantly lower than the numbers obtained from lymph nodes in both groups of mice treated with AmBisome at 15 mg/kg ($P \leq 0.001$), and 8 mg/kg ($P \leq 0.05$). However, no difference was observed between treatments (see Figure 5-7, panel B). Parasites from the control groups (both footpad and lymph nodes) could not be recovered. The fact that the numbers of parasites recovered from primary lesions were lower than with lymph nodes, suggests the possibility that parasites migrated from infected inflammatory cells, i.e. monocyte-derived dendritic cells (moDCs) localised at the site of infection. Although the basis of the immune response is fully understood, some species causing VL such as, *L. donovani* and *L. infantum*, infect and replicate in lymphoid tissues, e.g. spleen, liver, lymph nodes, bone marrow), causing a severe symptomatology, whereas cutaneous species (such as *L. mexicana*), responsible for CL, cause lesions that are mainly restricted to the skin, possibly, after the inhibition of the host immune response (Torres-Guerrero et al. 2017). For instance, the protective response of DC infected with *L. braziliensis* can be inhibited, here upregulation of major histocompatibility complex class II (MHC-II) and the secretion of IL-2 are absent. A similar inhibition of the MHC-II has been observed in spleens infected with *L. donovani*, and in macrophages in which their lysosomal properties are

inhibited by promastigotes (Kaye and Scott 2011). Other investigators have re-isolated viable amastigotes of cutaneous species (*L. mexicana*) from lymph node macerates in murine experimental models (Kaye and Scott 2011), suggesting that inflammatory monocytes (macrophages and moDCs), can facilitate the traffic of parasites to the draining lymph nodes. See section 5.2.7.1 (Kaye and Scott 2011; Thalhoffer et al. 2011). Differences in the lesion size can also be related with the the inflammatory response which influenced the activity and accumulation of AmBisome at infection site (Voak et al. 2018; Wijnant et al. 2018; Wijnant et al. 2018). For this reason, I recovered tissue (lymph nodes, footpads, liver, and spleen) from all of the infected animals. This tissue was stored in ethanol for future examination using histology (as with all four AmBR lines previously described (Figure 5-6), in combination with qPCR (to confirm parasite burden and replication) and immunohistochemistry (see details in section 5.2.7.1). These data, however, were not obtained here, due to limitations of time.

5.2.6 Retention of AmB resistance after infection *in vivo*

Considering the response to the treatment observed with both formulations of AmB, it was important to assess whether the resistance phenotype was retained in the AmBR lines after infection (see Figure 5-8). After being recovered from lesions, amastigotes were transformed into axenic promastigotes and the EC₅₀ was measured during the first or second passage. The EC₅₀ obtained with wild type promastigotes before ($0.060 \mu\text{M} \pm 0.0039$) and after ($0.0634 \mu\text{M} \pm 0.0076$) infection were similar (Figure 5-8, panel A, and Table 5-4). Similarly, all four AmBR resistant lines showed a comparable fold change with respect to their parental wild type, with values between 10- to 11.6-fold, and 7- to 13-fold, before and after infection, respectively (Table 5-4). Overall, no significant differences were observed between the EC₅₀ values before and post infection, indicating that all AmBR lines retained their resistant phenotype after being passaged, and recovered from mice. Previous studies have shown that AmBisome is up to 9 times more active than AmB *in vivo* (Adler-Moore et al. 2016). Interestingly, AmB deoxycholate was more active than AmBisome against *L. major* and *L. donovani*, in a macrophage model, i.e. peritoneal macrophages (Adler-Moore et al. 2016; Yardley and Croft 2000). A possible reason for this is that AmBisome might be internalized inside specific compartments within the macrophages, such as the phagolysosome, in a different manner between both *ex vivo* and *in vivo* macrophages, therefore, delivering variable concentrations of drug that target the amastigotes (Adler-Moore et al. 2016). Contrary to its higher activity *in vivo*, here, AmBisome was between 7.5-fold less active than AmB alone in wild type axenic promastigotes (*in vitro*). This difference was more pronounced in AmBR lines, in which

the activity of AmBisome was between 11.12- to 39-fold lower as compared with AmB alone (Figure 5-8, panel B, and Table 5-4).

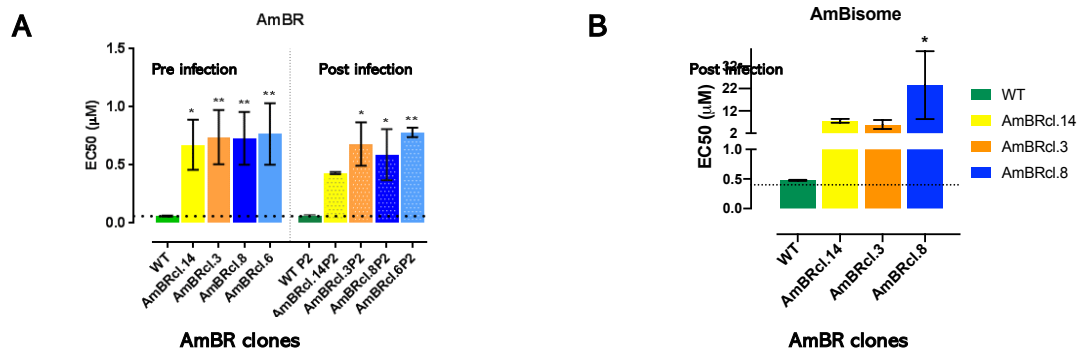


Figure 5-8. Susceptibility of AmBR lines of *L. mexicana* against AmB and AmBisome *in vitro*.

Mean EC₅₀ values of AmB (Panel A) and AmBisome (Panel B) are shown in µM with their standard deviation (bars).

The lower activity of AmBisome *in vitro* is, possibly, due to the fact that the MoA of AmBisome is based on the affinity of the liposome for the lipids in the membrane of the macrophage and the absence of endocytosis. Another possibility is that *in vitro*, AmB is not released from the liposome, at least at the same ratio than *in vivo*, and therefore lower amounts of drug are available to kill the promastigotes. The higher activity of AmB *in vitro*, has also been reported in other two strains of *L. donovani*. While AmB was between 3- to 6-fold more active than AmB in promastigotes, this difference was more pronounced, i.e. 3- to 9-fold, in macrophages infected with amastigotes (Yardley and Croft 1997). AmBisome was effective (EC₅₀ of 1.76- and 3.54 µM) against both wild type and AmBR *L. donovani* amastigotes intra-macrophage, however, the activity of AmBisome in axenic amastigotes, showed slightly better activity against wild type, but was inactive against AmBR amastigotes, with EC₅₀ values of 1.73- and >100 µM, respectively (Rochelle do Vale Morais et al. 2018).

Table 5-4. Susceptibility of AmBR lines of *L. mexicana* to AmB and AmBisome before and after infection in mice. Values in μM , Mean \pm Standard Deviation (SD). One-way ANOVA was performed independently for each compound to determine differences of the mean between groups. Tukey's multiple compared pairwise differences of resistant lines with respect the parental wild type. Statistical difference ($P < 0.05$, 95% Confidence Interval) is shown with stars as follows: ns non-significant or $P > 0.05$; * $P \leq 0.05$; ** $P \leq 0.01$; * $P \leq 0.001$; **** $P \leq 0.0001$. FC: Fold Change of AmBR lines is with respect their respective parental wild type (by column).**

AmB				AmBisome							
Pre infection				Post infection (P2)				Post Infection (P2)			
	Mean \pm SD	P value	FC		Mean \pm SD	P value	FC		Mean \pm SD	P value	FC
WT	0.0600 \pm 0.0039	-	-	WTP2	0.0634 \pm 0.0076	-	-	WTP2	0.4762 \pm 0.0082	-	-
AmBR line 14	0.6747 \pm 0.2158	0.0138 *	11.2	AmBRcl.14P2	0.4315 \pm 0.0099	0.3122 ns	6.84	AmBRcl.14P2	7.553 \pm 0.8734	0.6826 ns	15.9
AmBR line 3	0.7402 \pm 0.2335	0.0053 **	12.3	AmBRcl.3P2	0.6813 \pm 0.855	0.0125 *	10.8	AmBRcl.3P2	5.919 \pm 1.992	0.8204 ns	12.5
AmBR line 8	0.7297 \pm 0.2281	0.0062 **	12.1	AmBRcl.8P2	0.5890 \pm 0.2195	0.0458 *	9.34	AmBRcl.8P2	23.55 \pm 15.18	0.0255 *	49.3
AmBR line 6	0.7682 \pm 0.2642	0.0036 **	12.8	AmBRcl.6P2	0.7808 \pm 0.0410	0.0089 **	12.3	AmBRcl.6P2	Not determined	-	-

5.2.7 Histological analysis of mice infected with AmB resistant lines

Based on the macroscopic differences observed in the lesions caused by different AmB resistant lines of *L. mexicana*, I decided to explore in more depth if these changes were also different between lines at the histological level. Histological studies are an important tool to understand the pathogenesis of a disease, as this approach provides relevant biological information that cannot be distinguished macroscopically. Despite all of the advantages provided by other molecular tools that have progressed significantly in recent decades (Czapiński et al. 2017), the isolation of the pathogen is still considered the gold standard for the diagnosis of many infectious diseases and to understand their effects inside the host. With regard to leishmaniasis, histology is still extensively used for the study and identification of the intracellular form of the parasite within mammalian tissues, and a valuable tool to understand many aspects of the pathophysiology of the disease that cannot be determined using other techniques. Histopathology can be used to identify differences in the degree of the lesion and parasite burden (Passero et al. 2009), and to determine the degree of susceptibility between various strains of mice which have different genetic backgrounds. It has also revealed key information related to the visceralization and the distribution of different *Leishmania* spp. that cause cutaneous and visceral leishmaniasis, within the different organs of the animal (de Souza et al. 2018). In this study, I used histology to determine parasite burden and virulence, the latter being estimated from the number of inflammatory cells present within the tissues. Similarly, histology was used to identify if the acquisition of resistance and other traits, i.e. sterol profiles and the metabolome, were associated with fitness costs in these AmB resistant mutants. Other methods that have become standard to determine parasite load and replication, e.g. qPCR, are discussed further (see section 5.3)

As with other intracellular parasites, the granuloma is the typical lesion observed through histological analysis after infection with *Leishmania* spp. The granulomatous lesion results from the aggregation of inflammatory infiltrate which consist of macrophages and other inflammatory cells at the site of infection (Moreira et al. 2010). Histological analysis of the lesions can help to identify the nature of the alteration and to discriminate them from other alterations, i.e. increase of the lesion size, resulting from physiological processes other than an inflammatory response. Examples of this are a transudate and an exudate. The former is a non-inflammatory accumulation of liquid in a compartment of the body due to an increased hydrostatic pressure or low oncotic pressure derived from obstruction of the lymphatic draining system or other physiological causes. On the other hand, the exudative occurs only as a consequence of an infection. While both the transudate and the exudate

can cause an increase in size of an organ or tissue (as in the increase of the footpad lesions observed in this study), only in the latter, the augmented size is the direct consequence of the involvement of inflammatory cells, such as macrophages, dendritic cells and histiocytes. These cells release inflammatory mediators (e.g. bradykinin, histamine), causing dilation of blood vessels and other signs of inflammation, including increased blood flow, increased temperature, redness, tumour and pain (Kasper et al. 2015).

Although these signs can be observed clinically (macroscopically), the use of histology becomes necessary to confirm the presence of the amastigotes and the inflammatory cells within the host. Moreover, leishmaniasis can be misdiagnosed due to the clinical and histological similarities with other inflammatory and neoplastic diseases such as leprosy, paracoccidioidomycosis and tuberculosis among others (Daneshbod et al. 2011; Handler et al. 2015; Hepburn 2000). Other approaches are therefore necessary (see 5.3 for a more complete description).

5.2.7.1 Histopathology of footpads and lymph nodes infected with AmBR *Leishmania mexicana*.

The increase in size and other haemorrhagic and inflammatory changes are frequently observed in lymph nodes and organs that are located near the centre of the infection. Although all of the superficial lymph nodes (and footpads) are bilateral (Nomina Anatomica Veterinaria; <http://www.wava-amav.org/wava-documents.html>), in this study, I only recovered and analysed tissue from primary lesions, i.e. footpad (FP), and from popliteal lymph nodes (PLN) from the same side (right) of the site of inoculation. The enlargement of other deep lymph nodes, e.g. mesenteric, deep cervical, and renal (Van den Broeck, Derore, and Simoens 2006), and from other organs, was not recorded. However, analysis of samples from both sides of the animal, and from other organs can be useful. Tissue samples from the opposite uninfected side can be useful as a control. Similarly, should amastigotes and inflammatory cells appear in tissues from these organs it would indicate an ability of the parasite to migrate to other tissues.

After infection in mice, I also measured the EC_{50} of AmB in parasites (all lines) recovered from both FP and PLN (and transformed into promastigotes) and found that all lines retained their resistance (Table 5-4 and Figure 5-8). Given the biological value of this biological material, and following the findings observed with the first two infections in BALB/c mice (section 5.2.3), fragments of tissue or the whole organs, liver, kidney, spleen, left hind footpad and popliteal lymph node, were surgically removed from all mice infected in the third experiment (section 5.2.5). These samples were stored in ethanol for the quantification of parasites using histology and qPCR, the latter can detect amounts as low as 100 fg of DNA of the parasites within tissues (Antonia, Wang, and Ko 2018; Galluzzi et al. 2018; Nicolas, Prina, and Lang 2002). These tissue samples were not qPCR/histology processed due to limitations of time during the course of this project and therefore, these data were not included in this PhD Thesis. Processing these samples would be informative for future work.

While all lines were from an identical parental line, infectivity showed notable differences associated with their sterol profile (see Figure 5-3). Histological analysis of primary lesions (FP) revealed histiocytic infiltration and a granulomatous reaction with a density of amastigotes notably higher (Figure 5-9, panels A1-2 and B1-2 versus panels D1-2 and E1-2) in mice infected with lines, AmBRcl.14 and AmBRcl.3, in which the primary lesions were larger than in mice infected with WT and lines AmBRcl.8 and AmBRcl.6, in which the lesion showed no increase in size and no amastigotes were detected, possibly, due to a density of parasites below the limit of detection, i.e. 1×10^5 , by microscopy (Figure 5-9, panels D1-2 and E1-2). With respect to the number of amastigotes between the two virulent resistant lines, the number of parasites at microscopy, appeared comparable, i.e. between 7 to 30 parasites per macrophage (Figure 5-9) to those numbers observed in tissue infected with wild type parasites, although variability between samples was considerable. Moreover, the accuracy of light microscopy and the approach used here are limited (see explanation below).

While the identification of the parasite is a confirmative diagnosis (Koçarslan et al. 2013), the opposite cannot be ruled out when parasites are not detected (false negatives can be diagnosed). In agreement with this, in this study, I recovered viable parasites from FP and PLN homogenates, from all mice infected with all four AmBR lines and wild type (Figure 5-10), including those in which parasites were not identified by microscopy. Another change accompanying the increase in the density of parasites in FP lesions was the presence of a hyperkeratotic epidermis, which was observed in mice infected with both resistant lines, AmBRcl.14 and AmBRcl.3, and with wild type (Figure 5-9, panels A2 and

C2). Although the number of parasites can be determined by microscopy, this approach is a qualitative or semi-quantitative estimation of their total numbers. In this study, parasites were recovered without quantifying their exact density within tissues. Parasite burden can be estimated using a limiting dilution assay (De Souza et al. 2018), placing infected tissues into tissue culture medium and counting the numbers of promastigotes that can be recovered as growing over time. This method is, however, laborious, time consuming and can give inaccurate numbers, depending on the amount of tissue recovered, the region of the organ that is dissected, and other factors related to the culture such as the medium used and the phenotype of the strain, and other technical limitations such as the quality of the staining, the resolution of the microscope (and images), and the histological expertise of the investigator.

Unlike the FP lesions which varied in size, there was no difference between the size of PLN from mice infected with AmBR lines and wild type, and no parasites were identified within the PLN tissue. However, viable parasites were recovered in cultures from all PLN irrespective of their size or their identification by microscopy. Other histological changes observed in PLN were the presence of mononuclear and inflammatory cells and other alterations resembling cytosolic lipid droplets (LDs). The increase in number and size of the LD observed in the footpad from one mouse infected with AmBcl.3 (see Figure 5-9, B2), was more pronounced and observed in most of the samples of lymph nodes from mice infected with AmBR- cl.14 and -cl.3 (see chapter 5, section 5.2.7.1, Figure 5-9 and 5-10).

Interestingly, inflammatory cells were more abundant in PLN from mice infected with the attenuated lines (Figure 5-10, panels E1 and F1). The fact that the viable parasites were recovered from PLN, suggests that infected inflammatory cells, i.e. monocyte-derived dendritic cells (moDCs), localised at the site of infection, can facilitate their migration to the draining lymph nodes via lymphatic system. These findings are in agreement with those reported experimentally in a murine model in which viable amastigotes of *L. mexicana* were isolated from lymph node macerates (Kaye and Scott 2011).

The absence of amastigotes identified within the PLN can be explained, at least in part, by the fact that cutaneous species are mainly restricted to the skin and are not described to replicate within other lymphoid tissues (i.e. spleen, liver, lymph nodes, bone marrow) like those species causing VL such as, *L. donovani* and *L. infantum*, which are known to inhibit the host immune response after infection (Kaye and Scott 2011; Thalhoffer et al. 2011). This inhibition of the immune system by *Leishmania* has also been reported in dogs with

visceral leishmaniasis in which a severe granulomatous response was accompanied by higher parasite load, and associated with lymphoid atrophy (Moreira et al. 2010).

With regard to the presence of lipid droplets, these structures are present in most cell types, and consist of a heterogeneous structure predominantly formed by triglycerides and sterol esters, which are surrounded by a monolayer of phospholipids (Carr and Ahima 2016). In other studies, accumulation of lipid storage bodies has been observed in *L. amazonensis* promastigotes after the treatment with thiosemicarbazones (Britta et al. 2014).

In my study, I also screened a library of these compounds in some lines (not included in this Thesis due to time limitations). The formation of lipid bodies is indicative of cellular stress (Lee et al. 2013). Interestingly, LDs were more numerous in the two AmBR virulent lines (Figure 5-10, panels A1-2 and B1-2), in which other significant alterations in the metabolism of lipids (including triglycerides), and oxidative stress, were also identified with LC-MS, after the treatment with AmB (5 x the EC₅₀). A detailed description of these changes, and other metabolites, is discussed further (see Chapter 7).

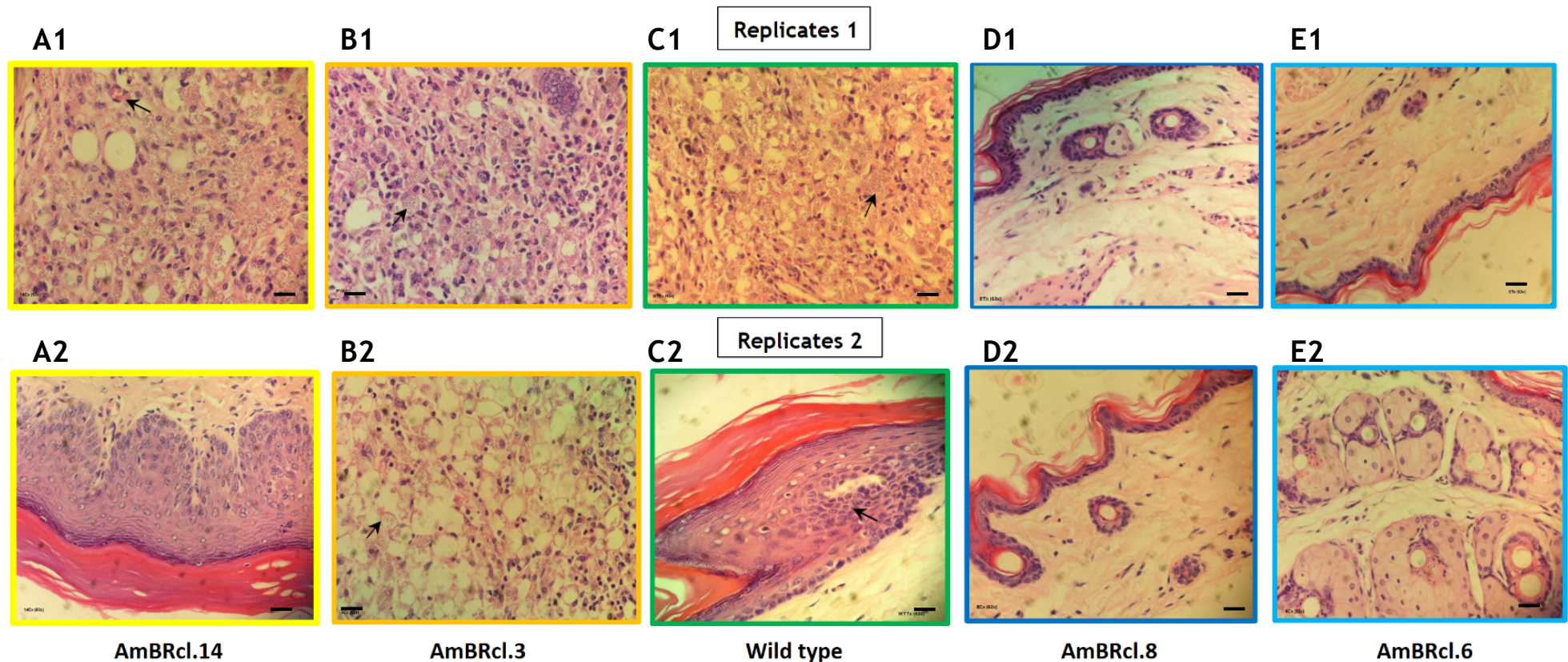


Figure 5-9. Histopathology of primary lesions (footpad) of BALB/c mice inoculated with AmBR lines of *L. mexicana*. Slides are representative of changes in two mice after 12 weeks of infection. Hematoxylin-eosin (H&E). Scale bar = ~10 μ m Objective ~63x. A1-2 and B1-2: AmBRcl.14, AmBRcl.3 (yellow and orange) show skin histiocytes with intense parasitism and inflammatory infiltrate reaction with granulocytes and eosinophilic cytoplasm (arrow) and some vacuolated macrophages. C1-2: Wild type (green) show very similar load of parasites with some macrophages and diffuse inflammatory infiltration with internalised amastigotes (top image) and (bottom image) and parasites (arrow) among muscular fibres. D1-2 and E1-2: AmBRcl.8 and AmBRcl.6 (dark and light blue) some discreet areas of inflammatory reaction localised in papillary dermis without visible parasites.

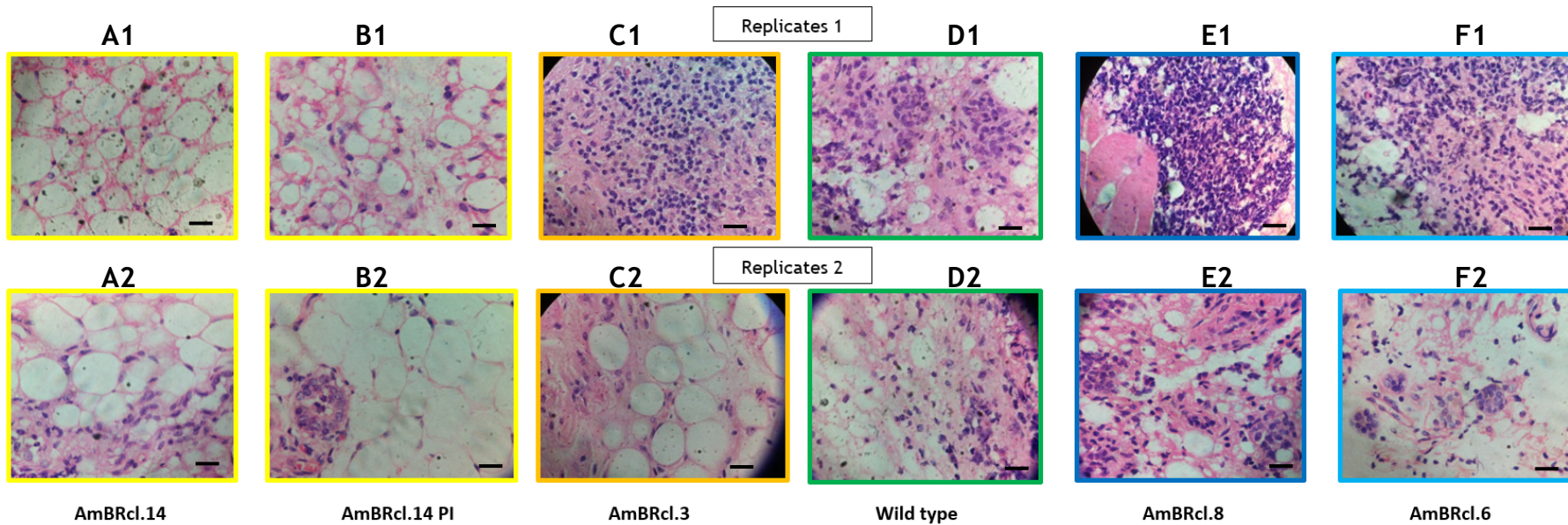


Figure 5-10. Histopathology of lymph nodes of BALB/c mice infected with AmBR lines of *L. mexicana*.

Slides are representative of changes in draining lymph nodes of two mice after 12 weeks of infection. Hematoxylin-eosin (H&E). Scale bar = ~10 μ M Objective ~60x. In A1-2 and B1-2: AmBRcl.14 (yellow), C1-2: AmBRcl.3 (orange), skin histiocytes with intense parasitism and inflammatory infiltrate reaction with granulocytes and eosinophilic cytoplasm (arrow), and some vacuolated macrophages are shown. D1-2: Wild type (green) show less intense parasitism with some macrophages and diffuse inflammatory infiltration with internalised parasites. E1-2 and F1-2: AmBRcl.8 and AmBRcl.6 (dark and light blue) some discrete areas of inflammatory reaction localised in papillary dermis without visible parasites.

Table 5-5. Summary of the mutations identified in genes of the sterol pathway in AmB resistant promastigotes of *Leishmania* spp., coupled with their sterol profile (GC-MS) and their phenotype in a murine model.

Gene annotations were obtained from the TriTrypDB database (<https://tritrypdb.org/tritrypdb/>).

Gene	Mutation and lines in this study	Changes in other genes	Sterol intermediates identified (GC-MS)	Similar changes described in other studies	Phenotype <i>in vivo</i> (lesions)	Histological changes
C5DS	1- V74E(T221A) in line AmBRcl.3	Not additional changes associated	Loss of wild type ergosterol, and cholestane intermediates with an increase of ergosta-7,22-dien-3-ol to 96 - 96.7%	- A mutation G139R (G415C) in AmBRA/cl1. This residue is localized between His residues that are predicted to be enzymatically relevant (1).	Both lines were slightly more virulent in mice (relative to the parental wild type, with significant increase of the lesion size indicating parasite burden	Presence of amastigotes in footpad's tissue, inflammatory cells. Recovery of viable parasites from footpad and lymph nodes from all mice.
	2- M93del (277-279delATG) R244L (G731T) in line AmBRcl.14			- increase of ergosta-7,22-dien-3-ol to 97.9% in one clone AmBRA/cl1 (1).		
	3- R244L (G731T) in lines AmBRcl.14 and AmBRcl.3			- reduction of ergosterol (2-fold), with a significant increase of ergosta-7,22-dien-3-ol from 1.7% and 0.84% to 6.5% and 20.6%, in avirulent- and avirulent log and stationary promastigotes of <i>L. infantum</i> (8). This study did not analyse mutations.		
	4- A95del in NysRcl.B2					
C24SMT	1. V321I (G961A) homozygous (I/I (A/A) in LmxM.36.2390 in three clones: - Two clones from line AmBRcl.8 (A11 and E12), and - One clone from line AmBRcl.6	Loss of miltefosine transporter (LmxM.13.1530), and the neighbouring gene downstream (LmxM.13.1540) In both lines	Loss of wild type ergosterol and ergostane intermediates, with an increase of cholesta-5,7,22-trienol to 86 - 87%	- Similar substitution V321I (G961A) homozygous (I/I (A/A) in three clones, AmBRB/cl2, AmBRC/cl3 and AmBRD/cl2, with increase of cholesta-5,7,22-trienol between 80 to 86.5% (1). - Similar substitution V321I, in three AmBR lines with loss of ergostanes and increase of cholesta-5,7,22-trienol to 87.4 to 93% (2). - A novel mutation, A325V (C974T) associated with a similar loss of the miltefosine transporter (2). I analysed the ORF of this new SNP, the mutation corresponds to the second letter of the codon (GCT/GTT) resulting into a silent mutation (substitution from Alanine to Valine, both non-polar residues) (2). - Abundance of cholestanes (6) after structural changes in C24SMT (suggested) (3, 6). - Loss of C24SMT, AmB resistance (1, 2, 3). - Loss of miltefosine transporter in (1, 2). - Mutation (deletion) of the miltefosine transporter (4). - Modification of C24SMT activity (<i>L. major</i>), loss of expression of one transcript (5, 6). - C24SMT null-mutants (<i>L. major</i>) showed loss of ergosterol and increase of cholestanes (7). I also observed the same effect in a C24SMT KO created with CRISPR (see Chapter 6). - Loss of all C-24 methylated sterols (ergostanes) with increase of cholestanes in AmBR <i>L. mexicana</i> promastigotes (62.4%) and amastigotes (97%). In this study, changes in C24SMT were not determined (9).	Both lines shown an attenuated phenotype in mice with no growth of the lesion size. Other studies showed total loss (7) or reduced infectivity in 2 of 3 AmBR lines (1) associated with loss of expression of C24SMT. AmBR promastigotes and amastigotes were attenuated <i>in vivo</i> (9).	No amastigotes observed in tissue from primary lesions, inflammatory infiltrate in lymph nodes. Recovery of viable parasites from footpad and lymph nodes from all mice.

References: (1) Pountain et al., 2019, (2) PhD Thesis Dr Raihana Binti, Barrett Lab, unpublished, (3) Pourshafie et al., 2004, (4) Fernandez-Prada et al. 2016, (5) Mbongo et al., 2004, (6) Purkait et al., 2012, (7) Mukherjee et al. 2018, (8) (Yao and Wilson 2016), (9) Al-Mohammed, et al. 2005.

Table 5-6. GC-MS profiling of *Leishmania* spp. amastigotes and promastigotes.

Samples from this study were *L. mexicana* log phase promastigotes, and amastigotes, and are compared with *L. infantum* log promastigotes from (Yao and Wilson 2016), and promastigotes and amastigotes from (Al-Mohammed et al. 2005). **LOG Prom: Logarithmic promastigotes growth in HOMEM.** In this study the ergosterol was ergosta-5,7,24(28)-trien-3 β -ol (a.k.a. 5-dehydroepisterol), which in the study of (Al-Mohammed et al. 2005) was ergosta-5,7,24(24¹)-trienol, and the study of Yao and Wilson, discriminates two ergosterol isomers (type I and II). Similarly, here we identified ergosta-7,22-dien-3-ol, which is identified as ergosta-7,24(24¹)-dienol (Al-Mohammed et al), and two isomers, i.e. ergosta-7,22-dien-3B-ol I and II, respectively (Yao and Wilson). All isomers reported in the latter if these studies have different RT. ** Statistically significant (P<0.05). Values of intermediates from this study are the mean of either the two attenuated-, or the two virulent lines, respectively.

Peak of Sterol (%) (alternative name)	LOG Prom (this study)			LOG Prom (Yao and Wilson. 2016)		LOG Prom (Al-Mohammed et al. 2005)		Amastigotes				
	WT HP	Attenuated	Virulent	Avirulent	Virulent	WT	AmB resistant	(this study)			(Al-Mohammed et al. 2005)	
								WT	AmB cl.8	AmB cl.14	WT	AmB resistant
Lanosterol	0.41	0.285	0.315	0.0	0.0	-	-	0.3	0.0	0.0	-	-
Lanosta-8,24-dienol						0.0	31.1	0.0	0.0	0.0	0.0	1.3
4,14,dimethyl-cholesta-8,24-dienol						0.0	62.4	0.0	0.0	0.0	0.0	97.3
4,14,dimethyl-cholesta-7,24-dienol						0.0	6.5	0.0	0.0	0.0	0.0	1.3
4,4-dimethylcholesta-5,7,9(11)-trien-3-ol or 4,4-dimethylcholesta-5,7,24-trien-3-ol, or 4,4-dimethyl-5 α -cholesta-8,14,24-trien-3 β -ol.	2.20	0.0	0.0	-	-	-	-	11.6	12.9	0.0	-	-
(22Z)-Cholesta-5,7,22-trien-3-ol	1.28	82.4	0.0	-	-	-	-	0.0	2.7	0.0	-	-
Cholesta-5,7,24-trien-3-ol		-	-			-	-	0.0	1.2	0.0	-	-
C27 dienol-cholesta-5,7-dienol	0.77	3.7	0.395	-	-	-	-	-	-	-	-	-
Zymosterol	0.0	0.0	0.0	0.0	0.0	-	-	-	-	-	-	-
Ergosta-8,24(28)-diene (Fecosterol)	0.0	0.0	1.28	-	-	-	-	-	-	-	-	-
Ergosta-7,22-dien-3-ol, (3 β ,22E) or any isomers (ergosta-5,7,24(241)-trienol, or ergosta-5,7,24(28)-trien-3 β -ol, or *	10.95	0.0	96.5	5.6 type I 1.7 type II	4.76 type I 6.6 type II**	4.2	0.0	25.8	18.5	43.0	4.6	0.0
ERGOSTEROL or any of the <i>Leishmania</i> spp. isomers *	81.63	0.4	0.25	28.6 type I 39.9 type II	30.92 type I 39.1 type II	85.1	0.0	41.4	48.6	0.0	40.9	0.0
Stigmasta-5,7-dien-3-ol	0.0	0.0	0.0	4.1	0.63	10.6	0.0	8.0	6.0	50.0	47.2	0.0
Cholesterol	3.9	1.6	6.4	16.7	14.6	0.0	0.0	12.2	10.2	7.3	0.0	0.0
Ergostatetraenol	-	-	-	3.27	3.38	-	-	-	-	-	-	-

5.3 Discussion

The lesions observed in mice infected with AmBR lines in this study are contradictory. On the one hand, two virulent lines triggered an exacerbated inflammatory response, indicating a higher parasite burden which was estimated by the higher increase in the primary lesions alongside with other histological alterations. On the other hand, in the other two attenuated lines, the absence of lesions was observed, resembling some of the clinical signs observed in the disseminated form of cutaneous leishmaniasis in which only few parasites are detected with histology, nevertheless, other diagnostic tests, e.g. *Leishmania* skin test (LST) and antileishmanial antibodies, are positive (Burza, et al. 2014). The acquisition of drug resistance in the attenuated lines resembles the fitness cost that has been observed in naturally resistant strains of *L. donovani* in which the development of resistance in the field is, in some cases, associated with treatment failure in endemic regions where resistance is prevalent (Vanaerschot et al. 2018). This fitness cost does not explain, however, the phenotype observed in the other two virulent lines that showed an advantage over the wild type. Similarly, a higher parasite burden was also observed in mice infected with antimonial resistant lines of *L. donovani* (Ouakad et al. 2011). It is possible that the attenuation is derived from long term culture rather than the selection for resistance alone. Alternatively, the specific genetic and metabolic changes associated with resistance vary between strains, and it could be that these underlie resistance. The increase in the lesion size is, however, indicative of the inflammatory response and parasite load. Using qPCR can detect amounts as low as 100 fg of DNA of the *Leishmania* parasites within tissues (Antonia et al. 2018; Galluzzi et al. 2018; Nicolas et al. 2002) and has become the standard practice for confirmation of intra-macrophages parasite replication (Ponte-Sucre et al. 2017). The use of qPCR in animal models of CL treated with liposomal amphotericin B has shown (in *L. mexicana*, *L. major* and *L. donovani*) that the inflammatory response has an effect on the activity of AmBisome and the accumulation of the drug within the site of infection (footpads in my study) (Voak et al. 2018; Wijnant et al. 2018; Wijnant et al. 2018), therefore some of the differences in lesion size observed in this study are possibly due to pro-inflammatory differences at the site of infection.

As summarized in Table 5-5 and Table 5-6, in this and other studies, there is a clear evidence of the role of mutations in two genes, C24SMT and C5DS, which are directly correlated with the presence of specific sterol intermediates that lack the C24 alkylation in the side chain in the former, and the $\Delta 5,7$ double bond in the latter (Pountain et al. 2019a). The evidence of these mutations with regard to their phenotype is, however, scarce and the few studies available, are more heterogeneous with regard to the species studied, their

analytical methods (e.g. standards), and the intermediates identified, therefore, a comparison between studies is a challenge. The accumulation of cholestane intermediates was also observed in a C24SMT-null mutants of *L. major* promastigotes. In addition to the loss of ergosterol, these changes lead to AmBR resistance and higher susceptibility to other lipid inhibitors (Mukherjee et al. 2018). Similar observations have been reported in *L. donovani* selected *in vitro* to AmB (Pourshafie et al. 2004), and in *L. infantum* after the loss of expression of C24SMT (LINF_360031200 in *L. infantum*) (Rastrojo, et al. 2018). These changes were also observed in AmBR line of *L. infantum* (Supplementary file 5), (see page 8) and in two additional studies with AmBR-*L. mexicana*. In the latter two of these studies, cholesta-5,7,22-trienol was between 80 and 86.5% in three clones (AmBRB/cl2, AmBRC/cl3 and AmBRD/cl2) (Pountain et al. 2019), and between 87.4 to 93%, in another three AmBR lines (PhD Thesis Dr Raihana Binti 2019, Barrett Lab, unpublished), which presented similar mutations in C24SMT (i.e. V321I). In both cases, the loss of ergostanes was also notable. Moreover, these findings are in agreement with the accumulation of cholestane-based sterols (90.8 to 91.2%) observed here in a C24SMT knockout, which was created using CRISPR-Cas9 system (Beneke et al. 2017), which GC-MS profile is discussed further (see Chapter 6).

In this study, the difference between virulent and attenuated phenotypes was related to the sterol profiling which derived from the mutations identified in two enzymes, i.e. C24SMT and C5DS, of the sterol biosynthetic pathway, and other changes associated with the loss of the miltefosine transporter (see Chapter 4). Moreover, the loss of the wild type ergosterol in all four AmBR resistant lines, was associated with resistance *in vivo* and *in vitro*. This is supported by the both, the macroscopic and histological findings in mice infected with AmBR lines, suggesting that the resistance of AmBR lines is carried forward from *in vitro* selection to *in vivo*, irrespective that a dose to cure was not achieved with either AmB deoxycholate or AmBisome. A clear description of the relationship between these mutations, and the sterols and phenotype *in vivo*, derived, including a comparison with similar changes reported elsewhere is summarised in Table 5-5. A similar explanation of the relationship between gene mutations, and changes in the metabolome in two AmBR lines (AmBRcl.14 and AmBRcl.8) is discussed in chapter 7.

6 Drug screening of a new class of sterol inhibitors in *Leishmania* promastigotes

6.1 Introduction

Azasterols (AZA) have been explored as C24SMT-specific inhibitors in *Leishmania* spp. (Contreras, Vivas, and Urbina 1997; Gigante et al. 2010; Gros et al. 2006; Haughan, Chance, and Goad 1995; Jiménez-Jiménez et al. 2008; Liendo et al. 1999; Lorente et al. 2004b; Magaraci et al. 2003; Rodrigues et al. 2007). AZA are active against the C24SMT in *Leishmania* spp. and its orthologues in *T. cruzi* (Magaraci et al. 2003), *T. brucei* (bloodstream form) (Gros et al. 2006; Lorente et al. 2004b), and *T. gondii* (Martins-Duarte et al. 2011). C24SMT plays a key role in the biosynthesis of ergosterol and other 24-methylated intermediates, and is related to drug resistance in *Leishmania* spp., particularly to AmB and nystatin which bind to ergostane type sterols (Pourshafie et al., 2004; Purkait et al., 2012; Pountain et al., 2019).

Deletion of both copies of this gene in *L. major*, resulted in the loss of the virulence *in vivo* (Mukherjee et al. 2018). The loss of expression of C24SMT is also related with AmB resistance in *L. infantum* (Rastrojo, et al. 2018), and in *L. mexicana* (Pountain *et al.*, 2019). The latter of these studies showed that AmB resistance was also associated with gene-amplification and duplication events within the C24SMT locus which contains two closely related genes expressed at different levels, and the presence of SIDER1 retrotransposon elements seemed to be related to these recombination related events. Another common feature observed in all these C24SMT mutants is the replacement of ergosterol by cholestane-type intermediates.

In my study, genomic alterations identified in C24SMT lead to AmB resistance, increase in cholestanes with a concomitant loss of the wild type ergosterol, and a loss of virulence *in vivo* (in a murine model) (chapter 5, section 5.2.3), in two AmBR lines (see Chapter 4 for details). The replacement of ergosterol by cholestanes was more pronounced (>90%), in a C24SMT-knockout (C24SMTKO) (Figure 6-10 and Table 6-3) developed here with CRISPR-Cas9 (Beneke *et al.*, 2017) (see chapter 2, section 2.8.4 for details). Accumulation of cholestanes has also been observed in *L. major* and *T. cruzi*, after the treatment with C24SMT inhibitors such as AZA (Magaraci et al. 2003), imipramine (IMI) and α -tomatidine (TOM), which have been found to disrupt the synthesis of sterols in *L. amazonensis* promastigotes (Andrade-Neto, Pereira, Do Canto-Cavalheiro, et al. 2016; Medina et al. 2012). Other potential MoA of IMI and TOM are discussed in detail later

(section 6.3). For this reason, I decided to investigate potential C24SMT inhibitors other than AZA. First, I tested two compounds, IMI and TOM, followed by the screening of a new library of sterol inhibitors, 1,2,3-triazolylsterols (TAZ), which have structural similarities to AZA (Porta et al. 2014). I then used GC-MS to validate if sterol changes are similar to those described with other C24SMT-mutants.

With regard to the screening of the TAZ inhibitors, I first tested three compounds, 2DR, 2ER and 2ES, in four AmBR lines, followed by the screening of the complete library (N=16) (Table 6-1). For this second part, I made a rational selection of cell lines and mutants, as follows: two AmBR lines were selected considering their mutations in C5DS (AmBRcl.14), and in C24SMT (AmBRcl.8), respectively. Since all four NysR clones showed a similar sterol profile (chapter 5), I selected the two most resistant clones, NysR-clB2 and -cl.E1, with the highest fold change (FC) in their EC₅₀ to nystatin (see section 3.2.3.3 and Figure 3-8). As the enzymes C24SMT and C14DM have been proposed as potential targets of TAZ, I included a third AmBR clone with EC₅₀ to AmB of 0.270 μM (3-fold) and with a mutation (N176I) in C14DM, that had been developed by a former member within the Barrett Lab (Mwenechanya et al. 2017). A C24SMT-overexpressor (C24SMT) (Figure 6-7), and a -knockout, named C24SMTKO herein, were also included.

Importantly, TAZ were also assayed for specific inhibition of the recombinant *L. mexicana* C24SMT (LmxM.36.2380), using zymosterol as the preferred substrate (others substrates were also tested). Enzymatic assays were performed by Boden Vanderloop from the David Nes Lab at the Texas Tech University Lubbock, and Dr Minu Chaudhuri, from the Meharry Medical College, USA, and are part of a collaborative effort between the Barrett-, Labadie- and Nes Labs, from Glasgow-, Argentina and Texas Tech Universities, respectively. Except for two inhibitors that are shown here to illustrate the activity of these compounds (Figure 6-6), these data are reserved for a manuscript (in preparation), and are not included in this Thesis. After analysing the similarity in the EC₅₀ obtained *in vitro* and the IC₅₀ found in enzymatic assays (Table 6-2), the two most potent compounds were selected, to determine their time- and dose-to-kill (Figure 6-9), before assessing their effect on the content of sterols in *L. mexicana* promastigotes (section 6.2.3, and Figure 6-10).

6.2 Results

6.2.1 Tricyclic antidepressants

IMI, a tricyclic antidepressant (TCA), is also active *in vivo* (in mice and hamsters), against antimonial-resistant and -sensitive promastigotes and with higher potency in amastigotes (IMI inhibits trypanothione reductase) (Mukherjee et al. 2012; Sarkar and Manna 2015). Other effects of IMI and other TCAs (e.g. clomipramine), are the disruption of the membrane proton pumps (and cellular pH), the inhibition of the transport of L-proline (Zilberstein and Dwyer 1984; Zilberstein, Liveanu, and Gepstein 1990), and the binding to lipid bilayers that is derived from its affinity for some lipid components of the membranes, i.e. phosphatidylcholine and phosphatidylethanolamine. I tested IMI considering its potential to inhibit C24SMT (Viana Andrade-Neto et al. 2016a), IMI also targets other methyl transferases related with the methylation of phospholipids (Mukherjee et al. 2012). In *L. donovani*, IMI decreased the mitochondrial transmembrane potential and caused apoptosis (Mukherjee et al. 2012), while in *L. mexicana* promastigotes and amastigotes, inhibition of the uptake of D-glucose (2-deoxy-D-[1,2-³H]glucose) was observed (Burchmore and Hart 1995). The antileishmanial properties of IMI have been demonstrated in other *Leishmania* spp (Mukherjee et al. 2012; Sarkar and Manna 2015; Viana Andrade-Neto et al. 2016b). These studies also showed that IMI has a good selectivity index and can be administered orally, which is an attractive property of this compounds, considering that to the present, MF is the only oral antileishmanial available (Sunyoto, et al., 2018).

IMI triggered a significant inhibition of the growth rate in wild type and two AmBR lines of *L. mexicana* promastigotes between 24 to 48 hours post treatment (ANOVA $P < 0.0001$; all pairwise comparisons were also significant, $P < 0.05$) (see supplementary 6) (see page 8). Notably, this effect was more dramatic between days 5 to 7, and more pronounced in both AmBR lines than in wild type (Figure 6-1, panels A to C). In comparison, inhibition of growth was partial or absent in wild type and the two AmBR lines, AmBRcl.8 and AmBRcl.3, after the treatment with 100- and 150 nM of AmB, respectively. While growth of the wild type was restored after day 4 to 5 (Figure 6-1 Panel A), the absence of growth inhibition indicates higher resistance of both AmBR lines. Moreover, the addition of ergosterol (80 μ M) in the culture medium, prevented the inhibition of growth in wild type treated with AmB, possibly due to its sequestration, and accelerated the growth rate in AmBRcl.3 (with mutations in C5DS) to a level comparable to untreated cells. However, the addition of ergosterol did not show any restoration of growth in AmBRcl.8 (with mutations in C24SMT and deletion of the miltefosine transporter). Interestingly, ergosterol

did not restore the growth in the wild type or any of the resistant lines after the treatment with IMI (100 μ M) (Figure 6-1, panels A to C).

The fact that wild type promastigotes restored their growth after 4-5 days after the treatment with AmB, even in the absence of ergosterol, can be explained by the fact that AmB is, possibly, degraded or inactivated in culture conditions at 26 °C. AmB is stable for one week at 2-8 °C, and for only 24 hours at room temperature (25 °C)

(<https://toxnet.nlm.nih.gov/cgi-bin/sis/search2/r?dbs+hsdb:@term+@rn+@rel+1397-89-3>),

and is also indicative that some of the wild type parasites, possibly persister-like populations (Barrett, et al., 2019), tolerated AmB at the concentration added here (the EC₅₀ of AmB in wild type is between 60 to 100 nM). Conversely, the sustained inhibitory effect of IMI is, possibly, due to the fact that its metabolite, desipramine, is also active in promastigotes (Evans and Croft 1994; Sarkar and Manna 2015). Following these observations, I suggested testing IMI in four other AmBR lines selected by a former member within the Barrett Lab (Pountain *et al.*, 2019). Interestingly, all of these lines, which were defective in ergosterol production, showed significant increase in susceptibility to IMI (P= 0.0217 to 4.51 x 10⁻⁴), irrespective of the presence of mutations in different enzymes of sterol synthesis, i.e. C24SMT and C5DS (Dr Andrew Pountain PhD Thesis, University of Glasgow).

In my study, all four AmBR lines were cross resistant to IMI, with AmBR- cl.8 and -cl.6 being slightly more resistant than AmBR- cl.14 and -cl.3 (chapter 3, Figure 3-6), however, all differences in EC₅₀ between AmBR lines and wild type were non-significant (see Table 3-2). Similarly, both lines, C24SMT-overexpressor (P=0.2290) and C24SMTKO (P=0.8421), were slightly more resistant to IMI than their respective parental wild type (Figure 6-2, panel B). I also tested other two compounds with a some structural similarities to IMI, i.e. desipramine and trimipramine (TRIMI), the former is the resulting metabolite of IMI (after a demethylation reaction) and is also active, whereas the latter is a derivative of IMI with a methyl group incorporated to its side chain (Figure 6-2, panel A). While the activity of TRIMI was similar across all lines, no activity was observed with desipramine (Figure 6-2, panel B). Previously, no increase in resistance to other C24SMT inhibitors, e.g. 22,26-azasterol, was observed in *L. major* promastigotes transfected with C24SMT, irrespective of the overproduction of the enzyme (Jiménez-Jiménez et al. 2008).

Following the experiments with ergosterol, I tested different concentrations (50, 25, 12.5 and 6.25%) of foetal bovine serum (FBS) in the culture medium and measured the EC₅₀ of AmB. A concentration dependent correlation was observed in wild type (R²= 0.96), and to

a lesser extent, in AmBcl.8 ($R^2= 0.64$) (Figure 6-1, panels D and E). These assays suggest that the content of cholesterol and other components in the serum (see below), can affect the susceptibility of *Leishmania* to AmB. Previous studies showed that *Leishmania* spp., can uptake exogenous cholesterol to its advantage (Andrade-Neto et al. 2011), and compensate the loss of ergosterol derived from the binding with AmB, which is the main MoA of AmB (see chapter 1, section 1.6.6.1, and Table 1-2, for a detailed description on the MoA).

Another possible explanation is the sequestration of AmB by cholesterol and other lipoproteins present in the plasma serum (Janina Brajtburg et al. 1984), which has been observed with both formulations, AmB deoxycholate and AmBisome (Bekersky et al. 2002). Additional experiments adding different concentrations of cholesterol, are needed to clarify the effect of both, ergosterol and cholesterol, in AmBR lines. All four AmBR clones were tested again for AmB, confirming the resistance observed in previous assays (see Chapter 3), interestingly, the two lines with mutations in C24SMT and with a deletion of the miltefosine transporter, were both more resistant to AmB, than the other two lines which have defects in C5DS. No change was found in the C24SMT-overexpressor (EC_{50} between 40 to 70 nM), while the C24SMTKO was 6-, 10-, and 2.3-fold resistant to AmB ($P < 0.0001$), AmBisome ($P = 0.0116$), and Nys ($P = 0.0131$), respectively, with respect to its parental line (Figure 6-2, panel B).

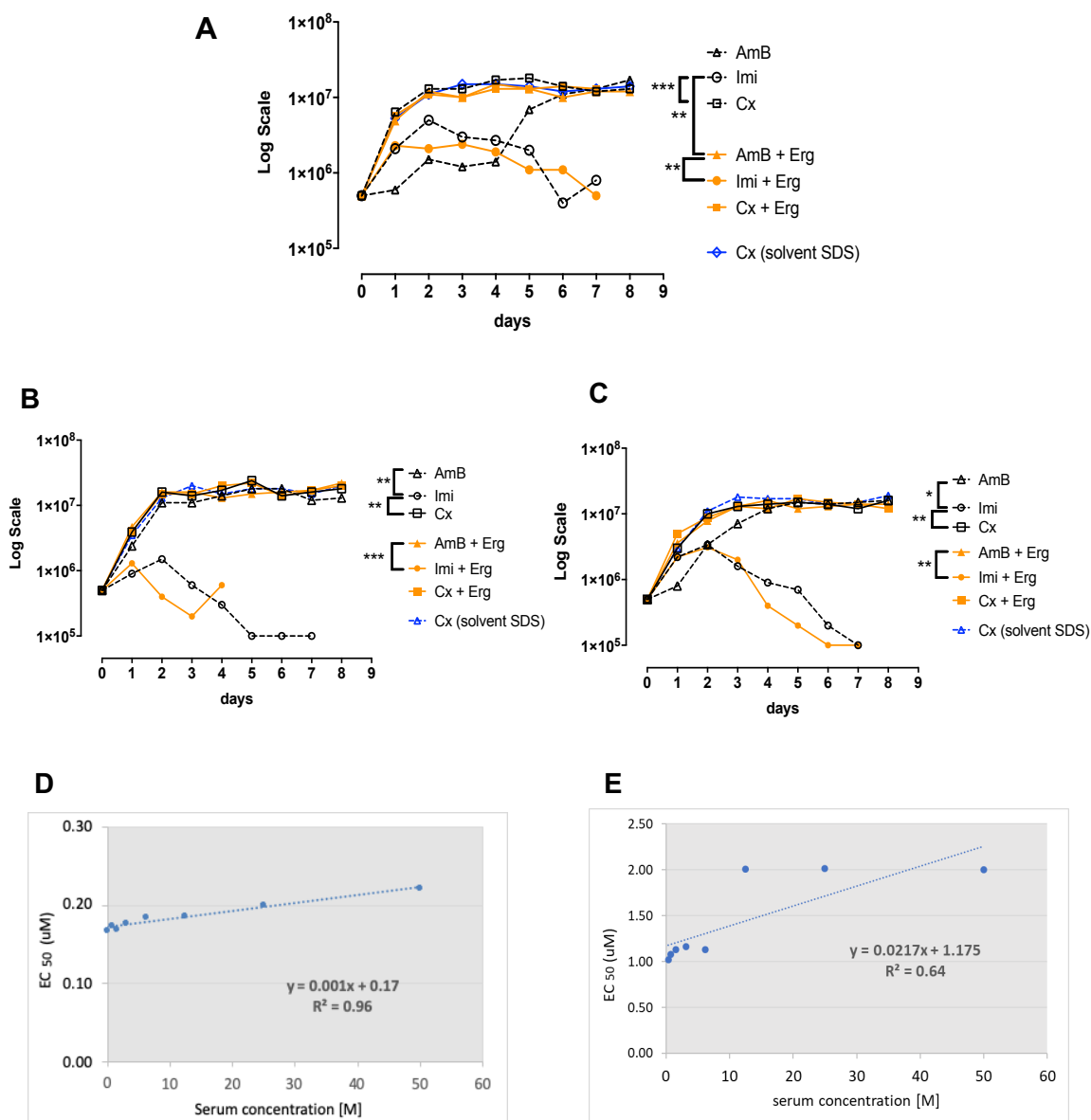


Figure 6-1. Effect of ergosterol in wild type and AmBR lines of *L. mexicana* after the treatment with sterol inhibitors
 Treatment with AmB and IMI was followed by the addition of ergosterol (80 μM) in the culture medium. Starting density of promastigotes for these assays was 5×10^5 per ml. Growth rate of wild type (**Panel A**); resistant lines AmBRcl.8 and AmBRcl.3, respectively (**Panels B and C**); correlation coefficient between the concentration of FBS in the culture medium and the EC₅₀ of AmB in wild type (**Panel D**) and in AmBRcl.8 (**Panel E**). Figures are representative of one biological replicate. Ergosterol was diluted in sodium dodecyl sulfate (SDS) 2.5% in PBS (v/v). Final concentration of the solvent in the assay was <1% (0.25%).

6.2.2 Sterol inhibitors, 1,2,3-triazolysterols

Compounds, 1,2,3-triazolysterols (TAZ), are sterol derivatives with heteroatoms or heterocycles on their side chain (Table 6-1). In a previous study, some of these compounds showed sub-micromolar potency (EC₅₀ 2DR: 1.14 μM , 2ER: 1.94 μM and 2ES: 1.35 μM) in *L. donovani* promastigotes, although their target was unknown (Porta et al. 2014, 2017). In my study, TAZ inhibitors were very stable (in DMSO) with good reproducibility

between assays. However, the potency of these three TAZ compounds in *L. mexicana* promastigotes, was between 5 to 20-fold lower than in the study of Porta and colleagues. Differences in activity between different leishmania species, however, is not uncommon and has been observed with many antileishmanials (Croft et al. 2006), including AmB (Franco-Muñoz, Manjarré S-Estremor, and Ovalle-Bracho 2018; Zauli-Nascimento et al. 2009). Similarly, in my study, TAZ were all less active than PENT and AmB (Table 3-2), which were used as in the study of Porta et al. While the most potent TAZ in *L. donovani* was 2DR (Porta et al., 2014), in my study, 2ES ($EC_{50} 7.5 \pm 0.7$) was between 3 to 5-fold more active than its isomers 2ER ($EC_{50} 22.4 \pm 0.7$) and 2DR ($EC_{50} 36.1 \pm 9.2$) in wild type *L. mexicana* promastigotes (Figure 6-2, panel C).

While Porta and colleagues tested TAZ (2DR, 2ER, 2ES) only in wild type (*L. donovani*), here, I showed their activity in wild type plus four AmBR lines, and two C24SMT-mutants. TAZ inhibitor 2ES was slightly less active in three AmB resistant lines, AmBRcl.14, AmBRcl.3 and AmBRcl.6, showing no significant difference with respect to wild type ($P \geq 0.2265$). No change in susceptibility was seen with AmBRcl.8, and with the C24SMTKO, while the C24SMT-overexpressor showed a marginal increase in susceptibility to this compound. The other two TAZ inhibitors, 2ER and 2DR, were more active in all four AmB resistant lines than in wild type. The former was 2-fold more potent in all AmBR lines ($P \leq 0.0019$), and the latter was ~ 1.7 -fold more potent in lines AmBRcl.14 and AmBRcl.3 ($P \geq 0.0894$), and ~ 3.1 -fold more potent in lines AmBRcl.8 and AmBRcl.6 ($P \leq 0.0061$), suggesting a C24SMT-specific activity. Additionally, the activity of 2DR in C24SMTKO was comparable to that found in wild type, while in the C24SMT-overexpressor, 2DR was ~ 6 -fold more potent than in the parental line ($P=0.0009$), although the effect in latter line was surprising (if the target is C24SMT, less potency is expected in an over-expressor), however, an alternative MoA of these inhibitors could explain this (Figure 6-2, panel C). All the EC_{50} values (mean \pm SD) are provided in a separate file (see Supplementary 6) (see page 8). Following the screening of the first three TAZ inhibitors, 2DR, 2ER and 2ES, I tested another sixteen analogues (Table 6-1). All of these compounds were less active than AmB (Figure 6-3), with five compounds showing statistical significance, B2N, B5, 90.A, 90.B ($P < 0.0001$) and C4 ($P = 0.0349$).

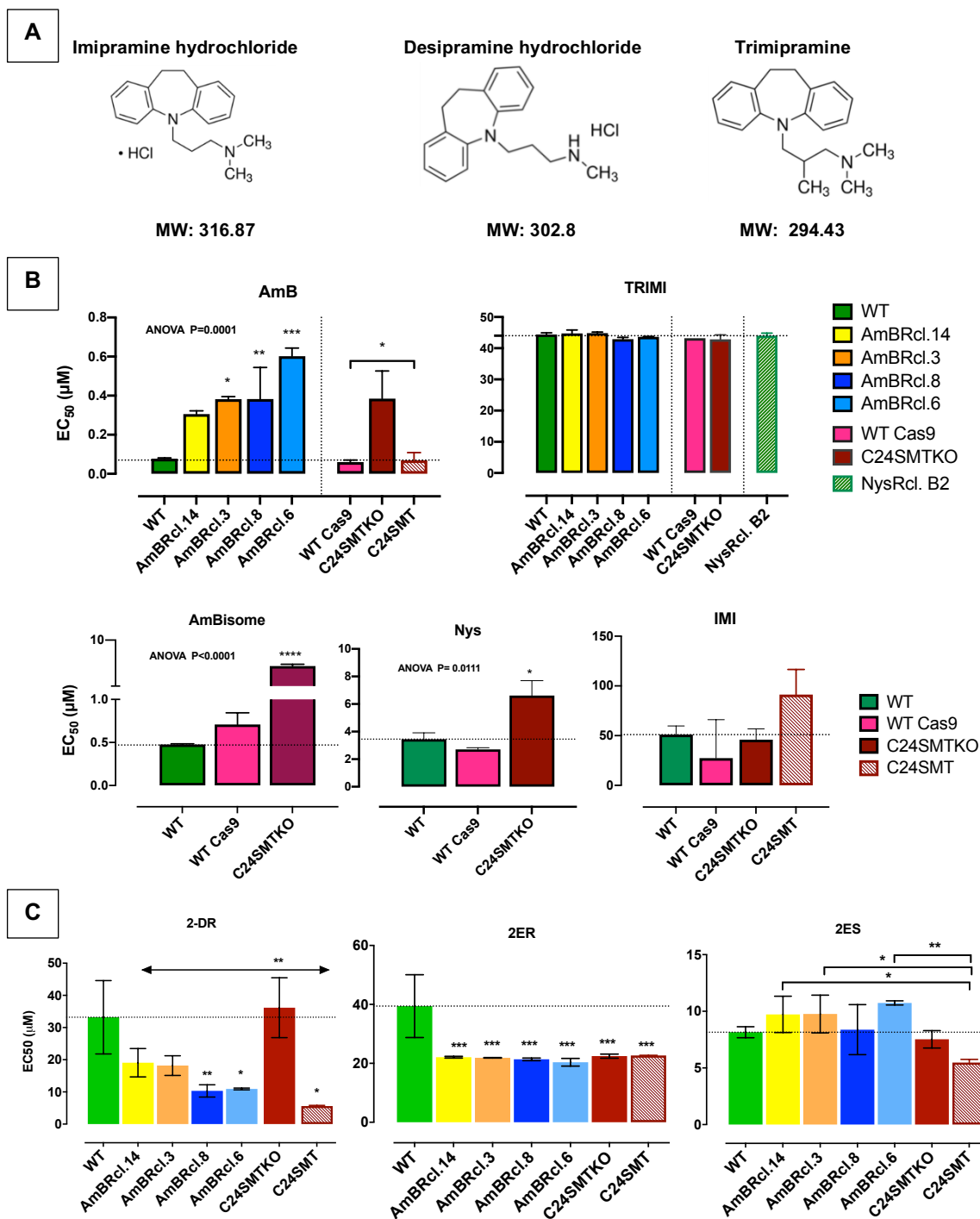


Figure 6-2. Susceptibility of AmBR lines of *L. mexicana* to 1,2,3-triazolylsterol inhibitors. **Panel A:** the structure of TCAs, imipramine (IMI), desipramine, and trimipramine (TRIMI) are shown with their respective molecular weight (MW). EC_{50} of IMI, clomipramine and mianserin, in AmBR and NysR lines is shown in chapter 3 (Figures 3-5 and Figures 3-7). **Panels B and C:** Mean EC_{50} values \pm standard deviation (bars) are from three replicates (TRIMI in WTCas9 is from one replicate). A one-way ANOVA test was performed per each compound to determine the difference of the mean between groups. Tukey's multiple comparison test was used to find pairwise differences. Statistically significant values ($P < 0.05$, 95% Confidence Interval) are shown with stars: * $P \leq 0.05$, ** $P \leq 0.01$, *** $P \leq 0.001$, **** $P \leq 0.0001$). A complete list of all values is provided in Supplementary file 6-1 (see page 8). WT is the parental wild type, AmBRcl.14, AmBRcl.3, AmBRcl.8 and AmBRcl.6 are AmB resistant, and NysRcl.B2 is nystatin resistant. WTCas9 is the wild type expressing Cas9, C24SMTKO is a knockout of C24-sterol methyl transferase (section 2.8.4). Nystatin (Nys).

Comparisons between the activity of TAZ compounds showed that 156.D and 156.E were the two most potent inhibitors with an EC₅₀ of 3.7- and 3.1 μ M, respectively (Figure 6-3, highlighted in red), although the difference was not statistically significant with respect to those compounds with EC₅₀ values within the same range, i.e. 5.0 to 16.7 μ M. Compounds 90.A and 90.B, were notably the two least active ($P < 0.0001$). Similarly, the activity of B5 and B2N, was significantly lower in all cell lines tested in comparison to the other TAZ compounds ($P = 0.0274$ to < 0.0001). While the difference between compounds was significant ($P < 0.0001$), the effect on different cell lines, and the interaction between compounds and different cell lines, were both non-significant ($P = 0.3101$ to 0.9288). The individual EC₅₀ values of the TAZ tested in this study in each of the nine cell lines, is discussed below (Figure 6-4). A list of all the EC₅₀ values (mean \pm SD), and statistical analyses, is provided (Supplementary 6) (see page 8). Two inhibitors, B2N ($P = 0.5732$) and C4 ($P = 0.1315$), were notably more active in the AmBR line with a mutation in C14DM (AmB 0.27 μ M) than in the wild type.

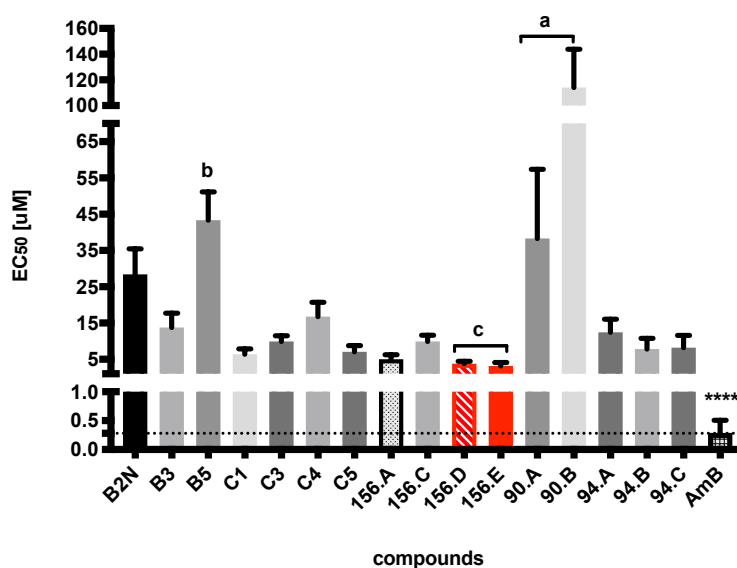
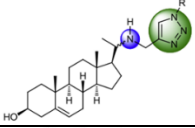
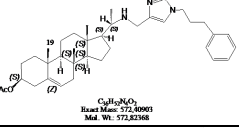
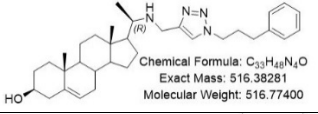

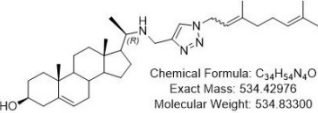
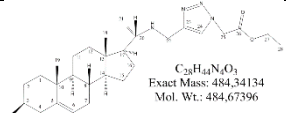
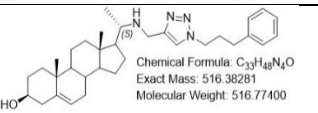
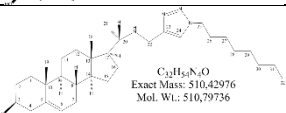
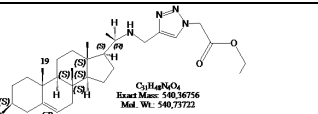
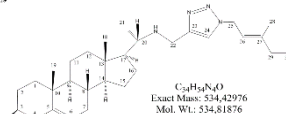
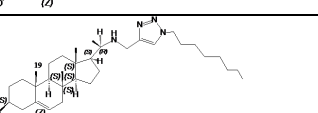
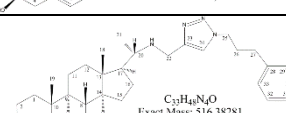
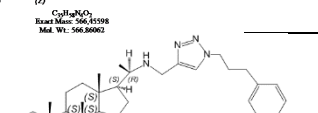
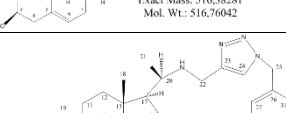
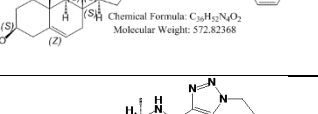
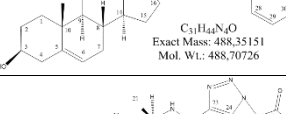
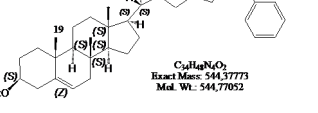
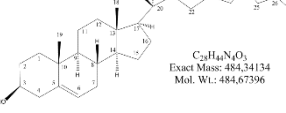
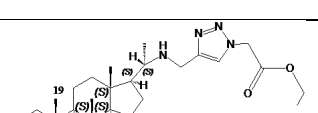
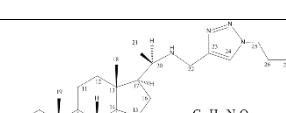
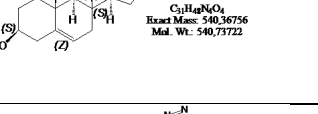
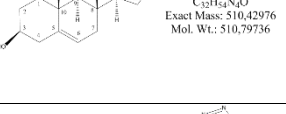


Figure 6-3. Susceptibility of AmBR lines of *L. mexicana* to 1,2,3-triazolylsterol inhibitors. Mean EC₅₀ values are shown in μ M with their standard deviation (bars). All values are from three biological replicates. A two-way ANOVA test showed the difference of the mean between compounds (95% Confidence Interval) significant values are shown with stars: **** $P \leq 0.0001$. Tukey's multiple comparison test was used to find pairwise differences between compounds. Statistically significant values ($P < 0.05$, 95% Confidence Interval) are: a $P \leq 0.0001$; b $P \leq 0.05$; c $P > 0.05$. A detailed list of all values is shown in Supplementary file 6-1. The two most active TAZ are highlighted in red. The EC₅₀ values of each compound in each cell line separately (nine cell lines in total), is shown in Figure 6-4.

Table 6-1. Chemical structure of the library of heterocyclic steroids from pregnenolone. The chemical steps for preparation of these compounds from pregnenolone (top left structure) were detailed elsewhere (Porta et al., 2014). All the structures and chemical details of these inhibitors were kindly provided by Dr Guillermo Labadie, from The University of Rosario, Argentina. The three compounds (2ER, 2DR and 2ES) that were studied in the initial stage of this screening are highlighted in grey.

CODE	STRUCTURE	CODE	STRUCTURE
Pregnenolone		C5	 C ₂₇ H ₄₂ N ₂ O ₂ Exact Mass: 572.30991 Mol. Wt.: 572.2168
2ER (YZ-1-13)	 Chemical Formula: C ₃₃ H ₄₈ N ₄ O Exact Mass: 516.38281 Molecular Weight: 516.77400	156.A	 C ₃₁ H ₄₄ N ₂ O Exact Mass: 488.3151 Mol. Wt.: 488.70726
2DR (YZ-1-15)	 Chemical Formula: C ₃₂ H ₄₄ N ₄ O Exact Mass: 534.42976 Molecular Weight: 534.83300	156.B	 C ₂₈ H ₄₄ N ₂ O ₃ Exact Mass: 484.34134 Mol. Wt.: 484.67396
2ES	 Chemical Formula: C ₃₃ H ₄₈ N ₄ O Exact Mass: 516.38281 Molecular Weight: 516.77400	156.C	 C ₃₁ H ₄₄ N ₂ O Exact Mass: 510.42976 Mol. Wt.: 510.79736
B2N	 C ₃₁ H ₄₄ N ₂ O ₄ Exact Mass: 540.36756 Mol. Wt.: 540.73722	156.D	 C ₃₄ H ₅₄ N ₂ O Exact Mass: 534.42976 Mol. Wt.: 534.81876
B3	 C ₃₃ H ₄₈ N ₂ O Exact Mass: 566.45598 Mol. Wt.: 566.86062	156.E	 C ₃₃ H ₄₈ N ₂ O Exact Mass: 516.38281 Mol. Wt.: 516.76042
B5	 Chemical Formula: C ₃₂ H ₄₂ N ₂ O ₂ Molecular Weight: 572.82368	90.A	 C ₃₁ H ₄₄ N ₂ O Exact Mass: 488.3151 Mol. Wt.: 488.70726
C1	 C ₃₄ H ₄₈ N ₂ O ₂ Exact Mass: 544.37773 Mol. Wt.: 544.77052	90.B	 C ₂₈ H ₄₄ N ₂ O ₃ Exact Mass: 484.34134 Mol. Wt.: 484.67396
C2N	 C ₃₁ H ₄₄ N ₂ O ₄ Exact Mass: 540.36756 Mol. Wt.: 540.73722	94.A	 C ₃₃ H ₄₄ N ₂ O Exact Mass: 510.42976 Mol. Wt.: 510.79736
C3	 C ₃₃ H ₄₈ N ₂ O ₂ Exact Mass: 566.45598 Mol. Wt.: 566.86062	94.B	 C ₃₁ H ₄₄ N ₂ O Exact Mass: 534.42976 Mol. Wt.: 534.81876
C4	 C ₃₂ H ₄₂ N ₂ O ₂ Exact Mass: 590.45598 Mol. Wt.: 590.88202	94.C	 C ₃₂ H ₄₀ N ₂ O Exact Mass: 530.39846 Mol. Wt.: 530.787

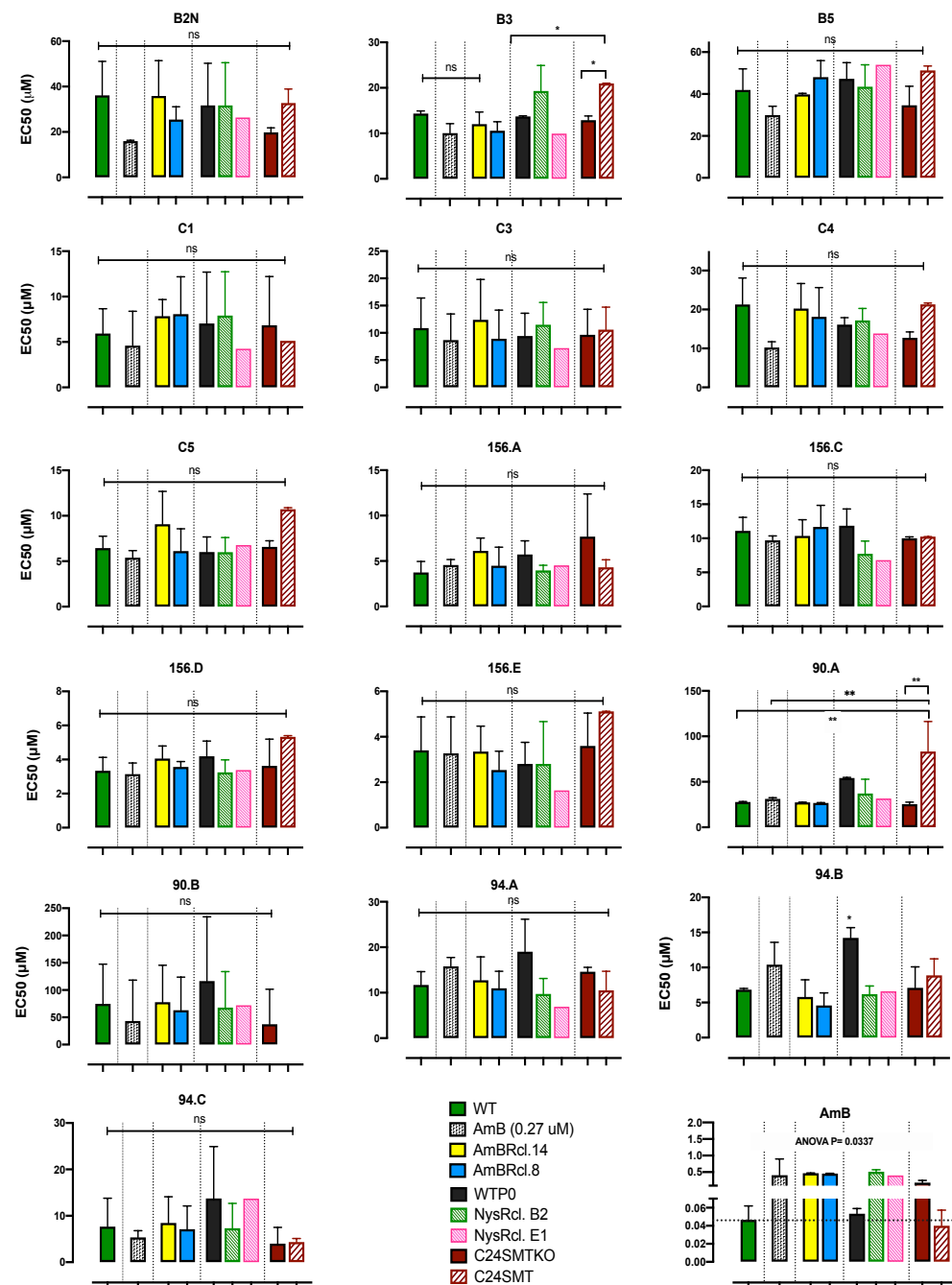


Figure 6-4. Susceptibility of AmBR lines of *L. mexicana* to 1,2,3-triazolylsterol inhibitors. Mean EC₅₀ values are shown in µM with their standard deviation (bars). All values are from three biological replicates (NysRcl.E1 is from one replicate). A one-way ANOVA test was performed for each compound to determine the difference of the mean between groups. Tukey's multiple comparison test was used to find pairwise differences between lines. Statistically significant values ($P < 0.05$, 95% Confidence Interval) are shown with stars: * $P \leq 0.05$, ** $P \leq 0.01$, *** $P \leq 0.001$, **** $P \leq 0.0001$). A detailed list of all values is provided separately (Supplementary file 6-1) (see page 8). Polyene resistant lines are: AmB 0.27 µM; AmBR *L. mex* clone with a mutation in C14DM (Mwenechanya et al., 2017); AmBRcl.14 and AmBRcl.8, and NysRclB2 and NysRcl.E1 are AmBR and nystatin resistant, respectively (see chapter 3); WT and WT P0 are two wild type parental lines, and C24SMT and C24SMTKO are an overexpressor- and knockout created using CRISPR-Cas9 (Beneke, et al. 2017) of C24-sterol methyl transferase

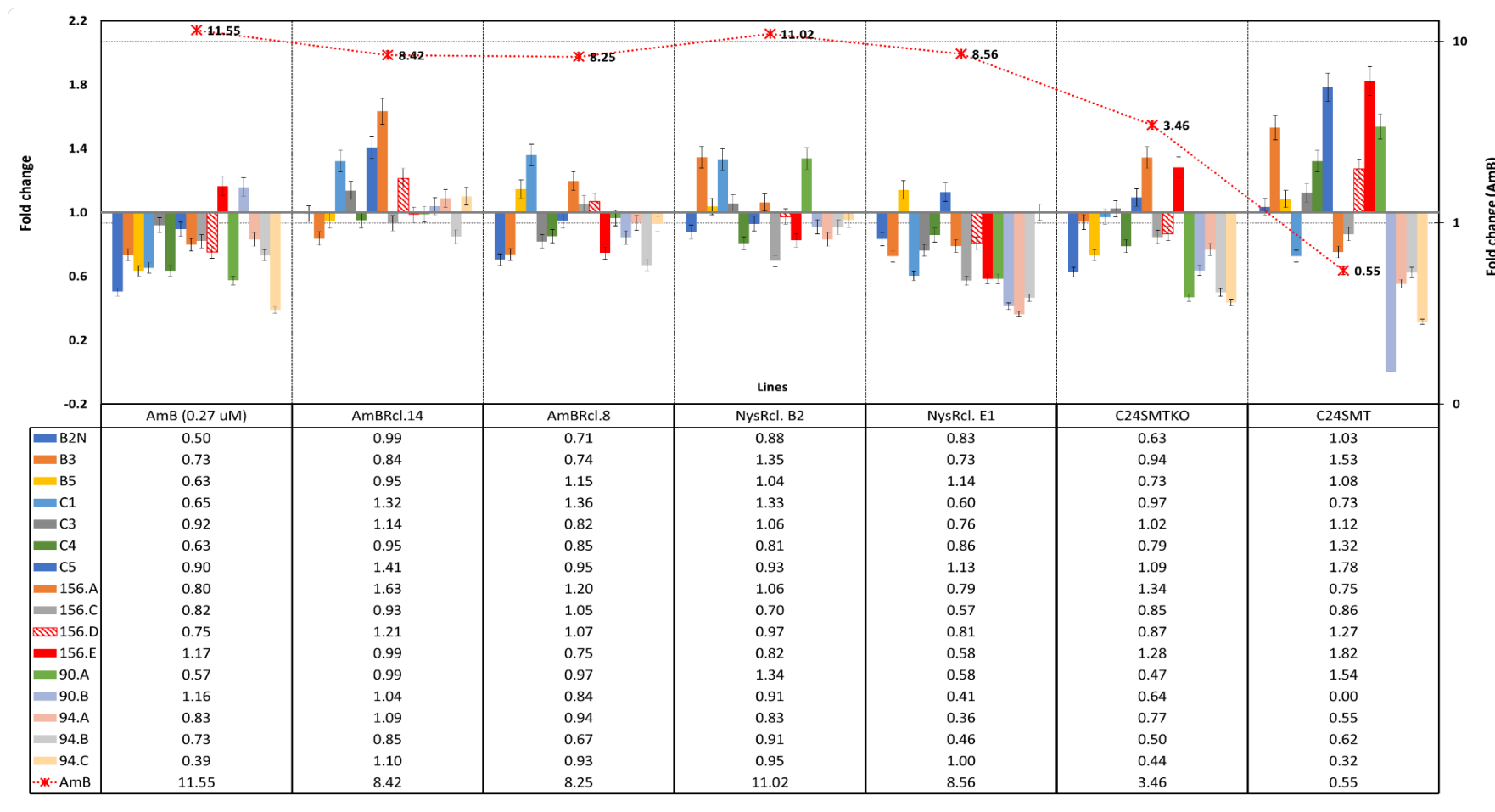


Figure 6-5. Fold changes to 1,2,3-triazolylsterol inhibitors in different sterol resistant lines of *L. mexicana* promastigotes. Fold changes (FC) in the mean EC_{50} are with respect to their parental wild type. Bars indicate the standard deviation expressed as percentage (5%). The structure of these compounds is shown Table 6-1. Abbreviations of the different cell lines is as shown in Figure 6-4. Except for AmB (control), which FC-scale is shown in the right y-axis, the FC of all the TAZ compounds, refers to the scale from the x-axis. A full list with all the EC_{50} values is provided separately (Supplementary file 6-1) (see page 8).

Except for compounds B3 ($P \leq 0.05$) and 90.A ($P \leq 0.01$) that were slightly less active in the C24SMT-overexpressor (relative to WT), none of the other TAZ inhibitors showed significant difference between wild type and each individual cell line (Figure 6-4). The C24SMT-specific activity of the TAZ was assessed against the recombinant protein and enzymatic assays (performed elsewhere but included here to help interpret my observations). Briefly, LmxM.36.2380 was cloned in *E. coli* and the expression of the recombinant protein was verified (unpublished data). Substrate specific assays were then performed using different substrates, including zymosterol that is the preferred substrate for C24SMT (David Nes et al. 2002; Nes et al. 1999). A preliminary screening identified those compounds with a K_m/V_{max} and IC_{50} values lower than $100 \mu\text{M}$. Twelve out of twenty compounds ($\geq 60\%$ of activity with respect the control) were then selected for a complete screening, comprising eleven data points (from 400- to $1.6 \mu\text{M}$) and three biological replicates. The two TAZ with the lowest- and highest activity are shown here (Figure 6-6 and Table 6-2). As mentioned in section 6.1, these assays were performed by Boden Vandeloop and Dr Minu Chaudhuri from David Nes's Lab.

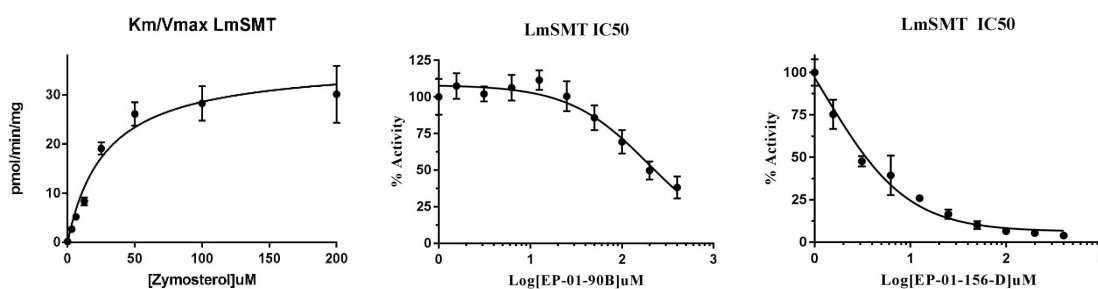


Figure 6-6. Activity of TAZ compounds with the recombinant C24SMT *L. mexicana*. **Left Panel:** Michaelis Menten kinetics of C24SMT against zymosterol (fixed SAM at $150 \mu\text{M}$, $K_m = 28.41$, $V_{max} = 36.65$). **Middle and right panels:** enzyme kinetics (IC_{50}) of 90.B and 156.D against zymosterol (eleven serial dilutions within the range 400- to $1.6 \mu\text{M}$ and control without inhibitor). Assays were performed by Boden Vanderloop from the Texas Tech University Lubbock, and Dr Minu Chaudhuri from the Meharry Medical College. Data were provided by David Nes as a collaborative effort between the Barrett-, Guillermo Labadie- and David Nes Labs, for the screening of the whole library (not included in this Thesis).

The EC_{50} values in promastigotes *in vitro* were comparable to those found with their IC_{50} in enzymatic assays in 62.5% ($n = 10$ out of 16 –four were not included in the enzymatic assays) of the compounds, indicative of their activity against C24SMT. I then selected the two most active, 156.D and 156.E, the former was 6-fold more active against the recombinant protein irrespective of showing equivalent activity against promastigotes (3.5 and $3.0 \mu\text{M}$, respectively), suggesting that their MoA is, at least in part, independent of the C24SMT inhibition. The low amount of 156.E remaining was deemed insufficient for further analysis (Note that GC-MS experiments require large quantities of compound and high cell numbers, 3×10^8). For this reason, I included the third most potent, 156.A (4.5

μM in promastigotes) for the following experiments (time- and dose-to-kill), before the extraction of sterols for GC-MS.

Table 6-2. EC₅₀ of the 1,2,3-triazolylsterol inhibitors (TAZ) in *L. mexicana*, and with the recombinant *L. mexicana* C24SMT-protein.

Azasterols compounds with known activity against C24SMT were used as controls. Compounds highlighted in red were not determined (ND) in either, the *L. mexicana* promastigotes *in vitro*, or in the enzymatic assay. Compounds in bold were the two most active in both assays. Compounds with poor activity in the preliminary enzymatic assay, were excluded (E). The last column on the right shows the match (ticks), between EC₅₀ (*in vitro*) and IC₅₀ (enzymatic assays). IC₅₀ assays were provided by Boden Vanderloop (Texas Tech University Lubbock, USA) and by Dr Minu Chaudhuri (Meharry Medical College, USA) from David Nes Lab.

Compounds	MW	IC ₅₀ enzymatic assays μM	EC ₅₀ <i>in vitro</i> <i>Leishmania</i>	IC ₅₀ and EC ₅₀ values match
Azasterols (controls)				
24,25-epiminolanosterol	441		-	-
25-azalanosterol	429		-	-
25-azacholsterol	387		-	-
25-thiolanosterol salt	414		-	-
Library of TAZ tested				
90-A	502	39	35	X
90-B	470	195	150	✓
94-A	510	109	15	✓
94-B	534	33	10	X
94-C	530	52	10	✓
156-B	484	136	ND	ND
156-C	510	8	11	✓
156-D	534	1	3.5	✓
156-E	516	6	3.0	✓
B2N	540	101	32	✓
B3	566	E	14	X
C1	572	E	6.0	X
B5	-	E	45	ND
C2N	542	E	ND	ND
C3	566	E	8.6	X
C4	590	E	20	✓
C5	572	E	6.0	✓
156.A	-	E	4.5	ND
2DR	534	38	10	✓
2ES	516	167	10	X

As with IMI (section 6.2.1), no additional resistance with respect to wild type, was found with most of the TAZ compounds from this library in the line overexpressing C24SMT, possibly, due to alternative MoA or other unknown targets. Another explanation to the lack of fitness in this line can be the lack of expression of the C24SMT gene. For this reason, I assessed the overexpression of the wild type copy of C24SMT (LmxM.36.2380) using qPCR and RNA-seq transcriptomics analysis (Figure 6-7). While the former showed a

17.5-fold difference in DNA abundance (Delta Ct threshold (δCt) of -4.13 for C24SMT; a δCt value of 6 was used as reference (section 2.8.3 and Supplementary 7) (see page 8), RNA-seq (section 2.9.2) showed a 3.67-fold change in expression ($SE \pm 0.1103$, $p < 8.88E-244$). A similar increase, 3.52 Log₂ FC ($SE \pm 0.1331$, $p < 2.87E-154$), was obtained with a parallel analysis using Galaxy (Afgan et al. 2018). Moreover, I confirmed (with RNA-seq only) that the other copy of C24SMT, LmxM.36.2390, was poorly expressed (Log₂ FC 0.1437; $SE \pm 0.1631$, $p < 3.78E-01$) (Figure 6-7, panel C), suggesting that transcript abundance associated with changes in drug resistance is associated with the LmxM.36.2380 copy that was transfected (section 2.8.2). RNA-seq, however, does not indicate the presence (or activity) of more protein, which needs to be determined using western blot. Although RNA-seq showed a large number of genes were differentially expressed, these changes remained within the range ± 1 log₂ fold change that of the wild type (Figure 6-7, panel B). A full list of the fold changes of all genes is included (supplementary file 8, see page 8).

Overexpressing C24SMT (6-fold increase in protein abundance shown by western-blot) in *L. major*, showed no additional resistance against 22,26 azasterols (C24SMT-specific), and to other sterol inhibitors (e.g. ketoconazole) (Jiménez-Jiménez et al. 2008). In their work, Jiménez-Jiménez and colleagues did not mention which transcript of C24SMT was transfected (Jiménez-Jiménez et al. 2008). This can be relevant considering that this gene has two copies arranged in tandem (positions, LmxM.20:950,430-951,491 and LmxM.20:954,192-955,253, respectively). Although both copies are of identical size (1.462 kb) and have similar function, LmxM.36.2390, has been shown to compensate when the dominant copy, LmxM.36.2380, is downregulated (Pountain *et al.*, 2019). In my study, I did not measure the overexpression of protein (hence the presence of active enzyme within the parasite is unknown), which in *Leishmania* is relevant given the post-transcriptional or post-translational changes that can occur and inactivate the product (Ivens et al. 2005b; Kazemi 2011).

The C24SMTKO showed an increase in resistance (3.8 to 4.3-fold, $P = 0.0116$) to AmB ($EC_{50} \sim 300$ nM), AmBisome (7.1-fold, $P < 0.0001$), and to nystatin (2.5-fold, $P = 0.0131$), in comparison to the parental wild type (here WT *L. mexicana* line expressing Cas9) (Figure 6-2, panel B and C). The reduced susceptibility to polyenes in this C24SMTKO line confirms the role of C24SMT with regard to AmB resistance. In my study, the maximum increase in resistance observed in four AmBR lines selected *in vitro* over nine months of drug exposure, was between 10 to 11-fold (chapter 3, Figure 3-1).

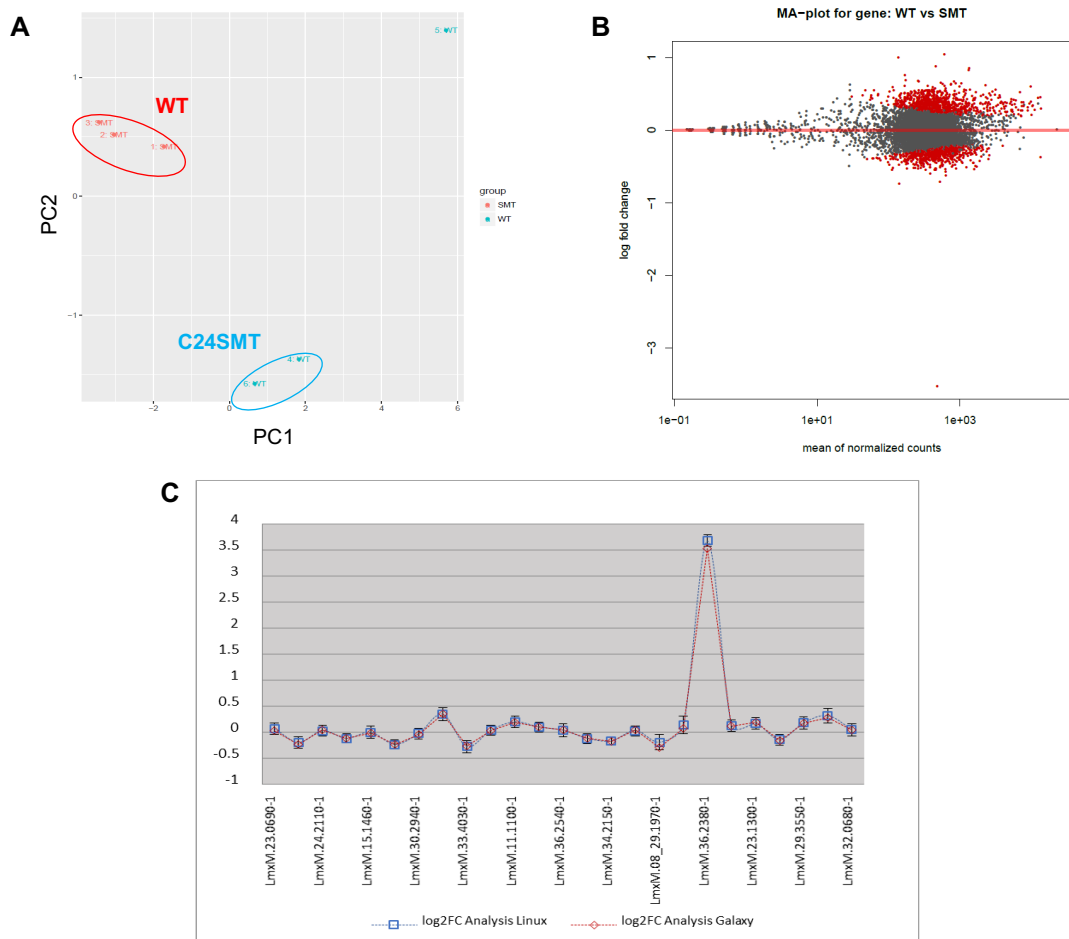


Figure 6-7. RNA-seq dataset of the C24SMT-overexpressor *L. mexicana*
Panel A: Principal component analysis (PCA) of RNA-seq abundance in wild type (control, red circle) and C24SMT-transfected parasites (blue circle). **Panel B:** RNA-seq data distribution of expression changes (MAP Log fold change) analysed with DESeq2 (Love, et al., 2014). Significantly differentially expressed genes (adjusted P value <0.1) are shown in red points. **Panel C:** RNaseq Log fold change was analysed with Linux (blue) and Galaxy (red) (Afgan et al. 2018), see section 2.9.2 for details, x-axis shows the genes of the sterol pathway from LmxM.23.0690 (left) to LmxM.32.0680 (right). Abbreviations: WT, wild type; SMT, transfected parasites. MAP, maximum *a posteriori* Log fold change.

A similar increase in resistance (4-fold) to both polyenes, AmB and Nys, has been described in various species of yeast (e.g. *S. cerevisiae*, *C. albicans*, *Kluyveromyces lactis*) lacking the C24SMT orthologue (ERG6 in fungi) (<http://www.yeastgenome.org>; Konecna, et al., 2016). In addition, polyene resistance was accompanied by dramatic changes in the sterols profiling of this mutant (Figure 6-10B, and Table 6-3), suggesting a disruption of the synthesis of 24-methylated sterols (section 6.2.3). To validate that changes in EC₅₀ were not related to differences in growth between C24SMTKO and the parental line, I assessed the growth rate of all the *L. mexicana* wild type expressing Cas9 and all the C24SMTKO mutants. All cell lines cultured in HOMEM showed a log- and stationary phase with no difference (P=0.8931) with respect to the parental wild type, i.e. WT-expressing Cas9, and to other wild type included for comparison (Figure 6-8). As with all

the other wild type- and polyene resistant-lines, none of the C24SMTKOs cultured in DM (a FBS-free culture medium), showed evidence of a log phase (cell densities were $\leq 5 \times 10^5$ per ml during five days, suggesting that some of the components found in FBS are essential for the parasite (Figure 6-8).

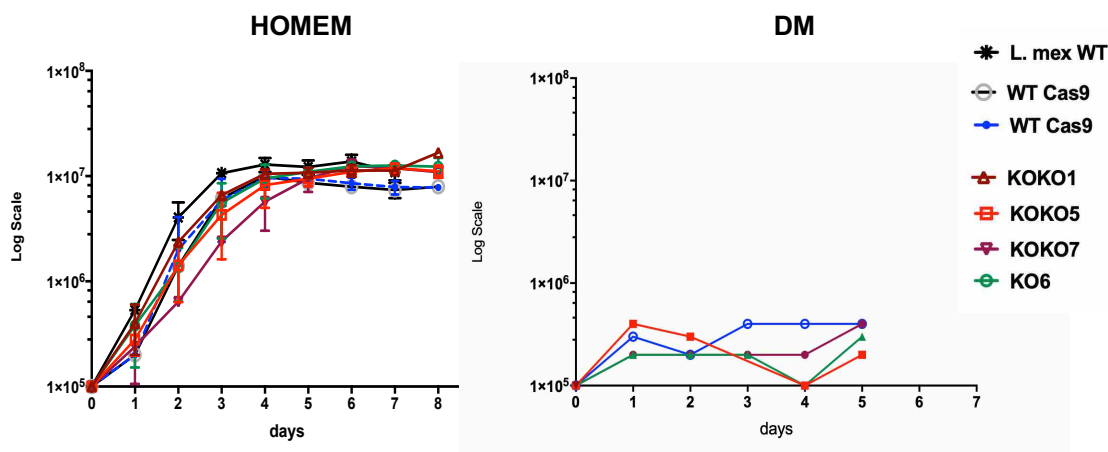


Figure 6-8. Growth curve of C24SMTKOs of *L. mexicana* promastigotes in HOMEM and DM. Starting density of 1×10^5 cells/ml. Left panel shows growth in HOMEM (i.e. *L. mexicana* wild type (*L. mex* WT), *L. mexicana* expressing Cas9 (WT Cas9) and all the C24SMTKOs (see section 2.8.4 for details). Right panel shows the same lines cultured in Defined Medium (DM). Mean values are shown with their standard deviation (bars). One-way ANOVA was performed independently for each compound to determine differences of the mean between groups. Tukey's multiple comparison test was used to find pairwise differences between lines. Statistically significant values ($P < 0.05$, 95% Confidence Interval) are indicated with a star.

6.2.3 Effect of the 1,2,3-triazolylsterol inhibitors on the sterol profiling of *Leishmania*

Although the most potent TAZ inhibitor (in promastigotes) was 156.E ($3.0 \mu\text{M}$), I selected compounds, 156.A and 156.D, with comparable potency (Figure 6-4), for further analysis, given the insufficient amount of the former. *L. mexicana* promastigotes were treated with different concentrations of these two compounds added into the culture medium in 24-well plates, and further incubated for 2, 6, 8, 16 and 24 hours (see section 2.5 for details). The morphology and number of parasites were examined at each of these time points. While the treatment with $5 \times \text{EC}_{50}$ showed dead cells after two hours, a concentration of $1 \times \text{EC}_{50}$ caused changes in morphology (round cells) in approximately 50% of the promastigotes at eight hours post treatment. The number of swollen cells increased up to 95% after 16 hours of drug exposure. For this reason, twelve hours of drug exposure (Figure 6-9), was the cut-off time point selected (Maes et al. 2017), before the extraction of sterols. Considering the cost of GC-MS and the number of drugs remaining, only one compound, 156.D, was used to assess its effects on the content of sterols using GC-MS. As described in section 6.2.2,

156.D was the most potent TAZ in the enzymatic assays, and the second most potent against promastigotes *in vitro* (Table 6-2). *L. mexicana* wild type and two resistant lines, AmBRcl.14 and AmBRcl.8 (these two lines showed mutations in C5DS and C24SMT, respectively, see chapter 3 for details) were treated with two different concentrations of 156.D, i.e. 3.5 μM (1 x EC_{50}) and 1.6 μM (MIC). Sterols were extracted from whole lysates of parasites, and analysed with GC-MS, as described before (section 2.8).

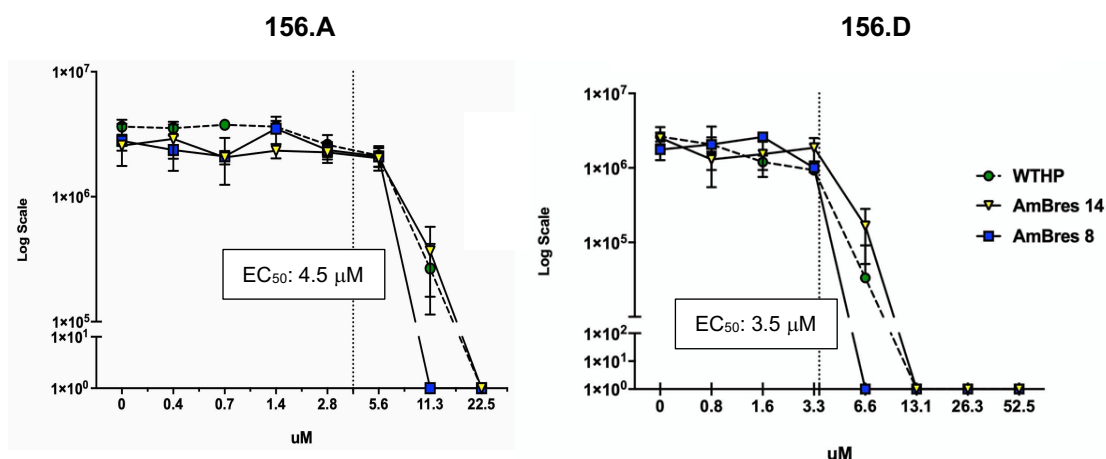


Figure 6-9. Treatment with TAZ inhibitors for 12 hours in wild type and two AmBR lines of *L. mexicana* promastigotes. Cell density and morphology were assessed with a haemocytometer. Starting density of 1×10^6 cells/ml and cells were cultured in HOMEM at 26 °C. Measurements are the median of three biological replicate, bars represent standard deviation. No significant difference was found between groups ($P= 0.5846$ and $P= 0.9885$, for compounds 156.A and 156.D, respectively).

Overall, a reduction in some sterol intermediates (mainly ergostanes) and a corresponding increase in the relative proportion of cholestanes indicated that 156.D, and potentially other TAZ analogues, have a direct effect in altering the synthesis of sterols, targeting the C24SMT. Other C24SMT inhibitors, i.e. AZA, have also shown good activity against the recombinant enzyme, and triggered dramatic changes on the growth rate and composition of sterol profile in *L. major* and *T. cruzi* (Magaraci et al. 2003).

In my study, an inhibitory effect on the growth rate was observed with both, 156.D and 156.A (Figure 6-9). Also, the morphological alterations showed that promastigotes developed a round shape after two hours of drug exposure. After confirmation of the C24SMT-specific activity of the TAZ inhibitors (Figure 6-6), the changes on the sterol composition after treatment with 156.D were surprising. No significant changes were found in wild type or either of the AmBR lines analysed. Interestingly, a mild increase of dimethylcholesta-5,7,24-trien-3-ol and cholesta-5,7,24-trienol in wild type and AmBRcl.14 were noted. On the other hand, AmBRcl.8, showed a reduction of ergosterol (and its

isomer 5-dehydroepisterol), and other ergostanes, from 13% to 0.5%, and of cholesta-5,7,24-trienol from 21% to 16%, accompanied by a moderate increase in cholestane-5,7,22,triene-3-ol from 60% to 70%. Note that the latter of these lines was only treated with the MIC dose.

The results from GC-MS analysis, and a breakdown of all the sterols identified (percentage \pm SD) are provided (Figure 6-10, panel B, and Table 6-3). Irrespective of the small changes in sterols, an accumulation of zymosterol was observed after the treatment with both concentrations of 156.D (EC_{50} and MIC). Although the relative abundance of this intermediate was very low ($< 1\%$), this marginal increase in zymosterol in wild type and AmBRcl.14 (Table 6-3), is in agreement with the specific activity shown with the recombinant protein (Figure 6-6), and with the EC_{50} reported here in all lines of *L. mexicana* (Figure 6-4).

The content of cholestanes in AmBRcl.8 increased only by 4% after exposure to 156.D (this line was only treated with MIC), in comparison with the untreated parasites. Considering that the abundance of cholestanes in these lines was of 82% before the treatment, this small increase in cholestanes was expected, however, the concomitant loss of other ergostanes is indicative of the C24SMT inhibitory activity of 156.D.

Also, an increase in cholesterol was observed in this line after the treatment, suggesting possible uptake of this sterol from the medium (Andrade-Neto *et al.*, 2011; De Cicco *et al.*, 2012; Ghosh *et al.*, 2012a) and host macrophages (Ginger *et al.* 1999), to compensate the loss of ergosterol and other sterols from the membrane. Notably, C24SMTKO and C24SMT over-expressor showed opposite changes in their content of sterols. While the former KO had a dramatic increase in cholestanes (91%), these intermediates were present in only 1.6% in the latter. Moreover, the content of ergostanes in these lines was of 0- and 90%, respectively. The increase of cholestanes is expected from C24SMT null mutants and after the treatment with C24SMT-inhibitors such as azasterols (AZA). This has been extensively studied in various species of *Leishmania* (Haughan, *et al.*, 1995; Contreras, *et al.*, 1997; Liendo *et al.*, 1999; Magaraci *et al.*, 2003; Lorente *et al.*, 2004a; Gros *et al.*, 2006; Rodrigues *et al.*, 2007; Jiménez-Jiménez *et al.*, 2008; Gigante *et al.*, 2010).

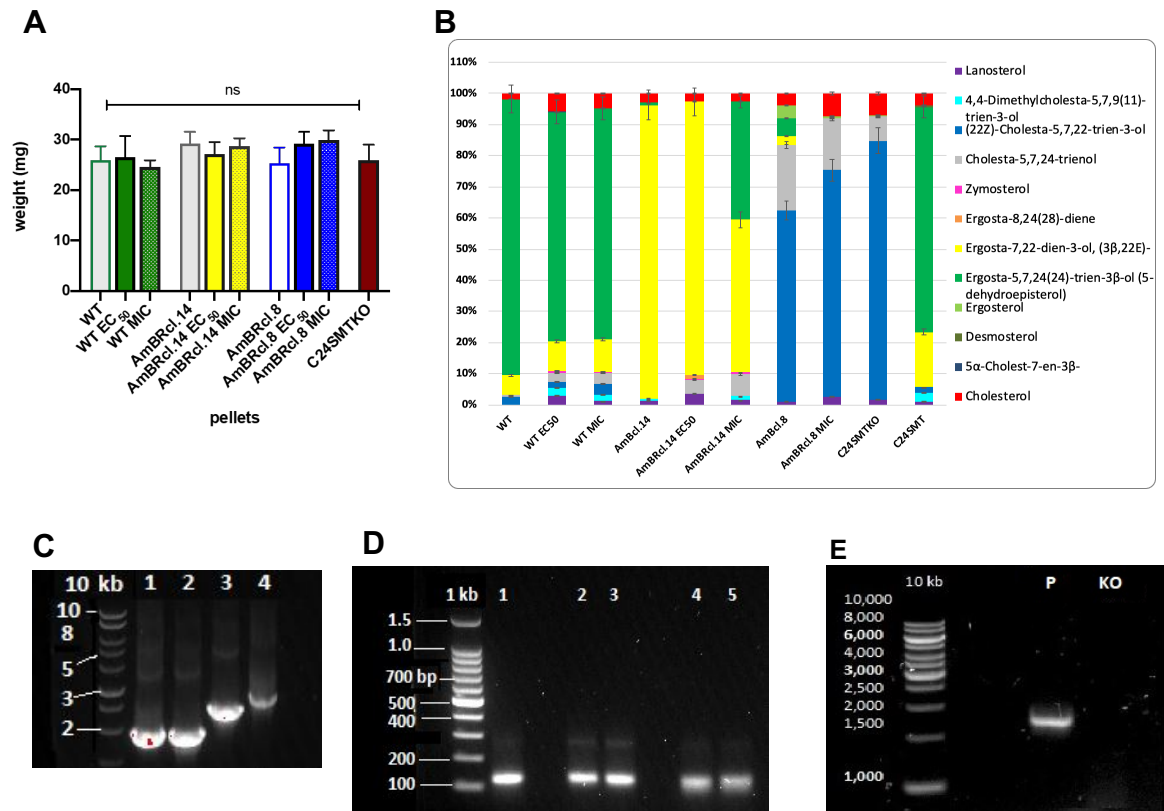


Figure 6-10. Characterisation of AmBR lines, and C24SMT and C24SMTKO mutants of *L. mexicana*, using GC-MS (sterols) and RNA-seq.

Panel A: *L. mexicana* promastigotes (3×10^8 parasites) were treated with the inhibitor 156.D for 12 hours at $3.5 \mu\text{M}$ (EC_{50}) and $1.6 \mu\text{M}$ (MIC). Controls were treated with the same volume of solvent (DMSO). Pellets were weighed before GC-MS analysis, to estimate the content of sterols per 100 parasites, bars indicate the standard deviation of the mean of three biological replicates. **Panel B:** names and content of sterols is shown as percentage. Mean values and standard deviation (SD), are shown in detail in Table 6-3. C24SMT-overexpressor-, and a C24SMTKO-lines, are included for comparison. Panels of gels are from one representative biological replicate. The paralyzed flagella protein 16 gene, LmxM.20.1400 (PF16) was used as positive control (Beneke et al. 2016). **Panel C:** DNA donors (repairing cassettes) were run in 1% agarose gel for 45' at 90 V, Lanes: 10 kb ladder, 1) pTpPF16, 2) pTpC24SMTKO, 3) pPLOTp.mNG.C24SMT.N-term (2.3 kb), 4) pPLOTp.mNeonGreenC24SMT.C-term (2.7 kb). **Panel D:** 5'- and 3' sgRNAs templates, samples were run in 2% agarose gel at 100 V for 60 min, Lanes: 1 kb ladder, 1)3'sgRNAPF16 (126 bp), 2 and 3) 5'sgRNAC24SMT, 4 and 5) 3'sgRNAC24SMT (126 bp). **Panel E:** PCR diagnostic of the *L. mexicana* C24SMTKO cell line showing the approximate expected presence/absence of C24SMT-specific bands for any of the two gene copies, i.e. LmxM.36.2380/90 (~1.1 kb). PCR products were run on agarose gel 2%. Lanes: 1 kb DNA ladder; P, parental cell line WT-Cas9 *L. mexicana*; KO, C24SMTKO population (non-clonal). Primers used were FP1 and RP1. PCR reactions and expected band size are as described in section 2.8.4 (Table 2-1). Table 6-3. Sterol profiling by GC-MS (derivatization with trimethylsilyl, TMS) in *L. mexicana* promastigotes treated with C24SMT inhibitors.

Table 6-3. Sterol profiling by GC-MS (derivatization with trimethylsilyl, TMS) in *L. mexicana* promastigotes treated with C24SMT inhibitors. Content of each sterol is the percentage of the total of the raw peak area detected per line \pm standard deviation of three independent biological replicates. Standards used were: cholesterol, desmosterol, 5 α -Cholest-7-en-3 β -ol, ergosterol, stigmasterol, β -sitosterol, lanosterol, 4,4-dimethyl-5 α -cholesta-8,14,24-trien-3 β -ol, and zymosterol (Source: Glasgow Polyomics). Peaks that did not match any standard were determined by comparing with the NIST spectral libraries with the ion trap mass spectrometer. The identification of peak 4, and a complete description of the sterols identified, i.e. major frag mass m/z , molecular ion m/z , TMS m/z , chemical formula, and retention time RT/min, are described in Chapter 5 (Table 5-1). ND: non detected.

Sterol intermediate	WT	WT EC ₅₀	WT MIC	AmBRcl.14	AmBRcl.14 EC ₅₀	AmBRcl.14 MIC	AmBcl.8	AmBRcl.8 MIC	C24SMTKO	LmC24SMT
Peak 1 Cholesta-5,7,22-trienol	2.66 \pm 0.09	1.93 \pm 0.50	3.61 \pm 0.97	0.27 \pm 0.19	ND	ND	61.05 \pm 6.57	70.35 \pm 4.90	82.92 \pm 0.77	1.66 \pm 0.35
Peak 2 Cholesta-5,7,24-trienol	0.44 \pm 0.38	3.06 \pm 0.41	3.48 \pm 0.50	ND	4.62 \pm 0.31	5.88 \pm 0.56	21.04 \pm 4.39	16.11 \pm 0.80	7.82 \pm 0.48	ND
Peak 3 Ergosta-8,24(28)-dienol	ND	ND	ND	ND	1.13 \pm 0.09	ND	ND	ND	ND	ND
Peak 4 Ergosta-5,7,24(28)-trienol (5-dehydroepisterol)	88.17 \pm 1.02	73.71 \pm 1.87	74.61 \pm 0.18	0.65 \pm 0.63	0.10 \pm 0.09	31.86 \pm 0.55	5.65 \pm 0.55	ND	ND	72.24 \pm 4.85
Peak 5 Ergosta-7,22-dienol	6.38 \pm 0.54	9.43 \pm 1.31	10.55 \pm 2.13	93.9 \pm 1.41	87.65 \pm 2.14	41.04 \pm 0.08	2.87 \pm 4.96	ND	ND	17.75 \pm 2.50
Cholesterol	1.80 \pm 0.04	5.81 \pm 0.49	4.70 \pm 0.20	3.01 \pm 0.59	2.44 \pm 0.22	2.13 \pm 0.04	3.90 \pm 1.47	7.04 \pm 0.28	7.04 \pm 0.69	3.73 \pm 0.52
Ergosterol							4.09 \pm 1.39	0.53 \pm 0.12	0.41 \pm 0.25	
Peak 6 Dimethylcholesta-5,7,24-trien-3-ol)	ND	2.35 \pm 0.39	2.00 \pm 0.18	0.38 \pm 0.66	ND	1.14 \pm 0.99	ND	ND	ND	3.01 \pm 2.70
Desmosterol										0.55 \pm 0.51
Lanosterol	ND	3.00 \pm 0.72	1.20 \pm 0.21	1.46 \pm 0.30	3.49 \pm 2.09	1.25 \pm 0.52	1.16 \pm 0.56	2.51 \pm 0.41	1.79 \pm 0.29	0.98 \pm 0.95
5 α -Cholest-7-en-3 β -	ND	0.12 \pm 0.20	0.11 \pm 0.11	ND	0.11 \pm 0.09	0.06 \pm 0.10	ND	0.20 \pm 0.18	ND	0.08 \pm 0.13
Zymosterol	ND	0.55 \pm 0.17	0.39 \pm 0.07	ND	0.33 \pm 0.03	0.54 \pm 0.23	ND	ND	ND	ND

6.3 Discussion

The potency of TAZ inhibitors was lower than that reported previously (Porta et al. 2014). Similarly, other C24SMT inhibitors, e.g. AZA and TOM, have previously shown to be more active in *Leishmania* (EC_{50} in the nanomolar range), than any of the TAZ tested here (Magaraci et al. 2003; Medina et al. 2012). Various AZA analogues used as controls in the enzymatic assays were also more potent than TAZ in the recombinant protein assays (unpublished). Libraries of AZA were designed following the hypothesis of Nes, et al., i.e. that 22,26 azasterol is a inhibitor of C24SMT (Nes 2000; Nes et al. 2009). These libraries spanned multiple combinations of substituents introduced in the side chain of the sterol molecule (Magaraci et al. 2003; Porta et al. 2014). In this study a broad range of activity against *L. mexicana* promastigotes *in vitro* (EC_{50} values from 5-, to >100 μ M) was noted across the different substituents of the lateral chain in the TAZ (Figure 6-3, Figure 6-4 and Figure 6-5). Importantly, these EC_{50} values (Table 6-2) were very similar to those obtained with the recombinant enzyme (Figure 6-6, only two compounds are shown in this Thesis), and with the dose-to-kill assays (Figure 6-9). Although the potency of TAZ was lower than expected, this study provides valuable information for further chemogenic and drug design studies, however, their potency needs to be tested using the amastigotes macrophages model *in vitro*. Some of the inhibitors tested in this Thesis, i.e. IMI, 2DR, 2ER, 2ES, have shown a good therapeutic window (Mukherjee et al. 2012; Porta et al. 2014), the former can moreover, be administered orally (Mukherjee et al. 2012). Here, I did not analyse the toxicity and other pharmacokinetic- or pharmacological properties that are essential for the characterisation of any drug candidate, particularly, considering that all the antileishmanials currently used are toxic, and have complex and long therapeutic schemes that can, in some cases, contribute to treatment failure and, possibly, drug resistance (Ponte-Sucre et al. 2017). TAZ inhibitors showed specific activity against C24SMT, however, other potential targets, e.g. C14DM, cannot be ruled out. Likewise, we cannot conclude on the sterol-specific activity (and other membrane lipids) of IMI given its numerous MoA (section 6.2.1). In the study of Porta and colleagues, and in other works with similar compounds (Haughan et al. 1995; Porta et al. 2017; Usachev 2018), C14DM was suggested as a potential target. In fact, in my study, I showed that the AmBR line with the mutation N176I in C14DM (Mwenechanya et al. 2017), was more sensitive than wild type, to B2N and C4, although the difference was not significant (Figure 6-3). Further enzymatic assays can help to determine if TAZ can inhibit other targets, including C14DM. In my study, the overexpression of C24SMT was confirmed with qPCR and RNA-seq (but not followed up at the level of enzyme activity), however, only four TAZ, B3, 90.A, 2DR and 2ES, showed a significant difference between their EC_{50} in the

C24SMT overexpressor over the wild type (and differences in susceptibility were relatively minor). This lack of correlation between the over-expression of transcripts of C24SMT in *Leishmania*, and the EC₅₀ values of inhibitors C24SMT-specific is not well understood and has been described with another AZA (Jiménez-Jiménez et al., 2008). An explanation of this can be that given that this gene has two copies, the effect exerted by these inhibitors may be redundant. During my studies, I realised that there are no reports of resistance against C24SMT-inhibitors. In fact, I tried to select some IMI-Res lines of *L. mexicana* without detecting an increase in resistance to IMI or AmB (data not included). Nevertheless, additional experiments are needed to understand this in more depth. I did not attempt to induce resistance with any of the TAZ compounds (due to time constraints), but this could be informative to pursue. I also noted that inhibitors have not been designed and tested against C5DS in *Leishmania* spp., which is one of the few enzymes of the sterol pathway (post squalene) that has been related with AmB resistance in both, *Leishmania* spp. and fungi. One reason is that the role of C5DS in resistance in *Leishmania* was unknown until recently (Pountain et al. 2019). Also, to the best of my knowledge, the structure of C5DS is not available. I found only one study (in cardiovascular diseases), in which a new class of inhibitors of C5DS (EC 1.14.21.6), showed increase of lathosterol (Giera et al. 2008).

Accumulation of cholestanes can result from the treatment of *Leishmania* spp. with C24SMT inhibitors, and from genetic manipulations. In the first case, AZA (Magaraci et al. 2003), IMI and TOM (Medina et al. 2012; de Souza and Rodrigues 2009a), are inhibitors that deplete 24-alkylated sterols and 5-dehydroepisterol (the most abundant sterol in wild type *Leishmania* also known as 24-methylene-cholesta-5, 7-dien-3 β -ol), and accumulation of cholesta-5,7,22-trien-3 β -ol, cholesta-7-24-dien-3 β -ol (Viana Andrade-Neto et al. 2016a), and of zymosterol (cholesta-8, 24-dien-3 β -ol). 156.D showed a mild increase of cholestanes (Figure 6-10B), indicating some activity targeting C24SMT, other MoA cannot be excluded, however. Another possible explanation of the lack of a clear change in sterols can be that the time point and the concentrations used here (12 hours, MIC and EC₅₀) were insufficient to trigger sterol modifications. This could be assessed by increasing the concentration, e.g. 5 x EC₅₀ (as with our experiments of LCMS). TOM proved inactive in both, WT and resistant lines. This was unexpected and is not well understood, considering that in previous studies, this steroidal glycoalkaloid showed nanomolar potency (EC₅₀ 124 nM in *L. amazonensis* promastigotes). TOM causes mitochondrial damage and increase of ROS, and other alterations such as the accumulation of bulky vacuoles and lipid droplets in the cytoplasm (Medina et al., 2012), which was also observed in promastigotes of *L. amazonensis* (Lorente et al. 2004a), and *L. donovani*

(Haughan et al. 1995; Lorente et al. 2004a), after the treatment with AZA, suggesting that the alteration of the metabolism of lipids, is possibly, related with the disruption of C24SMT. In my study, I described an increase in the number and size of lipid droplets in tissue from mice infected with AmB resistant lines of *L. mexicana*, being this change more prominent in lymph nodes than in footpad lesions (see chapter 5, section 5.2.7.1, Figure 5-9 and 5-10). However, there is no evidence indicating that changes observed in mice are related with the MoA of AZA found in the parasite.

Regarding the accumulation of cholestanes in *Leishmania* spp. after the deletion of the two C24SMT alleles (Mukherjee et al. 2018), and with other mutants with defects in this enzyme (Pountain, et al., 2019), I found a similar sterol profiling in two AmBR lines (see chapter 4 for details of lines AmBRcl.8 and AmBRcl6), and in a C24SMTKO generated with CRISPR-Cas9 (Beneke, et al., 2017), in which cholestanes increased notably (Figure 6-10B and Table 6-3). In addition, C24SMTKO displayed a similar fold change in resistance to polyene antifungals (Figure 6-2B) comparable to that described after the loss of expression of C24SMT in *L. infantum* (Rastrojo, et al. 2018), in *L. mexicana* (Pountain et al., 2019), and also in yeast with a deletion of the orthologue (<http://www.yeastgenome.org>), suggesting a disruption of the synthesis of 24-methylated sterols (section 6.2.3).

Further characterisation of the C24SMTKO is essential. In particular, the confirmation of the deletion (and expression) of both copies of the gene. Considering that C24SMT has two copies arranged in tandem that are identical in their sequence (except by one nucleotide) (Pountain et al., 2019), this represents a particular challenge. A combination of different primers (Table 2-1) and other tools, e.g. qPCR and Sanger sequencing, can also help to determine the nature of genomic changes present. Furthermore, testing the infectivity *in vivo*, and in macrophages, will contribute to further characterise if the deletion of C24SMT carries some fitness cost, as it was noted with *L. major* (the deletion of both copies caused the loss of virulence in mice) (Mukherjee et al. 2018). Interpretation of the susceptibility to TAZ identified in this study, however, requires a better understanding of the regulation of the biochemical pathways in *Leishmania* spp., and an enhanced approach using a combination of genetically modified parasites. In general, TAZ show an activity within the micromolar range, most likely with a pleomorphic MoA partially related with the inhibition of sterols in *L. mexicana*.

7 Metabolic effects of AmB in the *Leishmania mexicana* promastigotes.

7.1 Introduction

In previous chapters, I presented evidence on the development of resistance to polyene antifungals in eight independent lines of *L. mexicana* promastigotes selected *in vitro*, by increasing the concentration of drug in the culture medium in a step-wise manner (section 3.2.1). These polyene-resistant lines were then screened against a series of compounds, including the antileishmanials (chapter 3) and a new library of sterol inhibitors (chapter 6). Furthermore, genomic alterations (chapter 4) in two sterol enzymes, C24SMT and C5DS, lead to resistance against polyenes, AmB, nystatin and natamycin, and to cross-resistance and higher susceptibility towards other compounds. In agreement with other studies, here I described a significant increase in susceptibility against oxidative stress agents, such as PENT, methylene blue (Mbongo et al., 1998; Pountain et al., 2019), and hydrogen peroxide (Mwenechanya et al., 2017) in all four AmBR lines of *L. mexicana* (section 3.2.3.4). Targeted metabolomics using GC-MS, established two sterols profiles correlated with the genomic changes in C24SMT and C5DS (chapter 5), whereas complementary studies in a murine model revealed a relationship between these two sterols signatures, and parasite infectivity *in vivo*. Notably, the replacement of the wild type ergosterol by ergostanes and cholestanes, was associated with a virulent and an attenuated phenotype, respectively. We further confirmed the retention of resistance (*in vitro*) of all four AmBR lines after the treatment of mice with AmB (1 mg per kg) (section 5.2.3).

The use of metabolomics for the deconvolution of the MoA and resistance of antiparasitic drugs was discussed in detail in chapter 1 (section 1.8.3.1). LC-MS has pinpointed alterations of several metabolites and metabolic pathways after drug treatment (Vincent and Barrett 2015). For instance, antimonials (*L. donovani*) (Berg et al. 2015), MF (Vincent et al., 2014b), and AmB (Mwenechanya et al., 2017; Pountain et al., 2019), disrupted metabolic pathways that are relevant for the defences of the parasite against ROS (Wyllie et al., 2010; Kaur and Rajput, 2014), although it remains uncertain if such changes are a direct effect of the treatment or they resulted from a general stress response (M.-C. Brotherton et al. 2014). The MoA by which AmB generates oxidative damage (Anderson et al. 2014; Gray et al. 2012; Mesa-Arango et al. 2012) seems to be related to the disruption of other metabolic pathways, including the pentose phosphate pathway (PPP) (Fan et al., 2014), the polyamine-trypanothione pathway (PTP) (Purkait et al., 2012; Manta et al., 2013; Mandal et al., 2017). LC-MS also helped to identify that the metabolism of

phospholipids and other membrane lipids that interact with ergosterol, play a key role in the susceptibility to AmB. For instance, lower abundance of ergosterol (relative to wild type), was observed in a mutant (LCB2) lacking the sphingolipids pathway (SLP) (Armitage et al. 2018; Collett et al. 2019; Denny, Goulding, Michael A. J. Ferguson, et al. 2004), which was reflected in significant fold-changes in susceptibility to AmB in this mutant (unpublished data). In another study, other membrane proteins (e.g. flippases), phospholipid flippases and the miltefosine transporter, were related to the MoA and resistance to AmB in *T. brucei* (Collett et al. 2019). Finally, peroxidation of the membrane lipids has also been related to AmB resistance in pathogenic fungi, e.g. *Candida* (Bolard, 1986; Bolard et al., 1991; Walsh et al., 1990), but has not been studied in *Leishmania* spp.

The sterol biosynthetic pathway (SBP), arguably the most relevant pathway related to AmB resistance in *L. mexicana* (Mwenechanya et al. 2017; Pountain et al. 2019a), and the genomic alterations in this pathway that derived in dramatic changes in sterols, were discussed in detail elsewhere (section 4.1.3 and 5.2.1.1). While the loss of ergosterol (and other sterol intermediates) in AmBR lines was expected (based on previous findings), changes in other metabolites appeared more heterogeneous and are less well studied.

In order to identify changes in the metabolome of *L. mexicana* promastigotes, after short time exposure (15 min) to high concentrations of AmB (see section 2.5 for methods), that can provide hints towards understanding the MoA- and resistance-associated phenotype, I used LC-MS to interrogate broader changes in the metabolome in two AmBR lines selected in parallel. These lines were nominated for LC-MS analysis on the basis of their respective mutations in the enzymes of the sterol pathway, i.e. C5DS (AmBRcl.14) and C24SMT (AmBRcl.8). A third line of *L. mexicana* lacking the enzyme transketolase (TKT-KO), along with its parental line (WT) and the add-back (named R18 herein), were also included for comparison. The LC-MS approach (chloroform:methanol:water 1:3:1) used in this thesis (Creek, Anderson, et al. 2012), was developed and optimized by former members of the Barrett Lab, providing a high coverage of the *Leishmania* (and in *Trypanosoma* spp.) metabolome (Kovářová et al. 2018; Vincent et al. 2012, 2014), including five AmBR lines of *L. mexicana* (Mwenechanya et al. 2017; Pountain et al. 2019), and allowing for the detection of metabolites present in samples in low abundance (nanomolar to picomolar range) (Monteiro et al. 2013).

7.2 Results

Extraction of both polar and nonpolar metabolites was performed in four biological replicates per group (section 2.7). Peaks were then analysed based on their mass, and mass/retention time (RT) match, to a list of known standards. Identified peaks are those which both retention time and mass matched to a known standard, whereas annotated peaks are assigned putatively on the basis of mass alone. Datasets of AmBRcl.14 and AmBRcl.8 were mutually processed using IDEOM (Creek et al., 2012; and Creek et al. 2012b) and PiMP (Gloaguen et al., 2017) pipelines (<http://polyomics.mvls.gla.ac.uk>). Datasets generated in IDEOM are provided as supplementary 10 (AmBRcl.8) and supplementary 11 (TKTKO) (see page 8). In order to assess their quality, a principal component analysis (PCA) was performed for each dataset (Batushansky et al. 2019). A good separation between experimental groups was found in both resistant lines (Figure 7-1). Note that although the PCA from AmBRcl.14 performed with PiMP (Figure 7-1B) showed an overlap between two samples from both groups, wild type (WTTx) and AmBR (AmBRTx), which were treated with AmB, the PCA obtained with IDEOM confirmed a strong separation across all groups. While the first principal component (PC1), showed a clear effect (separation) of the treatment with AmB on the metabolic profiling, the PC2 showed a clear difference between AmB resistant lines and wild type in both datasets (Figure 7-1D). PCA has been previously shown its power for the separation of metabolic profiling between groups analysed with LC-MS (Barisón et al. 2017). Following the assessment of peaks quality, PiMP then performs a retention time alignment of mzXML files using the OrbiWarp algorithm (<http://polyomics.mvls.gla.ac.uk>).

The number of metabolites with significant fold-changes after the treatment with AmB, was considerably higher in the AmBRcl.14 dataset in comparison with AmBRcl.8. Initial targeting with PiMP detected a total of 5,001 and 2,246 peaks with a mass accuracy of 2 ppm (entries), from which only 33 (AmBRcl.14) and 47 (AmBRcl.8) metabolites, matched to a known standard (i.e. identified peaks). The remaining peaks (4,968 and 2,199, respectively) from each group were annotated as putative. The identity of some peaks was annotated in PiMP as numbers (peak ID 1, 2, etc.), these unidentified hits were then manually inspected, allowing the identification of additional relevant metabolites related with AmB resistance, such as, amphotericin B, xanthine, hypoxanthine, D-fructose, inositol-1-phosphate, phosphatidyl inositol, L-proline, D-glucose, myo-inositol, L-histidine, and some amino acids. The identity of some peaks, however, remained undetermined or redundant. This is related to the fact that a standard was not included, a poor quality of peaks, or because the peaks did not match the known standard. Also, in

some cases, some peaks with similar mass were listed by PiMP several times. To my knowledge, some of these repeated peaks correspond to isomers and manual inspection of these was necessary, however, curation of hundreds of hits is challenging and adds to time, considerably.

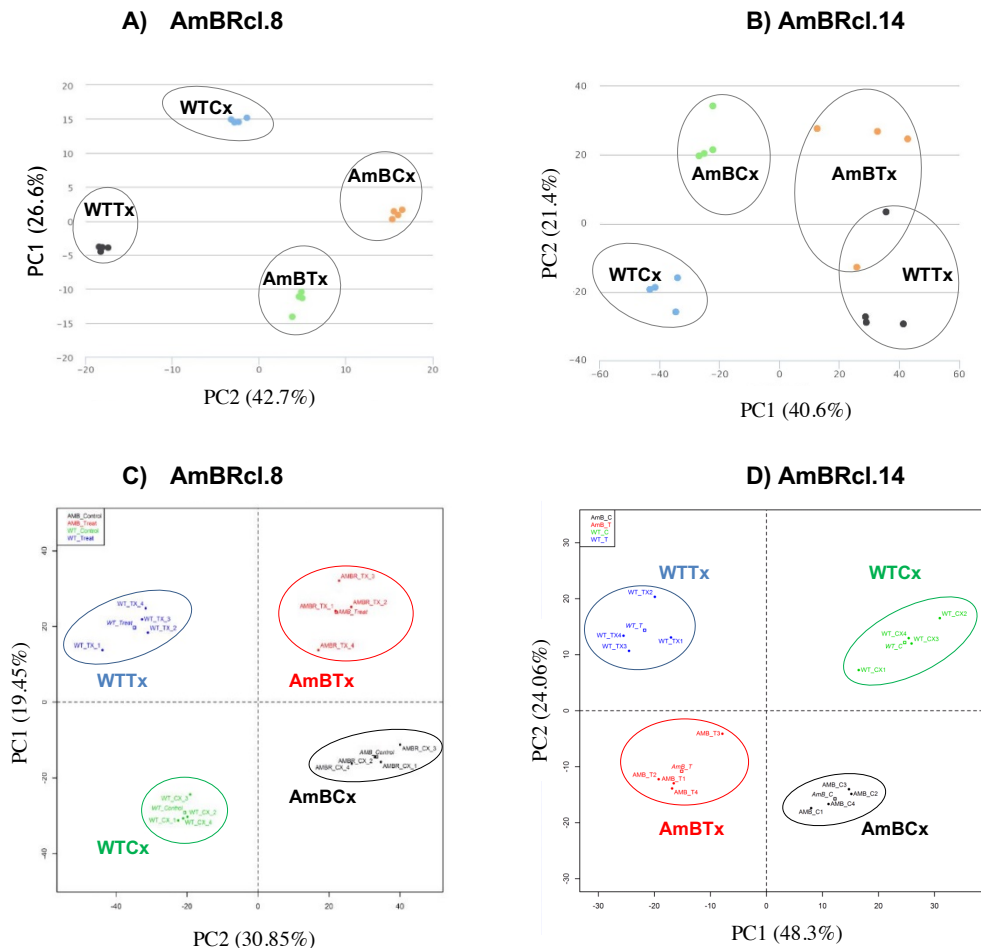


Figure 7-1. Principal component analysis (PCA) of two AmBR lines of *L. mexicana* promastigotes treated with AmB.

Top (A and B) and bottom (C and D) panels, show the PCA obtained with PiMP (Gloaguen et al., 2017) and IDEOM (Creek et al., 2012; and Creek et al. 2012b) platforms, respectively (see section 2.7 for details on the method). AmBRcl.8 is shown in the left panels (A and C) and AmBRcl.14 is shown in the right panels (B and D). Mid log phase *L. mexicana* promastigotes (1×10^8) were treated with a concentration of AmB $5 \times EC_{50}$ of each line (600 nM for wild type and $3 \mu\text{M}$ for both AmBR lines), for 15 minutes (section 2.5) and the metabolome was extracted as described before (section 2.7). Each dataset was performed in four biological replicates. Abbreviations: WTTx: wild type-treated (blue circles); WTCx: wild type-control (untreated) (green circles); AmBTx: AmBR lines-treated (red circles); AmBCx: AmBR lines-control (black circles).

Metabolites with significant fold-changes (P adjusted < 0.05) in each dataset, were identified by performing four pairwise comparisons, as follows: 1) AmBR control (AmBCx) relative to wild type control (WTCx); 2) wild type treated (WTTx) relative to WTCx; 3) AmBR lines treated (AmBTx) relative to AmBCx, and 4) AmBTx relative to

WTTx. Metabolites with significant changes in all four comparisons are listed in Supplementary 9, Table 1 and 2 (see page 8). The ten most significant hits of all four comparisons can be visualized in the volcano plots obtained from each pairwise comparison (Figure 7-2, red and blue circles). Given that the aim of my study is to investigate the effects of the treatment with AmB on the metabolome of *Leishmania*, the analysis of the abundance of metabolites was focused on peaks resulting from the pairwise comparisons 2 and 3. Similarly, the most significant hits (identified and annotated) altered after the treatment with AmB, in wild type and in both resistant lines (comparisons 2 and 3), are enlisted in Table 7-1. Three of these hits, i.e. sn-glycero-3-phosphocholine, L-proline, and hypoxanthine, were significantly changed in wild type, and in both resistant lines (Table 7-1). With regard to AmB, fold change in Table 7-1 indicate the identification in treated cells relative to control without drug (total absence) of peak 349, although the annotation of five other peaks as AmB, is discussed further (Figure 7-13). Identified and putative metabolites from AmBRcl.14 and AmBRcl.8, mapped to 232 and 208 KEGG metabolic maps (pathways), with only a small fraction (8 and 6 maps, respectively), showing $\geq 75\%$ of coverage. Some examples of these high-coverage pathways are: D-arginine and D-ornithine metabolism (90% and 80% coverage), valine, leucine and isoleucine biosynthesis (87% and 74% coverage) and the Pentose Phosphate Pathway (PPP) (76.5% for AmBRcl.14). In all cases, map coverage was higher in AmBRcl.14 than in AmBRcl.8, including the PPP that had a coverage of only 41% in the latter. Coverage of all the other pathways was lower (25 to 75%). Comparison of metabolites with significant fold changes ($P < 0.05$) in all four pairwise comparisons, showed a total of 319 and 202 identified/putative metabolites. Of these, 181 and 64 peaks were detected only in AmBRcl.14 and AmBRcl.8, respectively, with 138 metabolites shared between both datasets (Figure 7-3A). To better understand the nature of these changes, I clustered metabolites into four groups, i.e. carbohydrates, amino acids, lipids, and other groups. The latter includes, energy-, nucleotide-, purines-, pyrimidines-, and nicotinate and nicotinamide- metabolism. (Figure 7-3, B and C). Carbohydrates (32-39%) and amino acids (30-38.1%) were the two most abundant, while ‘other groups’ (20-27%), and lipids (12-13%), were less abundant. After clustering metabolites into four groups, a slightly higher number of hits was noted, due to 27 (AmBRcl.14) and 7 (AmBRcl.8) hits, e.g. acetyl-CoA, D-glucose, and L-serine, which are key metabolites central to various pathways (see Figure 7-3, panels B and C, and Supplementary 9) (see page 8).

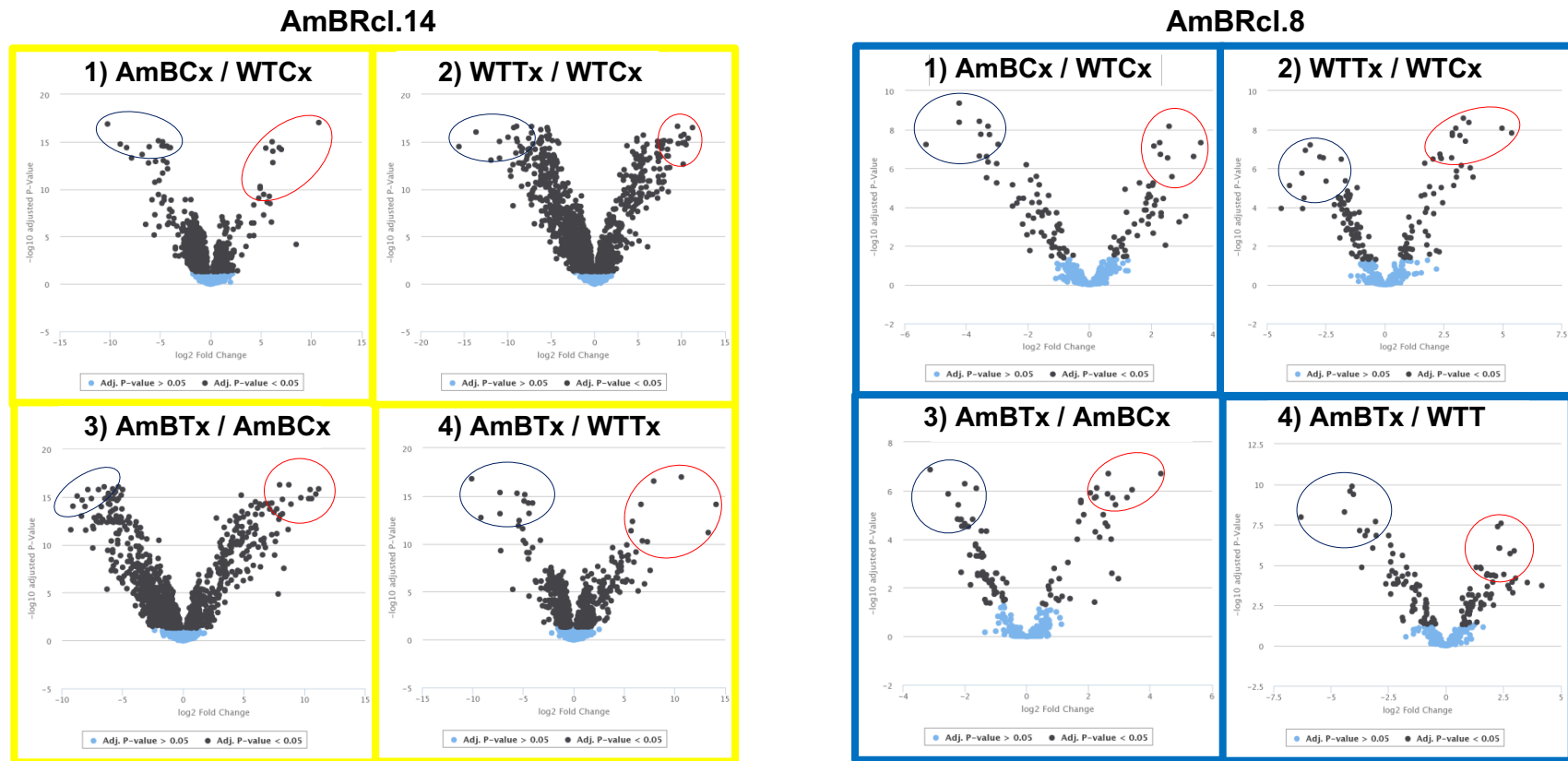


Figure 7-2. Volcano plots of metabolites with fold-change after the treatment with AmB in *L. mexicana* wild type and AmBR promastigotes. Mid log phase *L. mexicana* promastigotes (1×10^8) were treated with a concentration of AmB 5 \times EC₅₀ of each line (600 nM for wild type and 3 μ M for both AmBR lines), for 15 minutes (section 2.5) and the metabolome was extracted as described before (section 2.7). Four pairwise comparisons were performed as follows: 1) AmBR control (AmBCx) relative to wild type control (WTCx); 2) wild type treated (WTTx) relative to WTCx; 3) AmBR lines treated (AmBTx) relative to AmBCx, and 4) AmBTx relative to WTTx. AmBRcl.14 is and AmBRcl.8 are shown in the panels from the left (yellow) and right (blue), respectively. Volcano plots show statistical significance ($P < 0.05$), and fold-change in the y- and x-axes, respectively. Each dataset was performed in four biological replicates. Abbreviations: WTTx: wild type-treated; WTCx: wild type-control; AmBTx: AmBR lines-treated; AmBCx: AmBR lines-control. Circles highlight the ten most significant hits that are down- (blue) and up-regulated (red).

Table 7-1. Metabolites (identified / annotated) significantly (P<0.05) altered in wild type and AmBR lines treated with AmB.

Mid log phase *L. mexicana* promastigotes (1 x 10⁸) were treated with a concentration of AmB 5 x EC₅₀ of each line (600 nM for wild type and 3 μM for both AmBR lines), for 15 minutes (section 2.5). Abbreviations: WTTx/WTCx: wild type-treated relative to wild type control (untreated); AmBTx/AmBCx: AmBR lines-treated relative to AmBR lines-control (untreated). *AmB peak 349 was the best hit (mass 924.49, RT 275.26). See Figure 7 13 for other peaks found for AmB. Values from additional peaks found (isomers) are shown in brackets.

Compound	AmBRcl.14			AmBRcl.8		
	Peak (s)	Log FC	Adj. P-Value	Peak	Log FC	Adj. P-Value
Pairwise comparison 2) WTTx / WTCx						
Hypoxanthine	131 (2005)	8.45 to 9.65	3.3E-14-1.65E-15	528	3.75	0.0000028
Glucosamine / D-Glucosamine	337	7.76	5.1E-15	169	2.19	0.003
Betaine	1465 (76)	-3.84 to -4.64	1.8E-08 6.6E-08			
L-Proline	1	-4.21	3.4E-09	481 (10)	-3.37	0.00000012
sn-glycero-3-Phosphocholine	443	4.04	2.9e-06	23	2.06	0.00022
L-Leucine	1489	-3.71	1.4e-06			
L-Valine	309	-3.43	4.7e-07			
Isonicotinic acid / nicotinate				128 (565)	3.03	0.0000014
Glucose 6-phosphate / D-Glucose 6-phosphate				515	2.39	0.0000099
UTP (uridine triphosphate)	1996	-5.4	1.70E-09			
uridine 5'-diphosphate				547	-4.04	7.70E-06
Pairwise comparison 3) AmBTx / AmBCx						
Isonicotinic acid / nicotinate				128 (565)	3.41	9.10E-07
Adenine				530	2.97	0.0042
Hypoxanthine	131	5.21	1.60E-11	55	2.74	0.0001
sn-glycero-3-Phosphocholine	443	6.39	2.00E-08	23	2.62	2.90E-05
Glucose 6-phosphate / D-Glucose 6-phosphate				515	2.48	9.70E-06
L-Proline				481 (10)	-2.23	1.50E-05
L-Glutamic acid / L-Glutamate				451 (53)	-2.11	1.50E-05
5-Oxoproline				66	1.86	9.70E-06
Guanine	400	10.18	2.3E-13			
Glucosamine / D-Glucosamine	337	7.15	1.90E-14			
Betaine	1465	-4.65	9.00E-08			
L-Leucine	1489	-4.11	5.80E-07			
L-Valine	309	-3.92	1.40E-07			
N-Acetylneuraminic acid	2927	3.44	5.00E-09			
amphotericin B	349 *	10.96	5.10E-16			
l-pipecolic acid	30	-3.43	0.00019			

Further analysis consisted in the partitioning of all metabolites from these four groups, into 25 individual pathways, numbered as follows: 1) Glycolysis and Gluconeogenesis; 2) TCA cycle; 3) Pentose Phosphate Pathway (PPP); 4) Pentose and glucuronate; 5) fructose and mannose; 6) inositol phosphate; 7) Pyruvate, 8) amino sugar and nucleotide sugar, 9) Fatty acids (FA-) biosynthesis; 10) FA-elongation; 11) FA-degradation; 12) glycerolipids (GLs);

13) glycerophospholipids (GPLs); 14) sphingolipids (SPLs); 15) terpenoids; 16) purines and pyrimidines; 17) Alanine, aspartate, glutamate; 18) Glycine, serine, threonine; 19) glutathione, cysteine and methionine; 20) valine, leucine, isoleucine; 21) arginine and proline; 22) histidine; 23) energy metabolism and oxidative phosphorylation; 24) lipopolysaccharide (LPS); and 25) nicotinate and nicotinamide. A complete list of fold changes from all four pairwise comparisons of all the identified/putative metabolites, is provided by individual pathway (Supplementary 9, Tables 1 to 3) (see page 8).

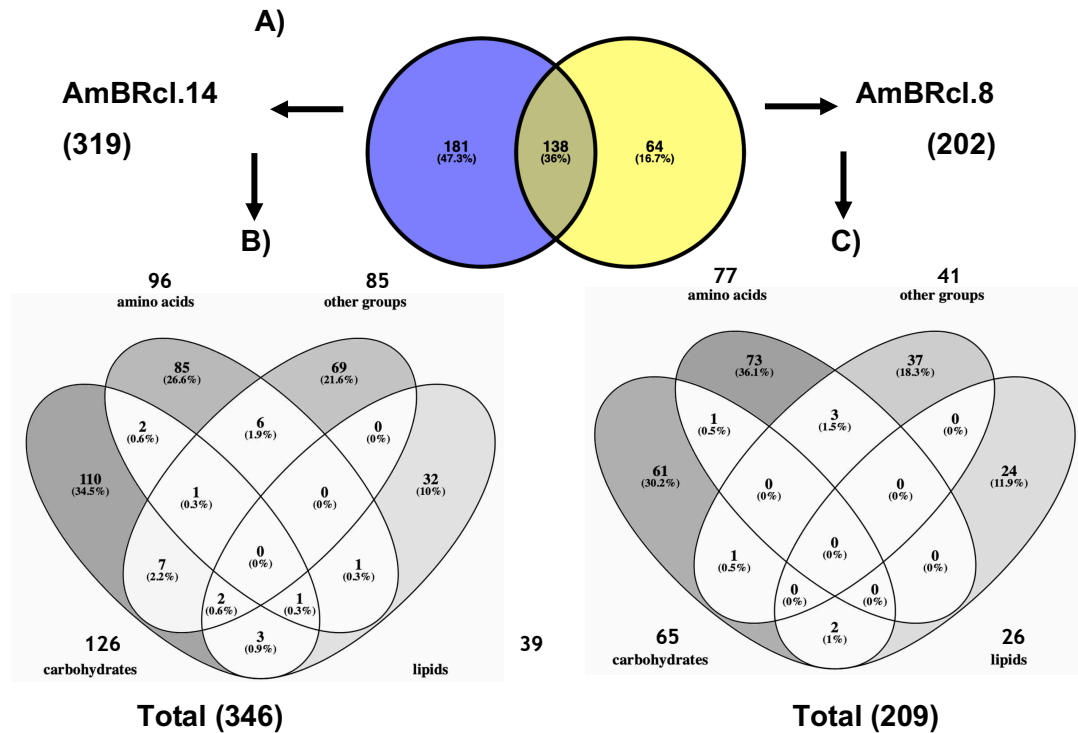


Figure 7-3. Distribution of classes of metabolites in two resistant lines of *L. mexicana* promastigotes treated with AmB.

Mid log phase *L. mexicana* promastigotes (1×10^8) were treated with a concentration of AmB $5 \times EC_{50}$ of each line (600 nM for wild type and 3 μ M for both AmBR lines), for 15 minutes (section 2.5). Panel A) overlap between metabolites significantly ($P < 0.05$) altered in both datasets. Panel B) Venn diagrams of the distribution and overlap of metabolites shown in Panel A, after being clustered into four groups (see text for details). Diagrams were constructed using Venny v2.1 tool (Oliveros 2015; <https://bioinfogp.cnb.csic.es/tools/venny/>). A full list with names of all metabolites is provided (see Supplementary 9, Table 1, 2 and 3) (see page 8).

7.2.1 Lipid metabolism

In this thesis, LC-MS data were acquired using a ZIC-pHILIC column along with a mobile phase consisting of water/acetonitrile, with this approach, highly polar metabolites are retained in the column for longer time, while those semi-polar/hydrophobic metabolites (as with lipids) are eluted earlier, this explains, at least in part, the fact that lipids classes were the less abundant group (Figure 7-3, B-C), and with the lowest coverage (12-13%). Other

methods, e.g. reverse-phase columns, and capillary electrophoresis–mass spectrometry (CE-MS) coupled with LC-MS, can detect lipids such as fatty acids, sphingolipids and glycerophospholipids (saponifiable), and other non-saponifiable species, i.e. sterols (Barbas-Bernardos et al. 2016). More recently, both polar and semi-polar metabolites have been analysed by performing a single extraction using a biphasic solvent, i.e. methyl tert-butyl ether:ethanol (3:1 v/v) (Fauland et al. 2011; Rampler et al. 2018). The latter of these methods, has shown good results in kinetoplastids (Dr. Paul Denny's Lab, unpublished data). Sterols are preferably analysed using GC-MS (as in my study, see Chapter 5), which is the standard method for identification of this group (Goad and Akihisa 1997).

Performing a targeted lipidomics analysis can confirm these lipid classes described here using LC-MS, which are of biological relevance, and account for 5–15% of the cellular and membrane lipids, e.g. inositol phosphoryl ceramide (IPC), in *Leishmania* (Kaneshiro, Jayasimhulu, and Lester 1986). Treatment with AmB altered several pathways related with the metabolism of lipids, i.e. GLs, GPLs, linoleic acid, arachidonic acid, FA- biosynthesis, -elongation, -degradation, and biosynthesis of unsaturated FA (UFAs). Overall, these changes are indicative that these species are implicated in the response of *L. mexicana*, to the treatment with high concentrations of this polyene and other drugs, e.g. miltefosine, targeting the membrane, possibly, due to their role in the regulatory function of the membrane that is related with the sterols in this structure (Gulati et al. 2010; Varga et al. 2006). In spite of the limitations of LC-MS to detect lipids, 39 and 26 peaks, showed significant fold changes in AmBRcl.14 and AmBRcl.8, respectively (Figure 7-3, B and C). With regard to saponifiable lipids, some patterns were noted in both datasets. Although undetected in AmBRcl.8, sn-glycerol-3-phosphoethanolamine showed a dramatic increase of 5.95 and 7.5-fold in AmBRcl.14 and its parental line, conversely, all the other GLs, GPLs and SPLs, e.g. choline, sn-glycerol 3-phosphate, and sn-glycerol 1-phosphate, showed a decrease (0.5 to 2.9-fold) in this line (Figure 7-4). In AmBRcl.8, three metabolites related with SPLs, showed an increase after being exposed to AmB, being these p-benzoquinone (2.2-3.2-fold), glycerophosphocholine and sn-glycero-3-phosphocholine (2.0-2.6-fold for both metabolites). Similar downregulation of the order of 2-fold was observed in some SPLs, e.g. sphinganine and sphingosine, in another AmBR line exposed AmB at similar concentrations ($5 \times EC_{50}$), with the difference that this line, was developed and treated in a serum-free medium (named DM) (PhD Thesis Dr Raihana Nithin, 2019, unpublished). Another work identified a similar increase in sn-glycero-3-phosphocholine and glycerophosphocholine in three AmBR lines (Dr Andrew Pountain, PhD Thesis, 2018), these changes altogether, suggest that GPLs and SPLs, alongside with sterols (see chapter 5), are involved in the response to the treatment with AmB (Gulati et al. 2010). Additional changes in lipids from the FA cohort, i.e. linoleic acid, showed a

clear increase in abundance in both resistant lines and their respective parental wild types (2.8- and 4.9-fold in AmBRcl.8 and WT, respectively), although this change was more pronounced in AmBRcl.14 (4.27 to 4.78-fold). Another FA, eicosapentanoic acid (EPA), also increased notably (8.3-fold), in AmBRcl.14, but was not detected in the other line. The increase of linoleic acid was also noted in the work of Dr Raihana Nithin, although in her work, AmBR cells were selected and treated in a serum-free medium, named defined medium (DM). Similarly, abundance of fatty acids increased from 4 to 57% in WT and AmBR, respectively and cholesta-5, 7, 24-trien-3 β -ol (as in the study of Pountain and in my study in two lines -AmBRcl.8 and AmBRcl.6-). The latter was described to contribute to the permeability of the membrane in *L. donovani* (Mbongo et al. 1998b).

Previous work has analysed sterols in *Leishmania* using LC-MS (Andrade-Neto, Pereira, Canto-Cavalheiro, et al. 2016; Jara et al. 2017), however, interpretation of these lipid-species should be considered with caution. LC-MS also detected some sterol peaks. Some examples are, 2-C-methyl-D-erythritol 4-phosphate, an intermediate of the non-mevalonate pathway (this alternative route for the synthesis of isoprenoids is present in *E. coli*, *M. tuberculosis*, *Plasmodium* spp., and other protozoan, albeit to the best of my knowledge, its presence in *Leishmania* spp. is unknown), which increased by 1.0-1.76, and 2.55-2.79 in AmBRcl.14 and AmBRcl.8, respectively. Although only detected in AmBcl.8, other 16 sterol peaks were detected with LCMS (Figure 7-5B). 7 of these showed a 3.35 to 3.75-fold decrease in abundance after AmB exposure, while others remain unaltered. A list with their full names is provided in Supplementary 9 (see page 8). Similar observations were found in the levels of sterol precursors of the terpenoid pathway (mevalonate) and sterol biosynthesis pathway. Interestingly, short-time exposure to AmB reduced the abundance of acetyl-CoA, L-leucine, L-isoleucine and mevalonic acid in all wild types (Figure 7-5). Similarly, a reduction in mevalonic acid (0.59-2.99-fold) and acetyl-CoA (0.59-2.0-fold), was found after exposure to AmB, in AmBcl.14. This was accompanied by a 1.9-fold decrease of another precursor of isoprenoids, glyceraldehyde-3-phosphate (G3P) (annotated as D-glyceraldehyde-3-phosphate). Neither mevalonic acid (mevalonate) nor acetyl-CoA were altered in AmBRcl.8 (-0.5 to 0.03-fold) as an effect of the short treatment with AmB, however, the former was 1.63-1.92-fold less abundant than in their respective WT, in both untreated lines, AmBcl.8 and AmBRcl.14, possibly, as a result of the selection for AmB-resistance over 9-months (see section 3.2.1).

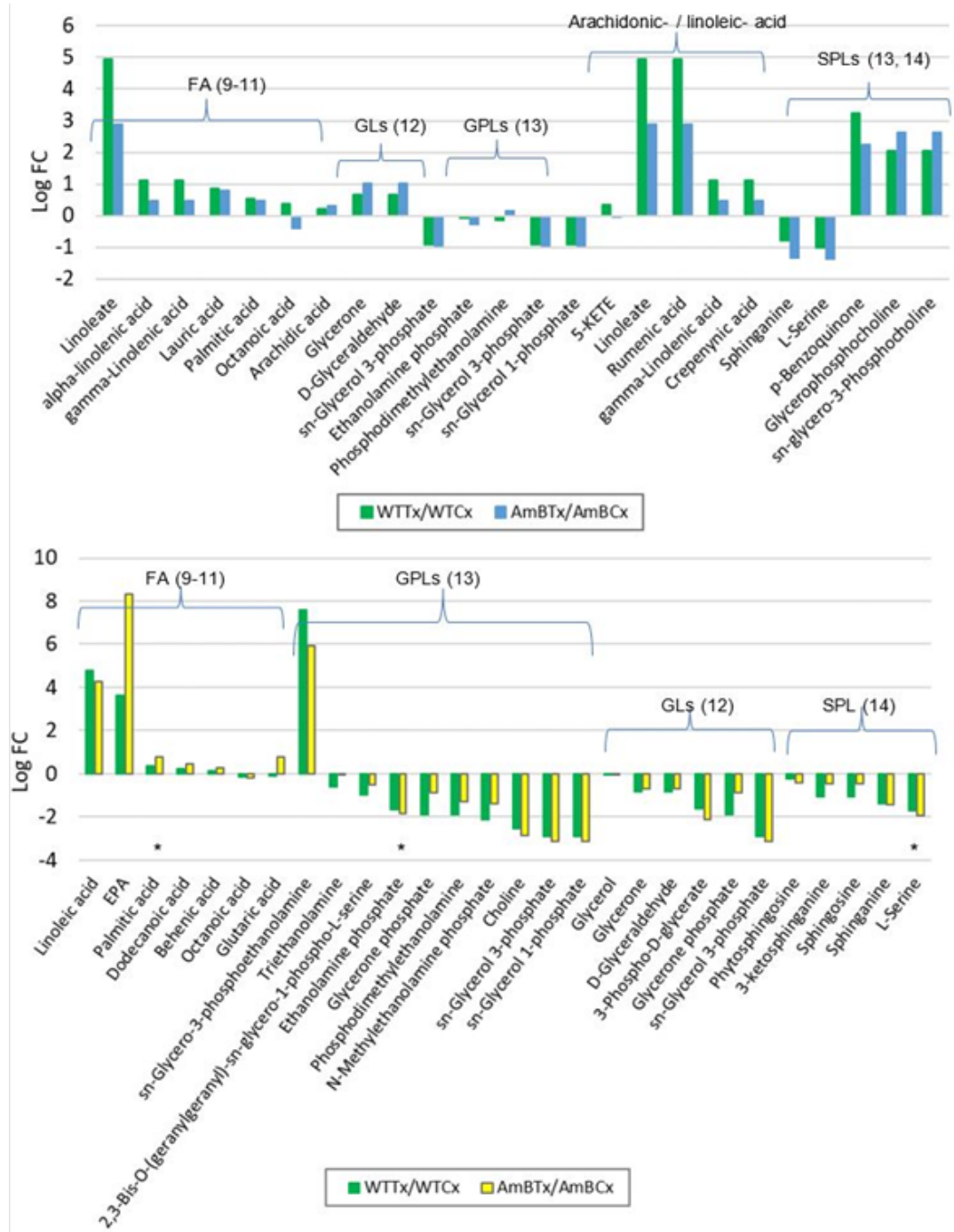


Figure 7-4. Lipid changes as detected by LC-MS.

The parental wild type (green in both panels) and resistant lines AmBRcl.14 (bottom, yellow) and AmBRcl.8 (top, blue), were treated with 5 x EC₅₀ (50 nM for wild type and 3 μM for the resistant lines). Significant fold changes (Log FC, P < 0.05) are relative to untreated cells (y-axis). Each dataset included four biological replicates. Numbers of individual pathways shown here are: 9) Fatty acid (FA-) biosynthesis; 10) FA-elongation; 11) FA-degradation; 12) glycerolipids (GLs); 13) glycerophospholipids (GPLs); and 14) sphingolipids (SPLs). *stars indicate metabolites that are related to other pathways. Abbreviations: WTTx/WTCx: wild type-treated relative to wild type control (untreated); AmBTx/AmBCx: AmBR lines-treated relative to AmBR lines-control (untreated). Some peaks, e.g. glycerophosphocholine and sn-glycero-3-phosphocholine are isomers with similar formula that PiMP cannot discriminate, and in some cases, are listed in more than one pathway.

The lower abundance of this sterol intermediates is probably related to the reduction of L-leucine in both lines, with this effect being up to 3-fold more pronounced in AmBRcl.14 (3.06-3.39-fold decrease with respect to wild type) than in AmBRcl.8 (Figure 7-5A). This is of particular relevance as in *Leishmania* spp., ergosterol derives mainly from this amino acid (up to 70-77% in *L. mexicana*), before entering the isoprenoid pathway (Ginger et al. 2000; Ginger, et al., 1999). In their study, Ginger et al., used ^{14}C and ^{13}C -labelled acetate, glucose and leucine as substrates. To the best of my knowledge, this approach has never been attempted in AmBR lines, which could provide hints in understanding more on the MoA and resistance to this polyene. In my study, leucine, and L-isoleucine, both matched to the reference standard, and showed significant fold change in both, PiMP and IDEOM pipelines (Figure 7-5). Contrary to L-leucine, isoleucine is poorly incorporated into lipids (in *L. mexicana*) (Ginger, et al., 1999).

Other sterol peaks have been previously detected using LCMS in AmBR lines (Figure 7-5B). Particularly, an increase in cholestanes was described in another study from a former member of our group. Interestingly, one of these two intermediates (cholesta-5,7,22-trienol, $\text{C}_{27}\text{H}_{42}\text{O}$) was further identified with GC-MS (Dr Andrew Pountain, PhD Thesis, 2018). Also using GC-MS, the latter was the predominant intermediate in lines, AmBRcl.8 and cl.6 (see section 5.2.1). However, none of the sterols detected with LC-MS were similar to those reported by Dr Pountain with this platform, nor to those identified with GCMS in both studies. From those identified here with LC-MS, only one with the formula $\text{C}_{20}\text{H}_{30}\text{O}_3$ showed a 2-fold increase, while seven other peaks (formulae $\text{C}_{28}\text{H}_{44}\text{O}_4$, $\text{C}_{28}\text{H}_{42}\text{O}_2$ and $\text{C}_{28}\text{H}_{42}\text{O}_3$) were decreased by 3.5-fold, and another eight all with formulae $\text{C}_{28}\text{H}_{44}\text{O}_3$, were unaltered (0.035 to 0.08-fold). A list with their full names (and the isomers identified) is provided in supplementary 9 (see page 8).

7.2.2 Carbohydrates and energy metabolism

Changes observed in some carbohydrate related pathways, e.g. glycolysis, Pentose Phosphate Pathway (PPP), were between 2.37 to 2.91-fold after the treatment with AmB, suggesting that AmB exposure in *L. mexicana* increases their flux as a response to an oxidative stress-environment (Maugeri and Cazzulo 2004; Purkait et al. 2012). In general, both AmBRcl.14 and AmBRcl.8 showed some evidence of changes in carbohydrates, being these changes with a similar pattern to that observed in their respective parental WT (Figure 7-6 and Figure 7-7). I therefore addressed these changes in carbohydrates by comparing both individual resistant lines, for simplification purposes. Evidently, “carbohydrates” represented the group with the largest difference in the number of

metabolites between both lines (126 in AmBRcl.14 and 65 AmBRcl.8).

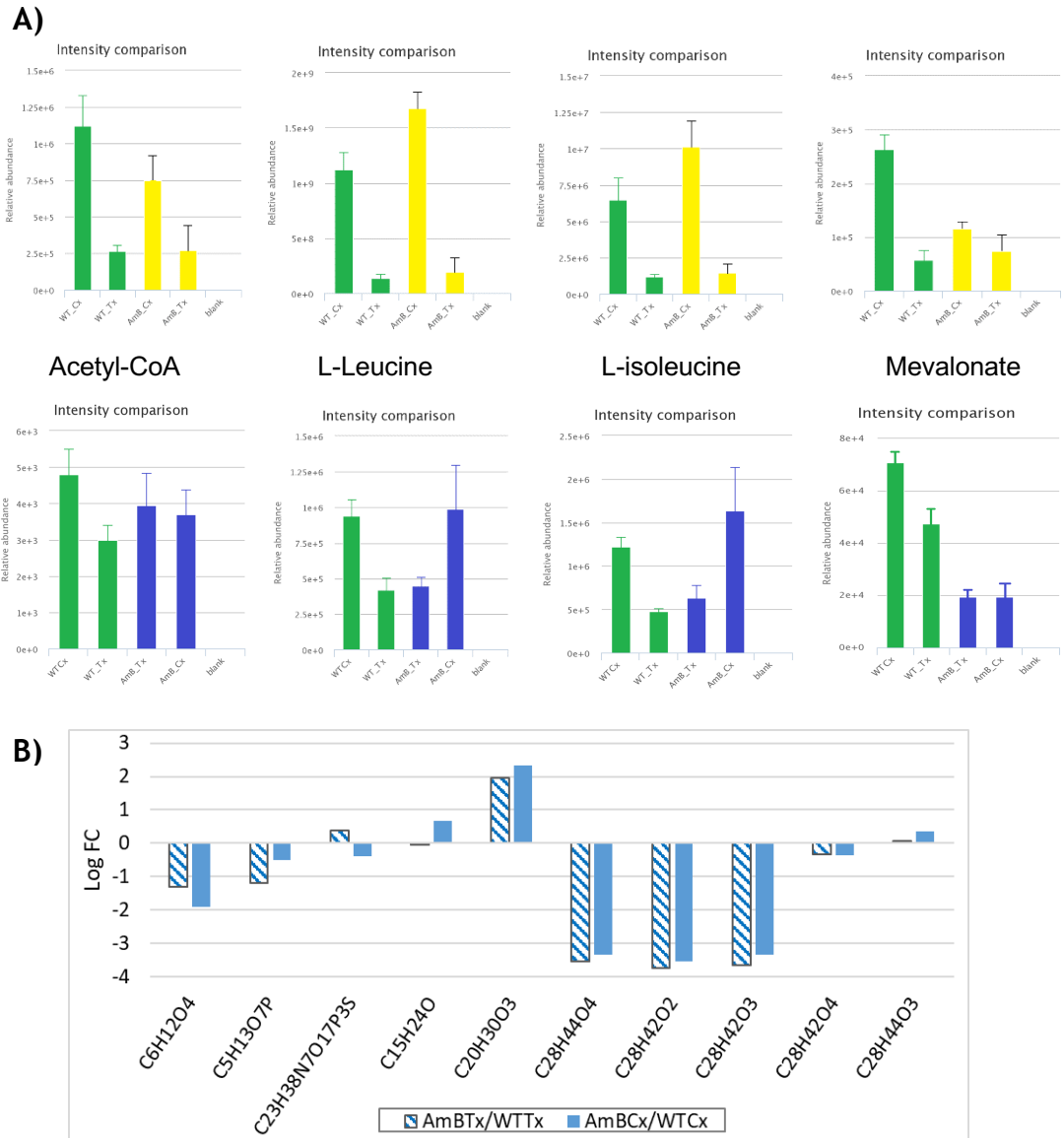


Figure 7-5. Perturbation of metabolites related with the sterol biosynthesis. Wild type (green) and AmBR lines of *L. mexicana* promastigotes were treated with AmB (5 x EC₅₀) and the abundance of metabolites was measured. **PANEL A)** AmBRcl.14 (yellow) and AmBRcl.8 (blue) are shown. L-Leucine and L-isoleucine matched to their respective standards, while acetyl-CoA and mevalonate were putatively annotated. **PANEL B)** shows the abundance of sterol intermediates in AmBRcl.8, a full list of their names is shown in Supplementary 9 (see page 8), here their chemical formulas are used for convenience. Data were processed with PiMP pipeline (Gloaguen, 2017). Mean values from four replicates are plotted with their standard deviation (bars). Abbreviations: WT_Tx: wild type treated; WT_Cx: wild type control; AmB_Tx: AmBR line treated; AmB_Cx: AmBR line control.

Contrary to the a previous study with AmBR lines in which upregulation of glycolysis and TCA (in *L. infantum*) were observed (M.-C. Brotherton et al. 2014), in this study, glycolysis showed a decrease in abundance (from 1.5 to 4.5-fold) in AmBRcl.14, no decrease was found in AmBRcl.8. In both resistant lines, D-glucose 1-P and D-glucose 6-P showed a similar pattern (1.68- and ~2.5-fold increase, in AmBRcl.14 and AmBRcl.8,

respectively). D-fructose 6-P also increases by 1.68-fold, albeit only in the former. Except for succinic acid that showed dramatic reduction (15-fold) in AmBRcl.14 (in WT it was reduced only 1.5-fold), no other prominent changes were present in metabolites of the TCA cycle. Changes in other carbohydrates observed in AmBRcl.14 and AmBRcl.8 were variable (Figure 7-6 and Figure 7-7). In both datasets, change in metabolites related to pyruvate was heterogeneous. From those metabolites related with fructose and mannose, sorbose 1-P, beta-D-fructose 2-P, beta-D-fructose 6-P, D-allulose 6-P, D-allose 6-P, D-mannose 1-P, D-mannose 6-P, and D-fructose 1-P, showed a similar pattern of increase in abundance from 1.61- to 1.68, and from 2.39 to 2.48-fold, in AmBRcl.14 and cl.8, respectively. Other members in this pathway decreased (only in AmBRcl.14) between 2 to 4.51-fold. With regard to the inositol phosphate metabolism, some interesting changes were noted, in particular, four peaks (C₆H₁₃O₉P) that can be either myo-inositol 1-phosphate, myo-inositol 4-phosphate, D-Glucose 6-phosphate or inositol 1-phosphate (average of 1.68 to 2.48-fold rise), in WT and resistant lines from both datasets. In agreement with these changes, an AmBR-*L. infantum* with mutations in the miltefosine transporter (MT), also observed both increases and decreases in various inositol-associated metabolites (Fernandez-Prada et al. 2016). A direct comparison with this study is however, difficult, considering differences between the methodology of the study of Fernandez-Prada et al., and that used in this thesis, i.e. GCMS and LCMS, respectively. The precise identification of these isomers without a standard is, however, problematic.

Pentose phosphate pathway (PPP) is related with redox oxidative protection (Ghosh et al. 2015; Kovářová and Barrett 2016) since NADPH, produced by the oxidative branch dehydrogenases, is the key electron donor in reductive processes (Figure 7-9). PPP metabolites were detected in higher amounts in AmBRcl14 than in AmBRcl.8 (21 vs 7) (see Supplementary 9 for a full list; see page 8). D-ribulose 5-phosphate showed an increase (three isomers with similar formula C₅H₁₁O₈P and fold-change were found, namely D-Xylulose 5-phosphate, and the bis-phosphorylated forms, alpha-D-ribose 1-P, D-ribose 5-P. D-gluconic acid, beta-D-fructose 6-P (and its isomer beta-D-glucose 6-P with formula C₆H₁₃O₉P), D-arabino-hex-3-ulose 6-P (an isomer with formula C₆H₁₃O₉P, alpha-D-glucose 6-P was found), showed an increase (from 1.6- to 3.98-fold), while four hits were decreased between 1.98 to 6.94-fold. This pattern of changes was consistent in both the WT and AmBRcl.14. In the other line, AmBRcl.8, only sedoheptulose 7-P, increased (in average ~2.45-fold), while other PPP metabolites showed no change (Figure 7-6). NADPH was notably reduced (in average 2-fold) in AmBRcl.14 (two peaks with mass 746.097 were found), but appeared undetected in the dataset of AmBRcl.8. The PPP is the main source of NADPH, hence this reduced cofactor is of significant relevance in

drug resistance that protects the parasite against oxidative stress. The abundance of NADPH (in AmBRcl.14) along with the two enzymatic steps in the PPP from which is produced, i.e. glucose-6-phosphate dehydrogenase (G6PDH) and 6-phosphogluconate dehydrogenase (6PGDH), are shown in Figure 7-9.

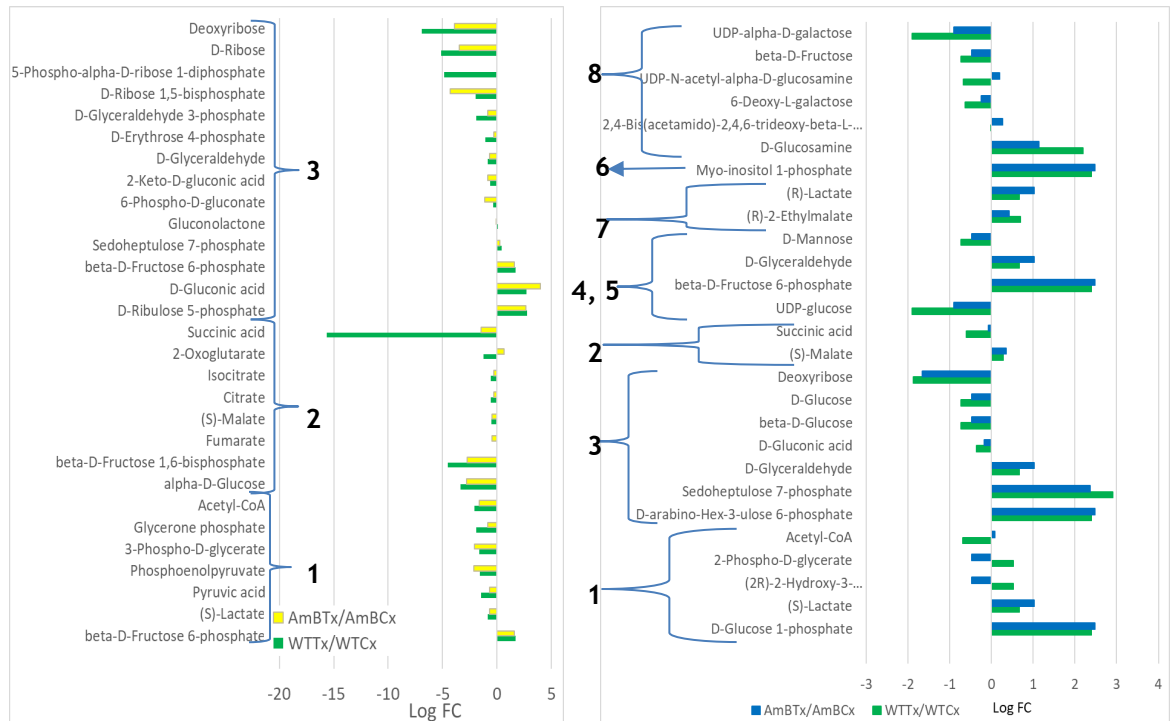


Figure 7-6. Changes in carbohydrates metabolism. Numbers of pathways are as follows: 1) Glycolysis/Gluconeogenesis; 2) TCA cycle; 3) Pentose Phosphate Pathway (PPP); 4) Pentose and gluconate; 5) fructose and mannose; 6) inositol phosphate; 7) Pyruvate, 8) amino sugar and nucleotide sugars. Abbreviations: WTTx: wild type-treated; WTCx: wild type-control (untreated); AmBTx: AmBR lines-treated; AmBCx: AmBR lines-control. Fold changes are relative to each pairwise comparison and only significant changes ($P < 0.05$) are shown. A full list of all metabolites is provided in Supplementary 9 (see page 8). Peaks were analysed and filtered using PIMP pipeline (Gloaguen et al. 2017).

A TKT-KO *L. mexicana* cell line along with the parental WT and the add-back line, were all exposed to similar concentrations of AmB, i.e. 5 x their respective EC_{50} (Figure 7-8B). The PCA of this dataset showed a clear separation of samples from all six groups, PC1 separated treated cells from the untreated controls in all groups. Similarly, PC2 showed a clear separation of the TKO-KO from both clusters formed the parental WT and the add-back (R18) (Figure 7-8A). In this dataset, the coverage of the PPP was of 61.7%, and the hexose (D-glucose) was the only metabolite validated by a standard (i.e. identified), while all the other 20 peaks in this pathway were putative. Contrary to the rise seen in some PPP metabolites in both resistant lines (and in their WTs), TKT-KO showed a general decrease in abundance (between 0.72 to 4.21-fold) across all the PPP metabolites.

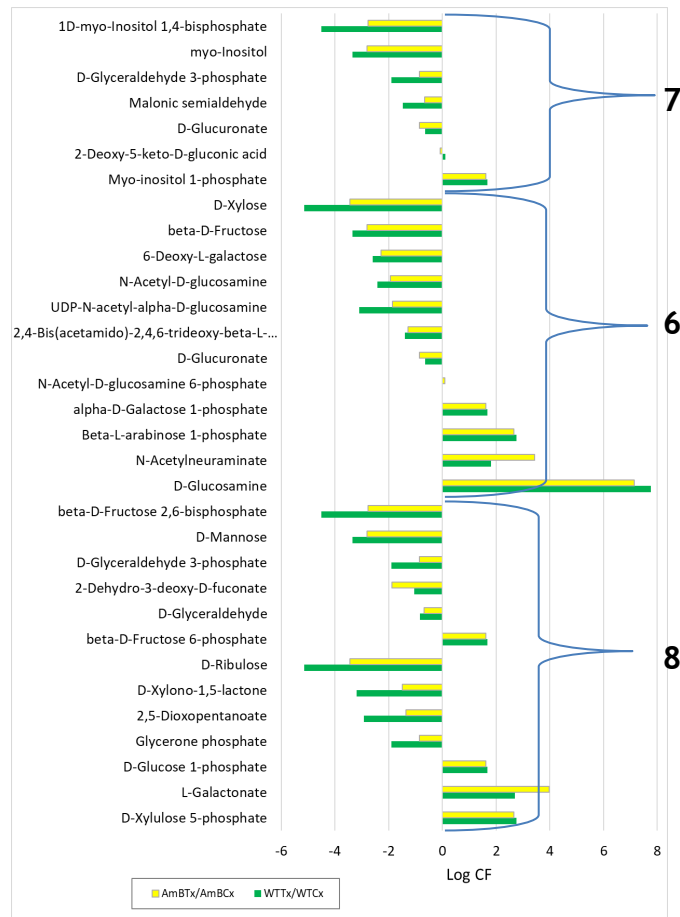


Figure 7-7. Additional changes in the metabolism of carbohydrates in AmBRcl.14. Fold changes are relative to each pairwise comparison and only significant changes ($P < 0.05$) were selected. See Figure 7-6 for a full description, and for numbers of individual pathways.

Those metabolites that decreased in WT, R18 and TKT-KO (and in both resistant lines) were, deoxyribose, D-ribose (undetected in AmBRcl.8), beta-D-glucose, and D-glucose. All changes found in TKT-KO, the parental WT and the add-back (R18) are listed in Table 7-2. Other changes in the TKT-KO were the decrease in some metabolites from oxidative phosphorylation (3 to 5-fold decrease in ADP and ATP), arginine metabolism (e.g. L-proline 2.77-fold, L-glutamic acid 3.28-fold, and S-adenosyl-L-methionine 3.36-fold) and in other amino acids. The decrease in the arginine pathway, including the arginine pool that is an essential amino acid for promastigotes in culture (Muxel et al. 2018; Westrop et al. 2015), was in agreement with those findings from the study of Dr Raihana Nithin in WT and one AmBR line that were both grown in defined medium, DM (a serum free culture medium). Changes in amino acids in both AmBR lines is discussed further (section 7.2.4). AmB also caused a decrease in the abundance of lactate, a product of the anaerobic branch of glycolysis, in all samples from the TKT experiment (also observed in AmBRcl.14), although this was opposite to the increase observed in AmBRcl.8, and in four other AmBR lines selected in our group (PhD Thesis, Dr A Pountain, University of Glasgow). Changes

in nicotinate and nicotinamide, which are precursors for the generation of NAD⁺ and NAP⁺, and in energy metabolism, are essential for redox metabolism. Nicotinate increased 3.0 to 3.4-fold in AmBRcl.8 (also in the parental WT) while in AmBRcl.14 this rise was moderate (0.7 to 1.1-fold). Interestingly, both WT and the AmBRcl.8 had a pronounced depletion of nicotinate (3.2-3.5-fold) as a result of the drug selection (this is in untreated cells), which was also observed, albeit to a lesser extent, in AmBRcl.14.

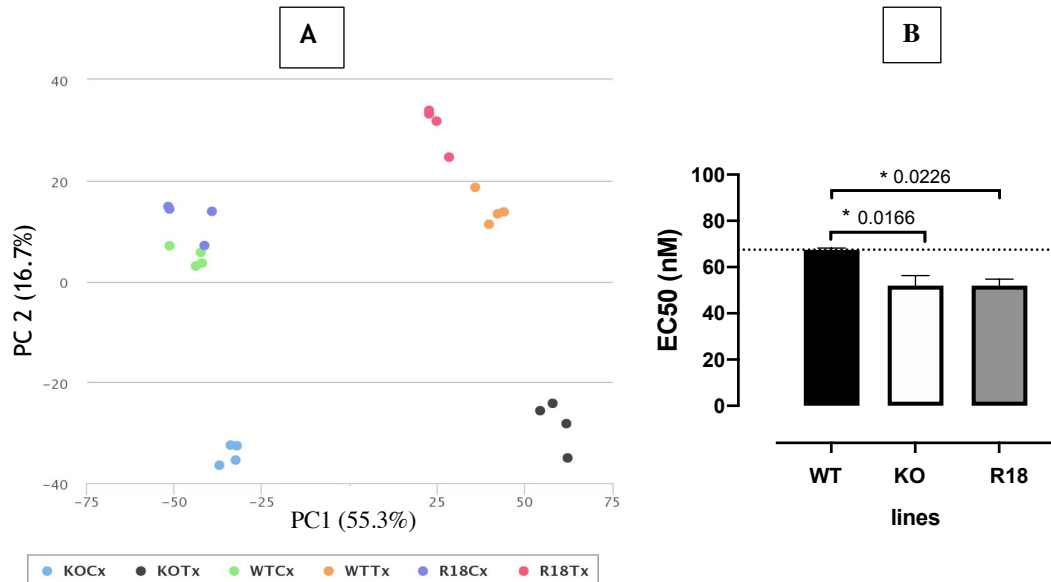


Figure 7-8. PCA and AmB EC₅₀ of WT, Δ TKT and add-back-TKT *L. mexicana* promastigotes. PANEL A: principal component analysis (PCA) of wild type (WT), knockout (KO) and add-back-back (R18), treated (-Tx) with AmB, and control groups (-Cx). PANEL B: the mean EC₅₀ values are shown in μ M with their standard deviation (bars). Tukey's multiple comparison test measured pairwise differences between each resistant line compared with wild type. Statistically significant values ($P < 0.05$, 95% Confidence Interval) are shown with stars: * $P \leq 0.05$, ** $P \leq 0.01$, * $P \leq 0.001$, **** $P \leq 0.0001$). The mean EC₅₀ \pm SD for each group was 67 ± 0.70 nM (WT), 52 ± 4.3 nM (KO), and 52 ± 2.8 nM (R18). These values were increased 5 x (300 nM for the TKT, and 250 nM for the other two groups), for the treatment of cells during 15 min, then the metabolome was analysed using LC-MS (see sections 2.5 and 2.7). Data from panels A and B were processed with PiMP pipeline (Gloaguen et al., 2017), and Prism 8.0, respectively.**

With regard to the energy metabolism in AmBRcl.8, a decrease in ATP (2.15-fold) and ADP (1.35-fold) were noted. This low abundance was more pronounced in AmBRcl.14 (ATP 4.23-fold, ADP 2.14-fold). Reduction of NADPH was found between the same ranges (2.07-2.28-fold) and these changes were accompanied by a dramatic reduction (15.5-fold) in succinic acid in AmBRcl.14, which was reduced only by 1.48-fold in the parental line and remained unaltered in AmBRcl.8 (0.07 to 0.6-fold). Other metabolites of the nicotinate and nicotinamide metabolism that were reduced in AmBRcl.14 and its WT were, 4-methylaminobutyrate (3.4-3.5-fold), L-aspartate (5.7-7.4-fold), and maleamate (8.7-8.8-fold).

Figure 7-9. Metabolic changes in the PPP after the treatment with AmB in *L. mexicana*. Glycolysis (boxed in blue), the oxidative- (boxed in green) and non-oxidative (boxed in purple) –branches of PPP are shown. The enzymes glucose-6-phosphate dehydrogenase (G6PDH, green box), and 6-phosphogluconate dehydrogenase (6PGDH, blue box), and transketolase (TKT, grey boxes) are highlighted. Pie chart shows the map coverage. The two enzymatic steps (G6PDH and 6PGDH) that produce NADPH are also indicated by green long arrows. Significant ($P < 0.05$) fold changes after the treatment with AmB (see section 2.5) are shown in arrows and equal signs, indicating increase (up arrows), decrease (down arrows) or no change (equal signs), observed in the two resistant lines, AmBcl.14 (black arrows) and AmBcl.8 (blue arrows), and the TKT-KO (red arrows). ** Values of fold changes in AmBcl.14 and AmBcl.8 are included for comparison (blue boxes-black numbers indicate decrease and yellow boxes-red numbers indicate increase). Bar graphs at the top show abundance of NADPH (only in AmBcl.14 dataset), and Lactate, after AmB-exposure, in WT (green), AmBcl.14 (yellow), AmBcl.8 (blue), TKT-KO (red), R18 (black). Annotated and identified (only D-glucose) metabolites are highlighted in the pathway by the yellow- and grey dots, respectively. Adapted from KEGG maps). Analysis was performed with PiMP (Gloaguen et al. 2017).

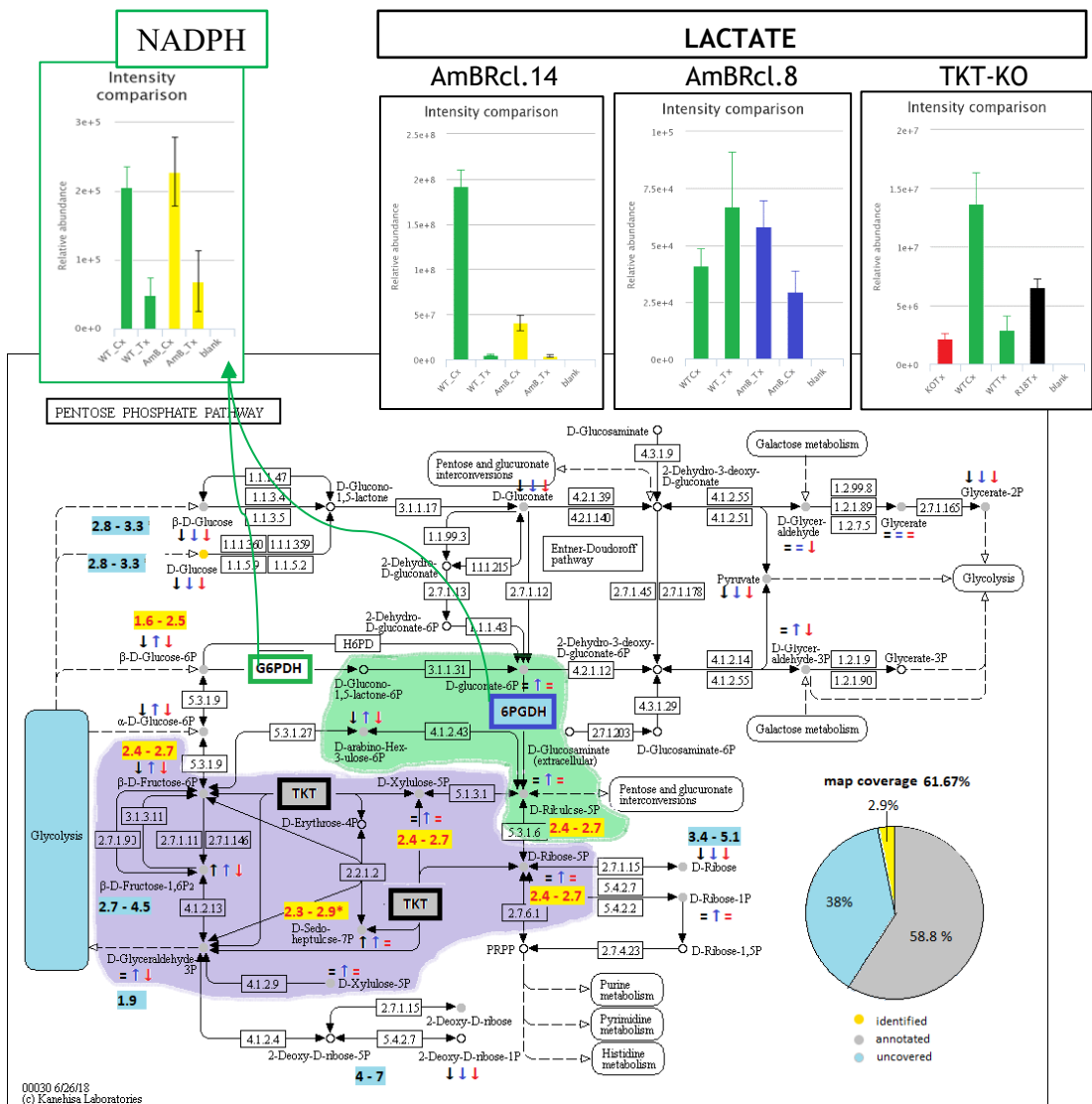


Table 7-2. Effects of AmB on the Pentose Phosphate Pathway in a TKTKO of *L. mexicana* *L. mexicana* promastigotes lacking the transketolase (KO) gene (parental WT and add-back (R18) were included for comparison), were treated with AmB as described in Figure 7-8 and section 2.5 and 2.7. Abbreviations: WTTx: wild type-treated; WTCx: wild type-control; R18Tx and R18Cx: add-back-treated and control; KOTx and KOCx: transketolase KO-treated and control. Fold changes (LogFC P<0.05) from each pairwise comparison shows a decrease (red) and increase (blue) in abundance relative to control (untreated) cells. Data processed with PiMP pipeline (Gloaguen et al. 2017). Except for D-glucose that matched a reference standard (Identified, boxed in yellow), some metabolites (here in red) with similar formula (e.g. C6H12O6, C6H13O9P and C5H11O8P) are putatively annotated and these peaks can be any of the isomers.

Name	Formula	logFC WTTx / WTCx	logFC R18Tx / WTCx	logFC KOTx / WTCx	Identification
Deoxyribose	C5H10O4	-2.71	-2.60	-4.21	annotated
D-Gluconic acid	C6H12O7	-1.69	-0.78	-2.47	annotated
D-Ribose	C5H10O5	-1.47	-1.07	-2.35	annotated
beta-D-Glucose	C6H12O6	-1.27	-0.73	-1.75	annotated
D-glucose	C6H12O6	-1.27	-0.73	-1.75	identified
2-Phospho-D-glycerate	C3H7O7P	-1.24	-0.15	-1.56	annotated
Pyruvic acid	C3H4O3	-0.45	-0.30	-1.15	annotated
alpha-D-Glucose 6-phosphate	C6H13O9P	-0.28	0.89	-0.92	annotated
beta-D-Fructose 6-phosphate	C6H13O9P	-0.28	0.89	-0.92	annotated
beta-D-Glucose 6-phosphate	C6H13O9P	-0.28	0.89	-0.92	annotated
D-arabino-Hex-3-ulose 6-phosphate	C6H13O9P	-0.28	0.89	-0.92	annotated
6-Phospho-D-gluconate	C3H6O3	-0.04	0.38	-0.72	annotated
D-Glyceraldehyde	C3H7O6P	0.13	0.69	-0.45	annotated
D-Glycerate	C7H15O10P	0.84	1.73	-0.36	annotated
D-Glyceraldehyde 3-phosphate	C6H13O10P	-0.22	1.57	-0.34	annotated
alpha-D-Ribose 1-phosphate	C6H14O12P2	1.19	2.00	-0.22	annotated
D-Ribose 5-phosphate	C3H6O4	0.03	0.27	0.00	annotated
D-Ribulose 5-phosphate	C5H11O8P	0.47	0.85	0.11	annotated
D-Xylulose 5-phosphate	C5H11O8P	0.47	0.85	0.11	annotated
Sedoheptulose 7-phosphate	C5H11O8P	0.47	0.85	0.11	annotated
beta-D-Fructose 1,6-bisphosphate	C5H11O8P	0.47	0.85	0.11	annotated

7.2.3 Nucleotide metabolism

As with the metabolism of some amino acids, e.g. L-arginine, *Leishmania* is auxotrophic for purine bases which need to be salvaged from the host, involving uptake via nucleoside transporters (Aoki et al. 2018; Monzani et al. 2007). Some purine analogues, e.g. allopurinol, are currently used as antileishmanials (canine leishmaniasis), and the purine salvage pathway is of great interest for potential drug targets (Croft and Coombs 2003). Figure 7-10 shows changes in both resistant lines related to purine and pyrimidine metabolism. In AmBRcl.14, dramatic increases were observed in the purines guanine (8.3- to 10.4-fold), xanthine (3.5- in WT and 11.3-fold in AmBRcl.14), hypoxanthine (5.2 to 8.4-fold), and guanosine (6.7- to 8.4-fold). Other purines with moderate increases in this line were adenosine and deoxyguanosine (both with 2.7- to 3.6-fold). On the other hand, a dramatic decrease in abundance was also seen in glycine (4.3- to 5.16-fold), deoxyinosine (7.8- to 9.2-fold) and 5-Phospho-alpha-D-ribose 1-diphosphate (4.8-fold only in

AmBRcl.14). In turn, dGDP, ADP, adenosine 3',5'-bisphosphate showed a more moderate reduction (all with 1.17- in WT and 2.17-fold in AmBRcl.14), while other metabolites remained with little or no change.

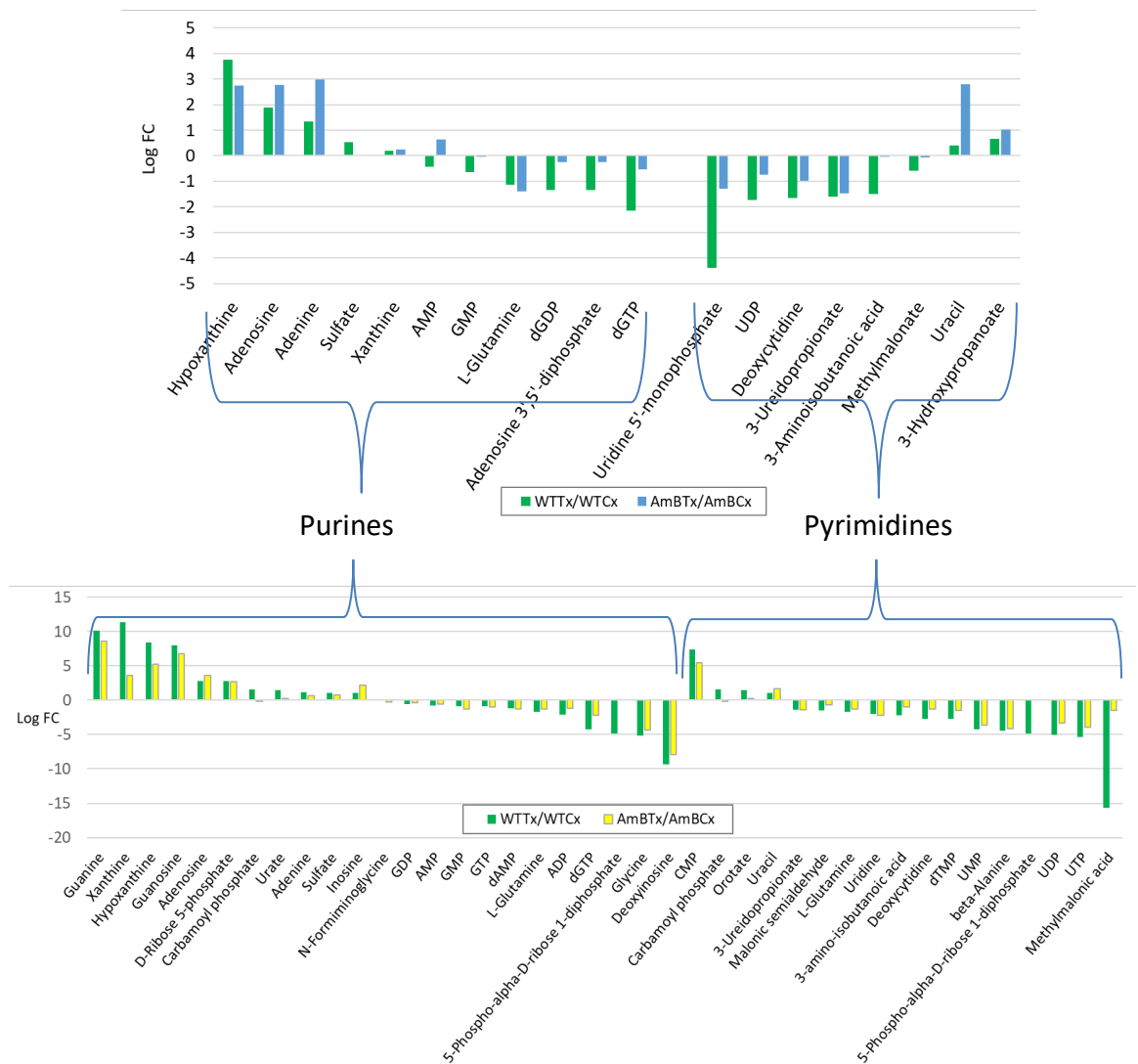


Figure 7-10. Changes in nucleotides (purines and pyrimidines) metabolism. Numbers of pathways are as follows: 16) Purine and pyrimidines. Abbreviations: WTTx: wild type-treated; WTCx: wild type-control AmBTx: AmBR lines-treated; AmBCx: AmBR lines control. Wild type is shown in green. AmBRcl.14 and AmBRcl.8 are shown in yellow (bottom panel) and blue (top panel), respectively. Fold changes are relative to each pairwise comparison and only significant changes ($P < 0.05$) are shown. A full list of all metabolites is provided in Supplementary 9 (see page 8). Peaks were analysed and filtered using PiMP platform <http://polyomics.mvls.gla.ac.uk> (Gloaguen et al. 2017).

Notably, the pyrimidine CMP, also increased significantly (5.4- to 7.3-fold), while the opposite was observed with UDP and UTP, which decreased by 3.3- to 5.4-fold, and a dramatic lower abundance in methylmalonic acid (15.6-fold) was also found. UMP, 3'-UMP, pseudouridine 5'-phosphate and beta-alanine all showed a similar decrease (between 3.65- to 4.25-fold). Although to a lesser extent, a similar pattern of changes was observed in AmBRcl.8. Likewise, in AmBRcl.14, hypoxanthine showed the most pronounced rise

(2.7- to 3.7-fold in AmBRcl.8), followed by adenosine (and another peak annotated as deoxyguanosine with similar formula, C₁₀H₁₃N₅O₄) (both with 1.8- to 2.7-fold), and adenine, C₅H₅N₅ (1.3- to 2.97-fold). Interestingly, in this line, xanthine remained unchanged as an effect of the short-term exposure to AmB. However, this purine was reduced ~4.1-fold in the untreated AmBRcl.8 with respect to WT, possibly derived from the long-term exposure (9 months) to this polyene. Also reduced were the pyrimidines uridine 5'-monophosphate (the isomers 3'-UMP and pseudouridine 5'-phosphate with formula C₉H₁₃N₂O₉P were also detected), all with 1.2- in WT and 4.39-fold in AmBRcl.8. UDP, deoxycytidine, 3-Ureidopropionate, and 3-aminoisobutanoic acid, which were less abundant (1.4- to 1.7) only in AmBRcl.8, but not in its parental line.

7.2.4 Amino acid and polyamine-trypanothione pathway

Along with carbohydrates, amino acids were the second group in which many metabolites were detected with LC-MS. 96 and 77 peaks showed significant changes after the treatment with AmB, in AmBRcl.14 and AmBRcl.8, respectively (Figure 7-12). Moreover, two pathways in this group (D-arginine and D-ornithine with 80-90%, and valine, leucine and isoleucine with 74-87%), showed the highest coverage in both datasets (Figure 7-3). As with the PPP and arginine-metabolism, amino acids and the polyamines-trypanothione pathway (PTP), are essential for the capacity of *Leishmania* to resist oxidative stress generated by AmB (Gray *et al.*, 2012; Anderson *et al.*, 2014) and may contribute to resistance to other antileishmanials (Mbongo *et al.*, 1998a; Brotherton *et al.*, 2014), e.g. pentamidine (Basselin *et al.*, 1997; Ouellette, *et al.* 2004; Díaz *et al.*, 2014; Kaur and Rajput, 2014), and antimonials (Wyllie, *et al.* 2004; Singh, *et al.* 2012). The PTP is also essential for the production of nitric oxide (NO) that is key for the differentiation of promastigotes into the intracellular stage, although the production of NO by *Leishmania* is controversial, given that NO is produced by the macrophages to eliminate the parasite (Aoki *et al.* 2018). Figure 7-11 shows the PTP-enzymes needed to produce the polyamines, putrescine, spermidine and spermine, and trypanothione (see section 1.7.3), as well as the precursors, i.e. L-arginine, L-serine, L-ornithine, that are also crucial for the correct functioning of the *Leishmania*-reducing machinery (Manta *et al.* 2013). Additional to the changes in L-isoleucine and L-leucine related with the sterol synthesis described before (section 7.2.1), numerous changes were observed in the metabolism of other amino acid groups (Figure 7-12). From those related with the PTP, no changes were found in other amino acids involved in the reverse trans-sulfuration pathway, serine, methionine (1.4-fold rise only in AmBRcl.8), and homocysteine. Similarly, L-arginine and L-ornithine (both identified by

standards), precursors of the synthesis of spermidine, appeared without changes (a decrease of 1.12-fold was seen in the latter amino acid only in AmBRcl.14).

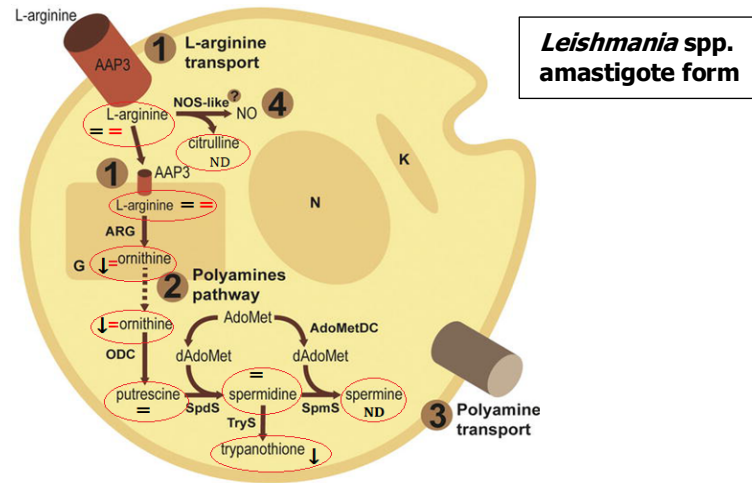


Figure 7-11. Metabolic changes in the PTP in *L. mexicana* after AmB-exposure. 1) L-arginine uptake is via the permease AAP3 in the cell- and glycosome- membranes; 2) inhibition of PTP can occur by inhibiting the different enzymes involved ARG, ODC and AdoMetDC, SpdS, SpmS and TryS (red circles); prevents replication; Metabolites (red circles) with significant ($P < 0.05$) fold changes after the treatment with AmB (see section 2.5 for details) observed in two resistant lines: AmBcl.14 (in black) and AmBRcl.8 (in red). Arrows and equal signs, indicate increase (up arrows), decrease (down arrows) or no change (equal signs). ND-not detected. Modified from (Aoki et al. 2018).

Although ZIC-HILIC column is valuable to detect polyamines (Westrop et al. 2015), these are detected poorly with LCMS pHILIC chromatography approach used here (presumed to be retained by the column). Using the latter of these methods, we found no increase in spermidine and putrescine, while a reduced abundance (1.76- to 2.62-fold) was seen in trypanothione disulfide (this was detected only in AmBRcl.14) (Figure 7-11). This may relate to lower abundance of the amino acids involved in glutathione biosynthesis, e.g. glutamate (1.37-fold) and glycine 4.3- to 5.16-fold), observed in this line. Also, in AmBcl.14 (and WT) and in agreement with this, glutathione was reduced (2.44- to 2.55-fold). Interestingly, gamma-L-glutamyl-L-cysteine was unchanged (0.15-fold - AmBRcl.14-), while L-cysteine increased notably (5.27- to 6.38-fold), but cysteine was not detected in this dataset. Glutathione was also detected in AmBRcl.8 albeit without change (0.33 to 0.37-fold). Other changes to the arginine and proline metabolism were highly significant. Some examples are L-citrulline, L-proline, hydroxyproline, L-aspartate, and carboxynor-spermidine, which showed decreased levels of 2.0-, 4.2-, 5.4-, 7.5-, and 7.9-fold, respectively.

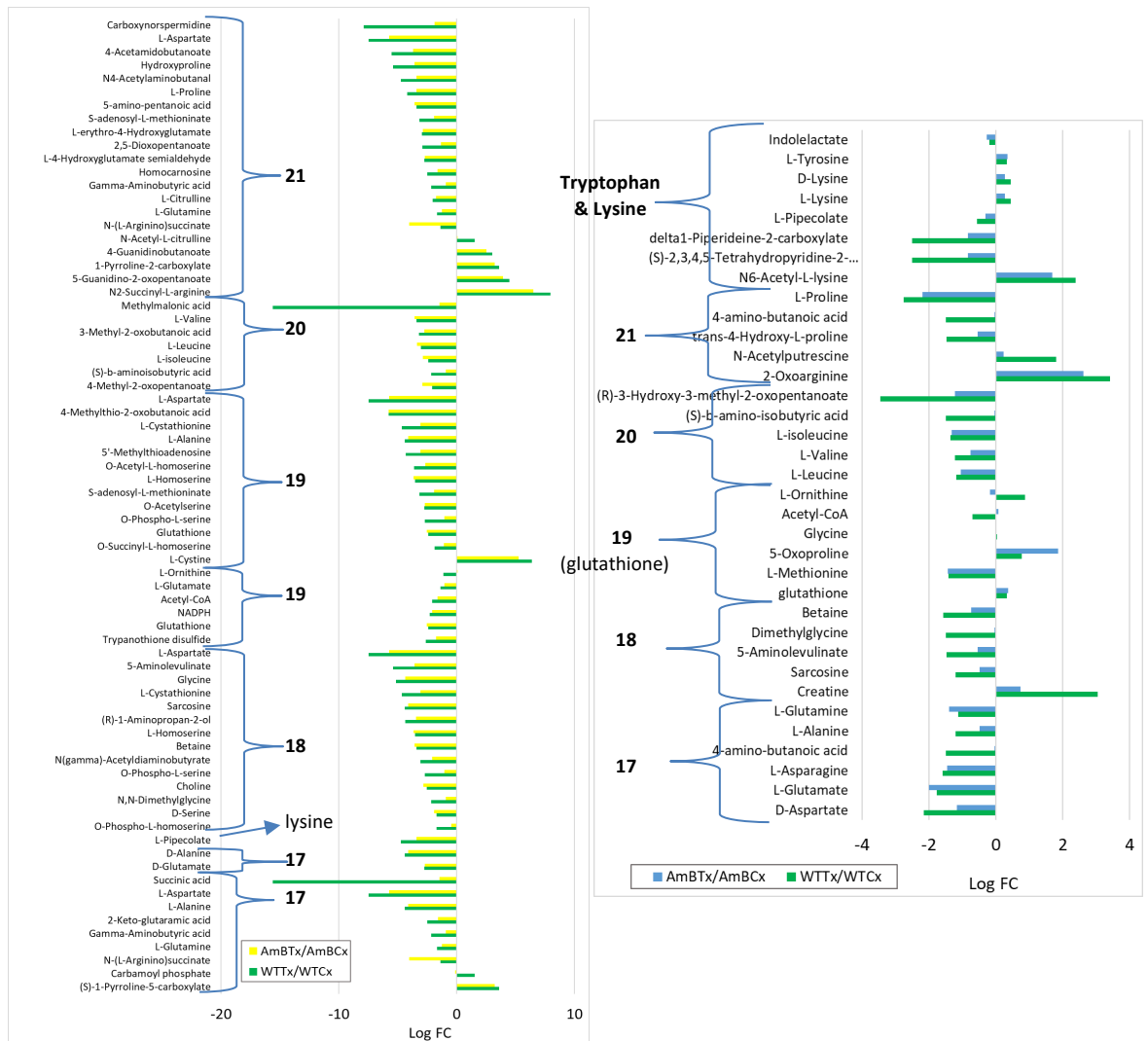


Figure 7-12. Changes in amino acids and polyamines metabolism.

Wild type (green in both panels), and resistant lines AmBRcl.14 (left panel, in yellow) and AmBRcl.8 (right panel in blue), were treated with 5 \times EC₅₀ (50 nM for wild type and 3 μ M for both resistant lines). Significant fold changes (Log FC, $P < 0.05$) are relative to untreated cells (x -axis). Each dataset is from four biological replicates. Numbers of individual pathways are: 17) Alanine, aspartate, glutamate; 18) Glycine, serine, threonine; 19) Glutathione, cysteine and methionine; 20) valine, leucine, isoleucine; 21) arginine and proline; 22) histidine. Abbreviations: WTTx/WTCx: wild type-treated relative to wild type untreated; AmBTx/AmBCx: AmBR lines-treated relative to AmBR untreated.

Other related metabolites followed the same trend in AmBRcl.14 and to a lesser extent in AmBRcl.8 (see Supplementary 9, Table 1 and page 8). The opposite trend was observed in a number of amino acids in this group, e.g. 2-oxoarginine (6.5- to 7.9-fold increase) and N2-succinyl-L-arginine (2.6- to 3.4-fold increase), in AmBRcl.8 and AmBRcl.14, respectively. The increase of N2-succinyl-L-arginine serves as substrate for the production of L-glutamate followed by the biosynthesis of arginine and proline, which requires NADPH. Likewise, the clear increase of 2-oxoarginine is also indicative of the catabolism of arginine. Signs of changes in disruption in other amino acid groups were also detected as were changes to the levels of some thiols and polyamines. Arginine and proline are of

particular interest, as they are related with the protection against ROS via the production of trypanothione, additionally the decrease of these amino acids, a clear signature between both resistant lines was not obvious and would require the addition of reference standards, however. In another study in *L. infantum* treated with miltefosine, depletion of these two groups was suggested to derive from their release from the cytoplasm after membrane damage (Vincent et al. 2014) which is an alternative explanation for AmB. Altogether this shows that short term treatment (15 min) with AmB has a significant impact on the fate of PTP metabolites, fitting with the hypothesis that AmB induces changes in the oxidative metabolism and causing an increase of ROS, and altering various pathways including, PPP, and PTP.

AmB is a good example of the redundancy of some peaks that are called by PiMP twice (or more). The mass of AmB is 924.1 g/mol based on the empirical formula, four peaks (peak ID numbers 349, 362, 1083 and 1257) were identified in the AmBRcl.14 dataset. The two formers showed a similar mass of 924.49 but differ in their RT (275.26 and 421.04). Likewise, the two latter had a similar mass of 946.47 and different RT values (424.8 and 277.19). Strikingly, two more peaks were manually found upon the basis of mass and RT, i.e. peaks 1952 and 1963, again, their mass was similar (922.48) and discrepancy between their RT values was observed (275 and 420.38) (Figure 7-13A). The fact that the first four peaks were identified in the positive-, as were the latter two in the negative polarity, can be attributed to the amphiphilic properties of AmB.

Neither mass nor RT identified AmB in the AmBRcl.8 experiment, possibly because this line has a deletion of the miltefosine transporter (MT), which is implicated in the susceptibility and resistance to AmB (Collett et al. 2019; Fernandez-Prada et al. 2016). AmBRcl.8 (and cl.6) was found to have the deletion of this transporter and was more resistant to miltefosine than WT (P values 0.0446 - 0.069), and with respect to the other two lines without this deletion (see section 3.2.3.2 for details). Similarly, AmBRcl.8 was significantly more resistant to AmB ($P \leq 0.0001$), than WT and both AmBR- cl.14 and - cl.3 ($P \leq 0.001$) (Figure 7-13B). Another reason for the less abundant amount of AmB in this line, can be that the exposure time of 15 min was very short, and as both lines had a significant loss of cellular ergosterol in the membrane, there is significant less target for AmB to bind, or a combination of both mechanisms which synergism prevented the uptake and binding of the drug, due to changes in the composition and fluidity of the membrane, although this is evidently, unexpected in the wild type.

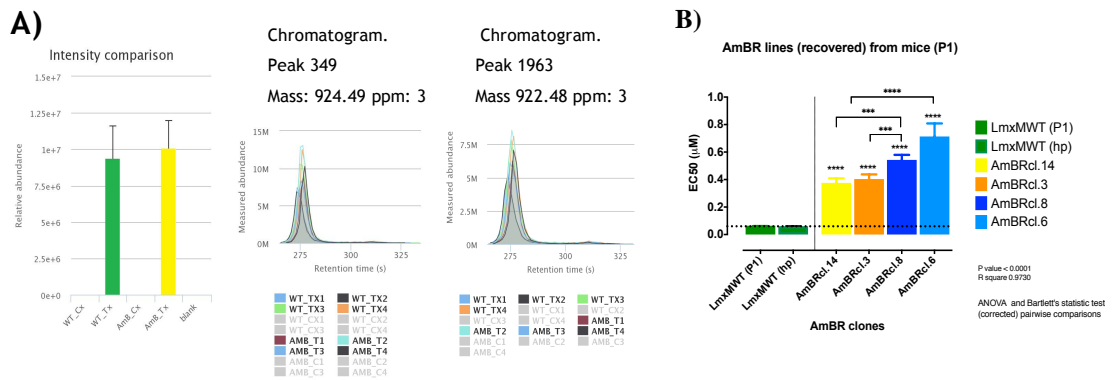


Figure 7-13. AmB abundance and susceptibility (EC₅₀) in the experimental groups. **PANEL A)** Data were processed with PiMP pipeline (Gloaguen, 2017). Mean values from four replicates are plotted with their standard deviation (bars). Significant fold changes after the treatment (WTTx relative to WTCx and AmBRTx relative to AmBRCx) are discussed in the text and showed in Supplementary 9 (see page 8). **PANEL B)** Mean EC₅₀ values are shown in µM with their standard deviation (bars). Tukey's multiple comparison test measured pairwise differences between each resistant line compared with wild type. Statistically significant values (P<0.05, 95% Confidence Interval) are shown with stars: *P ≤ 0.05, **P ≤ 0.01, ***P ≤ 0.001, ****P ≤ 0.0001). Here four AmBR lines (named cl.14, cl.8, cl.3 and cl.6 are shown). A full characterisation of these lines is discussed in chapters 3 to 5. Two wild types were tested here, P1-passage 1 after infection in mice, and hp-high passage (this was maintained in culture for at least 20 passages).

7.3 Discussion

This study provides insights upon the metabolic effects derived from the short-time (15 min) exposure to high concentrations (5 x EC₅₀) of the polyene AmB, in *L. mexicana* promastigotes. It is noteworthy that the changes observed here are representative of the effects of AmB in both, the two AmBR-lines that were selected for AmB-resistance over a period of nine months, and in the parental wild type cultured in parallel in the absence of drug (section 3.2.1.1, Figure 3-1). The use of the parental WT allows for the elimination, at least partially, those changes that arose stochastically as part of the long-term culture. Ideally, one should compare the parental WT from passage number one (at the beginning of the experiment) against the same cell line (without drug exposure) at the end of the experiment, this was beyond the aim of this thesis, however. Also, these datasets provide information on the changes derived from the long-term drug pressure alone (Supplementary 9, see pairwise comparison 1: AmBRCx versus WTCx from in each dataset) (see page 8). Also important (not analysed here), is to notice that some differences were observed between WT in both datasets, although this was a bit surprising, considering that the same parental line was used in both experiments. These changes reflect however, the variability that can be found between experiments. Evidently, many peaks were annotated as putative whereas others remained unidentified, however, authenticated annotations of the total metabolome that comprises hundreds or in some cases, thousands

of detected peaks is complex, and is beyond the aim of this thesis. Moreover, some peaks annotated several times under different names correspond isomers, albeit it is not possible to discriminate between them. Nonetheless, I provide the full lists of peaks, irrespective if they are annotated twice or more, which is of great value to understand the metabolome in a broader context. The use of targeted approaches, e.g. lipidomics, can however, help to corroborate the identity of specific peaks of interest.

Untargeted metabolomics identified some similarities in the pattern of changes observed between WT and AmBR lines, which strongly suggest that alternative MoA might be operating as a response to this polyene, and that these are independent of the binding to ergosterol, arguably, the main MoA of AmB in *Leishmania*. Although some differences between both lines tested, AmBRcl.14 and AmBRcl.8, were noticeable, these results also raise the hypothesis that the other MoA suggested in this study, are moreover independent of the sterol intermediates that replaced the wild type ergosterol (sterol profiling with GCMS is amply discussed in chapter 5). Of particular interest here, is the analysis of changes arose in lipid species other than sterols, as these molecules comprise the main structural components of the cell membrane, therefore relevant with respect to the MoA of AmB. Providing evidence that leads to hypothesize alternative MoA is one of the main contributions of using metabolomics in this study. Irrespective of the limitations of the method used here for the detection of lipids mentioned above (section 7.2.1), we identified disruption of the lipid metabolism after exposure to AmB, including GLs, GPLs and SLPs. These lipids interact with sterols in the membrane and are involved in the virulence of *Leishmania* (Ferguson 1999; Spath et al. 2003; Zhang et al. 2005; Zhang and Beverley 2010), and in other signalling functions (Guan and Mäser 2017). Ergosterol along with the polar lipids (phosphatidylcholine, phosphatidyl-ethanolamine and phospholipids), both are the major components of the *Leishmania* membranes (Rakotomanga, et al. 2005; Saint-Pierre-Chazalet et al. 2009). In my study, both these lipid classes decreased in AmBRcl.14, although a dramatic increase (5-fold) in sn-glycero-3-phosphoethanolamine was observed in this line. In AmBRcl.8, GLs and GPLs remained generally unaltered, but various SLPs increased notably. In the study of Fernandez-Prada and co-workers, an increase in phosphatidylethanolamine was also reported (Fernandez-Prada et al. 2016).

A limitation of the approach used here is, however, that cannot differentiate between isomers of these lipid classes (Figure 7-6), which identification is challenging due to the complexity of their large molecules. Altogether, these studies show the degree of complexity of the interaction between these lipid species, which is one possible source of the heterogeneity of changes identified. This is further supported by the fact that although

the loss of ergosterol is the main signature in all AmBR lines studied so far (Mbongo et al. 1998b; Mwenechanya et al. 2017; Pountain et al. 2019a; Purkait et al. 2012), this decrease is, however, not exclusive of the resistance to this polyene alone. In fact, decrease in ergosterol has been observed with other drugs, e.g. miltefosine. In the same trend, in this thesis I provide evidence that this loss of ergosterol also occurred in four lines selected for resistance to another polyene, nystatin (Nys) (section 3.2.1.2, Figure 3-3). Even though the latter was not surprising, considering that both AmB and Nys have a similar MoA (Table 1-2), this is, to the best of my knowledge, the first evidence of resistance against Nys in *Leishmania mexicana*.

Another notable finding of this study, was the notable changes in abundance related to the metabolism of these structural components of the *Leishmania* membrane observed in this study, are the pronounced decrease in the abundance of leucine. This amino acid is an essential precursor for the synthesis of both, sterols and phospholipids in *L. mexicana*. Also related is the decrease in the abundance of Acetyl-CoA, glyceraldehyde-3-phosphate and mevalonate (Figure 7-5). These three metabolites are essential for the synthesis of ergosterol. As shown in Figure 1-14, Acetyl-CoA is used by 3-hydroxy-3-methylglutaryl-CoA synthase (HMGS) to form HMG-CoA, which is then converted into mevalonate by the enzyme HMG-CoA reductase (HMGR), a NADPH dependent enzyme, and a rate-limiting step in the biosynthesis of ergosterol. After its synthesis within the mitochondrion, mevalonate is further metabolized in the glycosome. This sequence of reactions above described, can be related with the also significant reduced abundance of NADPH in one of these lines (Figure 7-9), thus confirming the central role of the PPP as the main source of this reduced cofactor and in the response in *Leishmania* to AmB.

It is relevant to remember that HMGR has been explored extensively as a potential drug target in *Leishmania* spp. (Dinesh et al. 2015; Sarkar and Manna 2015; Singh and Babu 2018). Moreover, in section 1.7.1, I presented evidence on the role of the sterol regulatory element-binding proteins (SREBPs) (Quan-zhen, Yan and Yuan-ying, 2016), which modulate LDL receptors and the enzyme HMGS (the previous step to HMGR in the SBP). Also present in *Leishmania*, SREBPs are involved in the protection of the parasite against ROS (Basu Ball et al., 2014). HMGR itself was upregulated after infection of macrophages with *L. mexicana* amastigotes (Semini et al., 2017). The increase of EPA in AmBRcl.14 was higher than in the WT. The lack of studies with regard to the role of EPA further complicates the interpretation of the increased observed here in AmBRcl.14, moreover, it is unknown if *Leishmania* can produce EPA. Currently, a group from the state of Bahia in the Northeast of Brazil, (<https://app.dimensions.ai/details/grant/grant.6941633>), is currently investigating

the role of these lipid mediators, EPA and DHA and their role in the host-pathogen interaction. Another study showed that this natural lipid, conjugated-EPA, has an effect on both, *L. donovani* promastigotes and the purified *Leishmania*-topoisomerase I (Vassallo, et al. 2011). The role of these metabolites in the MoA of AmB merits further investigation. Additionally, untargeted metabolomics provided evidence on the effects of AmB in the carbohydrates metabolism in wild type and AmBR parasites ergosterol-deficient. Although in general glycolysis shows a trend to the decrease, this could suggest that those metabolites that flux through the PPP have been consumed in response to the demand of production of NADPH by the PPP, leading to an increase in abundance of ROS from the respiratory chain that correspond to the increase in the flux through PPP. Interestingly, all PPP metabolites augmented in AmBRcl.8, while in the AmBRcl.14, only one metabolite from the non-oxidative branch, sedoheptulose-7-P, increased its abundance. The other products of the PPP in the latter of these lines were more similar to those changes found in the TKT-KO cell line, which in all cases, were more to the decrease trend. To the best of my knowledge, this is the first study in which the effects of AmB on the PPP have been confirmed using a TKT-KO.

The overexpression of the PPP enzymes, GPDH and 6PGDH (Figure 7-9), was accompanied by an increased consumption of glucose after exposing *L. donovani* to oxidative stress (Ghosh et al. 2015). This suggests that AmB exerts a similar increase in ROS, and these findings are in agreement with those from a previous report in AmBR of *L. mexicana* (PhD Thesis, Dr Raihana Nithin, unpublished). Interestingly, this upregulation of the PPP was absent in promastigotes cultured a serum-free culture medium, defined medium (DM), resembling that phenotype described above in the TKT-KO. While the AmBR line grown in DM developed resistance to AmB more gradually (and slowly) reaching a maximum level of resistance 4-fold lower than all four AmBR lines studied here (AmBRcl.14 and AmBRcl.8 were grown in HOMEM), some differences can be related to the lack of FBS (10%) in DM (see section 6.2.1 for the role of FBS on the MoA of AmB). This chapter provides a comprehensive list of metabolites useful as a platform for further analysis on alterations in metabolic pathways, in particular PTP and PPP, as a response to AmBR-exposure in both, wild type and laboratory generated AmBR mutants of *L. mexicana*.

8 General Discussion

Figure 8-1 provides a graphical overview of the scope of this thesis, chapters (Ch.-) 1 and 2, are not considered in this diagram.

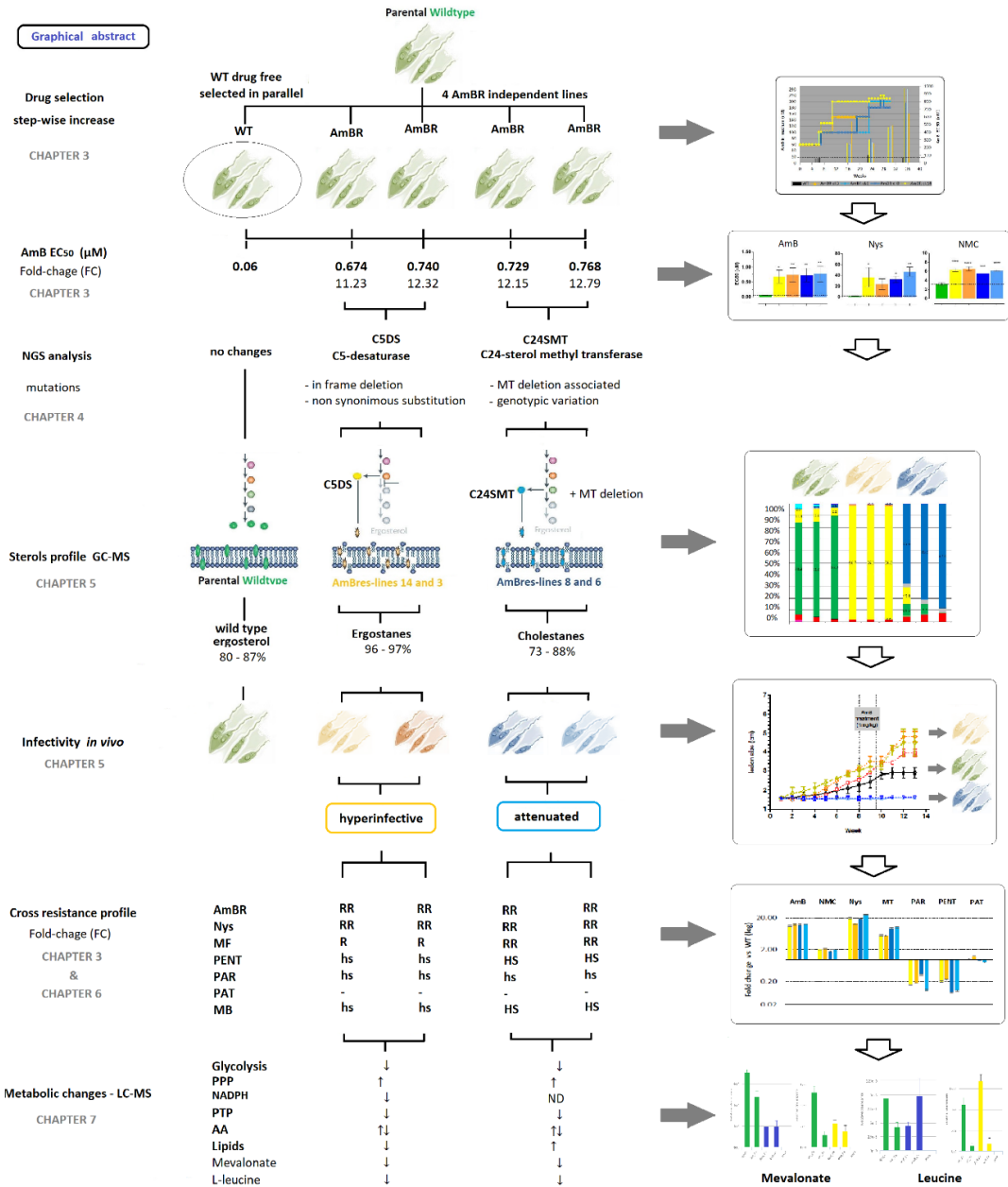


Figure 8-1. Graphical abstract of this Thesis.

Briefly, eight polyene-resistant lines were selected in parallel. Cross-resistance to antileishmanials and other compounds was performed (Ch.3). NGS identified genomic changes in two sterol genes (Ch.4) that triggered changes in cellular sterols (GCMS), which derived in two sterol-signatures that correlated with two reproducible phenotypes *in vivo*, i.e. virulent and attenuated (Ch.5). A new class of sterol-inhibitors was also investigated (Ch.6). Finally, untargeted metabolomics (LCMS) interrogated the MoA of AmB in two resistant-cell lines (Ch.7). RR: highly resistant, R: resistant, hs: hypersusceptible. Up- and down-arrows (↑ ↓) are increase and decrease, respectively. ND: not determined.

8.1 Drug susceptibility of amphotericin B resistant lines against different compounds

Although the definitive MoA of AmB is still unknown, this polyene is still the drug of choice for the treatment of the fatal form of the disease, Visceral leishmaniasis (VL). Other species that cause the cutaneous form, such as *L. mexicana*, are of similar importance, considering the social stigmatization and other mental health consequences that they generate (Bailey et al. 2019). Irrespective of the global prevalence of leishmaniasis showing a decreasing trend, and the progress achieved in recent years, some evidence shows increasing figures in some endemic areas (Table 1-1). The relatively infrequent resistance against AmB found in clinical isolates, has generated the perception that resistance against this polyene is unfeasible (Fairlamb, et al. 2016). Conversely, other work has identified AmB-resistance in clinical isolates (Purkait et al. 2012), including studies from non-endemic areas (Srivastava et al., 2011), and others in which AmB resistance was recognized from clinical cases identified before AmB became the frontline therapy for VL (Durand et al., 1998; Giorgio, 1999; Chakravarty and Sundar, 2010). In addition to this, there is evidence of intrinsic resistance to AmB and oxidative stress in some fungi. For instance, *Trichosporon beigelii* and *Aspergillus terreus*, have normal concentrations of ergosterol and high levels of catalase, respectively. Also, an increasing number of reports indicating resistance, and a recognition that methods to diagnose resistance in fungal strains are often flawed, complicates this picture (McCarthy et al. 2017). While the study of fungi is beyond the aims of this thesis, in *Leishmania* spp., a number of studies have also shown the feasibility of the appearance of AmB-resistance in laboratory strains (section 1.6.6.3). In addition to the AmBR lines developed, this thesis provides, to the best of my knowledge, the first evidence of the development of resistance to another polyene, nystatin (Nys), in *Leishmania* spp.

The methodology for the selection of drug resistance in *Leishmania* used in this study was similar for both polyenes. Promastigotes were cultured under drug pressure with AmBR and NysR over 30 and 20 weeks, respectively. Cross resistance profiling of all resistant mutants was then assessed for the antileishmanials, miltefosine (MF), pentamidine (PENT), paromomycin (PAR) and antimonials. Resistance against other polyenes was higher in all AmBR- compared to NysR-lines. Also, notable, was the small fold change (FC) observed with natamycin (NMC), a small polyene with a potentially different MoA than large polyenes, observed in AmBR- in comparison to NysR-lines. In a previous study in yeast, a similar inhibition pattern was observed between Nys and NMC, however, mutants lacking the sterol enzymes, C5-desaturase (C5DS) and C8-isomerase (C8SI),

triggered a loss of inhibition with both polyenes, indicating that the presence of double bonds within the sterol ring are implicated in the susceptibility to both antifungals (Te Welscher et al. 2010). While the role of the double bonds within the sterol ring is key for the binding of AmB (Hsuchen and Feingold, 1973), the role of the double bond at carbon 5,6 (performed by C5DS) the loss of which leads to AmB resistance, was recently identified for the first time in *L. mexicana* (Pountain et al. 2019b). In my study, five novel mutations were identified in C5DS (AmBRcl.14, AmBRcl.3 and NysRcl.B2) (section 4.1.5, Figure- 4-6 and 4-7). No evidence linking drug resistance to the double bond at position 7,8 of the sterol ring (C8SI-specific), has been found in *Leishmania* spp.

With regard to miltefosine, the higher levels of resistance observed in lines AmBRcl.8 and AmBRcl.6, was attributed to the deletion of the miltefosine transporter (MT) identified in these lines (Figure 4-4). Interestingly, other AmBR lines with a MT-deletion showed an increase of resistance within the range of 2-fold (Pountain et al. 2019b), while the values shown here (9.2 to 10-fold) in these two lines, are comparable to those reported in a MF-resistant line of *L. infantum* (11.95-fold) (Vincent et al. 2014). Changes in the MT have been previously found in other AmBR lines of *L. mexicana* (Pountain et al. 2019; PhD Thesis Dr. Raihana Ithinin, unpublished), suggesting that the MT is implicated in selection of resistance to AmB in some (but not all) AmBR lines. As with my study, the work of Pountain et al. and of Dr Ithinin, showed that the deletion of MT was accompanied by genomic changes in the C24-sterol methyltransferase (C24SMT), which resulted in the loss of expression of the latter and an altered sterol metabolism (increase of cholestane-like intermediates). The resistance derived from the loss of ergosterol is expected and has also been found in other MF-resistant cell lines of *L. infantum* (Fernandez-Prada *et al.*, 2016) and *L. donovani* (Rakotomanga, et al., 2005; Rakotomanga *et al.*, 2007). In the latter of these species, moreover, C24-alkylated sterols that are produced by C24SMT, were dramatically reduced in abundance (43%) after the treatment with MF, possibly because the substrate of C24SMT, zymosterol, is a membrane component that depends on sphingolipids (Veen and Lang 2005). More recently, a chemogenomic work in *T. brucei* confirmed the role of the MT, and other membrane associated hits, in the susceptibility to both, MF and AmB (Collett *et al.*, 2019). Other modes of resistance to AmB, e.g. efflux via multidrug resistant proteins 1 (MDR1), that are upregulated in some AmBR lines (*L. donovani*) (Purkait et al. 2012), cannot be ruled out, however.

A significant signature in all polyene resistant lines was the increase in susceptibility to PENT and PAR, identified across all eight selected lines and regardless of their mutations in different sterol-genes. In a similar trend, was the increase susceptibility found in all

AmBR-lines against methylene blue, an oxidative stress inducer (Kelner and Alexander, 1985). Intriguingly, the two lines with a deletion in the MT referred to above, were more sensitive to PENT and methylene blue, than the other two lines, AmBR- cl.14 and cl.3, with mutations in C5DS. Similar agment in susceptibility to PENT and methylene blue was reported previously in AmBR lines of *L. mexicana* (Mwenechanya et al. 2017; Pountain et al. 2019b), and in the work of another member from the Barrett Lab (PhD Thesis Dr. Raihana Ithinin, unpublished), suggesting a connection between polyene resistance and susceptibility to PENT, possibly related to modifications in the cell membrane of the parasite, e.g. ergosterol content, and possibly, other structural lipids. As with all four AmBR lines from my study, a clear signature of increased susceptibility towards PENT was consistent across all four NysR mutants (Figure 3-8). Considering that both polyenes AmB and Nys have presumably a MoA in *Leishmania* spp., targeting ergosterol in the membrane, and that the loss of the wild type ergosterol was also the main feature in these lines (Figure 5-5), this increased susceptibility is, possibly, related with the oxidative stress induced by PENT (Mehta and Shaha 2004), and to other metabolic alterations induced by AmB identified with LCMS (chapter 7), although further investigation is needed.

As resistance to existing drugs spreads, exploring new classes of compounds is essential. For this reason, I explored a library of new sterol inhibitors, 1,2,3-triazolylsterols (TAZ), with potential activity against C24SMT in *Leishmania* spp. Although very stable, TAZ inhibitors showed less potency in assays against *L. mexicana* promastigotes than that reported previously in other *Leishmania* species (Porta et al., 2014, 2017). TAZ inhibitors are analogues of azasterols (AZA) (Haughan, et al. 1995; Contreras, et al., 1997), however, no clear differences were identified between resistant lines, and in other mutants either lacking or over-expressing C24SMT. Two compounds were significantly less potent than all the other AZA-inhibitors, whereas non-significant differences between wild type and any of the mutant lines tested, were identified among those inhibitors that were more active (Figure 6-3). TAZ inhibitors showed activity against the recombinant *L. mexicana*-C24SMT in enzymatic assays and with comparable EC₅₀ values to those obtained in promastigotes *in vitro*, however, other potential MoAs of these compounds cannot be excluded. In agreement with this on-target activity, cholestane-type intermediates showed a marginal increase after exposure to the most potent compound from this library (Figure 6-10B). The increase of cholestanes is expected from C24SMT inhibitors, i.e. AZA (Magaraci et al., 2003). Accumulation of the preferred substrate of C24SMT, zymosterol, was also poor, possibly because the exposure-time to the compounds was insufficient to trigger sterol changes. These results suggest that TAZ compounds probably have other, as yet unknown targets, such as C14-sterol demethylase (C14DM) (Porta et al. 2017) and

even targets outside of the sterol biosynthesis pathway. Additional experiments are needed to further understand the MoA of these inhibitors in *Leishmania* spp.

8.2 Untargeted and targeted metabolomics in AmBR *Leishmania*

Untargeted metabolomics identified patterns of change between WT and two AmBR lines of *L. mexicana* promastigotes, after short-time exposure (15 min) to high concentrations (5 x EC₅₀) of AmB. These changes suggest that alternative routes independent of the binding to ergosterol and other sterol intermediates that replaced it AmBR lines (Figure 5-3), arguably the main MoA of AmB, might be operating in *Leishmania* (and possibly in fungi) as a response to AmB. Considering that AmBRcl.14 (virulent) triggered a higher inflammatory response in comparison with WT and two other AmBR lines (AmBRcl.8 and cl.6) that were non-pathogenic (avirulent) in mice (section 5.2.3, Figure 5-6), I speculated on the possibility of EPA being used by the parasite to inhibit the immune response and to facilitate its replication within the host macrophages, as identified by histology from tissue lesions (footpads) from infected mice (Figure 5-9). In the context of the interaction with the host, *Leishmania* interacts with macrophages by first avoiding the inflammatory phenotype of the macrophages (M1) and subsequently, when macrophages change into an anti-inflammatory phenotype (M2), they produce cytokines and other lipids such as arachidonic-, eicosapentaenoic, and docosahexaenoic-acids (AA, EPA and DHA), to diminish the inflammation (Das 2018). The loss or increase of ergostanes cannot be considered as the sole cause of the absence of virulence, it could be associated with the loss of some virulence factors found in the membrane of the parasite (GP63, lipophosphoglycan (LPG) and lipopolysaccharides (LPS) (Denny et al., 2004), although the latter is not present in *L. mexicana* (Torres-Guerrero et al. 2017). In the same sense, LCMS identified significant alterations of membrane lipids, such as GLs, GPLs and SLPs, which are known to interact with sterols and be related with the virulence of *Leishmania* (Ferguson 1999; Spath et al. 2003; Zhang et al. 2005; Zhang and Beverley 2010). The increase of ergosta-7,22-dien-3-ol is stage specific, increasing in stationary parasites (*L. infantum* virulent strain) (Yao and Wilson 2016). Although I did not measure the variation of sterols across the different growth phases of promastigotes, doing this can help to determine if a similar increase occurs in *L. mexicana*, and to determine if this differs in AmBR lines.

The reduced abundance of metabolites from glycolysis and TCA along with the increase of some enzymes from the PPP found in this study, are in agreement with the study of Dr Ithinin in AmBR-*L. mexicana*. Similar findings were observed in *L. donovani* after

oxidative stress exposure (Ghosh et al. 2015), but not in serum free medium nor in the TK-TKO, confirming the role of PPP in the response to AmBR ROS-generation. A role for enzymes of the glucose metabolism pathways has previously been related to the virulence of promastigotes in *L. mexicana* (Naderer et al. 2006). This central role of the PPP in the response in *Leishmania* to AmB is also related with the low abundance of mevalonate which is a product of the enzyme HMGR, which requires NADPH (NAPDH itself was also diminished after amphotericin B exposure).

8.3 Sterol profile and virulence of AmBR-resistant *Leishmania* in vivo

In previous studies, mutations in other enzymes such as C14DM, caused a similar loss of ergosterol in *L. mexicana* (Mwenechanya et al. 2017) and in *L. major*. In the latter of these mutants, an increase in the membrane fluidity, disruption of lipid rafts, and other morphological- and growth defects were concomitant with the loss of ergosterol (Xu et al. 2014). The loss of ergosterol has also been found in *L. infantum* resistant to MF (Fernandez-Prada et al. 2016), and in another mutant cell line of *L. major* (Δ LCB2) lacking the sphingolipid pathway (Armitage et al. 2018; Denny, et al. 2004). These studies highlight the importance of the interplay between these two lipid components of the membrane with respect to the MoA of AmB. Interestingly, ergosterol, and other membrane lipids (fatty acids), decrease during the transformation of promastigotes into amastigotes (Bouazizi-Ben Messaoud et al. 2017).

The role of the lipid membrane is intriguing, particularly if we consider that in my study, I also identified an attenuated phenotype in AmBRcl.8 and AmBRcl.6, which considering the absence of gross (lesions) and microscopic (histopathology) findings, most likely failed to replicate *in vivo* albeit remained viable within the host (amastigotes were also recovered post-infection from these two lines). The role of the parasite persistence factors was previously described in a cell line of *L. major* (also a cutaneous specie) lacking phosphoglycans and which was non-pathogenic within the host (Spath et al. 2003). A similar attenuated phenotype (absence of lesions) was described in another work with *L. mexicana* and the authors suggested that this lack of infectivity was related with the down regulation of virulence factors such as Th2 associated cytokines, which were on the other hand, were upregulated in virulent parasites (Ali et al. 2013). Other studies have described avirulent phenotypes after exposure to gentamycin (Daneshvar et al. 2009; Daneshvar et al., 2010), and to the chelating agent, methyl-beta-cyclodextrin (M β CD) that depletes ergosterol and other sterols after 1 hour (Yao et al. 2013).

The attenuated phenotype resembles that observed in persister-cells, although the latter are non-mutant cells, instead persister-cells are acknowledged as dormant phenotype that have evolved sophisticated immune evasion mechanisms (Fairlamb et al. 2016; Melorose, et al. 2015). In fungi, persister-cells are commonly found in biofilms. Interestingly, these fungi have up-regulation of some ergosterol-related genes (Silva et al. 2017). Although little has been investigated in *Leishmania*, this intriguing persister-like phenotype in protozoa was recently addressed to be related with drug treatment failure (Barrett et al. 2019). In my study, I identified a similar phenotype in axenic wild type promastigotes cultured *in vitro*, which after being exposed to different inhibitors, e.g. imipramine and AmB, restarted normal growth after three or four days (Figure 6-1, panels A to C).

The virulent and attenuated phenotypes, correspond to a dramatic accumulation of ergosta-7,22-dien-3-ol (96-97%) and cholesta-5,7,22-trienol (86-88%), respectively. While the increase of the latter has been associated with loss of expression and disruption of C24SMT (Gigante et al. 2009; Gros et al. 2006; Jiménez-Jiménez et al. 2008; Lorente et al. 2004; Magaraci et al. 2003), the accumulation of ergostane-type intermediates is less well studied but has been related with a hypervirulent phenotype in *L. infantum* metacyclic promastigotes (Yao and Wilson 2016). The study that identified the role of C5DS in AmB resistance in *L. mexicana* is currently the only evidence of this (Pountain et al. 2019b). While the study of Pountain et al., addressed the role of C5DS in AmB resistance, in their work, no clear association is presented with regard to the role of the accumulation of ergostanes *in vivo*. This is the first study showing evidence of a similar increase in resistance to AmB and ergostanes, derived from selection for resistance against Nys, in *Leishmania* spp. In the present study, however, ergostane-like intermediates accumulated in two AmBR lines (increase of ergostanes was also seen in all four NysR lines) which phenotype was preserved *in vitro* and *in vivo*. In this study, five novel mutations were identified in C5DS in two mutants (M93del in AmBRcl.14, V74E in AmBRcl.3, and R244L in both these lines) (section 5.2.3, Table 4-2). Similarly, ergosta-7,22-dien-3-ol was the most abundant sterol intermediate (up to 80.2-89.1%) in all four lines selected for nystatin, presumably derived from mutations in C5DS. Interestingly, NGS of the most resistant clone, NysRcl.B2, also showed novel mutations (e.g. A95del) in C5DS (sequencing of all clones was not possible due to costs) (see Figure 4-7). In this study, and others performed by former members of the Barrett Lab, we have shown that the emergence of resistance against polyene anti-leishmanials is feasible *in vitro* and with relative ease. Moreover, this study shows an association between sterol intermediates and virulence *in vivo*.

In addition, response to treatment with AmB (as deoxycholate) was noted in the parental wild type, while AmBRcl.14 and AmBRcl.3, and were both unresponsive to AmB *in vivo*, confirming that the resistant phenotype can be retained within the host. Furthermore, retention of resistance post-infection was confirmed *in vitro* (Alamar blue assay, section 2.4) in all four AmBR lines, using both AmB (as deoxycholate) and the liposomal formulation of AmB, AmBisome. While the EC₅₀ values of AmB were consistent with those found before infecting mice (Figure 5-8A, and 7-13B), AmBisome also showed an increase in resistance in all AmBR lines tested between 12- and 49-fold (Table 5-4). A separate experiment assessed the response to AmBisome *in vivo*. In this experiment, a higher number of parasites was recovered from footpad lesions than from lymph nodes, however, treatment with AmBisome (8 and 15 mg/kg) showed no effect in the reduction of WT- in comparison with AmBR-parasites. The lack of efficacy of AmBisome in this experiment was unexpected. Moreover, we were not able to recover tissue from untreated mice (placebo group injected with dextrose 5%), which further complicates the interpretation of results from this experiment.

With regard to the infectivity/virulence (both which are different concepts), it is necessary to assess the response to treatment and retention of resistance in amastigotes macrophage *in vitro* models. Likewise, quantification of parasite replication using qPCR will test the capacity of the parasites to replicate intra-macrophages (Ponte-Sucre et al. 2017) and to differentiate from other pro-inflammatory factors and from accumulation of the drug at the infection site involved which can influence the immune response (in *L. major*) and the activity of liposomal amphotericin B (Voak et al. 2018; Wijnant et al. 2018; Wijnant et al. 2018). In these studies, the response to treatment with AmBisome (and other liposomal formulations), was shown to be dependent on concentration and formulation of AmB, alongside with the disease stage, *Leishmania* spp., tissue inflammation and infection site.

8.4 Conclusions and future work

This study adds to the field in providing evidence on the risk of emergence of AmB (and other polyenes) resistance in *Leishmania*, which conveys the risk of cross resistance with other antileishmanials currently in use, such as miltefosine. The increase in susceptibility identified in all AmBR and NysR lines, to pentamidine and to paromomycin, is indicative that alternative treatments might be considered should AmB resistance emerge in the field. On the contrary, a role of the deletion of the miltefosine transporter was associated with

increase in resistance to both AmBR and MF, indicating a possible risk of (occasional) cross resistance emerging between these drugs.

Characterisation of four AmBR and four NysR lines identified an association between the genomic changes in two sterol enzymes, C24SMT (only in AmBR-lines) and C5DS and their sterol profiling in *Leishmania mexicana* and *L. infantum*. Notably, this is the first study in which resistance towards a polyene other than AmB, i.e. nystatin, has been achieved in *Leishmania* spp. and the implications related with AmB resistance were until now, unknown.

Importantly, novel mutations in C5DS derived from selection for resistance to Nys were also associated with the loss of the wild type ergosterol (as with all AmBR lines), alongside with the increase in ergostane-intermediates requires further characterisation of these four NysR clones in the context of *in vitro* and *in vivo* models. These additional studies would be of relevance towards a better understanding on the appearance of polyene-resistance in *Leishmania* spp.

Additional approaches (e.g. CRISPRcas9 multiplex in 96-wells plates) would allow for the screening of the entire library KOs lacking the genes of the sterol pathway, as well as gene editing of known SNPs and indels which were identified in this thesis, with further functional validation of the role of these changes in the context of resistance towards AmB (the drug of choice in visceral leishmaniasis) using other genetic tools, i.e. gene complementation.

Moreover, this study shows that AmBR resistance can be carried *in vivo*, however, additional investigation is recommended in order to understand the mechanism of this resistance and to differentiate the virulent/attenuated phenotypes from other pro-inflammatory changes. Our *in vivo* model showed that AmBR parasites are adaptable *in vivo* and that the attenuated phenotype, cannot be unequivocally associated with fitness cost, particularly, after viable parasites recovered from tissue showed a similar retention of resistant to those lines with virulent phenotype.

The use of other models is also essential to expand the characterisation of these resistant lines, such as: drugs susceptibility to the antileishmanials in the amastigote macrophage *in vitro* model and other animal models (Wijnant et al. 2018) which use different infection sites and qPCR to determine parasite replication. Moreover, a full characterisation of the phenotype both *in vitro* and *in vivo* of all four AmBR- and nystatin-mutants, is also crucial to be carried out.

List of References

- Abongomera, Charles, Tullia Battaglioli, Cherinet Adera, and Koert Ritmeijer. 2019. "Severe Post-Kala-Azar Dermal Leishmaniasis Successfully Treated with Miltefosine in an Ethiopian HIV Patient." *International Journal of Infectious Diseases* 81:221–24.
- Abongomera, Charles, Ermias Diro, Alan de Lima Pereira, Jozefien Buyze, Kolja Stille, Fareed Ahmed, Johan van Griensven, and Koert Ritmeijer. 2018. "The Initial Effectiveness of Liposomal Amphotericin B (AmBisome) and Miltefosine Combination for Treatment of Visceral Leishmaniasis in HIV Co-Infected Patients in Ethiopia: A Retrospective Cohort Study." *PLoS Neglected Tropical Diseases* 12(5):1–19.
- Abuaita, Basel H., Tracey L. Schultz, and Mary X. O'Riordan. 2018. "Mitochondria-Derived Vesicles Deliver Antimicrobial Reactive Oxygen Species to Control Phagosome-Localized Staphylococcus Aureus." *Cell Host & Microbe* 24(5):625–636.e5.
- Adler-Moore, Jill P., Jean Pierre Gangneux, and Peter G. Pappas. 2016. "Comparison between Liposomal Formulations of Amphotericin B." *Medical Mycology* 54(3):223–31.
- Adler-Moore, Jill P. and R. T. Proffitt. 2008. "Amphotericin B Lipid Preparations: What Are the Differences?" *Clinical Microbiology and Infection* 14(SUPPL. 4):25–36.
- Afgan, Enis, Dannon Baker, B er enice Batut, Marius van den Beek, Dave Bouvier, Martin  ech, John Chilton, Dave Clements, Nate Coraor, Bj orn A. Gr uning, Aysam Guerler, Jennifer Hillman-Jackson, Saskia Hiltemann, Vahid Jalili, Helena Rasche, Nicola Soranzo, Jeremy Goecks, James Taylor, Anton Nekrutenko, and Daniel Blankenberg. 2018. "The Galaxy Platform for Accessible, Reproducible and Collaborative Biomedical Analyses: 2018 Update." *Nucleic Acids Research* 46(W1):W537–44.
- Ait-Oudhia, K., E. Gazanion, D. Sereno, B. Oury, J. P. Dedet, F. Pratlong, and L. Lachaud. 2012. "In Vitro Susceptibility to Antimonials and Amphotericin B of Leishmania Infantum Strains Isolated from Dogs in a Region Lacking Drug Selection Pressure." *Veterinary Parasitology* 187(3–4):386–93.
- Akhoundi, Mohammad, Katrin Kuhls, Arnaud Cannet, Jan Votypka, Pierre Marty, Pascal Delaunay, and Denis Sereno. 2016. "A Historical Overview of the Classification, Evolution, and Dispersion of Leishmania Parasites and Sandflies." *PLoS Neglected Tropical Diseases* 10(3):1–40.
- Akpunarielva, Snezhana, Stefan Weidt, Dhilia Lamasudin, Christina Naula, David Henderson, Michael Barrett, Karl Burgess, and Richard Burchmore. 2017. "Integration of Proteomics and Metabolomics to Elucidate Metabolic Adaptation in Leishmania." *Journal of Proteomics* 155:85–98.
- Al-Mohammed, Hamdan I., Michael L. Chance, and Paul A. Bates. 2005. "Production and Characterization of Stable Amphotericin-Resistant Amastigotes and Promastigotes of Leishmania Mexicana." *Antimicrobial Agents and Chemotherapy* 49(8):3274–80.
- Alcazar-Fuoli, Laura and Emilia Mellado. 2012. "Ergosterol Biosynthesis in Aspergillus Fumigatus: Its Relevance as an Antifungal Target and Role in Antifungal Drug Resistance." *Frontiers in Microbiology* 3(JAN):1–6.
- Alcazar-Fuoli, Laura, Emilia Mellado, Guillermo Garcia-Effron, Maria J. Buitrago, Jordi F. Lopez, Joan O. Grimalt, J. Manuel Cuenca-Estrella, and Juan L. Rodriguez-Tudela. 2006. "Aspergillus Fumigatus C-5 Sterol Desaturases Erg3A and Erg3B: Role in Sterol Biosynthesis and Antifungal Drug Susceptibility." *Antimicrobial Agents and Chemotherapy* 50(2):453–60.
- Ali, K. S., R. C. Rees, C. Terrell-Nield, and S. A. Ali. 2013. "Virulence Loss and Amastigote Transformation Failure Determine Host Cell Responses to Leishmania Mexicana." *Parasite Immunology* 35(12):441–56.
- Ali, S. Atif, Bashir Ahmad, and M. Masoom. 1998. *A SEMISYNTHETIC FETAL CALF SERUM-FREE LIQUID MEDIUM FOR IN VITRO CULTIVATION OF LEISHMANIA PROMASTIGOTES*. Vol. 59.
- Altschul, Stephen F., John C. Wootton, E. Michael Gertz, Richa Agarwala, Aleksandr Morgulis, Alejandro A. Sch affer, and Yi-Kuo Yu. 2005. "Protein Database Searches Using Compositionally Adjusted Substitution Matrices." *The FEBS Journal* 272(20):5101–9.
- Anders, S., P. T. Pyl, and W. Huber. 2015. "HTSeq--a Python Framework to Work with High-Throughput Sequencing Data." *Bioinformatics* 31(2):166–69.
- Anderson, Thomas M., Mary C. Clay, Alexander G. Cioffi, Katrina A. Diaz, Grant S. Hisao, Marcus D. Tuttle, Andrew J. Nieuwkoop, Gemma Comellas, Nashrah Maryum, Shu Wang, Brice E. Uno, Erin L. Wildeman, Tamir Gonen, Chad M. Rienstra, and Martin D. Burke. 2014. "Amphotericin Forms an Extramembranous and Fungicidal Sterol Sponge." *Nature Chemical Biology* 10(5):400–406.
- Andrade-Narv ez, Fernando J., Alberto Vargas-Gonz alez, Silvia B. Canto-Lara, and Alma G. Dami an-Centeno. 2001. "Clinical Picture of Cutaneous Leishmaniasis Due to Leishmania (Leishmania) Mexicana in the Yucatan Peninsula, Mexico." *Memorias Do Instituto Oswaldo Cruz* 96(2):163–67.
- Andrade-Neto, Valter Viana, Herbert Leonel de Matos-Guedes, Daniel Cl audio de Oliveira Gomes, Marilene Marcuzzo do Canto-Cavalheiro, Bartira Rossi-Bergmann, and Eduardo Caio Torres-Santos. 2012. "The Stepwise Selection for Ketoconazole Resistance Induces Upregulation of C14-Demethylase (CYP51) in Leishmania Amazonensis." *Memorias Do Instituto Oswaldo Cruz* 107(3):416–19.
- Andrade-Neto, Valter Viana, Nuccia Nicole Theodore Cicco, Ed ezio Ferreira Cunha-Junior, Marilene Marcuzzo Canto-Cavalheiro, Georgia Correa Atella, and Eduardo Caio Torres-Santos. 2011. "The Pharmacological Inhibition of Sterol Biosynthesis in Leishmania Is Counteracted by Enhancement of LDL Endocytosis." *Acta Tropica* 119:194–98.
- Andrade-Neto, Valter Viana, Th ais Martins Pereira, Marilene do Canto-Cavalheiro, and Eduardo Caio Torres-Santos. 2016. "Imipramine Alters the Sterol Profile in Leishmania Amazonensis and Increases Its Sensitivity to Miconazole." *Parasites & Vectors* 9(1):183.
- Antonia, Alejandro L., Liuyang Wang, and Dennis C. Ko. 2018. "A Real-Time PCR Assay for Quantification of Parasite Burden in Murine Models of Leishmaniasis." *PeerJ* 6(CI):e5905.
- Aoki, Juliana Ide, Sandra Marcia Muxel, Juliane Cristina Ribeiro Fernandes, and Lucile Maria Floeter-Winter. 2018. "The Polyamine Pathway as a Potential Target for Leishmaniasis Chemotherapy." P. 13 in *Leishmaniasis as Re-emerging Diseases*. Vol. i. InTech.
- Arango Duque, Guillermo and Albert Descoteaux. 2015. "Leishmania Survival in the Macrophage: Where the Ends Justify the Means." *Current Opinion in Microbiology* 26:32–40.
- Arjmand, Mohammad, Azadeh Madrakian, Ghader Khalili, Ali Najafi Dastnaee, Zahra Zamani, and Ziba Akbari. 2016. "Metabolomics-Based Study of Logarithmic and Stationary Phases of Promastigotes in Leishmania Major By1H NMR Spectroscopy." *Iranian Biomedical Journal* 20(2):77–83.
- Armitage, Emily G., Amjed Q. I. Alqaisi, Joanna Godziel, Imanol Pe a, Alison J. Mbekeani, Vanesa Alonso-Herranz, Angeles L opez-Gonz alez, Julio Mart ın, Raquel Gabarro, Paul W. Denny, Michael P. Barrett, and Coral Barbas.

2018. "Complex Interplay between Sphingolipid and Sterol Metabolism Revealed by Perturbations to the Leishmania Metabolome Caused by Miltefosine." *Antimicrobial Agents and Chemotherapy* 62(5):1–12.
- Atan, Nasrin Amiri Dash, Mehdi Koushki, Nayeb Ali Ahmadi, and Mostafa Rezaei-Tavirani. 2018. "Metabolomics-Based Studies in the Field of Leishmania/Leishmaniasis." *Alexandria Journal of Medicine* 54(4):383–90.
- Azas, N., C. Di Giorgio, F. Delmas, M. Gasquet, and P. Timon-David. 2001. "No Evidence of Oxidant Events in Amphotericin B Cytotoxicity versus *L. Infantum* Promastigotes." *Parasite* 8(4):335–41.
- Baginski, Maciej, Haluk Resat, and Edward Borowski. 2002. *Comparative Molecular Dynamics Simulations of Amphotericin B-Cholesterol/Ergosterol Membrane Channels*.
- Bailey, Freddie ID, Karina Mondragon-Shem, Lee Rafuse Haines, Amina Olabi, Ahmed AlorfiID, José Antonio Ruiz-Postigo, Jorge Alvar, Peter Hotez, Emily R. Adams, Ivá D. Vélez, Waleed Al-Salem, Julian Eaton, Ivaro Acosta-SerranoID, and David H. Molyneux. 2019. "Cutaneous Leishmaniasis and Co-Morbid Major Depressive Disorder: A Systematic Review with Burden Estimates."
- Baker, J. R. 1969. *Parasitic Protozoa*. London: Hutchinson University Library.
- Banerjee, Antara, Jayeeta Roychoudhury, and Nahid Ali. 2008. "Stearylamine-Bearing Cationic Liposomes Kill Leishmania Parasites through Surface Exposed Negatively Charged Phosphatidylserine." *Journal of Antimicrobial Chemotherapy* 61(1):103–10.
- Bansal, Ruby, Shib Sankar Sen, Rohini Muthuswami, and Rentala Madhubala. 2019. "A Plant like Cytochrome P450 Subfamily CYP710C1 Gene in Leishmania Donovanii Encodes Sterol C-22 Desaturase and Its Over-Expression Leads to Resistance to Amphotericin B" edited by H. L. Nakhasi. *PLOS Neglected Tropical Diseases* 13(4):e0007260.
- Barbas-Bernardos, Cecilia, Emily G. Armitage, Antonia García, Salvador Mérida, Amparo Navea, Francisco Bosch-Morell, and Coral Barbas. 2016. "Looking into Aqueous Humor through Metabolomics Spectacles – Exploring Its Metabolic Characteristics in Relation to Myopia." *Journal of Pharmaceutical and Biomedical Analysis* 127:18–25.
- Bard, M., N. D. Lees, T. Turi, D. Craft, L. Cofrin, R. Barbuch, C. Koegel, and J. C. Loper. 1993c. "Sterol Synthesis and Viability Of erg11 (Cytochrome P450 Lanosterol Demethylase) Mutations In *Saccharomyces Cerevisiae* And *Candida Albicans*." *Lipids* 28(11):963–67.
- Bari, Vinay K., Sushma Sharma, Md Alfatah, Alok K. Mondal, and K. Ganesan. 2015. "Plasma Membrane Proteolipid 3 Protein Modulates Amphotericin B Resistance through Sphingolipid Biosynthetic Pathway." *Scientific Reports* 5.
- Barisón, María Julia, Ludmila Nakamura Rapado, Emilio F. Merino, Elizabeth Miekó Furusho Pral, Brian Suarez Mantilla, Leticia Marchese, Cristina Nowicki, Ariel Mariano Silber, and Maria Belen Cassera. 2017. "Metabolomic Profiling Reveals a Finely Tuned, Starvation-Induced Metabolic Switch in *Trypanosoma Cruzi* Epimastigotes." *Journal of Biological Chemistry* 292(21):8964–77.
- Barker, Katherine S., Sarah Crisp, Nathan Wiederhold, Russell E. Lewis, Bart Bareither, James Eckstein, Robert Barbuch, Martin Bard, and P. David Rogers. 2004. "Genome-Wide Expression Profiling Reveals Genes Associated with Amphotericin B and Fluconazole Resistance in Experimentally Induced Antifungal Resistant Isolates of *Candida Albicans*."
- Barratt, Joel, Alexa Kaufner, Bryce Peters, Douglas Craig, Andrea Lawrence, Tamalee Roberts, Rogan Lee, Gary McAuliffe, Damien Stark, and John Ellis. 2017. "Isolation of Novel Trypanosomatid, *Zelonía Australiensis* Sp. Nov. (Kinetoplastida: Trypanosomatidae) Provides Support for a Gondwanan Origin of Digenous Parasitism in the Leishmaniinae." *PLoS Neglected Tropical Diseases* 11(1):1–26.
- Barrett, Michael P. and Simon L. Croft. 2012. "Management of Trypanosomiasis and Leishmaniasis." *British Medical Bulletin* 104(1):175–96.
- Barrett, Michael P., Dennis E. Kyle, L. David Sibley, Joshua B. Radke, and Rick L. Tarleton. 2019. "Protozoan Persister-like Cells and Drug Treatment Failure." *Nature Reviews Microbiology* 17(10):607–20.
- Basselin, Badet-Denisot, Lawrence, and Robert-Gero. 1997. "Effects of Pentamidine on Polyamine Level and Biosynthesis in Wild-Type, Pentamidine-Treated, and Pentamidine-Resistant *Leishmania*." *Experimental Parasitology* 85(3):274–82.
- Basselin, Mireille, † Hubert Denise, Graham H. Coombs, and Michael P. Barrett. 2002. "Resistance to Pentamidine in *Leishmania Mexicana* Involves Exclusion of the Drug from the Mitochondrion." *ANTIMICROBIAL AGENTS AND CHEMOTHERAPY* 46(12):3731–38.
- Bastin, Philippe, André Stephan, Jayne Raper, Jean-Marie Saint-Remy, Frederik R. Opperdoes, and Pierre J. Courtoy. 1996. "An Mr 145000 Low-Density Lipoprotein (LDL)-Binding Protein Is Conserved throughout the Kinetoplastida Order." *Molecular and Biochemical Parasitology* 76(1–2):43–56.
- Basu Ball, Writoban, Madhuchhanda Mukherjee, Supriya Srivastav, and Pijush K. Das. 2014. "*Leishmania Donovanii* Activates Uncoupling Protein 2 Transcription to Suppress Mitochondrial Oxidative Burst through Differential Modulation of SREBP2, Sp1 and USF1 Transcription Factors." *The International Journal of Biochemistry & Cell Biology* 48:66–76.
- Bates, P. A., C. D. Robertson, L. Tetley, and G. H. Coombs. 1992. "Axenic Cultivation and Characterization of *Leishmania Mexicana* Amastigote-like Forms." *Parasitology* 105 (Pt 2):193–202.
- Bates, P. A. and L. Tetley. 1993. "*Leishmania Mexicana*: Induction of Metacyclogenesis by Cultivation of Promastigotes at Acidic PH." *Experimental Parasitology* 76(4):412–23.
- Bates, Paul A. 2018. "Revising *Leishmania*'s Life Cycle." *Nature Microbiology* 3(5):529–30.
- Batushansky, Albert, Satoshi Matsuzaki, Maria F. Newhardt, Melinda S. West, Timothy M. Griffin, and Kenneth M. Humphries. 2019. "GC-MS Metabolic Profiling Reveals Fructose-2,6-Bisphosphate Regulates Branched Chain Amino Acid Metabolism in the Heart during Fasting." *Metabolomics* 15(2):18.
- Bekersky, Ihor, Robert M. Fielding, Dawna E. Dressler, Jean W. Lee, Donald N. Buell, and Thomas J. Walsh. 2002. "Plasma Protein Binding of Amphotericin B and Pharmacokinetics of Bound versus Unbound Amphotericin B after Administration of Intravenous Liposomal Amphotericin B (AmBisome) and Amphotericin B Deoxycholate." *Antimicrobial Agents and Chemotherapy* 46(3):834–40.
- Ben-Ami, R., R. E. Lewis, and D. P. Kontoyiannis. 2008. "Immunocompromised Hosts: Immunopharmacology of Modern Antifungals." *Clinical Infectious Diseases* 47(2):226–35.
- Beneke, T., R. Madden, L. Makin, Valli J, J. Sunter, and Gluenzm E. 2016. "A CRISPR-Cas9 High-Throughput Genome Editing Toolkit for Kinetoplastids: Supplementary Information." *Handbook of Generation IV Nuclear Reactors* 859–69.
- Beneke, Tom, Ross Madden, Laura Makin, Jessica Valli, Jack Sunter, and Eva Gluenz. 2017b. "A CRISPR Cas9 High-Throughput Genome Editing Toolkit for Kinetoplastids." *Royal Society Open Science* 4(5):170095.
- Berens Randy, Brun Reto, and Krassner Stuart. 1976. "A Simple Monophasic Medium for Axenic Culture of Hemoflagellates Author (s): Randy L . Berens , Reto Brun and Stuart M . Krassner Published by : Allen Press on Behalf of The American Society of Parasitologists Stable URL : <http://www.jstor.org/stable/32>." *THE JOURNAL OF PARASITOLOGY* 62(3):360–65.
- Berg, Maya, Raquel García-Hernández, Bart Cuppers, Manu Vanaerschot, José I. Manzano, José A. Poveda, José A.

- Ferragut, Santiago Castanys, Jean-Claude Dujardin, and Francisco Gamarro. 2015. "Experimental Resistance to Drug Combinations in *Leishmania Donovanii*: Metabolic and Phenotypic Adaptations."
- Bhandari, Vasundhara, Arpita Kulshrestha, Deepak Kumar Deep, Olivia Stark, Vijay Kumar Prajapati, V. Ramesh, Shyam Sundar, Gabriele Schonian, Jean Claude Dujardin, and Poonam Salotra. 2012. "Drug Susceptibility in *Leishmania* Isolates Following Miltefosine Treatment in Cases of Visceral Leishmaniasis and Post Kala-Azar Dermal Leishmaniasis."
- Bhandari, Vasundhara, Shyam Sundar, Jean Claude Dujardin, and Poonam Salotra. 2014. "Elucidation of Cellular Mechanisms Involved in Experimental Paromomycin Resistance in *Leishmania Donovanii*." *Antimicrobial Agents and Chemotherapy* 58(5):2580–85.
- Biagi. 1974. *Enfermedades Parasitarias*. Fournier.
- Birkholtz, Lyn-Marie, Marni Williams, Jandeli Niemand, Abraham I. Louw, Lo Persson, and Olle Heby. 2011. "Polyamine Homeostasis as a Drug Target in Pathogenic Protozoa: Peculiarities and Possibilities." *Biochemical Journal* 438(2):229–44.
- Blankenberg, Daniel, Gregory Von Kuster, Nathaniel Coraor, Guruprasad Ananda, Ross Lazarus, Mary Mangan, Anton Nekrutenko, and James Taylor. 2010. "Galaxy: A Web-Based Genome Analysis Tool for Experimentalists." in *Current Protocols in Molecular Biology*. Hoboken, NJ, USA: John Wiley & Sons, Inc.
- Blum, J. J. 1993. "Intermediary Metabolism of *Leishmania*." *Parasitology Today* 9(4):118–22.
- Boggiatto, Paola Mercedes, Katherine Nicole Gibson-Corley, Kyle Metz, Jack Michael Hostetter, Kathleen Mullin, and Christine Anne Petersen. 2011. "Transplacental Transmission of *Leishmania Infantum* as a Means for Continued Disease Incidence in North America" edited by M. Boelaert. *PLoS Neglected Tropical Diseases* 5(4):e1019.
- Bolard. 1986. *How Do the Polyene MacroUde Antibiotics Affect the Cellular Membrane Properties?* Vol. 864.
- Bolard, J., P. Legrand, F. Heitz, and B. Cybulska. 1991. "One-Sided Action of Amphotericin B on Cholesterol-Containing Membranes Is Determined by Its Self-Association in the Medium." *Biochemistry* 30(23):5707–15.
- Bonneau, Laurent, Patricia Gerbeau-Pissot, Dominique Thomas, Christophe Der, Jeannine Lherminier, Stéphane Bourque, Yann Roche, and Françoise Simon-Plas. 2010. "Plasma Membrane Sterol Complexation, Generated by Filipin, Triggers Signaling Responses in Tobacco Cells." *BBA - Biomembranes* 1798:2150–59.
- Borowski, Edward, Natalia Salewska, Joanna Boros-Majewska, Marcin Serocki, Izabela Chabowska, Maria J. Milewska, Dominik Zietkowski, and Sławomir Milewski. 2018. "The Substantial Improvement of Amphotericin B Selective Toxicity upon Modification of Mycosamine with Bulky Substituents." *Medicinal Chemistry* 15.
- Bouazizi-Ben Messaoud, Hana, Marion Guichard, Philippe Lawton, Isabelle Delton, and Samira Azzouz-Maache. 2017. "Changes in Lipid and Fatty Acid Composition During Intramacrophagic Transformation of *Leishmania Donovanii* Complex Promastigotes into Amastigotes." *Lipids* 52(5):433–41.
- Boukari, Khaoula, Sébastien Balme, Jean Marc Janot, and Fabien Picaud. 2016. "Towards New Insights in the Sterol/Amphotericin Nanochannels Formation: A Molecular Dynamic Simulation Study." *Journal of Membrane Biology* 249(3):261–70.
- Brajtburg, J. S., Elberg, J. Bolard, G. S. Kobayashi, R. A. Levy, R. E. Ostlund, D. Schlessinger, and G. Medoff. 1984. "Interaction of Plasma Proteins and Lipoproteins with Amphotericin B." *The Journal of Infectious Diseases* 149(6):986–97.
- Brajtburg, Janina and Jacques Bolard. 1996. "Carrier Effects on Biological Activity of Amphotericin B." *Clinical Microbiology Reviews* 9(4):512–31.
- Brajtburg, Janina, Svetlana Elberg, Jacques Bolard, George S. Kobayashi, Richard A. Levy, Richard E. Ostlund, David Schlessinger, and Gerald Medoff. 1984. *Interaction of Plasma Proteins and Lipoproteins with Amphotericin B*. Vol. 149.
- Branco, J., M. Ola, R. M. Silva, E. Fonseca, N. C. Gomes, C. Martins-Cruz, A. P. Silva, A. Silva-Dias, C. Pina-Vaz, C. Erraught, L. Brennan, A. G. Rodrigues, G. Butler, and I. M. Miranda. 2017. "Impact of ERG3 Mutations and Expression of Ergosterol Genes Controlled by UPC2 and NDT80 in *Candida Parapsilosis* Azole Resistance." *Clinical Microbiology and Infection* 23(8):575.e1-575.e8.
- Brand, Theodor Von. 1966. "The Physiology of *Leishmania*." 14.
- Bridges, D. J., M. K. Gould, B. Nerima, P. Maser, R. J. S. Burchmore, and H. P. de Koning. 2007. "Loss of the High-Affinity Pentamidine Transporter Is Responsible for High Levels of Cross-Resistance between Arsenical and Diamidine Drugs in African Trypanosomes." *Molecular Pharmacology* 71(4):1098–1108.
- Britta, Elizandra Aparecida, Débora Botura Scariot, Hugo Falzirolli, Tânia Ueda-Nakamura, Cleuza Conceição Silva, Benedito Prado Dias Filho, Redouane Borsali, and Celso Vataru Nakamura. 2014. "Cell Death and Ultrastructural Alterations in *Leishmania Amazonensis* Caused by New Compound 4-Nitrobenzaldehyde Thiosemicarbazone Derived from S-Limonene." *BMC Microbiology* 14(1).
- Van den Broeck, Wim, Annie Derore, and Paul Simoons. 2006. "Anatomy and Nomenclature of Murine Lymph Nodes: Descriptive Study and Nomenclatory Standardization in BALB/CANCrI Mice." *Journal of Immunological Methods* 312(1–2):12–19.
- Brooks, Darrell N., Renata V Weber, Jerome D. Chao, Brian D. Rinker, Jozef Zoldos, Michael R. Robichaux, Sebastian B. Ruggeri, Kurt A. Anderson, Ekkehard E. Bonatz, Scott M. Wisotsky, Mickey S. Cho, Christopher Wilson, Ellis O. Cooper, John V Ingari, Bauback Safa, Brian M. Parrett, and Gregory M. Buncke. 2012. "Processed Nerve Allografts for Peripheral Nerve Reconstruction: A Multicenter Study of Utilization and Outcomes in Sensory, Mixed, and Motor Nerve Reconstructions." *Microsurgery* 32(1):1–14.
- Brotherton, Marie Christine, Sylvie Bourassa, Danielle Légaré, Guy G. Poirier, Arnaud Droit, and Marc Ouellette. 2014. "Quantitative Proteomic Analysis of Amphotericin B Resistance in *Leishmania Infantum*." *International Journal for Parasitology: Drugs and Drug Resistance* 4(2):126–32.
- Buchholz, Kathrin, R. Heiner Schirmer, Jana K. Eubel, Monique B. Akoachere, Thomas Dandekar, Katja Becker, and Stephan Gromer. 2008. "Interactions of Methylene Blue with Human Disulfide Reductases and Their Orthologues from *Plasmodium Falciparum*." *Antimicrobial Agents and Chemotherapy* 52(1):183–91.
- Burchmore, Richard J. S. and Michael P. Barrett. 2001. "Life in Vacuoles - Nutrient Acquisition by *Leishmania* Amastigotes." *International Journal for Parasitology* 31(12):1311–20.
- Burchmore, Richard J. S. and David T. Hart. 1995. "Glucose Transport in Amastigotes and Promastigotes of *Leishmania Mexicana Mexicana*." *Molecular and Biochemical Parasitology* 74(1):77–86.
- Burza, Sakib, Simon L. Croft, and Marleen Boelaert. 2018. "Leishmaniasis." *The Lancet* 392(10151):951–70.
- Burza, Sakib, Prabhat K Sinha, Raman Mahajan, Maria Angeles Lima, Gaurab Mitra, Neena Verma, Manica Balasegaram, and Pradeep Das. 2014. "Five-Year Field Results and Long-Term Effectiveness of 20 Mg/Kg Liposomal Amphotericin B (AmBisome) for Visceral Leishmaniasis in Bihar, India." *PLoS Negl. Trop. Dis.*
- Burza, Sakib, Prabhat Kumar Sinha, Raman Mahajan, Marta González Sanz, Maria Angeles Lima, Gaurab Mitra, Neena Verma, and Pradeep Das. 2014. "Post Kala-Azar Dermal Leishmaniasis Following Treatment with 20 Mg/Kg

- Liposomal Amphotericin B (Ambisome) for Primary Visceral Leishmaniasis in Bihar, India." *PLoS Neglected Tropical Diseases* 8(1):e2611.
- Bussotti, Giovanni, Evi Gouzelou, Mariana Côrtes Boité, Ihcen Kherachi, Zoubir Harrat, Naouel Eddaikra, Jeremy C. Mottram, Maria Antoniou, Vasiliki Christodoulou, Aymen Bali, Fatma Z. Guerfalli, Dhafer Laouini, Maowia Mukhtar, Franck Dumetz, Jean-Claude Dujardin, Despina Smirlis, Pierre Lechat, Pascale Pescher, Adil El Hamouchi, Meryem Lemrani, Carmen Chicharro, Ivonne Pamela Llanes-Acevedo, Laura Botana, Israel Cruz, Javier Moreno, Fakhri Jeddi, Karim Aoun, Aïda Bouratbine, Elisa Cupolillo, Gerald F. Späth, Citation G. Bussotti, Côrtes M. Boité, Dujardin J-c, and El A. Hamouchi. 2018. "Leishmania Genome Dynamics during Environmental Adaptation Reveal Strain-Specific Differences in Gene Copy Number Variation, Karyotype Instability, and Telomeric Amplification."
- Canuto, Gisele A. B., Emerson A. Castilho-Martins, Marina F. M. Tavares, Luis Rivas, Coral Barbas, and Angeles López-González. 2014. "Multi-Analytical Platform Metabolomic Approach to Study Miltefosine Mechanism of Action and Resistance in Leishmania." *Analytical and Bioanalytical Chemistry* 406(14):3459–76.
- Cardona-Arias, Jaiberth Antonio, Iván Darío Vélez, and Liliana López-Carvajal. 2015. "Efficacy of Thermoherapy to Treat Cutaneous Leishmaniasis: A Meta-Analysis of Controlled Clinical Trials." *PLoS One* 10(5):e0122569.
- Carnielli, Juliana B. T., Kathryn Crouch, Sarah Forrester, Vladimir Costa Silva, Sílvia F. G. Carvalho, Jeziel D. Damasceno, Elaine Brown, Nicholas J. Dickens, Dorcas L. Costa, Carlos H. N. Costa, Reynaldo Dietze, Daniel C. Jeffares, and Jeremy C. Mottram. 2018. "A Leishmania Infantum Genetic Marker Associated with Miltefosine Treatment Failure for Visceral Leishmaniasis." *EBioMedicine* 36:83–91.
- Carr, Rotonya M. and Rexford S. Ahima. 2016. "Pathophysiology of Lipid Droplet Proteins in Liver Diseases." *Experimental Cell Research* 340(2):187–92.
- Carrero-Lérida, Juana, Guiomar Pérez-Moreno, Víctor M. Castillo-Acosta, Luis M. Ruiz-Pérez, and Dolores González-Pacanowska. 2009. "Intracellular Location of the Early Steps of the Isoprenoid Biosynthetic Pathway in the Trypanosomatids Leishmania Major and Trypanosoma Brucei." *International Journal for Parasitology* 39(3):307–14.
- de Cássia Orlandi Sardi, Janaina, Diego Romário Silva, Maria José Soares Mendes-Giannini, and Pedro Luiz Rosalen. 2018. "Candida Auris: Epidemiology, Risk Factors, Virulence, Resistance, and Therapeutic Options." *Microbial Pathogenesis* 125:116–21.
- Castanho, M. A. R. B., S. Lopes, and M. Fernandes. 2003. "Using UV-Vis. Linear Dichroism to Study the Orientation of Molecular Probes and Biomolecules in Lipidic Membranes." *Spectroscopy-an International Journal* 17(2–3):377–98.
- Chakravarty, Jaya and Shyam Sundar. 2010. "Drug Resistance in Leishmaniasis." *Journal of Global Infectious Diseases* 2(2):167.
- Chang, Zanetta, R. Blake Billmyre, Soo Chan Lee, and Joseph Heitman. 2019. "Broad Antifungal Resistance Mediated by RNAi-Dependent Epimutation in the Basal Human Fungal Pathogen Mucor Circinelloides." *PLoS Genetics* 15(2):e1007957.
- Chauhan, Indira Singh, Jaspreet Kaur, Shagun Krishna, Arpita Ghosh, Prashant Singh, Mohammad Imran Siddiqi, and Neeloo Singh. 2011. "Evolutionary Comparison of Prenylation Pathway in Kinetoplastid Leishmania and Its Sister Leptomonas."
- Chawla, Bhavna and Rentala Madhubala. 2010. "Drug Targets in Leishmania." *Journal of Parasitic Diseases* 34(1):1–13.
- Chiou, C. C., A. H. Groll, and T. J. Walsh. 2000. "New Drugs and Novel Targets for Treatment of Invasive Fungal Infections in Patients with Cancer." *Oncologist*. 5(2):120–35.
- Choi, Jun Yong, Larissa M. Podust, and William R. Roush. 2014. "Drug Strategies Targeting CYP51 in Neglected Tropical Diseases."
- De Cicco, Nuccia N. T., Miria G. Pereira, José R. Corrêa, Valter V. Andrade-Neto, Felipe B. Saraiva, Alessandra C. Chagas-Lima, Katia C. Gondim, Eduardo C. Torres-Santos, Evelize Folly, Elvira M. Saraiva, Narcisa L. Cunha-e-Silva, Maurilio J. Soares, and Georgia C. Atella. 2012. "LDL Uptake by Leishmania Amazonensis: Involvement of Membrane Lipid Microdomains." *Experimental Parasitology* 130(4):330–40.
- Clayton, Christine and Michal Shapira. 2007. "Post-Transcriptional Regulation of Gene Expression in Trypanosomes and Leishmanias." *Molecular and Biochemical Parasitology* 156(2):93–101.
- Coelho, Adriano C., Nadine Messier, Marc Ouellette, and Paulo C. Cotrim. 2007. "Role of the ABC Transporter PRP1 (ABCC7) in Pentamidine Resistance in Leishmania Amastigotes." *ANTIMICROBIAL AGENTS AND CHEMOTHERAPY* 51(8):3030–32.
- Collett, Clare F., Carl Kitson, Nicola Baker, Heather B. Steele-Stallard, Marie-Victoire Santrot, Sebastian Hutchinson, David Horn, and Sam Alsford. 2019. "Chemogenomic Profiling of Anti-Leishmanial Efficacy and Resistance in the Related Kinetoplastid Parasite Trypanosoma Brucei." *Antimicrobial Agents and Chemotherapy* (June).
- Colotti, Gianni and Andrea Ilari. 2011. "Polyamine Metabolism in Leishmania: From Arginine to Trypanothione." *Amino Acids* 40(2):269–85.
- Contreras, Lellys Mariela, Julio Vivas, and Julio A. Urbina. 1997. "Altered Lipid Composition and Enzyme Activities of Plasma Membranes from Trypanosoma (Schizotrypanum) Cruzi Epimastigotes Grown in the Presence of Sterol Biosynthesis Inhibitors." *Biochemical Pharmacology* 53(5):697–704.
- Cosentino, Raúl O. and Fernán Agüero. 2014. "Genetic Profiling of the Isoprenoid and Sterol Biosynthesis Pathway Genes of Trypanosoma Cruzi." *PLoS ONE* 9(5).
- Costa, Fernanda Cristina, Amanda Fortes Francisco, Shiromani Jayawardhana, Simone Guedes Calderano, Michael D. Lewis, Francisco Olmo, Tom Beneke, Eva Gluenz, Jack Sunter, Samuel Dean, John Morrison Kelly, and Martin Craig Taylor. 2018. "Expanding the Toolbox for Trypanosoma Cruzi: A Parasite Line Incorporating a Bioluminescence-Fluorescence Dual Reporter and Streamlined CRISPR/Cas9 Functionality for Rapid in Vivo Localisation and Phenotyping." *PLoS Neglected Tropical Diseases* 12(4):1–21.
- Creek, Darren J., Jana Anderson, Malcolm J. McConville, and Michael P. Barrett. 2012. "Metabolomic Analysis of Trypanosomatid Protozoa." *Molecular and Biochemical Parasitology* 181(2):73–84.
- Creek, Darren J. and Michael P. Barrett. 2014. "Determination of Antiprotozoal Drug Mechanisms by Metabolomics Approaches." *Parasitology* 141(1):83–92.
- Creek, Darren J., Achuthanunni Chokkathukalam, Andris Jankevics, Karl E. V Burgess, Rainer Breitling, and Michael P. Barrett. 2012. "Stable Isotope-Assisted Metabolomics for Network-Wide Metabolic Pathway Elucidation." *Anal. Chem* 84:45.
- Croft, Simon L. and Graham H. Coombs. 2003. "Leishmaniasis - Current Chemotherapy and Recent Advances in the Search for Novel Drugs." *Trends in Parasitology* 19(11):502–8.
- Croft, Simon L., Shyam Sundar, and Alan H. Fairlamb. 2006. "Drug Resistance in Leishmaniasis." *CLINICAL MICROBIOLOGY REVIEWS* 19(1):111–26.
- Cuypers, Bart, Maya Berg, Hideo Imamura, Franck Dumetz, Géraldine De Muylder, Malgorzata A. Domagalska, Suman Rijal, Narayan Raj Bhattarai, Ilse Maes, Mandy Sanders, James A. Cotton, Pieter Meysman, Kris Laukens, and Jean Claude Dujardin. 2018. "Integrated Genomic and Metabolomic Profiling of ISC1, an Emerging Leishmania Donovanii Population in the Indian Subcontinent." *Infection, Genetics and Evolution* 62:170–78.

- Czapiński, Jakub, Michał Kielbus, Joanna Kalaft, Michał Kos, Andrzej Stepulak, and Adolfo Rivero-Müller. 2017. "How to Train a Cell-Cutting-Edge Molecular Tools." *Frontiers in Chemistry* 5(March).
- Damasceno, Jeziel D., Ricardo Obonaga, Gabriel L. A. Silva, João L. Reis-Cunha, Samuel M. Duncan, Daniella C. Bartholomeu, Jeremy C. Mottram, Richard McCulloch, and Luiz R. O. Tosi. 2018. "Conditional Genome Engineering Reveals Canonical and Divergent Roles for the Hus1 Component of the 9–1–1 Complex in the Maintenance of the Plastic Genome of *Leishmania*." *Nucleic Acids Research* 1–12.
- Daneshbod, Yahya, Ahmad Oryan, Mehdi Davarmanesh, and Sadegh Shirian. 2011. "Mucosal Leishmaniasis and Literature Review." *Cytologic Diagnosis of Mucosal Leishmaniasis* 135(April):478–82.
- Daneshvar, H., Z. Mahmmodi, H. Kamiabi, R. S. Phillips, and R. Burchmore. 2014. "Dogs Vaccinated with Gentamicin-Attenuated *Leishmania Infantum* or Infected with Wild-Type Parasite Can Be Distinguished by Western Blotting." *Parasite Immunology* 36(5):218–24.
- Daneshvar, H., M. M. Molaei, H. Kamiabi, R. Burchmore, P. Hagan, and R. Stephen Phillips. 2010. "Gentamicin-Attenuated *Leishmania Infantum*: Cellular Immunity Production and Protection of Dogs against Experimental Canine Leishmaniasis." *Parasite Immunology* 32(11–12):722–30.
- Daneshvar, Hamid, Graham H. Coombs, Paul Hagan, and R. Stephen Phillips. 2003. "*Leishmania Mexicana* and *Leishmania Major*: Attenuation of Wild-Type Parasites and Vaccination with the Attenuated Lines." *The Journal of Infectious Diseases* 187(10):1662–68.
- Daneshvar, Hamid, Mohammad M. Molaei, Reza Malekpour Afshar, Hosein Kamiabi, Richard Burchmore, Paul Hagan, and R. Stephen Phillips. 2009. "Gentamicin-Attenuated *Leishmania Infantum*: A Clinicopathological Study in Dogs." *Veterinary Immunology and Immunopathology* 129(1–2):28–35.
- Daneshvar, Hamid, Mohammad Javad Namazi, Hossein Kamiabi, Richard Burchmore, Sarah Cleaveland, and Stephen Phillips. 2014. "Gentamicin-Attenuated *Leishmania Infantum* Vaccine: Protection of Dogs against Canine Visceral Leishmaniasis in Endemic Area of Southeast of Iran." *PLoS Neglected Tropical Diseases* 8(4):2–8.
- Daneshvar, Hamid, Farnaz Sedghy, Shahriar Dabiri, Hossein Kamiabi, Mohammad M. Molaei, Stephen Phillips, and Richard Burchmore. 2012. "Alteration in Mononuclear Cell Subpopulations in Dogs Immunized with Gentamicin-Attenuated *Leishmania Infantum*." *Parasitology* 139(13):1689–96.
- Dantas-Torres, Filipe. 2009. "Canine Leishmaniasis in South America." *Parasites and Vectors* 2(SUPPL.1):1–8.
- Das, Undurti N. 2018. "Arachidonic Acid and Other Unsaturated Fatty Acids and Some of Their Metabolites Function as Endogenous Antimicrobial Molecules: A Review." *Journal of Advanced Research* 11:57–66.
- Das, Vidya Nand Rabi, Niyamat Ali Siddiqui, Biplab Pal, Chandra Shekhar Lal, Neena Verma, Ashish Kumar, Rakesh Bihari Verma, Dharendra Kumar, Pradeep Das, and Krishna Pandey. 2017. "To Evaluate Efficacy and Safety of Amphotericin B in Two Different Doses in the Treatment of Post Kala-Azar Dermal Leishmaniasis (PKDL)." *PLoS ONE* 12(3):1–13.
- Dashatan, Nasrin Amiri, Mostafa Rezaie Tavirani, Hakimeh Zali, Mehdi Koushki, and Nayebali Ahmadi. 2018. "Prediction of *Leishmania Major* Key Proteins Via Topological Analysis of Protein-Protein Interaction Network." 129(July):27–34.
- David Nes, W., Julie A. Marshall, Zhonghua Jia, Tahhan T. Jaradat, Zhihong Song, and Pruthvi Jayasimha. 2002. "Active Site Mapping and Substrate Channeling in the Sterol Methyltransferase Pathway*." .
- Dean, Samuel, Jack Sunter, Richard J. Wheeler, Ian Hodgkinson, Eva Gluenz, and Keith Gull. 2015. "A Toolkit Enabling Efficient, Scalable and Reproducible Gene Tagging in Trypanosomatids." *Open Biology* 5(1):140197.
- Debnath, Anjan, Josefino B. Tunac, Silvia Galindo-Gómez, Angélica Silva-Olivares, Mineko Shibayama, and James H. McKerrow. 2012. "Corifungin, a New Drug Lead against *Naegleria*, Identified from a High-Throughput Screen." *Antimicrobial Agents and Chemotherapy* 56(11):5450–57.
- Deep, Deepak Kumar, Ruchi Singh, Vasundhara Bhandari, Aditya Verma, Vanila Sharma, Saima Wajid, Shyam Sundar, V. Ramesh, Jean Claude Dujardin, and Poonam Salotra. 2017. "Increased Miltefosine Tolerance in Clinical Isolates of *Leishmania Donovanii* Is Associated with Reduced Drug Accumulation, Increased Infectivity and Resistance to Oxidative Stress." *PLoS Neglected Tropical Diseases* 11(6):1–16.
- Denny, Paul W., David Goulding, Michael A. J. Ferguson, and Deborah F. Smith. 2004. "Sphingolipid-Free *Leishmania* Are Defective in Membrane Trafficking, Differentiation and Infectivity." *Molecular Microbiology* 52(2):313–27.
- Denny, Paul W., Hosam Shams-Eldin, Helen P. Price, Deborah F. Smith, and Ralph T. Schwarz. 2006. "The Protozoan Inositol Phosphorylceramide Synthase A NOVEL DRUG TARGET THAT DEFINES A NEW CLASS OF SPHINGOLIPID SYNTHASE*." .
- Diaz-albiter, Hector M., Clément Regnault, Edubiel A. Alpizar-sosa, Dagmara Mcguinness, Michael Barrett, and Rod J. Dillon. 2018. "Non-Invasive Visualisation and Identification of Fluorescent *Leishmania Tarentolae* in Infected Sand Flies [Version 1 ; Referees : Awaiting Peer Review]." (0):1–7.
- Díaz-Albiter, Hector Manuel, Tainá Neves Ferreira, Samara Graciane Costa, Gustavo Bueno Rivas, Marcia Gumiel, Danilo Rufino Cavalcante, Márcio Galvão Pavan, Marcelo Salabert Gonzalez, Cícero Brasileiro De Mello, Viv Maureen Dillon, Rafaela Vieira Bruno, Eloi De Souza Garcia, Marli Maria Lima, Daniele Pereira De Castro, Rod James Dillon, Patricia De Azambuja, and Fernando Ariel Genta. 2016. "Everybody Loves Sugar: First Report of Plant Feeding in Triatomines." *Parasites and Vectors* 9(1):1–8.
- Díaz, María V., Mariana R. Miranda, Carolina Campos-Estrada, Chantal Reigada, Juan D. Maya, Claudio A. Pereira, and Rodrigo López-Muñoz. 2014. "Pentamidine Exerts in Vitro and in Vivo Anti Trypanosoma Cruzi Activity and Inhibits the Polyamine Transport in Trypanosoma Cruzi." *Acta Tropica* 134(1):1–9.
- Dinesh, Neeradi, Dheeraj Sree Ram Pallerla, Preet Kamal Kaur, Neerupudi Kishore Babu, and Sushma Singh. 2014. "Exploring *Leishmania Donovanii* 3-Hydroxy-3-Methylglutaryl Coenzyme A Reductase (HMGR) as a Potential Drug Target by Biochemical, Biophysical and Inhibition Studies." *Microbial Pathogenesis* 66:14–23.
- Dinesh, Neeradi, Neelagiri Soumya, and Sushma Singh. 2015. "Antileishmanial Effect of Mevastatin Is Due to Interference with Sterol Metabolism." *Parasitology Research* 114(10):3873–83.
- Diro, Ermias, Severine Blesson, Tansy Edwards, Koert Ritmeijer, Helina Fikre, Henok Admassu, Aderajew Kibret, Sally J. Ellis, Clelia Bardonneau, Eduard E. Zijlstra, Peninah Soipei, Brian Mutinda, Raymond Omollo, Robert Kimutai, Gabriel Omwalo, Monique Wasunna, Fentahun Tadesse, Fabiana Alves, Nathalie Strub-Wourgaft, Asrat Hailu, Neal Alexander, and Jorge Alvar. 2019. "A Randomized Trial of AmBisome Monotherapy and AmBisome and Miltefosine Combination to Treat Visceral Leishmaniasis in HIV Co-Infected Patients in Ethiopia" edited by E. M. Carvalho. *PLOS Neglected Tropical Diseases* 13(1):e0006988.
- Dorfman, Louis. 1953. *ULTRAVIOLET ABSORPTION OF STEROIDS*.
- Dostálová, Anna and Petr Volf. 2012. "Leishmania Development in Sand Flies: Parasite-Vector Interactions Overview." *Parasites and Vectors* 5(1):1–12.
- Duncan, Samuel M., Elmarie Myburgh, Cintia Philipon, Elaine Brown, Markus Meissner, James Brewer, and Jeremy C. Mottram. 2016. "Conditional Gene Deletion with DiCre Demonstrates an Essential Role for CRK3 in *Leishmania Mexicana* Cell Cycle Regulation." *Molecular Microbiology*.
- Durand, Remy, Muriel Paul, Francine Pratlong, Daniele Rivollet, Marie Laure Dubreuil-Lemaire, Rene Houin, Alain Astier,

- and Michele Deniau. 1998. "Leishmania Infantum: Lack of Parasite Resistance to Amphotericin B in a Clinically Resistant Visceral Leishmaniasis." *Antimicrobial Agents and Chemotherapy* 42(8):2141–43.
- El-Sayed, Najib M., Gaëlle Blandin, Jonathan Crabtree, Elisabet Caler, Elodie Ghedin, Daniella C. Bartholomeu, Brian J. Haas, Jennifer R. Wortman, Samuel Angiuoli, Jonathan Badger, Jane M. Carlton, Gustavo C. Cerqueira, Todd Creasy, Arthur L. Delcher, Appolinaire Djikeng, Christopher Hauser, Jeremy Peterson, Steven L. Salzberg, Joshua Shallom, Joana C. Silva, Jaideep Sundaram, Scott Westenberger, Owen White, Peter J. Myler, Gautam Aggarwal, Elizabeth A. Worthey, Atashi Anupama, Eithon Cadag, Kenneth D. Stuart, Matthew Berriman, Hubert Renauld, Christiane Hertz-Fowler, Christopher Peacock, Alasdair C. Ivens, Neil Hall, Anh-Nhi Tran, Daniel Nilsson, Björn Andersson, U. Cecilia M. Alsmark, T. Martin Embley, Frederic Bringaud, Sarah K. Kummerfeld, Jose B. Pereira-Leal, Sara E. Melville, and John E. Donelson. 2005. "Comparative Genomics of Trypanosomatid Parasitic Protozoa." *Science* 309(5733):404–10.
- Emami, Saeed, Pegah Tavangar, and Masoud Keighobadi. 2017. "An Overview of Azoles Targeting Sterol 14 α -Demethylase for Antileishmanial Therapy." *European Journal of Medicinal Chemistry* 135:241–59.
- European Medicines Agency. 2018. *Committee for Medicinal Products for Human Use (CHMP), Assessment Report, Perjeta.*
- Evans, A. Tudo. and Simon L. Croft. 1994. "Antileishmanial Actions of Tricyclic Neuroleptics Appear to Lack Structural Specificity." *Biochemical Pharmacology* 48(3):613–16.
- Fadili, Karima El, Nadine Messier, Philippe Leprohon, Gaétan Roy, Chantal Guimond, Nathalie Trudel, Nancy G. Saravia, Barbara Papadopoulou, Danielle Légaré, and Marc Ouellette. 2005. "Role of the ABC Transporter MRPA (PGPA) in Antimony Resistance in Leishmania Infantum Axenic and Intracellular Amastigotes." *ANTIMICROBIAL AGENTS AND CHEMOTHERAPY* 49(5):1988.
- Fairlamb, Alan H. and Anthony Cerami. 1992. *METABOLISM AND FUNCTIONS OF TRYPANOTHIONE IN THE KINETOPLASTIDA.*
- Fairlamb, Alan H., Neil A. R. Gow, Keith R. Matthews, and Andrew P. Waters. 2016. "Drug Resistance in Eukaryotic Microorganisms." *Nature Microbiology* 1(7).
- Fan, Jing, Jiangbin Ye, Jurre J. Kamphorst, Tomer Shlomi, Craig B. Thompson, and Joshua D. Rabinowitz. 2014. "Quantitative Flux Analysis Reveals Folate-Dependent NADPH Production."
- Farjami, Elaheh, Lilia Clima, Kurt V. Gothelf, and Elena E. Ferapontova. 2010. "DNA Interactions with a Methylene Blue Redox Indicator Depend on the DNA Length and Are Sequence Specific." *The Analyst* 135(6):1443.
- Fauland, Alexander, Harald Köfeler, Martin Trötz Müller, Astrid Knopf, Jürgen Hartler, Anita Eberl, Chandramohan Chitiraju, Ernst Lankmayr, and Friedrich Spener. 2011. "A Comprehensive Method for Lipid Profiling by Liquid Chromatography-Ion Cyclotron Resonance Mass Spectrometry." 52.
- Ferguson, Michael A. J. 1999. "The Structure, Biosynthesis and Functions of Glycosylphosphatidylinositol Anchors, and the Contributions of Trypanosome Research." *Journal of Cell Science* 112:2799–2809.
- Fernandez-Prada, Christopher, Isabel M. Vincent, Marie Christine Brotherton, Mathew Roberts, Gaétan Roy, Luis Rivas, Philippe Leprohon, Terry K. Smith, and Marc Ouellette. 2016. "Different Mutations in a P-Type ATPase Transporter in Leishmania Parasites Are Associated with Cross-Resistance to Two Leading Drugs by Distinct Mechanisms." *PLoS Neglected Tropical Diseases* 10(12):1–20.
- Fernández, Marisa M., Emilio L. Malchiodi, and Israel D. Algranati. 2011. "Differential Effects of Paromomycin on Ribosomes of Leishmania Mexicana and Mammalian Cells." *Antimicrobial Agents and Chemotherapy* 55(1):86–93.
- Fiebig, Michael, Steven Kelly, and Eva Gluenz. 2015. "Comparative Life Cycle Transcriptomics Revises Leishmania Mexicana Genome Annotation and Links a Chromosome Duplication with Parasitism of Vertebrates." *PLoS Pathogens* 11(10):1–28.
- Flórez, Andrés F., Daeui Park, Jong Bhak, Byoung-Chul Kim, Allan Kuchinsky, John H. Morris, Jairo Espinosa, and Carlos Muskus. 2010. "Protein Network Prediction and Topological Analysis in Leishmania Major as a Tool for Drug Target Selection." *BMC Bioinformatics* 11(1):484.
- Forrester, Sarah, Karin Siefert, Helen Ashwin, Najmeeyah Brown, Andrea Zelmar, Sally James, Dimitris Lagos, Jon Timmis, Mitali Chatterjee, Jeremy C. Mottram, Simon L. Croft, and Paul M. Kaye. 2019. "Tissue-Specific Transcriptomic Changes Associated with AmBisome® Treatment of BALB/c Mice with Experimental Visceral Leishmaniasis." *Wellcome Open Research* 4:198.
- Franco-Muñoz, Carlos, Merab Manjarré S-Estremor, and Clemencia Ovalle-Bracho. 2018. "Intraspecies Differences in Natural Susceptibility to Amphotericin B of Clinical Isolates of Leishmania Subgenus Viannia."
- Frézard, Frédéric, Cynthia Demicheli, and Raul R. Ribeiro. 2009. "Pentavalent Antimonials: New Perspectives for Old Drugs." *Molecules* 14(7):2317–36.
- Fügi, Matthias A., Kapila Gunasekera, Torsten Ochsenreiter, Xueli Guan, Markus R. Wenk, and Pascal Mäser. 2014. "Genome Profiling of Sterol Synthesis Shows Convergent Evolution in Parasites and Guides Chemotherapeutic Attack." *Journal of Lipid Research* 55(5):929–38.
- Gachotte, D., C. A. Pierson, N. D. Lees, R. Barbuch, C. Koegel, and M. Bard. 1997. "A Yeast Sterol Auxotroph (Erg25) Is Rescued by Addition of Azole Antifungals and Reduced Levels of Heme." *Proceedings of the National Academy of Sciences* 94(21):11713–78.
- Galluzzi, Luca, Marcello Ceccarelli, Aurora Diotallevi, Michele Menotta, and Mauro Magnani. 2018. "Real-Time PCR Applications for Diagnosis of Leishmaniasis." *Parasites and Vectors* 11(1):1–13.
- Ganapathy, Kulothungan, Christopher W. Jones, Camille M. Stephens, Rit Vatsyayan, Julie A. Marshall, and W. David Nes. 2008. "Molecular Probing of the Saccharomyces Cerevisiae Sterol 24-C Methyltransferase Reveals Multiple Amino Acid Residues Involved with C2-Transfer Activity." 1781(6–7):344–51.
- Gangneux, Jean-Pierre, Annie Sulahian, Yves Jean-Francois Garin, Robert Farinotti, and Francis Derouin. 1996. *Therapy of Visceral Leishmaniasis Due to Leishmania Infantum: Experimental Assessment of Efficacy of AmBisome.* Vol. 40.
- García-Hernández, R., J. I. Manzano, S. Castany, and F. Gamarro. 2012. "Leishmania Donovanii Develops Resistance to Drug Combinations." *PLoS Negl Trop Dis* 6(12):1974.
- Garcia, A., J. P. Adler-Moore, and R. T. Proffitt. 2000. "Single-Dose AmBisome (Liposomal Amphotericin B) as Prophylaxis for Murine Systemic Candidiasis and Histoplasmosis." *Antimicrobial Agents and Chemotherapy* 44(9):2327–32.
- Geber, A., C. A. Hitchcock, J. E. Swartz, F. S. Pullen, K. E. Marsden, K. J. Kwon-Chung, and J. E. Bennett. 1995. "Deletion of the Candida Glabrata ERG3 and ERG11 Genes: Effect on Cell Viability, Cell Growth, Sterol Composition, and Antifungal Susceptibility." *Antimicrobial Agents and Chemotherapy* 39(12):2708–17.
- Geilen, C. C., T. Wieder, and C. E. Orfanos. 1996. "Phosphatidylcholine Biosynthesis as a Target for Phospholipid Analogues." *Advances in Experimental Medicine and Biology* 416:333–36.
- Genois, Marie-Michelle, Eric R. Paquet, Marie-Claude N. Laffitte, Ranjan Maity, Amélie Rodrigue, Marc Ouellette, and Jean-Yves Masson. 2014. "DNA Repair Pathways in Trypanosomatids: From DNA Repair to Drug Resistance." *Microbiology and Molecular Biology Reviews: MMBR* 78(1):40–73.
- Ghazanfar, Mobeen and Muhammad Faheem Malik. 2016. "Sandfly and Leishmaniasis: A Review." *Journal of Ecosystem &*

Ecography 6(3).

- Ghosh, Ayan K., Abul H. Sardar, Abhishek Mandal, Savita Saini, Kumar Abhishek, Ashish Kumar, Bidyut Purkait, Ruby Singh, Sushmita Das, Rupkatha Mukhopadhyay, Syamal Roy, and Pradeep Das. 2015. "Metabolic Reconfiguration of the Central Glucose Metabolism: A Crucial Strategy of *Leishmania Donovanii* for Its Survival during Oxidative Stress." *The FASEB Journal* 29(5):2081–98.
- Ghosh, June, Shantanabha Das, Rajan Guha, Debopam Ghosh, Kshudiram Naskar, Anjan Das, and Syamal Roy. 2012b. "Hyperlipidemia Offers Protection against *Leishmania Donovanii* Infection: Role of Membrane Cholesterol." *Journal of Lipid Research* 53(12):2560–72.
- Giera, Martin, Delphine Renard, Florian Plössl, and Franz Bracher. 2008. "Lathosterol Side Chain Amides—A New Class of Human Lathosterol Oxidase Inhibitors." *Steroids*.
- Gigante, Federica, Marcel Kaiser, Reto Brun, and Ian H. Gilbert. 2009. "SAR Studies on Azasterols as Potential Anti-Trypanosomal and Anti-Leishmanial Agents." *Bioorganic and Medicinal Chemistry* 17(16):5950–61.
- Gigante, Federica, Marcel Kaiser, Reto Brun, and Ian H. Gilbert. 2010. "Design and Preparation of Sterol Mimetics as Potential Antiparasitics." *Bioorganic and Medicinal Chemistry* 18(20):7291–7301.
- Ginger, M L, M. L. Chance, and L. J. Goad. 1999. "Elucidation of Carbon Sources Used for the Biosynthesis of Fatty Acids and Sterols in the Trypanosomatid *Leishmania Mexicana*." *The Biochemical Journal* 342 (Pt 2)(2):397–405.
- Ginger, M. L., M. L. Chance, I. H. Sadler, and L. J. Goad. 2001. "The Biosynthetic Incorporation of the Intact Leucine Skeleton into Sterol by the Trypanosomatid *Leishmania Mexicana*." *The Journal of Biological Chemistry* 276(15):11674–82.
- Ginger, Michael L. 2005. "Trypanosomatid Biology and Euglenozoan Evolution: New Insights and Shifting Paradigms Revealed through Genome Sequencing." *Protist* 156(4):377–92.
- Ginger, Michael L, Michael L. Chance, and L. John Goad. 1999. "Sterols in the Trypanosomatid *Leishmania Mexicana*." *Society* 405:397–405.
- Ginger, Michael L., Mark C. Prescott, David G. Reynolds, Michael L. Chance, and L. John Goad. 2000. "Utilization of Leucine and Acetate as Carbon Sources for Sterol and Fatty Acid Biosynthesis by Old and New World *Leishmania* Species, *Endotrypanum Monrogeii* and *Trypanosoma Cruzi*." *European Journal of Biochemistry* 256(9):2555–66.
- Giorgio, C. 1999. "Flow Cytometric Assessment of Amphotericin B Susceptibility In." 71–76.
- Gloaguen, Yoann, Fraser Morton, Rónán Daly, Ross Gurden, Simon Rogers, Joe Wandy, David Wilson, Michael Barrett, and Karl Burgess. 2017. "PiMP My Metabolome: An Integrated, Web-Based Tool for LC-MS Metabolomics Data" edited by J. Wren. *Bioinformatics* 33(24):4007–9.
- Goad and Akihisa. 1997. "Gas—Liquid Chromatography of Sterols." Pp. 115–43 in *Analysis of Sterols*. Dordrecht: Springer Netherlands.
- Goad, L. John. and Toshihiro. Akihisa. 1997. *Analysis of Sterols*. Springer Netherlands.
- Goad, L. John, George G. Holz, and David H. Beach. 1984. "Sterols of *Leishmania* Species, Implications for Biosynthesis." *Molecular and Biochemical Parasitology* 10(2):161–70.
- Gonçalves, Sheila Viana Castelo Branco and Carlos Henrique Nery Costa. 2018. "Treatment of Cutaneous Leishmaniasis with Thermo-therapy in Brazil: An Efficacy and Safety Study." *Anais Brasileiros de Dermatologia* 93(3):347–55.
- Gossage, Sharon M., Matthew E. Rogers, and Paul A. Bates. 2003. "Two Separate Growth Phases during the Development of *Leishmania* in Sand Flies: Implications for Understanding the Life Cycle." *International Journal for Parasitology* 33(10):1027–34.
- Gray, K. C., D. S. Palacios, I. Dailey, M. M. Endo, B. E. Uno, B. C. Wilcock, and M. D. Burke. 2012. "Amphotericin Primarily Kills Yeast by Simply Binding Ergosterol." *Proceedings of the National Academy of Sciences* 109(7):2234–39.
- van Griensven, Johan, Manica Balasegaram, Filip Meheus, Jorge Alvar, Lutgarde Lynen, and Marleen Boelaert. 2010. "Combination Therapy for Visceral Leishmaniasis." *The Lancet Infectious Diseases* 10(3):184–94.
- Grill, Fabio and Marcela Zurmendi. 2017. *Leishmaniasis Visceral En Uruguay Visceral Leishmaniasis in Uruguay*.
- Grimaldi, Gabriel and Justus Schottelius. 2001. "Leishmaniasis – Their Relationships to Monoxenous and Dixenous Trypanosomatids." *Medical Microbiology and Immunology* 190(1–2):3–8.
- Gros, Ludovic, Silvia Orenes Lorente, Carmen Jimenez, Vanessa Yardley, Lauren Rattray, Hayley Wharton, Susan Little, Simon L. Croft, Luis M. Ruiz-Perez, Dolores Gonzalez-Pacanowska, and Ian H. Gilbert. 2006. "Evaluation of Azasterols as Anti-Parasitics." *Journal of Medicinal Chemistry* 49(20):6094–6103.
- Grover, Neeta D. 2010. "Echinocandins: A Ray of Hope in Antifungal Drug Therapy." *Indian Journal of Pharmacology* 42(1):9–11.
- Guan, Xue Li and Pascal Mäser. 2017. "Comparative Sphingolipidomics of Disease-Causing Trypanosomatids Reveal Unique Lifecycle- and Taxonomy-Specific Lipid Chemistries." *Scientific Reports* 7(1):13617.
- Gulati, S., Y. Liu, A. Munkacsi, L. Wilcox, and S. Stephen. 2010. "Sterols and Sphingolipids: Dynamic Duo or Partners in Crime?" *Prog Lipid Res.* 49(4):353–65.
- Gupta, Swati, Ajay Pal, and Suresh P. Vyas. 2010. "Drug Delivery Strategies for Therapy of Visceral Leishmaniasis." *Expert Opinion on Drug Delivery* 7(3):371–402.
- Gutarowska, Beata and Zofia Zakowska. 2010. "Estimation of Fungal Contamination of Various Plant Materials with UV-Determination of Fungal Ergosterol." *Annals of Microbiology* 60(3):415–22.
- Hailu, Asrat, Ahmed Musa, Monique Wasunna, Manica Balasegaram, Sisay Yifru, Getahun Mengistu, Zewdu Hurissa, Workagegnehu Hailu, Teklu Weldegebreal, Samson Tesfaye, Eyasu Makonnen, Eltahir Khalil, Osama Ahmed, Ahmed Fadlalla, Ahmed El-Hassan, Muzamil Raheem, Marius Mueller, Yousif Koummuki, Juma Rashid, Jane Mbui, Geoffrey Mucee, Simon Njoroge, Veronica Manduku, Alice Musibi, Geoffrey Mutuma, Fredrick Kirui, Hudson Lodenyo, Dedan Mutea, George Kirigi, Tansy Edwards, Peter Smith, Lawrence Muthami, Catherine Royce, Sally Ellis, Moses Alogo, Raymond Omollo, Josephine Kesusu, Rhoda Owiti, and John Kinuthia. 2010. "Geographical Variation in the Response of Visceral Leishmaniasis to Paromomycin in East Africa: A Multicentre, Open-Label, Randomized Trial." *PLoS Neglected Tropical Diseases* 4(10).
- Handler, Marc Z., Parimal A. Patel, Rajendra Kapila, Yasin Al-Qubati, and Robert A. Schwartz. 2015. "Cutaneous and Mucocutaneous Leishmaniasis: Differential Diagnosis, Diagnosis, Histopathology, and Management." *Journal of the American Academy of Dermatology* 73(6):911–26.
- Handman, Emanuela and Denise V. R. Bullen. 2002. "Interaction of *Leishmania* with the Host Macrophage." *Trends in Parasitology* 18(8):332–34.
- Haughan, P. A., M. L. Chance, and L. J. Goad. 1995. "Effects of an Azasterol Inhibitor of Sterol 24-Transmethylation on Sterol Biosynthesis and Growth of *Leishmania Donovanii* Promastigotes." *Biochem J* 308(Part 1):31–38.
- Hendrickx, S., J. Beyers, A. Mondelaers, E. Eberhardt, L. Lachaud, P. Delputte, P. Cos, and L. Maes. 2016. "Evidence of a Drug-Specific Impact of Experimentally Selected Paromomycin and Miltefosine Resistance on Parasite Fitness in *Leishmania Infantum*." *Journal of Antimicrobial Chemotherapy* 71(7):1914–21.
- Hendrickx, S., E. Eberhardt, A. Mondelaers, S. Rijal, N. R. Bhattarai, J. C. Dujardin, P. Delputte, P. Cos, and L. Maes. 2015. "Lack of Correlation between the Promastigote Back-Transformation Assay and Miltefosine Treatment Outcome."

- Journal of Antimicrobial Chemotherapy* 70(11):3023–26.
- Hendrickx, Sarah, Annelies Leemans, Annelies Mondelaers, Suman Rijal, Basudha Khanal, Jean Claude Dujardin, Peter Delpitte, Paul Cos, and Louis Maes. 2015. "Comparative Fitness of a Parent *Leishmania* Donovanii Clinical Isolate and Its Experimentally Derived Paromomycin-Resistant Strain." *PLoS ONE* 10(10):1–14.
- Hepburn, N. 2000. "Cutaneous Leishmaniasis." *Annales de Dermatologie et de Venerologie* 146(3):232–46.
- Horton, J. and I. Shimomura. 1999. "Sterol Regulatory Element-Binding Proteins: Activators of Cholesterol and Fatty Acid Biosynthesis.Pdf."
- Hsuchen, Chuen-Chin and David S. Feingold. 1973. *Selective Membrane Toxicity of the Polyene Antibiotics: Studies on Lecithin Membrane Models (Liposomes)*.
- Hu, Ping, Wenhua Zhang, Hongbo Xin, and Glenn Deng. 2016. "Single Cell Isolation and Analysis." *Frontiers in Cell and Developmental Biology* 4:116.
- Inbar, Ehud, V. Keith Hughitt, Laura A. L. Dillon, Kashinath Ghosh, Najib M. El-Sayed, and David L. Sacks. 2017. *The Transcriptome of Leishmania Major Developmental Stages in Their Natural Sand Fly Vector*.
- Ishemgulova, Aygul, Jana Hlaváčková, Karolína Majerová, Anzhelika Butenko, Julius Lukeš, Jan Votýpka, Petr Volf, and Vyacheslav Yurchenko. 2018. "CRISPR/Cas9 in *Leishmania mexicana*: A Case Study of LmxBTN1." *PLoS ONE* 13(2):1–17.
- IUPAC-IUB Comm. on Biochem. Nomencl. IUPAC-IUB Comm. on Biochem. 1970. "IUPAC-IUB Commission on Biochemical Nomenclature. Abbreviations and Symbols for the Description of the Conformation of Polypeptide Chains. Tentative Rules (1969)." *Biochemistry* 9(18):3471–79.
- Ivens, Alasdair C., Christopher S. Peacock, Elizabeth A. Worthey, Lee Murphy, Gautam Aggarwal, Matthew Berriman, Ellen Sisk, Marie Adele Rajandream, Ellen Adlem, Rita Aert, Atashi Anupama, Zina Apostolou, Philip Attipoe, Nathalie Bason, Christopher Bauser, Alfred Beck, Stephen M. Beverley, Gabriella Bianchetti, Katja Borzym, Gordana Bothe, Carlo V. Bruschi, Matt Collins, Eithon Cadag, Laura Ciarloni, Christine Clayton, Richard M. R. Coulson, Ann Cronin, Angela K. Cruz, Robert M. Davies, Javier De Gaudenzi, Deborah E. Dobson, Andreas Duesterhoeft, Gholam Fazelina, Nigel Fosker, Alberto Carlos Frasc, Audrey Fraser, Monika Fuchs, Claudia Gabel, Arlette Goble, André Goffeau, David Harris, Christiane Hertz-Fowler, Helmut Hilbert, David Horn, Yiting Huang, Sven Klages, Andrew Knights, Michael Kube, Natasha Larke, Lyudmila Litvin, Angela Lord, Tin Louie, Marco Marra, David Masuy, Keith Matthews, Shulamit Michaeli, Jeremy C. Mottram, Silke Müller-Auer, Heather Munden, Siri Nelson, Halina Norbertczak, Karen Oliver, Susan O'Neil, Martin Pentony, Thomas M. Pohl, Claire Price, Bénédicte Purnelle, Michael A. Quail, Ester Rabinowitsch, Richard Reinhardt, Michael Rieger, Joel Rinta, Johan Robben, Laura Robertson, Jeronimo C. Ruiz, Simon Rutter, David Saunders, Melanie Schäfer, Jacquie Schein, David C. Schwartz, Kathy Seeger, Amber Seyler, Sarah Sharp, Heesun Shin, Dhileep Sivam, Rob Squares, Steve Squares, Valentina Tosato, Christy Vogt, Guido Volckaert, Rolf Wambutt, Tim Warren, Holger Wedler, John Woodward, Shiguo Zhou, Wolfgang Zimmermann, Deborah F. Smith, Jenefer M. Blackwell, Kenneth D. Stuart, Bart Barrell, and Peter J. Myler. 2005b. "The Genome of the Kinetoplastid Parasite, *Leishmania major*." *Science* 309(5733):436–42.
- Iwaki, T., H. Iefuji, Y. Hiraga, A. Hosomi, T. Morita, Y. Giga-Hama, and K. Takegawa. 2008. "Multiple Functions of Ergosterol in the Fission Yeast *Schizosaccharomyces Pombe*." *Microbiology (Reading, England)* 154(Pt 3):830–41.
- Jain, Vineet and Keerti Jain. 2018. "Molecular Targets and Pathways for the Treatment of Visceral Leishmaniasis." *Drug Discovery Today* 23(1):161–70.
- Janson, Eric M., Robert J. Grebenok, Spencer T. Behmer, and Patrick Abbot. 2009. "Same Host-Plant, Different Sterols: Variation in Sterol Metabolism in an Insect Herbivore Community." *Journal of Chemical Ecology* 35(11):1309–19.
- Jara, Marlene, Maya Berg, Guy Caljon, Geraldine de Muylder, Bart Cuyper, Denis Castillo, Ilse Maes, Maria del Carmen Orozco, Manu Vanaerschot, Jean-Claude Dujardin, and Jorge Arevalo. 2017. "Macromolecular Biosynthetic Parameters and Metabolic Profile in Different Life Stages of *Leishmania braziliensis*: Amastigotes as a Functionally Less Active Stage" edited by V. Yurchenko. *PLOS ONE* 12(7):e0180532.
- Jhingran, Anupam, Bhavna Chawla, Shailendra Saxena, Michael Peter Barrett, and Rentala Madhubala. 2009. "Paromomycin: Uptake and Resistance in *Leishmania donovani*." *Molecular and Biochemical Parasitology* 164(2):111–17.
- Jiménez-Jiménez, Carmen, Juana Carrero-Lérida, Marco Sealey-Cardona, Luis Miguel Ruiz Pérez, Julio Alberto Urbina, and Dolores González Pacanowska. 2008. "Δ24 (25)-Sterol Methenyltransferase: Intracellular Localization and Azasterol Sensitivity in *Leishmania major* Promastigotes Overexpressing the Enzyme." *Molecular and Biochemical Parasitology* 160(1):52–59.
- Jones, Nathaniel G., Carolina M. C. Catta-Preta, Ana Paula C. A. Lima, and Jeremy C. Mottram. 2018. "Genetically Validated Drug Targets in *Leishmania*: Current Knowledge and Future Prospects." *ACS Infectious Diseases* 4(4):467–77.
- Joseph-home, Timothy, Nigel J. Manning, Derek Hollomon, and Steven L. Kelly. 1995. "Defective Sterol Δ5(6)Desaturase as a Cause of Azole Resistance in *Ustilago maydis*." *FEMS Microbiology Letters* 127(1–2):29–34.
- Kamhawi, Shaden. 2006. "Phlebotomine Sand Flies and *Leishmania* Parasites: Friends or Foes?" *Trends in Parasitology* 22(9):439–45.
- Kanafani, Zeina A. and John R. Perfect. 2010. "Resistance to Antifungal Agents: Mechanisms and Clinical Impact." *Chinese Journal of Infection and Chemotherapy* 10(4):320.
- Kaneshiro, Edna S., Koka Jayasimhulu, and Robert L. Lester. 1986. *Characterization of Inositol Lipids from Leishmania donovani Promastigotes: Identification of an Inositol Sphingophospholipid*. Vol. 27.
- Karimkhani, Chante, Valentine Wanga, Paria Naghavi, Robert P. Dellavalle, and Mohsen Naghavi. 2017. "Global Burden of Cutaneous Leishmaniasis." *The Lancet Infectious Diseases* 17(3):264.
- Kaufer, Alexa, John Ellis, Damien Stark, and Joel Barratt. 2017. "The Evolution of Trypanosomatid Taxonomy." *Parasites and Vectors* 10(1):1–17.
- Kaur, Gagandeep and Bhawana Rajput. 2014. "Comparative Analysis of the Omics Technologies Used to Study Antimonial, Amphotericin b, and Pentamidine Resistance in *Leishmania*." *Journal of Parasitology Research* 2014.
- Kaye, Paul and Phillip Scott. 2011. "Leishmaniasis: Complexity at the Host-Pathogen Interface." *Nature Reviews Microbiology* 9(8):604–15.
- Kazemi, B. 2011. "Genomic Organization of *Leishmania* Species." *Iranian Journal of Parasitology* 6(3):1–18.
- Kelly, S. L., D. C. Lamb, D. E. Kelly, N. J. Manning, J. Loeffler, H. Hebart, U. Schumacher, and H. Einsele. 1997. "Resistance to Fluconazole and Cross-Resistance to Amphotericin B in *Candida albicans* from AIDS Patients Caused by Defective Sterol Delta5,6-Desaturation." *FEBS Letters* 400(1):80–82.
- Kelly, Steven L., David C. Lamb, Mark Taylor, Andrew J. Corran, Brian C. Baldwin, and William G. Powderly. 1994. "Resistance to Amphotericin B Associated with Defective Sterol Δ8,7, Isomerase in a *Cryptococcus neoformans* Strain from an AIDS Patient." *FEMS Microbiology Letters* 122(1–2):39–42.
- Kelner, Michael J. and Nicholas M. Alexander. 1985. *THE JOURNAL OF BIOLOGICAL CHEMISTRY Methylene Blue Directly Oxidizes Glutathione without the Intermediate Formation of Hydrogen Peroxide*; Vol. 260.

- Khalil, Eltahir A. G., Teklu Weldegebreal, Brima M. Younis, Raymond Omollo, Ahmed M. Musa, Workagegnehu Hailu, Abuzaid A. Abuzaid, Thomas P. C. Dorlo, Zewdu Hurissa, Sisay Yifru, William Haleke, Peter G. Smith, Sally Ellis, Manica Balasegaram, Ahmed M. EL-Hassan, Gerard J. Schoone, Monique Wasunna, Robert Kimutai, Tansy Edwards, and Asrat Hailu. 2014. "Safety and Efficacy of Single Dose versus Multiple Doses of AmBisome® for Treatment of Visceral Leishmaniasis in Eastern Africa: A Randomised Trial." *PLoS Neglected Tropical Diseases*.
- Khan, Imran, Momin Khan, Muhammad Naveed Umar, Deog-Hwan Oh, Muhammad Naveed Umar, and Deog-Hwan Oh. 2016. "Attenuation and Production of the Amphotericin B-Resistant *Leishmania Tropica* Strain." *Jundishapur Journal of Microbiology* 9(6):32159.
- Kitajima, Yasuo, Takashi Sekiya, and Yosi-Hnori Nozawa. 1976. *FREEZE-FRACTURE ULTRASTRUCTURAL ALTERATIONS INDUCED BY FILIPIN, PIMARICIN, NYSTATIN AND AMPHOTERICIN B IN THE PLASMA MEMBRANES OF EPIDERMOPHYTON, SACCHAROMYCES AND RED BLOOD CELLS. A PROPOSAL OF MODELS FOR POLYENE-ERGOSTEROL COMPLEX-INDUCED MEMBRANES*.
- Kloehn, J., M. Blume, S. A. Cobbold, E. C. Saunders, M. J. Dagley, and M. J. McConville. 2016. "Using Metabolomics to Dissect Host-Parasite Interactions." *Current Opinion in Microbiology* 32:59-65.
- Kloehn, Joachim, Eleanor C. Saunders, Sean O'Callaghan, Michael J. Dagley, and Malcolm J. McConville. 2015. "Characterization of Metabolically Quiescent *Leishmania* Parasites in Murine Lesions Using Heavy Water Labeling." *PLoS Pathogens* 11(2):1-19.
- Koçarslan, Sezen, Enver Turan, Turan Ekinci, Rabia Apari, and Yavuz Yesilova. 2013. "Clinical and Histopathological Characteristics of Cutaneous Leishmaniasis in Sanliurfa City of Turkey Including Syrian Refugees." *Indian Journal of Pathology and Microbiology* 56(3):211.
- Koek, Maud M., Renger H. Jellema, Jan van der Greef, Albert C. Tas, and Thomas Hankemeier. 2011. "Quantitative Metabolomics Based on Gas Chromatography Mass Spectrometry: Status and Perspectives." *Metabolomics* 7(3):307-28.
- Konecna, Alexandra, Nora Toth Hervay, Alexandra Bencova, Marcela Morvova, Libusa Sikurova, Iva Jancikova, Dana Gaskova, and Yvetta Gbelska. 2018. "Erg6 Gene Is Essential for Stress Adaptation in *Kluyveromyces Lactis*." *FEMS Microbiology Letters* 365(23):1-8.
- Kontoyiannis, Dimitrios P. and Russell E. Lewis. 2002. "Antifungal Drug Resistance of Pathogenic Fungi." *The Lancet* 359(9312):1135-44.
- Kovářová, Julie and Michael P. Barrett. 2016. "The Pentose Phosphate Pathway in Parasitic Trypanosomatids." *Trends in Parasitology* 32(8):622-34.
- Kovářová, Julie, Andrew W. Pountain, David Wildridge, Stefan Weidt, Frédéric Bringaud, Richard J. S. Burchmore, Fiona Achcar, and Michael P. Barrett. 2018. *Deletion of Transketolase Triggers a Stringent Metabolic Response in Promastigotes and Loss of Virulence in Amastigotes of Leishmania Mexicana*. Vol. 14.
- Kristan, Katja and Tea Lanišnik Rižner. 2012a. "Steroid-Transforming Enzymes in Fungi." *Journal of Steroid Biochemistry and Molecular Biology* 129(1-2):79-91.
- Kristan, Katja and Tea Lanišnik Rižner. 2012b. *Steroid-Transforming Enzymes in Fungi*. Vol. 129. Pergamon.
- De Kruijff, B., W. J. Gerritsen, A. Oerlemans, R. A. Demel, and L. L. M. van Deenen. 1974. "Polyene Antibiotic-Sterol Interactions in Membranes of *Acholeplasma Laidlawii* Cells and Lecithin Liposomes. I. Specificity of the Membrane Permeability Changes Induced by the Polyene Antibiotics." *Biochimica et Biophysica Acta (BBA) - Biomembranes* 339(1):30-43.
- Laffitte, Marie-Claude N., Philippe Leprohon, Barbara Papadopoulou, and Marc Ouellette. 2016. "Plasticity of the *Leishmania* Genome Leading to Gene Copy Number Variations and Drug Resistance." *F1000Research* 5:2350.
- Lakhani, Prit, Akash Patil, and Soumyajit Majumdar. 2019. "Challenges in the Polyene- and Azole-Based Pharmacotherapy of Ocular Fungal Infections." *Journal of Ocular Pharmacology and Therapeutics* 35(1):6-22.
- Lebowitz, Jonathan H., Hong Q. Smith, Laura Rusche, and Stephen M. Beverley. 1993. "Coupling of p. O I Y (A .) Site . Selection and t r a n s - s p u c m g m L e z s h m a m A." 996-1007.
- Lee, Seon Jin, Jinglan Zhang, Augustine M. K. Choi, and Hong Pyo Kim. 2013. "Mitochondrial Dysfunction Induces Formation of Lipid Droplets as a Generalized Response to Stress." *Oxidative Medicine and Cellular Longevity* 2013.
- Leprohon, P., D. Legare, F. Raymond, E. Madore, G. Hardiman, J. Corbeil, and M. Ouellette. 2009. "Gene Expression Modulation Is Associated with Gene Amplification, Supernumerary Chromosomes and Chromosome Loss in Antimony-Resistant *Leishmania Infantum*." *Nucleic Acids Research* 37(5):1387-99.
- Leprohon, Philippe, Christopher Fernandez-Prada, Élodie Gazanion, Rubens Monte-Neto, and Marc Ouellette. 2015. "Drug Resistance Analysis by next Generation Sequencing in *Leishmania*." *International Journal for Parasitology: Drugs and Drug Resistance* 5(1):26-35.
- Lewis, D. J. 1971. "Phlebotomid Sandflies." *Bulletin of the World Health Organization* 44(4):535-51.
- Li, H. and R. Durbin. 2009. "Fast and Accurate Short Read Alignment with Burrows-Wheeler Transform." *Bioinformatics* 25(14):1754-60.
- Li, H., B. Handsaker, A. Wysoker, T. Fennell, J. Ruan, N. Homer, G. Marth, G. Abecasis, and R. Durbin. 2009. "The Sequence Alignment/Map Format and SAMtools." *Bioinformatics* 25(16):2078-79.
- Liarte, Daniel B. and S. M. F. Murta. 2010. "Selection and Phenotype Characterization of Potassium Antimony Tartrate-Resistant Populations of Four New World *Leishmania* Species." *Parasitology Research* 107(1):205-12.
- Liendo, Andreina, Gonzalo Visbal, Marta M. Piras, Romano Piras, and Julio A. Urbina. 1999. "Sterol Composition and Biosynthesis in *Trypanosoma Cruzi* Amastigotes." *Molecular and Biochemical Parasitology* 104(1):81-91.
- Liu, Teresa T., Robin E. B Lee, Katherine S. Barker, Richard E. Lee, Lai Wei, Ramin Homayouni, and P. David Rogers. 2005. "Genome-Wide Expression Profiling of the Response to Azole, Polyene, Echinocandin, and Pyrimidine Antifungal Agents in *Candida Albicans* †." *ANTIMICROBIAL AGENTS AND CHEMOTHERAPY* 49(6):2226-36.
- Lohner, Karl. 2014. "Antimicrobial Mechanisms: A Sponge against Fungal Infections." *Nature Chemical Biology* 10(6):411-12.
- Lopes, S. and M. A. R. B. Castanho. 2002. "Revealing the Orientation of Nystatin and Amphotericin B in Lipidic Multilayers by UV-Vis Linear Dichroism." *Journal of Physical Chemistry B* 106(29):7278-82.
- Lorente, Silvia Orenes, Juliany C. F. Rodrigues, Carmen Jiménez Jiménez, Miranda Joyce-Menekse, Carlos Rodrigues, Simon L. Croft, Vanessa Yardley, Kate De Luca-Fradley, Luis M. Ruiz-Pérez, Julio Urbina, Wanderley De Souza, Dolores González Pacanowska, and Ian H. Gilbert. 2004a. "Novel Azasterols as Potential Agents for Treatment of Leishmaniasis and Trypanosomiasis." *Antimicrobial Agents and Chemotherapy* 48(8):2937-50.
- Love, Michael I., Wolfgang Huber, and Simon Anders. 2014. "Moderated Estimation of Fold Change and Dispersion for RNA-Seq Data with DESeq2." *Genome Biology* 15(12):550.
- Lye, L. F., K. Owens, H. Shi, Smf M. F. Murta, and A. C. Vieira. 2010. "Retention and Loss of RNA Interference Pathways in Trypanosomatid Protozoans." *PLoS Pathog* 6(10):1001161.
- De Macedo-Silva, Sara Teixeira, Julio A. Urbina, Wanderley De Souza, and Juliany Cola Fernandes Rodrigues. 2013. "In Vitro Activity of the Antifungal Azoles Itraconazole and Posaconazole against *Leishmania Amazonensis*." *PLoS ONE*

8(12).

- Maes, L., J. Beyers, A. Mondelaers, M. Van den Kerkhof, E. Eberhardt, G. Caljon, and S. Hendrickx. 2017. "In Vitro 'Time-to-Kill' Assay to Assess the Cidal Activity Dynamics of Current Reference Drugs against *Leishmania Donovanii* and *Leishmania Infantum*." *Journal of Antimicrobial Chemotherapy* 72(2):428–30.
- Magaraci, Filippo, Carmen Jimenez Jimenez, Carlos Rodrigues, Juliana C. F. Rodrigues, Marina Vianna Braga, Vanessa Yardley, Kate De Luca-Fradley, Simon L. Croft, Wanderley De Souza, Luis M. Ruiz-Perez, Julio Urbina, Dolores Gonzalez Pacanowska, and Ian H. Gilbert. 2003. "Azasterols as Inhibitors of Sterol 24-Methyltransferase in *Leishmania* Species and *Trypanosoma Cruzi*." *Journal of Medicinal Chemistry* 46(22):4714–27.
- Mandal, Goutam, Vaidya Govindarajan, Mansi Sharma, Hiranmoy Bhattacharjee, and Rita Mukhopadhyay. 2017. "Drug Resistance in *Leishmania*." Pp. 649–65 in *Antimicrobial Drug Resistance*, edited by Mayers Douglas L., J. D. and Sobel, and O. Marc, and K. K. S., and M. Dror. Cham: Springer International Publishing.
- Manta, Bruno, Marcelo Comini, Andrea Medeiros, Martín Hugo, Madia Trujillo, and Rafael Radi. 2013. "Trypanothione: A Unique Bis-Glutathionyl Derivative in Trypanosomatids." *Biochimica et Biophysica Acta - General Subjects* 1830(5):3199–3216.
- Marchese, Leticia, Janaina Nascimento, Flávia Damasceno, Frédéric Bringaud, Paul Michels, and Ariel Silber. 2018. "The Uptake and Metabolism of Amino Acids, and Their Unique Role in the Biology of Pathogenic Trypanosomatids." *Pathogens* 7(2):36.
- Marr, Alexandra K., Julia L. Maclsaac, Ruiwei Jiang, Adriana M. Airo, Michael S. Kobor, and W. Robert McMaster. 2014. "Leishmania Donovanii Infection Causes Distinct Epigenetic DNA Methylation Changes in Host Macrophages." *PLoS Pathogens* 10(10).
- Marr, Kieren A. 2004. "Invasive Candida Infections: The Changing Epidemiology." *Oncology (Williston Park, N.Y.)* 18(14 Suppl 13):9–14.
- Marshall, Julie A. and W. Davi. Nes. 1999. "Isolation and Characterization of an Active-Site Peptide from a Sterol Methyl Transferase with a Mechanism-Based Inhibitor." *Bioorganic & Medicinal Chemistry Letters* 9(11):1533–36.
- Martel, Claire M., Josie E. Parker, Oliver Bader, Michael Weig, Uwe Gross, Andrew G. S. Warrilow, Diane E. Kelly, and Steven L. Kelly. 2010. "A Clinical Isolate of *Candida Albicans* with Mutations in ERG11 (Encoding Sterol 14alpha-Demethylase) and ERG5 (Encoding C22 Desaturase) Is Cross Resistant to Azoles and Amphotericin B." *Antimicrobial Agents and Chemotherapy* 54(9):3578–83.
- Martel, Claire M., Josie E. Parker, Oliver Bader, Michael Weig, Uwe Gross, Andrew G. S. Warrilow, Nicola Rolley, Diane E. Kelly, and Steven L. Kelly. 2010. "Identification and Characterization of Four Azole-Resistant Erg3 Mutants of *Candida Albicans*." *Antimicrobial Agents and Chemotherapy* 54(11):4527–33.
- Martínez-Calvillo, Santiago, Juan C. Vizuet-De-Rueda, Luis E. Florencio-Martínez, Rebeca G. Manning-Cela, and Elisa E. Figueroa-Angulo. 2010. "Gene Expression in Trypanosomatid Parasites." *Journal of Biomedicine and Biotechnology* 2010.
- Martínez, Dalila Y., Kristien Verdonck, Paul M. Kaye, Vanessa Adauí, Katja Polman, Alejandro Llanos-Cuentas, Jean-Claude Dujardin, and Marleen Boelaert. 2018. "Tegumentary Leishmaniasis and Coinfections Other than HIV."
- Martins-Duarte, Érica S., Leandro Lemgruber, Silvia Orenes Lorente, Ludovic Gros, Filippo Magaraci, Ian H. Gilbert, Wanderley de Souza, and Rossiane C. Vommaro. 2011. "Evaluation of Three Novel Azasterols against *Toxoplasma Gondii*." *Veterinary Parasitology* 177(1–2):157–61.
- Matrangolo, Fabiana S. V., Daniel B. Liarte, Laila C. Andrade, Melina F. De Melo, Juvana M. Andrade, Rafael F. Ferreira, André S. Santiago, Carlos P. Pirovani, Rosiane A. Silva-Pereira, and Silvana M. F. Murta. 2013. "Comparative Proteomic Analysis of Antimony-Resistant and-Susceptible *Leishmania Braziliensis* and *Leishmania Infantum* Chagasi Lines." *Molecular and Biochemical Parasitology* 190(2):63–75.
- Maugeri, Dante A. and Juan J. Cazzulo. 2004. "The Pentose Phosphate Pathway in *Trypanosoma Cruzi*." *FEMS Microbiology Letters* 234(1):117–23.
- Mayers, D. L. 2017. *Antimicrobial Drug Resistance: Mechanism of Drug Resistance*. Vol. 1. edited by Douglas Mayers, S. Jack, M. Ouellette, K. Kaye, and D. Marchaim. Springer US.
- Mayers, Douglas and SpringerLink. 2009. *Antimicrobial Drug Resistance Handbook*.
- Mbongo, Nicolas, Philippe M. Loiseau, Marie A. Billion, and Malka Robert-Gero. 1998a. "Mechanism of Amphotericin B Resistance in *Leishmania Donovanii* Promastigotes." *Antimicrobial Agents and Chemotherapy* 42(2):352–57.
- McCammon, M. T., M. A. Hartmann, D. K. Bottema, and L. W. Parks. 1984. "Sterol Methylation in *Saccharomyces Cerevisiae*." *Journal of Bacteriology* 157(2):475–83.
- McConville, Malcolm J. 2016. "Metabolic Crosstalk between *Leishmania* and the Macrophage Host." *Trends in Parasitology* 32(9):666–68.
- McConville, Malcolm J. and Emanuela Handman. 2007. "The Molecular Basis of *Leishmania* Pathogenesis." *International Journal for Parasitology* 37(10):1047–51.
- McConville, Malcolm J., Eleanor C. Saunders, Joachim Kloehn, and Michael J. Dagley. 2015. "Leishmania Carbon Metabolism in the Macrophage Phagolysosome- Feast or Famine?" *F1000Research* 4:1–11.
- McConville, Malcolm J., David de Souza, Eleanor Saunders, Vladimir A. Likic, and Thomas Naderer. 2007. "Living in a Phagolysosome; Metabolism of *Leishmania Amastigotes*." *Trends in Parasitology* 23(8):368–75.
- McKenna, Aaron, Matthew Hanna, Eric Banks, Andrey Sivachenko, Kristian Cibulskis, Andrew Kernysky, Kiran Garimella, David Altshuler, Stacey Gabriel, Mark Daly, and Mark A. DePristo. 2010. "The Genome Analysis Toolkit: A MapReduce Framework for Analyzing next-Generation DNA Sequencing Data." *Genome Research* 20(9):1297–1303.
- Mckenna, Myles, Charalampos Attipa, Severine Tasker, and Monica Augusto. 2019. "Leishmaniasis in a Dog with No Travel History Outside of the UK."
- Medina, J. M., J. C. F. RODRIGUES, W. DE SOUZA, G. C. ATELLA, and H. BARRABIN. 2012. "Tomatidine Promotes the Inhibition of 24-Alkylated Sterol Biosynthesis and Mitochondrial Dysfunction in *Leishmania Amazonensis* Promastigotes." *Parasitology* 139(10):1253–65.
- Mehta, Ashish and Chandrima Shaha. 2004. "Apoptotic Death in *Leishmania Donovanii* Promastigotes in Response to Respiratory Chain Inhibition." *Journal of Biological Chemistry* 279(12):11798–813.
- Melrose, J., R. Perroy, and S. Careas. 2015. *Antibiotic Resistance: Implications for Global Health and Novel Intervention Strategies*. Vol. 1.
- Merlen, Tjmothee, Denis Sereno, Nathalie Brajon, and Florence Rostand. 1999. *Leishmania Spp.; : Completely Defined Medium without Serum and Macromolecules (CDM/LP) for the Continuous in Vitro Cultivation of Infective Promastigote Forms*. Vol. 60.
- Mesa-Arango, Ana C., Liliána Scorzoni, and Oscar Zaragoza. 2012. "It Only Takes One to Do Many Jobs: Amphotericin B as Antifungal and Immunomodulatory Drug." *Frontiers in Microbiology* 3(AUG):1–10.
- Michel, Grégory, Christelle Pomares, Bernard Ferrua, and Pierre Marty. 2011. "Importance of Worldwide Asymptomatic Carriers of *Leishmania Infantum* (L. Chagasi) in Human." *Acta Tropica* 119:69–75.

- Mikus, Judith and Dietmar Steverding. 2000. "A Simple Colorimetric Method to Screen Drug Cytotoxicity against Leishmania Using the Dye Alamar Blue®." *Parasitology International* 48(3):265–69.
- Miller, Walter L. and Richard J. Auchus. 2011. "The Molecular Biology, Biochemistry, and Physiology of Human Steroidogenesis and Its Disorders." *Endocrine Reviews* 32(1):81.
- Misra, Biswapriya B., Carl Langefeld, Michael Olivier, and Laura A. Cox. 2018. "Integrated Omics: Tools, Advances and Future Approaches." *Journal of Molecular Endocrinology* (2016):R21–45.
- Miyazaki, Yoshitsugu, Antonia Geber, Haruko Miyazaki, Derek Falconer, Tanya Parkinson, Christopher Hitchcock, Brian Grimberg, Katherine Nyswaner, and John E. Bennett. 1999. *Cloning, Sequencing, Expression and Allelic Sequence Diversity of ERG3 (C-5 Sterol Desaturase Gene) in Candida Albicans*. Vol. 236.
- Mo, Caiqing and Martin Bard. 2005b. "A Systematic Study of Yeast Sterol Biosynthetic Protein–Protein Interactions Using the Split-Ubiquitin System." *Biochimica et Biophysica Acta (BBA) - Molecular and Cell Biology of Lipids* 1737(2–3):152–60.
- Mo, Caiqing and Martin Bard. 2005c. "Erg28p Is a Key Protein in the Yeast Sterol Biosynthetic Enzyme Complex." *Journal of Lipid Research* 46(9):1991–98.
- Mo, Caiqing, Martin Valachovic, and Martin Bard. 2004. "The ERG28-Encoded Protein, Erg28p, Interacts with Both the Sterol C-4 Demethylation Enzyme Complex as Well as the Late Biosynthetic Protein, the C-24 Sterol Methyltransferase (Erg6p)." *Biochimica et Biophysica Acta - Molecular and Cell Biology of Lipids*.
- Mohamed-Ahmed, Abeer H. A., Karin Seifert, Vanessa Yardley, Hollie Burrell-Saward, Stephen Brocchini, and Simon L. Croft. 2013. "Antileishmanial Activity, Uptake, and Biodistribution of an Amphotericin B and Poly(α -Glutamic Acid) Complex." *Antimicrobial Agents and Chemotherapy* 57(10):4608–14.
- Mohammed, Aml. 2012. "Glucocorticoids: Biochemical Group That Play Key Role in Fetal Programming of Adult Disease." *Glucocorticoids - New Recognition of Our Familiar Friend* (8).
- Mondelaers, Annelies, Maria P. Sanchez-Cañete, Sarah Hendrickx, Eline Eberhardt, Raquel Garcia-Hernandez, Laurence Lachaud, James Cotton, Mandy Sanders, Bart Cuyppers, Hideo Imamura, Jean-Claude Dujardin, Peter Delputte, Paul Cos, Guy Caljon, Francisco Gamarro, Santiago Castanys, and Louis Maes. 2016. "Genomic and Molecular Characterization of Miltefosine Resistance in Leishmania Infantum Strains with Either Natural or Acquired Resistance through Experimental Selection of Intracellular Amastigotes" edited by A. R. Satoskar. *PLOS ONE* 11(4):e0154101.
- Moné, Yves, Guillaume Mitta, David Duval, and Benjamin E. F. Gourbal. 2010. "Effect of Amphotericin B on the Infection Success of Schistosoma Mansoni in Biomphalaria Glabrata." *Experimental Parasitology* 125(2):70–75.
- Monteiro, M. S., M. Carvalho, M. L. Bastos, and P. Guedes de Pinho. 2013. "Metabolomics Analysis for Biomarker Discovery: Advances and Challenges." *Current Medicinal Chemistry* 20(2):257–71.
- Monzani, Paulo S., Stefano Trapani, Otavio H. Thiemann, and Glaucius Oliva. 2007. "Crystal Structure of Leishmania Tarentolae Hypoxanthine-Guanine Phosphoribosyltransferase." *BMC Structural Biology* 7(1):59.
- Monzote, Lianet, Marley García, Ramón Scull, Armando Cuellar, and William N. Setzer. 2014. "Antileishmanial Activity of the Essential Oil from Bixa Orellana." *Phytotherapy Research* 28(5):753–58.
- de Moraes-Teixeira, Eliane, Mariana Kolos Gallupo, Lucas Fonseca Rodrigues, á Ivoro José Romanha, and Ana Rabello. 2014. "In Vitro Interaction between Paromomycin Sulphate and Four Drugs with Leishmanicidal Activity against Three New World Leishmania Species." *Journal of Antimicrobial Chemotherapy* 69(1):150–54.
- Moreira, Pamela Rodrigues Reina, Lais Mendes Vieira, Mariana Mac Edo Costa De Andrade, Marcio De Barros Bandarra, Gisele Fabrino MacHado, Danísio Prado Munari, and Rosemeri De Oliveira Vasconcelos. 2010. "Immune Response Pattern of the Popliteal Lymph Nodes of Dogs with Visceral Leishmaniasis." *Parasitology Research* 107(3):605–13.
- Moreira, W., P. Leprohon, and M. Ouellette. 2011. "Tolerance to Drug-Induced Cell Death Favours the Acquisition of Multidrug Resistance in Leishmania." *Cell Death and Disease* 2(9):e201-8.
- Morio, F., F. Pagniez, C. Lacroix, M. Miegerville, and P. Le Pape. 2012. "Amino Acid Substitutions in the Candida Albicans Sterol 5,6-Desaturase (Erg3p) Confer Azole Resistance: Characterization of Two Novel Mutants with Impaired Virulence." *Journal of Antimicrobial Chemotherapy* 67(9):2131–38.
- Mudavath, Shyam Lal, Mahe Talat, Madhukar Rai, Onkar Nath Srivastava, and Shyam Sundar. 2014. "Characterization and Evaluation of Amine-Modified Graphene Amphotericin B for the Treatment of Visceral Leishmaniasis: In Vivo and in Vitro Studies." *Drug Design, Development and Therapy* 8:1235–47.
- Mukherjee, Angana, Lance D. Langston, and Marc Ouellette. 2011. "Intrachromosomal Tandem Duplication and Repeat Expansion during Attempts to Inactivate the Subtelomeric Essential Gene GSH1 in Leishmania." *Nucleic Acids Research* 39(17):7499–7511.
- Mukherjee, Madhuchanda, Writoban Basu Ball, and Pijush K. Das. 2014. "Leishmania Donovanii Activates SREBP2 to Modulate Macrophage Membrane Cholesterol and Mitochondrial Oxidants for Establishment of Infection." *The International Journal of Biochemistry & Cell Biology* 55:196–208.
- Mukherjee, Sandip, Budhaditya Mukherjee, Rupkatha Mukhopadhyay, Kshudiram Naskar, Shyam Sundar, Jean Claude Dujardin, Anjan Kumar Das, and Syamal Roy. 2012. "Imipramine Is an Orally Active Drug against Both Antimony Sensitive and Resistant Leishmania Donovanii Clinical Isolates in Experimental Infection." *PLoS Neglected Tropical Diseases* 6(12).
- Mukherjee, Sumit, Wei Xu, Fong Fu Hsu, Jigesh Patel, Juyang Huang, and Kai Zhang. 2018. "Sterol Methyltransferase Is Required for Optimal Mitochondrial Function and Virulence in Leishmania Major." *Molecular Microbiology* 0:1–17.
- Munday, Jane C., Anthonius A. Eze, Nicola Baker, Lucy Glover, Caroline Clucas, David Aguinaga Andrés, Manal J. Natto, Ibrahim A. Tekka, Jennifer McDonald, Rebecca S. Lee, Fabrice E. Graf, Philipp Ludin, Richard J. S. Burchmore, C. Michael R. Turner, Andy Tait, Annette Macleod, Pascal Mäser, Michael P. Barrett, David Horn, and Harry P. De Koning. 2014. "Trypanosoma Brucei Aquaglyceroporin 2 Is a High-Affinity Transporter for Pentamidine and Melaminophenyl Arsenic Drugs and the Main Genetic Determinant of Resistance to These Drugs." *Journal of Antimicrobial Chemotherapy* 69(3):651–63.
- Munday, Jane C., Luca Settimo, and Harry P. de Koning. 2015. "Transport Proteins Determine Drug Sensitivity and Resistance in a Protozoan Parasite, Trypanosoma Brucei." *Frontiers in Pharmacology* 6(MAR):1–10.
- Muxel, Sandra M., Juliana I. Aoki, Juliane C. R. Fernandes, Maria F. Laranjeira-Silva, Ricardo A. Zampieri, Stephanie M. Acuña, Karl E. Müller, Rubia H. Vanderlinde, and Lucile M. Floeter-Winter. 2018. "Arginine and Polyamines Fate in Leishmania Infection." *Frontiers in Microbiology* 8(JAN):1–15.
- Mwenechanya, Roy, Julie Kovářová, Nicholas J. Dickens, Manikhandan Mudaliar, Pawel Herzyk, Isabel M. Vincent, Stefan K. Weidt, Karl E. Burgess, Richard J. S. Burchmore, Andrew W. Pountain, Terry K. Smith, Darren J. Creek, Donghyun Kim, Galina I. Lepesheva, and Michael P. Barrett. 2017. "Sterol 14 α -Demethylase Mutation Leads to Amphotericin B Resistance in Leishmania Mexicana" edited by J. Raper. *PLOS Neglected Tropical Diseases* 11(6):e0005649.
- Naderer, Thomas, Miriam A. Ellis, M. Fleur Sernee, David P. De Souza, Joan Curtis, Emanuela Handman, and Malcolm J. Mcconville. 2006. *Virulence of Leishmania Major in Macrophages and Mice Requires the Gluconeogenic Enzyme Fructose-1,6-Bisphosphatase*. Vol. 103.

- Nakagawa, Yasuo, Yuichi Umegawa, Tetsuro Takano, Hiroshi Tsuchikawa, Nobuaki Matsumori, and Michio Murata. 2014. "Effect of Sterol Side Chain on Ion Channel Formation by Amphotericin B in Lipid Bilayers." *Biochemistry* 53(19):3088–94.
- Nayak, Archana, Snezhana Akpunarlieva, Michael Barrett, and Richard Burchmore. 2018. "A Defined Medium for Leishmania Culture Allows Definition of Essential Amino Acids." *Experimental Parasitology* 185:39–52.
- Nes, W. David, and Edward J. Parish. 1989b. *Analysis of Sterols and Other Biologically Significant Steroids*. Academic Press.
- Nes, W. David. 2000. "Sterol Methyl Transferase: Enzymology and Inhibition." *Biochimica et Biophysica Acta - Molecular and Cell Biology of Lipids* 1529(1–3):63–88.
- Nes, W. David. 2011. "Biosynthesis of Cholesterol and Other Sterols." *Chemical Reviews* 111(10):6423–51.
- Nes, W. David, Brian S. McCourt, Julie A. Marshall, Jianzhong Ma, Allen L. Dennis, Monica Lopez, Haoxia Li, and Ling He. 1999. "Site-Directed Mutagenesis of the Sterol Methyl Transferase Active Site from *Saccharomyces Cerevisiae* Results in Formation of Novel 24-Ethyl Sterols." *Journal of Organic Chemistry* 64(5):1535–42.
- Nes, W. David, Wenxu Zhou, Kulothungan Ganapathy, Jia Lin Liu, Rit Vatsyayan, Swetha Chamala, Keven Hernandez, and Mayra Miranda. 2009. "Sterol 24-C-Methyltransferase: An Enzymatic Target for the Disruption of Ergosterol Biosynthesis and Homeostasis in *Cryptococcus Neoformans*." *Archives of Biochemistry and Biophysics* 481(2):210–18.
- Nicolas, Luc, Eric Prina, and Thierry Lang. 2002. "Real-Time PCR for Detection and Quantitation Of." *Society* 40(5):1666–69.
- Nolan, Thomas John and Robert Herman. 1985. "Effects of Long-Term In Vitro Cultivation on *Leishmania Donovanii* Promastigotes." *The Journal of Protozoology* 32(1):70–75.
- O. Vassallo, S. Castelli, A. Biswas, S. Sengupta, P. K. Das, I. D'Annessa, F. Oteri, A. Leoni, P. Tagliatesta, H.K. Majumder, A. Desideri. 2011. "Conjugated Eicosapentaenoic Acid (CEPA) Inhibits L. *Donovani* Topoisomerase I and Has an Antiproliferative Activity Against L. *Donovani* Promastigotes." *The Open Antimicrobial Agents Journal* 3(1):23–29.
- O'Day, D. M. and W. S. Head. 2006. "Foundation Volume 2, Chapter 62 Ocular Pharmacology of Antifungal Drugs." *Duane's Ophthalmology, 2006 Edition* 2.
- O'day, Denis M., W. Steven Head, Richard D. Robinson, and Jeffrey A. Clanton. 1986. "Corneal Penetration of Topical Amphotericin b and Natamycin." *Current Eye Research*.
- O'Keeffe, Alec, Lauren Hyndman, Sean McGinty, Alaa Riezak, Sudaxshina Murdan, and Simon L. Croft. 2019. "Development of an In Vitro Media Perfusion Model of *Leishmania* Major Macrophage Infection." *PLoS ONE* 14(7).
- Oppendoes, Fred R. and Graham H. Coombs. 2007. "Metabolism of *Leishmania*: Proven and Predicted." *Trends in Parasitology* 23(4):149–58.
- Oppendoes, Fred R. and Paul A. M. Michels. 2010. "METABOLISM OF TRYPANOSOMATID PARASITES AND DRUG DISCOVERY Glycolytic Enzymes." 56–65.
- Otranto, Domenico and Filipe Dantas-Torres. 2013. "The Prevention of Canine Leishmaniasis and Its Impact on Public Health." *Trends in Parasitology* 29(7):339–45.
- Ouakad, M., M. Vanaerschot, S. Rijal, S. Sundar, N. Speybroeck, L. Kestens, L. Boel, S. De Doncker, I. Maes, S. Decuyper, and J. C. Dujardin. 2011. "Increased Metacyclogenesis of Antimony-Resistant *Leishmania Donovanii* Clinical Lines." *Parasitology* 138(11):1392–99.
- Ouameur, Amin Ahmed, Isabelle Girard, Danielle Légaré, and Marc Ouellette. 2008. "Functional Analysis and Complex Gene Rearrangements of the Folate/Biopterin Transporter (FBT) Gene Family in the Protozoan Parasite *Leishmania*." *Molecular and Biochemical Parasitology* 162(2):155–64.
- Ouellette M, Haimeur A, Grondin K, Légaré D, and Papadopolou B. 1998. "Amplification of ABC Transporter Gene PgpA and of Other Heavy Metal Resistance Genes in *Leishmania Tarentolae* and Their Study by Gene Transfection and Gene Disruption." *ABC Transporters: Biochemical, Cellular, and Molecular Aspects* 292(1993):182–93.
- Ouellette, Marc, Jolyne Drummelsmith, and Barbara Papadopolou. 2004. "Leishmaniasis: Drugs in the Clinic, Resistance and New Developments." *Drug Resistance Updates* 7(4–5):257–66.
- De Pablos, L. M., T. R. Ferreira, and P. B. Walrad. 2016. "Developmental Differentiation in *Leishmania* Lifecycle Progression: Post-Transcriptional Control Conducts the Orchestra." *Current Opinion in Microbiology* 34(Figure 1):82–89.
- Pan, Alfred A. 1984. "*Leishmania Mexicana*: Serial Cultivation of Intracellular Stages in a Cell-Free Medium." *Experimental Parasitology* 58(1):72–80.
- Parmar, Arpan, Kulbir Singh, Anita Bahadur, Gerrard Marangoni, and Pratap Bahadur. 2011. "Interaction and Solubilization of Some Phenolic Antioxidants in Pluronic@micelles." *Colloids and Surfaces B: Biointerfaces* 86(2):319–26.
- Parreira De Arruda, Maria Sueli, Maria Esther, Salles Nogueira, and Ana Paula Bordon. 2002. *Histological Evaluation of the Lesion Induced by Inoculation of Leishmania Mexicana in the Cheek Pouch of the Hamster Avaliação Histológica Da Lesão Induzida Pela Inoculação de Leishmania Mexicana Na Bolsa Jugal Do Hamster*. Vol. 35.
- Passero, L. F. D., Juliano V. Sacomori, Thaise Yumie Tomokane, C. E. P. Corbett, Fernando Tobias Da Silveira, and Márcia Dalastra Laurenti. 2009. "Ex Vivo and in Vivo Biological Behavior of *Leishmania* (*Viannia*) *Shawi*." *Parasitology Research* 105(6):1741–47.
- Patterson G. 1971. *Relation between Structure and Retention Time of Sterols in Gas Chromatography*. Vol. 43.
- Peacock, Christopher S., Kathy Seeger, David Harris, Lee Murphy, Jeronimo C. Ruiz, Michael A. Quail, Nick Peters, Ellen Adlem, Adrian Tivey, Martin Aslett, Arnaud Kerhornou, Alasdair Ivens, Audrey Fraser, Marie Adele Rajandream, Tim Carver, Halina Norbertczak, Tracey Chillingworth, Zahra Hance, Kay Jagels, Sharon Moule, Doug Ormond, Simon Rutter, Rob Squares, Sally Whitehead, Ester Rabbinowitsch, Claire Arrowsmith, Brian White, Scott Thurston, Frédéric Bringaud, Sandra L. Baldauf, Adam Faulconbridge, Daniel Jeffares, Daniel P. Depledge, Samuel O. Oyola, James D. Hilley, Loislene O. Brito, Luiz R. O. Tosi, Barclay Barrell, Angela K. Cruz, Jeremy C. Mottram, Deborah F. Smith, and Matthew Berriman. 2007. "Comparative Genomic Analysis of Three *Leishmania* Species That Cause Diverse Human Disease." *Nature Genetics* 39(7):839–47.
- Pech-May, Angélica, F. J. Escobedo-Ortegón, M. Berzunza-Cruz, and Eduardo Alfonso Rebollar-Téllez. 2010. "Incrimination of Four Sandfly Species Previously Unrecognized as Vectors of *Leishmania* Parasites in Mexico." *Medical and Veterinary Entomology* 24(2):150–61.
- Pérez-Victoria, F. Javier, María P. Sánchez-Cañete, Karin Seifert, Simon L. Croft, Shyam Sundar, Santiago Castanys, and Francisco Gamarro. 2006. "Mechanisms of Experimental Resistance of *Leishmania* to Miltefosine: Implications for Clinical Use." *Drug Resistance Updates* 9:26–39.
- Petersen, Christine A. and Stephen C. Barr. 2009. "Canine Leishmaniasis in North America: Emerging or Newly Recognized?" *The Veterinary Clinics of North America. Small Animal Practice* 39(6):1065–74, vi.
- Petterson, Eric F., Thomas D. Goddard, Conrad C. Huang, Gregory S. Couch, Daniel M. Greenblatt, Elaine C. Meng, and Thomas E. Ferrin. 2004. "UCSF Chimera - A Visualization System for Exploratory Research and Analysis." *Journal of*

Computational Chemistry.

- Phelouzat, Marie-Anne, Françoise Lawrence, and Malka Robert-Gero. 1993. *Parasitology Research Characterization of Sinefungin-Resistant Leishmania Donovanii Promastigotes*. Vol. 79.
- Pike, Linda J. 2003. "Lipid Rafts: Bringing Order to Chaos." *Journal of Lipid Research* 44(4):655–67.
- Piscopo, T. and Mallia C. 2006. "Leishmaniasis Tonio V Piscopo, Charles Mallia Azzopardi." *Postgrad Med J* 82:649–57.
- Pomel, Sébastien, Sandrine Cojean, and Philippe M. Loiseau. 2015. *Targeting Sterol Metabolism for the Development of Antileishmanials*. Vol. 31. Elsevier Current Trends.
- Ponte-Sucre, Alicia, Francisco Gamarro, Jean Claude Dujardin, Michael P. Barrett, Rogelio López-Vélez, Raquel García-Hernández, Andrew W. Pountain, Roy Mwenechanya, and Barbara Papadopoulou. 2017. "Drug Resistance and Treatment Failure in Leishmaniasis: A 21st Century Challenge." *PLoS Neglected Tropical Diseases* 11(12):1–24.
- Porta, Exequiel O. J., Paulo B. Carvalho, Mitchell A. Avery, Babu L. Tekwani, and Guillermo R. Labadie. 2014. "Click Chemistry Decoration of Amino Sterols as Promising Strategy to Developed New Leishmanicidal Drugs." *Steroids* 79:28–36.
- Porta, Exequiel O. J., Sebastián N. Jäger, Isabel Nocito, Galina I. Lepesheva, Esteban C. Serra, Babu L. Tekwani, and Guillermo R. Labadie. 2017. "Antitrypanosomal and Antileishmanial Activity of Prenyl-1,2,3-Triazoles." *MedChemComm* 8(5):1015–21.
- Pountain, Andrew W., Stefan K. Weidt, Clément Regnault, Paul A. Bates, Anne M. Donachie, Nicholas J. Dickens, and Michael P. Barrett. 2019b. "Genomic Instability at the Locus of Sterol C24-Methyltransferase Promotes Amphotericin B Resistance in Leishmania Parasites" edited by M. P. Pollastri. *PLoS Neglected Tropical Diseases* 13(2):e0007052.
- Pourshafie, Mohammad, Stanislas Morand, Alain Virion, Michaëlle Rakotomanga, Corinne Dupuy, and Philippe M. Loiseau. 2004. "Cloning of S-Adenosyl-L-Methionine:C-24- Δ -Sterol-Methyltransferase (ERG6) from Leishmania Donovanii and Characterization of MRNAs in Wild-Type and Amphotericin B-Resistant Promastigotes." *Antimicrobial Agents and Chemotherapy* 48(7):2409–14.
- Pund, Swati and Amita Joshi. 2017. "Nanoarchitectures for Neglected Tropical Protozoal Diseases: Challenges and State of the Art." Pp. 439–80 in *Nano- and Microscale Drug Delivery Systems: Design and Fabrication*. Elsevier.
- Purkait, Bidyut, Ashish Kumar, Nilay Nandi, Abul Hasan Sardar, Sushmita Das, Sudeep Kumar, Krishna Pandey, Vidyannanda Ravidas, Manish Kumar, Tripti De, Dharmendra Singh, and Pradeep Das. 2012. "Mechanism of Amphotericin B Resistance in Clinical Isolates of Leishmania Donovanii." *Antimicrobial Agents and Chemotherapy* 56(2):1031–41.
- Purkait, Bidyut, Ruby Singh, Kirti Wasnik, Sushmita Das, Ashish Kumar, Mark Paine, Manas Dikhit, Dharmendra Singh, Abul H. Sardar, Ayan K. Ghosh, and Pradeep Das. 2015. "Up-Regulation of Silent Information Regulator 2 (Sir2) Is Associated with Amphotericin B Resistance in Clinical Isolates of Leishmania Donovanii." *Journal of Antimicrobial Chemotherapy* 70(5):1343–56.
- Qiao, Xue, Wei Song, Qi Wang, Ke-di Liu, Zheng-xiang Zhang, Tao Bo, Ren-yong Li, Li-na Liang, Yew-min Tzeng, De-an Guo, and Min Ye. 2015. "Comprehensive Chemical Analysis of Triterpenoids and Polysaccharides in the Medicinal Mushroom Antrodia Cinnamomea." *RSC Advances* 5(58):47040–52.
- Quan-zhen, Lv, Lan Yan, and Jiang Yuan-ying. 2016. "The Synthesis, Regulation, and Functions of Sterols in Candida Albicans: Well-Known but Still Lots to Learn." *Virulence* 7(6):649–59.
- Rajasekaran, Rajalakshmi and Yi Ping Phoebe Chen. 2015. "Potential Therapeutic Targets and the Role of Technology in Developing Novel Antileishmanial Drugs." *Drug Discovery Today* 20(8):958–68.
- Rakotomanga, M., S. Blanc, K. Gaudin, P. Chaminade, and P. M. Loiseau. 2007. "Miltefosine Affects Lipid Metabolism in Leishmania Donovanii Promastigotes." *Antimicrobial Agents and Chemotherapy* 51(4):1425–30.
- Rakotomanga, M., M. Saint-Pierre-Chazalet, and P. Loiseau. 2005. "Alteration of Fatty Acid and Sterol Metabolism in Miltefosine-Resistant Leishmania Donovanii Promastigotes and Consequences for Drug-Membrane Interactions Alteration of Fatty Acid and Sterol Metabolism in Miltefosine-Resistant Leishmania Donovanii Promasti." *Antimicrob. Agents Chemother.* 49(September 2016):2677–2686.
- Ralton, Julie E., Thomas Naderer, Helena L. Piraino, Tanya A. Bashtannyk, Judy M. Callaghan, and Malcolm J. McConville. 2003. "Evidence That Intracellular B1-2 Mannan Is a Virulence Factor in Leishmania Parasites." *Journal of Biological Chemistry* 278(42):40757–63.
- Ramplé, Evelyn, Harald Schoeny, Bernd M. Mitic, Yasin El Abiead, Michaela Schwaiger, and Gunda Koellensperger. 2018. "Simultaneous Non-Polar and Polar Lipid Analysis by on-Line Combination of HILIC, RP and High Resolution MS †." *Cite This: Analyst* 143:1250.
- Rao, B. Sashidha., V. Sudersha. Rao, Y. Ramakrishna, and Ramesh V. Bhat. 1989. "Rapid and Specific Method for Screening Ergosterol as an Index of Fungal Contamination in Cereal Grains." *Food Chemistry* 31(1):51–56.
- Rastrojo, Alberto, Raquel García-Hernández, Paola Vargas, Esther Camacho, Laura Corvo, Hideo Imamura, Jean Claude Dujardin, Santiago Castanys, Begoña Aguado, Francisco Gamarro, and Jose M. Requena. 2018. "Genomic and Transcriptomic Alterations in Leishmania Donovanii Lines Experimentally Resistant to Antileishmanial Drugs." *International Journal for Parasitology: Drugs and Drug Resistance* 8(2):246–64.
- Rezende, Antonio M., Edson L. Folador, Daniela de M. Resende, and Jeronimo C. Ruiz. 2012. "Computational Prediction of Protein-Protein Interactions in Leishmania Predicted Proteomes" edited by J. Parkinson. *PLoS ONE* 7(12):e51304.
- Ribeiro, Raul Rio, Marilene Suzan Marques Michalick, Manoel Eduardo da Silva, Cristiano Cheim Peixoto dos Santos, Frédéric Jean Georges Frézard, and Sydnei Magno da Silva. 2018. "Canine Leishmaniasis: An Overview of the Current Status and Strategies for Control." *BioMed Research International* 2018:1–12.
- Rico, Eva, Laura Jeacock, Julie Kovářová, and David Horn. 2018. "Inducible High-Efficiency CRISPR-Cas9-Targeted Gene Editing and Precision Base Editing in African Trypanosomes." *Scientific Reports* 8(1):1–10.
- Rigden, Daniel J., Simon E. V. Phillips, Paul A. M. Michels, and Linda A. Fothergill-Gilmore. 1999. "The Structure of Pyruvate Kinase from Leishmania Mexicana Reveals Details of the Allosteric Transition and Unusual Effector Specificity." *Journal of Molecular Biology* 291(3):615–35.
- Rijal, Suman, Bart Ostyn, Surendra Uranw, Keshav Rai, Narayan Raj Bhattarai, Thomas P. C. Dorlo, Jos H. Beijnen, Manu Vanaerschot, Saskia Decuyper, Subodh S. Dhakal, Murari Lal Das, Prahlad Karki, Rupa Singh, Marleen Boelaert, and Jean-Claude Dujardin. 2013. "Increasing Failure of Miltefosine in the Treatment of Kala-Azar in Nepal and the Potential Role of Parasite Drug Resistance, Reinfection, or Noncompliance." *Clinical Infectious Diseases* 56(11):1530–38.
- Roberts, C. W., R. McLeod, D. W. Rice, M. Ginger, M. L. Chance, and L. J. Goad. 2003. "Fatty Acid and Sterol Metabolism: Potential Antimicrobial Targets in Apicomplexan and Trypanosomatid Parasitic Protozoa." *Molecular and Biochemical Parasitology* 126(2):129–42.
- Rochelle do Vale Morais, Andreza, André Leandro Silva, Sandrine Cojean, Kaluvu Balaraman, Christian Bories, Sébastien Pomel, Gillian Barratt, Eryvaldo Sócrates Tabosa do Egito, and Philippe M. Loiseau. 2018. "In-Vitro and in-Vivo Antileishmanial Activity of Inexpensive Amphotericin B Formulations: Heated Amphotericin B and Amphotericin B-Loaded Microemulsion." *Experimental Parasitology* 192(June):85–92.

- Rodrigues, Juliany C. F., Celene F. Bernardes, Gonzalo Visbal, Julio A. Urbina, Anibal E. Vercesi, and Wanderley de Souza. 2007. "Sterol Methenyl Transferase Inhibitors Alter the Ultrastructure and Function of the *Leishmania Amazonensis* Mitochondrion Leading to Potent Growth Inhibition." *Protist* 158(4):447–56.
- Roger, François Louis, Philippe Solano, Jérémy Bouyer, Vincent Porphyre, David Berthier, Marisa Peyre, and Pascal Bonnet. 2017. "Advocacy for Identifying Certain Animal Diseases as 'Neglected.'" *PLOS Neglected Tropical Diseases* 11(9):e0005843.
- Rogers, Matthew B., James D. Hilley, Nicholas J. Dickens, Jon Wilkes, Paul A. Bates, Daniel P. Depledge, David Harris, Yerim Her, Pawel Herzyk, Hideo Imamura, Thomas D. Otto, Mandy Sanders, Kathy Seeger, J. C. Jean-Claude Dujardin, Matthew Berriman, Deborah F. Smith, Christiane Hertz-Fowler, and Jeremy C. Mottram. 2011. "Chromosome and Gene Copy Number Variation Allow Major Structural Change between Species and Strains of *Leishmania*." *Genome Research* 21(12):2129–42.
- Rogers, Matthew E. and Paul A. Bates. 2007. "Leishmania Manipulation of Sand Fly Feeding Behavior Results in Enhanced Transmission." *PLoS Pathogens* 3(6):0818–25.
- Rojo, David, Gisele A. B. Canuto, Emerson A. Castilho-Martins, Marina F. M. Tavares, Coral Barbas, Ángeles López-González, and Luis Rivas. 2015. "A Multiplatform Metabolomic Approach to the Basis of Antimonial Action and Resistance in *Leishmania Infantum*." *PLoS ONE*.
- Roque, André Luiz R. and Ana Maria Jansen. 2014. "Wild and Synanthropic Reservoirs of *Leishmania* Species in the Americas." *International Journal for Parasitology: Parasites and Wildlife* 3(3):251–62.
- Rosenzweig, Doron, Derek Smith, Fred Opperdoes, Shay Stern, Robert W. Olafson, and Dan Zilberstein. 2008. "Retooling *Leishmania* Metabolism: From Sand Fly Gut to Human Macrophage." *The FASEB Journal* 22(2):590–602.
- Sadlova, Jovana, Petr Volf, Kathleen Victoir, Jean-Claude Dujardin, and Jan Votykpa. 2006. "Virulent and Attenuated Lines of *Leishmania* Major: DNA Karyotypes and Differences in Metalloproteinase GP63." *Folia Parasitologica* 53(2):81–90.
- Sagatova, Alia A., Mikhail V. Keniya, Rajni K. Wilson, Brian C. Monk, and Joel D. A. Tyndall. 2015. "Structural Insights into Binding of the Antifungal Drug Fluconazole to *Saccharomyces Cerevisiae* Lanosterol 14 α -Demethylase." *Antimicrobial Agents and Chemotherapy* 59(8):4982–89.
- Saint-Pierre-Chazalet, M., M. Ben Brahim, L. Le Moyec, C. Bories, M. Rakotomanga, and P. M. Loiseau. 2009. "Membrane Sterol Depletion Impairs Miltefosine Action in Wild-Type and Miltefosine-Resistant *Leishmania* *Donovani* Promastigotes." *Journal of Antimicrobial Chemotherapy* 64(5):993–1001.
- Sánchez-Valdéz, Fernando J., Angel Padilla, Wei Wang, Dylan Orr, and Rick L. Tarleton. 2018. "Spontaneous Dormancy Protects *Trypanosoma Cruzi* during Extended Drug Exposure." *ELife* 7:1–20.
- Dos Santos Ferreira, Cláudio, Patricia Silveira Martins, Cynthia Demicheli, Christian Brochu, Marc Ouellette, and Frédéric Frézard. 2003. "Thiol-Induced Reduction of Antimony(V) into Antimony(III): A Comparative Study with Trypanothione, Cysteinyl-Glycine, Cysteine and Glutathione." *BioMetals* 16(3):441–46.
- Santos, Renato E. R. S., Gabriel L. A. Silva, Elaine V. Santos, Samuel M. Duncan, Jeremy C. Mottram, Jeziel D. Damasceno, and Luiz R. O. Tosi. 2017. "A DiCre Recombinase-Based System for Inducible Expression in *Leishmania* Major." *Molecular and Biochemical Parasitology* 216:45–48.
- Sarkar, Paramita and Madhumita Manna. 2015. "Anti Leishmanial Activities of Some Antidepressant Drugs."
- Satragno, Dinora, Paula Faral-Tello, Bruno Canneva, Lorenzo Verger, Alejandra Lozano, Edgardo Vitale, Gonzalo Greif, Carlos Soto, Carlos Robello, and Yester Basmdjjan. 2017. "Autochthonous Outbreak and Expansion of Canine Visceral Leishmaniasis, Uruguay." *Emerging Infectious Diseases* 23(3):536–38.
- Saunders, Eleanor C., Thomas Naderer, Jenny Chambers, Scott M. Landfear, and Malcolm J. McConville. 2018. "*Leishmania Mexicana* Can Utilize Amino Acids as Major Carbon Sources in Macrophages but Not in Animal Models." *Molecular Microbiology* 108(2):143–58.
- Seifert, Karin, Sangeeta Matu, F. Javier Pérez-Victoria, Santiago Castanys, Francisco Gamarro, and Simon L. Croft. 2003. "Characterisation of *Leishmania* *Donovani* Promastigotes Resistant to Hexadecylphosphocholine (Miltefosine)." *International Journal of Antimicrobial Agents* 22(4):380–87.
- Seitz, L. M., H. E. Mohr, R. Burroughs, and D. B. Sauer. 1977. "Ergosterol as an Indicator of Fungal Invasion in Grains." *Cereal Chem* 54:1207–17.
- Seitz, L. M., D. B. Sauer, R. H. Burroughs, E. Mohr, and J. D. Hubbard. 1979. "Ergosterol as a Measure of Fungal Growth." *Phytopathology* 69(11):1202–3.
- Semini, Geo, Daniel Paape, Athina Paterou, Juliane Schroeder, Martin Barrios-Llerena, and Toni Aebischer. 2017. "Changes to Cholesterol Trafficking in Macrophages by *Leishmania* Parasites Infection." *MicrobiologyOpen* 6(4):1–13.
- Serafim, Tiago D., Iliano V. Coutinho-Abreu, Fabiano Oliveira, Claudio Meneses, Shaden Kamhawi, and Jesus G. Valenzuela. 2018. "Sequential Blood Meals Promote *Leishmania* Replication and Reverse Metacyclogenesis Augmenting Vector Infectivity." *Nature Microbiology* 3(5):548–55.
- Serhan, George, Colin M. Stack, Gabriel G. Perrone, and Charles O. Morton. 2014. "The Polyene Antifungals, Amphotericin B and Nystatin, Cause Cell Death in *Saccharomyces Cerevisiae* by a Distinct Mechanism to Amphibian-Derived Antimicrobial Peptides." *Annals of Clinical Microbiology and Antimicrobials* 13(1):1–4.
- Shalev, Moran, Haim Rozenberg, Boris Smolkin, Abedelmajeed Nasereddin, Dmitry Kopelyanskiy, Valery Belakhov, Thomas Schrepfer, Jochen Schacht, Charles L. Jaffe, Noam Adir, and Timor Baasov. 2015. "Structural Basis for Selective Targeting of *Leishmania* Ribosomes: Aminoglycoside Derivatives as Promising Therapeutics." *Nucleic Acids Research* 43(17):8601–13.
- Sharma, Umakant, Dharmendra Singh, Parveen Kumar, M. P. Dobhal, and Sarman Singh. 2011. "Antiparasitic Activity of Plumericin & Isoplumericin Isolated from *Plumeria Bicolor* against *Leishmania* *Donovani*." *Indian Journal of Medical Research* 134(11):709–16.
- Shaw, C. D., J. Lonchamp, T. Downing, H. Imamura, T. M. Freeman, J. A. Cotton, M. Sanders, G. Blackburn, J. C. Dujardin, S. Rijal, B. Khanal, C. J. R. Illingworth, G. H. Coombs, and K. C. Carter. 2016. "In Vitro Selection of Miltefosine Resistance in Promastigotes of *Leishmania* *Donovani* from Nepal: Genomic and Metabolomic Characterization." *Molecular Microbiology* 99(6):1134–48.
- Shimony, Orly and Charles L. Jaffe. 2008. "Rapid Fluorescent Assay for Screening Drugs on *Leishmania* Amastigotes." *Journal of Microbiological Methods* 75(2):196–200.
- Da Silva, Rosangela and David L. Sacks. 1987. *Metacyclogenesis Is a Major Determinant of Leishmania Promastigote Virulence and Attenuation Downloaded From*. Vol. 55.
- Silva, Sónia, Célia Rodrigues, Daniela Araújo, Maria Rodrigues, and Mariana Henriques. 2017. "Candida Species Biofilms' Antifungal Resistance." *Journal of Fungi* 3(1):8.
- Singh, Nisha, Manish Kumar, and Rakesh Kumar Singh. 2012. "Leishmaniasis: Current Status of Available Drugs and New Potential Drug Targets." *Asian Pacific Journal of Tropical Medicine* 5(6):485–97.
- Singh, Sushma and N. Kishore Babu. 2018. "3-Hydroxy-3-Methylglutaryl-CoA Reductase (HMGR) Enzyme of the Sterol Biosynthetic Pathway: A Potential Target against Visceral Leishmaniasis." P. 13 in *Leishmaniasis as Re-emerging*

Diseases. Vol. i. InTech.

- Singh, Sushma, Neeradi Dinesh, Preet Kamal Kaur, and Baigadda Shamiulla. 2014. "Ketanserin, an Antidepressant, Exerts Its Antileishmanial Action via Inhibition of 3-Hydroxy-3-Methylglutaryl Coenzyme A Reductase (HMGR) Enzyme of *Leishmania Donovanii*." *Parasitology Research* 113(6):2161–68.
- Smith, Deborah F., Christopher S. Peacock, and Angela K. Cruz. 2007. "Comparative Genomics: From Genotype to Disease Phenotype in the Leishmaniases." *International Journal for Parasitology* 37(11):1173–86.
- Smith, Martin, Frédéric Bringaud, and Barbara Papadopoulou. 2009. "Organization and Evolution of Two *SIDER* Retroposon Subfamilies and Their Impact on the *Leishmania* Genome."
- Smith, S. J., J. H. Crowley, and L. W. Parks. 1996. "Transcriptional Regulation by Ergosterol in the Yeast *Saccharomyces Cerevisiae*." *Molecular and Cellular Biology* 16(10):5427–32.
- Sokol-Anderson, M. L., J. Brajtburg, and G. Medoff. 1986. "Amphotericin B-Induced Oxidative Damage and Killing of *Candida Albicans*." *The Journal of Infectious Diseases* 154(1):76–83.
- Sollelis, Lauriane, Mehdi Ghorbal, Cameron Ross Macpherson, Rafael Miyazawa Martins, Nada Kuk, Lucien Crobu, Patrick Bastien, Artur Scherf, Jose Juan Lopez-Rubio, and Yvon Sterkers. 2015. "First Efficient CRISPR-Cas9-Mediated Genome Editing in *Leishmania* Parasites." *Cellular Microbiology* 17(10):1405–12.
- Soto, Jaime, Paula Soto, Andrea Ajata, Carmelo Luque, Carlos Tintaya, David Paz, Daniela Rivero, and Jonathan Berman. 2018. "Topical 15% Paromomycin-Aquaphilic for Bolivian *Leishmania Braziliensis* Cutaneous Leishmaniasis: A Randomized, Placebo-Controlled Trial." *Clinical Infectious Diseases (Xx)*:1–6.
- De Souza, Celeste da Silva Freitas, Kátia da Silva Calabrese, Ana Lúcia Abreu-Silva, Luiz Otávio Pereira Carvalho, Flávia de Oliveira Cardoso, Maria Elizabeth Moraes Cavalheiros Dorval, Elisa Teruya Oshiro, Patrícia Flávia Quaresma, Célia Maria Ferreira Gontijo, Raquel da Silva Pacheco, Maria Isabel Doria Rossi, Sylvio Celso Gonçalves Da Costa, and Tânia Zaverucha Do Valle. 2018. "Leishmania Amazonensis Isolated from Human Visceral Leishmaniasis: Histopathological Analysis and Parasitological Burden in Different Inbred Mice." *Histology and Histopathology* 33(7):705–16.
- de Souza, Dziejdom K. and Thomas P. C Dorlo. 2018. "Safe Mass Drug Administration for Neglected Tropical Diseases."
- de Souza, Wanderley and Juliany Cola Fernandes Rodrigues. 2009a. "Sterol Biosynthesis Pathway as Target for Anti-Trypanosomatid Drugs." *Interdisciplinary Perspectives on Infectious Diseases* 2009:642502.
- de Souza, Wanderley and Juliany Cola Fernandes Rodrigues. 2009b. "Sterol Biosynthesis Pathway as Target for Anti-Trypanosomatid Drugs." *Interdisciplinary Perspectives on Infectious Diseases* 2009:1–19.
- Spath, G. F., Hiroaki Segawa Lon-Fey Lye, David L. Sacks, Salvatore J. Turco, Stephen M. Beverley, Gerald F. Spath, Lon-Fey Lye, Hiroaki Segawa, David L. Sacks, Salvatore J. Turco, and Stephen M. Beverley. 2003. "Persistence Without Pathology in Phosphoglycan-Deficient *Leishmania Major*." *Science* 301(5637):1241–43.
- Spies, Hendrik S. C. and Daniel J. Steenkamp. 1994. "Thiols of Intracellular Pathogens: Identification of Ovoidiol A in *Leishmania Donovanii* and Structural Analysis of a Novel Thiol from *Mycobacterium Bovis*." *European Journal of Biochemistry* 224(1):203–13.
- Srivastava, Pankaj, Vijay Kumar Prajapati, Madhukar Rai, and Shyam Sundar. 2011. "Unusual Case of Resistance to Amphotericin B in Visceral Leishmaniasis in a Region in India Where Leishmaniasis Is Not Endemic." *Journal of Clinical Microbiology* 49(8):3088–91.
- Srivastava, Saumya, Jyotsna Mishra, Anil Kumar Gupta, Amit Singh, and Sarman Singh. 2017. "Laboratory Confirmed Miltefosine Resistant Cases of Visceral Leishmaniasis from India."
- Stagljär, Igor, Chantal Korostensky, Nils Johnsson, and Stephan Te Heesen. 1998. *A Genetic System Based on Split-Ubiquitin for the Analysis of Interactions between Membrane Proteins in Vivo*. Vol. 95.
- Steverding, Dietmar. 2017. "The History of Leishmaniasis." *Parasites and Vectors* 10(1):1–10.
- Stuart, Ken, Reto Brun, Simon Croft, Alan Fairlamb, Ricardo E. Gürtler, Jim McKerrow, Steve Reed, and Rick Tarleton. 2008. "Kinetoplastids: Related Protozoan Pathogens, Different Diseases." *Journal of Clinical Investigation* 118(4):1301–10.
- Subramanian, A., J. Jhavar, and R. R. Sarkar. 2015. "Dissecting *Leishmania Infantum* Energy Metabolism—A Systems Perspective." *PLoS ONE* 10(9):137976.
- Sun, Xianyun, Wenzhao Wang, Kangji Wang, Xinxu Yu, Jie Liu, Fucai Zhou, Baogui Xie, and Shaojie Li. 2013. "Sterol C-22 Desaturase ERG5 Mediates the Sensitivity to Antifungal Azoles in *Neurospora Crassa* and *Fusarium Verticillioides*." *Frontiers in Microbiology* 4:127.
- Sundar, Shyam. 2001. "Drug Resistance in Indian Visceral Leishmaniasis." *Tropical Medicine and International Health* 6(11):849–54.
- Sundar, Shyam and Jaya Chakravarty. 2013. "Leishmaniasis: An Update of Current Pharmacotherapy." *Expert Opinion on Pharmacotherapy* 14(1):53–63.
- Sundar, Shyam and Jaya Jaya. 2010. "Liposomal Amphotericin B and Leishmaniasis: Dose and Response." *Journal of Global Infectious Diseases* 2(2):159.
- Sundar, Shyam, T. K. Jha, Chandreshwar P. Thakur, Prabhat K. Sinha, and Sujit K. Bhattacharya. 2007. "Injectable Paromomycin for Visceral Leishmaniasis in India." *NEJM* 257:1–81.
- Sundar, Shyam, Anup Singh, Madhukar Rai, Vijay K. Prajapati, Avinash K. Singh, Bart Ostyn, Marleen Boelaert, Jean-Claude Dujardin, and Jaya Chakravarty. 2012. "Efficacy of Miltefosine in the Treatment of Visceral Leishmaniasis in India After a Decade of Use."
- Sundar, Shyam, Kumar Sinha, Madhukar Rai, Kumar Verma, Kumar Nawin, Shanawwaj Alam, Jaya Chakravarty, Michel Vaillant, Neena Verma, Krishna Pandey, Poonam Kumari, Chandra Shekhar Lal, Rakesh Arora, Bhawna Sharma, Sally Ellis, Nathalie Strub-Wourgaft, Manica Balasegaram, Piero Olliaro, Pradeep Das, and Farrokh Modabber. 2011. "Comparison of Short-Course Multidrug Treatment with Standard Therapy for Visceral Leishmaniasis in India: An Open-Label, Non-Inferiority, Randomised Controlled Trial." *www.thelancet.com* 377.
- Sunyoto, Temmy, Julien Potet, and Marleen Boelaert. 2018. "Why Miltefosine—a Life-Saving Drug for Leishmaniasis—Is Unavailable to People Who Need It the Most." *BMJ Global Health* 3(3):e000709.
- Szklarczyk, Damian, Andrea Franceschini, Michael Kuhn, Milan Simonovic, Alexander Roth, Pablo Minguéz, Tobias Doerks, Manuel Stark, Jean Muller, Peer Bork, Lars J. Jensen, and Christian Von Mering. 2011. "The STRING Database in 2011: Functional Interaction Networks of Proteins, Globally Integrated and Scored." *Nucleic Acids Research* 39(SUPPL. 1):561–68.
- Szklarczyk, Damian, Andrea Franceschini, Stefan Wyder, Kristoffer Forslund, Davide Heller, Jaime Huerta-Cepas, Milan Simonovic, Alexander Roth, Alberto Santos, Kalliopi P. Tsafou, Michael Kuhn, Peer Bork, Lars J. Jensen, and Christian Von Mering. 2015. "STRING V10: Protein-Protein Interaction Networks, Integrated over the Tree of Life." *Nucleic Acids Research* 43(D1):D447–52.
- Taramino, S., M. Valachovic, S. Oliaro-Bosso, F. Viola, B. Teske, M. Bard, and G. Balliano. 2010. "Interactions of Oxidosqualene Cyclase (Erg7p) with 3-Keto Reductase (Erg27p) and Other Enzymes of Sterol Biosynthesis in Yeast." *Biochimica et Biophysica Acta - Molecular and Cell Biology of Lipids* 1801(2):156–62.

- Taton, Maryse and Alain Rahier. 1996. *Plant Sterol Biosynthesis: Identification and Characterization of Higher Plant Delta7-Sterol C5(6)-Desaturase*. Vol. 325.
- Tesh, R. B. 1995. "Control of Zoonotic Visceral Leishmaniasis: Is It Time to Change Strategies?" *American Journal of Tropical Medicine and Hygiene* 52(3):287–92.
- Teske, B., S. Taramino, M. S. A. Bhuiyan, N. S. Kumaraswami, S. K. Randall, R. Barbuch, J. Eckstein, G. Balliano, and M. Bard. 2008. "Genetic Analyses Involving Interactions between the Ergosterol Biosynthetic Enzymes, Lanosterol Synthase (Erg7p) and 3-Ketoreductase (Erg27p), in the Yeast *Saccharomyces Cerevisiae*." *Biochimica et Biophysica Acta - Molecular and Cell Biology of Lipids* 1781(8):359–66.
- Tetaud, Emmanuel and Alan H. Fairlamb. 1998. "Cloning, Expression and Reconstitution of the Trypanothione-Dependent Peroxidase System of *Crithidia Fasciculata*." *Molecular and Biochemical Parasitology* 96(1–2):111–23.
- Thalhofer, Colin J., Yani Chen, Bayan Sudan, Laurie Love-Homan, and Mary E. Wilson. 2011. "Leukocytes Infiltrate the Skin and Draining Lymph Nodes in Response to the Protozoan *Leishmania Infantum* Chagasi." *Infection and Immunity* 79(1):108–17.
- Thomas, James, Nicola Baker, Sebastian Hutchinson, Caia Dominicus Id, Anna Trenaman, Lucy Glover Id, Sam Alsford Id, and David Horn Id. 2018. "Insights into Antitrypanosomal Drug Mode-of- Action from Cytology-Based Profiling." 1–19.
- Thompson, Julie, Desmond Higgins, and Toby Gibson. 1994. "CLUSTAL W: Improving the Sensitivity of Progressive Position-Specific Gap Penalties and Weight Matrix Choice Multiple Sequence Alignment through Sequence Weighting." 22(22):4673–80.
- Tinoco, Herlandes Penha, Maria Elvira Loyola Teixeira da Costa, Angela Tinoco Pessanha, Carlyle Mendes Coelho, Tatiane Furtado de Carvalho, Juliana Pinto da Silva Mol, Agostinho Gonçalves Viana, Lilian Lacerda Bueno, Ricardo Toshio Fujiwara, and Renato Lima Santos. 2018. "Visceral Leishmaniasis in an Infant Gorilla (*Gorilla Gorilla Gorilla*): Clinical Signs, Diagnosis, and Successful Treatment with Single-Dose Liposomal Amphotericin B." *Journal of Medical Primatology* 47(6):416–18.
- Tirmenstein, M. A., P. I. Plews, C. V. Walker, M. D. Woolery, H. E. Wey, and M. A. Toraason. 1995. "Antimony-Induced Oxidative Stress and Toxicity in Cultured Cardiac Myocytes." *Toxicology and Applied Pharmacology* 130(1):41–47.
- Tollemar, J., L. Klingspor, and O. Ringdén. 2001. "Liposomal Amphotericin B (AmBisome) for Fungal Infections in Immunocompromised Adults and Children." *Clinical Microbiology and Infection* 7:68–79.
- Torrelee, Els, Bernadette Bourdin Trunz, David Tweats, Marcel Kaiser, Reto Brun, Guy Mazué, Michael A. Bray, and Bernard Pécoul. 2010. "Fexinidazole - a New Oral Nitroimidazole Drug Candidate Entering Clinical Development for the Treatment of Sleeping Sickness." *PLoS Neglected Tropical Diseases* 4(12):1–15.
- Torres-Guerrero, Edoardo, Marco Romano Quintanilla-Cedillo, Julieta Ruiz-Esmenjaud, and Roberto Arenas. 2017. "Leishmaniasis: A Review." *F1000Research* 6(May):750.
- Trapnell, Cole, Adam Roberts, Loyal Goff, Geo Pertea, Daehwan Kim, David R. Kelley, Harold Pimentel, Steven L. Salzberg, John L. Rinn, and Lior Pachter. 2012. "Differential Gene and Transcript Expression Analysis of RNA-Seq Experiments with TopHat and Cufflinks."
- Trochine, Andrea, Darren J. Creek, Paula Faral-Tello, Michael P. Barrett, and Carlos Robello. 2014. "Benznidazole Biotransformation and Multiple Targets in *Trypanosoma Cruzi* Revealed by Metabolomics." *PLoS Neglected Tropical Diseases* 8(5).
- Turner, Kimbra G., Paola Vacchina, Maricela Robles-Murguía, Mariha Wadsworth, Mary Ann McDowell, and Miguel A. Morales. 2015. "Fitness and Phenotypic Characterization of Miltefosine-Resistant *Leishmania Major*." *PLoS Neglected Tropical Diseases* 9(7):1–15.
- Tutaj, Krzysztof, Radoslaw Szlajak, Joanna Starzyk, Piotr Wasko, Wojciech Grudzinski, Wieslaw I. Gruszecki, and Rafal Luchowski. 2015. "The Orientation of the Transition Dipole Moments of a Polyene Antibiotic Amphotericin B under UV-VIS Studies." *Journal of Photochemistry and Photobiology B: Biology* 151:83–88.
- Ubeda, Jean-Michel, Frédéric Raymond, Angana Mukherjee, Marie Plourde, Hélène Gingras, Gaétan Roy, Andréanne Lapointe, Philippe Leprohon, Barbara Papadopoulou, Jacques Corbeil, and Marc Ouellette. 2014. "Genome-Wide Stochastic Adaptive DNA Amplification at Direct and Inverted DNA Repeats in the Parasite *Leishmania*" edited by P. J. Hastings. *PLoS Biology* 12(5):e1001868.
- Ubeda, Jean Michel, Danielle Légaré, Frédéric Raymond, Amin Ahmed Ouameur, Sébastien Boisvert, Philippe Rigault, Jacques Corbeil, Michel J. Tremblay, Martin Olivier, Barbara Papadopoulou, and Marc Ouellette. 2008. "Modulation of Gene Expression in Drug Resistant *Leishmania* Is Associated with Gene Amplification, Gene Deletion and Chromosome Aneuploidy." *Genome Biology* 9(7).
- Usachev, Boris I. 2018. "Chemistry of Fluoroalkyl-Substituted 1,2,3-Triazoles." *Journal of Fluorine Chemistry*.
- Vacchina, P., B. Norris-Mullins, M. A. Abengózar, C. G. Viamontes, J. Sarro, M. T. Stephens, M. E. Pfrender, L. Rivas, and M. A. Morales. 2016. "Genomic Appraisal of the Multifactorial Basis for In Vitro Acquisition of Miltefosine Resistance in *Leishmania Donovanii*." *Antimicrobial Agents and Chemotherapy* 60(7):4089–4100.
- Vacchina, P., B. Norris-Mullins, E. S. Carlson, and M. A. Morales. 2016. "A Mitochondrial HSP70 (HSPA9B) Is Linked to Miltefosine Resistance and Stress Response in *Leishmania Donovanii*." *Parasites and Vectors* 9(1):1–15.
- Valdivia, Hugo O., Laila V. Almeida, Bruno M. Roatt, João Luís Reis-Cunha, Agnes Antônia Sampaio Pereira, Celia Gontijo, Ricardo Toshio Fujiwara, Alexandre B. Reis, Mandy J. Sanders, James A. Cotton, and Daniella C. Bartholomeu. 2017. "Comparative Genomics of Canine-Isolated *Leishmania* (*Leishmania*) *Amazonensis* from an Endemic Focus of Visceral Leishmaniasis in Governador Valadares, Southeastern Brazil." *Scientific Reports* 7(1):40804.
- Vale-Silva, L. A., A. T. Coste, F. Ischer, J. E. Parker, S. L. Kelly, E. Pinto, and D. Sanglard. 2012. "Azole Resistance by Loss of Function of the Sterol 5,6-Desaturase Gene (ERG3) in *Candida Albicans* Does Not Necessarily Decrease Virulence."
- Vanaerschot, Manu, Franck Dumetz, Marlene Jara, Jean-Claude Dujardin, and Alicia Ponte-Sucre. 2018. "The Concept of Fitness in *Leishmania*." Pp. 341–66 in *Drug Resistance in Leishmania Parasites*. Cham: Springer International Publishing.
- Varela-M, Rubén E., Janny A. Villa-Pulgarín, Edward Yepes, Ingrid Müller, Manuel Modolell, Diana L. Muñoz, Sara M. Robledo, Carlos E. Muskus, Julio López-Abán, Antonio Muro, Iván D. Vélez, and Faustino Mollinedo. 2012. "In Vitro and in Vivo Efficacy of Ether Lipid Edelfosine against *Leishmania* Spp. and SbV-Resistant Parasites." *PLoS Neglected Tropical Diseases* 6(4).
- Varga, Mónika, Tibor Bartók, and Ákos Mesterházy. 2006. "Determination of Ergosterol in *Fusarium*-Infected Wheat by Liquid Chromatography–Atmospheric Pressure Photoionization Mass Spectrometry." *Journal of Chromatography A* 1103(2):278–83.
- Vargas-Zepeda, Jesús, Alejandro V Gómez-Alcalá, José Alfonso Vázquez-Morales, Leonardo Licea-Amaya, Johan F. De Jonckheere, and Fernando Lares-Villa. 2005. "Successful Treatment of *Naegleria Fowleri* Meningoencephalitis by Using Intravenous Amphotericin B, Fluconazole and Rifampicin." *Archives of Medical Research* 36:83–86.
- Veen, M. and C. Lang. 2005. *Interactions of the Ergosterol Biosynthetic Pathway with Other Lipid Pathways*. Vol. 33.
- Verlinde, Christophe L. M. J., Véronique Hannaert, Casimir Blonski, Michèle Willson, Jacques J. Périé, Linda A. Fothergill-

- Gilmore, Fred R. Opperdoes, Michael H. Gelb, Wim G. J. Hol, and Paul A. M. Michels. 2001. "Glycolysis as Drug Target in Trypanosomes Glycolysis as a Target for the Design of New Anti-Trypanosome Drugs."
- Vermeersch, Marieke, R. I. Da Luz, Kim Toté, Jean Pierre Timmermans, Paul Cos, and Louis Maes. 2009. "In Vitro Susceptibilities of Leishmania Donovanii Promastigote and Amastigote Stages to Antileishmanial Reference Drugs: Practical Relevance of Stage-Specific Differences." *Antimicrobial Agents and Chemotherapy* 53(9):3855–59.
- Viana Andrade-Neto, Valter, Thais Martins Pereira, Marilene Do Canto-Cavalheiro, and Eduardo Caio Torres-Santos. 2016a. "Imipramine Alters the Sterol Profile in Leishmania Amazonensis and Increases Its Sensitivity to Miconazole." *Parasites and Vectors*.
- Viana Andrade-Neto, Valter, Thais Martins Pereira, Marilene Do Canto-Cavalheiro, and Eduardo Caio Torres-Santos. 2016b. "Imipramine Alters the Sterol Profile in Leishmania Amazonensis and Increases Its Sensitivity to Miconazole." *Parasites and Vectors* 9(1):183.
- Vijayakumar, Saravanan and Pradeep Das. 2018. "Recent Progress in Drug Targets and Inhibitors towards Combating Leishmaniasis." *Acta Tropica* 181(February):95–104.
- Vincent, Benjamin Matteson, Alex Kelvin Lancaster, Ruth Scherz-Shouval, Luke Whitesell, and Susan Lindquist. 2013. "Fitness Trade-Offs Restrict the Evolution of Resistance to Amphotericin B" edited by A. P. Mitchell. *PLoS Biology* 11(10):e1001692.
- Vincent, Isabel M. and Michael P. Barrett. 2015. "Metabolomic-Based Strategies for Anti-Parasite Drug Discovery." *Journal of Biomolecular Screening* 20(1):44–55.
- Vincent, Isabel M., Darren J. Creek, Karl Burgess, Debra J. Woods, Richard J. S. Burchmore, and Michael P. Barrett. 2012. "Untargeted Metabolomics Reveals a Lack Of Synergy between Nifurtimox and Eflornithine against Trypanosoma Brucei."
- Vincent, Isabel M., Darren Creek, David G. Watson, Mohammed A. Kamleh, Debra J. Woods, Pui Ee Wong, Richard J. S. Burchmore, and Michael P. Barrett. 2010. "A Molecular Mechanism for Eflornithine Resistance in African Trypanosomes." *PLoS Pathogens* 6(11).
- Vincent, Isabel, Stefan Weidt, Luis Rivas, Karl Burgess, Terry Smith, and Marc Ouellette. 2014. "Untargeted Metabolomic Analysis of Miltefosine Action in Leishmania Infantum Reveals Changes to the Internal Lipid Metabolism." *International Journal for Parasitology: Drugs and Drug Resistance* 4(1):20–27.
- Voak, Andrew A., Joseph F. Standing, Nuno Sepúlveda, Andy Harris, Simon L. Croft, and Karin Seifert. 2018. "Pharmacodynamics and Cellular Accumulation of Amphotericin B and Miltefosine in Leishmania Donovanii-Infected Primary Macrophages." *Journal of Antimicrobial Chemotherapy* 73(5):1314–23.
- Walsh, Thomas J., Gregory P. Melcher, Michael G. Rinaldi, Julius Leccionese, Deanna A. MCGough, Patrick Kelly, James Lee, Diana Callender, Marc Rubin, Philip A. Pizzo', and Audie L. Murphy. 1990. *Trichosporon Beigelii, an Emerging Pathogen Resistant to Amphotericin B*. Vol. 28.
- Webster, Joanne P., David H. Molyneux, Peter J. Hotez, and Alan Fenwick. 2018. "The Contribution of Mass Drug Administration to Global Health: Past, Present and Future."
- Welscher, Yvonne M. te. 2010. "The Antifungal Activity of Natamycin." *Igitur-Archive.Library.Uu.Nl*.
- Welscher, Yvonne M. te, Hendrik H. ten Napel, Miriam Masià Balagué, Cleiton M. Souza, Howard Riezman, Ben de Kruijff, and Eefjan Breukink. 2008. "Natamycin Blocks Fungal Growth by Binding Specifically to Ergosterol without Permeabilizing the Membrane." *Journal of Biological Chemistry* 283(10):6393–6401.
- Te Welscher, Yvonne M., Hendrik H. Ten Napel, Miriam Masià Balagué, Cleiton M. Souza, Howard Riezman, Ben De Kruijff, and Eefjan Breukink. 2008. "Natamycin Blocks Fungal Growth by Binding Specifically to Ergosterol without Permeabilizing the Membrane." *Journal of Biological Chemistry* 283(10):6393–6401.
- Te Welscher, Yvonne Maria, Lynden Jones, Martin Richard Van Leeuwen, Jan Dijksterhuis, Ben De Kruijff, Gary Eitzen, and Eefjan Breukink. 2010. "Natamycin Inhibits Vacuole Fusion at the Priming Phase via a Specific Interaction with Ergosterol." *Antimicrobial Agents and Chemotherapy* 54(6):2618–25.
- Westrop, Gareth D., Roderick A. M. Williams, Lijie Wang, Tong Zhang, David G. Watson, Ana Marta Silva, and Graham H. Coombs. 2015. "Metabolomic Analyses of Leishmania Reveal Multiple Species Differences and Large Differences in Amino Acid Metabolism." *PLoS ONE* 10(9).
- Wheeler, Richard J., Eva Gluenz, and Keith Gull. 2011. "The Cell Cycle of Leishmania: Morphogenetic Events and Their Implications for Parasite Biology." *Molecular Microbiology* 79(3):647–62.
- Wijnant, Gert-Jan, Katrien Van Bocxlaer, Vanessa Yardley, Andy Harris, Mo Alavijeh, Rita Silva-Pedrosa, Sandra Antunes, Isabel Mauricio, Sudaxshina Murdan, and Simon L. Croft. 2018. "Comparative Efficacy, Toxicity and Biodistribution of the Liposomal Amphotericin B Formulations Fungisome® and AmBisome® in Murine Cutaneous Leishmaniasis."
- Wijnant, Gert Jan, Katrien Van Bocxlaer, Amanda Fortes Francisco, Vanessa Yardley, Andy Harris, Mo Alavijeh, Sudaxshina Murdan, and Simon L. Croft. 2018. "Local Skin Inflammation in Cutaneous Leishmaniasis as a Source of Variable Pharmacokinetics and Therapeutic Efficacy of Liposomal Amphotericin B." *Antimicrobial Agents and Chemotherapy* 62(10).
- Wilson, W. David, Ferial A. Taniou, Amanda Mathis, Denise Tevis, James Edwin Hall, and David W. Boykin. 2008. "Antiparasitic Compounds That Target DNA." *Biochimie* 90(7):999–1014.
- Wyllie, Susan, Mark L. Cunningham, and Alan H. Fairlamb. 2004. "Dual Action of Antimonial Drugs on Thiol Redox Metabolism in the Human Pathogen Leishmania Donovanii." *Journal of Biological Chemistry* 279(38):39925–32.
- Wyllie, Susan, Goutam Mandal, Neeloo Singh, Shyam Sundar, Alan H. Fairlamb, and Mitali Chatterjee. 2010. "Elevated Levels of Tryparedoxin Peroxidase in Antimony Unresponsive Leishmania Donovanii Field Isolates." *Molecular and Biochemical Parasitology* 173(2):162–64.
- Wyllie, Susan, Tim J. Vickers, and Alan H. Fairlamb. 2008. "Roles of Trypanothione S-Transferase and Tryparedoxin Peroxidase in Resistance to Antimonials." *Antimicrobial Agents and Chemotherapy* 52(4):1359–65.
- Xiang, Ming Jie, Jin Yan Liu, Pei Hua Ni, Shengzheng Wang, Ce Shi, Bing Wei, Yu Xing Ni, and Hai Liang Ge. 2013. "Erg11 Mutations Associated with Azole Resistance in Clinical Isolates of Candida Albicans." *FEMS Yeast Research* 13(4):386–93.
- Xu, W, F. F. Hsu, E. Baykal, J. Huang, and K. Zhang. 2014. "Sterol Biosynthesis Is Required for Heat Resistance but Not Extracellular Survival in Leishmania." *PLoS Pathog* 10(10):1004427.
- Yao, Chaoqun, Upasna Gaur Dixit, Jason H. Barker, Lynn M. Teesch, Laurie Love-Homan, John E. Donelson, and Mary E. Wilson. 2013. "Attenuation of Leishmania Infantum Chagasi Metacyclic Promastigotes by Sterol Depletion" edited by J. H. Adams. *Infection and Immunity* 81(7):2507–17.
- Yao, Chaoqun and Mary E. Wilson. 2016. "Dynamics of Sterol Synthesis during Development of Leishmania Spp. Parasites to Their Virulent Form." *Parasites and Vectors* 9(1):1–12.
- Yardley, Vanessa and Simon L. Croft. 1997. "Activity of Liposomal Amphotericin B against Experimental Cutaneous Leishmaniasis." *Antimicrobial Agents and Chemotherapy* 41(4):752–56.
- Yardley, Vanessa and Simon L. Croft. 2000. "A Comparison of the Activities of Three Amphotericin B Lipid Formulations against Experimental Visceral and Cutaneous Leishmaniasis." *International Journal of Antimicrobial Agents*

- 13(4):243–48.
- Yoon, S. A., J. A. Vazquez, P. E. Steffan, J. D. Sobel, and R. A. Akins. 1999. "High-Frequency, in Vitro Reversible Switching of *Candida Lusitaniae* Clinical Isolates from Amphotericin B Susceptibility to Resistance." *Antimicrobial Agents and Chemotherapy* 43(4):836–45.
- Young, Laura Y., Christina M. Hull, and Joseph Heitman. 2003. "Disruption of Ergosterol Biosynthesis Confers Resistance to Amphotericin B in *Candida Lusitaniae*." *Antimicrobial Agents and Chemotherapy* 47(9):2717–24.
- Zakir Hossain, Md and Tetsuhisa Goto. 2015. "A Rapid Determination of Ergosterol in Grains Using Gas Chromatography-Mass Spectrometry Method Without Derivatization." *Food Anal. Methods* 8:1021–26.
- Zarate, Erica, Veronica Boyle, Udo Rupprecht, Saras Green, Silas G. Villas-Boas, Philip Baker, and Farhana R. Pinu. 2016. "Fully Automated Trimethylsilyl (TMS) Derivatization Protocol for Metabolite Profiling by GC-MS." *Metabolites* 7(1).
- Zauli-Nascimento, Rogéria C., Danilo C. Miguel, Jenicer K. U. Yokoyama-Yasunaka, Ledice I. A. Pereira, Milton A. Pelli de Oliveira, Fátima Ribeiro-Dias, Miriam L. Dorta, and Silvia R. B. Uliana. 2009. "In Vitro Sensitivity of *Leishmania (Viannia) Braziliensis* and *Leishmania (Leishmania) Amazonensis* Brazilian Isolates to Meglumine Antimoniate and Amphotericin B." *Tropical Medicine & International Health* 15(1):68–76.
- Zeiman, Einat, Charles L. Greenblatt, Sharona Elgavish, Ina Khozin-Goldberg, and Jacob Golenser. 2008. "Mode of Action of Fenarimol Against *Leishmania* Spp." *Journal of Parasitology* 94(1):280–86.
- Zhang, Kai and Stephen M. Beverley. 2010. "Phospholipid and Sphingolipid Metabolism in *Leishmania*." *Molecular and Biochemical Parasitology* 170(2):55–64.
- Zhang, Kai, Fong-Fu Hsu, David A. Scott, Roberto Docampo, John Turk, and Stephen M. Beverley. 2005. "Leishmania Salvage and Remodelling of Host Sphingolipids in Amastigote Survival and Acidocalcisome Biogenesis." *Molecular Microbiology* 55(5):1566–78.
- Zhang, Wen Wei and Greg Matlashewski. 2015. "CRISPR-Cas9-Mediated Genome Editing in *Leishmania Donovanii*." *MBio* 6(4):1–14.
- Zhang, Wen Wei, Laura Isobel McCall, and Greg Matlashewski. 2013. "Role of Cytosolic Glyceraldehyde-3-Phosphate Dehydrogenase in Visceral Organ Infection by *Leishmania Donovanii*." *Eukaryotic Cell* 12(1):70–77.
- Zhang, Y., Z. Li, D. S. Pilch, and M. J. Leibowitz. 2002. "Pentamidine Inhibits Catalytic Activity of Group I Intron Ca.LSU by Altering RNA Folding." *Nucleic Acids Res.* 30(1362–4962):2961–71.
- Zhou, Wenxu, George A. M. Cross, and W. David Nes. 2007. "Cholesterol Import Fails to Prevent Catalyst-Based Inhibition of Ergosterol Synthesis and Cell Proliferation of *Trypanosoma Brucei*."
- Zhou, Wenxu, Galina I. Lepesheva, Michael R. Waterman, and W. David Nes. 2006. "Mechanistic Analysis of a Multiple Product Sterol Methyltransferase Implicated in Ergosterol Biosynthesis in *Trypanosoma Brucei*." *Journal of Biological Chemistry* 281(10):6290–96.
- Zilberstein, Dan and Dennis M. Dwyer. 1984. "Antidepressants Cause Lethal Disruption of Membrane Function in the Human Protozoan Parasite *Leishmania*." *Science* 226(4677):977–79.
- Zilberstein, Dan, Varda Liveanu, and Amira Gepstein. 1990. *TRICYCLIC DRUGS REDUCE PROTON MOTIVE FORCE IN LEISHMANIA DONOVANI PROMASTIGOTES*. Vol. 39.